Vol. 191, December 31, 1986
Complete in one issue
ISSN 0003-2670
Special Issue

THIRD INTERNATIONAL CONFERENCE ON CHEMOMETRICS IN ANALYTICAL CHEMISTRY, LERICI, ITALY, MAY 25–30, 1986

ANALYTICA CHIMICA ACTA

International journal devoted to all branches of analytical chemistry

ELSEVIER

ANALYTICA CHIMICA ACTA

International journal devoted to all branches of analytical chemistry
Revue internationale consacrée à tous les domaines de la chimie analytique
Internationale Zeitschrift für alle Gebiete der analytischen Chemie

PUBLICATION SCHEDULE FOR 1987

	J	F	M	A	M	J	J	A	S	O	N	D
Analytica Chimica Acta	192	193	194	195	196	197	198	199	200	201	202	203

Scope. *Analytica Chimica Acta* publishes original papers, short communications, and reviews dealing with every aspect of modern chemical analysis both fundamental and applied.

Submission of Papers. Manuscripts (three copies) should be submitted as designated below for rapid and efficient handling:

Papers from the Americas to: Professor Harry L. Pardue, Department of Chemistry, Purdue University, West Lafayette, IN 47907, U.S.A.

Papers from all other countries to: Dr. A. M. G. Macdonald, Department of Chemistry, The University, P.O. Box 363, Birmingham B15 2TT, England. Papers dealing particularly with computer techniques to: Professor J. T. Clerc, Universität Bern, Pharmazeutisches Institut, Baltzerstrasse 5, CH-3012 Bern, Switzerland.

Submission of an article is understood to imply that the article is original and unpublished and is not being considered for publication elsewhere. Upon acceptance of an article by the journal, authors will be asked to transfer the copyright of the article to the publisher. This transfer will ensure the widest possible dissemination of information.

Information for Authors. Papers in English, French and German are published. There are no page charges. Manuscripts should conform in layout and style to the papers published in this Volume. Authors should consult Vol. 190 for detailed information. Reprints of this information are available from the Editors or from: Elsevier Editorial Services Ltd., Mayfield House, 256 Banbury Road, Oxford OX2 7DE (Great Britain).

Reprints. Fifty reprints will be supplied free of charge. Additional reprints (minimum 100) can be ordered. An order form containing price quotations will be sent to the authors together with the proofs of their article.

Advertisements. Advertisement rates are available from the publisher.

Subscriptions. Subscriptions should be sent to: Elsevier Science Publishers B.V., Journals Department, P.O. Box 211, 1000 AE Amsterdam, The Netherlands. Tel: 5803 911, Telex: 18582.

Publication. *Analytica Chimica Acta* appears in 12 volumes in 1987. The subscription for 1987 (Vols. 192–203) is Dfl. 2700.00 plus Dfl. 300.00 (p.p.h.) (total approx. US $1333.30). All earlier volumes (Vols. 1–191) except Vols. 23 and 28 are available at Dfl. 231.00 (US $102.70), plus Dfl. 15.00 (US $6.70) p.p.h., per volume.

Our p.p.h. (postage, packing and handling) charge includes surface delivery of all issues, except to subscribers in the U.S.A., Canada, Japan, Australia, New Zealand, P.R. China, India, Israel, South Africa, Malaysia, Thailand, Singapore, South Korea, Taiwan, Pakistan, Hong Kong, Brazil, Argentina and Mexico, who receive all issues by air delivery (S.A.L. — Surface Air Lifted) at no extra cost. For the rest of the world, airmail and S.A.L. charges are available upon request.

Claims for issues not received should be made within three months of publication of the issues. If not they cannot be honoured free of charge.

For further information, or a free sample copy of this or any other Elsevier Science Publishers journal, readers in the U.S.A. and Canada can contact the following address: Elsevier Science Publishing Co. Inc., Journal Information Center, 52 Vanderbilt Avenue, New York, NY 10017, U.S.A., Tel: (212) 916-1250.

ANALYTICA CHIMICA ACTA
VOL. 191 (1986)

ANALYTICA CHIMICA ACTA

International journal devoted to all branches of analytical chemistry

ELSEVIER Amsterdam–Oxford–New York–Tokyo

0003-2670/86/$03.50

Printed in The Netherlands

SPECIAL ISSUE

CHEMOMETRICS IN ANALYTICAL CHEMISTRY III

Proceedings of a Conference held in San Terenzo di Lerici,
La Spezia, Italy, May 25–30, 1986

CONTENTS

(Abstracted, Indexed in: Anal. Abstr.; Biol. Abstr.; Chem. Abstr.; Curr. Contents Phys. Chem. Earth Sci.; Life Sci.; Index Med.; Mass Spectrom. Bull.; Sci. Citation Index; Excerpta Med.)

Special issue on Chemometrics in Analytical Chemistry III, Proceedings of a Conference held in San Terenzo di Lerici, La Spezia, Italy, May 25–30, 1986

Editorial

The 3rd International Conference on Chemometrics in Analytical Chemistry was held in Lerici (Italy) during May 26—29, 1986. On the one hand, the conference indicated significant progress in this general area. Chemometrics is no longer a synonym for the dilettante application of sophisticated statistical methods to chemical problems, but has grown into a recognized branch of analytical chemistry. On the other hand, many of the over 150 participants were probably made well aware of a fundamental problem of the field. Chemometrics has tended to become an autonomous discipline developing its own language, which is often hardly understood by the average analytical chemist. By publishing a selection of the papers presented at this conference in a journal devoted to all branches of analytical chemistry, the editors of Analytica Chimica Acta hope to make the general analytical chemist more aware of the new concepts that are being developed by chemometricians and to give the chemometrician a better perception of the problems that general analytical chemists have to solve in their everyday work.

J. T. Clerc
A. M. G. Macdonald
H. L. Pardue
A. Townshend

Analytica Chimica Acta, 191 (1986) 1–16
Elsevier Science Publishers B.V., Amsterdam — Printed in The Netherlands

SUPERVISED PATTERN RECOGNITION: THE IDEAL METHOD?

M. P. DERDE and D. L. MASSART

Pharmaceutical Institute, Vrije Universiteit Brussel, Laarbeeklaan 103, B-1090 Brussels (Belgium)

(Received 11th July 1986)

SUMMARY

The different criteria that should be considered in selecting a supervised pattern recognition technique for a particular application are discussed. An overview is given of the most important and most frequently-used supervised techniques and the extent to which they meet these criteria. The possibilities of two rule-building expert systems are also discussed.

Supervised pattern recognition covers many different techniques, and can be applied in many fields of scientific research. This paper deals first with the different criteria that should be kept in mind in order to select the pattern recognition techniques to be used for a given application. Next, an overview is given of the most important and most frequently-used supervised techniques and the extent to which they meet the selection criteria is discussed.

SELECTION CRITERIA

The classification rules derived should enable as correct as possible classification decisions to be made and should be easy to apply in daily practice. Obviously, the criteria are two-fold: technical (mathematical) aspects and practical aspects.

Technical aspects

Optimal boundaries. The general aim of supervised pattern recognition is to develop rules for the classification of samples of unknown origin, on the basis of a group of samples with known classification which have been characterized by a number of measurements (parameters, features). The success of classification depends on whether the classification rules are optimal for the problems under study. Optimal rules mean optimal boundaries. In multivariate data analysis, each object can be seen as a point in a multidimensional pattern space, the axes coinciding with the different variables. If the variables used in the classification problem are appropriately chosen, then objects belonging to different classes are situated in separate subspaces of the pattern space. The classification rules developed by supervised methods

0003-2670/86/$03.50

correspond to boundaries that implicitly or explicitly divide the pattern space into several subspaces.

Optimal boundaries can be obtained only if the situation of the different classes in the pattern space is exactly known. This is only possible if the shape of the distribution of the population in the pattern space is known, and if the distribution parameters of the population are known. Theoretically, then, optimal boundaries can be obtained only if each class is represented by an infinite number of samples, which is of course impossible. In practice, the population distribution and distribution parameters are estimated on the basis of a sample of restricted size. It is clear that this sample should be representative of the classes and that the sample size should be sufficiently large because the estimation of the population parameters becomes more accurate as larger samples are taken.

A first distinction can be made between techniques that take account of information on the population distribution and those that do not. The non-parametric techniques (e.g., KNN, ALLOC, PRIMA) make no assumptions on the population distribution (i.e., do not take information on the population distribution into account) while parametric techniques (e.g., LDA, UNEQ, SIMCA) do. The parametric techniques are based on a well defined distribution. LDA and UNEQ, for instance, are based on the assumption that the population distributions are multivariate normally distributed. Consequently they yield optimal boundaries only if the populations are indeed multinormal. If information is available on the shape of the distributions and on the distribution parameters, it is advisable to make use of a technique that takes this information into account. The efficiency of parametric techniques is greater than that of non-parametric techniques, especially when only small samples are used.

If no such information is present or no technique exists that takes account of the particular distribution of the population, then non-parametric techniques should be used. But when parametric techniques are applied to cases in which there are large deviations from the assumptions made about the population distribution, the boundaries obtained will be far from optimal.

Overlapping regions. As stressed above, an appropriate choice of the parameters used in the classification is necessary to obtain good results. If one wants to discriminate groups that resemble each other closely, it becomes impossible to find a combination of parameters that allows complete discrimination. In this case, the subspaces in the pattern space where the individual classes are situated overlap. An example is the classification of South Italian olive oils according to the region from which they derive, on the basis of their percentage distribution of 8 fatty acids [1, 2]. Visualization of the data set (consisting of 117 olive oil samples originating from three different regions in Italy) by means of a LDA display (Fig. 1a) indicates that some of these classes are discriminated (e.g., Calabria and North Apulia), while others overlap (e.g., Sicily and Calabria).

The classification rules derived with discriminating techniques correspond

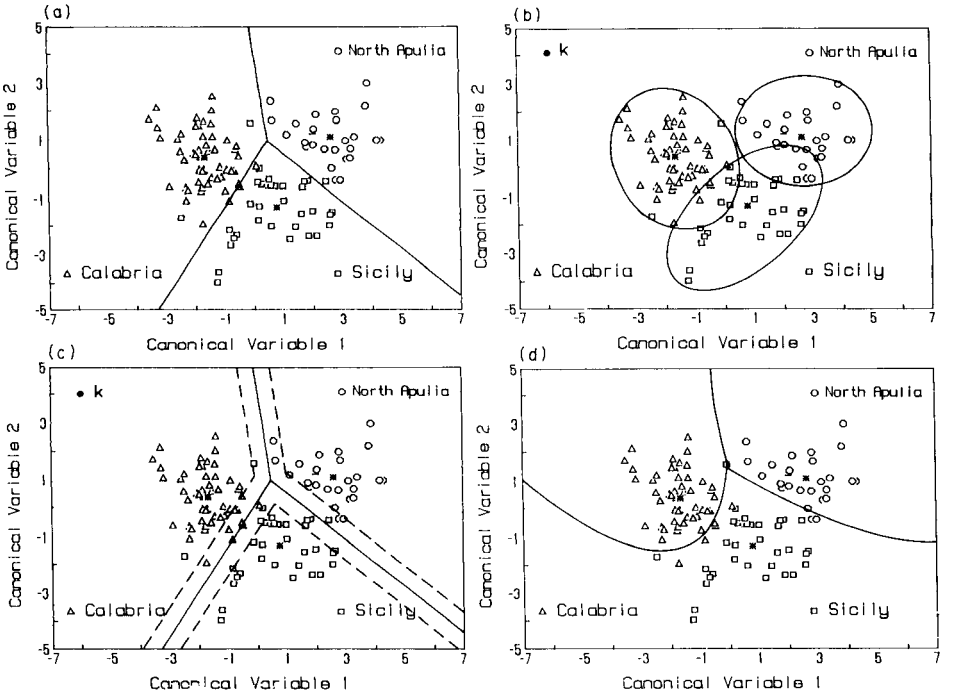

Fig. 1. (a) LDA display of 117 samples of olive oils originating from three different regions in Italy and characterized by their percentage distribution of 8 fatty acids. The straight lines are the decision boundaries obtained with LDA; they are situated halfway between the centroids of the classes (indicated by *). (b) Illustration of a class-modelling approach: for each class separately, a class box is defined that surrounds the location of the class in the pattern space by a closed boundary. Test object *k* falls outside all class boxes, and so will be classified as an outlier, i.e., not belonging to one of the three training classes. (c) With discriminating techniques, probabilistic classifications are obtained by using Bayes' theorem; stating that the empirically-established probability must at least equal a predefined threshold value (e.g., 0.95) corresponds to the creation of regions of doubt around the boundaries. (d) Illustration of discriminating boundaries as obtained with QDA.

to boundaries that subdivide the pattern space in as many regions as there are classes in the training set (e.g., KNN, LDA and ALLOC). For a three-group problem, for example, the pattern space is divided into three subspaces. When a discriminating technique is used for the classification of objects into overlapping classes, the decision boundary is forced through the overlapping region, so that some samples are misclassified. An illustration is given in Fig. 1(a).

The emphasis in class-modelling techniques lies on the modelling of each of the classes of the training set on the basis of the similarities between the objects within a class (e.g., UNEQ, SIMCA and PRIMA). The decision rules defined by these techniques are closed boundaries, one for each of the training classes separately. They envelop the class subspaces, thus defining a

'class box' for each of the classes. An illustration is given in Fig. 1(b). The construction of a class box for a particular class involves two steps. Based on the training objects for that class, the class is first modelled by a representative point or interval (M). This estimates the location of the class population in the pattern space. The data for each training object ($\mathbf{X}_k$) belonging to the class, can thus be split into a part explained by the model (M), and a residual, unexplained, part (E_k): $\mathbf{X}_k = M + E_k$. The residuals measure the degree of dispersion of the class around the class model. They are used to construct class boundaries around the class model. This involves the construction of some kind of a confidence interval. If classes overlap, so will their class boxes. When a test object falls inside the overlapping region of the class boxes, the classification decision will be that there is not sufficient evidence to clasify it unambiguously. Thus, for applications where classes resemble each other closely, a modelling technique should be preferred to a discriminating one because it recognizes overlapping regions.

Estimation of the degree of certainty of a classification. A third possible distinction between techniques is based on their deterministic (e.g., KNN and PRIMA) or probabilistic character (e.g., UNEQ and SIMCA). With a deterministic technique an object is classified in one and only one of the training classes and the degree of reliability of this decision is not measured. Probabilistic techniques provide an estimate of the reliability of the classification decision.

Probabilistic properties are introduced in different ways for discriminating techniques and modelling techniques. Probabilistic discriminating techniques make use of Bayes' theorem. Once an object k has been classified into a class ($\mathbf{Q}_q$), the posterior probability of class membership is estimated on the basis of the Bayes equation.

$$P(\mathbf{Q}_q/\mathbf{X}_k) = \left[P(\mathbf{X}_k/\mathbf{Q}_q)\,P(\mathbf{Q}_q)\right] \Big/ \left[\sum_{l=1}^{r} P(\mathbf{X}_k/\mathbf{Q}_l)P(\mathbf{Q}_l)\right] \tag{1}$$

where $P(\mathbf{Q}_l)$ is the prior probability of class $\mathbf{Q}_l$, $P(\mathbf{X}_k/\mathbf{Q}_l)$ the probability density of class $\mathbf{Q}_l$ in position $\mathbf{X}_k$, and r the number of classes in the training set. On the basis of the posterior class membership probabilities, $P(\mathbf{Q}_q/\mathbf{X}_k)$, regions of doubt can be constructed around the boundaries (Fig. 1c); they can consist, for example, of those regions where the posterior probability for any class is less than 0.95.

In probabilistic modelling techniques, the boundaries of the class box correspond to confidence limits defined on a statistical basis. They are constructed in such a way that a predefined fraction $(1 - \alpha)$ of the class falls inside the boundaries of the class box. These methods are based on the assumption that the distance towards the class model of objects belonging to this class, follows a known distribution (e.g., a χ^2-distribution). On the basis of this known distribution, the probability density of the class in $\mathbf{X}_k$ can be estimated; $[1 - P(\mathbf{X}_k/\mathbf{Q}_q)]$ is a measure of class membership of the

concerned object and can thus be used as a measure of the probability of correct classification.

Outlier detection. An important shortcoming of discriminating techniques is that the whole measurement space is completely assigned to the classes of the training set, so that an object cannot belong to a class not included in the training set. The aberrant object must be classified in one of the training classes. This is illustrated by object *k* in Fig. 1(c). Though this object is assigned to the class of Calabrian oils, it really is an outlier.

In many applications, it is impossible to include training objects for all possible classes in the training set. Furthermore, with real data, outliers occur through faulty experiments. To detect such errors, it is necessary to use methods that are able to detect outliers. When, with a modelling technique, an object is situated within none of the class boxes (e.g., object *k* in Fig. 1(b)), this object can be suspected of being an outlier. With a discriminating approach, using only Bayes' theorem, it is not possible to detect outliers. The probability density of the Calabrian class in the position of object *k* is very small, but the probability densities of the other classes in this point will be even smaller. The resulting posterior probability of each of the classes in point *k* will thus be in favour of Calabria, i.e., will be larger than the predefined level of confidence (e.g., 95%). Outlier detection becomes possible, however, if one states that the probability density of the class in which an object is classified should, in the position of the object, at least be equal to a predefined threshold value (e.g., 0.05). In this way, modelling aspects are given to basically discriminating techniques. In contrast, modelling techniques obtain discriminating characteristics when, for the classification of an object situated in an overlap region, Bayes' theorem is used in order to derive to which of the overlapping classes it is most similar.

In general, the distinctions that have been made between modelling and discriminating techniques on the one hand and probabilistic and deterministic on the other hand, and their resulting suitability for outlier detection or use with overlapping regions, are only first and rough approximations. As shown below, modifications of most existing techniques are possible such that they show both modelling as well as discriminating aspects. Still, when the accent is on discrimination or modelling, it is preferable to use a technique originally developed for that purpose. In the same way, methods developed on a probabilistic basis are to be preferred when one desires results in terms of probabilities.

Practical aspects

The following enumeration of practical aspects that should be considered in selecting a technique is not limitative. The list merely points out some of the most important general practical aspects.

Updates. In selecting a technique, one should wonder whether it is possible that new training classes will be added later to the training set. In that case, it is advisable to use a modelling technique. Modelling techniques are

disjoint techniques which means that the decision rules for each class are independent from the other classes in the training set. This avoids repeating the learning process for all the training classes each time a new group is introduced. When it is possible that the training set will be updated with new objects, it is preferable to use a technique (such as the nearest-neighbour methods) in which classification is performed on the basis of a direct comparison of the pattern vector to be classified with those of the training objects.

Variables of mixed type. In most applications, in analytical chemistry, only continuous variables are used. However, there are applications where nominal or ordinal data may also be interesting. In medical decision-making, for example, important information may be included in the patient's symptom record. For such applications, techniques should be used that allow the use of variables of mixed types.

Irrelevant parameters. It may be that not all of the parameters measured are necessary for the classification problem under study. Moreover, in general, the reliability of the classification functions decreases when irrelevant parameters are introduced or when too many parameters are used. Indeed, the reliability usually increases with an increasing ratio of number of objects in the training classes to the number of parameters used. For LDA, this has been discussed in more detail by Lachenbruch [3]. This implies that for a given sample size the reliability is inversely proportional to the number of parameters. It is therefore advisable to eliminate irrelevant parameters.

Ease of use. People applying the decision rule in practice are not necessarily experts in the field of pattern recognition. Therefore, the decision rules should be easy to handle and the methods used to derive them should not be too sophisticated, at least in concept, so that the user understands how they work.

SUPERVISED TECHNIQUES — AN OVERVIEW

In this section, an overview is given of the most frequently used supervised pattern-recognition techniques in analytical chemistry and the extent to which they meet the criteria enumerated in the previous section. Extensive information on the mathematical background of the methods can be found in the references given for each of the methods.

Discriminating techniques

The most important discriminating techniques are discriminant analysis, the nearest-neighbour methods and the potential function classifiers.

Discriminant analysis [3]. Discriminant analysis, i.e., LDA (linear discriminant analysis) and QDA (quadratic discriminant analysis) are probably the best known and most extensively used supervised pattern-recognition techniques. They both are parametric probabilistic discriminating tech-

niques. They are parametric because they make assumptions about the population distributions. The assumptions made by LDA are that the classes are multivariate normally distributed and have equal variance/covariance matrices, i.e., that the internal dispersion of all the classes is identical. Both requirements are not absolute but should be considered as conditions for achieving optimal boundaries.

In discriminant analysis, the decision rules are defined in a reduced space, the axes of which are obtained by optimizing the criterion so that in this space as much of the discrimination between the different classes will be preserved. This corresponds to the optimization of the ratio of between-classes to within-classes dispersion as observed in this reduced space. The dimension of the reduced space (given by the discriminant axes or canonical variables) is one less than the number of classes in the training set, or equal to the number of variables, whichever is smaller. In the computation of the canonical variables, stepwise selection criteria can be used in order to include only those variables that are relevant for the discrimination. Discriminant analysis thus offers the possibility of eliminating redundant parameters. In LDA, the boundaries between the different classes are situated halfway between the centroids of the classes. This is rarely optimal in practice. In medical decision-making, for instance, where the classification often concerns the discrimination between healthy and ill people, the healthy group is often much more condensed than the ill group. The decision rule obtained with LDA is then situated too near to the more heterogeneous class so that some objects are classified erroneously in the most condensed class. The use of QDA in which there is no requirement for equal dispersion of the classes is then to be preferred (Fig. 1d).

Both methods are of the probabilistic type. Using Bayes' theorem, the posterior probability may be used in order to estimate the degree of reliability of the classification. As these techniques are of the discriminating type, outlier detection is not directly possible. However, it becomes possible if one states that the probability density for the class at the location of a test object, may not be less than a predefined threshold value.

Because the decision rules are based on all the classes in the training set, updating with new objects and/or new classes requires that the classification rules be completely redetermined. As it is assumed that the classes are multivariate normally distributed, only variables measured on an interval or ratio scale can be used in the classification problem.

The KNN method [4—6]. The simplest KNN method classifies a test object in the learning class to which the majority of the K training objects which are closest to the test object belong (Fig. 2). The appropriate K value can be selected by means of the leave-one-out procedure. Usually, the euclidian distance (on the raw data, on autoscaled data or on range-scaled data) is used as the distance measure. However, other measures of distance can also be used. If the objects are characterized by parameters of mixed types, a distance measure can be used which combines mixed-type variables [7].

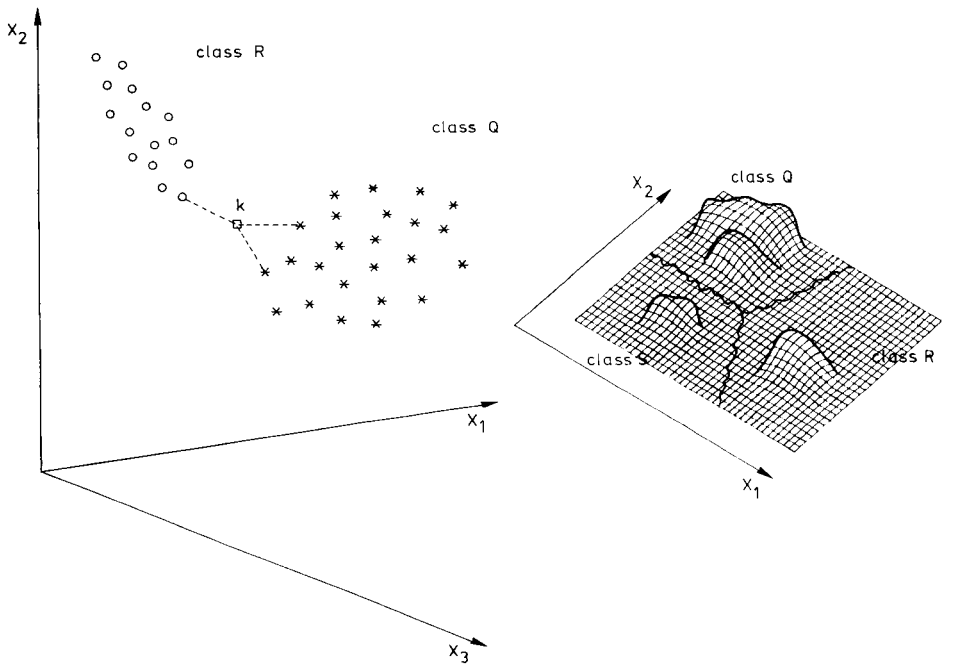

Fig. 2. 3-NN classification: object k is classified in class **Q** because, from its 3 nearest neighbours, two belong to this class.

Fig. 3. Illustration of the ALLOC method for a two-dimensional classification problem. The lines correspond to the decision boundaries between the three classes (adapted from [11]).

In its simplest form, KNN is non-parametric (no assumptions on the shape of the population distribution or on the distribution parameters), deterministic and discriminating. As classification is done by direct comparison of the pattern vector of a test object with the pattern vectors of the training objects, the boundaries that subdivide the pattern space are not explicitly formulated by means of a set of mathematical functions. Therefore, updating with new training objects or training classes is easy. This, together with its mathematical simplicity, is the major advantage of this technique.

Many modifications of these methods have been proposed that make them more attractive. In order to detect overlapping regions, the following approach can be used: an object is classified in a class if out of its K neighbours at least L (with $L > K/2$) belong to that class. Otherwise it is assigned to a region of doubt. Extensions of the basic version of KNN in order to give the method probabilistic properties have been proposed by Loftsgaarden and Quesenberry [8] and by Coomans and Massart [5, 6]. As for all dis-

criminating techniques, this probabilistic character is obtained by using Bayes' theorem (Eqn. 1). As KNN is a non-parametric technique, the probability density of the different classes for test object k, $P(\mathbf{X}_k/\mathbf{Q}_l)$, is not based on any assumption about the population distribution, but is estimated directly by means of the training set.

This leaves the problem of outlier detection. Again one can think of modifications to give the method possibilities for outlier detection. In a 1-NN classifier, for instance, this could be achieved by comparing the distance of the test object to its nearest neighbour, $d(k,1\text{-NN})$, with the distribution of the distances observed between each training object and its nearest neighbour belonging to that class. If $d(k,1\text{-NN})$ appears to be much larger than the largest distance observed between the training objects of any particular class, then the object can be suspected of being an outlier.

Potential function classifiers — ALLOC [9, 10]. The potential function methods, of which the best known in analytical chemistry is ALLOC, can be considered as generalizations of the KNN methods. In ALLOC each object of the learning set is considered as a point in the pattern space surrounded by a potential field. The highest potential is observed at the position of the object and the potential decreases with the distance from the object. The classification of an object from the test set into one of the learning classes is determined by means of the cumulative potential of the learning class in the position of the test object. The cumulative potential is obtained by adding up the individual potentials developed by the objects of the learning class in the position of the test object. The test object is classified into the class which gives rise to the largest cumulative potential. The boundary between two classes thus coincides with the positions where the cumulative potentials caused by the learning classes have the same value. ALLOC therefore belongs to the group of discriminating techniques (see Fig. 3).

ALLOC is designed to perform classifications in a probabilistic way. Using Bayes' theorem (Eqn. 1), the posterior probability that the test object belongs to a class can be calculated. This probability is not based on an assumption on the shape of the distribution of the population as in LDA, but on the basis of the mean potential of training objects of class Q_l in the position k.

ALLOC is a non-parametric technique. As different types of functions can be used to create a potential field around the training objects, functions can be applied which allow the combined use of variables expressed on different types of scales [10]. Used as such, ALLOC does not allow detection of outliers. However, as with LDA, outlier detection becomes possible if one states that an object may only be classified into a class if the probability density of that class in the position of the test object exceeds a given threshold value, as defined on the basis of the training objects of that class. Because ALLOC performs the classification of a test object in a direct way, updating of the training set with new examples is easy to perform.

As illustrated by Coomans et al. [11], potential function classifiers

are sensitive to irrelevant parameters. Therefore a feature-selection procedure, such as the one included in the ALLOC package which is based on the concept of potential functions, should be used in the training procedure. Besides the 'pure' potential function classifiers as described above, associations with other supervised techniques such as LDA [12] and SIMCA [13, 14] also seem to be promising.

Modelling techniques

UNEQ [15]. As said before, the construction of the class box for a class (Q_q) involves two steps. First, the class is modelled. In UNEQ, the class model consists of a single point, the class centroid. The distance of samples towards the class centroid is measured as the generalized distance $\tilde{d}(k,M_q)$:

$$\tilde{d}(k,M_q) = \left\{d^2(n_q - p - 2)/n_q - (p/n_q)\right\}^{1/2}$$

with $d^2 = (\mathbf{X}_k - \bar{\mathbf{X}}_q)' \, \mathbf{S}_p^{-1} \, (\mathbf{X}_k - \bar{\mathbf{X}}_q)$; $\mathbf{X}_k$ is the pattern vector of object k, $\bar{\mathbf{X}}_q$ the mean vector of class Q_q, $\mathbf{S}_p$ the sample variance/covariance matrix of class Q_q, p the number of variables used to construct the model, and n_q the number of training objects in class Q_q.

One of the interesting properties of this distance is that it takes the correlations between the variables into account in the computation of the distance between an individual sample and the centroid.

In UNEQ class models are developed for each class of the training set separately, thus the training classes may have different dispersions, i.e., different variance/covariance matrices. UNEQ therefore stands for UNEQual dispersed classes. UNEQ is a parametrical technique. It assumes that the classes are multivariate normally distributed. If this assumption applies, then the square of the generalized distance of objects belonging to the class follows a χ-square distribution with p degrees of freedom. The class boundary around the class model coincides with a confidence interval developed at a predefined α% significance level. Mathematically, the boundary is defined by a value d_{crit}; d^2_{crit} is the value for which the probability is $(1 - \alpha)$ that a χ-square distributed variable has a value less than d^2_{crit}. Geometrically, a UNEQ class box thus coincides with a (hyper)-ellipsoid with the population mean as its centroid and its size defined by d_{crit} (Fig. 4). Although UNEQ is parametrical and needs multivariate normally distributed data, the requirements are less drastic than for LDA. This is due to the disjoint character of the method.

UNEQ is a probabilistic technique. If the distribution of $\tilde{d}^2$ is known, it is also possible to associate with each value of $\tilde{d}^2(k,M_q)$ the probability $P[\chi^2_p < \tilde{d}^2(k,M_q)]$. This is the probability that an object that belongs to the population is situated nearer to the population mean than the object k; $1 - P[\chi^2_p < \tilde{d}^2(k,M_q)]$ is the degree of class membership.

SIMCA [16]. In SIMCA, each class of the training set is modelled by a principal component (PC) model. The number of significant components for class Q_q, a_q, can be defined on the basis of several criteria. In SIMCA, the

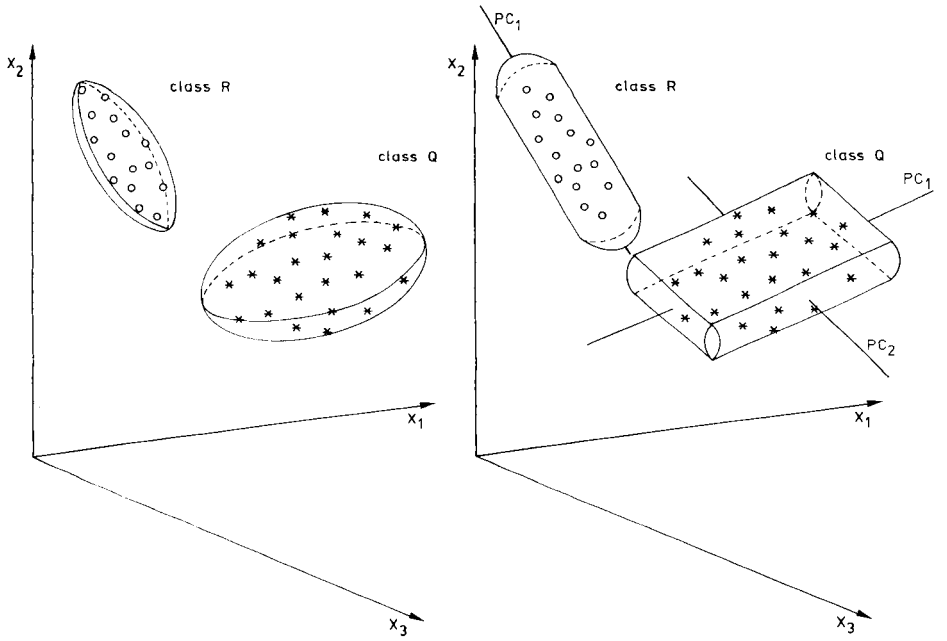

Fig. 4. Geometrical illustration of the shape of class boxes obtained with the UNEQ method.

Fig. 5. Geometrical illustration of the shape of class boxes obtained with the SIMCA method. Class **Q** is described by a 2-PC model ($a_q = 2$), and class **R** by a 1-PC model ($a_r = 1$).

cross-validation procedure is recommended for this purpose. The combination of the a_q significant PC's defines an a_q dimensional plane in the pattern space. The situation of the class model in this plane is further defined by the range of the scores of the training objects along each of the significant PC's. According to the number of components used to model a class, the shape of the class model can be a point ($a_q = 0$), a line segment ($a_q = 1$), a rectangle ($a_q = 2$), and so on. The distance between an object and the class model is given by $s_k(q)$ (residual standard deviation for object k towards the class model of class Q_q).

$$s_k^2(q) = \sum_{j=1}^{p} e_{jk}^2/(p - a_q)$$

$s_k(q)$ is a measure of how well object k is explained by the class model. Geometrically it corresponds to the orthogonal distance between the object and the plane defined by the significant components.

SIMCA is a parametric technique. It assumes that the residuals are normally distributed. Therefore, the ratio $s_k^2(q)/s_0^2(q)[= F_k(q)]$ for objects belonging to class Q_q is expected to follow an F-distribution, with $(p - a_q)$

and $(p - a_q)(n_q - a_q - 1)$ degrees of freedom; $s_0(q)$ measures the mean distance between objects belonging to the class and the class model. This makes it possible to define which is the largest value that F may have (say F_{crit}) in order that an object will be classified in that class. F_{crit} is the value for which $(1 - \alpha)\%$ of the objects belonging to the class have an F value less than F_{crit}. From F_{crit} the value s_{crit} can be derived, i.e., the distance defining the boundaries of the class box:

$$s_{crit} = [F_{crit}\, s_0^2(q)]^{1/2}$$

Geometrically, the structure of the class box obtained with SIMCA depends on the number of components used to define the class model (Fig. 5).

SIMCA is also a probabilistic technique. On the basis of the F distribution, it is possible to associate with each F_k ratio the probability $P[F < F_k(q)]$ that an object belonging to the class is situated nearer to the class model than the classified object k; $1 - P[F < F_k(q)]$ is again the degree of class membership of object k.

At first sight one may have the impression that UNEQ and SIMCA use completely different approaches but there are some points of resemblance. As will be explained in detail at a later date, it can be proven that in case of uncorrelated variables with equal standard deviation, classes are spherical and will thus with SIMCA be modelled by a single point, namely the class centroid. In this situation, there is a simple relationship existing between the distance of an object towards the SIMCA model and the distance of that object towards the UNEQ model. In case of correlated variables, SIMCA models a class by at least one principal component, thus yielding differently shaped models compared with UNEQ. However, the PC's computed with SIMCA coincide with the major axes of the (hyper)-ellipsoid that defines the UNEQ class boundaries. In fact, UNEQ is intrinsically based on principal components analysis (PCA) while PCA is used explicitly in SIMCA. This implies that both methods not only enable classifications to be performed but also allow the relationship between the variables in each class to be explored, by interpreting the loadings of the variables on the significant PC's and to define important directions within each class. This makes them particularly useful for some specific analytical applications in which it is important to have an idea about the direction within the classes. One type of classification problem in food research for instance concerns the identification of adulteration, e.g., the adulteration of orange juice by cheaper products such as apple juice. For such an application, the training set will consist of samples of pure orange juice prepared with oranges having a specific origin. Though the origin of the fruit will influence the class model, the use of mixtures of oranges from different origins is legally allowed (at least in Belgium). Therefore when different classes of orange juice, each with a specific origin, are modelled, the fact that a test sample falls outside all class models does not necessarily mean that it is not a pure juice but can also indicate that the sample is a mixture. Information on the direction in which this sample is

outlying, i.e., the position of the sample on the PC's can reveal whether the sample is situated far away from all 'pure' orange juice classes, in which case it probably is adulterated, or situated somewhere between the 'pure' classes in which case it may be a mixture. Another example in which the interpretation of the directions within the classes is important concerns medical diagnosis. Indeed, the degree of illness of patients generally coincides with one of the main directions in the disease class [17]. When a patient is classified into a disease class, it is important to know where he is placed along this direction.

PRIMA [18]. As in UNEQ, PRIMA models the classes by the class centroid. The spread of the class around this modelling point is measured by the dispersion of the individual parameters, i.e., by their standard deviation. The resemblance between an object and the class model for class Q_q is measured as the euclidian distance calculated on the autoscaled variables:

$$d(k,M_q) = \left\{ \sum_{j=1}^{p} [x_{jk} - \bar{x}_j(q)]^2 / s_j^2(q) p \right\}^{1/2}$$

In contrast to UNEQ, correlations between the parameters are thus not taken into account. The class boxes defined with PRIMA therefore have a spherical shape around the class centroid (Fig. 6). The radius of these spheres is defined by a value d_{crit}. As stated by Juricskay and Veress [18], d_{crit}

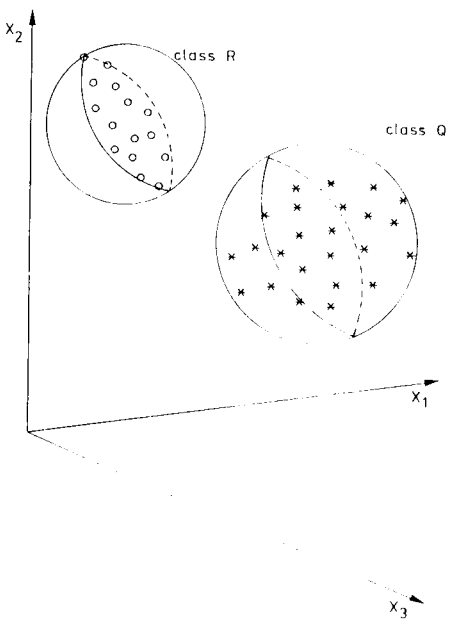

Fig. 6. Geometrical illustration of the shape of class boxes obtained with the PRIMA method. The class box for class **R** is less suitable as the variables are strongly correlated. This problem can be overcome by decorrelating the variables by means of PCA.

should be a suitably selected limiting value, evaluated iteratively on the basis of the recognition rate. This means that a value should be sought such that an optimal recognition ability is obtained for all the training classes under consideration. This is an essential difference from UNEQ and SIMCA in which the class boundaries are defined on the basis of an underlying distribution. Therefore, PRIMA is a non-parametric method. It also is a deterministic method as no information is obtained on the reliability of the classification decision.

Another essential difference is that PRIMA ignores the correlations between the variables. The PRIMA class boxes might therefore be less suitable when some of the variables are strongly correlated. This problem can however easily be overcome by applying PRIMA on decorrelated variables, obtained by an orthogonal transformation of the original variables (i.e., on the principal component scores) rather than on the original variables. In contrast to UNEQ and SIMCA which, because of the assumptions they are based on, can only be used with continuous variables, PRIMA can also be used with mixed-type variables, provided that a suitable measure of distance is used.

EXPERT SYSTEMS

Appropriate selection of a technique for a given application is not easy for non-experts in this field. The use of expert systems might therefore be an attractive alternative. Expert systems are software products that incorporate the knowledge of the expert and try to make consistent decisions on the basis of this knowledge. An expert system consists of two parts: the knowledge base and the inference machine that makes decisions on the basis of the content of the knowledge base. In the so-called rule-building expert systems, the knowledge can be entered as examples, i.e., as a data base consisting of a set of observations made on several objects with a known "decision", i.e., a known classification.

Typically, this is the kind of information one starts from in a supervised application. As the final purpose of supervised pattern-recognition techniques and the rule-building expert systems is the same, namely a classification, the performance of two such commercially available systems, EXTRAN (J. Perrone and Associates, San Francisco, CA 94114; 1985) and TIMM (General Research, Santa Barbara, CA 93105; 1985), was investigated. Both systems were compared for their performance on a data set to which several pattern-recognition techniques had already been applied, i.e., the classification of olive oils characterized by the percentage distribution of fatty acids and originating from different regions in Italy. Full detail will be given at a later date, but some general conclusions can be summarized.

EX-TRAN. EX-TRAN is an expert system that generates a decision-tree set of rules. The program searches the variables one at a time to identify the one with which it can best separate one class from another. The choice is

based on an information theoretical measure. The program splits the training set into a number of subgroups on the basis of this parameter. Objects with a parameter value less than the value midway between the two closest objects of the subgroups are assigned to one subgroup and those greater than or equal to the threshold value are assigned to the other. For each subgroup separately, this procedure is repeated until all objects within a subgroup belong to the same class. Thus EX-TRAN is a sequential univariate classification method. EX-TRAN clearly belongs to the group of discriminating techniques. It creates, piecewise, linear boundaries with the directions of the different parts of the boundaries orthogonal to the variable axes. As an illustration, Fig. 7 gives the decision rule obtained for the discrimination between East and West Ligurian olive oils. As no indication is obtained on the probability of having made the correct classification decision, EX-TRAN only allows a "black/white" classification. Outlier detection is not directly possible.

The fact that this system clearly belongs to the group of non-parametric deterministic discriminating techniques, makes it appropriate only for classification problems in which there is little noise in the data set, i.e., for applications where the classes are separable to a high degree. EX-TRAN has some attractive practical advantages: as it is designed for use by non-experts, it is extremely user-friendly; variables of mixed types can be used; and it uses only as many variables as necessary in order to define the boundaries. This indicates that it contains a built-in feature-reduction procedure.

TIMM. The user manual of TIMM is much less clear about the algorithm used to derive the decision rules. The fact that this program is presented as a black box is a serious disadvantage. TIMM uses some kind of nearest neigh-

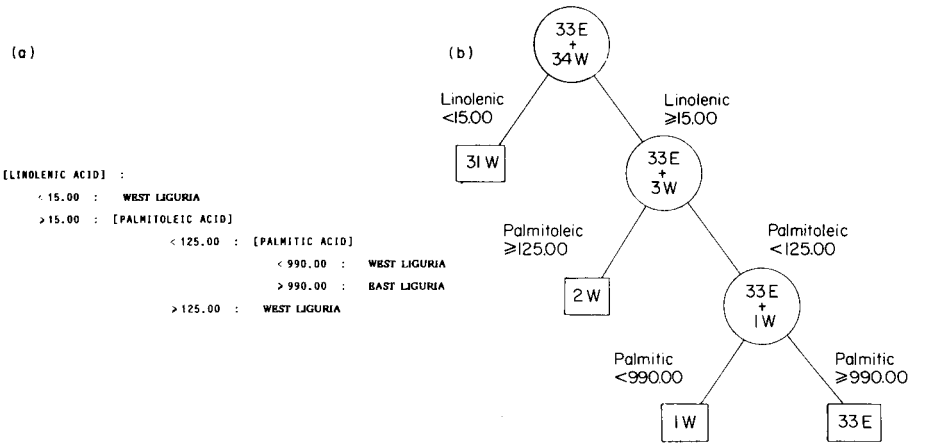

Fig. 7. (a) Decision tree sets of rules derived with EX-TRAN for the discrimination between East and West Ligurian olive oils. (b) The training set, consisting of 33 East and 34 West Ligurian oils is split stepwise into subgroups until all of splinter groups contain only samples from the same origin. Though the samples are characterized by 8 fatty acids, only three are used for the discrimination.

bour algorithm with the euclidian distance based on range-scaled variables as distance measure. After the objects have been classified, a reliability value is given to the classification. Again, insufficient information is given on how this reliability is computed. Anyway, this parameter seems to have no statistical background. Like EX-TRAN, TIMM thus belongs to the group of non-parametric deterministic discriminating techniques. As TIMM basically uses a nearest neighbour approach, it has the same advantages and disadvantages: features of mixed types can be used (nominal, ordinal, numeric); updating is easy; and the program is easy to use and to understand.

Conclusion

The commercially available rule-building expert systems appear to be extremely user-friendly, which is an important advantage, but the algorithms used in order to derive the decision rules are not optimal for all applications. Very powerful supervised techniques are available, such as the probabilistic modelling techniques. Thus a combination of the advantages of both, namely the incorporation of modelling algorithms into an expert system framework, would yield very attractive and powerful tools for most supervised applications.

The authors thank the Fonds voor Geneeskundig en Wetenschappelijk Onderzoek and Lotto for financial support.

REFERENCES

1 M. Forina and C. Armanino, Ann. Chim. (Rome), 72 (1982) 127.
2 M. Forina and E. Tiscornia, Ann. Chim. (Rome), 72 (1982) 143.
3 P. A. Lachenbruch, Discriminant Analysis, Hafner Press, New York, 1975.
4 D. L. Massart, A. Dijkstra and L. Kaufman, Evaluation and Optimization of Laboratory Methods and Analytical Procedures, Elsevier, Amsterdam, 1978.
5 D. Coomans and D. L. Massart, Anal. Chim. Acta, 136 (1982) 15.
6 D. Coomans and D. L. Massart, Anal. Chim. Acta, 138 (1982) 153.
7 L. Kaufman and P. Rousseeuw, Finding Groups in Data, Wiley, New York, in press.
8 D. O. Loftsgaarden and C. P. Quesenberry, Ann. Math. Stat., 36 (1965) 1049.
9 J. Hermans and J. D. F. Habbema, Manual for ALLOC Discriminant Analysis Program, Department of Medical Statistics, University of Leiden, The Netherlands, 1973.
10 D. Coomans and I. Broeckaert, Potential Pattern Recognition, Wiley, New York, 1986.
11 D. Coomans, M. P. Derde, D. L. Massart and I. Broeckaert, Anal. Chim. Acta, 133 (1981) 241.
12 D. Coomans, I. Broeckaert and D. L. Massart, Anal. Chim. Acta, 132 (1981) 69.
13 H. Van Der Voet and D. A. Doornbos, Anal. Chim. Acta, 161 (1984) 115.
14 H. Van Der Voet and D. A. Doornbos, Anal. Chim. Acta, 161 (1984) 125.
15 M. P. Derde and D. L. Massart, Anal. Chim. Acta, 184 (1986) 33.
16 S. Wold, M. Sjostrom, in B. R. Kowalski (Ed.), Chemometrics: Theory and Application, American Chemical Society, Washington, 1977, p. 243.
17 D. Coomans, A. Bossuyt, I. Broeckaert, M. Ingels, M. Jonckheer, D. L. Massart, W. Musch and S. Wold, Medinfo, January (1983).
18 I. Juricskay and G. E. Veress, Anal. Chim. Acta, 171 (1985) 61.

Analytica Chimica Acta, 191 (1986) 17—32
Elsevier Science Publishers B.V., Amsterdam — Printed in The Netherlands

MULTIVARIATE DESIGN

SVANTE WOLD*, MICHAEL SJÖSTRÖM, ROLF CARLSON, TORBJÖRN LUNDSTEDT, SVEN HELLBERG, BERT SKAGERBERG, CONNY WIKSTRÖM and JERKER ÖHMAN

Department of Organic Chemistry, Umeå University, S-901 87 Umeå (Sweden)

(Received 26th May 1986)

SUMMARY

In multivariate data analysis such as principal components analysis (PCA) and projections to latent structures (PLS), it is essential that the training set systems (objects) are selected to provide data with substantial information for model parametrization, and to represent properly any future situations where the multivariate model is used for predictions. In the framework of multivariate projections (PCA, SIMCA and PLS), elementary concepts of statistical design (fractional factorials and composite designs) can be used with the latent variables (PC or PLS scores) as design variables. The plan of action thus becomes: (1) problem formulation (specify aim and model, make a conceptual division of the investigated system into subsystems); (2) collection of multivariate data on a range of subsystems; (3) estimation of the practical dimensionality of the data for each type of subsystems by PC or PLS analysis; (4) use of the PC or PLS scores (t) as design variables in the combination of subsystems to systems in the training set; (5) measurement of responses (Y); (6) analysis of data by PCA or PLS; (7) interpretation of results with possible feedback to steps 1, 2 or 3. The procedures are illustrated by two problems: a structure/activity relationship for a family of peptides, and optimization of an organic synthesis with respect to system variables (solvent, substrate, co-reactant) and process variables (temperature, reactant concentrations).

Chemists have only recently realized that it is inefficient to change one "factor" at a time when investigating a system by a series of experiments [1]. As an illustration, consider a simple process influenced by only two factors (Fig. 1). By changing all variables simultaneously by factorial or fractional designs [1] or simplex designs [2], the experimental domain can be scanned efficiently and the real optimum reached. In this way, the optimum is reached with fewer experiments than are usually needed with the "one variable at a time" (OVAT) approach [1].

A second area where OVAT has been shown to be inefficient is in multivariate analysis, i.e., the analysis of data tables. The essence of multivariate analysis is to look at all data simultaneously, e.g., as points in a space with as many dimensions as there are variables (see Fig. 5, below). With more than three variables, projections of the multidimensional space give patterns, views of the data, which display the essential information in the data [3]. A consequence of the superior information content of multivariate data is that any

0003-2670/86/$03.50

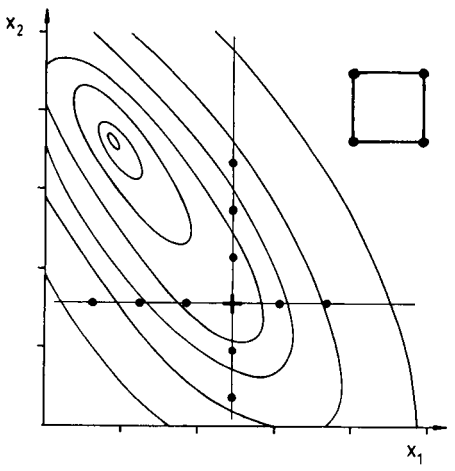

Fig. 1. A simple process influenced by only two variables. Making experiments by changing one variable at a time (OVAT) leads to a false optimum, +, far from the real optimum. When the first variable is changed, one finds the ridge, but when thereafter the second variable is changed, one falls off the ridge again. This is because it is necessary to have a step length which is large enough to allow noticeable differences in response between the experiments. Only by changing both variables simultaneously with, for instance, a factorial design, can the real optimum be reached. This is because such designs give information about favourable directions in any angle to the coordinate axes. The upper right in figure contains a factorial design, a square in the case of two variables.

chemical "effect" or response should be described, quantified, characterized, by a multitude of variables. The projection of this multitude of measurements will provide a better response variable than a single measurement [4—6].

In the construction of a training set for a data analytical projection, it is essential that this set of objects spans the pertinent experimental region properly. If not, the resulting model will give bad predictions in parts of the region; i.e., the training set must be selected according to a statistical design. In the context of multivariate analysis, this training set selection is usually not as easy as an ordinal statistical design. What can be experimentally manipulated is often a change of subsystems; e.g., change between different solvents and catalysts, or the change of a substituent in a reactant. These changes often do not correspond directly to the individual factors of the problem, but involve the simultaneous change of several factors. Thus, for instance, the change of solvent in a synthesis may involve the change of polarity, hydrogen-bonding ability, charge-transfer complexing ability and still other factors. It is difficult to make a change so that only one of these factors changes and the others remain constant.

With multivariate projection methods, however, one can see a solution to this problem of multivariate design, namely a design in terms of the latent variables resulting from an initial projection of a multivariate characterization of the involved subsystems. This is the aim of the present paper. The

illustrations given include: (i) the design of series of compounds for the development of structure/activity relationships; and (ii) the design of series of experiments for the optimization of a chemical synthesis with respect to the choice of solvent, coreactant and substrate.

STATISTICAL DESIGN

Beginning with the pioneering work of Fisher [7], it has become clear that in the experimental investigation of a system, all variables influencing the system must be changed simultaneously in order to make the measured data contain information about the position of the system optimum. Figure 1 above is a geometrical demonstration of this well known fact.

The simultaneous change of all variables demands a strict mathematical protocol in order not to lose experimental control. For this purpose, Yates [8], Finney [9], Plackett and Burman [10], and Box and Wilson [11] developed the protocols of factorial designs, fractional factorial designs, and composite designs. Several good text books present the methodology in detail [1, 12, 13].

Two-level factorial designs form the basis for these schemes. Each variable that is changed (pH and T in Fig. 1) is changed between two and only two levels, denoted by + and − (high and low). A complete factorial design (CFD) in two variables is given by the four experiments ++, +−, −+ and −−. In general, with K variables, 2^K experiments are made in a CFD. These can be visualized as the corners of a K-dimensional super-cube. Figure 2 shows this design for three variables. In a composite design, the factorial design is expanded with experiments on the variable axes, such as (0, 0, 0), (0, 0, 1.3),

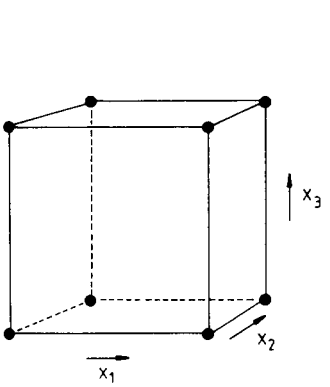

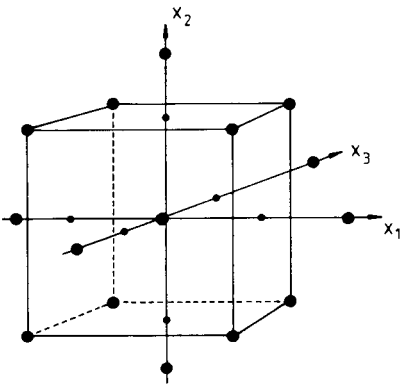

Fig. 2. The eight experiments in a 2^3 complete factorial design (CFD) are performed in the corners of a cube. In p variables, the CFD is a hypercube in p dimensions.

Fig. 3. A composite design is a factorial design expanded with additional experiments on the variable axes.

(0, 1.3, 0) and (1.3, 0, 0), (0, 0, −1.3), ... for the case with three dimensions (Fig. 3).

With many variables, however, the 2^K CFD and its composite extension correspond to an impossibly large number of experiments. For K = 10, for instance, 2^{10} equals 1024, which might need years of experimentation. For this case, the fractional factorial designs (FFD) provide relief.

If it can be assumed that part of the variables, regardless of which, has only slight influence on the studied process, it is sufficient to make a fraction of the experiments of a CFD and still get almost the same information (Fig. 4). For multidimensional designs, this can lead to an enormous reduction in the number of experiments. Instead of making 1024 experiments in a 2^{10} CFD, a FFD with 16 carefully selected experiments may give sufficient information.

Box and Meyer [14] have recently reviewed the application of FFD and found that a reduction factor of about 0.20 is typical in practice. Thus only about a fifth of the variables has substantial influence on a typical process and therefore a large reduction is usually possible, i.e., using 2^{K-r} FFDs.

How to apply statistical designs in multivariate modelling

The basic difficulty in applying statistical designs in multivariate analysis is that the factors that the investigator can manipulate separately are often not the same as those thought to influence the investigated system.

In peptides, for instance, the investigator can with some difficulty change one amino acid to another in a given compound. But the factors believed to

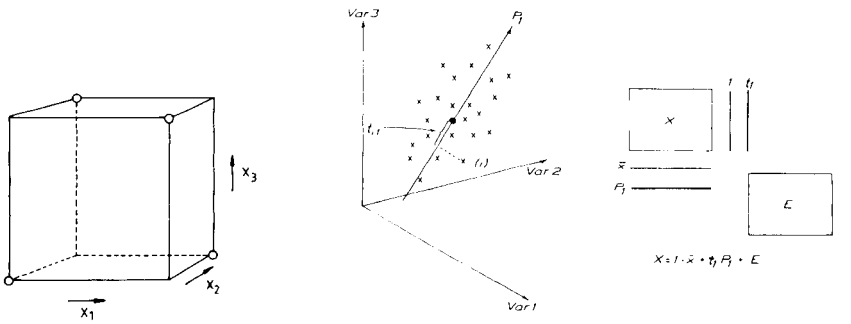

Fig. 4. A fractional factorial design, FFD (here half factorial) in three variables.

Fig. 5. A 3-space with a swarm of points approximated by a one-dimensional PC model (a straight line). The direction coefficients of the line comprise the loading vector **p**, and the coordinates of the projections of the points down on this line comprise the score vector **t**. The values of the latter are measured from the middle point of the data so that t_i is zero in this middle point as indicated in the figure. In one direction from the middle point, t_i is positive and, in the other direction, t_i is negative. Spaces with more than three dimensions have fundamentally the same properties as a 3-space with respect to such geometrical concepts as points, lines, planes, angles, and distances. Hence, 3-spaces can be used as conceptual models for M-spaces with 4, 5, 6, or any finite number of dimensions.

influence the biological properties of the peptide are lipophilicity, size, electronic inductive effect, hydrogen bonding, etc. And when the amino acid at one position is changed, all these factors change. It is more or less impossible to make a structural change in a peptide so that only one factor, say lipophilicity, is varied.

Similarly, in the second example discussed below, that of organic synthesis, the change of solvent or substrate involves the simultaneous change of a number of microscopic factors such as polarity, hydrogen bonding, solubility, etc., factors that cannot be individually manipulated in experiments.

A solution to these difficulties in applying statistical designs to multivariate problems has been outlined by Hellberg et al. [15] and Carlson and co-workers [16, 17]. The subsystems that can be changed in the experiments (amino acids in the peptide structure or the solvent and reactants in the synthesis) are characterized by a broad range of multivariate data. These multivariate data are then projected down on few-dimensional subspaces, separately for each type of subsystems. Thereafter, the coordinates in these subspaces (the latent variables, here called "principal properties") are used as design variables. Indeed, this gives a plan which works in practice as will be seen below, but first we shall briefly rehearse this approach to multivariate analysis.

It should be noted, however, that there are important applications of multivariate analysis in chemistry where the involved factors can be directly controlled and manipulated and where consequently ordinary designs in these variables can be used. Multivariate calibration in analytical chemistry is an example of this case. The concentrations of the analytes can be set to any desired value in the standard samples. A design, say a composite design, in these analyte concentrations will provide a good and informative calibration set. The only slightly unusual point in this calibration situation is that the design is made on the **Y** matrix instead of on the **X** matrix, but this is a natural consequence of the use of the inverse calibration approach.

MULTIVARIATE ANALYSIS

As discussed by Wold and co-workers [5, 6], all common problems in multivariate data analysis, i.e., the analysis of data tables, can be approached by means of projections. Different types of problem correspond to different projections.

Principal components analysis (PCA) provides the basic projection of a data table with the aim to get an overview and a good approximation of the table. Principal components analysis can be regarded geometrically as finding the linear structure (line, plane or hyperplane) that adequately approximates the swarm of data points in the K-dimensional measurement space (M-space). Though an M-space with more than three dimensions cannot be directly visualized, 3-spaces serve as good models of higher-dimensional spaces, in that all basic concepts such as points, lines, planes, angles, and distances have the same properties in both 3-spaces and M-spaces with any finite number of dimensions.

Although the PC model is a linear geometrical structure, it is capable of good approximation of non-linear data structures. Thus, for instance, a curve in M-space is well approximated locally by a plane. The PC model is a local linearization of arbitrarily complex data structures which is powerful as long as the data structures can be seen as generated by a continuous and differentiable process. In this way PC and PLS models (see below) of data matrices correspond to polynomial expansions of bivariate (x, y) data. In M-space, each object (row in the data table) is represented as a point and hence the data table is a swarm of points and the PC model is a line or plane or hyperplane (Fig. 5).

Mathematically, PCA corresponds to the decomposition of the data matrix **X** into a mean vector plus a score matrix **T** times a loading matrix **P**′ plus residuals **E**.

$$\mathbf{X} = 1\bar{x} + \mathbf{T}\mathbf{P}' + \mathbf{E}$$

The dimensionality of the PC model, A, corresponds to the number of columns in **T** and rows in **P**′. It can be shown that, provided that the objects represented in the data matrix **X** are similar to each other, the dimensionality A is small [18]. A good way to establish an adequate dimensionality for a given data set is cross-validation [19, 20]. This gives the dimensionality that corresponds to the best predictions of data elements deleted from the matrix.

The loading matrix **P** is a projection matrix with orthogonal columns that projects **X** on a hyperplane giving the projection coordinates **T**. The score matrix **T** also has orthogonal columns. This projection can be considered as constructing a window with A dimensions in M-space and looking at the data through this window. Plotting the columns in **T** against each other gives the view through this window (see Figs. 7 and 8 below).

In the present context PCA is used to reduce the dimensionality of data matrices characterizing the changing subsystems of an investigated system. The score vectors **t** are few and orthogonal and summarize the properties of the subsystems. Hence, these t-scales can be used as design variables governing how the subsystems should be combined to give an informative training set of systems.

Example 1. Principal components analysis of a property matrix for 20 amino acids

To get an idea of the complexity involved when one amino acid is changed to another in a protein or in a peptide, Hellberg et al. [15] collected a matrix of 29 physical and chemical measurements such as pK_a, pI, ^{13}C-n.m.r. of the α-carbon and the carboxyl carbon, ^{1}H-n.m.r. of the α-hydrogen, and various hydrophilicity scales, for the 20 amino acids coded by RNA in the amino acid synthesis.

A PC model with three significant dimensions (cross-validation) was obtained, explaining together about 60% of the variance of the data. The three score vectors (t_1 — t_3 in Table 1) can be regarded as "principal properties"

TABLE 1

Values of the principal properties t_1, t_2 and t_3, resulting as scores from a principal components analysis of a data matrix of 29 variables for the twenty "natural" amino acids. These scales are tentatively interpreted as hydrophilicity (negative lipophilicity), bulk and electronic effect, respectively

Amino acid	t_1	t_2	t_3	Amino acid	t_1	t_2	t_3
Ala A	0.07	−1.73	0.09	His H	2.41	1.74	1.11
Val V	−2.69	−2.53	−1.29	Gly G	2.23	−5.36	0.30
Leu L	−4.19	−1.03	−0.98	Ser S	1.96	−1.63	0.57
Ile I	−4.44	−1.68	−1.03	Thr T	0.92	−2.09	−1.40
Pro P	−1.22	0.88	2.23	Cys C	0.71	−0.97	4.13
Phe F	−4.92	1.30	0.45	Tyr Y	−1.39	2.32	0.01
Trp W	−4.75	3.65	0.85	Asn N	3.22	1.45	0.84
Met M	−2.49	−0.27	−0.41	Gln Q	2.18	0.53	−1.14
Lys K	2.84	1.41	−3.14	Asp D	3.64	1.13	2.36
Arg R	2.88	2.52	−3.44	Glu E	3.08	0.39	−0.07

of the amino acids, i.e., principal properties that summarize most properties of the amino acids. Thus most measurements on an amino acid are fairly well described as linear combinations of these three scales.

Partial least-squares projections. With PC projections, it was possible to obtain a representation of the variation in the matrix **X** as **TP'** with the only aim that this would provide a good approximation of **X**. This PC projection is useful for getting a representation of **X** and also for obtaining models of separate classes of objects when the aim is classification or discrimination between classes of objects (the SIMCA method [5, 6]).

A common problem in multivariate data analysis is to search for correlations between batteries, blocks, of variables with the scope either to predict one block from the other or to seek any joint information in the blocks.

Optimization is a typical PLS application, where a block of *X*-variables is manipulated experimentally to change the performance of a system and a block of *Y*-variables measure the response of the system with respect to properties of interest, e.g., the biological effect of a compound, or the yield of a synthesis. A model predicting **Y** from **X** then gives information on how to change **X** to improve **Y**.

The appropriate projection methodology for these problems was developed by H. Wold [21] and is called PLS (partial least-squares modelling in latent variables, or projections to latent structures). Splitting the data matrix **Z** variable-wise into the two blocks **X** and **Y**, the PLS method projects each of the blocks onto a model of the same form as the PC model:

$$\mathbf{X} = 1\bar{x} + \mathbf{TP}' + \mathbf{E}$$

$$\mathbf{Y} = 1\bar{y} + \mathbf{UQ}' + \mathbf{F}$$

In the case for which the **Y** block consists of a single variable (corresponding to multiple regression), **Y** is not projected but **U** is identical to **Y**. When the aim is to predict **Y** from **X** (predictive PLS or PPLS), there is also an inner predictive relation for each pair (dimension index a) of column vectors in **U** and **T**: $\mathbf{u}_a = b_a\mathbf{t}_a + \mathbf{h}_a$. Here $\mathbf{h}_a$ is a vector of residuals and b_a is a regression coefficient.

For correlative PLS, also called consensus PLS (CPLS), each pair of column vectors in **U** and **T** are instead modelled by a common component v ($\mathbf{g}_a$ and $\mathbf{h}_a$ are vectors of residuals and b_a and c_a are loading coefficients): $t_a = b_a\mathbf{v}_a + \mathbf{g}_a$ and $\mathbf{u}_a = c_a\mathbf{v}_a + \mathbf{h}_a$. As for PCA, the appropriate dimensionality of PLS models can be established by cross-validation.

Example 2. A structure/activity relationship for a peptide family

For a family of $N = 15$ pentapeptides, Ufkes et al. [22] measured the bradykinin potentiating activity. Hellberg et al. [15] parametrized the peptide structure by describing each amino acid position by the three principal property scales (see Example 1). Thus, the structure of each peptide is quantified in terms of fifteen numbers (5 positions × three scales).

A PLS model between the (15 × 15) structure matrix **X** and the (15 × 1) biological activity matrix **Y** gave two significant dimensions explaining 97% of the variance in **Y**. The resulting model was used to predict the bradykinin potentiating activity for another set of pentapeptides [22] as shown in Fig. 6.

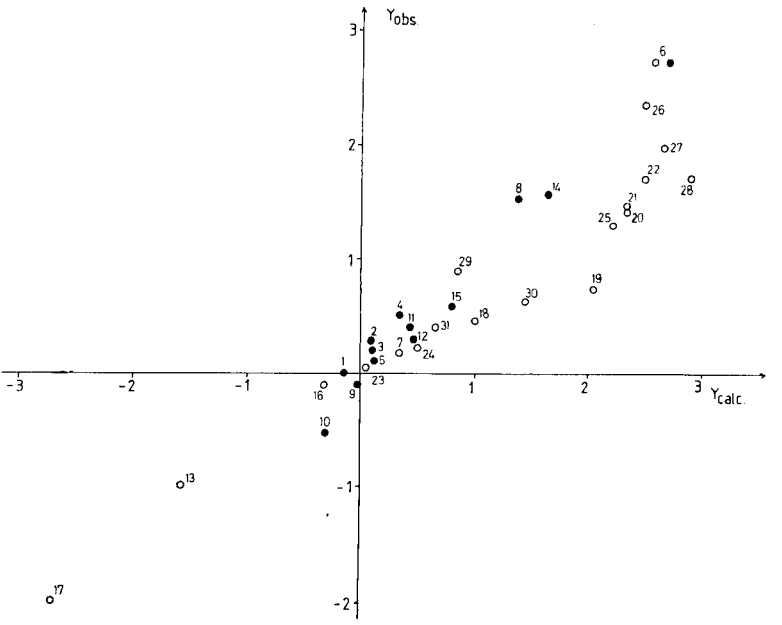

Fig. 6. Predicted activity plotted against observed activity for the pentapeptides of Ufkes et al. [22]: (•) the 15 compounds included in the development of the PLS model (training set); (○) prediction set of compounds not included in the model development.

Model dimensions, factors, latent variables. In Example 1, the score vectors (columns in **T**) were seen as new variables that were latent (hidden) in the original set of variables, **X**. A projection by PCA or PLS of a property matrix uncovers these latent variables and gives them a quantitative meaning. In a way, these latent variables, often also called factors, can be regarded as more fundamental than the original measured variables; they represent the underlying structure of the investigated system.

The latent variables have the interesting property of being fairly independent of the number of original variables. With an increasing number of measured variables, K, the latent variables t_a become better determined. The only change with K is that for some large K values, minor latent variables can become statistically significant.

The design problem. If a set of penta-peptides were to be constructed for investigating a structure/activity relationship, then the initial prototype would not be, say, Ala-Ala-Ala-Ala-Ala and one amino acid position at a time would not be changed among a set of possibilities, to give for instance:

1. Ala-Ala-Ala-Ala-Ala
2. Leu-Ala-Ala-Ala-Ala
3. Ser-Ala-Ala-Ala-Ala
4. Glu-Ala-Ala-Ala-Ala
5. Phe-Ala-Ala-Ala-Ala
6. Ala-Leu-Ala-Ala-Ala
7. Ala-Ser-Ala-Ala-Ala
8. Ala-Glu-Ala-Ala-Ala
9. Ala-Phe-Ala-Ala-Ala
10. Ala-Ala-Leu-Ala-Ala
11. Ala-Ala-Ser-Ala-Ala
12. Ala-Ala-Glu-Ala-Ala
13. Ala-Ala-Phe-Ala-Ala
14. Ala-Ala-Ala-Leu-Ala
15. Ala-Ala-Ala-Ser-Ala
16. Ala-Ala-Ala-Glu-Ala
17. Ala-Ala-Ala-Phe-Ala
18. Ala-Ala-Ala-Ala-Leu
19. Ala-Ala-Ala-Ala-Ser
20. Ala-Ala-Ala-Ala-Glu
21. Ala-Ala-Ala-Ala-Phe

This "design" (or rather lack of design) is obviously a variant of the old OVAT approach. It is also easy to see that this set of peptides has the same problem as the OVAT "design" in Fig. 1, i.e., it lacks information about the direction leading to higher response, here biological activity Y. If, for instance, Glu-Phe-Ala-Leu-Ser is the "best" peptide, this cannot be inferred from data measured on the above set of 21 members.

The deplorable design exemplified above may be christened the COST design (change one substituent at a time). Yet, this COST design has surprisingly been recommended for the investigation of peptides and proteins [23, 24]. The frequent use of the COST design for constructing compound sets for structure/activity investigations is a probable reason for the common lack of success in this area.

The use of latent variables as design variables. Once some idea has been obtained as to what is changing when one amino acid is replaced by another, i.e., the three principal properties t_1—t_3, a better design would be obtained by the following procedure.

(a) Use the principal properties t_1—t_3 as design variables. This gives 15 variables for the set of penta-peptides.

(b) Make a fractional factorial design (FFD) in these variables. This design must have a minimum of 16 members because there are 15 variables. The FFD is generated in the standard way [1]:

```
 1. +++ +++ +++ +++ +++
 2. +++ −++ −+− −+− −−−
 3. ++− ++− +−+ −−+ −−−
 4. ++− −+− −−− +−− +++

 5. +−+ +−+ +−− +−− +−−
 6. +−+ −−+ −−+ −−+ −++
 7. +−− +−− ++− −+− −++
 8. +−− −−− −++ +++ +−−

 9. −++ +−− −++ +−− −+−
10. −++ −−− ++− −−+ +−+
11. −+− +−+ −−+ −+− +−+
12. −+− −−+ +−− +++ −+−

13. −−+ ++− −−− +++ −−+
14. −−+ −+− +−+ −+− ++−
15. −−− +++ −+− −−+ ++−
16. −−− −++ +++ +−− −−+
```

Thereafter columns 1—3 are identified with the amino acid in position one, columns 4—6 with position two, etc., and the amino acid with the most similar sign pattern in t is selected from the table of t values (Table 1). In this similarity, t_1 is more important than t_2 which, in turn, supersedes t_3. This gives for peptide no. 1, for instance, Asp-His-Asn-His-Asp, and for peptide no. 2, Asp-Trp-Tyr-Tyr-Val.

(c) Include a centre point (here a peptide with amino acids with t values near zero, say Ala-Ala-Ala-Ala-Ala) plus some randomly generated numbers to account for the fact that the latent variables may not be a complete description of the peptide structural change.

This set of penta-peptides with around 20 members will give dramatically more information about the relation between structural change and change in biological activity than the COST set of 21 peptides in the preceding section. The development of "principal properties" of amino acids and the following design of informative sets of peptides is very recent, and therefore the third step, the essential one, has not yet been taken. So far, nobody has made such a designed set of peptides and analyzed its information content with respect to a biological test system.

THE INTEGRATED MULTIVARIATE APPROACH: $MV^3 = MVC \times MVD \times MVA$

With the amino acid/peptide example in mind, the following conclusion can be drawn. To investigate complicated systems like the relationship between structure and activity, or the influence of solvent and substrate on a chemical synthesis (see below), there are three concepts that should be approached multivariately. These are multivariate characterization (MVC),

multivariate design (MVD), and multivariate analysis (MVA). Each of these forms a cornerstone in the MV^3 approach and each is critically dependent on the other two; they form a triangle rather than a ladder.

A further example will serve as an illustration to this approach.

Example 3. Optimization of the Willgerodt-Kindler reaction

This example seems to be the first complete application of the MV^3 strategy to a chemical problem. The Willgerodt-Kindler reaction is a complicated heterogeneous reaction with no well established mechanism, where an aromatic ketone in the presence of sulphur reacts with an amine and rearranges to a carboxylic acid thioamide. For a given selection of solvent, ketone and amine, the reaction is influenced by the continuous variables temperature (T), amount of sulphur (S) and the ratio amine/ketone (R).

Multivariate characterization (MVC)

Chemical structure, biological activity, solvent influence, substrate properties and other complicated issues cannot be quantified in terms of a single variable. Rather, as many relevant measurements as possible should be used for this characterization, to provide a possibility for multivariate analysis to extract stable latent variables, "principal properties" for the actual systems.

The scope of a multivariate characterization may be regarded as quantifying analogy. It can be shown that any variable measured on an ensemble of similar objects (e.g., peptides in a structural family or synthetic runs which are modifications of the same "prototype synthesis") is correlated to any other variable measured on the same ensemble according to a simple factor structure [18]. Hence, if (a) the investigated system is conceptually divided into subsystems, and (b) a sufficiently broad multivariate characterization of these subsystems is produced, then the battery of variables comprising the characterization will contain "all essential factors", including those influencing the response variables Y (biological activity of the peptides or the yield of the synthesis).

For the characterization of the amino acids 20 measured variables were initially used, but the inclusion of additional carefully selected and measured properties indeed made the latent variables more stable [15]. To include the choice of solvent and co-reagent as design variables for a given substrate in the Willgerodt-Kindler reaction, a multivariate characterization of 82 solvents by 10 variables and of 29 co-reagents (amines) by 8 variables was first made. The PCA of the two resulting matrices gave two significant principal properties in both cases (Figs. 7 and 8).

The substrates were of four types depending on the *para*-substituent in the aromatic ring (alkyl, donor, acceptor or halogen). A few representatives of each of the four types of substrates were first subjected to a series of pilot experiments to study the feasibility of the approach. It was found that when the *para*-substituent was an acceptor, the reaction took a completely different route giving another type of product. The other three types of substrates

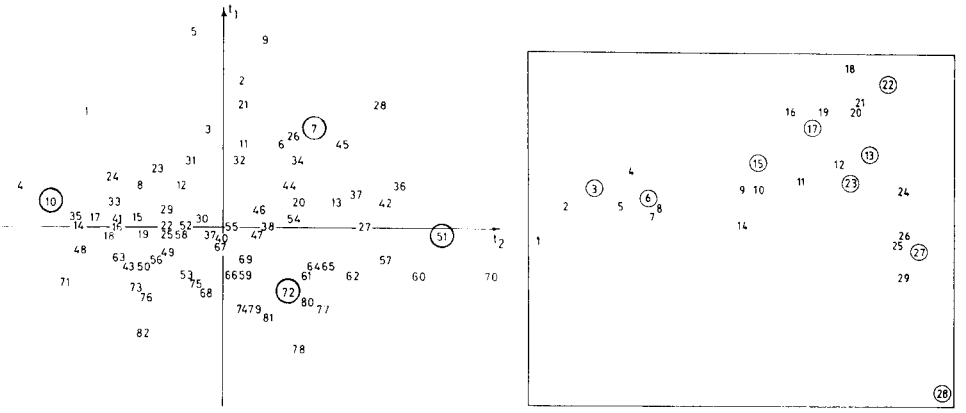

Fig. 7. Principal components projection of the ten variables characterizing 82 solvents commonly used in organic synthesis. The resulting scores (latent variables) t_1 and t_2 can be seen as "principal properties" of the solvents and can be used to select solvents that well span the range of interest. In the Willgerodt-Kindler application, the four circled solvents 7 (triethylene glycol), 10 (ethanol), 51 (quinoline) and 72 (benzene) were chosen as design points. Because the latent variables t_1 and t_2 are orthogonal, any four points spanning the plane of these variables are good design points.

Fig. 8. Principal components projection of the eight variables characterizing 29 possible Willgerodt-Kindler co-reactants (amines). The resulting latent variables t_1 and t_2 were used to select amines fully spanning the amine "domain". The four amines 3 (isopropylamine), 15 (diethylamine), 22 (dipentylamine) and 28 (morpholine) were chosen as design points.

with alkyl, halide and donor substituents in the *para*-position gave normal products. These substituents were thereafter described by the two system variables σ_I (inductive effect) and π (lipophilicity). Altogether, this resulted in the use of six system variables describing the qualitative change of solvent, co-reagent (amine) and substrate (*para*-substituted aromatic ketone).

In the peptide example, the response, the biological activity, was expressed as a single variable. This is an inefficient reminiscence from the old days when multivariate data were computationally intractable, but today there is no reason to limit the response to one variable.

Multiple responses provide the possibility to obtain essential information about the homogeneity of the objects, i.e., if the peptides are active according to the same biological mechanism. In addition, multiple responses give an independent estimate of how much of the variation in the data is systematic. This can then be compared with how much is "explained" by the model $\mathbf{X} \rightarrow \mathbf{Y}$, which gives indications of where model deficiencies should be sought [25, 26]. In the chemical synthesis example, where the experiments were under proper control, the response was indeed multivariate with four measurements describing yield and the coordinates of the optimal conditions in R, S and T.

Multivariate design (MVD)

The use of latent variables as design variables is an obvious approach if the latent variables can be accepted as describing the fundamental structure of the investigated system. As shown by Carlson, Lundstedt and co-workers [16, 17], this indeed works in practice. Because, for complicated systems, measured properties usually vary collinearly to each other, a design in the measured variables is intractable. In particular, for variables that cannot be manipulated, but just measured, a design is impossible. The design in terms of latent variables solves these problems in a simple and straightforward way.

However, the design in latent variables is not always easily and rapidly achieved. One must first collect a relevant data set to estimate the latent variables; for both the amino acids, solvents and substrates this has taken a long time and much effort, and the work is not yet complete. The presently used "principal properties" of these systems may have to be extended to more "factors" and their numerical values may change slightly when more precise and possibly more relevant variables are included in the data matrices.

In the synthesis example, a 2^{6-3} FFD was constructed in the six-system variables for solvent, substrate (ketone) and co-reactant (amine). Thus totally eight (2^3) design points were constructed. For each design point, a response surface optimization [1] was based on a composite design in the three continuous variables R, S and T.

Multivariate analysis (MVA)

The role of multivariate analysis in terms of projections is central in the MV^3 approach. First, the principal properties are estimated from the subsystem property matrices. Secondly, multivariate models are formulated between the designed set of objects (peptides or synthetic runs) and the measured responses Y, and are thereafter estimated by PLS. The ability of multivariate projection methods such as PCA and PLS to operate regardless of the number of variables in relation to the number of objects is essential. This was demonstrated above in the peptide QSAR (Example 2). Also, the simple and stable handling of missing data in these methods is an advantage because real data sets are never quite complete.

In the synthesis optimization, the multivariate analysis was used in three stages. First, the principal properties, latent variables, were calculated for the solvents and co-reactants by PCA (see Figs. 7 and 8). Secondly, a response surface model in the continuous variables R, S and T was calculated by PLS for each design point in the system variables. This gave the coordinates for optimum yield for the variables R, S, and T, which was also confirmed by experiment. Thirdly, modelling of the influence of the system variables on yield and the position of the optimum was modelled by PLS. This produced, among other things, optimum conditions for both system and continuous variables, which were again confirmed by experiments. The results were highly satisfactory. High yields were obtained for each substrate, but for different values of R, S and T and with different solvents and co-reagents (Table 2).

TABLE 2

Optimal conditions for the Willgerodt-Kindler reaction as a result of the MV³ investigation of Carlson, Lundstedt and co-workers [16, 17]

Reaction system			Optimum conditions			
Substrate	Amine	Solvent	Molar ratio		T (°C)	Yield (%)
			Sulphur/ketone	Amine/ketone		
p-Cl	(15) DEA	(7) TEG	8.4	5.3	123	89
p-H	(3) iPr	(51) Quin.	10.25	4.75	133	89
p-MeO	(3) iPr	(10) EtOH	3.8	6.61	80	91
p-Phenoxy	(15) DEA	(72) Benzene	9.6	5.8	80	85
p-Cl	(22) DPe	(72) Benzene	13.6	8.5	80	68
p-H	(28) Mor	(10) EtOH	3.7	13.4	80	86
p-MeO	(28) Mor	(51) Quin.	9.3	8.9	130	100
p-Phenoxy	(22) DPe	(7) TEG	13.0	8.3	118	73

One conclusion is that the common practice of evaluating the feasibility of an organic synthesis under so-called standardized conditions easily leads to wrong conclusions; each variant of the synthesis must be optimized both with respect to qualitative system variables and quantitative continuous variables if the results are to have any value in decision-making. And because there are strong interactions between the variables influencing the synthesis, the optimizations must be based on statistical designs.

Summary of MV³

The general outline of MV³ exemplified by peptide family and synthesis, is as follows.

(1) Problem formulation: varying subsystems (amino acids, solvents, substrates, . . .).

(2) Characterization of subsystems: "model" reactions, properties, . . . (analogy concept); multivariate data, span latent variable (factor) space, e.g., amino acids in each varied position, solvents, substrates, or co-reactants.

(3) First projection (PCA → principal properties).

(4) Design in principal properties gives the **X** matrix (FFD + centre point + a few random).

(5) Experiment, measurements (responses Y).

(6) Data analysis (second projection): PLS gives relation between **X** and **Y**; number of factors estimated; any points grossly deviating found (indications of more dimensions, change in mechanism, . . .); plots (grouping in score plot, etc.).

(7) Interpretation, feedback, predictions, etc.

CONCLUSIONS

The combination of multivariate characterization, analysis and design provides a handle on complexity. The characterization is made of subsystems of the studied process, subsystems that should be chosen to be fairly large "chunks" of the total system. Thus amino acids are subsystems of peptides, but not the only ones; dipeptides and selected tripeptides may be better candidates, but unfortunately less available and with very little literature data.

By projecting the data matrix resulting from the multivariate characterization by PCA, "principal properties" of the subsystems are obtained. These principal properties can then be used as ordinary continuous design variables to get objects that broadly span the abstract space of the studied process.

A basic difficulty is that the real latent variables in an application may be unrepresented in the characterization "battery" or appear far down in the sequence of PCs [27]. Then the design does not span all relevant factors and an incomplete model results in the last stage of the analysis. Therefore the inclusion of randomly chosen objects in the training set is recommended, to guard at least to some extent against these problems.

An approximation to this strategy of multivariate characterization followed by the calculation of "principal properties by PCA, may be to use a few carefully selected properties as design variables; for solvents, refractive index and dielectric constant may suffice, and for the amines, their pK_a and solubility in water. If these properties are well chosen, they may approximately span the same subspace as the principal properties and thus lead to a good design.

The difference between the design stage and the data analysis stage must be emphasized with respect to the system description. In the design stage, a few latent variables are used for the selection of systems. In the data analysis stage, numerous variables are used to get a rich description of the systems in the **X** matrix; only practicalities like the size of computer memory limit the number of X-variables at this stage.

The number of possible applications in chemistry of the MV^3 approach is large; the investigation or optimization of any complex system with respect to any desirable property can be approached in this way. A short list of systems would include polymers, proteins, complicated products such as paints, mixed wines, blended whisky and food, syntheses, structure/property relationships, quality control, and process optimization.

We are grateful for support from the Swedish Natural Science Research Council (NFR), the Swedish Board for Technical Development (STU), and the Swedish Council for Planning and Coordination of Research (FRN).

REFERENCES

1 G. E. P. Box, W. G. Hunter and J. S. Hunter, Statistics for Experimenters, Wiley, New York, 1978.
2 S. N. Deming and L. R. Parker, Jr., Crit. Rev. Anal. Chem., Sept. 1978, 187.

3 K. V. Mardia, J. T. Kent and J. M. Bibby, Multivariate Analysis, Academic Press, New York, 1979.
4 G. E. P. Box, W. J. Hunter, J. F. MacGregor and J. Erjavec, Technometrics, 15 (1973) 33.
5 S. Wold, C. Albano, W. J. Dunn, III, U. Edlund, K. Esbensen, P. Geladi, S. Hellberg, E. Johansson, W. Lindberg and M. Sjöström, in B. R. Kowalski (Ed.), Chemometrics: Mathematics and Statistics in Chemistry, D. Reidel, Dordrecht, 1984.
6 S. Wold, Pattern Recognition, 8 (1976) 127.
7 R. A. Fisher, The Design of Experiments, Oliver and Boyd, Edinburgh, 1935.
8 F. Yates, J. Roy. Stat. Soc. Suppl., 2 (1935) 181.
9 D. J. Finney, Ann. Eugen., 12 (1945) 291.
10 R. L. Plackett and J. P. Burman, Biometrika, 33 (1946) 305.
11 G. E. P. Box and K. B. Wilson, J. Roy. Stat. Soc. B, 13 (1951) 1.
12 O. L. Davies (Ed.), Design and Analysis of Industrial Experiments, Hafner, New York, 1954.
13 W. G. Cochran and G. M. Cox, Experimental Designs, 2nd edn., Wiley, New York, 1957.
14 G. E. P. Box and R. D. Meyer, Technometrics, 28 (1986) 11.
15 S. Hellberg, M. Sjöström, B. Skagerberg, C. Wikström and S. Wold, Acta Pharm. Jugosl., (1987) in press.
16 R. Carlson, T. Lundstedt and C. Albano, Acta Chem. Scand. B, 39 (1985) 79.
17 T. Lundstedt, R. Carlson and R. Shabana, Acta Chem. Scand., (1987) in press.
18 S. Wold, Chem. Scr., 5 (1974) 97.
19 S. Wold, Technometrics, 20 (1978) 397.
20 H. T. Eastment and W. J. Krzanowski, Technometrics, 24 (1982) 73.
21 See, e.g., H. Wold, in K. G. Jöreskog and H. Wold (Eds.), Systems under Indirect Observation, Vol. 2, North-Holland, Amsterdam, 1982.
22 J. G. R. Ufkes, B. J. Visser, G. Heuver, C. Van Der Meer and H. J. Wynne, Eur. J. Pharmacol., 50 (1978) 119; 79 (1982) 155.
23 J. Rudinger, in E. J. Ariens (Ed.), Drug Design, Academic Press, New York, 1971, p. 319.
24 P. S. Farmer, in E. J. Ariens (Ed.), Drug Design, Academic Press, New York, 1980, p. 119.
25 W. J. Dunn, III, S. Wold, U. Edlund, S. Hellberg and J. Gasteiger, Quant. Struct-Act. Relat., 3 (1984) 131.
26 S. Wold, W. J. Dunn, III and S. Hellberg, Environ. Health Persp., 61 (1985) 257.
27 I. T. Joliffe, Appl. Stat., 31 (1982) 300.

Analytica Chimica Acta, 191 (1986) 33—45
Elsevier Science Publishers B.V., Amsterdam — Printed in The Netherlands

THE CLAS PROGRAM FOR CLASSIFICATION AND EVALUATION

JAN B. HEMEL*

Central Laboratory for Clinical Chemistry, University Hospital, P.O. Box 30001, NL-9700 RB Groningen (The Netherlands)

HILKO VAN DER VOET

Chemometrics Research Group, Pharmaceutical Laboratories, A. Deusinglaan 2, NL-9713 AW Groningen (The Netherlands)

(Received 29th May 1986)

SUMMARY

Multivariate classification methods are needed to assist in extracting information from analytical data. The most appropriate method for each problem must be chosen. The applicability of a method mainly depends on the distributional characteristics of the data population (normality, correlations between variables, separation of classes, nature of variables) and on the characteristics of the data sample available (numbers of objects, variables and classes, missing values, measurement errors). The CLAS program is designed to combine classification methods with evaluation of their performance, for batch data processing. It incorporates two-group linear discriminant analysis (SLDA), independent class modelling with principal components (SIMCA), kernel density estimation (ALLOC), and principal component class modelling with kernel density estimation (CLASSY). Most of these methods are implemented so as to give probabilistic classifications. Multiple linear regression is provided for, and other methods are scheduled. CLAS evaluates the classification method using the training set data (resubstitution), independent test data, and pseudo test data (leave-one-out method). This last method is optimized for faster computation. Criteria for classification performance and reliability of the given probabilities, etc. are determined. The package contains flexible possibilities for data manipulation, variable transformation and missing data handling.

Analytical chemical and especially clinical chemical laboratories have seen major changes in assay techniques, including the introduction of highly sophisticated instrumentation and automation. The voluminous data flow thus obtained has to be processed and reduced to useful information, so that there has been accompanying growth in data-handling techniques. Many of those techniques are based on multivariate statistical methods, including multiple regression (linear and nonlinear), cluster analysis, construction of multidimensional reference areas, principal components analysis, etc.

Distinctions between two or more groups of samples are often important, e.g., samples from different diagnostic groups or classes of chemical compounds or wines from different regions. Many methods are available for such classifications into a priori defined groups. All these multivariate classification

0003-2670/86/$03.50

methods require a training set of data, which consists of a matrix of n objects, each with p measured variables, and each of known class. The training set must contain all classes that are to be distinguished. Some classification rule constructed on the basis of this training set is then used to classify new objects of unknown class (the test set).

For an individual problem, it is often difficult to choose the best classification method. Rather than looking for the best method for general use, attempts should be made to establish the method best equipped for the problem at hand, because the applicability of a multivariate classification method depends mainly on two data aspects. First, distributional characteristics of the data population are important. Some methods require that the population underlying the data is normal; others require independence between the variables. The degree to which the classes are separated from each other always governs the classification results to a large extent, but some methods are more sensitive than others. Most methods require quantitative numerical variables; qualitative variables then have to be coded numerically (dummy variables), which endangers any assumption about distribution. Secondly, the characteristics of the available training sample must be considered. A large sample size (many objects) usually yields better results than a small training set. However, most methods become very time-consuming with growing sample size, because of extensive calculations. The optimum sample size, as well as the optimum ratio of number of objects to number of variables (the n/p ratio) may differ between multivariate methods. Most of these methods do not allow missing values in either training or test set. The degree of precision with which the variables are measured may favour a particular method.

A totally different aspect of the choice of method is whether probabilistic classification is needed or not. Especially if one is interested in each individual object, as a physician is in every patient, probabilistic classification is preferable. To a physician it makes a large difference whether the probability of a diagnosis is 100% or 51%, although the chosen diagnosis (the classification) itself remains the same. If one is interested in classification of a group as a whole, individual probabilities may be of less importance, and non-probabilistic classification (just choosing the most probable group) will do. Not all multivariate methods yield a probabilistic classification.

To choose the best method for a certain classification problem, comparative evaluation of the results is needed. Criteria for classification performance have been derived by Hilden et al. [1]. They distinguish discriminatory ability (whether the objects are classified into the right group) from sharpness of classification (sharpness is obtained when the attached probabilities differ greatly). In a classification method that is trustworthy, there should be agreement between the number of classification errors made and the degree of certainty (i.e., attached probabilities) of the system. A reliability score can be derived from the discriminatory ability and sharpness scores. In a practical situation, one can choose the most appropriate multivariate method by comparing the criteria calculated for different methods. One can evaluate

the classification rule obtained by applying it to the training data. This evaluation method (resubstitution), which is very popular, can sometimes be strongly biased if used with small samples [2, 3], but it is very simple to apply as no additional sampling is needed. The most objective evaluation is accomplished by application of the classification rule to newly sampled data, the test set. As data sampling is often costly, it is tempting to add the extra samples to the training set, so that the classification rule is based on more data, but the independence of the test data is then lost. Randomly splitting the available data into training and test sets offers the possibility of real test data evaluation, but leaves fewer data for model construction.

An intermediate solution to this evaluation problem is given by the leave-part-out algorithm. This algorithm splits the data set into k parts and uses a rotating scheme; in every cycle, a different part of the data is used as test set while the other parts constitute the training set. The disadvantage of this method is the fact that every cycle uses a different training set, and so a different classification rule. If only one object is used as test set in every cycle, n cycles are needed to complete the leave-one-out scheme, and the training sets differ only slightly. However, in principle, a full classification including the classification rule construction must be repeated n times, which is very time-consuming. Lachenbruch [3] showed that this leave-one-out method (LOOM) is almost unbiased, while it requires no extra data sampling.

Many computer programs for multivariate analysis are available today. The Statistical Package for the Social Sciences (SPSS) [4], and the BMDP Biomedical Computer Programs [5] are almost classical, but offer few multivariate classification methods, mainly statistical linear discriminant analysis (SLDA). The ARTHUR program [6] offers many multivariate techniques, but is difficult to operate and lacks probabilistic techniques. For separate multivariate methods, programs have been written, such as SIMCA-3B for independent principal components class modelling [7], and ALLOC-80 for kernel density estimation [8]. Other programs, like MASLOC for cluster analysis [9], and DPP for processing of analytical data [10], cover fields of multivariate data analysis other than classification. Evaluation criteria and LOOM are seldom offered.

In this paper, the CLAS computer program is discussed. This program runs on a Control Data Cyber 170/760 mainframe computer under the NOS operating system. It is written in Pascal, using some Pascal 6000 [11] extensions that have analogs in most other Pascal versions. It is being adapted for use on a IBM-PC or IBM-AT microcomputer of moderate size, using IBM Pascal, to bring its facilities within wider reaches. CLAS performs some major multivariate classification techniques and is able to evaluate them, by using LOOM.

THEORY

There are three main purposes of the CLAS programming project. First, the CLAS computer program is meant to enable the suitability of a multivariate

classification method to be judged when applied to a certain data set; therefore, the incorporation of all major multivariate classification techniques is desirable. Secondly, probabilistic classification should be available in the program, and the resulting probabilities should be used in the evaluation procedure. And thirdly, the leave-one-out technique being very suitable for evaluation, should be provided. Further requirements are that CLAS should primarily be suitable for research; thus it should be easily adaptable and extendable (open-ended) to allow incorporation of newly developed methods. It should also include effective means for handling missing data, and its operation should be as simple as possible, whilst versatility is retained and output is compact, user-selectable, and self-explanatory.

Highly structured source code was considered to be essential for future extension and maintenance of the program. The programming language Pascal was chosen because of its structure-promoting qualities combined with its efficient code. To compensate for minor deficiencies of standard Pascal, some Pascal 6000 extensions were used; their analogies are supported by most compilers, thus the implementation on other computer systems should not pose too many problems. Because of the high computational demands of some classification and evaluation procedures, a batch system was chosen (see below). Output is in standard ASCII on a output file that may be previewed or printed separately. For the microcomputer version that is currently being prepared, the CLAS source is adapted to IBM-Pascal, which is a modular Pascal version.

Program structure

CLAS consists of a main program that serves as a driver for the various functions that are selected by the user. Almost every function is represented by its own Pascal main procedure. These main procedures comprise the procedures necessary to process the options pertaining exclusively to them. Utilities used in many procedures are declared in a global utility section. In the microcomputer version, every main procedure will fit in a module, and the utilities will be grouped into modules.

Currently CLAS can handle 250 objects, 35 variables and 10 classes, but these values can easily be adapted as required subject to the limitations of the computer system.

Command syntax

CLAS reads its input from an input file in which the user specifies every required function by a command. The command syntax is depicted in Fig. 1. The command consists of the command name and an optional set of function-dependent options enclosed in parentheses. The total command may cover several lines. The format of the command is free, provided that the set of options, if present, is enclosed in parentheses, and that all words and numbers are separated by separators. Separators include the end-of-line marker and all characters except letters, digits and some special characters. Commands, or

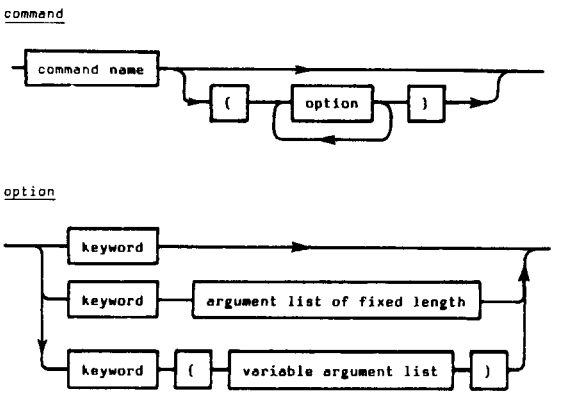

Fig. 1. Command syntax diagram of CLAS.

parts of commands, can be temporarily omitted by inserting the double quote (") character. The rest of the input line involved is ignored by CLAS. In this way, comments may be inserted as well.

Options can basically consist of one of four structures: (1) a keyword (e.g., LOOM for evaluation by the leave-one-out method); (2) a keyword followed by a fixed number of arguments (e.g., NAME=DATASET, to attach a name to a data set); (3) a keyword followed by an argument list of variable length which must be enclosed in parentheses [e.g., PRINT (EVALUATION, HORNSTEST, POSTERIOR): print evaluation output, results from Horn's test, and posterior probabilities]; and (4) a keyword followed by an option [e.g., SELECT VAR (1—3): selection of the variables 1, 2 and 3].

Only the first four letters of keywords are meaningful to CLAS. Names given to the data set, classes, objects and variables may contain up to ten significant characters. These names must start with a letter and may incorporate letters, digits, the plus (+), minus (—), asterisk (*), solidus (/), hat (^) and dash (') characters, as well as the underline (_), which represents a blank. Characters that cannot be interpreted by CLAS are skipped.

Data-base structure

The data base is contained in two Pascal variables (one for the training set and one for a test set) of the Pascal type "data type" which is a declared Pascal record composed of two parts. The first part is a heading of data-set name (user specified), number of objects (determined by CLAS), number of variables (determined by CLAS), identification of each variable (user specified), number of classes (determined by CLAS), identification of each class (user specified), size of each class (determined by CLAS), an indicator for the presence of missing data (determined by CLAS), and the number of times each variable is present in the data set (determined by CLAS). All parts in the heading that can be specified by the user are defaulted by CLAS.

The second part of the data-type record consists of a file of objects of the Pascal type "object type" which is a declared Pascal record consisting of object

index number (user specified), object name (user specified), number of measured variables (determined by CLAS), class index (only used internally, linked to user-specified class identification), and the measured variable values (user specified, not defaulted). Except for the measured variable values, defaults are provided for all user specified values.

Available functions

CLAS contains several functions; they are summarized in Table 1 and are discussed briefly below.

INPUT. In this procedure, the number of lines that is occupied by the first object in the data set must be specified to CLAS if it exceeds the default value of one. This enables the program to count the number of variables, and, assuming a constant order of the data for each object throughout the input file, to read all objects and count them. Except for the ordering of the object data and the constancy of the number of variables, there are no formatting requirements. Further, the data set, class and variable names can be specified for easy reference, the width (in columns) of the printed output and the number representing a missing value can be chosen. If the name of a variable is CLASS, the program assumes this variable to contain the class number, but any variable can be specified as such using the CLASS VARIABLE option.

INPUT reorders the objects to contiguous class number, if necessary. A test set may be created using the CHANGE function (see below). As an alternative, data may be read from a system file that has been prepared before (see LIST).

LIST. The function LIST is able to produce a complete listing of the data, including the names given to variables and classes. If desired, a listing in scientific notation can be given for maximum accuracy. LIST can also print line-printer plots of any variable versus any other, including the class number. These plots can be fully specified by the user and can have any size and resolution. Large plots will be printed in parts. As these plots are ASCII-coded, they can be printed by any printer. Another option of LIST is to prepare a system file that can be saved for later use (see INPUT). This system file is a fully legible, documented ASCII file.

NOISEDATA. This procedure is included in CLAS in order to have the possibility for simulation studies. Many aspects of the simulated data can be varied, such as number of objects, number of variables, number of classes, position of the centroids of the classes, and standard deviation of the simulated values. The construction of low-dimensional class models that are submerged in higher-dimensional data spaces is possible. In this case, one can choose the dimensionality of the class models and the ratio between the standard deviations of the class model dimensions and the overall noise. The algorithms implemented for generating random numbers are those described by Forsythe et al. [12] for uniform numbers and Brent [13] for Gaussian numbers.

CHANGE. The CHANGE procedure allows extensive data manipulation. Not only can part of the data set be deleted, but also a test set can be created from part of the data. Furthermore, variables can be transformed or renamed.

TABLE 1

Available CLAS functions

Input/output	Data manipulation	MCM[a]	Other
INPUT	CHANGE	ALLOC	STATISTICS
LIST	MISVAL	SIMCA	MLR
	SCALE	CLASSY	
	NOISEDATA	SLDA	

[a]Multivariate classification methods.

Transformations include addition, subtraction, division, multiplication, raising to a power, conditional substitution, natural and common logarithm, exponentiation, and absolute value. The value added to the variable(s) can be a constant number or the value of another variable. In the former case, a plus is added to the name of the variable. In the latter case, an extra variable with a new name, consisting of part of both the names of both variables separated by a plus, is formed. Analogous procedures are followed with subtraction, division, multiplication and raising to a power. The value of a variable can be substituted by another value if it equals a certain constant, or is greater or smaller than a constant. All transformations are adequately reflected in the new name of the variable name. Last, but not least, new variables can be created from existing ones, using the transformations mentioned above.

MISVAL. This function enables data gaps to be removed by either filling them with estimates or deleting the variables and/or objects that contain them. By now, a missing value can be estimated as the mean of the variable, this mean being based on the class from which the incomplete object stems or on the entire data set. Other methods of removing data gaps that are implemented are deletion of all variables or all objects that contain gaps, and stepwise deletion. Stepwise deletion [14] deletes some objects and some variables, retaining as many data-set values as possible and simultaneously sparing small classes. A minium n/p ratio can be specified.

SCALE. This procedure performs user-specified scaling of the data. Origin displacement as well as scaling factor can be independently chosen by the user in many different ways. They can be user-specified or calculated from the data in a user-specified way. Autoscaling (scaling all variables to an overall mean of zero and an overall standard deviation of one) and class scaling (autoscaling executed for every class separately) are available. If the intrinsic variability of the variables is known, reproducibility scaling can be applied.

STATISTICS. This procedure calculates simple univariate statistics on the training data: number of values, number of missing values (if any), minimum, maximum, median and mean value, standard deviation, relative standard deviation and variance, coefficients of skewness and kurtosis. These statistics are calculated on all selected objects, for every selected class separately and for

all together, for each variable. Furthermore, a correlation matrix of the selected classes, objects and variables can be produced, along with confidence intervals and tail probability values.

LINREG. This function performs (multiple) linear regression (MLR). A MLR case with only two different values for the dependent variable is recognized as a two-class linear discriminant analysis (SLDA) case and the typical SLDA output is added automatically. The significance of the regression and an ANOVA table are printed. For evaluation purposes, the LOOM and residuals output are available. The LOOM is implemented with computational efficiency. After LOOM calculations, the prediction sum of squares (PRESS) [15] is printed. It is possible to calculate a model without intercept. This may be of use in special cases like the analysis of mixture design models [16].

ALLOC. Classification by kernel density estimation is done by the ALLOC function. ALLOC constructs a model for every class by placing a gaussian density function around every training set point. The cumulated densities of all training points yield a sort of field strength at every point in the data space. At the coordinates of every test point, the field strengths of all class models are compared and the point is classified into the class with the highest strength.

The width of the elementary gaussian distribution (the smoothness parameter) is of major importance for the classification. In CLAS it can be specified by the user. The method is computationally equivalent to the implementation in the ALLOC-80 programs [8].

User-specified output, including evaluation results, probability densities, and posterior probabilities, are available for training and test set. Real LOOM evaluation is possible, in contrast to the ALLOC-80 programs in which only the smoothness parameter is chosen leaving-one-out.

SIMCA. Wold's SIMCA method [7], in which a principal component model is fitted for every class separately, is performed by the SIMCA function in CLAS. SIMCA is adapted especially for CLAS to perform probabilistic classification, as will be described elsewhere. User-specified output is available including LOOM evaluation results, probability densities, eigenvector matrices, Horn's test [17] for the number of principal components to be retained, and many more. For the LOOM evaluation, the principal component models are updated, if possible, by an efficient algorithm described by Bunch et al. [18].

The implementation is meant to produce the same non-probabilistic output as the SIMCA-3B programs [7], but the numerical results are sometimes different for two reasons. Firstly, the SIMCA-3B programs are written in a version of BASIC that does not provide enough numerical accuracy. Secondly, CLAS performs principal component analysis by applying singular value decomposition as in the algorithm of Householder described by Wilkinson and Reinsch [19]. This algorithm converges faster than the partial least-squares algorithm used in SIMCA-3B, and thus reduces rounding errors. As SIMCA-3B limits the maximum number of iterations to 20, the desired accuracy is not always attained.

CLASSY. The CLASSY method [20], which is a combination of SIMCA and ALLOC, is implemented in CLAS, too. The user-specified output is analogous to that from SIMCA and ALLOC.

RESULTS AND DISCUSSION

Figure 2 shows the printed output from an example data set in a sample run. All values and names are fictitious. The input file used is given in Table 2. Figure 2A shows the output from INPUT. If reordering is necessary to obtain contiguous classes, it is executed and reported. The data set structure is analysed and names and numbers of classes and variables are checked for duplication; if there is, changes are made automatically and a warning is issued. Every procedure ends with the CPU time used. The way CLAS lists a data set is depicted in Fig. 2B. The numbers of missing values per variable and per object are given only if the data set is incomplete. The output of the MISVAL (DELETE BOTH) command is shown in Fig. 2C. Figure 2D shows the default output of STATISTICS; univariate statistics (including the median) are given for each class as well as for the entire training set). The correlation matrix contains both confidence interval and tail probability for every correlation. As an example of the evaluation output of a classification method, the CLASSY print is shown using LOOM. The output contains not only relevant CLASSY model statistics but also posterior probabilities for all objects and all classes, by using resubstitution as well as LOOM. The command given was CLASSY (A=2, LOOM).

To compare the computational efficiency of CLAS with the SPSS and ARTHUR programs, some CLAS functions were selected that have almost equivalent counterparts in the other programs. The results are shown in Table 3. Comparisons like these, however, are always difficult to interpret, as procedures in different programs are not exactly the same and as not everything that is done by the program is shown in the output. SPSS differs so fundamentally in the way of processing the data that only a very gross comparison is justified. Notwithstanding this fact, CLAS seems to perform at least as well as the other programs. The strongest points of CLAS lie in evaluation, especially in its use of the LOOM. Performance comparison of CLAS with the other programs in this respect is not possible because SPSS and ARTHUR do not offer LOOM.

Examples of the LOOM evaluation capacity in CLAS are shown in Table 4. As the data set used contains 42 objects, and as LOOM evaluation yields not only the results per object but also the resubstitution results, the computing time should increase by a factor of 43 (neglecting some overhead). Clearly, the time needed for LOOM evaluation is far less than proportional. This improvement is reached partly by optimizing the necessary iterations, avoiding overhead as much as possible, and partly by applying algorithms that update intermediate statistics rather than recalculating them.

One of the main purposes of CLAS is assisting in the choice between multivariate classification techniques for a certain data set. The following

```
INPUT (NAME: DEMONSTRATION; VAR NAMES: (CLASS, CREATININE,
       LACTATEDEHYDROGENASE); CLASS NAMES: (LIVER, KIDNEY)
       MISSING=-99)
LIST
MISVAL (DELETE BOTH)
STATISTICS
CLASSY (A=2; LOOM)
```

(A)

```
PROCEDURE INPUTDATA    DATE: 86/05/22.   TIME: 13.24.39.
--------------------------------------------------------------------------------
VARIABLE 1 IS SPECIFIED AS CLASS DESIGNATION;

WARNING: THE OBJECTS ARE REORDERED TO CONTIGUOUS CLASSNUMBER
         THIS MAY HAVE CONSEQUENCES IF YOU SPECIFIED A SERIES
         OF OBJECTS AS A RANGE IN ONE OF THE FOLLOWING PROCEDURES.

DATASET DEMONSTRAT CONTAINS 2 CLASSES, 16 OBJECTS AND 3 VARIABLES
THERE ARE MISSING VALUES IN THIS DATASET

CLASS STRUCTURE:          CLASS NR  CLASS NAME     CLASS SIZE
                          ------------------------------------
                                1   LIVER               9
                                2   KIDNEY              7

WARNING: OBJECT NAMES AND NUMBERS ARE NOT CHECKED!

INPU----------------------------------------------------------------------37-MSEC
```

(B)

```
PROCEDURE LISTDATA     DATE: 86/05/22.   TIME: 13.24.39.   DATASET: DEMONSTRAT
--------------------------------------------------------------------------------
 CLASS NR  CLASS NAME
OBJ NUMBER OBJECTNAME MISS  CREATININ  LACTATEDE      VAR3
--------------------------------------------------------------------------------

        1 LIVER
        2 MISS LEV     1      -        195.000    102.000
        3 BLAUW-KN     -     72.000    548.000    344.000
        4 LEVERING     -     55.000    246.000    101.000
        5 V/D SLOK     -     73.000    363.000    108.000
        6 PALPABEL     -     44.000    382.000    225.000
       11 LEVERMA      -    456.000    234.000    123.000
       12 KNOOP-BL     -     67.000    567.000    345.000
       13 SLOKJENS     -     78.000    345.000    123.000
       14 TASTING      -     45.000    345.000    234.000

        2 KIDNEY
        7 NIERMAN      -    527.000    195.000     19.000
        8 VAN NIER     1    211.000      -         18.000
        9 NEFRONIU     1    657.000      -         17.000
       10 PIESTRA      2   1200.000      -          -
       15 NIEREMA      -    567.000    123.000     12.000
       16 NIERMISS     1    211.000    288.000      -
       17 URONIUS      -    678.000    123.000     12.000

            MISSING:   6      1          3          2

   (5 OBJECTS MISS ONE OR MORE VARIABLES)


LIST----------------------------------------------------------------------16-MSEC
```

(C)

```
PROCEDURE MISVAL       DATE: 86/05/22    TIME: 13.24.39.   DATASET: DEMONSTRAT
--------------------------------------------------------------------------------
MISSING DATA ARE REMOVED BY DELETING VARIABLES AND/OR OBJECTS SO AS TO MAXIMIZE
THE NUMBER OF VALUES REMAINING IN THE DATASET
NO VARIABLES WERE DELETED BECAUSE OF MISSING VALUES

THE FOLLOWING OBJECTS WERE DELETED BECAUSE OF MISSING VALUES:
        2 MISS LEV              8 VAN NIER              9 NEFRONIU
       10 PIESTRA              16 NIERMISS
DATASET DEMONSTRAT CONTAINS 2 CLASSES, 11 OBJECTS AND 3 VARIABLES

CLASS STRUCTURE:          CLASS NR  CLASS NAME     CLASS SIZE
                          ------------------------------------
                                1   LIVER               6
                                2   KIDNEY              5

MISV ----------------------------------------------------------------------13 MSEC
```

(D)

```
PROCEDURE STATISTICS   DATE: 86/05/22.   TIME: 13.24.40.   DATASET: DEMONSTRAT
--------------------------------------------------------------------------------
 VARIABLE      CLASS
NR  NAME     NR  NAME          NR.VALUES  MINIMUM     MEAN      MAXIMUM   MEDIAN
                               STAND.DEV  C.V.  PCT  VARIANCE  SKEWNESS  KURTOSIS
--------------------------------------------------------------------------------
1  CREATININE 1  LIVER              8      44.000    111.875    456.000    78.000
                                  139.786  124.977  19517.84    2.776     7.776
              2  KIDNEY           3      527.000   598.667    678.000   567.000
                                  78.233   13.245   6120.333    1.237      -
                        ALL:      11     44.000    242.455    678.000    77.000
                                  254.768  105.076  64982.87    0.000     -1.413
2  LACTATEDEH 1  LIVER             8      234.000   368.750    567.000   345.000
                                  125.514  34.030   15753.64    0.668     -0.542
              2  KIDNEY           3      123.000   147.000    195.000   123.000
                                  41.569   28.278   1728.000    1.732      -
                        ALL:      11     123.000   308.273    567.000   302.000
                                  148.667  48.226   22101.82    0.615     -0.277
3  VAR3       1  LIVER             8      101.000   208.375    345.000   174.000
                                  102.584  51.196   10523.41    0.598     -1.474
              2  KIDNEY           3      12.000    14.333     19.000    12.000
                                  4.041    28.196   16.333     1.732      -
                        ALL:      11     12.000    149.636    345.000   123.000
                                  122.153  81.633   14921.25    0.547     -0.885

                    C O R R E L A T I O N   M A T R I X

 VARIABLE      VAR  CONFIDENCE INTERVAL      PROB  VAR  CONFIDENCE INTERVAL      PROB
NR   NAME      NR  LO-----COR-----HI        VALUE  NR  LO-----COR-----HI        VALUE
--------------------------------------------------------------------------------
1  CREATININE  1    -       1       -

2  LACTATEDEH  1  -0.931  -0.7488  -0.278  0.004   2    -       1       -

3  VAR3        1  -0.923  -0.7229  -0.217  0.006   2   0.719   0.9213   0.988  0.000
               3    -       1       -

STAT----------------------------------------------------------------------103-MSEC
```

(E)

```
PROCEDURE CLASSY       DATE: 86/05/22.   TIME: 13.24.43.   DATASET: DEMONSTRAT
--------------------------------------------------------------------------------
                        CLASS MODEL LIVER
--------------------------------------------------------------------------------
PC VARIANCES OF CLASS MODEL LIVER:
     PC 1          PC 2          PC 3
--------------------------------------------
 286033.84521   28627.11424    2852.29855
--------------------------------------------

                        CLASS MODEL KIDNEY
--------------------------------------------------------------------------------
PC VARIANCES OF CLASS MODEL KIDNEY:
     PC 1          PC 2          PC 3
--------------------------------------------
 373898.72638    2845.94836     0.888885
--------------------------------------------

WARNING: FOR ONE OBJECT ALL DENSITIES ARE ZERO:
         THE PROBABILITIES ARE CONSIDERED EQUAL: 0.5000

CLASS   NO OF      68
MODEL   COMP.   (CLASS R&D)
-----------------------------
1         2     52.31049
2         2      0.00481

CLASSY POSTERIOR PROBABILITIES
--------------------------------------------------------------------------------
                                FIT                    LOOM
          CLASS MODEL:          1          2           1          2
--------------------------------------------------------------------------------
NR NAME      CLASS
3  BLAUW-KN    1          1.00000    0.00000    1.00000    0.00000
4  LEVERING    1          1.00000    0.00000    1.00000    0.00000
5  V/D SLOK    1          1.00000    0.00000    1.00000    0.00000
6  PALPABEL    1          1.00000    0.00000    1.00000    0.00000
11 LEVERMA     1          1.00000    0.00000    0.50000    0.50000
12 KNOOP-BL    1          1.00000    0.00000    1.00000    0.00000
13 SLOKJENS    1          1.00000    0.00000    1.00000    0.00000
14 TASTING     1          1.00000    0.00000    1.00000    0.00000
7  NIERMAN     2          0.00003    0.99997    0.99470    0.00530
15 NIEREMA     2          0.00001    0.99999    0.00084    0.99916
17 URONIUS     2          0.00000    1.00000    0.00016    0.99984

PROBABILISTIC EVALUATION CLASSY A=2                    FIT          LOOM
--------------------------------------------------------------------------------
NON-ERROR RATE (NER)                          Q6     1.00000      0.81818
AVERAGE PROBABILITY FOR THE PROPER CLASS      Q1     1.00000      0.86483
MODIFIED QUADRATIC (BRIER) SCORE              Q31    1.00000      0.68732
SAMPLE SKILL SCORE                            SSS    0.39669      0.17134
SHARPNESS OF CLASSIFICATION                   Q2     0.99999      0.95348
RELIABILITY                                   Q3     0.000004    -0.00938
S.D. OF Q3                                    Q4     0.00059      0.00214
STANDARDIZED RELIABILITY                      Q5     0.00645    -12.52631
                                                     RELIABLE OVER-CONFIDENT

CLAS----------------------------------------------------------------------393-MSEC


END OF RUN             DATE: 86/05/22.   TIME: 13.25.04.   DATASET: DEMONSTRAT
--------------------------------------------------------------------------------
THIS CLAS RUN TOOK 565 MSEC
```

Fig. 2. Example of a CLAS run with five procedures: (a) INPUTDATA; (b) LISTDATA; (c) MISVAL; (d) STATISTICS; (e) CLASSY.

TABLE 2

Command file for CLAS used to give the output of Fig. 2

```
INPUT (NAME: DEMONSTRATION; VAR NAMES: (CLASS, CREATININE,
       LACTATEDEHYDROGENASE); CLASS NAMES: (LIVER, KIDNEY)
       MISSING= — 99)
LIST
MISVAL (DELETE BOTH)
STATISTICS
CLASSY (A=2; LOOM)
```

TABLE 3

Comparison between different programs

Procedure	CPU time required (ms)[a]		
	ARTHUR	SPSS-X[b]	CLAS
Input	488	200	270
Variable deletion	131	—	30
Listing	75	110	156
Missing data handling (class mean substitution)	244	—	40
Variable transformation (ln, exp, adding a variable)	146	—	66
Autoscaling	92	—	15
Univariate statistics	217	410	526
Correlation matrix	333	230	258
Linear regression including plot of residuals	337	270	144
Whole run	2063	—	1505

[a] All times measured with the program running on a CDC Cyber 170/760 computer. The data set consisted of 42 objects, 3 classes and 27 variables. [b] The way in which SPSS-X processes data differs from that of the other programs so that a timable SPSS-X analog could not be found for every procedure.

example serves to illustrate such an evaluation. The IRIS data set [21] contains two classes of 50 objects each, with four measured vairables. The data are class-scaled. SIMCA and CLASSY models of three components are fitted to each class. ALLOC models are also constructed. LOOM evaluation using the CLAS program yields the results given in Table 5. It can be seen that, in this case, the CLASSY and ALLOC methods discriminate about equally well, i.e., the quadratic scores (Q_{31}) are almost the same [21] whereas discrimination with the SIMCA model is considerably worse. The seeming overconfidence of SIMCA and ALLOC (Q_5 negative [1]) and the diffidence found for CLASSY (Q_5 positive) are not significant (reliability (Q_5) is between −1.96 and +1.96).

It must be stressed that CLAS is not yet finished. Extensions and modifications are installed regularly. The microcomputer version is far from definite. Although the batch structure is considered to be mainly an advantage, freeing

TABLE 4

Comparison between resubstitution and LOOM

Procedure	CPU time required (ms)[a]		
	Resubstitution	LOOM	Factor[b]
Linear regression (n=42, p=27)	146	354	2.4
SIMCA (n=42, p=13, c=3)	597	4697	7.9
ALLOC (n=42, p=13, c=3)	651	3961	6.1
CLASSY (n=42, p=13, c=3)	935	7819	8.4

[a] All times measured with the program running on a CDC Cyber 170/760 computer. [b] If the leave-one-out algorithm is implemented as a straightforward repetition of the procedure, a factor of about 43 is expected.

TABLE 5

Example of evaluation

Procedure	Number of errors	Quadratic score (Q_{31})	Reliability (Q_5)
SIMCA (A=3)	20	0.873	−1.30
CLASSY (A=3)	4	0.971	+0.47
ALLOC	5	0.957	−1.17

the user from irritating waiting, it is clear that simple syntax errors may be recognized only after much calculation has been done. To compensate for this drawback, a procedure is planned that will allow interactive creation of the input file. This will prevent syntax errors and fully utilize the microcomputer capabilities of user friendliness. Some major techniques are still absent in CLAS. Multiclass SLDA will hopefully be implemented, as well as the K-nearest-neighbour method. Many procedures will be extended to increase flexibility and plotting output will be available from more procedures. Other aspects requiring attention are outlier detection and variable selection.

REFERENCES

1 J. Hilden, J. D. F. Habbema and B. Bjerregaard, Method Inf. Med., 17 (1978) 227, 238.
2 P. A. Lachenbruch and M. R. Mickey, Technometrics, 10 (1968) 1.
3 P. A. Lachenbruch, Biometrics, 23 (1967) 639.
4 N. H. Nie, C. Hadlai Hull, J. G. Jenkins, K. Steinbrenner and D. H. Bent, SPSS, Statistical Package for the Social Sciences, McGraw-Hill, New York, 1975.
5 W. J. Dixon, BMDP Biomedical Computer Programs, University of California Press, Los Angeles, 1975.
6 A. M. Harper, D. L. Duewer, B. R. Kowalski and J. L. Fasching, in B. R. Kowalski (Ed.), Chemometrics: Theory and Application, ACS Symposium Series 52, American Chemical Society, Washington DC, 1977, p. 14.

7 S. Wold and M. Sjöström, in B. R. Kowalski (Ed.), Chemometrics: Theory and Application, ACS Symposium Series 52, American Chemical Society, Washington DC, 1977, p. 241.
8 J. Hermans, J. D. F. Habbema, T. K. D. Kasanmoetalib and J. W. Raatgever, Manual for the ALLOC-80 Discriminant Analysis Program, Dept. of Medical Statistics, University of Leiden, 1982.
9 D. L. Massart and L. Kaufman, The Interpretation of Analytical Chemical Data by the use of Cluster Analysis, Wiley, New York, 1983.
10 P. van Espen, Anal. Chim. Acta, 165 (1984) 31.
11 J. P. Strait, A. B. Mickel and J. T. Easton, Pascal 6000 release 3, University of Minnesota, Minneapolis, 1979.
12 G. E. Forsythe, M. A. Malcolm and C. B. Moler, Computer Methods for Mathematical Computation, Prentice-Hall, Englewood Cliffs, NJ, 1977, 246.
13 R. P. Brent, Algorithm 488, Communications of the Association for Computing Machinery.
14 J. B. Hemel and H. van der Voet, Anal. Chim. Acta, 1987, to be published.
15 D. M. Allen, Technometrics, 16 (1974) 125.
16 R. D. Snee, Chem. Technol., (1979) 702.
17 P. E. Green, Analyzing Multivariate Data, Dryden Press, Hinsdale, 1978, p. 366.
18 J. R. Bunch, C. P. Nielsen and D. C. Sorensen, Numer. Math., 31 (1978) 31.
19 J. H. Wilkinson and C. Reinsch, Handbook for Automatic Computation, Vol. 2, Linear Algebra, Springer Verlag, Berlin, 1977.
20 H. van der Voet and D. A. Doornbos, Anal. Chim. Acta, 161 (1984) 115.
21 H. van der Voet and D. A. Doornbos, Anal. Chim. Acta, 161 (1984) 125.

Analytica Chimica Acta, 191 (1986) 47—62
Elsevier Science Publishers B.V., Amsterdam — Printed in The Netherlands

THE EVALUATION OF PROBABILISTIC CLASSIFICATION METHODS
Part 1. A Monte Carlo Study with ALLOC

HILKO VAN DER VOET*[a] and PIERRE M. J. COENEGRACHT

Chemometrics Research Group, Pharmaceutical Laboratories, A. Deusinglaan 2, NL-9713 AW Groningen (The Netherlands)

JAN B. HEMEL

Central Laboratory for Clinical Chemistry, University Hospital, P.O. Box 30001, NL-9700 RB Groningen (The Netherlands)

(Received 20th June 1986)

SUMMARY

Probabilistic classification (i.e., classification of individuals into one of several groups by assigning probabilities of classification to each individual) is desirable when the main interest is in individuals rather than the whole group. The evaluation of probabilistic assignments is described in detail, including statistical features such as measures for the sharpness of the classification, the predictive ability and the reliability of the probability values. In a simulation study, the influence of the objects—variable ratio and the interclass distance on the results was examined for the training data themselves (resubstitution method), an independent test set, and a pseudo-independent test set created from the training set (leave-one-out method). The results indicate that the leave-one-out method can often be used instead of an independent test set. In many cases, the assignments cited as probabilities are not probabilities at all, because the classification system is too over-confident.

Pattern recognition deals with situations where a class structure is assumed to be present in the problem investigated. This series of papers considers supervised pattern recognition, i.e., methods designed to classify objects from an unknown class into one of a number of previously defined classes. More specifically, it deals only with those methods that are able to give classification probabilities. When an object of unknown origin is examined by such a probabilistic method, the results can be presented as a set of statements of the form: "This object belongs to class c with probability P", where c varies over all classes that were previously defined.

There are many multivariate classification methods (MCM's) capable of producing probabilistic results. An optimal choice between them requires suitable criteria. Hilden et al. [1, 2] have described such criteria, but these seem to be not well known in chemometrics. Some of these criteria and also

[a]Present address: Agricultural Statistics Department, TNO Institute of Applied Computer Science (iTi-TNO), PO Box 100, NL-6700 AC Wageningen, The Netherlands.

0003-2670/86/$03.50

the important concepts of discriminatory ability and reliability are discussed in this paper. The results obtained by applying these criteria to practical data sets have raised several questions. One of the problems concerns the method of evaluation: Lachenbruch's leave-one-out method (see below) is often used when no independent test data are available, but "there is little theory to justify its use, insofar as performance criteria other than percentage correct answers are concerned" [3]. Another problem is exemplified by a statement of Templeton et al. [4], who used a simple method based on Bayes' formula for medical diagnosis and concluded from a reliability evaluation that "the numbers assigned by Bayesian diagnosis are not probabilities at all". Similar results have been reported by other researchers using more sophisticated MCM's [1, 3, 5, 6]. These and other problems suggested a study of probabilistic methods and their detailed evaluation by means of a Monte Carlo study. The design of this simulation study is described and some useful insights that have been acquired about the applicability of the evaluation methods and criteria are discussed.

THEORY

The need for evaluation of probabilistic classification

The need for probabilistic classification itself is best illustrated by an example. Table 1 shows how two wine samples, which are only part of a data set of 58 wine samples, are classified by the probabilistic method SLDA (statistical linear discriminant analysis). The classification rule gives probabilities for each of the three classes, that were represented in the training set, in this case the three possible regions of origin, Beaujolais, Bourgogne and Bordeaux. For both wine samples, the highest probability is given to the Bourgogne class, and as this is indeed the real origin of both, a non-probabilistic approach would consider both samples as correctly classified. But this approach would not disclose that the Bourgogne Pinot sample is classified with almost complete certainty, but that the Puligny Montrachet is a border case, a Bourgogne wine which is close in its characteristics to the Beaujolais samples. In fact, without knowing the real class of the wines, one could not exclude the possibility that the latter wine comes from the Beaujolais region.

TABLE 1

Probabilistic classification by SLDA of two French wine samples originating from the Bourgogne class (leave-one-out classification based on a data set of 58 French wines)

Wine sample	Probability for:		
	Beaujolais	Bourgogne	Bordeaux
Bourgogne Pinot 1979	0.0002	0.9998	0.0000
Puligny Montrachet 1973	0.3961	0.6039	0.0000

Doubt classification [7, 8] will not be discussed here but it should be noted that probabilistic methods are essential whenever the classification of the individual objects is important. If only the overall class separability is important, non-probabilistic methods may suffice.

It is necessary to evaluate probabilistic methods in practical situations. Although many people seem to think that one should try to find one classification method that is optimal in all situations, there are many factors that govern whether or not a particular method will perform well in a practical problem. Some of these factors are the number and type of chemical measurements made, the number of classes that are to be distinguished, the number of training objects that can reasonably be collected for each class, the appearance of missing values in the data matrix, the necessity for outlier detection, etc. The appropriateness of any particular classification method depends to a large extent on these factors, some of which will be known (although different for each problem) and some unknown (e.g., the statistical distribution of the variables or the amount of correlation between variables). Thus evaluation is not an academic problem, but a necessary step for anyone who wishes to apply pattern recognition techniques to a specific problem. The importance of this separate evaluation for each new problem should be stressed although a kind of evolutionary evaluation develops with experience.

Methods for evaluation

There are many different probabilistic MCM's that could be applied to a problem. Some of the more important are SLDA [9], ALLOC [10—12], SIMCA [13, 14] (made probabilistic [15]) and CLASSY [15]. Other methods were discussed by Coomans et al. [16], Titterington et al. [17] and Aitchison et al. [18]. In practical situations, there is plenty of choice, but this can also be dangerous, as pointed out by Wold et al. [19] who warned against applying different pattern recognition methods and then selecting the results that "look best". Not the best results, but the best method should be selected. There are two possible ways in which the best method can be selected. One way is to select a method or eliminate another for theoretical reasons without looking at empirical results. The method of centroid classification [20], for example, takes no account of the covariance structure of the classes and therefore seems a poor candidate for a good classification method. However, there are plenty of MCM's, which all are theoretically appealing, in different ways. The other way to select the best method without regard to the "best results" is to include a separate evaluation step in the process. As shown in Fig. 1a, the total pattern recognition process consists of an initial part (choice of data and MCM) and a routine part in which newly sampled data are presented to the MCM and new results are obtained. The extra step shown in Fig. 1(b) involves comparative evaluation in order to select the best method. At this stage, one certainly looks at the best results, but the evaluation is not a routine part of the process. Once the most appropriate method has been chosen for the particular problem and type of data,

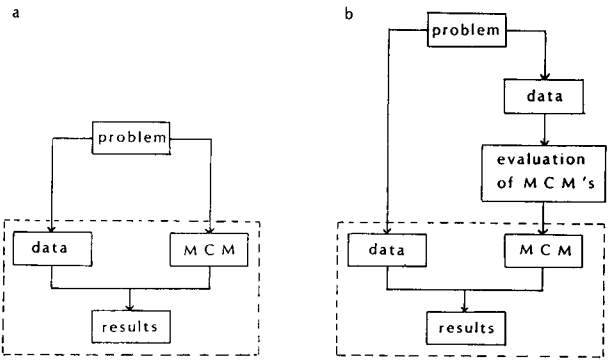

Fig. 1. Schematic representation of the application of pattern recognition. (a) Basic scheme; the routine part of the process is enclosed by a dashed line. (b) As (a) with a separate evaluation step added.

this method should be applied to all data sampled in the routine process. The rest of this paper is devoted to the evaluation step.

The best way to evaluate an MCM is to test the correctness of its predictions. For this purpose, there should ideally be enough data for both a training set and a test set. The test set is a collection of objects for which the real class membership is known to the evaluator, but not to the MCM. The fraction of correctly classified objects is called the non-error rate (NER). Unfortunately, it is often difficult to collect enough data for both a training and a test set. In such cases all available objects will be used to construct the classifier. Evaluation has then to be done on the objects of the training set itself. If this is done without further thought, the procedure is known as the resubstitution method for evaluation [21]. However, the results tend to give an overoptimistic view of the classificatory ability, because the classification rule was optimized for the training objects and newly sampled objects will generally not have exactly the same measurement values as the training objects.

An alternative way for evaluation is to delete one object from the training set, and then to classify this one object with a classification rule based on the remaining training objects. The disadvantage that the evaluation set consists of only one object can be removed by repeating the whole procedure N times, each time with a different object deleted from the training set. This is appropriately called the leave-one-out method and was introduced by Lachenbruch [21, 22]. Other names for this procedure are the hold-one-out method [23, 24], the leave-current-patient-out method (in medical statistics [3]), cross-validation [17, 25] and jack-knifing [7] (although the latter two terms are also used for other schemes). A more recent development in evaluation methods is Efron's bootstrap method [25—27]. Although this is a very interesting technique, it was not applied in the present study.

Criteria for evaluation

The most commonly used criterion for evaluation is the non-error rate (NER), the number of correctly classified objects divided by the total number of evaluation objects. The NER has the draw-back that it does not take into account that classification is done with probabilities. Thus one does not really evaluate in a probabilistic manner, but instead all methods are judged as if they were non-probabilistic.

Hilden et al. [1, 2] introduced criteria especially for the evaluation of probabilistic classification methods. Their work has its roots in the theory of subjective probability [28]: they consider the MCM as a black box producing numbers that are meant to be probabilities, even in situations where the objective definition of probability (i.e., as a frequency) cannot be applied directly. It is important to distinguish between two different aspects of the performance of classification methods: discriminatory ability and reliability. The distinction can be clarified by some artificial examples. The results of a probabilistic classification can always be displayed in a probability matrix. Table 2 shows the results of hypothetical classifications where six evaluation objects had to be classified in two classes. The real origin of the first 3 objects (unknown to the MCM) was class 1, the real origin of the last 3 objects was class 2. This is emphasized in the Table by underlining the entries for the correct class. Table 2(I) shows almost ideal results: all objects are classified correctly and with high probabilities. The results of Table 2(II) are less favourable: the objects B, C and E have the highest probability assignment for the wrong class, so that half the objects are misclassified, i.e., the discriminatory ability of the MCM is low. This lack of discrimination is reflected in the probability values themselves: they are all near 50%. In fact, the classification method can be said to have little confidence in its own discriminatory power; in this case it is right and the method is called reliable or well-calibrated [29]. Good reliability means that the discriminatory ability of the method

TABLE 2

Examples of probability matrices: (I) good discrimination and good reliability; (II) bad discrimination and good reliability; (III) bad discrimination and bad reliability (over-confidence); (IV) good discrimination and bad reliability (under-confidence)

Object	Matrix I Class		Matrix II Class		Matrix III Class		Matrix IV Class	
	1	2	1	2	1	2	1	2
A	0.99	0.01	0.52	0.48	0.99	0.01	0.52	0.48
B	0.99	0.01	0.43	0.57	0.02	0.98	0.57	0.43
C	0.98	0.02	0.49	0.51	0.01	0.99	0.55	0.45
D	0.00	1.00	0.49	0.51	0.00	1.00	0.30	0.70
E	0.01	0.99	0.60	0.40	0.94	0.06	0.45	0.55
F	0.01	0.99	0.44	0.56	0.02	0.98	0.47	0.53

should be reflected in the individual probability values, i.e., the numbers in the classification table can be regarded as real probabilities. Examples of classification that cannot be regarded as real probabilities are shown in Table 2(III) and (IV). Table 2(III) again shows a low discriminatory ability with 3 out of 6 objects misclassified but, if the real classes of the objects were unknown, the probability values would give the impression of a very secure classification, as all values are near 100% or 0%. This is called a sharp classification, as in the case of 2(I); in both cases, the classification method appears to be self-confident but in case 2(III) the self-confidence is clearly not justified and the method is called over-confident rather than reliable: the values are too sharp for real probabilities. Table 2(IV) shows another possibility: all objects are classified correctly, but the method hesitates, with probabilities all near 50%, and so is termed under-confident or diffident.

So far, the discussion of MCM performance has been qualitative. Some quantitative criteria discussed by Hilden et al. [1, 2] are summarized in Table 3. Some useful considerations about these criteria have been published [5, 16, 30—33]. Among the criteria for the discriminating ability are the non-error rate (which does not use the probabilistic information) and the average probability assigned to the proper class Q_1, which is easily computed as the average of all underscored values in any of the classification matrices shown

TABLE 3

Summary of some important criteria for the probabilistic evaluation of classification [1, 2]. Notation: P_{ik} is the assigned probability that object i belongs to class k; $d(i)$ is the real class of i. The number of evaluation objects is N, the number of classes is K. I is the indicator function: 1 if condition is true, 0 otherwise

Criteria for discriminatory ability	Range
Non-error rate $\mathrm{NER} = Q_0 = (1/N)\,\Sigma_i I\{P_{id(i)} = \max_k P_{ik}\}$	[0, 1]
Average probability for the proper class $Q_1 = (1/N)\,\Sigma_i P_{id(i)}$	[0, 1]
Brier score (quadratic score) $Q_{30} = (1/N)\,\Sigma_i[(1 - P_{id(i)})^2 + \Sigma_{k \neq d(i)} P_{ik}^2]$	[0, 2]
Modified Brier score $Q_{31} = 1 - Q_{30}/2 = Q_1 - Q_2/2 + 1/2 = (Q_1 + Q_3)/2 + 1/2$	[0, 1]
Criteria for sharpness and reliability	**Range**
Sharpness (self-confidence) $Q_2 = (1/N)\,\Sigma_i \Sigma_k P_{ik}^2$	$[1/K, 1]$
Reliability score (calibration score) $Q_3 = Q_1 - Q_2$	$[-1, (K-1)/(4K)]$
Standardized reliability score $Q_5 = Q_3/\{\Sigma_i \Sigma_k [P_{ik}(P_{ik} - \Sigma_h P_{ih}^2)^2]\}^{1/2}$	

in Table 2. Although Q_1 has a clear interpretation, it should not be used as a guide to find the optimal discriminating method because it is also influenced by the reliability of the results. In fact, as long as the majority of all objects is classified into the proper class, the criterion value increases whenever the probability values become sharper. So Q_1 as a criterion for discriminatory ability favours over-confident methods and is called a non-proper scoring rule [2].

Brier [34] introduced a criterion that can be shown to be a strictly proper scoring rule [2], implying that it attains an optimal value if the values given by a classifying person or computer program are equal to the real (although unknown) probabilities. This criterion has been extensively used in meteorology to assess the quality of weather predictions [35]. The Brier score, here designated by Q_{30}, is in essence a quadratic distance measure, so that 0 represents the optimal result. To bring it into the same range as Q_1 and the NER, Hilden et al. [2] applied a simple rescaling and obtained the modified Brier score Q_{31}, which equals $1 - Q_{30}/2$. It can also be expressed as a linear combination of the simple criterion Q_1 and the reliability measure Q_3 (see below) in such a way that the favouring of over-confident methods by Q_1 is corrected for.

A numerical measure for the sharpness of probabilistic predictions is Q_2 (see Table 3). This is again an average over the N evaluation objects, where for each object the contribution is the sum of the squared probabilities. Therefore, if the MCM has assigned 100% probability to one class (which may be right or wrong) the contribution to Q_2 is 1 for that object. The minimal value of Q_2 is obtained when all probability mass is distributed equally over the classes.

Sharpness can be regarded as the MCM's opinion of its own discriminatory ability (see above). For a measure of reliability, this can be contrasted with an expression for the real discriminatory ability. Taking Q_1 for the latter, it can be derived that the difference $Q_1 - Q_2$ should be approximately zero for an absolutely reliable system [1]. In more technical terms, Q_2 can be shown to be the expectation of Q_1 for a fixed probability matrix under the null hypothesis that the values in the table are real probabilities. The difference $Q_1 - Q_2$ is termed Q_3 and it is easily seen that over-confidence (too sharp probabilities) leads to negative values of Q_3, while under-confidence produces a positive reliability score. It is even possible to calculate the variance of Q_3 under the null hypothesis, so that by scaling one obtains a criterion, termed Q_5, that follows approximately a standard normal distribution [1].

Applications of the criteria discussed above, mainly to medical data sets, have been described in the literature [5, 6, 16, 17, 32, 33, 36].

In previous work [6], disturbing results were obtained with the reliability criteria. Over-confidence was commonly observed but it seemed to depend more on the data set investigated than on the classification method used. Inspection of the results both from that study and from the literature suggested some important factors that could be responsible for the appearance of over-confident predictions: especially the ratio between the number

of objects per class (n) and the number of measured (independent) variables (p) seemed to be important. To study this in more detail, the simulation study described below was planned.

EXPERIMENTAL

A simulation study was performed by using a Gaussian pseudo-random number generating algorithm [37] to construct data tables. Each data table consisted of $N = 2n$ rows, representing equal numbers of objects from two classes, and p columns, representing the measured variables. The number of objects per class (n) was varied systematically over the values 3, 5, 10, 20 and 40. The number of variables (p) was varied systematically over the values 1, 2, 5, 10 and 20. The distribution of the random numbers was Gaussian, so that the distance between the class centres could be quantified by the Mahalanobis distance Δ^2. In the simulations, the covariance matrix of the variables was taken equal to the identity matrix, so Δ was equal to the Euclidean distance. For a data matrix with p variables, the population centroids of the two classes were set at $(0, 0, \ldots, 0)$ and $[(\Delta^2/p)^{1/2}, (\Delta^2/p)^{1/2}, \ldots, (\Delta^2/p)^{1/2}]$, respectively. The population value Δ was varied systematically from 5 (standing for a reasonable separation between the two classes) via 2 and 1 down to 0 (i.e., no difference between the classes). Each of the possible combinations of n, p and Δ produced a data table that was used as a training set for multivariate classification. All results presented below were obtained with the ALLOC method.

The evaluation of the probabilistic classification results was done in three ways. Each generated data table with training objects was accompanied by another data table of the same dimensions, so that test set evaluation became possible. The training objects themselves were used for resubstitution evaluation and leave-one-out evaluation.

To reduce the variability of the results arising from the random numbers used, the whole classification and evaluation procedure was repeated 30 times for each combination of n, p and Δ. This also allowed the computation of empirical standard deviations in the calculated criteria. These criteria included the NER, Q_1, Q_{30} and Q_{31} for the evaluation of discriminatory ability, and Q_2, Q_3 and Q_5 for evaluation of sharpness and reliability.

All computations (simulation, classification and evaluation) were done with the CLAS program, which is designed especially for the comparative evaluation of probabilistic MCM's [38]. One of the features of this program is that it greatly reduces the computational costs of the otherwise time-consuming leave-one-out method.

RESULTS AND DISCUSSION

It is not possible in the present context to give details of all results from the experiments. Tables with the means and standard deviations of all criteria for the three evaluation methods and for each $n - p - \Delta$ combination are

available from the authors on request. Some of the more interesting results are presented here graphically and discussed in relation to the problems that motivated this study, namely, the regular occurrence of over-confidence and the relative merits of the resubstitution and leave-one-out methods of evaluation compared to the test-set method.

Reliability of the probabilities

Only results obtained with the test-set method are considered here. Figure 2 shows the reliability score Q_3 as a function of the dimensionality ratio n/p. The n/p axis is logarithmic so that the whole range of dimensionality ratios from 0.15 to 40 can be neatly shown. Each point is the average Q_3 score for 30 simulation runs. The results for $\Delta = 1$ have been omitted for clarity. It can be seen that the reliability score is effectively zero when n/p is large enough. According to the theory of Hilden et al., a classification method is only reliable if Q_3 is effectively zero. However, the lines diverge to over-confidence for low n/p ratios. This effect is most pronounced when the separation between the classes is bad. For $\Delta = 0$, the over-confidence is always significant in this study; for $\Delta = 2$, over-confidence is significant below a dimensionality ratio of about 5, and for $\Delta = 5$ this is so below $n/p = 1$ ($\alpha = 0.05$). Significance was detected by computing a t statistic for each point using the empirical standard deviations.

The reliability score Q_3 is thus very often significantly negative. At first sight, it may be tempting to conclude that the multivariate classification method ALLOC is therefore often not reliable, but experience with other methods, both on practical data sets and in preliminary simulation experiments, suggest that the pattern is the same: all probabilistic MCM's seem to be over-confident in certain difficult situations. Reliability can be otherwise formulated as the trustworthiness of the probability values. Thus, if a method

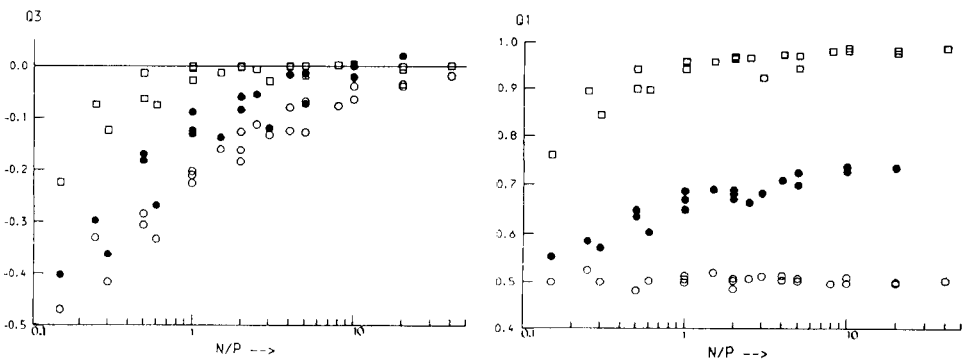

Fig. 2. Reliability score Q_3 as a function of the dimensionality ratio n/p for different Δ values: (○) 0; (●) 2; (□) 5.

Fig. 3. Average probability assigned to the proper class Q_1 as a function of the dimensionality ratio n/p for different Δ values. Symbols as in Fig. 2.

is found unreliable, this means that the values given in the output of the computer program cannot be trusted as being real probabilities. Therefore over-confidence seems to indicate that probabilistic classification is not possible. This will occur when the n/p ratio and the interclass distance are both small, i.e., when there is insufficient discriminatory information available in the data.

It is of interest to look at Q_1 and Q_2, the elements from which the reliability score is constructed (see Figs. 3 and 4). It should be recalled that sharpness can be considered as the expected value of Q_1 under the null hypothesis of reliability. For high n/p ratios, Q_1 and Q_2 are indeed approximately equal to each other and also to the NER. The limiting value, known as the optimal non-error rate, depends on the separation of the two populations. For Gaussian populations it has the value $\Phi(\Delta/2)$, where Φ represents the cumulative standard normal distribution [39, 40].

For $\Delta = 0$, Q_1 is close to the theoretically expected value of 50% over the whole range of n/p ratios. The sharpness Q_2, however, deviates sharply from this value for low dimensionality ratios, and this accounts for the observed over-confidence. The problem here is that the interpretation of sharpness as the expected value of Q_1 is valid only for a fixed probability matrix: it does not take into account the variations that can normally be expected with any classifier that makes use of the data. This kind of variation is the same as the observer variation discussed by Lindberg [33]. An example may clarify why probabilities are always too sharp in the case $\Delta = 0$. Table 4 contains two matrices with classification probabilities for the same kind of problem as Table 2. Elementary calculations show that the unrealistic results of Table 4 (Matrix I) with all values exactly equal to 0.50 is the only way to obtain a reliability score Q_3 of zero. With any random fluctuation in the probability values (e.g., Table 4 (Matrix II)), the sharpness increases and exceeds 0.5. Consequently, the reliability score becomes negative ($Q_3 = -0.045$ for the data given). Symmetric fluctuations in the probability values (which can be

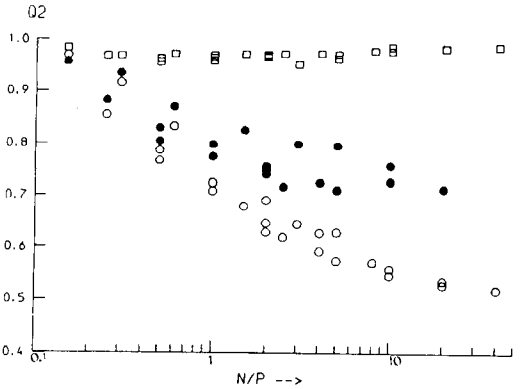

Fig. 4. Sharpness Q_2 as a function of the dimensionality ratio n/p for different Δ values. Symbols as in Fig. 2.

TABLE 4

Examples of probability matrices

Object	Matrix I[a]		Matrix II[b]	
	Class 1	Class 2	Class 1	Class 2
A	0.50	0.50	0.42	0.58
B	0.50	0.50	0.74	0.26
C	0.50	0.50	0.48	0.52
D	0.50	0.50	0.73	0.27
E	0.50	0.50	0.37	0.63
F	0.50	0.50	0.54	0.46

[a]Without random fluctuations around 0.50. $Q_1 = 0.50$, $Q_2 = 0.50$, $Q_3 = 0.00$. [b]With random fluctuations around 0.50. $Q_1 = 0.50$, $Q_2 = 0.545$, $Q_3 = -0.045$.

expected if the classification is based on randomly sampled data) do not lead to symmetric fluctuations in the reliability, but always to negative values of Q_3.

When the classes are reasonably well separated ($\Delta = 5$), the graphs of Q_1 and Q_2 are somewhat different: Q_2 is always very high in this case, and it is not increased sharpness that is primarily responsible for the observed overconfidence, but a decline in the average probability for the proper class at low n/p ratios. For intermediate values of the interclass distance, such as $\Delta = 2$, both effects occur: as n/p is lowered, Q_1 decreases and Q_2 increases.

Comparison of evaluation methods

In order to decide how satisfactory the leave-one-out and the resubstitution methods are as substitutes for the test-set method, all the different evaluation criteria could be considered individually. As the trend appears to be the same for NER, Q_1, Q_{31} and Q_3, however, only one of them (Q_1) is presented below. For one criterion, the sharpness Q_2, very little difference was found between the three evaluation methods. In fact, this explains the similar behaviour of Q_1, Q_3 (which equals $Q_1 - Q_2$) and Q_{31} (which equals $Q_1 - Q_2/2 + 1/2$).

Figure 5 shows for the cases $\Delta = 0$, $\Delta = 2$ and $\Delta = 5$, respectively, the significance of the differences between the resubstitution and test-set methods, and between the leave-one-out and test-set methods. The t statistics based on the 30 individual differences in Q_1 for each $n - p - \Delta$ combination are shown. Generally, there is a clear trend in the results: the resubstitution method tends to produce higher Q_1 scores than the test-set method (positive t statistics) and the leave-one-out method gives on average somewhat lower values than the test set method (negative t statistics). The latter result does not confirm the impression of Coomans [41] that the leave-one-out method would tend in some cases to give too optimistic a picture of the classificatory ability of a pattern recognition technique. On the contrary, while the resubstitution method suffers from optimistic bias, the leave-one-out method for

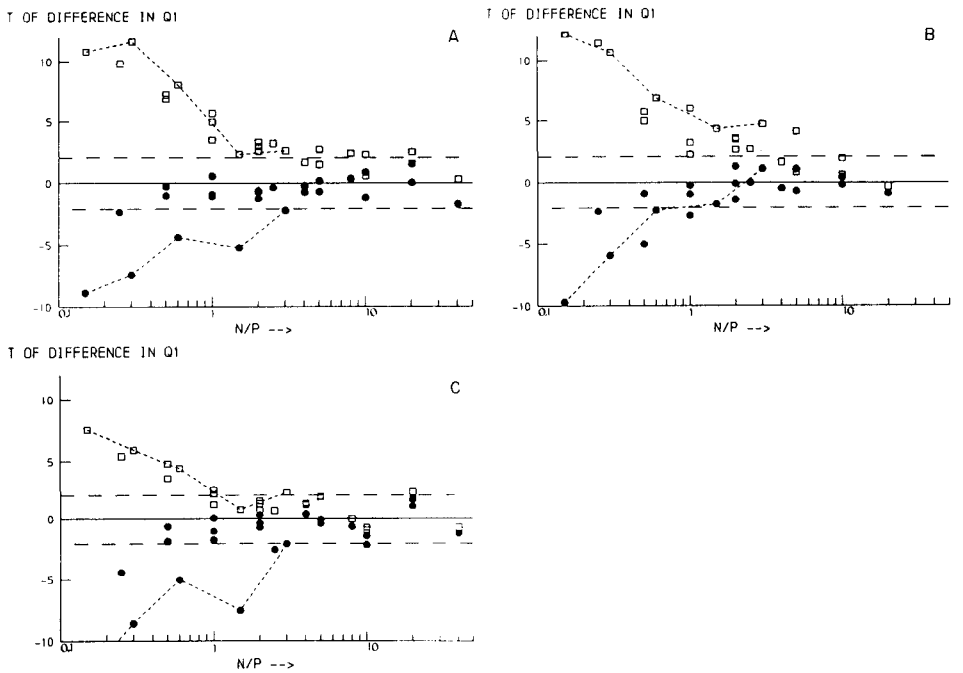

Fig. 5. Deviations of resubstitution and leave-one-out results from the test-set results for different values of Δ: (A) $\Delta = 0$; (B) $\Delta = 2$; (C) $\Delta = 5$. The t statistics (29 degrees of freedom) for the significance of the differences in Q_1 are shown. (□) Resubstitution—test; (•) leave-one-out—test. (——) 95% confidence limits around zero; (- - -) results from experiments with $n = 3$.

evaluation shows, if anything, a pessimistic bias. Both effects increase when the n/p ratio is lowered. The over-optimism of the resubstitution method also depends on the inter-class distance: when the classes are closer to one another, the over-optimism of evaluation by resubstitution increases. Figure 5 shows that for $\Delta = 0$ the optimistic bias of the resubstitution method is very often statistically significant ($\alpha = 0.05$), even for dimensionality ratios as high as $n/p = 20$. For $\Delta = 5$, this optimistic bias is less pronounced, although the general trend is clear. The leave-one-out method gives results that are rarely significantly different from the test-set results with one important exception; when the class size was only 3 objects, the Q_1 values were very negatively biased. It seems wise to restrict the use of this evaluation method to situations where the number of objects in each class is, say, not <5. If this condition is fulfilled, the claim of Lachenbruch [22] that the method is almost unbiased remains valid.

Theoretical reasons can be given for the biases found in the experiments. All MCM's apply statistical modelling to the training data and, depending on the complexity of the model and the degrees of freedom in the data, there is always the danger of over-fitting [42]. The resubstitution criteria are measures of fit rather than of predictive power, so clearly the over-fitting will translate

into an overly optimistic view of the predictive abilities. The pessimism of the leave-one-out method can be explained by considering the training set in just one step of the leave-one-out procedure: this training set is not exactly a random sample from the population of interest. In fact, the type of measurements found for the one object used for evaluation has a lower probability of being present in the training set (for this to occur, the relevant measurement vector would have to be duplicated in the data). Thus the left-out object is predicted with the use of a model which is optimal for a population with a somewhat smaller amount of objects of the type of the left-out object itself; thus the predictive ability is underestimated.

Another aspect of the comparison of evaluation methods concerns the variability of the results. The results found for the NER are used for this comparison, because this criterion has a very convenient statistical distribution in the case of independent test data. The NER can be considered as a count of N values, where each value is 1 or 0 (correctly or incorrectly classified), divided by a constant (N). Consequently, each individual contribution to the NER is binomially distributed with variance $\pi(1 - \pi)$, where π is the probability of correct classification. The NER evaluated on N objects has therefore a variance of $\pi(1 - \pi)/N$. From the experiments, both the NER as an estimate of π and the empirical standard deviation as an estimate of $[\pi(1 - \pi)/N]^{1/2}$ are available. Multiplying the empirical standard deviation by $N^{1/2}$ yields estimates for the one-object standard deviation that should depend only on π. Figure 6A shows a plot of this standard deviation against the NER itself for the test-set data; it can be seen that the empirical points are well spread around the theoretically predicted model. Figure 6B and C shows the results for the resubstitution and leave-one-out methods. There are three pertinent observations: (1) the theoretical model predictions for the standard deviation are exceeded for both methods; (2) the amount of excess is about the same for the resubstitution and leave-one-out methods; (3) the increase in the standard deviations, compared to the test-set results, is not large (on average a factor of about 1.3).

The comparison of evaluation methods indicates that a separate extra test set remains best. If this test set is not available, the leave-one-out method is a good alternative. The criteria computed in this way have a somewhat greater variability, and they may be slightly pessimistic, but this effect is rarely significant (except for very small class sizes). The resubstitution method also gives criteria values with a somewhat greater variability, but the over-optimism can be serious. Apart from the quantitative difference between the resubstitution and leave-one-out methods, it is generally better in practice to err on the safe side in estimating the discriminatory ability of a classification rule. Therefore the use of the resubstitution method should be discouraged; even when it might be applicable (at high n/p ratios), it is perhaps still better to split the data into separate training and test sets.

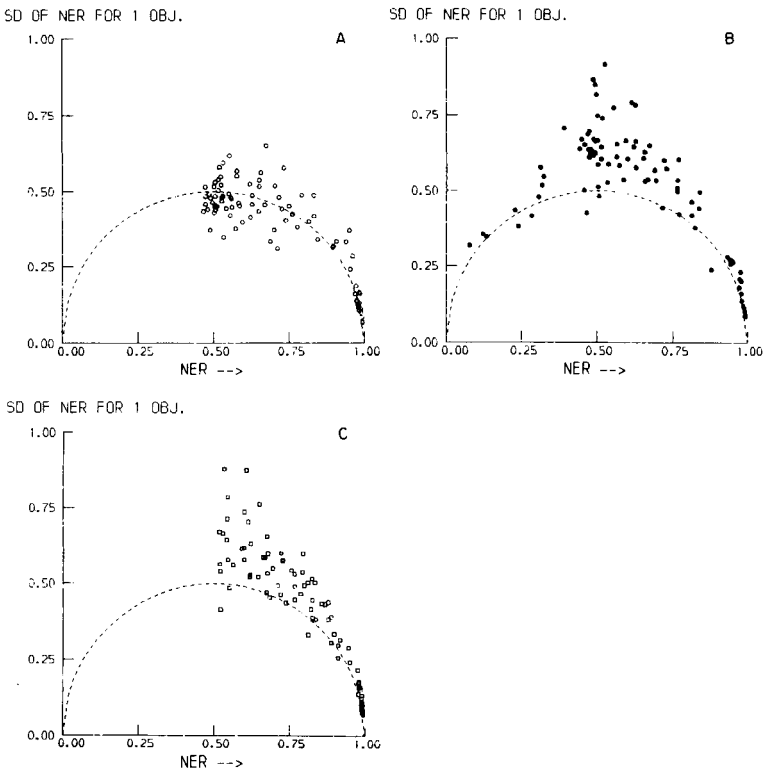

Fig. 6. Variation in the non-error rate: (A) for the test set results; (B) for the leave-one-out results; (C) for the resubstitution results. (———) Theoretical relation between the standard deviation and the mean of the NER score for one object; (○), (•) and (□) empirical results.

Conclusions

This work was done because probabilistic classification is often desirable; when the feature of interest is an individual, an either/or classification is too coarse and shades of grey are needed. The choice of MCM must be made in a separate evaluation step, whereas in routine applications a single MCM must be used. Practical performance must be evaluated by considering both the discriminatory ability and the reliability of the probabilities.

The main conclusions from this work can be summarized as follows. First, over-confidence is common; it occurs if both the n/p ratio and the interclass distance Δ are small. Secondly, over-confidence depends on the data: if insufficient information is present in the data, no method can extract it. Thirdly, the resubstitution method for evaluation is often too optimistic; this can be dangerous, so the method should not be used. Fourthly, the leave-one-out method is generally a good substitute for an independent test-set evaluation, although it tends to be slightly pessimistic. Finally, the leave-one-out method should not be used for very small class sizes (say, <5 objects), as it is then very pessimistically biased.

No conclusions are drawn regarding the possible superiority of one or other classification method, because only one method was used here. Although it is hoped to present results of MCM comparison at a later date, it is obvious that the performance of MCM's depends on many known and unknown factors in particular cases. Therefore the final choice of the most appropriate method for a particular problem must be made by the user.

REFERENCES

1 J. Hilden, J. D. F. Habbema and B. Bjerregaard, Meth. Inform. Med., 17 (1978) 227.
2 J. Hilden, J. D. F. Habbema and B. Bjerregaard, Meth. Inform. Med., 17 (1978) 238.
3 J. Hilden and B. Bjerregaard, in F. T. de Dombal and F. Grémy (Eds.), Decision Making and Medical Care: Can Information Science Help?, North-Holland, Amsterdam, 1976, p. 365.
4 A. W. Templeton, J. L. Lehr and C. Simmons, Radiology, 87 (1966) 658.
5 J. Hilden and J. D. F. Habbema, in A. Alpérovitch, F. T. de Dombal and F. Grémy (Eds.), Evaluation of Efficacy of Medical Action, North-Holland, Amsterdam, 1979, p. 123.
6 H. van der Voet, J. B. Hemel and P. M. J. Coenegracht, Anal. Chim. Acta, 191 (1986) 63.
7 J. D. F. Habbema, J. Hermans and A. T. van der Burgt, Biometrika, 61 (1974) 313.
8 J. D. F. Habbema, J. Hilden and B. Bjerregaard, Meth. Inform. Med., 17 (1978) 217.
9 D. Coomans, D. L. Massart and L. Kaufman, Anal. Chim. Acta, 112 (1979) 97.
10 J. D. F. Habbema and J. M. H. Hermans, Ph.D. thesis, University of Leiden, 1978, p. 22.
11 D. Coomans, D. L. Massart, I. Broeckaert and A. Tassin, Anal. Chim. Acta, 133 (1981) 215.
12 J. Hermans, J. D. F. Habbema, T. K. D. Kasanmoentalib and J. W. Raatgever, Manual for the ALLOC80 Discriminant Analysis Program, Dept. of Medical Statistics, University of Leiden, Leiden, 1982.
13 S. Wold, Pattern Recognition, 8 (1976) 127.
14 C. Albano, G. Blomqvist, D. Coomans, W. J. Dunn III, U. Edlund, B. Eliasson, S. Hellberg, E. Johansson, D. Johnels, B. Nordén, M. Sjöström, B. Söderström, H. Wold and S. Wold, in A. Höskuldsen, K. Conradsen, B. Sloth Jensen and K. Esbensen (Eds.), Proc. Symposium i anvent statistik, NEUCC, RECAU and RECKU, Copenhagen, 1981, p. 183.
15 H. van der Voet, J. B. Hemel and P. M. J. Coenegracht, Anal. Chim. Acta, 192 (1987) 63.
16 D. Coomans, I. Broeckaert, M. Jonckheer and D. L. Massart, Meth. Inform. Med., 22 (1983) 93.
17 D. M. Titterington, G. D. Murray, L. S. Murray, J. D. F. Habbema and G. J. Gelpke, J. R. Statist. Soc. A, 144 (1981) 145.
18 J. Aitchison, J. D. F. Habbema and J. W. Kay, Appl. Statist., 26 (1977) 15.
19 S. Wold, C. Albano, W. J. Dunn III, U. Edlund, K. Esbensen, P. Geladi, S. Hellberg, E. Johansson, W. Lindberg and M. Sjöström, in B. R. Kowalski (Ed.), Chemometrics, Mathematics and Statistics in Chemistry, D. Reidel, Dordrecht, 1984, p. 74.
20 K. Varmuza, Pattern Recognition in Chemistry, Springer-Verlag, Berlin, 1980, p. 18.
21 P. A. Lachenbruch and M. R. Mickey, Technometrics, 10 (1968) 1.
22 P. A. Lachenbruch, Biometrics, 23 (1967) 639.
23 K. H. Drechsler and R. J. Blomer, in F. T. de Dombal and F. Grémy (Eds.), Decision Making and Medical Care: Can Information Science Help?, North-Holland, Amsterdam, 1976, p. 499.
24 S. J. Pöppl, in F. T. de Dombal and F. Grémy (Eds.), Decision Making and Medical Care: Can Information Science Help?, North-Holland, Amsterdam, 1976, p. 477.

25 B. Efron, Ann. Statist., 7 (1979) 1.
26 B. Efron and G. Gong, Am. Statist., 37 (1983) 36.
27 B. Efron, J. Am. Statist. Assoc., 78 (1983) 316.
28 D. Kahneman and A. Tversky, in D. Kahneman, P. Slovic and A. Tversky (Eds.), Judgment under Uncertainty: Heuristics and Biases, Cambridge University Press, 1982, p. 32.
29 S. Lichtenstein, B. Fischoff and L. D. Phillips, in D. Kahneman, P. Slovic and A. Tversky (Eds.), Judgment under Uncertainty: Heuristics and Biases, Cambridge University Press, 1982, p. 306.
30 J. D. F. Habbema, J. Hilden and B. Bjerregaard, Meth. Inform. Med., 20 (1981) 97.
31 J. D. F. Habbema, Anal. Chim. Acta, 150 (1983) 1.
32 J. Hermans, B. van Zomeren, J. W. Raatgever, P. J. Sterk and J. D. F. Habbema, Meth. Inform. Med., 20 (1981) 207.
33 G. Lindberg, Meth. Inform. Med., 20 (1981) 163.
34 G. W. Brier, Monthly Weather Rev., 75 (1950) 1.
35 A. H. Murphy and R. L. Winkler, J. Am. Statist. Assoc., 79 (1984) 489.
36 D. Coomans and D. L. Massart, Anal. Chim. Acta, 138 (1982) 167.
37 R. P. Brent, Collected Algorithms from CACM, 488-P1.
38 J. B. Hemel and H. van der Voet, Anal. Chim. Acta, 191 (1986) 33.
39 O. J. Dunn, Technometrics, 13 (1971) 345.
40 J. T. Page, Technometrics, 27 (1985) 189.
41 D. Coomans, Ph.D. thesis, Vrije Universiteit Brussel, 1982, p. 267.
42 W. E. Larimore and R. K. Mehra, Byte, October 1985, p. 167.

Analytica Chimica Acta, 191 (1986) 63—73
Elsevier Science Publishers B.V., Amsterdam — Printed in The Netherlands

NEW PROBABILISTIC VERSIONS OF THE SIMCA AND CLASSY CLASSIFICATION METHODS
Part 2. Practical Evaluation†

HILKO VAN DER VOET*[a] and PIERRE M. J. COENEGRACHT

Chemometrics Research Group, Pharmaceutical Laboratories, A. Deusinglaan 2, NL-9713 AW Groningen (The Netherlands)

JAN B. HEMEL

Central Laboratory for Clinical Chemistry, University Hospital, P.O. Box 30001, NL-9700 RB Groningen (The Netherlands)

(Received 27th March 1986)

SUMMARY

The new probabilistic versions of SIMCA and CLASSY described in Part 1 are evaluated. Their classification performance is found to be generally better than those of the old versions. The results are also compared with those of the ALLOC and SLDA classification methods. General over-confident behaviour of the new SIMCA and CLASSY methods as well as ALLOC and SLDA is noted for two of the three data sets investigated (Iris and two wine data sets).

DATA AND EVALUATION METHODS

The evaluation was done with the same three data sets as used for the evaluation of the old probabilistic versions [2]. The Iris data set contained two classes of 50 objects each, with four measured variables. The wine data set had two classes of respectively 21 (Bordeaux) and 19 (Bourgogne) objects, and 20 variables. The Wine-HS data set contained values for 11 variables measured on the same 40 objects by head-space gas chromatography.

All data sets were examined by the leave-one-out method (LOOM) for an almost unbiased evaluation of the predictive power [3, 4]. To provide suitable comparisons, the Iris data were also examined by splitting the data set into two subsets in the same way as in previous work (leave-half-the-data-out method) [2].

Four criteria were used to evaluate the results:

(1) The number of erroneously classified objects (NE) in the data set. Erroneous classification occurs if an object is assigned a higher probability in a class other than the one to which it actually belongs.

(2) The modified Brier score or quadratic score (Q_{31}). The range of Q_{31} is

†For Part 1 see ref. 1.

[a]Present address: Agricultural Statistics Department, TNO Institute of Applied Computer Science (iTi-TNO), PO Box 100, NL-6700 AC Wageningen, The Netherlands.

0003-2670/86/$03.50

[0,1] with 1 indicating the optimal result. This score was shown by Hilden et al. [5] to be a good criterion for the judgment of predictive ability. The choice of A that leads to the highest Q_{31} score will be termed the optimal class model dimensionality.

(3) The sharpness of the classification (Q_2). This measure states how close the assigned probabilities lie to the extremities of the probability scale (0 and 1). The range for Q_2 is the interval $[1/K, 1]$ with K as the number of classes. Q_2 can be regarded as measuring the self-confidence of the classification method. A sharpness 1, for instance, is obtained only when the classification method is absolutely confident of the correctness of its assignments, i.e., when the assigned probabilities are all 1 or 0. Previously [2], a pattern of increasing sharpness was found for higher values of A. This was not observed for the new algorithms. Probably the effect was due to inconsistencies in the old algorithms. In the present study, no other interesting features were disclosed by studying Q_2, thus the Q_2 values are not presented here.

(4) The reliability score (Q_5). This criterion measures whether the sharpness of the classifications accords with the predictive ability. If so, the classification is said to give reliable or calibrated predictions (Q_5 equals zero plus or minus some random fluctuation). If not, the classification method is either diffident (sharpness too low, Q_5 positive) or over-confident (sharpness too high compared with the predictive ability, Q_5 negative). Q_5 is standardized, so that the values plus and minus 1.96 can be used for testing the null hypothesis of reliability on a 5% unconfidence level.

A more elaborate discussion of these evaluation criteria and the formulae by which they are computed can be found elsewhere [5–7].

Computer programs

All calculations with respect to SIMCA, CLASSY and ALLOC were made with the CLAS program, written in PASCAL-6000 and running on the CDC CYBER 170/760 computer of Groningen State University [8]. CLAS contains options for an automatic leave-one-out evaluation and then applies several computational shortcuts, thereby greatly reducing the run time and increasing the practicability of this technique. For example, the run time for a SIMCA ($A = 2$) analysis of the wine data set (40 objects, 20 variables, 2 classes) is 0.55 s for a normal run and only 4.5 s for a complete leave-one-out evaluation. This is only about a fifth of the time that would be required for 40 separate leave-one-out runs ($40 \times 0.55 = 22$ s). The corresponding run times for CLASSY ($A = 2$) are 0.81 s and 8.3 s (which is only about a quarter of 40×0.81). A version of CLAS for microcomputers is in preparation.

Statistical Linear Discriminant Analysis (SLDA) was done with SPSS version 9 [9]. SLDA was applied in two variations: (1) with all available variables, and (2) with an automatic procedure for variable selection, provided in the SPSS program (METHOD = MINRESID). These methods will be indicated in the following as SLDA and SLDA (v.s.) respectively. With SPSS, the leave-one-out method was applied in a literal sense (including the variable selection procedure).

RESULTS

Iris data

The probabilistic SIMCA and CLASSY classification methods were evaluated with two kinds of scaling and with the class model dimensionality A varied between 0 and 4. ALLOC was applied with all four variables; this was previously found to be the optimal number of variables for this method [2]. The results of the leave-one-out evaluation are shown in Table 1 and Fig. 1.

When class autoscaling is applied to the data before the evaluation, the optimal dimensionality for SIMCA appears to be $A = 0$. The quadratic score Q_{31} is then 0.945 and the method is slightly over-confident ($Q_5 = -2.18$). Class modelling with 1 or 2 dimensions does not lower the discriminating performance much, but modelling with $A = 3$ or 4 is disastrous. For $A = 0$, the SIMCA and CLASSY methods are identical, because no IMS exists. CLASSY however improves its results when A is increased; the discriminating ability does not differ much for $A = 1$, 2, 3 or 4. The optimal method with class-scaled data is CLASSY ($A = 3$) with $Q_{31} = 0.971$. This method gives reliable probabilities ($Q_5 = 0.47$).

The four variables of the Iris data set all have the same units and all values are of the same order of magnitude. Therefore the most rational choice for data scaling seems to be to omit all scaling. When the data analysis is applied to the unscaled data, the results do not differ much from the previous ones. The optimal methods are now SIMCA ($A = 1$) with $Q_{31} = 0.946$ and $Q_5 = -0.57$ (reliable) and CLASSY ($A = 3$) with $Q_{31} = 0.972$ and $Q_5 = 0.29$ (reliable). It can be concluded that the type of scaling is not very important

TABLE 1

Evaluation of SIMCA, CLASSY and ALLOC applied on the Iris data (with the leave-one-out method)[a]

		NE		Q_{31}		Q_5	
		(n)	(c)	(n)	(c)	(n)	(c)
SIMCA	$A = 0$	12	7	0.919	0.945	−2.83	−2.18
	$A = 1$	7	8	0.946	0.941	−0.57	−0.68
	$A = 2$	7	8	0.945	0.938	−0.91	−2.49
	$A = 3$	16	20	0.896	0.873	+0.10	−1.30
	$A = 4$	33	31	0.798	0.803	−1.51	−1.44
CLASSY	$A = 0$	12	7	0.919	0.945	−2.83	−2.18
	$A = 1$	5	5	0.953	0.966	−1.76	−0.81
	$A = 2$	3	5	0.969	0.961	−0.63	−2.73
	$A = 3$	4	4	0.972	0.971	+0.29	+0.47
	$A = 4$	5	5	0.968	0.968	+0.32	+0.32
ALLOC		5	5	0.957	0.957	−1.17	−1.17

[a](n) no scaling applied; (c) class autoscaling applied.

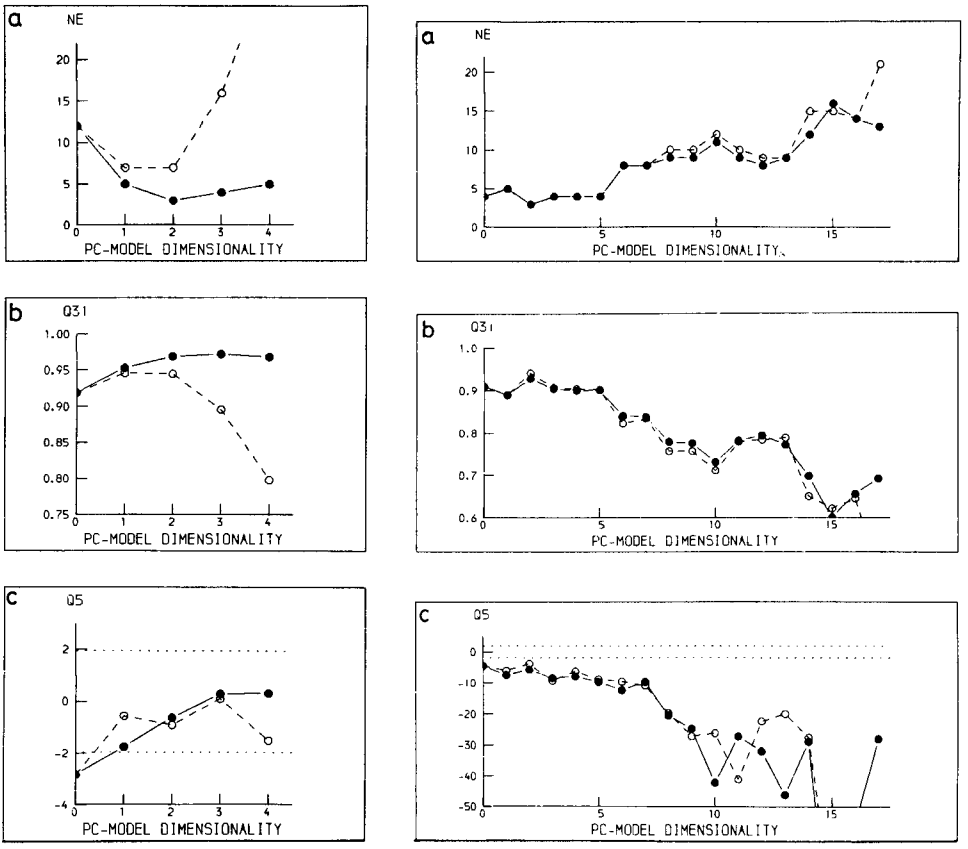

Fig. 1. Evaluation (leave-one-out method) of the unscaled Iris data for a varying number of PCs. Solid lines and symbols: CLASSY. Dashed lines and open symbols: probabilistic SIMCA. (a) NE, number of errors (out of 100); (b) Q_{31}, quadratic score; (c) Q_5, reliability score.

Fig. 2. Evaluation (leave-one-out method) of the class-scaled wine data for a varying number of PCs. Lines and symbols as in Fig. 1; (a) NE, number of errors (out of 40); (b) Q_{31}, quadratic score; (c) Q_5, reliability score.

for the Iris data. The method ALLOC is invariant under scaling and gives $Q_{31} = 0.957$ and $Q_5 = -1.17$.

A comparison between the three best methods is shown in Table 2. This comparison was done with paired t-tests on the individual Q_{31} values [2, 10]. CLASSY ($A = 3$, no scaling) is seen to have a significantly better discriminating performance than SIMCA ($A = 1$, no scaling). ALLOC falls between the two other methods, but differences were not significant. In conclusion, for the Iris data set, CLASSY (and perhaps also ALLOC) seems to perform better than SIMCA.

To compare the old and new probabilistic algorithms, evaluation was also done with a somewhat cruder cross-validation technique, the leave-half-the-

TABLE 2

Paired comparisons between the best SIMCA, CLASSY and ALLOC models in the leave-one-out evaluation of the Iris data

Method A	Method B	Mean dQ_{31} = $Q_{31}(B) - Q_{31}(A)$	Difference between A and B
SIMCA (A = 1) no scaling	CLASSY (A = 3) no scaling	0.026	Significant ($p \approx 0.02$)
SIMCA (A = 1) no scaling	ALLOC (4 variables)	0.011	Not significant ($p \approx 0.50$)
ALLOC (4 variables)	CLASSY (A = 3) no scaling	0.015	Not significant ($p \approx 0.14$)

data-out method, which was also used earlier [2]. The results in Table 3 indicate that the theoretical superiority of the new algorithms is only shown for A = 1. For higher class dimensionalities, no significant differences were observed.

Wine data

No less than 39 classification methods were applied to this data set: probabilistic SIMCA and CLASSY with class dimensionalities varied between A = 0 and A = 17, and in addition ALLOC and two versions of SLDA (full variable model and a model with an automatic variable selection). The results are presented in Table 4 and Fig. 2.

The differences between the results of the old and new algorithms of SIMCA and CLASSY are very large. SIMCA, which formerly attained a maximal quadratic score of 0.893 at A = 5 now has Q_{31} = 0.941 at A = 2. For CLASSY, there is almost no difference in the optimal quadratic score (0.928 for the new algorithm against 0.932 for the old version), but this maximum is attained at a much lower dimensionality of the class models (A = 2 instead of A = 10). In fact, as can be seen from Fig. 2, SIMCA and CLASSY now give almost identical results with an optimal predictive ability for low values of the class dimensionality (A = 0—5). The reliability analysis of the wine data gives somewhat embarrassing results: all methods are found to be over-confident, i.e., they make too sharp predictions. This over-confidence was moderate for ALLOC, SLDA (v.s.), and SIMCA and CLASSY with low dimensionalities (A = 0—7). SIMCA and CLASSY with $A > 7$ and SLDA without variable selection gave far more over-confident results.

Although the quadratic scores of SIMCA (A = 2), ALLOC and CLASSY (A = 2) were much higher than that of SLDA and SLDA (v.s.), none of the pairwise comparisons proved significant. An explanation for this is that different wines are misclassified by the different methods. Table 5 shows which wines are misclassified by ALLOC, SLDA, SLDA (v.s.) and the optimal SIMCA and CLASSY methods. It can be seen, for instance, that wines 16 and 37 are classified correctly by SLDA but wrongly by SIMCA and CLASSY

TABLE 3

Evaluation of SIMCA, CLASSY and ALLOC applied on the unscaled Iris data (using the leave-half-the-data-out method)[a]

		NE		Q_{31}	
		Old	New	Old	New
SIMCA	$A = 1$	5	5	0.936	0.953
	$A = 2$	2	7	0.951	0.949
	$A = 3$	14	13	0.882	0.906
	$A = 4$		25		0.874
CLASSY	$A = 1$	8	5	0.939	0.962
	$A = 2$	6	4	0.969	0.968
	$A = 3$	4	5	0.976	0.964
	$A = 4$	5	5	0.964	0.964
ALLOC		4		0.964	

[a]Old, result of old algorithms [2]; new, result of new algorithms [1].

TABLE 4

Evaluation of SIMCA, CLASSY, ALLOC and SLDA applied to the wine data (with the leave-one-out method). The results from the old algorithms of SIMCA and CLASSY are given in parentheses

	NE		Q_{31}		Q_5	
	SIMCA	CLASSY	SIMCA	CLASSY	SIMCA	CLASSY
$A = 0$	4	4	0.910	0.910	−4.49	−4.49
$A = 1$	5(5)	5(5)	0.890(0.838)	0.890(0.848)	−6.02(2.96)	−7.43(1.40)
$A = 2$	3(3)	3(9)	0.941(0.864)	0.928(0.818)	−3.79(3.00)	−5.73(0.06)
$A = 3$	4(4)	4(8)	0.907(0.875)	0.904(0.843)	−9.30(2.84)	−8.36(0.21)
$A = 4$	4(5)	4(10)	0.904(0.873)	0.900(0.855)	−6.21(2.53)	−7.88(0.27)
$A = 5$	4(4)	4(9)	0.902(0.893)	0.901(0.856)	−8.85(2.10)	−9.65(0.69)
$A = 6$	8(7)	8(4)	0.823(0.866)	0.841(0.928)	−9.52(1.71)	−12.4(1.34)
$A = 7$	8(4)	8(4)	0.834(0.883)	0.838(0.915)	−10.8(1.83)	−9.65(0.15)
$A = 8$	10(5)	9(4)	0.757(0.884)	0.779(0.921)	−19.6(1.55)	−20.4(−0.40)
$A = 9$	10(8)	9(4)	0.757(0.885)	0.776(0.925)	−27.1(0.86)	−24.8(−0.94)
$A = 10$	12(8)	11(3)	0.711(0.869)	0.731(0.932)	−26.2(−0.20)	−42.1(−1.13)
$A = 11$	10(9)	9(6)	0.780(0.849)	0.782(0.903)	−41.0(−2.10)	−27.1(−2.25)
$A = 12$	9(10)	8(8)	0.784(0.779)	0.794(0.843)	−22.3(−6.55)	−31.9(−7.00)
$A = 13$	9(10)	9(8)	0.789(0.770)	0.772(0.834)	−19.9(−8.26)	−46.0(−10.5)
$A = 14$	15(8)	12(8)	0.651(0.820)	0.698(0.830)	−27.5(−7.79)	−28.9(−14.7)
$A = 15$	15(8)	16(8)	0.622(0.826)	0.601(0.814)	−80.2(−7.55)	−99.1(−22.3)
$A = 16$	14(16)	14(15)	0.645(0.639)	0.656(0.685)	−114(−21.9)	−55.2(−21.0)
$A = 17$	21(7)	13(15)	0.475(0.826)	0.692(0.639)	−189(−20.8)	−27.9(−84.4)
ALLOC	2		0.933		−2.19	
SLDA						
all var.	5		0.870		−15.5	
var. sel.	6		0.879		−5.49	

TABLE 5

Index numbers of the misclassified objects from the wine data set

Method	Misclassified wines index numbers	Q_{31}	Q_s
SIMCA (A = 2)	16, 22, 37	0.941	−3.79
CLASSY (A = 2)	16, 22, 37	0.928	−5.73
ALLOC	16, 30	0.933	−2.19
SLDA	5, 12, 22, 24, 26	0.870	−15.5
SLDA (v.s.)	5, 8, 12, 22, 24, 26	0.879	−5.49

(and wine 16 is also misclassified by ALLOC). Wines 5, 12, 24 and 26 cause problems for both varieties of SLDA, but not for the other methods.

Wine-HS data

The classification techniques applied to this data set were SIMCA and CLASSY with class dimensionalities varied between A = 0 and A = 11, ALLOC, and again two versions of SLDA (full variable model and a model with an automatic variable selection). The results are presented in Table 6 and Fig. 3. The differences between the old and new algorithms of SIMCA and CLASSY are not as large as those observed for the wine data, but generally the new algorithms still have a higher predictive ability. The optimum found for SIMCA increases somewhat (Q_{31} = 0.950 at A = 3 against Q_{31} = 0.943 at A = 2 with the old method) and the optimum for CLASSY decreases slightly (Q_{31} = 0.968 at A = 10 against Q_{31} = 0.975 with the old method). At lower values of class dimensionality, however, there is a clear tendency to better performance of both methods.

Comparison of the new SIMCA and CLASSY algorithms with the other methods shows that all methods have about equal predictive abilities. None of the pairwise comparisons made between the methods in Table 7 resulted in significant differences. In the previous study [2], it was concluded that there were no really important differences between SIMCA, CLASSY and ALLOC, and this conclusion can now be extended to the new SIMCA and CLASSY algorithms and to SLDA. It should be noted, however, that this conclusion pertains to the general characteristics of the classification methods, but not to the individual classifications (see the indices of the misclassified objects in Table 7).

The reliability statistic Q_5 is again always negative, which indicates an overconfident behaviour of all the investigated methods.

DISCUSSION

The main motivation for this research was to formulate new (and better) algorithms for probabilistic classification methods. Only probabilistic methods

TABLE 6

Evaluation of SIMCA, CLASSY, ALLOC and SLDA applied to the wine-HS data (with the leave-one-out method). The results from the old algorithms of SIMCA and CLASSY are given in parentheses

	NE		Q_{31}		Q_5	
	SIMCA	CLASSY	SIMCA	CLASSY	SIMCA	CLASSY
$A = 0$	3	3	0.930	0.930	−9.29	−9.29
$A = 1$	2(3)	2(2)	0.946(0.937)	0.948(0.949)	−15.6(1.74)	−8.85(1.56
$A = 2$	2(3)	2(3)	0.950(0.943)	0.950(0.944)	−8.06(1.58)	−7.52(0.56
$A = 3$	2(4)	2(4)	0.950(0.942)	0.950(0.920)	−6.15(1.15)	−10.7(−2.2(
$A = 4$	2(4)	2(3)	0.948(0.943)	0.950(0.939)	−6.20(1.04)	−8.85(−1.(
$A = 5$	2(3)	3(3)	0.948(0.930)	0.926(0.940)	−3.53(0.01)	−6.75(−2.1
$A = 6$	3(3)	3(2)	0.930(0.925)	0.938(0.938)	−9.80(−1.31)	−5.25(−3.3
$A = 7$	3(4)	2(3)	0.934(0.915)	0.949(0.931)	−8.73(−2.76)	−4.73(−5.8
$A = 8$	5(4)	2(3)	0.885(0.894)	0.953(0.922)	−10.4(−4.75)	−4.35(−12
$A = 9$	6(12)	2(3)	0.887(0.772)	0.967(0.929)	−10.2(−9.26)	−5.00(−8.2
$A = 10$	5(14)	2(1)	0.884(0.693)	0.968(0.975)	−8.02(−17.1)	−4.72(−2.(
$A = 11$	6	3(2)	0.868	0.940(0.950)	−9.59	−12.6(−5.32
ALLOC	2		0.950		−4.85	
SLDA						
all var.	3		0.946		−3.44	
var. sel.	3		0.954		−4.57	

were considered because the availability of posterior probabilities is so essential in many applications of multivariate classification. Examples are medical diagnosis (e.g., the probability for a patient with data vector $\mathbf{X}_i$ to have disease c) and the detection of falsifications in food chemistry (e.g., the probability for a wine with data vector $\mathbf{X}_i$ to originate from region c). In these and many other instances, a simple all-or-nothing classification would not be detailed enough.

It is important to distinguish between the two aspects of performance, predictive ability on the one hand and reliability on the other. The former was evaluated by using the number of errors (NE) and the modified quadratic score (Q_{31}) and the latter by using the standardized reliability score (Q_5). The evaluation of reliability involves some problems; over-confidence is observed in almost every situation. This is true not only for the present results but also for earlier results [6, 11]. Hilden et al. [6] reported that interdependence between variables tends to make the results of the Bayes' classification algorithm (which supposes independence) over-confident. Currently, a simulation study is being done to establish more fundamental reasons why over-confidence is so often observed.

A more important aspect of performance is predictive ability. The new algorithms for SIMCA and CLASSY generally have a higher predictive ability than their predecessors, at least for low dimensionalities of the class models.

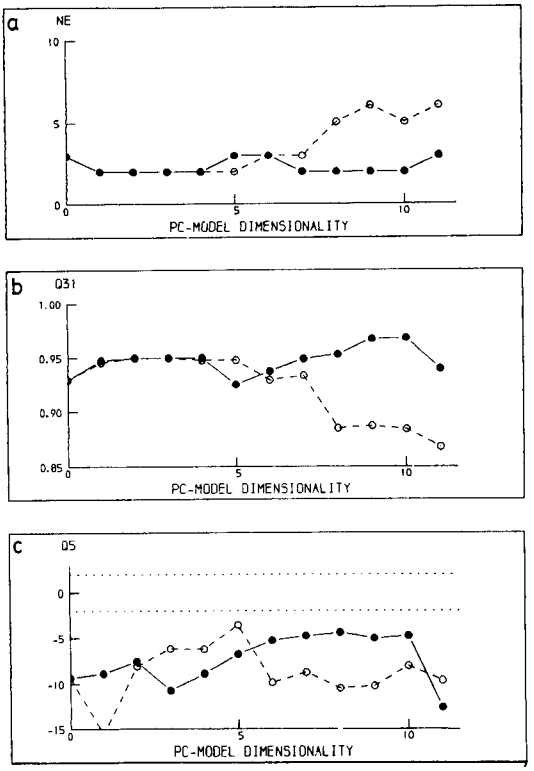

Fig. 3. Evaluation (leave-one-out method) of the class-scaled wine-HS data for a varying number of PCs. Solid lines and symbols: CLASSY. Dashed lines and open symbols: probabilistic SIMCA. (a) NE: number of errors (out of 40); (b) Q_{31}: quadratic score; (c) Q_5: reliability score.

TABLE 7

Index numbers of the misclassified objects from the wine-HS data set

Method	Misclassified wines index numbers	Q_{31}	Q_5
SIMCA (A = 3)	30, 35	0.950	−6.15
CLASSY (A = 10)	23, 35	0.968	−4.72
ALLOC	30, 35	0.950	−4.85
SLDA	1, 22, 35	0.946	−3.44
SLDA (v.s.)	1, 22, 35	0.954	−4.57

For SIMCA, the improvement is very clear (at least for the wine and wine-HS data), while the main effect on the CLASSY results is a shift of the optimum to lower values of A. This is not surprising because the improvements were chiefly made in the OMS part of the classification rule, thus strengthening

SIMCA as well as the OMS part of CLASSY. This OMS part plays a predominant role at low PC model dimensionalities, while the IMS part causes CLASSY to act more like ALLOC at high dimensionalities.

The question may be asked: if the superiority of CLASSY with respect to SIMCA, which was found previously, also applies to the new algorithms. The answer is generally no: SIMCA and CLASSY appear to perform about equally well as long as the chosen class dimensionality is at least 3 or 4 less than the number of variables. In fact, the results are similar for low values of A. This suggests that in these cases the OMS densities are important while the IMS densities contribute little to the result. This means that the extra sophistication of the CLASSY method turns out to be a mainly theoretical advantage for data sets such as the wine data. When A, the number of PCs, is chosen close to p, the total number of variables, the dimensionality of the OMS becomes small. This explains why SIMCA, which works mainly with OMS densities, produces low predictive abilities in these cases. In practice, this means that SIMCA has problems with low-dimensional data sets, such as the Iris set. In this four-dimensional case, CLASSY attained a significantly higher quadratic score, Q_{31}, than SIMCA.

The probabilistic SIMCA and CLASSY methods must also be compared with the other investigated methods. For this purpose the best results from SIMCA and CLASSY are compared to the results from ALLOC, SLDA and SLDA (v.s.). It should be noted that some bias in favour of SIMCA and CLASSY is introduced in this way, because it is not clear that an automatic procedure for selecting A would produce the same choice. However, such an automatic procedure would be able to improve the results by selecting different values of A for the diverse class models, a possibility not considered here. Work on the inclusion of Horn's method [12] for automatically selecting the number of PCs is in progress.

On average, all investigated methods show only small variations in predictive power, although the results for individual objects may be quite different. The only exception with respect to the average behaviour was SLDA (both with and without variable selection) which produced more errors than the other methods when applied to the wine data (see Table 5). But even in this case the difference could not be proved significant because of the large differences in the classifications of the individual objects. As an example, consider an object i that is misclassified by two methods and an object ii misclassified by only one of these methods; i's contribution to Q_{31} is low for both methods so the difference dQ_{31} for this object also tends to be small. Yet dQ_{31} tends to be large for ii, because for this object it is the difference between a relatively high and a relatively low Q_{31} value. In this way, the distribution of all individual differences dQ_{31} becomes diffuse, thereby reducing the statistical significance of the average difference in Q_{31} between the two methods.

It seems that the choice of a classification method can have a large impact on the result for one particular object but that for each method there will be

some difficult type of individuals. For example, objects that are relatively distant from training objects of the same class, but close to training objects from another class, will present difficulties for ALLOC, while SLDA will tend to misclassify objects that violate the assumptions of normality or equal class covariance-structure.

Conclusions

The main points emerging from this study can be summarized as follows. The new algorithms for probabilistic SIMCA and CLASSY have generally a better predictive ability than previous versions. With the new algorithms CLASSY only improves on the SIMCA results if there are few variables in the data set. There are only small differences between the investigated classification methods if their average performances are considered. For any particular object, however, the assigned probabilities can depend very much on the chosen technique. Finally, it is concluded that the situation with respect to evaluation of reliability is unsatisfactory. Over-confidence seems to be unavoidable in many situations. Further theoretical and empirical research on this topic is needed.

REFERENCES

1 H. van der Voet, J. B. Hemel and P. M. J. Coenegracht, Anal. Chim. Acta, 192 (1987) 63.
2 H. van der Voet and D. A. Doornbos, Anal. Chim. Acta, 161 (1984) 125.
3 P. A. Lachenbruch, Biometrics, 23 (1967) 639.
4 S. M. Snapinn and J. D. Knoke, Technometrics, 26 (1984) 371.
5 J. Hilden, J. D. F. Habbema and B. Bjerregaard, Meth. Inf. Med., 17 (1978) 238.
6 J. Hilden, J. D. F. Habbema and B. Bjerregaard, Meth. Inf. Med., 17 (1978) 227.
7 H. van der Voet and D. A. Doornbos, Anal. Chim. Acta, 161 (1984) 115.
8 J. B. Hemel and H. van der Voet, Anal. Chim. Acta, 191 (1986) 33.
9 N. H. Nie, C. H. Hull, J. G. Jenkins, K. Steinbrenner and D. H. Bent, SPSS: Statistical Package for the Social Sciences, 2nd edn., McGraw-Hill, New York, 1975.
10 J. Hilden and J. D. F. Habbema, in A. Alpérovitch, F. T. de Dombal and F. Grémy (Eds.), Evaluation of Efficacy of Medical Action, North-Holland, Amsterdam, 1979, p. 123.
11 J. Hilden and B. Bjerregaard, in F. T. de Dombal and F. Grémy (Eds.), Decision Making and Medical Care: Can Information Science Help?, North-Holland, Amsterdam, 1976, p. 365.
12 P. E. Green, Analyzing Multivariate Data, The Dryden Press, Hinsdale, IL, 1978, p. 366.

Analytica Chimica Acta, 191 (1986) 75—85
Elsevier Science Publishers B.V., Amsterdam — Printed in The Netherlands

THE UTILITY OF CORRESPONDENCE FACTOR ANALYSIS FOR MAKING DECISIONS FROM CHEMICAL DATA

MAX FEINBERG

Centre Informatique sur la Qualité des Aliments, 16 Rue Claude-Bernard, 75231 Paris Cedex 05 (France)

(Received 27th May 1986)

SUMMARY

Multivariate analysis is now conventional for data treatment. Available methods are classified according to the purpose of the study (prediction, decision making, clustering, classification) and the types of variable (the nature of the information) available. These aspects must be considered simultaneously. Within that frame, correspondence factor analysis (CFA) is proposed as a suitable method for handling categorial variables (qualitative or semiquantitative information) and descriptive decision-making (symmetry between lines and columns). The theoretical principles of CFA are outlined. The utility of CFA is illustrated by three examples: a complex sampling design related to use of sewage sludge, assessment of the selectivity of insect behaviour towards chemical products in trees, and an environmental study of mercury contamination of freshwater fish.

Multivariate factor analysis is now a conventional tool for examining chemical data. Several methods are available and new methods are published regularly by statisticians. They are often wrongly proposed as multi-purpose tools for data analysis, and chemists must themselves establish the correct conditions for applications to analytical data. Thus, it seems useful to suggest some rules for the selection of methods appropriate to the nature of the information, in order to avoid misinterpretation of results. The aim is to provide recommendations for classification based on the nature of the descriptors and on the goals to be attained.

In many ways, analytical chemists are decision-makers. Thus, decision-making is emphasized here and a factor analysis technique in accord with this target, correspondence factor analysis (CFA) [1], is considered. Several examples will be used for illustration.

VARIABLES AND MULTIVARIATE METHODS

Classification of multivariate methods can be based on two considerations: the nature of the information or the types of variables used to describe it; and the purpose of the study or the model proposed for structuring the data.

Six types of variables can be defined. Binary variables can take only two values, e.g., yes/no or 0/1. Second, ordered classes take n numeric or alphanu-

0003-2670/86/$03.50

TABLE 1

Transformation of one continuous variable to three binary variables

Continuous	Discrete	Ordered class	Class names	Three binary variables		
				High	Medium	Low
13.7	14	3	High	1	0	0
13.4	13	3		1	0	0
12.9	13	3		1	0	0
12.9	13	3		1	0	0
11.5	11	2	Medium	0	1	0
10.8	11	2		0	1	0
8.5	8	2		0	1	0
7.9	8	2		0	1	0
6.4	6	1	Low	0	0	1
3.2	3	1		0	0	1
3.1	3	1		0	0	1

meric values (e.g., low, medium and high, or grade 1, grade 2, etc.); the class names can be recoded as single integer variables. Third, unordered classes are used when there is no class hierarchy, such as different catalysts or chromatographic columns used in an experiment; these classes can be recoded as binary variables, one variable for each class (see Table 1). Fourth, integer or discrete variables take only numeric values, such as counts or dial settings. Fifth, continuous variables, which are the commonest, are used for chemical or physical measures. Sixth, there is the rank variable which is used for non-parametric statistical methods; but few examples of multivariate methods based on rank variables have been reported [2].

In large data sets, several types of variable may be encountered; it may then be necessary to transform some variables in order to obtain a homogeneous data table. This transformation can be done from the continuous type down to the binary type as indicated in Table 1. The reverse sequential transformation is usually impossible. Unfortunately, a given statistical method will not be able to process all kinds of variables. For instance, unordered class variables are not suited to principal components analysis. Therefore, the types of variable in the problem already limits the choice of method.

Multivariate methods

Four different types of problem can be tackled by multivariate study. Each of them corresponds to a model which is a description of the underlying structure of the data matrix. To describe these models, the data base **X** is assumed to contain n lines and p columns which can be split into, respectively, $k1$ and $k2$ subsets. The problems are as follows.

Prediction. A predictive quantitative relationship is fitted between one variable and others or among several groups of variables. This can be called the $n,p+1$ or $n,k2$ model.

Decision-making. A qualitative description of the relationships between variables and/or observations is sought. The decision will arise from a compromise between these relationships. This can be termed the n, p model as lines and columns are considered in the same way.

Grouping (or unsupervised learning). Clusters of similar observations are formed in order to define homogeneous groups from the data table. This is the (?), p model as the number of observation clusters is unknown.

Discrimination (or supervised learning). New observations are assigned to one or more predefined classes after computation of a membership probability. A previous learning procedure is necessary in order to obtain the discriminatory functions used to compute this membership probability. This is the $k1$, p model.

But it is usually impossible to achieve these different purposes directly with one statistical method. Table 2 is an attempt to classify some of the conventional methods according to the object of the work. Moreover, some methods only accept continuous variables, and sometimes distributional assumptions, such as normality, are necessary (Table 3). Thus, guidelines for method selection can be defined by correlating the variable types and the purpose of the study.

From these definitions, correspondence factorial analysis (CFA) or its derivative, multiple correspondence factorial analysis (MCFA), can be classed as good decision-making aids suitable for class or binary variables. As will be seen, they give no possibility for prediction, describing only the correspondences between the lines and the columns of the data table.

TABLE 2

Purposes attained depending on the selected multivariate method

Model	Methods	Purpose[a]			
		P	D	G	C
$n, p+1$	Multiple regression	+++	+	—	—
	Regression on principal components	+++	—	—	—
$n, k2$	Canonical correlation	++	++	—	—
	Partial least-squares	+++	+	—	—
n, p	Correspondence factor analysis	—	+++	+	—
	Principal component analysis	—	++	+	—
	Factor analysis	—	++	+	—
$n, k2$	Multiple correspondence factor analysis	—	+++	+	—
$k1, p$	Linear and factorial discriminant analysis	—	+	—	+++
	SIMCA, ALLOC	—	+	—	+++
(?), p	Partitioning classification	—	—	+++	—
	Hierarchical classification	—	—	+++	—

[a]P, prediction; D, description for decision-making; G, clustering of groups; C, classification.

TABLE 3

Multivariate methods and suitable types of variable

Methods	Types[a]			
	C	O	U	B
Multiple regression (MR)	+	+	—	—
Regression on principal components	+	—	—	—
Canonical correlation (CC)	+	—	—	—
Partial least-squares (PLS)	+	+	—	—
Correspondence factor analysis (CFA)	—	+	+	+
Principal component analysis (PCA)	+	—	—	—
Factor analysis (FA)	+	+	—	—
Multiple correspondence factor analysis (MCFA)	—	+	+	+
Linear and factorial discriminant (LDA)	+	+	—	—
SIMCA, ALLOC	+	—	—	—
Partitioning classification	+	—	—	—
Hierarchical classification (HC)	+	—	—	—

[a]C, Continuous; U, unordered class; O, ordered class; B, binary

This point is made clear from the background of CFA and MCFA, which were specially developed to deal with binary or class variables and were initially designed for use in marketing studies or opinion polls. They can also be applied successfully for exploring chemical information and will be adequate for solving many analytical problems. Given that a preliminary recoding of continuous variables to class variables, which may cause some loss of information, is a prerequisite for their application to analytical measurements, it is surprising how efficient these methods can be.

CORRESPONDENCE FACTOR ANALYSIS

The data table needed for CFA consists of class or binary variables. It is usually a frequency table; for instance, each cell could contain the number of peaks obtained from several experiments (lines) corresponding to different chromatographic conditions (columns), or the number of satisfactory results obtained by laboratories participating in interlaboratory studies. In fact, lines and columns can be transposed without changing the results.

The starting point of the numerical procedure is to compute a contingency table, i.e., a k-way table containing the relative frequencies of each cell (Fig. 1A).

This constraint explains the theoretical obligation to have class variables. Therefore, the words "observation" and "variable" common to other multivariate methods become meaningless; the terms "line-pattern" and "column-pattern" are preferred. It is clear that their roles are perfectly symmetrical. The contingency table can then be transformed to two distance tables computed either between line-patterns or column-patterns. When line-patterns are

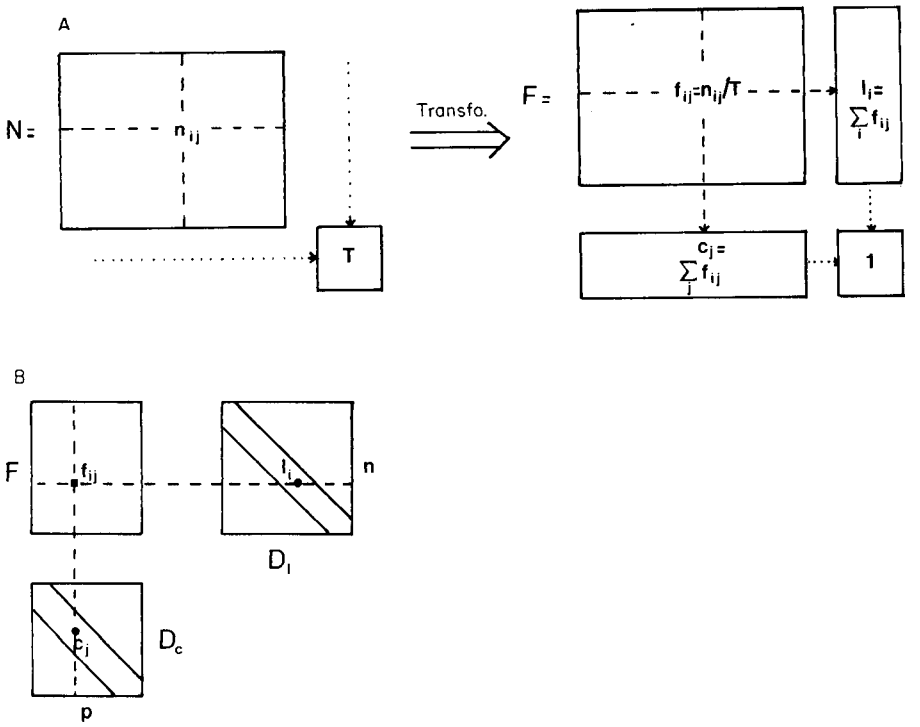

Fig. 1. Theoretical background of CFA. (A) Transformation of raw frequencies (n_{ij}) to relative frequencies. (B) Computation of χ^2 distance tables for lines and columns.

considered, a distance weighted by the sum of each column-pattern is used instead of the Euclidian distance in order to emphasize the role of the smallest column-populations. The role of this weight will be even more emphasized by squaring. Thus:

$$d^2_{1;2} = \sum_j (1/c_j)\,[(f_{1j}/l_1) - (f_{2j}/l_2)]^2$$

$$d^2_{1;2} = \sum_i (1/l_i)\,[(f_{i1}/c_1) - (f_{i2}/c_2)]^2$$

In the end, a generalized χ^2 distance table for line-patterns or column-patterns (Fig. 1B) is obtained. Eigenvalues and eigenvectors are extracted from this table in order to compute the projections of the line-patterns in a new factor space which minimizes the dispersion. It can be demonstrated that the χ^2 table for column-patterns has the same eigenvalues (except $n - p$ which are zero), and therefore line-patterns and column-patterns can be graphically represented on the same factor space as follows.

Given $Y = D_l^{-1}\, F\, D_c^{-1/2}$ with U eigenvectors of Y, $P_l = D_l^{-1}\, F\, D_c^{-1/2}\, U$. Symmetrically $P_c = D_c^{-1}\, F'\, D_l^{-1/2}\, V$. As U and V have the same eigenvalues, except for $(n - p)$ for V, if $n \geqslant p$. Thus $P_c = D_c^{-1}\, F'\, P_1 D_\lambda^{-1/2}$ with $\mathrm{tr}(V) = \chi^2_{(n-1)(p-1)}$.

One of the most interesting features of the method is that proximities between line- and column-patterns can be interpreted as similarities. The χ^2 tables present other interesting features: (a) the first eigenvalue is zero, corresponding to the loss of one dimension caused by weighting, and this implies that a special subroutine for eigenvalue extraction can be used in the software; (b) all eigenvalues are between 0 and 1; (c) the total dispersion of points (line- or column-patterns) around the centroid is equal to the global χ^2 of the table and can be used to test the independence of lines or columns. However, this test is meaningless if the variables are recoded continuous variables. More details about computations have been given [1, 2] and an extensive literature survey is available [3].

This method has also been developed in a multiple mode (MCFA), which is applied when columns can be split into several subsets. The analysis is then performed on each group followed by a canonical analysis of paired blocks of columns. Most available software allows the user to add supplementary columns or lines; these are not processed for the extraction of eigenvectors but their projections are computed. This scheme is very similar to the splitting of data base into training and prediction sets in pattern recognition.

Many CFA or MCFA have been applied in this laboratory. Some examples will give a better idea of their possible applications.

Preparation of a sampling design

The preparation of a sampling design is always difficult, as it can usually be optimized only at the end of the study. This particular study was concerned with the effects of repeated applications of sewage sludges to soils as fertilizer, and evaluation of the transfer of heavy metals from soil to plants. Before chemical analysis was started, it was necessary to select several sampling points representative of various historical, agricultural and soil conditions.

A questionnaire was given to 40 farmers concerning the history of about 100 fields where sewage sludges were used as fertilizer. For each field (line), information was obtained about the nature of the sludges used, the quantities, the years of spreading, the subsequent crop, and about the physical or chemical status (when available) of the soil (columns). All variables were homogenized to binary variables and recoded if necessary. Separate CFAs were performed for each kind of crop (e.g., corn, wheat, peas or sugar beet), as separate studies were planned.

A projection of line- and column-points was thus obtained on the two first factors, but the main interest lay in the spread of the fields (Fig. 2). From the several clusters observed, sampling points were selected so that varied situations would be represented. Altogether 40 interesting sampling points were kept for use in a complete chemical study. The study proved to be satisfactory and will be published elsewhere.

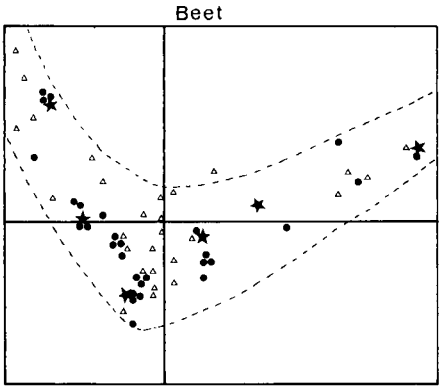

Fig. 2. Projections of the field samples relevant to sugar-beet (black symbols) and the descriptive variables (open triangles). The selected fields are marked by stars.

Description of the selectivity of insect behaviour

Certain species of insects (Scolytidae) devastate millions of hectares of trees (conifers) each year, being attracted by terpenes in the essential oils of the trees. The selectivity of this attraction for a given species of insect had to be confirmed in order to establish the chemical nature of the terpenes or terpene mixture present in the essential oil [4]. The data table consisted of the results of attraction tests for 9 insect species, belonging to 6 genus, performed on 10 tree species from 4 genus (Pinus, Cupressus, Abies and Picea). Each test was repeated three times on paired tree logs (i.e., 45 combinations); altogether 1215 sets of counts were obtained for the numbers of insects attracted by the first log and the second log and of those not attracted. The raw data table thus had 45 × 3 lines and 9 × 3 columns. The CFA on these data demonstrated the good repeatability of tests and the selectivity of the attraction. Some species attacked only one tree genus, e.g., Phloesinus on Cupressus, but others were less selective, as shown in Fig. 3.

In the subsequent study, the essential oils were determined by g.c./m.s. and the data were processed by cluster analysis. It should eventually be possible to indicate which terpenes are responsible for attracting a given insect genus. However, the analytical procedure itself is rather difficult as several extraction methods are necessary, and only some results are accessible [4].

Evaluation of an environmental pollution

This example is the most complex [5]. It relates to a study of the mercury pollution of rivers in the Alsace region, including the Rivers Rhine and Ill, which joins the Rhine near Strasbourg. Fish were used as biological pollution indicators, as it is very difficult to obtain consistent results from water or sediment samples. About 1500 fish samples were examined over a 5-year period after dissecting the muscle, gills, liver and kidney. As is usual for such expensive studies, several aims were proposed: (a) to map pollution from the

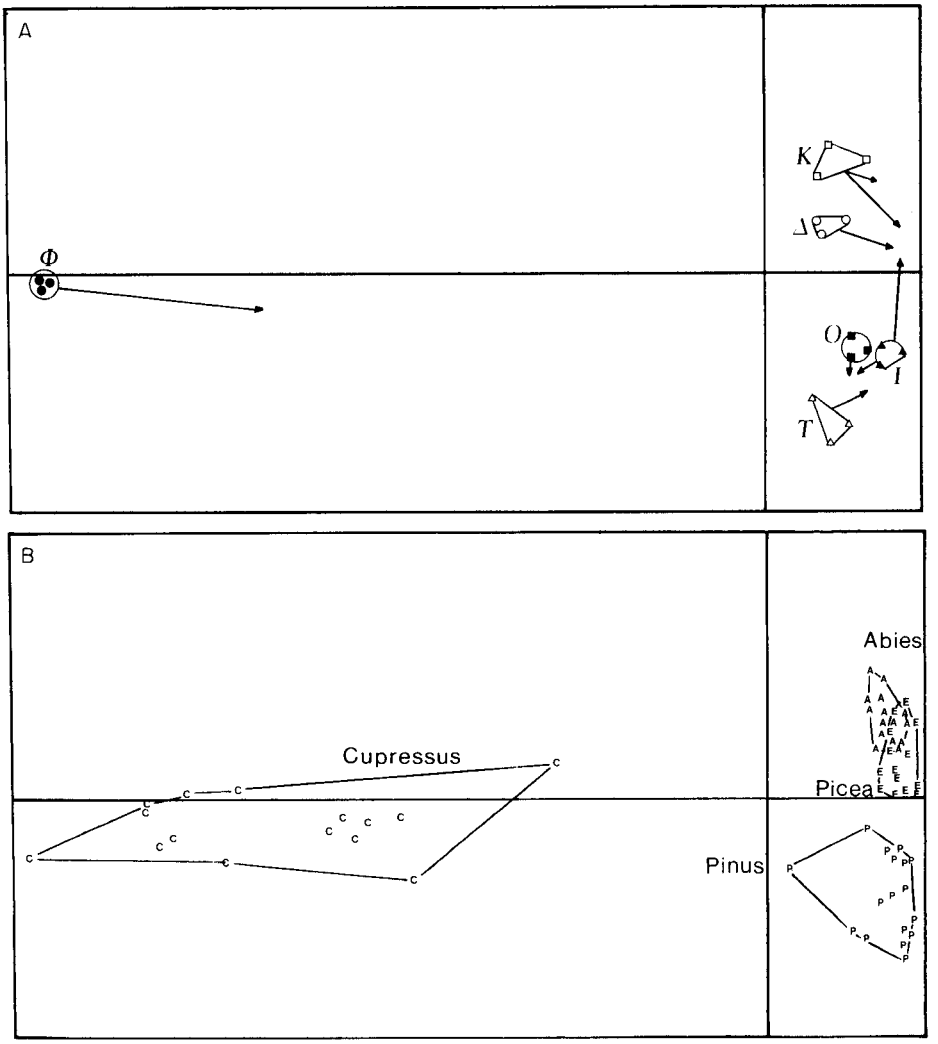

Fig. 3. Projections of insects and trees on two first factors. Arrows represent the selectivity of attraction, which was obtained by considering the proximities of clusters in the 3-factor space. Insects: (K) Cryphalus; (Δ) Dendroctomus; (I) Ips; (O) Orthomicus; (T) Tomicus; (Φ) Phloesinus. Trees: (P) Pinus; (C) Cupressus; (A) Abies; (E) Picea.

results observed at about 30 sampling stations; (b) to detect any decrease of pollution during the study period following new regulations on the industrial use of mercury; and (c) to check bio-accumulation of mercury depending on the trophic level of the varied fish species collected (about 15 species).

One of the greatest difficulties for such studies is the interaction between pollution mechanisms. For instance, mercury contamination of fish muscle depends not only on a pollution source being in the vicinity of a sampling

station, but also on the weight (or age) of the fish and on its feeding behaviour or trophic level (predators are more polluted than herbivores). The double weighting of χ^2 distance is a good way to take this complexity into account. MCFA was a possibility, as no model was available for a covariance analysis of the data.

Multiple CFA gave interesting results as it was done after the quantitative variables (concentrations and fish weight) had been coded to ordered class variables. Distributions were strongly skewed and a preliminary log transformation of quantitative data was used. Figure 4 shows a global MCFA of all available information from the study. The projections of the year variable indicate that the decrease of pollution was very poor despite the mercury regulations; this can be interpreted as a buffering effect of sediments. The correlation between muscle and gill contents also confirmed this hypothesis, as direct contact of gills with water or sediment enhances the contamination of animals; this was substantiated by the poor discrimination of fish species in all trophic levels.

The results shown in Fig. 5 concern only the five stations located on the river Ill, which is the main tributary of the Rhine in France. All the important cities and industrial plants in the region are situated along this river. Mapping of pollution according to station proved the efficiency of the water treatment plant located in Strasbourg, as the pollution level dramatically decreased downstream of this city. A better distribution of species depending on their trophic levels was also observed, but the differences were less significant than those suggested by the results of toxicologists using ecosystem modelling.

The results of MCFA gave good indications about the initial purposes of the study. The decrease in annual pollution was slower than expected. Possible interpretations are that the sediments still trapped a large quantity of mercury or that they may be naturally contaminated (analytical evidence for this is very difficult to obtain). The low efficiency of the bio-accumulation mechanism is also stressed by the abnormally high pollution level of some herbivorous species which feed on sieved microscopic algae or bacteria living in sediments.

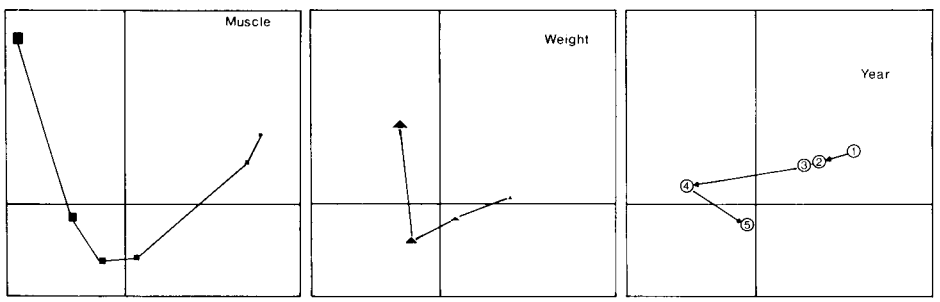

Fig. 4. Projections on the two first-factor space of the muscle mercury concentration classes (■), the weight classes (▲) and the year number (○).

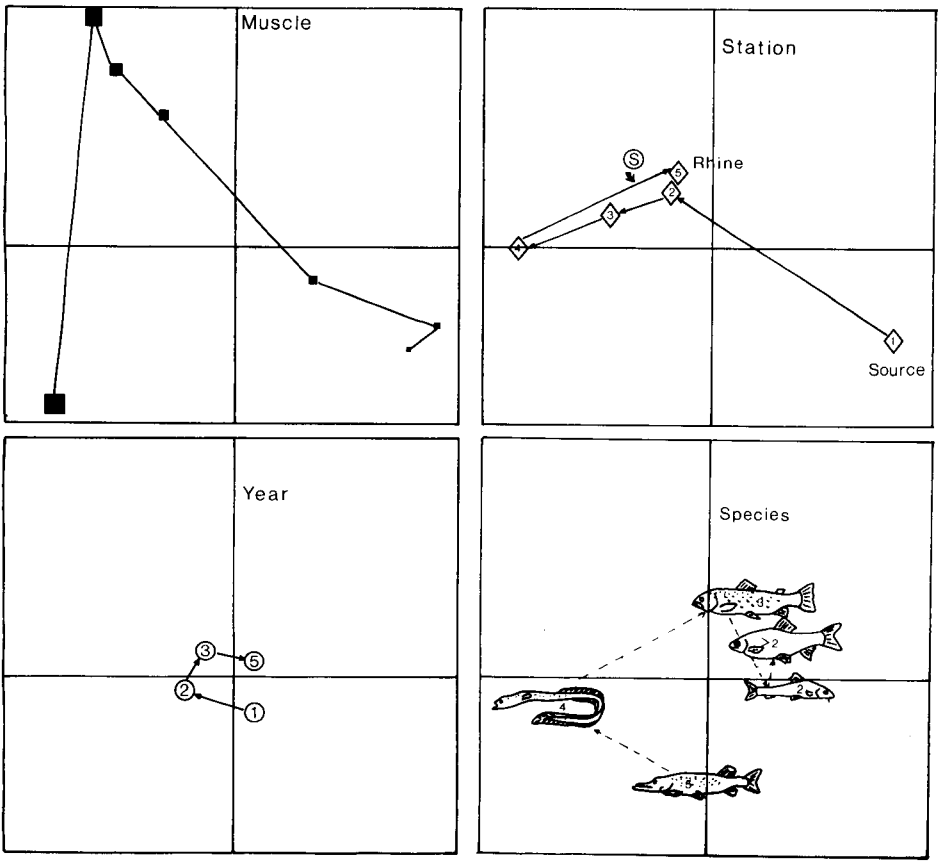

Fig. 5. Study of the Ill River: projections of classes corresponding to mercury in muscle, sampling stations from the source of the Ill (1) to the junction with the Rhine (5; S is Strasbourg), year and species (the trophic level is indicated on each species, pike, eel, trout, roach and gudgeon).

Conclusions

The usefulness of CFA in multivariate statistics has been demonstrated. Some guidelines for selecting suitable methods have been outlined. Compared to many methods giving predictive functions, CFA may seem relatively poor. But although coding data may lead to loss of information or to some bias, it is the only way of studying simultaneously different kinds of variables and assembling data which would otherwise remain unused. Moreover, the analytical chemist, as a problem solver, sometimes needs only to establish the general trends of the problem under study without finding the exact structure of the information. For those reasons, CFA can be considered as a very efficient tool which deserves more attention from chemometricians.

REFERENCES

1 J. P. Benzecri, l'Analyse des Correspondances, Vol. 2, 3rd edn., Dunod, Paris, 1980.
2 L. Lebart, A. Morineau and N. Tabard, Techniques de la Description Statistique, Dunod, Paris, 1977.
3 J. P. Fenelon, Qu'est-ce que l'Analyse des Donnees ?. Lefonen, Paris, 1981.
4 C. Chararas, C. Revolon, M. Feinberg and C. Ducauze, J. Ecol. Chem., 8 (1982) 1093.
5 M. Feinberg, G. Cumont and M. Chevalier, Int. Conf. on Heavy Metals in the Environment, Amsterdam, Commission of the European Communities, Brussels, Sept. 1981.

Analytica Chimica Acta, 191 (1986) 87—96
Elsevier Science Publishers B.V., Amsterdam — Printed in The Netherlands

VISUALIZING INFORMATION IN MULTIVARIATE DATA: APPLICATIONS TO PETROLEUM GEOCHEMISTRY
Part 1. Projection Methods

OLAV M. KVALHEIM*
Department of Chemistry, University of Bergen, N-5000 Bergen (Norway)
NILS TELNÆS
Norsk Hydro A/S, P.O. Box 4313, N-5001 Bergen (Norway)
(Received 27th May 1986)

SUMMARY

General procedures are developed for revealing and comparing the information carried by experimental data obtained for different petroleum fractions. Oblique rotation of principal components is used to obtain projections amenable to geochemical interpretation. A systematic method is given for selecting markers, i.e., compounds related to specific geochemical factors. By projecting samples onto axes defined by markers, their potential for describing a petroleum fraction can be evaluated. The similarity between samples or groups (classes) of samples is revealed by projecting samples onto "geochemical" axes and by comparing their residual distances to class models. In class modelling, projections on markers are proposed as a method for eliminating differences induced by alteration processes not related directly to the source of the oils, e.g., maturity.

The crude oil composition observed in reservoirs is generally governed by many factors, such as organic input, depositional environment, maturity, migration and various other alteration processes. Evaluation of source-specific parameters represents a major goal of petroleum geochemistry; the correlation of crude oils and their sources being of crucial importance in oil exploration [1]. Obviously, the solution to this problem requires all the basic ingredients of pattern recognition methods: classification, interpretation and prediction.

Among the pattern recognition methods proposed, principal component (PC) [2—4] and partial least-squares (PLS) [5, 6] modelling are extensively used both for exploratory data treatment [4] and for multivariate calibration [7]. Despite their powerful data-reduction facilities, these methods rarely provide direct answers to the major problems of petroleum geochemistry. Frequently, each sample is of considerable interest in itself, e.g., the pair-wise comparison of crude oil samples is important for revealing possible communication between wells [8]. Furthermore, factors not directly source-related, e.g., thermal maturation and migration, may profoundly influence the classification and should be accounted for. In such cases, classification

0003-2670/86/$03.50

may still be possible by using either PLS modelling [9] or the projection techniques proposed here. Finally, because of the varying influence of geochemical factors, two oil fractions may contain partly common, partly different information. Extraction of both unique and common information involves problems quite different from those of calibration where interpretation of the related matrices is of no concern [7].

The principal components are average, composite variables located in directions successively describing the maximum amount of variation in the data. Because of their average character, the principal components may not be amenable to geochemical interpretation. In a recent investigation of oil/oil correlations based on light hydrocarbons [8], comparison of principal component scores with ratios related to biodegradation and maturity established the first principal component as being related to biodegradation only, while source and maturity both contributed to the second component. Using similar comparisons in a correlation study based on sterane and triterpane distributions, Telnæs and Dahl [10] ascribed one principal component to thermal maturity.

The interpretation problem was early recognized in factor analysis [11, 12]. Thurstone [11] formulated a "simple structure" criterion which he used for finding interpretable components by a sequence of graphical rotations. Generally, these components were oblique, i.e., correlated. Thurstone's approach has inspired much work in the interpretation problem: Kaiser's orthogonal Varimax solution [13] and oblique solutions [14] such as Promax [15] and target rotations [16], are all based on some "simple structure" criterion. Malinowski and Howery [17] used chemical variables to define a target matrix, generally selected from the original data matrix. If the selected variables approximately span the principal component space, then they represent an oblique, simple and chemically interpretable decomposition of the data matrix.

The aim of the present work is to find general quantitative methods for the comparison and interpretation of composite samples. Various diagrams are proposed for revealing the information in each variable and for comparing samples or groups of samples; such diagrams can be used routinely for visualizing the information in multivariate data.

DATA TYPES AND DATA REPRESENTATION

Depending on the purpose of the analysis, one of three basic approaches are used to characterize crude oils and source rock extracts [1]: (1) isolation and determination of abundance of individual molecules; (2) distillation to obtain fractions within selected temperature windows followed by physical and chemical measurements on these fractions to obtain structural characteristics; (3) quantitative separation into fraction of molecules with similar chemical structure followed by determination of molecular distribution within each fraction using chemical methods.

For multivariate correlation, group-type separation of each sample is most useful. Quantitative structural information can then be obtained by a multitude of experimental techniques: gas chromatography (g.c.) and gas chromatography in combination with mass spectrometry (g.c./m.s.) for determination of the whole molecular distribution of a fraction, and nuclear magnetic resonance spectroscopy (n.m.r.), infrared spectroscopy (i.r.) and derived techniques for group-type characterization [8].

In computerized data acquisition, each chromatographic, fragmentographic or spectral profile can be represented by several thousand data points. Thus, an initial data reduction is usually necessary. Transforming the data to peak heights or peak areas gives a representation which is simple and also conserves most of the information. Peak heights or peak areas are then collected in tables (matrices), turning the problem of data interpretation into problems of finding useful decompositions of data matrices with respect to the information required.

DECOMPOSITION OF A DATA MATRIX

The interpretation and classification of multivariate samples rest on the decomposition of a data matrix into orthogonal matrices of lower dimensionality:

$$\mathbf{X}_{N \times I} = \mathbf{T}_{N \times K}\, \mathbf{G}^{1/2}_{K \times K}\, \mathbf{B}'_{K \times I} + \mathbf{E}_{N \times I} \qquad (1)$$

where $\mathbf{X}$ symbolises the centered data matrix (N samples and I constituents) after normalization, logarithmic conversion or other data-pretreatment procedures. The orthonormal matrices $\mathbf{B}$ and $\mathbf{T}$ contain normalized variable loadings and standardized sample scores, respectively; $\mathbf{G}$ is a diagonal matrix of variances accounted for by the K principal components, while $\mathbf{E}$ is the residual $N \times I$ matrix. The prime implies a transposed matrix. Matrix dimensions are included as subscripts.

Equation 1 corresponds to the singular-value decomposition of a rectangular matrix as proposed by Eckart and Young [18]. This formulation departs slightly from the expression commonly used in chemometric applications, e.g., by Wold et al. [4]. As shown below, the symmetric form of Eqn. 1 is necessary for the calculation of rotated scores and loadings. Equation 1 is also useful for selecting graphical representations which quantitatively display the relations between variables and samples.

CLASSIFICATION AND SAMPLE COMPARISONS

Principal component modelling can be done either disjointly by generating a separate model for each class [2], or jointly by treating several classes of samples in a single model [3, 4]. In disjoint modelling, the similarity between classes of samples is measured by the ratio between inter-class and intra-class residual distances [2]. The residual class distances should be corrected for effects of maturation and other alteration

processes not related to source differences. Esbensen et al. [9] used PLS modelling to correct for background processes in geochemical modelling. If the principal components are identical with the "geochemical" components, background processes can be corrected for directly by subtracting the product of scores and loadings on these dimensions from the data matrix. Projections on markers (see below) represent an alternative approach to removing the effects of background processes. Several geochemical processes can be corrected for by successively projecting the covariances between the other variables and the markers from the data matrix **X**. The similarity between classes is found by inspection of the matrix of corrected residual inter- to intra-class distances. The residual distances to the class models can be visualized in powerful diagrams [19].

In joint modelling, the relations between samples can be visualized in bivariate score plots either of principal components [3, 4] or of oblique components obtained by projections onto markers or by rotating the principal component. For PC plots, the coordinates are obtained from Eqn. 1 by post-multiplying the matrix **T** of standardized scores with $\mathbf{G}^{1/2}$. The case with oblique axes is discussed below.

Sample relations can also be displayed in bivariate object plots [20]. In these plots, pairs of objects represented by their original variable values are compared. We have found these plots useful for both (i) intra-class variable comparisons in order to reveal why some samples are outliers or to uncover systematic differences between replicates, and (ii) inter-class variable comparisons when the number of samples in each class is too small for separate modelling.

Figure 1 shows an object plot used for inter-class variable comparison. The diagram shows the absolute intensity distribution in the ^{13}C-n.m.r. spectra acquired from the naphtha fraction of two neighbouring oil wells [8]. Most intensities closely fit a straight line, implying a similar distribution of the constituents corresponding to these peaks. However, the peaks originating from n-alkanes are clearly more intense in the spectrum of the sample from well 4, implying that the oils differ in their relative abundance of n-alkanes, probably because of biodegradation [1].

INTERPRETATION OF PRINCIPAL AND ROTATED COMPONENTS

Interpretation of the classification in joint modelling can be made at two levels: (i) direct interpretation of principal components in terms of the loadings (weights) of each variable; and (ii) interpretation in terms of real geochemical processes. The second problem often requires rotations of the principal components [11—17].

Equation 1 is used for direct interpretation of principal components. The idea of weighting the loadings with the root of the variance of the principal components, i.e., $\mathbf{G}^{1/2}\mathbf{B}'$, follows naturally. The weighted loadings correctly account for the explained variances of the variables

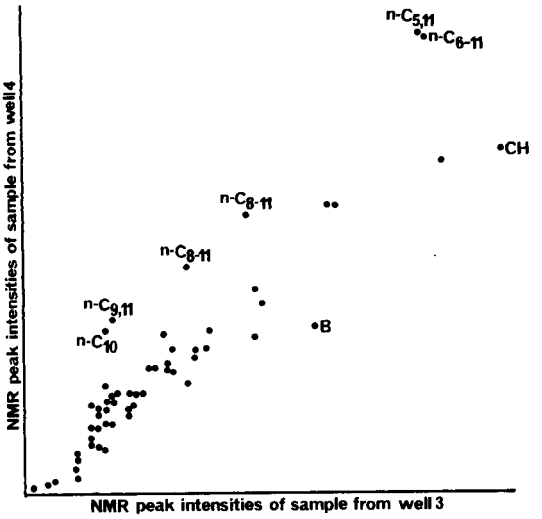

Fig. 1. Example of an object plot [20], samples from two oil wells, Nos. 3 and 4 [8].

$$s_i^2 = \sum_{k=1}^{K} g_k b_{ik}^2 \qquad (2)$$

Loading plots based on variance-weighted loadings have several advantages: (1) the significance of the variables in discriminating between samples is shown; (2) the covariance between variables is pictured correctly; (3) the distribution of the variance of each variable in the principal components is displayed, a useful feature in the selection of marker variables or ratios representing the principal components.

When rotated components or projections on markers are used, Eqn. 2 needs to be modified to account for the possibility of oblique axes. In this case, either so-called structure or pattern loadings on the oblique axes can be used [14, 20]. Figure 2 shows the two possibilities. The structure loadings are correlations between variables and rotated components, while the pattern loadings are coordinates. The two sets of loadings are connected through a simple matrix relation [14]. In the case of orthogonal axes, pattern and structure loadings coincide. In this work, the term loading is used to mean structure loading. As long as the obliqueness between rotated axes is small, statements 1—3 above are valid also in the oblique case.

INFORMATION CARRIED BY DIFFERENT FRACTIONS

Because the ultimate composition of crude oils is governed by equilibria simultaneously influenced by several processes, methods analogous to target rotation [17] may be necessary to extract geochemical information from oil

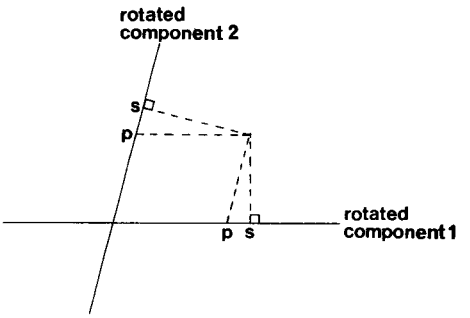

Fig. 2. Pattern (p) and structure (s) loadings on oblique axes [11, 12, 14].

fractions. The projection method developed below works both when the target matrix consists of variables or variable ratios obtained from the data matrix which has to be interpreted, and with variables obtained from other data matrices. However, in the following development, the targets are principal components amenable to "geochemical" interpretation. These principal components are assumed to contain partly the same information as the matrix to be investigated. This approach utilizes the fact that different petroleum fractions contain redundant information, all constituents being influenced, at least to some degree, by the same geochemical factors.

When one fraction can be resolved into interpretable principal components, projections onto axes with maximum correlation with these principal components should reveal the influence of the same geochemical factors on other fractions. Using standard notation the data matrices are decomposed, according to Eqn. 1:

$$\mathbf{X} = \mathbf{T}\,\mathbf{G}^{1/2}\,\mathbf{B}' \tag{3a}$$

$$\mathbf{Y} = \mathbf{U}\,\mathbf{H}^{1/2}\,\mathbf{C}' \tag{3b}$$

These equations give the singular-value decomposition of the $N \times I$ data matrix $\mathbf{X}$ and the $N \times J$ data matrix $\mathbf{Y}$.

The dimensions of $\mathbf{U}$, $\mathbf{H}$ and $\mathbf{C}$ are $N \times L$, $L \times L$ and $J \times L$, respectively. The two sets of principal components are connected by a $K \times L$ correlation matrix $\mathbf{R}$:

$$\mathbf{R} = \mathbf{T}'\,\mathbf{U}/(N-1) \tag{4}$$

The matrix $\mathbf{R}$ consists of L column matrices: $\mathbf{R} = [\mathbf{r}_1, \mathbf{r}_2, \ldots, \mathbf{r}_L]$. By squaring and summing over each of the L columns of the correlation matrix $\mathbf{R}$ (Eqn. 4), the squared multiple correlation coefficient (SMCC) [21] is obtained between each principal component of Y-space and the principal components of X-space:

$$r_l^2 = \mathbf{r}_l'\mathbf{r}_l \qquad (l = 1, 2, \ldots, L) \tag{5}$$

Because of the orthogonality between principal components, the SMCC represents a quantitative measure of the correlation between a principal

component of Y-space and the variance of X-space as described by the K principal components, i.e., the SMCC is a measure of congruence with values between zero and one. If the SMCC is equal to unity, then the information in that principal component of Y-space is completely accounted for by a rotated component of X-space, i.e., the principal component of Y-space is collinear with this rotated component. By summing the SMCC's multiplied by the variances along the principal components of Y-space, the total absolute variance of Y-space accountable for by the X-space can be obtained:

$$v_{Y \subset X} = \sum_{l=1}^{L} h_l r_l^2 \tag{6}$$

Now the rotated components of X-space most collinear with the principal components of Y-space can be established. The rotated components normalized to unit length are denoted by ($\mathbf{b}_l^*$, $l = 1, 2, \ldots, L$). The rotated components are described by linear combinations of variance-weighted principal components of X-space with coefficients equal to the correlation coefficients (r_{kl}, $k = 1, 2, \ldots, K$) normalized by r_l, the square root of the SMCC, i.e., $\mathbf{r}_l/(\mathbf{r}_l' \mathbf{r}_l)^{1/2}$. Thus, each normalized column of the correlation matrix $\mathbf{R}$ defines a possible rotated component in X-space.

Rotated components of X-space are determined only for principal components of Y-space which have large SMCC's with the principal components of X-space. This selection prevents information unique to Y-space being "blown up" in X-space. For a projection in X-space, variance-weighted loadings and standardized scores are determined from the original loadings and scores by use of the following relations:

$$(g_l^*)^{1/2} \mathbf{b}_l^* = \mathbf{r}_l' \mathbf{G}^{1/2} \mathbf{B}' / (\mathbf{r}_l' \mathbf{r}_l)^{1/2} \tag{7}$$

$$\mathbf{t}_l^* = \mathbf{T} \mathbf{r}_l / (\mathbf{r}_l' \mathbf{r}_l)^{1/2} \tag{8}$$

The variance $(g_l^*)^{1/2}$ accounted for by a rotated component, is given by the normalization condition for the transformed (structure) loadings or by the relation $g_l^* = \mathbf{r}_l' \mathbf{G} \mathbf{r}_l / \mathbf{r}_l' \mathbf{r}_l$. The correlation between two rotated components is calculated by use of Eqn. 8:

$$\phi_{mn}^* = \mathbf{r}_m' \mathbf{r}_n / (\mathbf{r}_m' \mathbf{r}_m)^{1/2} (\mathbf{r}_n' \mathbf{r}_n)^{1/2} \tag{9}$$

Rotated components defined by Eqn. 7 are generally oblique. If the variables of Y-space are orthogonal, e.g., principal components, the degree of obliqueness depends solely on the correlation between X-space and Y-space. Orthogonal rotated components are obtained in the special case when the principal components of Y-space are fully accounted for by X-space.

Bivariate score and loading plots are obtained for oblique components by a procedure slightly different from that used in the orthogonal case. Given that rotated components are represented by structure loadings (Eqn. 7),

Fig. 2 shows how to locate a variable in a bivariate oblique loading plot. Oblique score plots are obtained in complete analogy to oblique loading plots.

PROJECTION ONTO MARKERS

In addition to classifying samples, PC modelling and rotation can be useful for revealing clusters of interrelated variables. Variables with similar loading patterns may carry the same information, while different loadings patterns indicate different information content.

Because of the orthogonality between principal components, these statements can be extended. Variables with large loadings on one principal component and small loadings on the others contain information specific to that principal component. If the principal components are amenable to geochemical interpretation, and if the principal components account for the major part of the variances of these variables, so-called markers can be selected among these variables. Markers are variables that carry information related to one geochemical factor only. Increased sensitivity is obtained by using ratios between negatively correlated markers, but this is not recommended because such ratios always give non-linear relationships. The statements above hold also for oblique components if the degree of obliqueness is moderate.

Molecular markers or ratios between such markers have been used extensively in oil/oil and oil/source correlation studies [1]. Generally, these markers have been selected by successively comparing samples using one or two markers or combinations of markers to see whether a preconceived classification emerged. Projection onto markers represents a systematic approach to evaluating the potential of marker variables in describing a petroleum fraction. Furthermore, this type of projection reveals how the other constituents of a fraction have responded to the influence of the geochemical factor represented by the marker.

The scores and loadings on markers are calculated by a procedure similar to that of the trial vector method [12]. The vector $\mathbf{x}$ of values for a marker variable defines a latent variable. The loadings $\mathbf{b}'$ are determined by premultiplying the original data matrix $\mathbf{X}$ by the row vector $\mathbf{x}'$, i.e., $\mathbf{b}' = \mathbf{x}'\mathbf{X}/\mathbf{x}'\mathbf{x}$. Normalized loadings are then given by $\|\mathbf{b}\|^{-1}\ \mathbf{b}'$ and the scores by $\mathbf{t} = \|\mathbf{b}\|\ \|\mathbf{x}\|^{-1}\ \mathbf{x}$.

This procedure can be repeated to obtain markers for all relevant geochemical factors. Orthogonal components are obtained if the product $\mathbf{tb}'$ of scores and loadings is subtracted from the data matrix $\mathbf{X}$. If the original data matrix $\mathbf{X}$ is retained after each projection, components are obtained with exactly the same degree of obliqueness as that between the marker variables used. This last approach is preferable because correlations between geochemical processes are thus properly represented.

Projection onto markers can also be viewed as an "internal" PLS with one

dependent variable. The similarity to the PLS algorithm [22] is shown by selecting the PLS weightings equal to zero for all but the marker variable which is given a weighting of unity.

CONCLUSIONS

The overall plan adopted consists of four consecutive steps: (1) decomposition of each data matrix into principal components; (2) rotation of principal components to obtain components amenable to geochemical interpretation; (3) selection of geochemical markers; (4) projection of the original data onto markers to obtain condensed descriptions of fractions in geochemical terms.

Markers obtained can be used for extracting information about unresolved fractions using partial least squares or the projection method developed in this work. The methods shown should uncover similarities and differences in constituents caused by the various processes acting during petroleum generation and migration. Furthermore, in correlation studies it should be possible to account for migration effects, or, as indicated above, thermal maturation, revealing true source-specific effects. This is important, because case studies have shown that class modelling produced principal components which had to be attributed to correlated geochemical factors [19].

With the present approach, factorial invariance is achieved, i.e., the factors produced are hardly affected by inclusion or exclusion of a subset of variables [19]. Finally, the methods proposed account for the variation between fractions arising from the varying influence of geochemical factors.

The authors thank R. Eastgate, Norsk Hydro, Bergen, R. Manne, University of Bergen and S. Wold, University of Umeå for valuable suggestions and discussions.

REFERENCES

1 B. P. Tissot and D. H. Welte, Petroleum Formation and Occurrence — A New Approach to Oil and Gas Exploration. Springer Verlag, Heidelberg, 1984.
2 S. Wold, Pattern Recognition, 8 (1976) 127.
3 D. L. Massart and L. Kaufman, The Interpretation of Analytical Chemical Data by the Use of Cluster Analysis. Wiley, New York, 1983.
4 S. Wold, C. Albano, W. J. Dunn III, U. Edlund, K. Esbensen, P. Geladi, S. Hellberg, E. Johansson, W. Lindberg and M. Sjöström, in B. R. Kowalski (Ed.), Chemometrics — Mathematics and Statistics in Chemistry, Reidel, Dordrecht, 1984.
5 H. Wold, in K. G. Jöreskog and H. Wold (Eds.), Systems under Indirect Observation, Part 2, North-Holland, Amsterdam, 1982.
6 S. Wold, C. Albano, W. J. Dunn III, K. Esbensen, S. Hellberg, E. Johansson and M. Sjöström, in H. Martens and H. Russwurm, Jr. (Eds.), Food Research and Data Analysis. Applied Science Publishers, London, 1983, p. 147.
7 H. Martens, Dr. techn. thesis, Technical University of Norway, Trondheim, 1985.
8 O. M. Kvalheim, D. W. Aksnes, T. Brekke, M. O. Eide, E. Sletten and N. Telnæs, Anal. Chem., 57 (1985) 2858.

9 K. H. Esbensen, E. Johansson, S. Wold and K.-M. Drake, in Proc. Nordic Symp. on Applied Stat., 1983, p. 111.
10 N. Telnæs and B. Dahl, Org. Geochem., 10(1—3) (1985) 425.
11 L. L. Thurstone, Multiple-factor Analysis, The University of Chicago Press, Chicago, 1947.
12 R. B. Cattel, Factor Analysis: An Introduction and Manual for the Psychologist and Socialist Scientist, Harpers and Brothers, New York, 1952.
13 H. F. Kaiser, Psychometrika, 23 (1958) 187.
14 H. H. Harman, Modern Factor Analysis, The University of Chicago Press, Chicago, 2nd edn., 1967.
15 A. E. Hendrickson and P. O. White, Br. J. Statist. Psychol., 17 (1964) 65.
16 D. N. Lawley and A. E. Maxwell, Factor Analysis as a Statistical Method, Butterworth, London, 2nd edn., 1971.
17 E. R. Malinowski and D. G. Howery, Factor Analysis in Chemistry, Wiley, New York, 1980.
18 C. Eckart and G. Young, Psychometrika, 1 (1936) 211.
19 O. M. Kvalheim and N. Telnæs, Anal. Chim. Acta, 191 (1986) 97.
20 K. G. Jöreskog, J. E. Klovan and R. A. Reyment, Geological Factor Analysis, Elsevier, Amsterdam, 1976.
21 R. J. Rummel, Applied Factor Analysis, Northwestern University Press, Evanston, IL, 1970.
22 S. Wold, A. Ruhe, H. Wold and W. J. Dunn III, SIAM J. Sci. Stat. Comput., 5 (1984) 735.

Analytica Chimica Acta, 191 (1986) 97—110
Elsevier Science Publishers B.V., Amsterdam — Printed in The Netherlands

VISUALIZING INFORMATION IN MULTIVARIATE DATA: APPLICATIONS TO PETROLEUM GEOCHEMISTRY

Part 2. Interpretation and Correlation of North Sea Oils by Using Three Different Biomarker Fractions

OLAV M. KVALHEIM*
Department of Chemistry, University of Bergen, N-5000 Bergen (Norway)
NILS TELNÆS
Norsk Hydro A/S, P.O. Box 4313, N-5001 Bergen (Norway)
(Received 27th May 1986)

SUMMARY

Pentacyclic triterpanes, steranes and aromatic steroids of thirty-five North Sea crude oils are investigated for their usefulness in correlation and interpretation. Oblique components are necessary for obtaining data projections amenable to geochemical interpretation and for selecting molecular markers, i.e., compounds related to specific geochemical factors. Normoretane is shown to be a specific maturity parameter for the North Sea oils examined.

Steranes and pentacyclic triterpanes found in sedimentary organic matter are often termed biomarkers or geochemical fossils [1]. The terms stem from the assumption that many of these molecules originate directly from the building blocks of living organisms, their carbon skeleton remaining largely unaltered during the processes leading to petroleum formation [1]. Cholesterol, stigmastane and sitostane are biological precursors of the steranes, while tetrahydroxybacteriohopane has been proposed as precursor for some of the pentacyclic triterpanes found in oils (Fig. 1). Seifert and Moldowan [2, 3] showed that the relative abundances of steranes and terpanes in oils correlate with source input, maturation and migration. However, the various compounds were found to respond differently to these factors. Accordingly, groups of compounds could be selected as carriers of specific geochemical information.

Christie et al. [4] and Telnæs and Dahl [5] used the distribution of pentacyclic triterpanes and steranes in crude oils as input to principal component (PC) modelling. The distributions were evaluated by metastable ion monitoring for selected transitions [6]. Telnæs and Dahl [5] found that the sterane distribution was related to depositional environment and maturity. During diagenesis [1], sterenes are converted to diasteranes through clay mineral catalysis, while the conversion to α,α,α- and α,β,β-steranes is an effect of thermal maturation:

0003-2670/86/$03.50

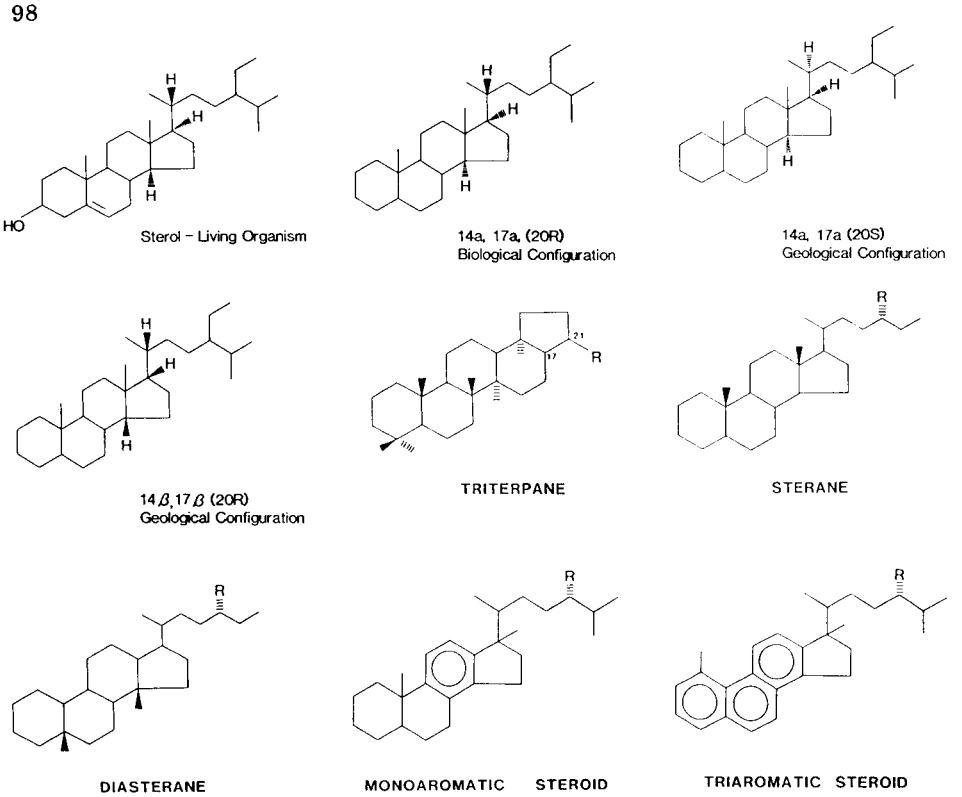

Fig. 1. Structures of some biomarkers and their biological precursors (cf. Tables 1–3).

$$\alpha,\beta,\beta\text{-steranes} \xleftarrow[\text{maturation}]{\text{thermal}} \alpha,\alpha,\alpha\text{-steranes} \xleftarrow[\text{maturation}]{\text{thermal}} \text{sterenes} \xrightarrow[\text{catalysis}]{\text{clay mineral}} \text{diasteranes}$$

These processes proceed to equilibrium. One further point should be mentioned. With increasing maturation, the relative concentration of biomarkers decreases, an effect ascribed mainly to dilution caused by the release of other petroleum constituents from the kerogen during generation.

Although some geochemical information could be deduced from the interpretation of principal components, Telnæs and Dahl [5] concluded that reduction of the number of dimensions represented the main achievement of principal component (PC) modelling. Accordingly, geochemical interpretation of the above-mentioned biomarkers was the aim of the present work. Applications to major problems in petroleum geochemistry are presented: the correlation of crude oils, and the establishment of molecular markers related to maturity, source input and depositional environment. The matter of molecular markers is emphasized here, but it should be realized that this is closely related to the correlation of crude oils, the ultimate goal being an understanding of the geochemical processes at a level where reliable statements can be made about the source of oils.

EXPERIMENTAL

The molecular distributions of 16 pentacyclic triterpanes (Table 1), 36 steranes (Table 2) and 14 mono- and tri-aromatic steroids (Table 3) in 35 crude oils from five fields in the Norwegian sector of the North Sea were examined. The sources of all the oils used were mainly from the Upper Jurassic Kimmeridge Clay Formation of the North Sea. The sterane and triterpane distribution was determined by metastable ion monitoring of selected transitions [6], while the aromatic steroids were determined by using selected ion monitoring of *m/z* 231 and *m/z* 253. Figure 2 shows typical fragmentograms of the three distributions. The percentages [7] converted into logarithms were used as input to multivariate data analysis.

Various procedures were used for correlating the oils and interpreting the different fractions. Correlation was done by disjoint class modelling, i.e., the SIMCA method [8], and by comparing the sample scores obtained for principal components, rotated components and components determined by marker projections [9]. For class modelling, cross-validation [10] was used to evaluate the dimensionality of the PC models. All calculations were done with the UIB-SIMCA package [11], a general-purpose program for multivariate statistics implemented on a VAX 11/750 and NORD-100 computer.

CORRELATION OF OILS BY DISJOINT PRINCIPAL COMPONENTS MODELLING

For successful correlation, differences in maturity, being unrelated to sources, must be eliminated prior to constructing class models. By projection onto a maturity-related marker [9], this source of variation can be removed. However, joint modelling of the sterane and triterpane distribution of the 35 samples showed that contributions from variations in maturity level were small. Indeed, 60.8% of the total variance in the data set was accounted for by the first principal component which, in line with previous results for similar oils [5], was attributed to variation in depositional environment.

TABLE 1

Triterpanes

No.	Compound	No.	Compound
1	17α(H)-bishomohopane (22S)	9	Normoretane
2	17α(H)-bishomohopane (22R)	10	C_{29} Triterpane
3	17α(H)-25,28,30-trisnorhopane	11	17α(H)-28,30-bisnorhopane
4	17α(H)-homohopane (22S)	12	C_{28} Triterpane
5	17α(H)-homohopane (22R)	13	C_{28} Triterpane
6	17α(H)-hopane	14	17α(H)-22,29,30-trisnorhopane
7	17α(H)-norhopane	15	18β(H)-22,29,30-trisnorhopane
8	C_{29} Triterpane	16	C_{27} Triterpane

TABLE 2

Steranes

No.	Compound	No.	Compound
1	C_{30} 13β(H), 17α(H)-diasterane (20S)	20	13β(H), 17α(H)-24-methyl-diacholestane (20S, 24S/R)
2	C_{30} 13β(H), 17α(H)-diasterane (20R)	21	13β(H), 17α(H)-24-methyl-diacholestane (20R, 24S/R)
3	C_{30} 13α(H), 17β(H)-diasterane (20S)	22	13β(H), 17α(H)-24-methyl-diacholestane (20R, 24S/R)
4	C_{30} 13α(H), 17β(H)-diasterane (20R)	23	13α(H), 17β(H)-24-methyl-diacholestane (20S)
5	C_{30} Sterane	24	13α(H), 17β(H)-24-methyl-diacholestane (20R)
6	C_{30} 5α(H), 14α(H), 17α(H)-sterane (20S)	25	5α(H), 14α(H), 17α(H)-24-methylcholestane (20S)
7	C_{30} 5α(H), 14β(H), 17β(H)-sterane (20R)	26	5α(H), 14β(H), 17β(H)-24-methylcholestane (20R)
8	C_{30} 5α(H), 14β(H), 17β(H)-sterane (20S)	27	5α(H), 14β(H), 17β(H)-24-methylcholestane (20S)
9	C_{30} 5α(H), 14α(H), 17α(H)-sterane (20R)	28	5α(H), 14α(H), 17α(H)-24-methylcholestane (20R)
10	13β(H), 17α(H)-24-ethyldiacholestane (20S)	29	13β(H), 17α(H)-diacholestane (20S)
11	13β(H), 17α(H)-24-ethyldiacholestane (20R)	30	13β(H), 17α(H)-diacholestane (20R)
12	C_{29} Sterane	31	13α(H), 17β(H)-diacholestane (20S)
13	13α(H), 17β(H)-24-ethyldiacholestane (20S)	32	13α(H), 17β(H)-diacholestane (20R)
14	13α(H), 17β(H)-24-ethyldiacholestane (20R)	33	5α(H), 14α(H), 17α(H)-cholestane (20S)
15	5α(H), 14α(H), 17α(H)-24-ethylcholestane (20S)	34	5α(H), 14β(H), 17β(H)-cholestane (20R)
16	5α(H), 14β(H), 17β(H)-24-ethylcholestane (20R)	35	5α(H), 14β(H), 17β(H)-cholestane (20S)
17	5α(H), 14β(H), 17β(H)-24-ethylcholestane (20S)	36	5α(H), 14α(H), 17α(H)-cholestane (20R)
18	5α(H), 14α(H), 17α(H)-24-ethylcholestane (20R)		
19	13β(H), 17α(H)-24-methyl-diacholestane (20S, 24S/R)		

TABLE 3

Mono- and tri-aromatic steroids

No.	Compound	No.	Compound
1	C_{21} 5β mono-aromatic steroid	8	C_{20} tri-aromatic steroid
2	C_{22} 5β mono-aromatic steroid	9	C_{21} tri-aromatic steroid
3	C_{27} 5β mono-aromatic steroid	10	C_{26} tri-aromatic steroid (20R + 20S)
4	C_{27} 5β mono-aromatic steroid (20R)	11	C_{27} tri-aromatic steroid (20S)
5	C_{28} 5α mono-aromatic steroid (20R) + C_{27} 5β mono-aromatic steroid (20S)	12	C_{28} tri-aromatic steroid (20S)
6	C_{29} 5β mono-aromatic steroid (20S)	13	C_{27} tri-aromatic steroid (20R)
7	C_{29} 5α mono-aromatic steroid (20R) + C_{29} 5β mono-aromatic steroid (20S)	14	C_{28} tri-aromatic steroid (20R)

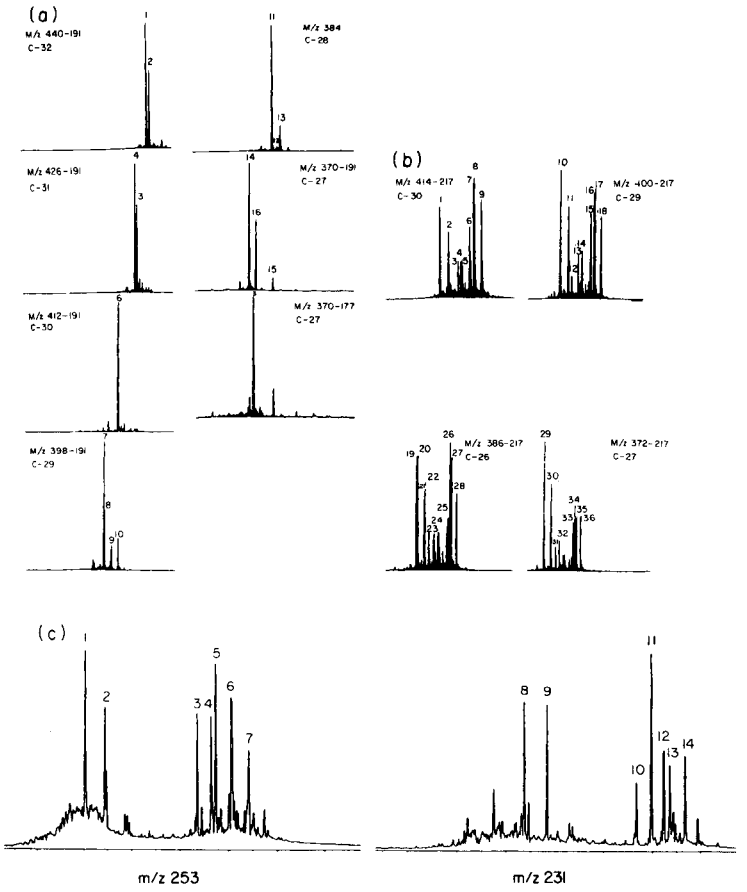

Fig. 2. Fragmentograms: (a) pentacyclic triterpanes; (b) steranes; (c) aromatic steroids.

Accordingly, correction for different maturity levels was not necessary for these oils.

Table 4 shows the average residual inter-class to intra-class distances [8] obtained by the separate modelling of five pre-established classes of oils using the distribution of pentacyclic triterpanes and steranes. Figure 3, which shows residual distances of the samples from the class models, makes a quantitative visual comparison possible. Only the nearest sample is included for oils belonging to any one of the other pre-established classes. The diagram shows that all samples are correctly classified, demonstrating the potential of the SIMCA method for classifying samples even when some classes show large systematic variances (class 2 and 4, see Table 4). Figure 3 also suggests that one of the samples of class 1 may be an outlier.

TABLE 4

Residual distances [2] between classes[a] of oils

Class no.	1	2	3	4	5
1	1.0				
2	4.4	1.0			
3	4.5	4.1	1.0		
4	5.8	6.2	3.4	1.0	
5	7.4	10.0	3.7	4.2	1.0

[a]Disjoint modelling with 0, 1, 0, 1, 2 principal components for classes 1 to 5.

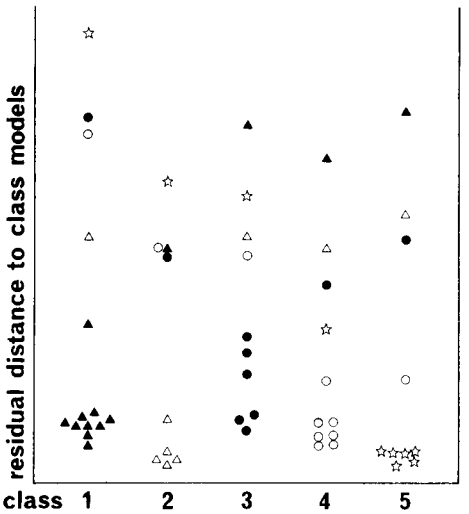

Fig. 3. Residual distances to class models.

Information carried by steranes

While joint modelling of the distribution of pentacyclic triterpanes and steranes showed that the first principal component (PC1) could be attributed to the influence of depositional environment only, the other principal components mixed the effects of maturity, organic input, etc. This is not surprising, because steranes and terpanes are likely to respond differently to primary formation processes. Accordingly, the sterane and triterpane distributions were individually normalized to 100% for separate data analysis. This renormalization leads to a minor loss of information, i.e., the information carried by the ratio between steranes and triterpanes is lost, but this is a worthwhile sacrifice if interpretation in geochemical terms is gained.

The sterane distribution gave three significant principal components which accounted for 79.6, 8.6 and 6.3%, respectively, of the total variance. Figure 4(a) displays the variable loadings in PC1 and PC2. The first PC, being dominated by a negative correlation between regular steranes and

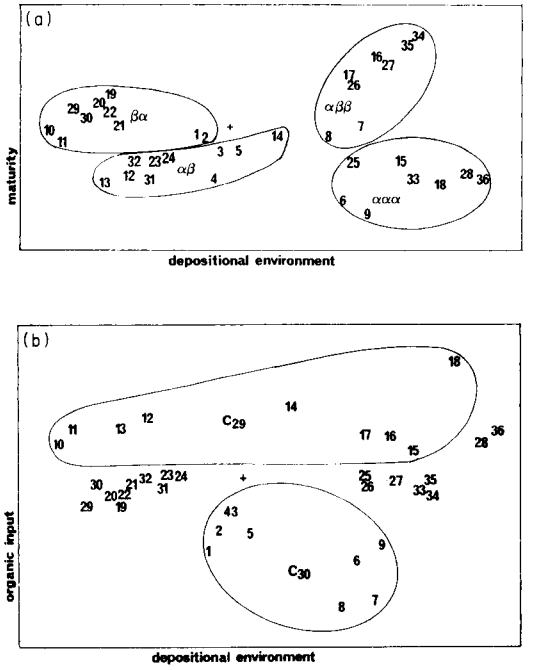

Fig. 4. Loadings from joint PC modelling of the sterane distribution: (a) PC1 vs. PC2; (b) PC1 vs. PC3.

diasteranes, can be interpreted as describing differences in depositional environment [5, 12]. The second PC is dominated by a negative correlation between α,α,α- and α,β,β-steranes together with a similar relation between β,α- and α,β-diasteranes. These conversions are well-known effects of maturation [2, 3, 13]. Figure 4(b) shows that PC3 is dominated by a negative correlation between C_{29} and C_{30} steranes. This correlation is interpreted in terms of differences in organic input. Oils originating from marine sediments are richer in C_{27} and C_{30} steranes relative to C_{29} steranes, when compared to oils from sources dominated by terrestrial organic matter [1].

Because PC2 of the sterane distribution can be attributed to differences in maturity, the scores on PC1 and PC3 are useful for correlating the oil on the basis of organic input and depositional environment alone. Figure 5(a) displays the oils on PC1 and PC2. Comparison with Fig. 5(b), which displays the samples on PC1 and PC3, shows that oils from class 3 partly coincide with those from classes 4 and 5 when the effect of different maturities is eliminated. All these oils were evidently formed within a similar depositional environment, class 3 containing oils slightly more mature than the others, but being between classes 4 and 5 with regard to relative input of marine organic matter, class 5 being the least marine.

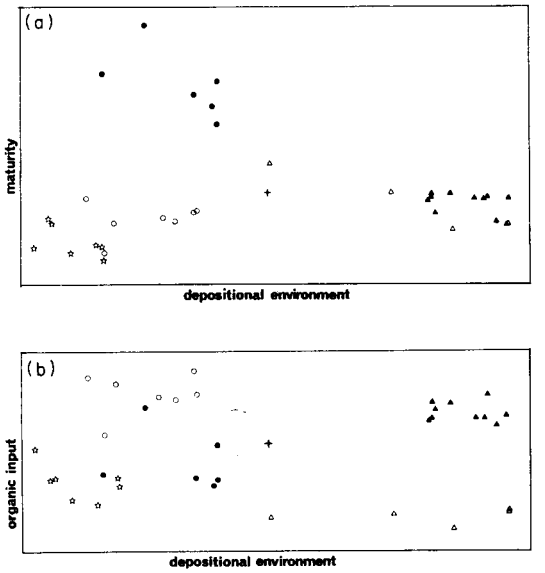

Fig. 5. Scores from joint PC modelling of the sterane distribution: (a) PC1 vs. PC2; (b) PC1 vs. PC3.

Information carried by triterpanes

The triterpanes gave four significant principal components accounting for 48.4, 29.1, 15.2 and 4.2%, respectively, of the total variance. Score plots for PC1, PC2 and PC3 (Fig. 6) showed a different picture from that given by the sterane distributions. This observation reflects the average character of principal components, and the fact that steranes and triterpanes do not carry quite the same information.

Because the variation in sterane distribution can be interpreted in terms of the extracted principal components, the projection methods [9] can be used. Table 5 shows the 4×3 correlation matrix and the squared multiple correlation coefficients (SMCC's) [9] calculated for the principal components obtained from the sterane and triterpane matrix, respectively. Several conclusions can be drawn from this table. First, the SMCC's for the triterpanes show that the three dominant principal components are distributed equally among the principal components extracted for the steranes, emphasizing the average character of the principal components obtained for the triterpanes. Secondly, the least significant principal component extracted for the triterpanes bears no relation at all to the steranes. Thirdly, the SMCC's of the sterane principal components with respect to the triterpane principal components reveal that the triterpanes investigated contain information about depositional environment and maturity, but little or no information about organic input. Finally, Table 5 shows that PC2 and PC3 for the triterpanes have most information in common with PC1 and PC2 for the steranes.

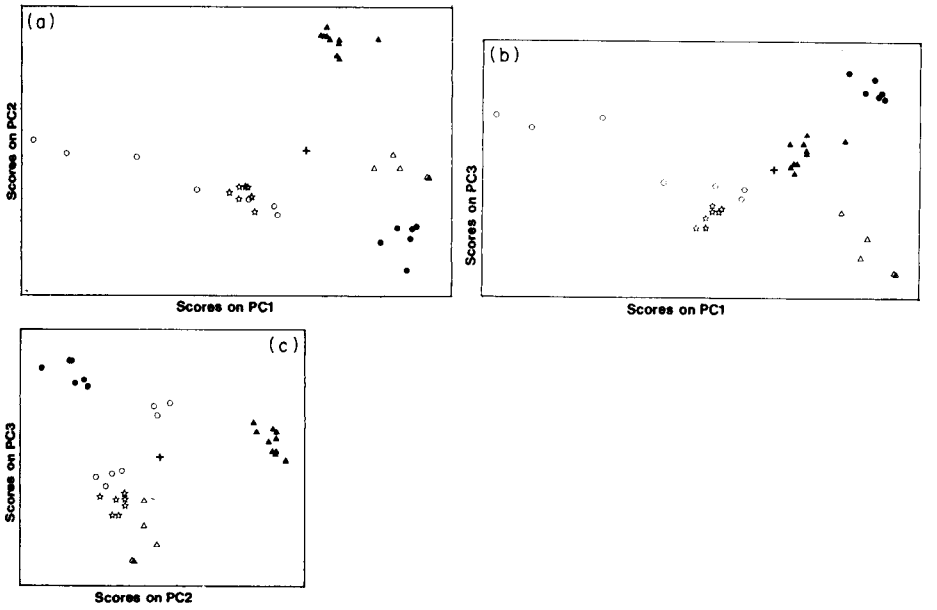

Fig. 6. Scores from joint PC modelling of the triterpane distribution: (a) PC1 vs. PC2; (b) PC1 vs. PC3; (c) PC2 vs. PC3.

TABLE 5

Correlations between principal components from steranes (horizontal), cumulative variance 94.6%, and triterpanes (vertical), cumulative variance 96.9%

PC no.	1	2	3	SMCC[a]
1	0.5474	0.5756	−0.4061	0.7960
2	0.7398	−0.3000	0.3370	0.7509
3	−0.1411	0.7143	0.4323	0.7170
4	−0.1926	−0.1138	0.1400	0.0696
SMCC	0.9040	0.9445	0.4850	2.3335[b]

[a]Squared multiple correlation coefficient. [b]Summed SMCC's.

Rotated components corresponding to depositional environment and maturity in triterpane space were then calculated by using the projection technique [9]. These components accounted for 35.2 and 28.9% of the original variance with an angle of 89.1° between them. Thus, the rotated triterpane components are nearly orthogonal, a consequence of the SMCC's being close to unity [9] for the depositional and maturity-related sterane principal components with triterpane principal components. Figure 7 shows the scores plotted on the slightly oblique axes. The similarity between this diagram and Fig. 5(a), based on the sterane matrix, is striking. The improved

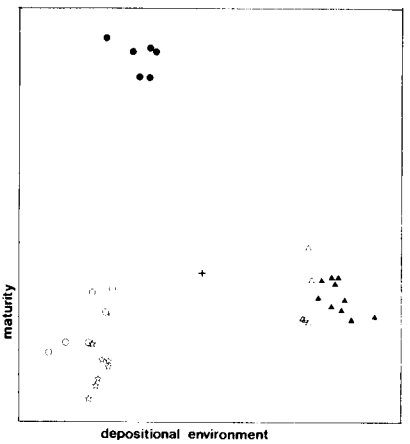

Fig. 7. Scores on oblique components on triterpane space.

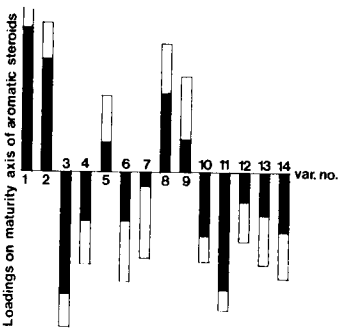

Fig. 8. Loadings (shaded) and original residuals for the aromatic steroids on the maturity component.

separation between classes (oil fields) on the rotated triterpane components compared to the corresponding sterane principal components, is due to reduced intra-class variances on the depositional and maturity-related triterpane projections.

Information content carried by aromatic steroids

Four significant principal components accounting for 61.4, 23.0, 5.2 and 4.0%, respectively, of the total variance were obtained for the distribution of the 14 mono- and tri-aromatic steroids listed in Table 3. The principal components were not amenable to geochemical interpretation. A faint similarity was observed when the distribution of samples along PC1 for this fraction was compared with the distribution along the maturity components obtained for the steranes and triterpanes. For the aromatic steroids, data were available for only 33 of the oils. Thus, the sterane distribution had to be remodelled for these 33 samples before the principal components were used as exploratory tools for revealing geochemical information carried by the aromatic steroids.

Table 6 shows the 4×3 correlation matrix and the SMCC's between the principal components of the aromatic steroids and steranes. The SMCC's reveal that a major part of the variation in the distribution of aromatic steroids is caused by factors other than those revealed by the steranes. For maturity, however, a strong relationship is observed, with a large contribution from the dominant principal component of the aromatic steroids. Variable loadings on the maturity component are shown in Fig. 8 so as to show mutual correlations between variables together with their original residual standard deviations. This projection accounts for 46.6% of the total original variance of the

TABLE 6

Correlations between principal components based on steranes (horizontal), cumulative variance 94.6%, and aromatic steroids (vertical), cumulative variance 93.4%

PC no.	1	2	3	SMCC[a]
1	0.0103	−0.7634	0.1710	0.6121
2	−0.3450	−0.1664	0.5770	0.4796
3	0.5903	−0.0890	0.2843	0.4372
4	0.1327	−0.4244	−0.2262	0.2489
SMCC	0.4852	0.7984	0.4941	1.7777[b]

[a]Squared multiple correlation coefficient. [b]Summed SMCC's.

aromatic steroids. Table 4 together with the loading pattern as displayed in the new type of diagram (Fig. 8) shows that this projection is related to the "cracking parameter" defined by Mackenzie et al. [13], which is a marker ratio based on reduction in the content of aromatic steranes with extended side-chains following increased thermal maturation. Figure 9 shows the good correlation between samples on the maturity component of the steranes and aromatic steroids.

Mono- and tri-aromatics are probably sensitive to migration phenomena. Their relative abundances may be seriously affected by "geo-chromatography", the tri-aromatics being more polar than the mono-aromatics. Thus, different migration paths and distances for the oils may account for the unresolved information of this aromatic fraction.

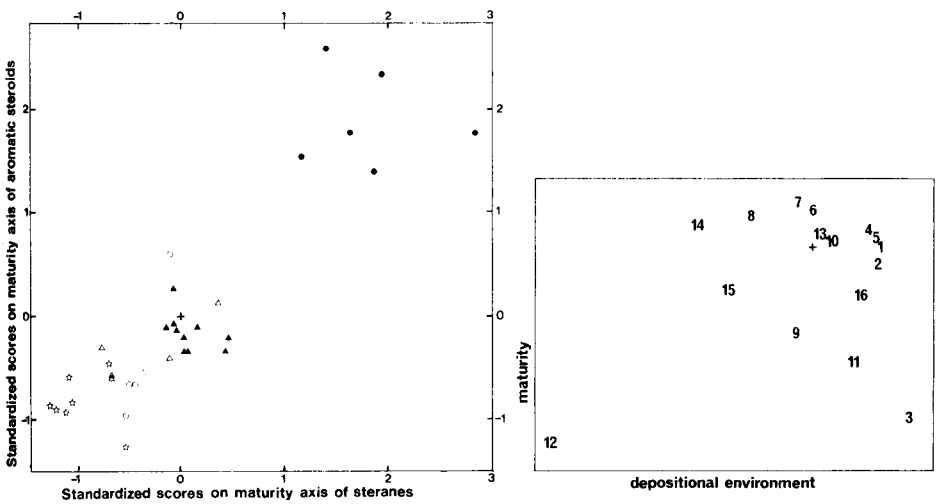

Fig. 9. Samples plotted on the maturity components of steranes and aromatic steroids.

Fig. 10. Loadings in oblique components (89.1°) of triterpane space.

SELECTION OF MARKERS

Because the principal components extracted from the sterane distribution can be directly interpreted in terms of geochemical processes, this fraction may be amenable to a condensed description in terms of marker compounds [9]. The loading plots (Fig. 4a,b) reveal that most steranes are influenced by more than one geochemical factor. Exceptions are the eight β,α-diasteranes (variables 10, 11 and 19–22 and 29, 30). Their relative occurrence appears to be related only to the depositional environment. The correlations between the percentage occurrences of these compounds and the environmentally related principal component (PC1) are all between —0.93 and —0.99. The best markers are probably 13β(H), 17α(H)-diacholestane 20S and 20R, both of which are major sterane constituents and highly selective. All variables with high loadings in the principal component related to maturity (PC2) have also high loadings in the principal component related to depositional environment (PC1). The same conclusion holds for the principal component related to organic input (PC3) with the sole exception of variable 5, a C_{30} sterane which seems to be a rather selective marker with respect to the ratio between marine and terrestrial source input. However, the low abundance of this compound (below 1% in all samples) makes it a poor marker. As mentioned in the experimental section, the oils used in this investigation were mainly from one source. Subtle differences in organic facies are thus expected, while major differences in organic input cannot possibly be detected from these oils.

Figure 10 displays the loadings on the two oblique projections in triterpane space which maximize the correlation with the environment and maturity-related principal components of the steranes. It can be observed that normoretane (variable 9) and 18β(H)-22, 29, 30-trisnorhopane (variable 15) are marker candidates for maturity and depositional environment, respectively. The correlation coefficient between the percent occurrences of normoretane and the positions (scores) on the maturity component of the steranes (Fig. 11) was —0.86. The corresponding calculation for 18β(H)-22, 29,30-trisnorhopane gave a correlation with the environment-related principal component of —0.77. This is poor compared to the markers found among the steranes.

Figure 12 displays the oils in components determined by using 13β(H), 17α(H)-diacholestane (20S) and normoretane for marker projections [9]. These components account for 45.6 and 11.3%, respectively, of the total variance of the normalized distributions of pentacyclic triterpanes and steranes. The angle of 82.5° shows the original correlation between 13β(H), 17α(H)-diacholestane and normoretane. Comparison of Fig. 12 with Fig. 4(a) shows that the oils investigated are amenable to a simple, condensed description in terms of markers which separate the oils according to depositional environment and maturity.

Finally, Fig. 8 shows that the variables 1, 2, 3 and 11 are marker candi-

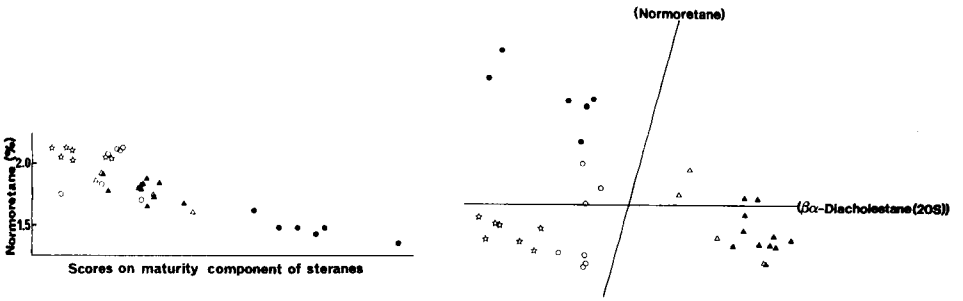

Fig. 11. Percent normoretane of total triterpanes plotted vs. the scores on PC2 (maturity) for the sterane matrix.

Fig. 12. Samples plotted on axes determined by marker projections based on normalized distribution of triterpanes and steranes. Markers used are normoretane (I) and 13β(H), 17α(H)-diacholestane (20S).

dates for maturity among the aromatic steroids. Correlation coefficients in the range 0.70—0.74 between these compounds and the maturity-related principal component of the non-aromatic steranes show that all these compounds are sensitive to other effects. Minor correlations with the environment and organic input-related principal components of the steranes strengthen the suspicion that migration phenomena influence this fraction. Accordingly, although the projection of the aromatic steroid distribution on variable 1 accounted for 65.7% of the total variance of this fraction, no single aromatic steroid appears to be a good molecular marker for maturity.

Conclusions

Projection techniques have proved useful for interpreting different biomarker fractions. Markers (i.e., variables carrying specific geochemical information) are revealed, and their potential for describing geochemical factors and whole fractions is evaluated. These markers can be used as exploratory tools for investigating the information of unresolved fractions. Further work is necessary on samples spanning a larger geographical area, both to obtain reliable source-specific parameters and to study the influence of migration, a process not well understood at present.

The authors thank R. Eastgate, Norsk Hydro, Bergen, R. Manne, University of Bergen and S. Wold, University of Umeå for valuable suggestions and discussions.

REFERENCES

1 B. P. Tissot and D. H. Welte, Petroleum Formation and Occurrence. A new approach to oil and gas exploration, Springer Verlag, Heidelberg, 1984.
2 W. K. Seifert and J. M. Moldowan, Geochim. Cosmochim. Acta, 42 (1978) 77.
3 W. K. Seifert and J. M. Moldowan, Geochim. Cosmochim. Acta, 43 (1979) 111.

4 O. H. J. Christie, T. Meyer and P. W. Brooks, Anal. Chim. Acta, 161 (1984) 75.
5 N. Telnæs and B. Dahl, Org. Geochem., 10(1—3) (1985) 425.
6 G. A. Warburton and J. E. Zumberge, Anal. Chem., 55 (1983) 123.
7 O. M. Kvalheim, Anal. Chim. Acta, 177 (1985) 71.
8 S. Wold, Pattern Recognition, 8 (1976) 127.
9 O. M. Kvalheim and N. Telnæs, Anal. Chim. Acta, 191 (1986) 87.
10 S. Wold, Technometrics, 20 (1987) 397.
11 O. M. Kvalheim, Simca user's guide, University of Bergen, 1985.
12 O. Sieskind, G. Joly and P. Albrecht, Geochim. Cosmochim. Acta, 43 (1979) 1675.
13 A. S. Mackenzie, C. F. Hoffmann and J. R. Maxwell, Geochim. Cosmochim. Acta, 45 (1981) 1345.

Analytica Chimica Acta, 191 (1986) 111—123
Elsevier Science Publishers B.V., Amsterdam — Printed in The Netherlands

ELUCIDATING CHEMICAL REACTIVITY BY PATTERN RECOGNITION METHODS

J. GASTEIGER*, H. SALLER[a] and P. LÖW[a]

Organisch-chemisches Institut, Technische Universität München, D-8046 Garching (Federal Republic of Germany)

(Received 15th July 1986)

SUMMARY

Methods have been developed that allow important chemical effects to be quantified. Parameters calculated with these procedures can be used to investigate both quantitative and qualitative information on chemical reactivity. A variety of statistical and pattern recognition methods is used for that purpose. These studies lead to reactivity functions that allow the prediction of the course of complex organic reactions.

Analytical chemists and organic chemists have quite different perspectives of their disciplines and different approaches to solving their problems. An analytical chemist heavily relies on instruments and bases his conclusions on the evaluation of many numbers. Modern spectrometers produce a profusion of data of high precision. Therefore, the analytical chemist must generally resort to powerful data-processing techniques to manage this large amount of information. An organic chemist, in contrast, bases his conclusions to a large extent on non-numerical information. Observations on the course of reactions have led the organic chemist to form concepts that allow him to order and explain the experimental events. These notions can be names given to reactions that share certain characteristics (Cannizzaro reaction), can specify net observations on reactions (substitution, elimination) or stereochemistry (suprafacial, enantioselective), or can express some physicochemical factor (inductive effect). These semantic models have created a world of their own, largely inaccessible to the uninitiated. However, it must be pointed out that these concepts are mostly used, even by the experts, only to explain observations in hindsight. It is difficult to make predictions with these concepts because, quite often, they are only defined in a qualitative manner.

To illustrate, Fig. 1 shows possible pathways for the reaction of an alkyl bromide with a nucleophile. Each of the branching points has been characterized by organic chemists with a specific name. However, it is not easy to decide which branch will be followed for a specific reaction with a given

[a]Present address: Chemodata Computer-Chemie GmbH, D8038 Gröbenzell, Federal Republic of Germany.

0003-2670/86/$03.50

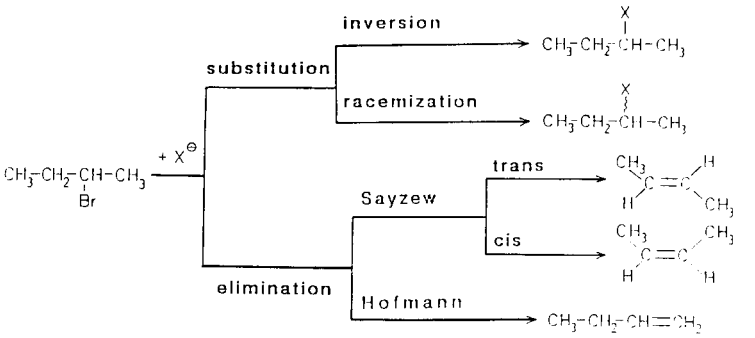

Fig. 1. Potential pathways for the reaction of an alkyl bromide with a nucleophile.

group R and nucleophile X in a particular solvent. At best, attempts can be made to assess the major pathway, far away from a quantitative prediction of the yields of the various products.

However different are the approaches of analytical and organic chemists to solving their problems, the nature of their problems has much in common. Both deal with multivariate problems for which the exact mathematical relationship is either not known or too complex to be explicitly solvable. Many analytical chemists are now routinely using multivariate data-processing methods for studying their problems. The question is therefore whether these methods can also be of benefit in the problems that organic chemists face. Many multivariate data-processing methods can in fact help in predicting the course and rate of organic reactions.

CHEMICAL REACTIVITY: A MULTIVARIATE PROBLEM

Chemical reactions are simultaneously influenced by many effects and they are so to various extents. This makes the quantitative treatment of chemical reactivity a difficult problem. The method most widely used for quantitative analysis of reactivity data is to establish a linear free enthalpy relationship (LFER). In the LFER treatment the reaction under investigation is compared with a reference system, either some physical data or another reaction. However, the basic assumption of LFER treatment, the separation of a system into substituent, skeleton, and reaction site is artificial and breaks down when the types of interactions between these subunits change within a series of compounds. The existence of several simultaneous interaction mechanisms has led to a profusion of different tables of substituent parameters making the selection of the appropriate scale for a specific problem a matter of chance.

A study was therefore undertaken to overcome the deficiences of LFER approaches. Rather than arbitrary separation of a molecule into skeleton, substituent and reaction site, it is considered necessary to treat each molecule as an integral entity, performing calculations on molecules as a whole. Even when effects can be located on specific atoms or bonds, accounting for the influence of more remote parts of the molecule was deemed necessary. Better

to describe the reacting species, organic molecules, the concepts that an organic chemist uses are a logical starting point. For these concepts, such as partial atomic charges, inductive effects, resonance effects, polarizability effects, bond dissociation energies, steric effect, and solvent effects, comprise a lot of chemical knowledge in a rather concise manner. As already mentioned, their biggest drawback, however, is that there is only a qualitative or, at the most, a semiquantitative feeling for the magnitude of these effects. The goal has therefore been to quantify the chemical effects.

From the outset, the treatment of large molecules and big data sets was envisaged. This requires rapid calculations to be able to handle so many large systems. Therefore, because of restraints on computer time, a quantum-mechanical treatment had to be rejected. Rather, it was necessary to develop novel methods. Because of the empirical nature of these methods, extensive comparisons with physical and chemical data were conducted to establish the significance of the values calculated for the various effects.

As most of the methods have been described in detail elsewhere, brief hints will suffice here. A broader overview of the methods and their application to reaction prediction is available [1].

Properties and effects utilized

Bond dissociation energies. The procedure for calculating bond dissociation energies (BDE) is basically an additivity scheme and works along similar lines as the method for obtaining reaction enthalpies [2]. The program contains tables of parameters for specific structural subunits. Each type of bond and radical center has a base value which is, however, modified depending on the substitution pattern. Thus, for example, the changes in the dissociation energy of a C—H bond in going from a primary to a secondary to a tertiary carbon atom are well reproduced. The values obtained for these bond dissociation energies are usually accurate within 1.0 kcal mol^{-1} [1].

Partial atomic charges, residual electronegativities and charge flow. The method for calculating partial atomic charges, q, in molecules starts from the electronegativity concept. The mutual dependence of electronegativity on charge and of charge transfer on electronegativity difference is solved by an iterative procedure [3]. This partial equalization of orbital electronegativity (PEOE) leads to partial charges on the atoms of a molecule that reflect both the type of atom and its molecular environment. Associated with this charge, each atom receives a uniquely defined residual electronegativity value, χ, that is a measure of the inductive effect. Furthermore, values for the amount of charge that is transferred over a certain bond, the charge flow, q_f, are obtained. It has been shown that with these charge values various physical data like dipole moments, ESCA binding energies, as well as ^{1}H- and ^{13}C-n.m.r. shifts can be calculated [3—6].

Resonance effect. For conjugated π-systems an extension of the above method had to be developed [7, 8]. Again, it was shown that the resulting π-charges can reproduce dipole moments, ESCA energies, and ^{13}C-n.m.r. shifts [8].

Polarizability effect. An effective polarizability, α_d, has been defined as a measure of the stabilization of a charge introduced into a molecule at a specific site [9]. Effective polarizability can be calculated from increments typical for an atom in a given valence state. These values are added in a manner that takes account of the distance of an atom from the charge center. Correlations with physical and chemical data have shown the significance of the values thus calculated.

To summarize, procedures have been developed that allow rapid assignment of quantitative values to important physicochemical effects used by the organic chemist to explain his observations. With these methods, parameters are obtained that allow a detailed description of energetic and electronic effects in molecules. Each atom and bond of a molecule is characterized by several readily calculated numbers (cf. Fig. 5). In the following paragraphs, it will be shown how these values can be used by multivariate data-processing methods to shed more light on chemical reactivity. However, it should also be pointed out that the calculations and correlations with physical data performed to establish the significance of the parameters and mentioned in the references are also of interest to the analytical chemist; for they allow the prediction of various spectroscopic data directly from structural information on molecules.

CHEMICAL REACTIVITY

Case 1: homogeneous set of quantitative data

Once the significance of the values calculated for the various chemical effects with physical data had been established, attention was turned to chemical reactivity data.

Initially, reactivity data on gas-phase reactions were chosen for several reasons. First, in the gas phase, the inherent reactivity of individual molecules is observed. Thus, the complicating effects of a solvent are absent and it can be hoped that the reactivity data can be reproduced with a few parameters only. Secondly, in recent years, many data of high numerical accuracy have been determined through new experimental techniques. Large series of compounds have been measured where the structure of the molecules was systematically changed. Thus, homogeneous sets of accurate data are available.

In this general context, application of multilinear regression analysis (MLR) is permissible. Standard precautions were taken. The number of parameters used was kept to a minimum. A particular parameter was only included if there was a definite indication of its relevance, on both physicochemical and statistical grounds. Furthermore, the sign of a coefficient had to correspond to the physicochemical interpretation of the particular parameter.

Several series of individual gas-phase reactions were studied independently. Most of the studies have been discussed thoroughly in papers already published [9—12]. Therefore, only a brief summary is given here.

Proton affinity of amines. Proton affinity (PA) values give the energy released on protonation in the gas phase. As long as the data set is restricted t

simple alkylamines (Fig. 2, reaction A), the PA values can be reproduced by a single parameter, the effective polarizability, α_d: PA = 209.2 + 2.70 α_d (n = 49, r = 0.984, s = 1.0 kcal mol^{-1}) [9].

When amines are included in the data set that also bear heteroatoms, the inductive effect of these heteroatoms has to be accounted for. This can be achieved by using an average value of the residual electronegativities, χ_{12}, of the atoms one and two bonds away from the nitrogen atom. This value is a measure of the electron-withdrawing power of the entire molecule exerted on the nitrogen atom. A two-parameter equation considering the values for the polarizability and the inductive effect can reproduce the experimental data of all 80 amines for which data were available at the time of investigation [10]:

$$PA = 343.0 + 2.99\,\alpha_d - 27.8\,\chi_{12}$$

(n = 80, r = 0.998, s = 1.33 kcal mol^{-1}). The signs of the coefficients express the fact that the protonated amine is stabilized by the polarizability effect whereas the inductive effect destabilizes the positive ion and therefore decreases the proton affinity.

Data on other gas-phase reactions. To explore the general validity of the parameters calculated for the various chemical effects, data for the other gas-phase reactions contained in Fig. 2 (B—E) were also studied by MLR. As above for the amines, two-parameter equations using the values of the polarizability and the inductive effect can reproduce both the proton affinities of

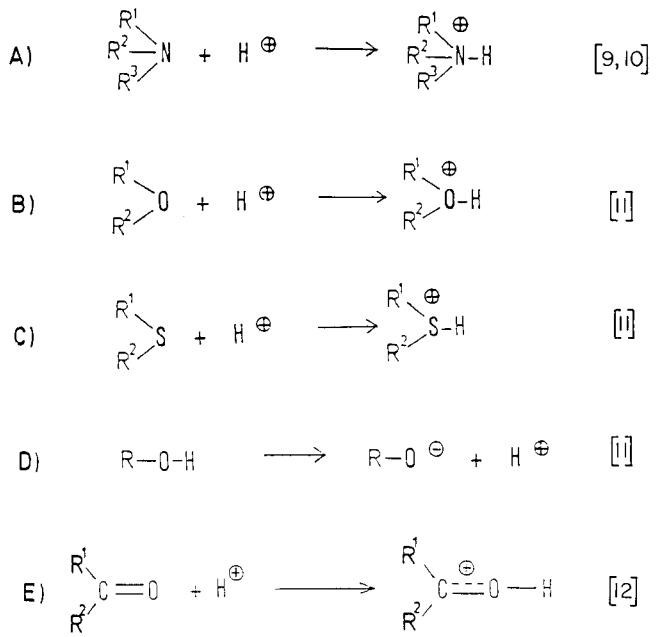

Fig. 2. Gas-phase reactions for which data have been analyzed by MLR.

alcohols and ethers (reaction B) as well as those of thiols and thioethers (C). The same two parameters, α_d and χ_{12}, are also sufficient for calculating values for reaction (D), the gas-phase acidity of alcohols. In this case, however, the coefficients have the same sign for both independent variables, reflecting that both effects tend to stabilize the resulting negative alkoxide ion. For the PA data of carbonyl compounds (reaction E), in addition to parameters for the polarizability and inductive effect, a measure of the hyperconjugation effect had to be included to account for its stabilizing effect on an empty orbital in the alkoxycarbenium ion.

The overall picture that emerges from these studies is that the parameters calculated for the various chemical effects are indeed able to reproduce quantitative data on chemical reactivity. Thus, the reactivities of some fundamental chemical reactions can be directly calculated from structural information on molecular species.

Case 2: qualitative information on reactive bonds

For the gas-phase reactions treated above, good quantitative data for rather extensive, homogeneous sets of molecules were available. This is a rather fortunate situation, not commonly met with organic reactions. For most organic reactions, knowledge on their reactivity is more qualitative in nature ("this compound is more reactive than the other"). In other cases, where quantitative values on reactivity are available, the data are of limited amount. The most serious problem is that the data are not statistically balanced and the data sets are inhomogeneous, i.e., the chemists ran their experiments under widely different conditions, changing too many parameters simultaneously. This precludes application of linear regression techniques.

Other ways were therefore sought to quantify chemical reactivity and to develop reactivity functions, even for those reactions where not enough quantitative experimental data are available. This certainly requires statistical methods more powerful than MLR. Detrimental as the lack of statistically balanced quantitative information on chemical reactivity is, there is also some positive point in analyzing chemical reactivity. Knowledge on chemical reactions is vast; chemists have studied very many reactions, and their investigations have shown the course of a large series of reactions. For many reactions, one knows which pathway, of the many conceivable ones, is actually followed. Thus, although the information on chemical reactions is qualitative in nature, but such information exists for a wide area of organic chemistry.

The reactivity space. In order to evaluate chemical reactivity even in those situations where only qualitative information (information about the groups or bonds that are reacting) is available, a variety of pattern recognition methods has been used. To do so, a space was first defined for applying these methods. As indicated above, methods for quantifying important chemical effects are available. The measures of these effects can be taken as coordinates of a space. Each bond of a molecule has uniquely defined values for these effects and is therefore represented by a clearly defined point in that space. As this space is used for studying chemical reactivity, it may be termed

the reactivity space. Figure 3 gives a simple three-dimensional space spanned by bond polarizability, charge difference, and electronegativity difference as coordinates. The bonds of iodine bromide and of hydrogen fluoride are taken as examples; iodine bromide has high bond polarizability but low charge and electronegativity difference, whereas the bond of hydrogen fluoride is characterized by a large charge and electronegativity difference but low polarizability.

Most organic reactions occur through heterolysis of bonds and formation of bonds between atoms of opposite polarity. However important these reactions are, quantitative understanding of these processes is not well developed. Investigations of heterolytic processes were therefore stressed. As a bond has two ways of breaking heterolytically (Fig. 4), each bond I—J will be represented by two points in a reactivity space, one corresponding to the charge pattern I(+) and J(—) and the other to I(—) and J(+).

In Fig. 5, the heterolysis of several single bonds of 2-cyclopentanone carboxylic acid is represented by points in a space defined by the resonance effect, R, bond dissociation energy, BDE, and charge flow, q_f. As an example, the two possibilities for the charge pattern in breaking the OH-bond are given by point 1 and point 7, respectively (Fig. 4). The difference between these two points can, to a large extent, be attributed to the charge flow; in the heterolysis corresponding to point 7, the charges are assigned to the atoms in a manner that is already outlined in the ground state, whereas in point 1, the charge is shifted against the initial polarity of that bond. Another major distinction between points 1 and 7 comes from the resonance effect. A negative charge on the oxygen atom of the carboxyl group can be better stabilized

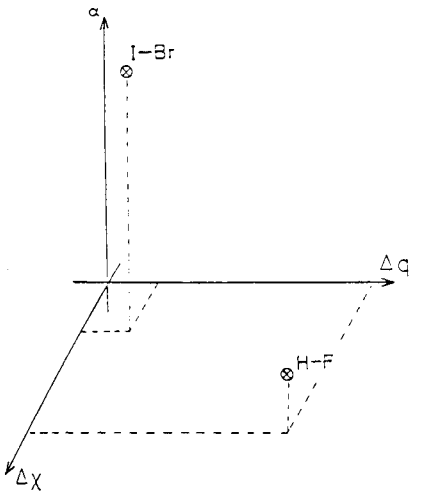

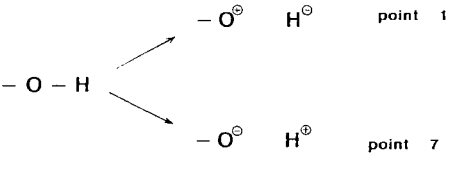

Fig. 3. Reactivity space defined by bond polarizability, charge and electronegativity difference.

Fig. 4. The alternatives for heterolysis of the OH-bond of 2-cyclopentanone carboxylic acid.

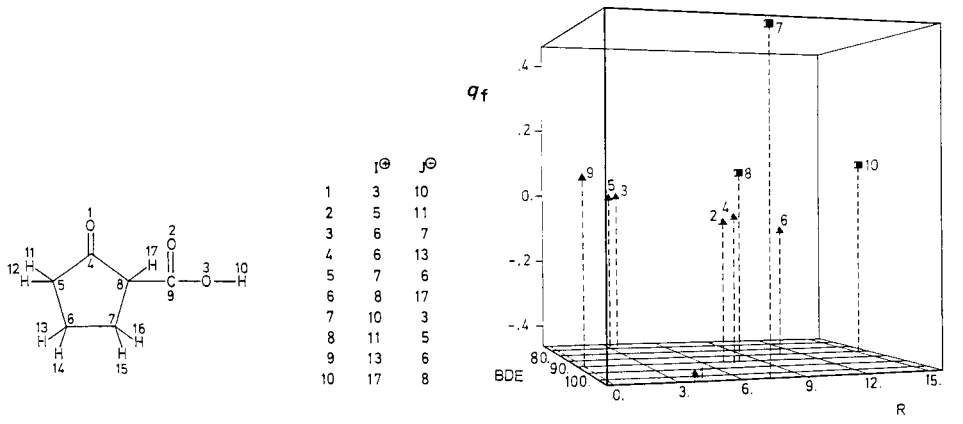

Fig. 5. Heterolysis of bonds of 2-cyclopentanone carboxylic acid in a reactivity space spanned by the resonance effect, R, bond dissociation energy, BDE, and charge flow, q_f. (■) Breakable bonds; (▲) unbreakable bonds (see text).

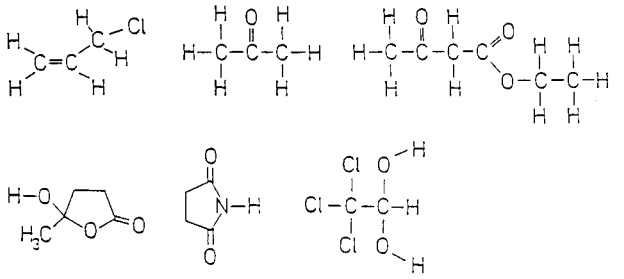

Fig. 6. Examples of molecules contained in the data set for representing aliphatic chemistry.

by the resonance effect than a positive charge on that atom. However, both points have the same value for the BDE, as this value refers to a homolysis of a bond, a process which is the same both for point 1 and for point 7.

As an additional feature, the points of Fig. 5 are marked according to whether the corresponding breaking of a bond is considered likely or not. Reactive bonds are distinguished by cubes, non-reactive bonds by square pyramids. With this molecule, the dissociation of a proton from three sites was considered likely, leading to the carboxylate (point 7), or to a carbanion at atom 5 (point 8) or atom 8 (point 10), respectively. Reactive and unreactive bonds clearly separate in this space. Furthermore, the more reactive a bond, the further away the corresponding point is found from the plane separating breakable and unbreakable bonds. From the chemical point of view, in 2-cyclopentanone carboxylic acid, acidity will decrease in the order OH > C_8—H > C_5—H. This sequence is indeed reflected in a decrease of the distance of point 7, point 10, and point 8, in that order, from the unreactive bonds. Thus, the reactivity observed in 2-cyclopentanone carboxylic acid is represented in that three-dimensional reactivity space of Fig. 5 quite well.

This promising result warranted investigation of a wider range of chemical reactivity. In addition, attempts were made to exploit the properties of reactivity spaces to arrive at quantitative functions expressing chemical reactivity. To investigate the reactivity of a broad range of aliphatic chemistry, 29 molecules were chosen as a data set to cover most functional groups and structural variations found in aliphatic compounds. Figure 6 gives some representative examples.

Altogether, these molecules contained 385 bonds. As each bond has two choices for shifting the charges on heterolysis, 770 bond breakings had to be considered. For each such bond breakage, the values of BDE, bond polarizability, σ-charge difference, charge flow, σ-electronegativity difference, and the resonance effect were calculated (Table 1). The large size of this data set and the many parameters for each bond again underscore the need for rapid calculations of all those chemical effects. Of these bonds, 116 bonds were selected for further investigation. Thus, the space for studying the reactivity of aliphatic bonds consisted of 116 points in a six-dimensional space.

Pattern recognition methods of unsupervised and supervised learning were applied to investigate this reactivity space and to get more insight into chemical reactivity. For the application of supervised learning techniques, the bonds were characterized as either reactive or unreactive. This classification rested on rather unequivocal chemical knowledge. Of the 116 bonds, 42 bonds were considered breakable and 74 unbreakable.

Unsupervised learning techniques

A principal component analysis showed two factors being of predominant importance with an additional third factor necessary to describe 85% of the variance in the data set (Table 2). Thus, a sizable reduction in the dimensionality of the reactivity space from six to three dimensions is possible without much loss of information. The first factor largely comprises effects in the σ-electron distribution, the second factor is predominantly loaded with BDE, bond polarizability and the resonance effect, and the third factor represents some other effects in σ-electron distribution.

In a cluster analysis, bonds of similar type and those belonging to the same functional groups are found in common clusters. The grouping of these clusters indicates interesting chemical relationships.

Supervised learning techniques

In these two studies, the overall structure of the reactivity space was investigated without making assumptions on the reactivity of bonds. In the following investigations, bonds were classified as either breakable or unbreakable and this information was used by supervised pattern recognition methods. Table 3 gives the results of a K-nearest neighbor analysis. Both breakable and unbreakable bonds can, to a large extent, be correctly classified over a broad range of the number, K, of neighbors being considered. This shows that reactive and unreactive bonds clearly separate in the six-dimensional reactivity space.

TABLE 1

The parameters for the chemical effects for two bonds of 2-chlorobutanoic acid: bond dissociation energy, BDE, bond polarizability, α, charge difference, Δq_σ, charge flow, q_f, electronegativity difference, $\Delta\chi_\sigma$, and resonance effect, R

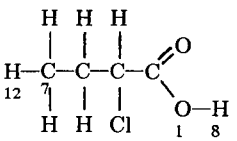

Parameter	7—12		1—8	
	C^+H^-	C^-H^+	O^+H^-	O^-H^+
BDE	98.67	98.67	108.13	108.13
α	4.41	4.41	3.60	3.60
$\Delta_{q\sigma}$	−0.086	0.086	−0.447	0.447
q_f	−0.046	0.046	−0.441	0.441
$\Delta\chi_\sigma$	0.10	−0.10	1.56	−1.56
R	3.84	0.0	3.69	7.25

TABLE 2

Results of a principal components analysis

Factor	% Variance	Cumulative %		Factor 1	Factor 2	Factor 3
1	38.9	38.9	BDE	0.129	−0.835	0.040
2	33.5	72.4	α	−0.126	0.849	−0.039
3	12.7	85.1	Δq_σ	0.845	0.113	0.500
			q_f	0.997	0.080	0.023
			$\Delta\chi_\sigma$	−0.749	−0.037	0.610
			R	0.024	0.449	0.068

There can be a sizeable reduction in the dimensionality of the reactivity space without much loss of capability for correct classification. This can be seen from linear discriminant analysis and logistic regression analysis. A linear discriminant analysis shows that even with two variables (resonance effect, R, and charge flow, q_f, a high degree of correct classification is obtained classified to a high degree (Table 4).

One method that has been found particularly useful is logistic regression analysis. In this method, an initial binary classification, in our case the classification of whether a bond is breakable or unbreakable, is considered as an input probability, P_o, that is modelled by a calculated probability P. P is taken as an exponential function $P = 1/[1 - \exp(-f)]$ where the exponent, f, is expanded as a linear function in the parameters x_i used: $f = c_0 + c_1x_1 + c_2x_2 + \ldots$. It is observed that, again, with the two variables resonance effect,

TABLE 3

Results of a K-nearest neighbor analysis

K	1	2	3	4	5	6	7	8
% correct classification	94.0	94.0	95.7	94.8	94.0	94.8	94.8	94.8

TABLE 4

Results of a linear discriminant analysis

	Group	% correct	Classified into group	
			0	1
Unbreakable	0	95.9	71	3
Breakable	1	83.3	7	35
Total		91.4	78	38

R, and charge flow, q_f, a high degree of correct classification is obtained (Table 5). As an additional benefit, a function, f, based on the above two parameters is obtained that performs the classification. It was mentioned in relation to Fig. 5 that the more reactive a bond, the farther it is from the unreactive bonds. This suggested the use of function f obtained through logistic regression analysis for the classification problem, as a quantitative measure of reactivity. Indeed, it has been observed that more reactive bonds are distinguished by higher values of f.

This function as developed by the above analysis, and a similar function obtained from investigation of a data set of organic ions and zwitterions have been applied to predict the most reactive bonds in neutral and charged organic species. This allowed prediction of the most likely reaction mechanisms of complex organic reactions. The course and outcome of organic reactions can be predicted.

Figure 7 shows such a network of reaction steps obtained for the problem of predicting the most likely product for Lewis acid-catalyzed rearrangement of the menthane-bis-epoxide (1). The intermediates of each reaction step are arranged from left to right with decreasing value of the function f. It is important to note that the charges on the structures of Fig. 7 only indicate the direction of charge shift in heterolysis of the corresponding bonds. They must not be taken at face value to correspond to the development of full unit charges. Overall, it is thus predicted that the bond-breaking pattern indicated with structure 2 is the most favored one. Making three bonds in the formal intermediate 2 leads to structure 3 as being predicted to be the most favored reaction product. This is a surprising result, as one of the oxirane rings is broken in a manner leading to the less stable carbenium ion, and above all,

TABLE 5

Results of logistic regression analysis[a]

Group	Classification	
	0	1
0	72	2
1	6	36

[a] $f = -4.87 + 37.33\, q_t + 0.256\, R$.

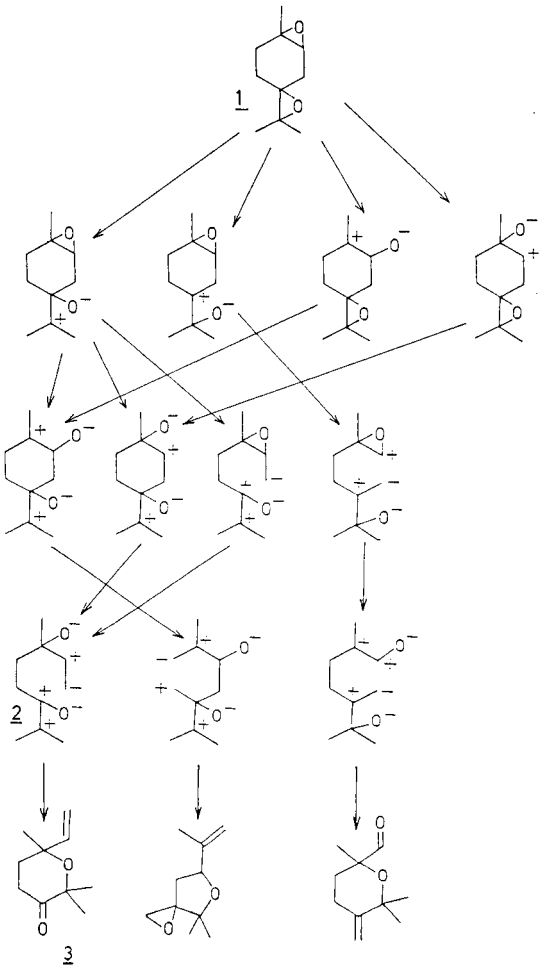

Fig. 7. Prediction of the network of reaction steps for the rearrangement of 1, 2: 4, 8-diepoxy-*p*-menthane (1).

it is predicted that even a CC-single bond in an unstrained six-membered ring should be broken. Indeed, this prediction is correct as 3 is the experimentally observed product [13].

Other examples for the correct prediction of the course and products of complex organic reactions have been reported [1].

CONCLUSION

It has been shown that the concepts that an organic chemist uses to order his observations and to discuss reaction mechanisms can be put on a quantitative basis. The procedures developed for that purpose provide parameters that can be used for studying information on chemical reactivity.

When a homogeneous set of enough quantitative data on chemical reactivity is available, multi-linear regression techniques might suffice. In other cases, more powerful statistical and pattern recognition methods have to be applied. With such methods it is even possible to transform qualitative information on whether bonds are reactive or not into reactivity functions that allow assignment of quantitative values for chemical reactivity. With such functions, correct predictions on the course and products of complex organic reactions can be made. Thus, the conceptual models of the organic chemists and the statistical models of chemometrics can be combined to further understanding of chemical reactivity.

Support of this research by Deutsche Forschungsgemeinschaft and by Imperial Chemical Industries plc, England is gratefully acknowledged. We thank Dr M. G. Hutchings for many interesting discussions.

REFERENCES

1 J. Gasteiger, M. G. Hutchings, B. Christoph, L. Gann, C. Hiller, P. Löw, M. Marsili, H. Saller and K. Yuki, Topics Curr. Chem., 137 (1987) 19.
2 J. Gasteiger, Comput. Chem., 2 (1978) 85; Tetrahedron, 35 (1979) 1419.
3 J. Gasteiger and M. Marsili, Tetrahedron, 36 (1980) 3219.
4 J. Gasteiger and M. D. Guillen, J. Chem. Res. (S) (1983) 304; (M) (1983) 2611.
5 J. Gasteiger and M. Marsili, Org. Magn. Reson., 15 (1981) 353.
6 J. Gasteiger and I. Suryanarayana, Magn. Reson. Chem., 23 (1985) 156.
7 M. Marsili and J. Gasteiger, Croat. Chem. Acta, 53 (1980) 601.
8 J. Gasteiger and H. Saller, Angew. Chem., 97 (1985) 699; Angew. Chem. Int. Ed. Engl., 24 (1985) 687.
9 J. Gasteiger and M. G. Hutchings, J. Chem. Soc., Perkin Trans. 2, (1984) 559.
10 M. G. Hutchings and J. Gasteiger, Tetrahedron Lett., 24 (1983) 2541.
11 J. Gasteiger and M. G. Hutchings, J. Am. Chem. Soc., 106 (1984) 6489.
12 M. G. Hutchings and J. Gasteiger, J. Chem. Soc., Perkin Trans. 2, (1986) 455.
13 T. L. Ho and C. J. Stark, Justus Liebigs Ann. Chem., (1983) 1446.

Analytica Chimica Acta, 191 (1986) 125—131
Elsevier Science Publishers B.V., Amsterdam — Printed in The Netherlands

THE PLAYGROUND OF CHEMOMETRICS

G. KATEMAN

Department of Analytical Chemistry, University of Nijmegen, Toernooiveld, 6525 ED Nijmegen (The Netherlands)

(Received 27th May 1986)

SUMMARY

A useful description of chemometrics is "the software part of analytical chemistry". This description opens wide fields of applications and does not contradict the more official definition of "statistical and mathematical methods". The typical systems approach allows the application of chemometric methods in such diverse fields as sampling, experimental design, pattern recognition and laboratory organization, some examples of which are given.

Analytical chemists try to obtain information from material systems or objects by chemical, physical or physicochemical techniques. These techniques are often very sophisticated, very precise and sensitive, and as a rule expensive. The input of analytical chemistry consists of samples, representative parts of the objects under investigation, which may be homogeneous, heterogeneous or correlated. The samples are subjected to preparation to convert them to a suitable form for measurements, and the data obtained are processed by more or less sophisticated techniques. This output is intended for sample description, or for process monitoring or control, at the behest of the principal, owner, controller or manager of the object or process.

Chemometrics plays in this field but, as chemometrics is rarely hampered by the use and needs of analytical instrumentation (hardware) and is concerned only with the data (software) in analytical chemistry, its field is somewhat wider. With a rather small collection of techniques, chemometrics tries to serve analytical chemistry but, as it is still a young part of chemistry, many think its practitioners are just playing around. The playground of chemometrics covers the terrain of the principal and his purposes, the object and its peculiarities, and analytical chemistry with its chemical preprocessing and physical measurements.

Taking chemometrics seriously, it must be stressed that one of the most urgent reasons for the introduction of chemometrics is the ever increasing pressure on the quality of analytical results. Quality can be defined as the (numerical) value of a set of wanted properties. The list of properties in analytical chemistry is not long, but difficult to describe in quantitative terms. Accuracy, precision, limit of detection and sensitivity are fairly well

0003-2670/86/$03.50

defined and partly quantifiable. Robustness, reliability, compatibility, difficulty, speed and even cost are much less easy to define or quantify.

As the purpose of analytical chemistry is the collection of information, it seems appropriate to try to use information as a common denominator for analytical quality. According to Shannon's definition, information is the difference between the entropy before and after a message or, translated into analytical language, information is what more is known about the object after the analysis than before it. As inexact as this definition seems to be, a mathematical description can be given [1]:

$$\text{entropy. } H = -\sum_{i=1}^{n} P_i \, ld \, P_i$$

$$\text{information: } I = H_{\text{before}} - H_{\text{after}}$$

where, for normal distributions,

$$P = (2\,\sigma^2\,\pi\,e)^{-1/2} \exp\left[-(c-\mu)^2/2\sigma^2\right]$$

$$H = ld\,\sigma\,(2\,\pi\,e)^{1/2}$$

$$I = ld\,(\sigma_{\text{before}}/\sigma_{\text{after}}) = -1/2\;ld\,R$$

where R is the variance reduction. In general, $I(\text{tot}) = \Sigma_{i=1}^{n} I + 1/2\;ld$ |correlation|.

A principal concern is then how to obtain more information, for less cost, with more confidence, and within possible physical boundaries (Table 1). As information is the difference between knowledge before and after measurements, an important influencing factor is the availability of prior knowledge, which can be exploited by several means. A quite new but quickly expanding technique is the expert system, which stores knowledge as rules and facts and which is able to search efficiently in these knowledge bases.

Like medicine, analytical chemistry is largely an art. That means that there are no scientific foundations to carry the entire analytical process from problem to solution. Most of the techniques are scientifically or technically sound and well founded, but it is not possible to predict which method will give the ultimate answer for which problem. This absence of theoretical rules can be compensated for by experience and so analytical chemistry depends on highly trained and experienced workers. They know the peculiarities of the sample and the instruments, they seek in the literature the most promising methods and choose one to the best of their knowledge. If the method shows unexpected deviations during its testing, they change conditions, reagents and instruments and obtain in most cases a result that can be trusted within known boundaries.

This art is difficult to teach and difficult to describe in clear unambiguous text. This is where expert systems may help. An expert system contains a rule base, a data base and an inference machine. The data base contains facts,

TABLE 1

Increasing the information yield

Use prior information	Expert systems; state estimation and prediction
Increase productivity	Curve resolution; pattern recognition
Increase relevancy	Measurability
Find cheaper ways of producing information	Laboratory organization; experimental design; optimization

e.g., the properties of an instrument or of chemicals and reagents; the rule base contains links between facts. The inference machine contains rules to find answers to questions. As the programming language allows manipulation of symbols (words, sentences) as well as data, and some systems allow manipulation of "fuzzy" answers (not only yes and no, but also "perhaps" or "maybe"), these systems can find their way through the input knowledge and produce reasonable answers and questions or suggest reasonable paths to solutions. With these systems, it is possible for instance to build a system that uses its input rules and facts to explain an infrared spectrum [2]. More sophisticated systems can interpret mass spectra and n.m.r. spectra [3]. Other systems can guide the medical doctor to the right medicine [4]. Because the interpretation of spectra is a mixture of art and science, as is the choice of the optimal method of analysis, it should be possible to use the program structure (often called an "empty shell") for the guidance of the analyst. Efforts to produce such expert systems are presently being made in many places. As these systems can "learn" (i.e., use the knowledge of the human analyst) they are a means of collecting knowledge or influencing the H_{before} factor. The effort to diminish remaining uncertainty can be fully exploited to produce information.

A totally different approach is not based on experience but on the exploitation of theory from other disciplines, in particular, statistics and operations research. One way is to use all knowledge that builds up during measurements. The basis is a simple and straightforward model of analytical chemical measurements:

$$x_k = F_k\, x_{k-1} + w_{k-1} \qquad \text{or } \mathbf{x}_k = \mathbf{F}_{k/k-1}\, \mathbf{x}_{k-1} + \mathbf{W}_{k-1}$$

$$y_k = B_k\, x_k + v_k \qquad \text{or } y_k = \mathbf{B}_k^T\, \mathbf{x}_k + v_k$$

$$Q_{k-1} = \text{var}\,(w_{k-1}) \qquad \text{or } \mathbf{Q}_{k-1} = \text{cov}\,(\mathbf{w}_{k-1})$$

$$R_k = \text{var}\,(v_k) \qquad \text{or } \mathbf{R}_k = \text{cov}\,(v_k)$$

The first equation describes the system under investigation. The symbol x represents a state, e.g., the concentration of a component. This can be one component as in the left-hand equation or a vector representation of a list of components as in the right-hand equation. Factor F denotes a transition coefficient; $F = 1$ means that the state does not change as a function of

k (k is, e.g., time or sequence). For autoregressive systems, F can be $F = \exp(-Tx^{-1})$, a measure of the speed of change. Symbol w_k denotes the statistical fluctuations in the state of the object. The second equation is a model of the measurements, where B denotes the calibration coefficient and v_k the measurement noise. A recursive description of the process of measurements and state estimation has been described by Kalman [5—7].

Given the knowledge acquired during the previous measurements, x_{k-1}, a prediction can be made of the state that is expected, using the model:

$$\bar{x}_k = F_k \hat{x}_{k-1} \qquad \text{or } \hat{\mathbf{x}}_{k/k-1} = \mathbf{F}_{k/k-1} \hat{\mathbf{x}}_{k-1/k-1}$$

This prediction is corrected by the measurements y and gives the best estimate:

$$\hat{x}_k = \bar{x}_k + G_k(y_k - B_k \bar{x}_k) \text{ or } \hat{x}_{k/k} = \hat{\mathbf{x}}_{k/k-1} + G_k (y_k - \mathbf{B}_k^T \hat{x}_{k/k-1})$$

where G_k is a proportionality factor. It should be noted that the estimate uses all previous knowledge and corrects this with the measurements, instead of using only the new measurements.

The variance in the estimate can be predicted by

$$\overline{P}_k = F_k \hat{P}_{k-1} + Q_{k-1} \quad \text{or} \quad P_{k/k-1} = \mathbf{F}_{k/k-1} P_{k-1/k-1} \mathbf{F}_{k/k-1}^T + Q_{k-1}$$

where Q is the system noise covariance, and the proportionality factor G can be estimated by

$$G_k = B_k \overline{P}_k (B_k^2 \overline{P}_k + R_k)^{-1} \quad \text{or} \quad G_k = \mathbf{P}_{k/k-1} B_k (\mathbf{B}_k^T P_{k/k-1} \mathbf{B}_k + R_k)^{-1}$$

where R is the measurement noise covariance. Finally, P can be estimated by

$$\hat{P}_k = \overline{P}_k - B_k G_k \overline{P}_k \quad \text{or} \quad P_{k/k} = \mathbf{P}_{k/k-1} - G_k \mathbf{B}_k^T P_{k/k-1}$$

The information $I_k = H_{k-1} - H_k$ and $I(\text{tot})_k = H_0 - H_{k-1} = \sum_{i=1}^{k} I_i$ can be calculated from the state estimate. If the probability density is assumed to be normally distributed, then

$$H_k = 1/2\ ld\ (2\pi e P_k) \quad \text{or} \quad H_k = 1/2\ ld\ [(2\pi e)^n |P_{k/k}|]$$

and $I_k = 1/2\ ld\ [(B \overline{P}_k / R_k) + 1]$

In analogous ways, state estimates can be used to predict the state one or more steps ahead and control the measurements. The total information $I(\text{tot})_k$ follows from the additive relation $I(\text{tot}) = I(\text{pred}) + I(\text{filt})$ and the calculated information yields [8, 9]:

$$I_k = 1/2\ ld\ (\hat{P}_{k-1}/\hat{P}_k)$$

$$= 1/2\ ld\ (\hat{P}_{k-1}/\overline{P}_k) + 1/2\ ld\ (B \overline{P}_k / R_k + 1) = I(\text{pred})_k + I(\text{filt})_k$$

This optimal way of obtaining information from measurements can be applied in many analytical processes, e.g., electroanalysis, optimal multicomponent analysis, optimal titrations or optimal recalibration decisions [10—13]. This last application is characteristic of the method: all knowledge

that can be obtained during a series of measurements is used to decide when to recalibrate the system, instead of basing this decision on more or less fuzzy feelings of urgency. Full details were reported recently [14].

Another approach to enhancing the information yield in analytical chemistry is to squeeze all information from the measurement. An example of this approach is demonstrated in the curve resolution of the two-dimensional data matrix obtained from high-performance liquid chromatography (h.p.l.c.) with diode-array u.v.-visible detection. With this method, one obtains many (digitized) spectra during a h.p.l.c. run. By applying principal components and iterative target transformation analysis, it is possible to deconvolute badly separated chromatographic peaks and to estimate the spectra of the components [15, 16]. Examples have been given for handling mixtures of polynuclear aromatic hydrocarbons and proteins [16].

Another way to use data to their full extent is to use pattern recognition. Roughly, this method has two aspects. The first is to "cluster" data in groups that seem to be related; during the process of clustering, the information that is represented by the grouped data changes. Using the degree of clustering with the highest information content seems appropriate, but it may not be certain that this information is relevant information, as the clustering may be superficial [17, 18]. The second aspect is the classification of data into categories that are known, possibly by the clustering method. In this way, relevance is enhanced as the meaningless array of data has been ordered. The techniques used in manipulating multidimensional data are similar to the methods used in curve-fitting procedures.

Increasing the information from analytical procedures can also be done by increasing the efficiency of the measurement. In fact, this means that only relevant information should be produced. In plain language, not referring to Shannon's definition, it is necessary to produce only information derived from "any difference that makes a difference". An example can be found in sampling and analyzing samples from a process that has to be controlled. By using the Kalman predictions mentioned above, it can be shown that the increase in certainty of a sampled process (in fact, the information) depends on a number of parameters. These parameters not only reflect classical analytical characteristics of the measurement, e.g., precision, but also such parameters as speed of analysis and sampling rate.

Stated more precisely, for a first-order autoregressive process (most processes comprising mixing of the object under investigation) that can be characterized with a correlation constant, Tx, the information yield is $I = 1/2ld(\mathrm{var}_{\mathrm{before}}/\mathrm{var}_{\mathrm{after}})$ where $\mathrm{var}_{\mathrm{before}}$ is the variance of the uncontrolled process and $\mathrm{var}_{\mathrm{after}}$ is the variance that is or can be obtained after control. The theory of measurability [19] is applicable. The measurability can be defined as $m^2 = (\mathrm{var}_{\mathrm{before}} - \mathrm{var}_{\mathrm{after}})/\mathrm{var}_{\mathrm{before}}$ and $I = -1/2\ ld\ (1 - m^2)$. Measurability can be split to $m_t = m_d m_a m_g m_n$, where $m_d = \exp(-d)$ and $d = Td/Tx$, $m_a = \exp(-a/2)$ and $a = Ta/Tx$, $m_g = \exp(-g/3)$ and $g = Tg/Tx$, and

$$m_n = \left\{[1 + a \text{ var } (s)]^{1/2} - [a^2 + a \text{ var } (s)]^{1/2}\right\} /(1 - a) = 1 - [a \text{ var } (s)]^{1/2}$$

for $a \ll 0.2$.

Here $s = (\text{var}_{\text{anal}}/\text{var}_{\text{before}})^{1/2}$; Td is the analysis time, Ta the sample distance and Tg the sample time, with Tx as the correlation time.

This approach allows the characterization of analytical methods in relation to the process to be measured by means of one parameter, information yield. The classical example is the ranking of analytical methods [19]. A similar general approach to characterization by information power can be extended to more complex systems such as complete laboratories. The organization of a laboratory is always such that the capacity to analyze samples is finite. Queueing theory then predicts that waiting times have a certain distribution and that the mean waiting time depends on the mean inter-arrival time and the utilization of the service system [20]. Combined with the aforementioned theory on information production in processes, it can be calculated that the information depends on the type of distribution of arriving samples, the type of distribution of the analysis times and the organization of the laboratory. In most cases, this leads to maximal information production at a laboratory utilization far below 100%, often between 40 and 60% [21]. The distribution of sample arrivals and of analysis times can be random (M) or deterministic (D); when in A/B/1, A denotes sample arrivals and B analysis times, the measurability and so the information yield can be calculated. For M/M/1 systems,

$$m^2 = (1 - \rho)(1 + 2\bar{a})^{-1}(\bar{d} - \rho + 1)^{-1}$$

For M/D/1 systems,

$$m^2 = 2\bar{a}(1 - \rho)(1 + 2\bar{a})^{-1}[(2a - 1)\exp(2\bar{d}) + 1]^{-1}$$

and for D/M/1 systems,

$$m^2 = (1 - \epsilon)[(1 - \epsilon) + 2\bar{d}]^{-1} \exp(-2\bar{a})$$

where $\bar{a}$ is the mean sample interval time/correlation time, $\bar{d}$ the mean analysis time/correlation time, $\rho = \bar{a}/\bar{d}$ is the utilization factor and ϵ is a numerically determined factor. Theoretical curves for information yield as a function of the utilization factor for different situations have been reported [21]. The laboratory capacity can be influenced by many factors. The most important ones are the regime of the batch-forming and the priority rules attached to the samples [22, 23]. These factors, and the fact that a real laboratory is a complex network with alternative routings, manifold service points, people, etc. mean that theoretically based algorithms are not yet available. A solution is simulation, by modelling the laboratory, its structure and components in (statistically) describable units that can be interlocked. Altering the parameters of the system gives diverse results, allowing an optimal configuration to be established [24]. It must be stressed, however,

that this way offers no large advances for two reasons. The first reason is a technical one. The estimation of all influencing parameters is a demanding task and many parameters will be known only approximately. The second reason is more fundamental to chemometrics. In order to obtain sufficient cooperation from the analyst, chemometrics must prove that its algorithms are optimal, that its rules and data bases are sound and tested, and that its models have a sufficiently wide span of action. If not, the human user of chemometrics will rightly state that in complex matters he is still superior and chemometric methods will not be accepted.

So the main challenges for chemometrics are twofold: lay a sturdy base that can move analytical chemistry from art to science, and persuade analytical chemists that chemometrics can be taken seriously by providing them with tested examples of chemometric expertise.

REFERENCES

1 K. Eckschlager and V. Stepanek, Analytical Measurements and Information, Research Studies Press, London, 1985.
2 H. B. Woodruff and G. M. Smith, Anal. Chem., 52 (1980) 2321.
3 R. K. Lindsay, B. G. Buchanan, E. A. Feigenbaum and J. Lederberg, Applications of Artificial Intelligence for Organic Chemistry — the Dendral Project, McGraw-Hill, New York, 1980.
4 E. H. Shortliffe, Computer-based medical consultations: MYCIN, Elsevier, Amsterdam, 1976.
5 R. E. Kalman, J. Basic Eng., 82 (1960) 35.
6 R. E. Kalman and R. S. Bucy, J. Basic Eng., 83 (1961) 95.
7 S. M. Bozic, Digital and Kalman Filtering, Arnold, London, 1979.
8 P. C. Thijssen, Anal. Chim. Acta, 162 (1984) 253.
9 P. C. Thijssen, G. Kateman and H. C. Smit, Anal. Chim. Acta, 173 (1985) 265.
10 H. N. J. Poulisse, Anal. Chim. Acta, 112 (1979) 361.
11 S. C. Rutan and S. D. Brown, Anal. Chim. Acta, 160 (1984) 99.
12 P. F. Seelig and H. N. Blount, Anal. Chem., 48 (1976) 252.
13 P. C. Thijssen, N. J. M. L. Janssen, G. Kateman and H. C. Smit, Anal. Chim. Acta, 177 (1985) 57.
14 P. C. Thijssen, L. T. M. Prop, G. Kateman and H. C. Smit, Anal. Chim. Acta, 174 (1985) 27.
15 B. A. Roscoe and P. K. Hopke, Comput. Chem., 5 (1981) 1.
16 B. G. M. Vandeginste, W. Derks and G. Kateman, Anal. Chim. Acta, 173 (1985) 253.
17 A. Eskes, P. F. Dupuis, A. Dijkstra, H. DeClercq and D. L. Massart, Anal. Chem., 47 (1975) 2168.
18 D. Wienke and K. Danzer, Anal. Chim. Acta, 184 (1986) 107.
19 F. A. Leemans, Anal. Chem., 43 (1971) 36A.
20 B. G. M. Vandeginste, Anal. Chim. Acta, 112 (1979) 253.
21 T. A. H. M. Janse and G. Kateman, Anal. Chim. Acta, 150 (1983) 219.
22 T. A. H. M. Janse and G. Kateman, Anal. Chim. Acta, 159 (1984) 181.
23 B. G. M. Vandeginste, Analusis, 12 (1984) 496.
24 B. van de Wijdeven, J. Lakeman, J. Klaessens, B. Vandeginste and G. Kateman, Anal. Chim. Acta, 184 (1986) 151.

Analytica Chimica Acta, 191 (1986) 133—148
Elsevier Science Publishers B.V., Amsterdam — Printed in The Netherlands

PARTIAL LEAST-SQUARES REGRESSION ON DESIGN VARIABLES AS AN ALTERNATIVE TO ANALYSIS OF VARIANCE

HARALD MARTENS[a], LUIS IZQUIERDO[b], MAGNY THOMASSEN and MAGNI MARTENS*[a]

Norwegian Food Research Institute, N-1432 Ås-NLH (Norway)

(Received 10th July 1986)

SUMMARY

The partial least-squares (PLS) algorithm has become popular for explorative multivariate data analysis and for multivariate calibration. The same PLS algorithm can also be used for confirmatory data analysis. The discussion is limited to analysis of a single response variable. A close correspondence of PLS1 regression to classical analysis of variance (ANOVA) is demonstrated. The design of an experiment is described in terms of discrete design variables for main effects and simple interactions (dummy variables). These are used as regressors $X = (x_1, x_2, \ldots,)$ for modelling the response variable of the experiment, y. As in conventional use of PLS1 regression, the algorithm gives a concentrated model or diagram of the most important, y-relevant variability types in the X-data. In the present case, this gives the combination of design variables that models the variations in y. A simple plot of the resulting factor loadings immediately reveals the important design variables. Statistical tests and confidence regions in the PLS solution give additional safeguards against interpretation of spurious effects. The method is applied to two data sets. One concerns assessment of personal preference for blackcurrant juice, studied in a 2^5 factorial experiment; these data are also studied with missing values and as fractional factorials. The other concerns spectrophotometric absorbance-based colour assessments of pigment in strawberry jam in a 3-factor design with 2, 2 and 3 levels in the respective factors.

Partial least-squares (PLS) regression is a relatively new approach to the analysis of experimental data. It is quite flexible, and it appears that a single PLS program can replace a number of different specialized programs for data analysis. This could be beneficial, especially for non-statisticians. The present paper shows that yet another type of data analysis, traditional confirmatory hypothesis testing, can be done with the PLS algorithm.

The basic PLS concept and algorithm was developed by H. Wold [1] for applications in the social sciences. The strength of his approach was its simplicity and versatility in seeking a valid empirical relationship between large, complicated, uncertain data structures in several different tables at the same time. In order to analyze the more precise data from chemistry and

[a]Present address: Norwegian Computing Center, Blindern, Oslo 3 (Norway).
[b]Present address: Instituto Agroquimica y Tecnologia de Alimentos, 46010 Valencia (Spain).

0003-2670/86/$03.50

physics, a particular version of the PLS regression method, the mode A multifactor two-block PLS regression, was developed after 1980 [2, 3]. In contrast to the original PLS concept, this algorithm is limited to the analysis of inter-relationships between two tables (blocks) of variables. But it allows mathematically correct modelling of data affected simultaneously by several underlying phenomena. This PLS algorithm, often termed PLS2, for modelling a set of j different y variables from k different x variables, is computationally simple, but does require iterative procedures. A special version of it, the PLS1 algorithm, for modelling a single y variable from a set of k x variables, is not iterative and so even simpler. The PLS1 algorithm exists in two versions, with orthogonal scores [3] and with non-orthogonal scores [4]. Helland [5] has recently proven earlier empirical observations [6] that the two versions are equivalent.

The mode A multifactor PLS method (PLS2) has proved to be quite successful for different practical applications. It was developed rather heuristically, based on practical experience with realistic data, in contrast to most statistical methods which rely on well defined, but possibly less realistic assumptions with regard to collinearities, measurement noise, outliers, and missing data. Therefore its theoretical properties have not yet been fully explored though theoretical studies of the PLS1 algorithm have been reported [2, 5, 7, 8]. One successful class of applications of PLS1 and PLS2 regression is soft modelling, i.e., exploratory data analysis [9], when the problems are to decide if there are any valid, underlying relationships between these two blocks of data and then to visualize them. The PLS regression has been used successfully not only in chemometrics [9—11] but in related fields like sensory chemical studies [12].

The main advantage of PLS regression over alternatives like multiple linear regression (MLR) and canonical correlation appears to be its ability to handle so-called "collinear" data, i.e., data tables containing two or more variables expressing the same type of information, for example, with more variables than there are observations. Another advantage is its ability to reduce complicated data structures to simple, two-dimensional diagrams of the main relevant phenomena in the data; prior knowledge and intuition may then be used in the final interpretation.

An important condition for its success has been S. Wold's implementation of PLS regression on microcomputers in the SIMCA package [13]. Wold has insisted on conservative modelling with predictive validity by including cross-validation to find the number of significant factors or phenomena that can be modelled from a given set of data. This has apparently reduced the frequency of uncritical misuse of the method, compared to how traditional statistical regression software is often misused by non-statisticians.

Another class of PLS applications has been in multivariate calibration, i.e., teaching the computer how to convert inselective measurements (x) to reliable, selective information (y). Using data from a representative training set with known qualities to be calibrated for, the PLS algorithm extracts the main

types of variation (factors) from a set of inselective but precise (x) variables (e.g., converting diffuse near-infrared reflectance spectra to quantitative information like protein, water, and lipid concentrations in food [6, 14—16]). If it is known that generally there is a good relationship between x-variables and y-variables. Though the actual relationship is unknown for a particular kind of samples, the problem is to find underlying harmonies between all the x variables that together give the best predictions of each of the y variables, and that automatically provide warning if a sample is abnormal. The main advantage of the PLS algorithm in this sort of application, compared to statistical methods such as MLR, is again its ability to handle collinear and noisy x variables, to give interpretable graphics of the main information, and to discover various types of outliers, both in the training set and in unknown samples. Compared to chemometric methods such as multicomponent curve-fitting, its advantage is that it will detect and model unexpected phenomena such as interferences and many types of nonlinearities. A general software package for multivariate calibration based on PLS regression, UNSCRAMBLER, has been developed [17].

The PLS regression has been recommended for classification (both disjoint classification and discriminant classification) as well as for time series analysis [10]. It can apparently replace multivariate techniques such as stepwise MLR, canonical correlation, multidimensional scaling, and analysis of variance (ANOVA) [12]. The present paper is an attempt to clarify the latter point in more detail. It will be shown that the PLS1 version is identical to the classical ANOVA of a single response variable y, in contrast to the other cases, where PLS regression is an alternative data analysis. It will also be shown how ANOVA parameters of factorial experiments can be obtained from PLS1 regression output, how missing values can be treated, and how simplifying reduced designs (fractional factorials) can be analyzed by the PLS1 algorithm. Finally, an example of a slightly more complicated design will be shown. The empirical data analyzed concern colour measurements in fruit juice and jams.

EXPERIMENTAL

The ANOVA and PLS1 programs applied in two types of experimental design.

(A) Factorial design with two level per factor (2^k). The response variable y referred to the assessments of personal preferences for blackcurrant juice. Twenty-four volunteers were asked to rate their preference for 32 samples on a 9-point scale (1 = dislike, 9 = like very much) [18]. The mean values over the 24 persons were used in the ANOVA and PLS1 computations.

Design variables corresponded to a factorial design of 5 factors (a—e) with two levels per factor (2^5): (a) time (evaluation before and after lunch), (b) acidity (regular and modified with citric acid), (c) temperature (5 and 20°C), (d) volume (15 and 25 ml), and (e) colour (regular, i.e., deep red,

and modified with a green dye). The values +1 and −1 were assigned to the first and second levels of each factor, respectively. For example, the sample tested before lunch, with modified acidity, at 5°C, 25 ml of volume and natural colour had +1, −1, +1, −1, +1 as values of the design variables. The values for the interactions were obtained by multiplying the values of these experimental factors implied in the interaction. So, the mentioned sample had the value 1 × (−1) = −1 for the interaction time × temperature [19].

(B) Factorial design with more than two levels per factor. In this case the response variable y referred to the absorbance ratio of pigments of 505/425 nm in strawberry jams, and design variables corresponded to a 3-factor design with 2, 2 and 3 levels: factories (2), storage temperature (5 and 20°C) and storage time (1, 3 and 6 months). Values +1 and −1 were assigned to the first and second levels of factories and temperatures. The time factor received +1, 0 and −1 (linear effect) and +1, −2, +1 (quadratic effect) for the first, second and third storage times, respectively [20].

RESULTS

Factorial design with two levels per factor

Design without missing values. Table 1 shows the preference assessments for the complete 32 (2^5) samples of blackcurrant juice and the design variables for the 5 studied factors and the 10 simple interactions. As each factor has two levels, there is one degree of freedom per factor, which makes it possible to analyze the linear effects (differences between the two levels +1 and −1).

Application of analysis of variance (ANOVA) to the preference assessments y gave the results shown in Table 2. Mean squares equalled sum of squares for all factors as there was only one degree of freedom per factor. The sum of squares for any factor (SS_m) is

$$SS_m = I \times \sum_{j=1}^{J} (\bar{y}_j - \bar{y})^2 \tag{1}$$

where I is the number of samples at each level (here, $I = 16$), $\bar{y}_j$ is the average for level j and $\bar{y}$ is the total average:

$$\bar{y}_j = I^{-1} \sum_{i=1}^{I} y_{ij} \text{ and } \bar{y} = J^{-1} \sum_{j=1}^{J} \bar{y}_j$$

When there are two levels per factor, $J = 2$ so Eqn. 1 can be written as

$$SS_m = I\,[(\bar{y}_{(+1)} - \bar{y})^2 + (\bar{y}_{(-1)} - \bar{y})^2] \tag{2}$$

where $\bar{y}_{(+1)}$ and $\bar{y}_{(-1)}$ are the averages for the first and second levels, respectively. These effects are tested against the residual sum of squares (RSS) in an F-test:

TABLE 1

Response and design variables for the study of preference for blackcurrant juice (sample numbers 1—32)

No.	Response variable y	Design variables														
		Main effects[a]					Simple interactions									
		a	b	c	d	e	$a \times b$	$a \times c$	$a \times d$	$a \times e$	$b \times c$	$b \times d$	$b \times e$	$c \times d$	$c \times e$	$d \times e$
1	6.38	1	1	1	1	1	1	1	1	1	1	1	1	1	1	1
2	5.23	1	1	1	1	−1	1	1	1	−1	1	1	−1	1	−1	−1
3	6.33	1	1	1	−1	1	1	1	−1	1	1	−1	1	−1	1	−1
4	5.46	1	1	1	−1	−1	1	1	−1	−1	1	−1	−1	−1	−1	1
5	6.38	1	1	−1	1	1	1	−1	1	1	−1	1	1	−1	−1	1
6	4.29	1	1	−1	1	−1	1	−1	1	−1	−1	1	−1	−1	1	−1
7	6.50	1	1	−1	−1	1	1	−1	−1	1	−1	−1	1	1	−1	−1
8	4.67	1	1	−1	−1	−1	1	−1	−1	−1	−1	−1	−1	1	1	1
9	5.17	1	−1	1	1	1	−1	1	1	1	−1	−1	−1	1	1	1
10	4.96	1	−1	1	1	−1	−1	1	1	−1	−1	−1	1	1	−1	−1
11	5.71	1	−1	1	−1	1	−1	1	−1	1	−1	1	−1	−1	1	−1
12	4.58	1	−1	1	−1	−1	−1	1	−1	−1	−1	1	1	−1	−1	1
13	5.54	1	−1	−1	1	1	−1	−1	1	1	1	−1	−1	−1	−1	1
14	4.63	1	−1	−1	1	−1	−1	−1	1	−1	1	−1	1	−1	1	−1
15	5.54	1	−1	−1	−1	1	−1	−1	−1	1	1	1	−1	1	−1	−1
16	5.13	1	−1	−1	−1	−1	−1	−1	−1	−1	1	1	1	1	1	1
17	6.25	−1	1	1	1	1	−1	−1	−1	−1	1	1	1	1	1	1
18	4.67	−1	1	1	1	−1	−1	−1	−1	1	1	1	−1	1	−1	−1
19	6.25	−1	1	1	−1	1	−1	−1	1	−1	1	−1	1	−1	1	−1
20	4.96	−1	1	1	−1	−1	−1	−1	1	1	1	−1	−1	−1	−1	1
21	5.46	−1	1	−1	1	1	−1	1	−1	−1	−1	1	1	−1	−1	1
22	4.17	−1	1	−1	1	−1	−1	1	−1	1	−1	1	−1	−1	1	−1
23	6.59	−1	1	−1	−1	1	−1	1	1	−1	−1	−1	1	1	−1	−1
24	4.62	−1	1	−1	−1	−1	−1	1	1	1	−1	−1	−1	1	1	1
25	5.83	−1	−1	1	1	1	1	−1	−1	−1	−1	−1	−1	1	1	1
26	4.25	−1	−1	1	1	−1	1	−1	−1	1	−1	−1	1	1	−1	−1
27	6.25	−1	−1	1	−1	1	1	−1	1	−1	−1	1	−1	−1	1	−1
28	4.83	−1	−1	1	−1	−1	1	−1	1	1	−1	1	1	−1	−1	1
29	5.75	−1	−1	−1	1	1	1	1	−1	−1	1	−1	−1	−1	−1	1
30	5.25	−1	−1	−1	+1	−1	1	1	−1	1	1	−1	1	−1	1	−1
31	5.46	−1	−1	−1	−1	1	1	1	1	−1	1	1	−1	1	−1	−1
32	5.17	−1	−1	−1	−1	−1	1	1	1	1	1	1	1	1	1	1

[a] Factors a—e are explained in the text and in Table 2.

TABLE 2

Analysis of variance of preference for blackcurrant juices

Source of variation		Sums of squares	Degrees of freedom	Mean squares	F
	Total (TSS)	15.98	31	—	
a	Time	0.0167	1	—	
b	Acidity	0.5434	1	—	
c	Temperature	0.1188	1	—	
d	Volume	0.4632	1	—	
e	Colour	10.7300	1	—	82.73[a]
$a \times b$	Time × acidity	0.4536	1	—	
$a \times c$	Time × temperature	0.0030	1	—	
$a \times d$	Time × volume	0.0413	1	—	
$a \times e$	Time × colour	0.0536	1	—	
$b \times c$	Acidity × temperature	0.4395	1	—	
$b \times d$	Acidity × volume	0.0488	1	—	
$b \times e$	Acidity × colour	0.9835	1	—	7.58[b]
$c \times d$	Temperature × volume	0.0102	1	—	
$c \times e$	Temperature × colour	0.0001	1	—	
$d \times e$	Volume × colour	0.0004	1	—	
	Residual (RSS)	2.0754	16	0.1297	
	Explained (ESS)	13.91			

[a] $p < 0.01$. [b] $p < 0.05$.

$$F = (SS_m / d.f.1)/(RSS/d.f.2)$$

In the present case, the degrees of freedom $d.f.1 = 1$ and $d.f.2 = 16$. As Table 2 shows, only the factor colour (e) is significant at the 99% level and the interaction (acidity × colour) at the 95% level.

For the application of the partial least-squares regression (PLS1) the 15 design variables (+1, —1) from Table 1 were taken as regressors $X = \{x_1, x_2, \ldots\}$ and the preference assessments as response variables y. Based on experience with PLS1 regression on empirical x data, one might have expected the present design matrix for the 2^5 experiment to give rise to as many "significant" (in the predictive sense) PLS factors as there are statistically significant effects in the data, and to converge to the MLR (and hence to the ANOVA) solution using the maximum possible number of PLS factors. However, in the present case, only the first PLS factor had predictive ability, so that this PLS solution already corresponded to the MLR (i.e., ANOVA) model. This effect appears to be a consequence of the fact that all the eigenvalues of the complete 2^5 design X matrix were identical [5], as is the case for X matrices where all the columns are orthogonal to each other and scaled to the same sum-of-squares. (This effect can also be seen for empirical X data in the PLS1 regression if their standardized principal component scores are used instead of the raw data themselves). In the present treatment therefore, only the first PLS factor is considered.

The first step of the PLS1 algorithm is the estimation of the regression weights, as elements of a row vector ($\mathbf{w}'$) of as many elements as there are design variables, using $\mathbf{w}' = \mathbf{y}' \times \mathbf{X}$, where $\mathbf{y}'$ is the row vector of the 32 centered response variable values and $\mathbf{X}$ the centered design variable matrix (32 rows and 15 columns). As the design variable values are +1 for the first level of each factor and −1 for the second level, the value of an element (w_m) of the vector $\mathbf{w}'$ is

$$w_m = \sum_{i=1}^{I} (y_{i(+1)}) - \sum_{i=1}^{I} (y_{i(-1)})$$

where $I = 16$ and $y_{i(+1)}$ or $y_{i(-1)}$ for each sample are the values of the response variable of the first or second level, respectively. This can also be written as

$$w_m = I \times (\bar{y}_{(+1)} - \bar{y}_{(-1)}) \tag{3}$$

The expression

$$w_m^2/2I = SS_m \tag{4}$$

relates an element of vector $\mathbf{w}'$ with the corresponding sum of squares obtained from ANOVA. This can be seen from the following. If $A = \bar{y}_{(+1)}$ and $B = \bar{y}_{(-1)}$, the square of Eqn. 3 is $w_m^2 = I^2(A^2 + B^2 - 2AB)$ and dividing by $2I$ gives

$$w_m^2/2I = (I/2)(A^2 + B^2 - 2AB)$$

But, replacing the value $\bar{y}$ (mean average) in Eqn. 2 by $(\bar{y}_{(+1)} + \bar{y}_{(-1)})/2$ or $(A + B)/2$ (mean of the two averages) gives

$$\begin{aligned} SS_m &= I\{[A - (A + B)/2]^2 + [B - (A + B)/2]^2\} \\ &= I\{[(A - B)/2]^2 + [(B - A)/2]^2\} \\ &= I\{[(A^2 + B^2 - 2AB)/4] + [(A^2 + B^2 - 2AB)/4]\} \\ &= (I/2)(A^2 + B^2 - 2AB) \end{aligned}$$

A positive sign of w_m means that the first level of the factor has a higher average than the second one, and vice versa.

The length (L) of vector $\mathbf{w}'$ is related to the explained sum of squares (ESS):

$$L = \sum_{m=1}^{M} w_m^2 = \sum_{m=1}^{M} SS_m \times 2I = ESS \times 2I \tag{5}$$

where M is the number of factors and interactions. The residual sum of squares (RSS) can easily be calculated from the PLS1 output by calculating ESS from L and subtracting it from the total sum of squares (TSS). The values for TSS, RSS and ESS are shown in Table 2.

Residual variance (RV, residual mean squares) is obtained by dividing RSS by the number of degrees of freedom (31 − 15 = 16 in this case). The effect of a given factor m is considered significant if the ratio between the mean square of the factor (MS_m) and RV is higher than the corresponding F value. In the present example, there is one degree of freedom per factor, so MS_m equals SS_m. The F value for 1 and 16 degrees of freedom is 4.49 at the 95% level.

An effect is considered significant if $SS_m > RV \times 4.49$. Replacing SS_m by its equivalent in Eqn. 4 gives $w_m^2 > 2I \times RV \times 4.49$, and the confidence interval $-(2I \times RV \times 4.49)^{1/2} < w_m < (2I \times RV \times 4.49)^{1/2}$ can be established for the elements of vector $\mathbf{w}'$. A factor is not significant at the 95% level if the value of its corresponding element w_m is inside the limits of the interval.

To standardize the vector $\mathbf{w}'$ to length 1, each element w must be divided by the square root of the length of the unstandardized $\mathbf{w}'$ vector. In such conditions, the interval is $-(2IRV4.49/L)^{1/2} < w_m/L^{1/2} (2IRV4.49/L)^{1/2}$. Replacing L in the limits of the interval by its value in Eqn. 5 gives $-(2IRV4.49/ESS2I)^{1/2} < w_m/L^{1/2} < (2IRV4.49/ESS2I)^{1/2}$ or $-(RV4.49/ESS)^{1/2} < w_m/L^{1/2} < (RV4.49/ESS)^{1/2}$.

In the present example the interval at the 95% level is $-0.204 < w_m/L^{1/2} < 0.204$ and at the 99% ($F = 8.53$) $-0.282 < w_m/L^{1/2} < 0.282$. Figure 1 shows the elements of vector $\mathbf{w}'$ (standardized in length 1) for all factors and interactions and the confidence intervals at 95% and 99% calculated as outlined above. Only the element of $\mathbf{w}'$ corresponding to factor colour (e) significantly differs from zero at 99%, and the element corresponding to the interaction acidity × colour at 95%, as was obtained by ANOVA.

One important feature of PLS regression is the estimation of sample scores for each factor (e.g., for factor 1, $t_1 = \mathbf{Xw}'$). The score vectors create a simplified diagram of the main relationships between the samples, suitable for visual interpretation. With only one relevant PLS factor in the present case, this can best be plotted against something else. Figure 2 shows the preference y_1 plotted against the PLS scores t_1; there is a linear relationship with a certain, apparently random, variability.

As implemented in the UNSCRAMBLER program, analysis of the PLS regression results leads to automatic outlier warnings to the user. These are particularly advantageous for multifactor PLS solutions that are difficult to visualize. But the present one-factor case illustrates two of the outlier detection methods: samples 22 and 3 are the ones that have highest leverage in $\mathbf{X}$, i.e., they represent the outer samples in the subspace t_1 from the $\mathbf{X}$ space. Sample 31 shows the largest deviation from the regression line of y on t_1. The detected outliers should be given particular attention by checking for errors, etc. But the samples detected here are very mild outliers, indicating that the data set is homogeneous and fits reasonably well to the model chosen.

Missing values. The PLS1 algorithm allows calculations on incomplete experimental designs with some values missing. But the validity of the

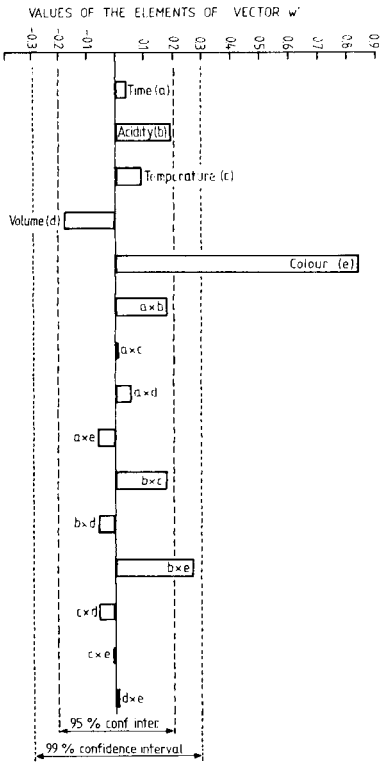

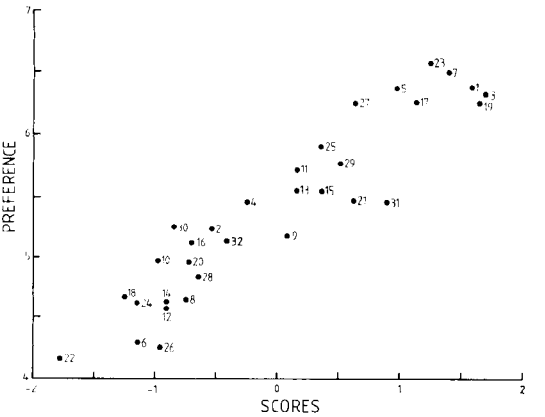

Fig. 1. Elements of vector **w**' for all factors and interactions and confidence intervals (95 and 99%).

Fig. 2. Preference y_1 plotted against PLS scores t_1 .

ensuing significance tests depends on how well balanced is the remaining design. This was studied by simulating incomplete experiments, i.e., randomly choosing subsets of observations y_i to be regarded as missing. Certain rows of the **X** and **Y** matrix corresponding to missing values were removed from the input data and the algorithm was applied without change. A total of 24 different calculations were performed, each for a different subset of missing values (Table 3) randomly taken from the 32 samples of the full design.

Although each of the design variables in **X** was scaled to the same sum-of-square before the PLS1 regression, two or more PLS factors now had predictive ability for **y**, in contrast to the previous, complete 2^5 design. The reason is probably that the design variables are no longer orthogonal, and so the eigenvalues of **X** are no longer identical. However, the first PLS factor was by far the greater contributor to the modelling ability for **y** and so only this factor is discussed here. The results showed good consistency between

TABLE 3

Missing values experiments

Exp. no.	No. of values missing	Sample numbers for missing values (Table 1)
1	4	13 20 22 26
2	4	16 18 22 27
3	4	9 14 17 29
4	4	4 11 28 31
5	4	3 24 25 32
6	4	5 10 19 30
7	4	2 6 12 15
8	4	1 7 8 12
9	6	7 11 16 21 24 28
10	6	13 4 20 25 26 30
11	6	4 6 8 9 12 15
12	6	3 10 23 27 29 32
13	6	1 2 17 18 22 31
14	8	1 8 9 11 13 14 30 31
15	8	7 10 16 17 23 25 26 29
16	8	2 5 12 18 20 24 28 32
17	8	3 4 6 12 15 19 22 27
18	10	1 5 9 12 17 19 23 27 31 32
19	10	2 6 10 11 13 14 15 22 26 29
20	10	3 7 8 16 18 20 21 24 25 28
21	12	2 3 4 5 6 12 15 16 21 24 26 32
22	12	1 10 17 18 19 20 22 23 25 28 29 31
23	14	1 3 9 12 14 18 20 21 22 23 24 29 30 31
24	14	2 5 6 7 10 11 13 15 16 17 19 25 26 27

ANOVA and PLS regression, even when the number of missing values was high. Figure 3 is a plot of the elements of vector $\mathbf{w}'$ for all these missing-values experiments. The colour effect came out as significant at 99%, as in the full design, except for the one simulated experiment with the most missing values (14 out of 32); even then the effect was significant at 95%. The interaction acidity × colour remains significant at 95% in 17 of the 24 missing-values experiments. Six of the other 7 cases for which the significance falls below the 95% are for 10 or more missing values. The acidity and volume effects, which were almost significant at 95% in the full design experiment, were now significant in 9 and 7 of the 24 missing-values tests, respectively. Only in one case for acidity and two cases for volume was a change in the sign of the corresponding element of vector $\mathbf{w}'$ observed, and none was significant. For time and temperature, the least significant effects in the complete design, many changes of sign were observed. But only three cases for temperature and one for time were significant at the 95% level.

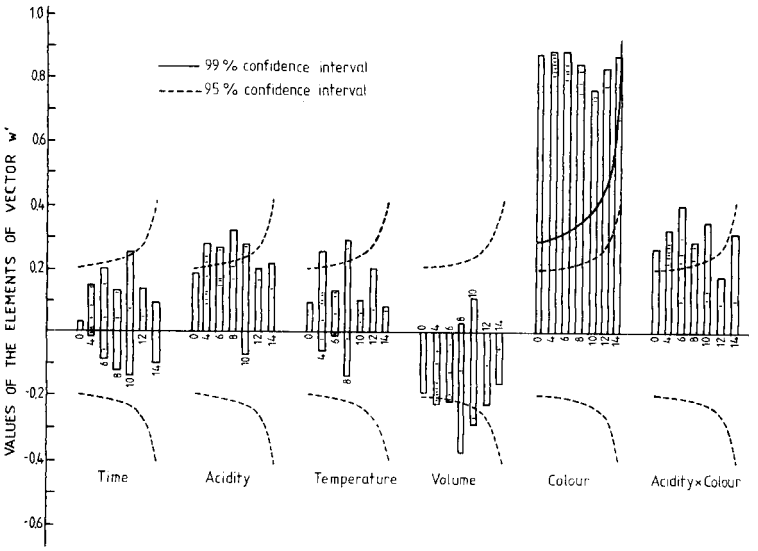

Fig. 3. Elements of vector **w** plotted for missing-value experiments (cf. Fig. 1).

As the number of missing values approaches 50% of the data, the F value required for significance increased sharply, because of lack of degrees of freedom. In 4 of the 24 experiments, apparent significances at the 95% level was found for main effects that showed almost no effect in the complete design. Three of these occurred with 30% missing values or more. In summary, in the ANOVA computation, based on PLS1 regression, similar conclusions could be drawn in most of the 24 simulated incomplete, 2^5 experiments as in the original experiment with complete design.

Fractional factorial designs. An important aspect of factorial experiments is the possibility of using fractionals, i.e., reduced designs that require fewer samples than the full experiment without becoming unbalanced and spurious like the random missing-values design. Factors not directly considered in the fractional can be studied convolved with interactions that are assumed to be less important than the simpler factor [19]. Fractionals of 16 and 8 samples from the full design of 32 (2^{5-1} and 2^{5-2}) were selected and analyzed with PLS1. Because these designs are balanced and orthogonal, all the eigenvalues of **X** are identical and only one PLS factor had predictive ability for **y**. Response and design variables for a 2^{5-1} fractional (16 samples) are shown in Table 4. The design was generated from the extra condition for the main design effects $X\ a \times b \times c \times d \times e = 1.0$. Hence, samples were chosen so that, e.g., the main effect "colour" (e) was convolved with the four-factor interaction of time × acidity × volume × temperature ($a \times b \times c \times d$). For the chosen samples, the values of the variables for this interaction and for the colour factor in the full factorial (Table 1) are the same. Likewise, pairs of two- and three-factor interactions were convolved. Results for the

TABLE 4

Design variables for main effects for a 2^{5-1} fractional

Sample no.[a]	Response variable y	Design variables[a] Main effects				
		a $b \times c \times d \times e$	b $a \times c \times d \times e$	c $a \times b \times d \times e$	d $a \times b \times c \times e$	e $a \times b \times c \times d$
1	6.38	1	1	1	1	1
4	5.46	1	1	1	−1	−1
6	4.29	1	1	−1	1	−1
7	6.50	1	1	−1	−1	1
10	4.96	1	−1	1	1	−1
11	5.71	1	−1	1	−1	1
13	5.54	1	−1	−1	1	1
16	5.13	1	−1	−1	−1	−1
18	4.67	−1	1	1	1	−1
19	6.25	−1	1	1	−1	1
21	5.46	−1	1	−1	1	1
24	4.62	−1	1	−1	−1	−1
25	5.83	−1	−1	1	1	1
28	4.83	−1	−1	1	−1	−1
30	5.25	−1	−1	−1	1	−1
31	5.46	−1	−1	−1	−1	1

[a]See Table 1 for sample numbers and meaning of factors a—e.

main effects (Fig. 4A) confirm the importance of colour, obviously assuming the high-order interaction $a \times b \times c \times d$ to be unimportant. The interaction terms in the model were not significant.

The 8-sample fractional design 2^{5-3} is shown in Table 5 and the results for the main effects in Fig. 4B. In this case, every main effect will be convolved with two- and three-factor interactions. For instance, colour is convolved with the interactions time × temperature and acidity × temperature × volume. As Fig. 4B shows, the importance of colour is still confirmed in this 2^{5-2} fractional consisting of only 8 observations.

In summary, the PLS1 regressions in the fractional experiments gave the expected results.

Factorial design with more than two levels per factor

When a quantitative factor with more than two levels is studied through ANOVA and differences among levels are found, additional calculations are normally used to determine the kind (linear, quadratic) of these differences. Through PLS1, the calculations can be done in a single step as is shown in the next example in which the absorbances (response variable y) of strawberry pigments are determined in jams produced in two factories (first factor, two levels), stored at 5 and 20°C (second factor, two levels)

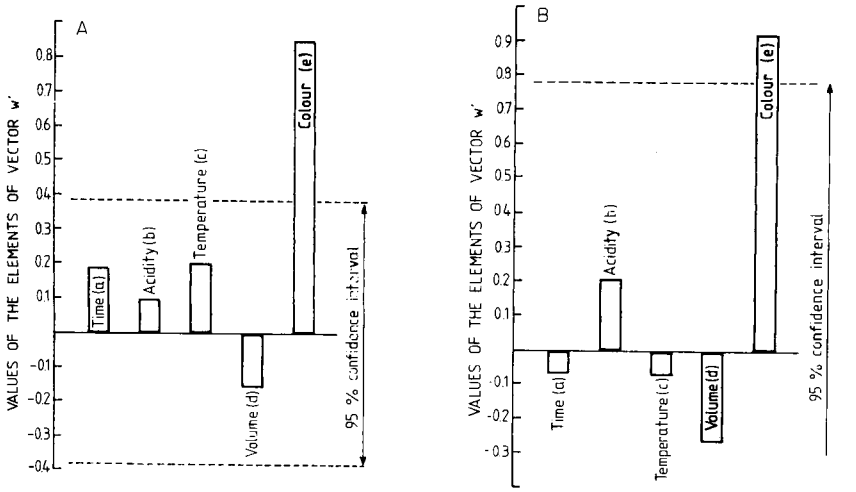

Fig. 4. Elements of vector $\mathbf{w}'$ plotted for fractional designs: (A) for 16 (2^{5-1}) samples; (B) for 8 (2^{5-2}) samples (cf. Fig. 1).

TABLE 5

Design variables for main effects for the 2^{5-2} fractional

Sample number (Table 1)	Response variable y	Design variables Main effects				
		a $c \times e$ $b \times d$	b $a \times d$ $c \times d \times e$	c $a \times e$ $b \times d \times e$	d $a \times b$ $b \times c \times e$	e $a \times c$ $b \times c \times d$
1	6.38	1	1	1	1	1
6	4.29	1	1	−1	1	−1
11	5.71	1	−1	1	−1	1
16	5.13	1	−1	−1	−1	−1
20	4.96	−1	1	1	−1	−1
23	6.59	−1	1	−1	−1	1
26	4.25	−1	−1	1	1	−1
29	5.75	−1	−1	−1	1	1

[a]Generating conditions: (1) $a \times c \times e = 1$; (2) $a \times b \times d = 1$; (3) $b \times c \times d \times e = 1$. [b]See Table 1 for sample numbers and meaning of factors a—e.

during 1, 3 and 6 months (third factor, three levels). So, the factor "time" has two degrees of freedom which allows the linear effect of absorbance variation to be studied during the storage (increase or decrease) as well as the quadratic effect (e.g., faster decrease at the start of storage than at the end). The same analysis can be done for the interactions involving time. The response variable is presented in the first column of Table 6 and the ANOVA results are shown in Table 7. The three simple factors and the interaction factories × temperature are significant at the 95% level whereas the interaction factories × time is not significant. The sum of squares of this inter-

TABLE 6

Response and design variables for the study of absorbances of strawberry jams

Response variable[a]	Simple factor[b]				Interactions		
	a	*b*	*c*	*d*			
			Time			Factory × Temp.	
	Factory	Temp.	Linear	Quadratic	Factor × Temp.	Linear	Quadratic
0.52	1	1	1	1	1	1	1
0.40	1	1	0	−2	1	0	−2
0.27	1	1	−1	1	1	−1	1
0.41	1	−1	1	1	−1	1	1
0.30	1	−1	0	−2	−1	0	−2
0.21	1	−1	−1	1	−1	−1	1
0.82	−1	1	1	1	−1	−1	−1
0.83	−1	1	0	−2	−1	0	2
0.48	−1	1	−1	1	−1	1	−1
0.57	−1	−1	1	1	1	−1	−1
0.46	−1	−1	0	−2	1	0	2
0.28	−1	−1	−1	1	1	1	−1

[a]Absorbances. [b]Assignment of values: (a) 1, First factory; −1, second factory. (b) 1, 5°C; −1, 20°C. (c) 1, 1 month; 0, 3 months; −1, 6 months. (d) 1, 1 month and 6 months; −2, 3 months.

TABLE 7

Analysis of variance for absorbances of strawberry jams

Source of variation	Sums of squares	Degrees of freedom	Mean squares	*F*	Decomposition of the sum-of-squares			
					Linear effects		Quadratic effects	
					Mean squares	*F*	Mean squares	*F*
Total	0.4479	11						
Factories	0.1519	1	0.1519	76**				
Time	0.1525	2	0.0763	38**	0.1458	73**	0.0067	3.4
Temperature	0.0990	1	0.0990	50**				
Factories × time	0.0114	2	0.0057	2.9	0.0041	2.0	0.0073	3.5
Factories × temp.	0.0252	1	0.0252	12.6*				
Residual	0.0079	4	0.0020					
Explained	0.4400							

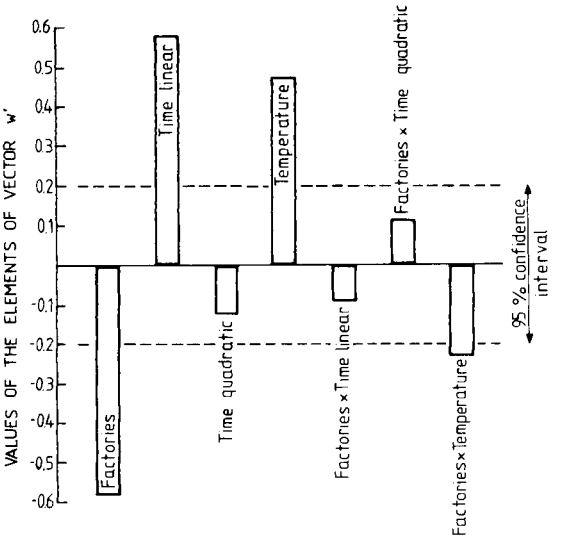

Fig. 5. Elements of vector **w**′ plotted for the strawberry jam example.

action and of the time factor are decomposed in the last columns of Table 7 to two effects, linear and quadratic. In the case of the time factor, only the linear effect is significant at the 95% level and in the case of the interaction factories × time neither the linear nor the quadratic effect is significant.

Table 6 shows the design variables for PLS1. In the case of the time factor and the interaction factories × time there are two design variables, corresponding to the two existing degrees of freedom, one for the linear effect (with values +1, 0, and −1 for respectively 1, 3 and 6 months) and another one for the quadratic effect (values +1, −2, +1). This again is a balanced orthogonal design, so that only the first PLS factor had predictive ability for **y**. The results are presented in Fig. 5. A positive sign of the corresponding element of the vector **w**′ means, for linear effects, a decrease of the mean value (a decrease of the absorbance during the storage in this case) and, for quadratic effects, a faster decrease at the beginning than at the end, and vice versa. Again the elements of vector **w**′ from the PLS1 analysis are found to be equivalent (as in the 2^5 design) to the sum of squares of ANOVA for each factor or for each effect in which the factor is decomposed.

Conclusion

A close correspondence between factorial analysis of variance and PLS1 regression has been demonstrated. Given the flexibility of the PLS algorithm and the geometric interpretability of its output, the PLS approach may offer certain practical advantages over the classical ANOVA modelling. The partial least-squares (PLS1) regression method has earlier proved helpful for other problems in data analysis. The possibility of solving many different problems with a single method in a single computer program seems advantageous.

One of the authors (L. I.) thanks the Consellería de Cultura, Educació y Ciencia de la Generalitat Valenciana for financial support during his stay in Norway.

REFERENCES

1 H. Wold, in J. Gani (Ed.), Perspectives in Probability and Statistics, Academic Press, London, 1975.
2 S. Wold, H. Wold, W. J. Dunn III and A. Ruhe, Report UMINF 83, Umeå University, Sweden, 2nd edn., 1983.
3 S. Wold, H. Martens and H. Wold, in A. Ruhe and B. Kaagstroem (Eds.), Proc. Conf. on Matrix Pencils, Piteaa, Sweden. Lecture Notes in Mathematics, Springer Verlag, Heidelberg, 1983, p. 286.
4 H. Martens and T. Naes, in P. Williams (Ed.), Near-infrared analysis, Am. Assoc. Cereal Chemists, St Paul, MN, 1987.
5 I. Helland, On the Structure of Partial Least Squares Regression, Report No. 21/86, Dept. of Mathematics and Statistics, Norwegian Agricultural University.
6 H. Martens and S. A. Jensen, in J. Holas and J. Kratochvil (Eds.), Progress in Cereal Chemistry and Technology 5a. Elsevier, Amsterdam, 1983, p. 607.
7 T. Naes and H. Martens, Commun. Statist., 14 (1985) 545.
8 T. Naes, C. Irgens and H. Martens, Appl. Statist., 35 (1986) 195.
9 S. Wold, C. Albano, W. J. Dunn III, K. Esbensen, S. Hellberg, E. Johansson and M. Sjøstrøm, in H. Martens and H. Russwurm Jr. (Eds.), Food Research and Data Analysis, Applied Science, London, 1983, p. 147.
10 S. Wold, C. Albano, W. J. Dunn III, U. Edlund, K. Esbensen, P. Geladi, S. Hellberg, E. Johansson, W. Lindberg and M. Sjøstrøm, in B. R. Kowalski (Ed.), Chemometrics, Mathematics and Statistics in Chemistry, NATO ASI-C-138, D. Reidel, Dordrecht, 1984.
11 E. Johansson, J. Persson and C. Albano, Determination of Water and Energy in Peat with Near Infrared spectroscopy. Report, National Swedish Laboratory for Agricultural Chemistry, S-900 05 Umeå, Sweden, 1985.
12 M. Martens and H. Martens, in J. R. Piggot (Ed.), Statistical Procedures in Food Research, Elsevier Applied Science, London, 1986.
13 S. Wold, SIMCA-3B & 3F. University of Umeå, Sweden (1985)
14 H. Martens and T. Naes, Trends Anal. Chem., 3 (1984) 204.
15 H. Martens, Dr. techn. thesis, Technical University of Norway, 1985.
16 T. Naes and H. Martens, Trends Anal. Chem., 3 (1984) 266.
17 UNSCRAMBLER User's Manual, CAMO A/S, P.O. Box 5115, N-7001 Trondheim, 1987.
18 M. Martens, E. Risvik and H. G. Schutz, in J. V. McLoughlin and B. M. McKenna (Eds.), Research in Food Science and Nutrition, Boote Press, Dublin, Vol. 2, 1983, p. 193.
19 J. S. Hunter, in B. R. Kowalski (Ed.), Chemometrics, Mathematics and Statistics in Chemistry, D. Reidel, Dordrecht, 1984, NATO ASI C, 138, pp. 1—15.
20 G. Snedecor, Statistical Methods Applied to Experiments in Agriculture and Biology, Iowa State University Press, Ames, IA, 1956.

Analytica Chimica Acta, 191 (1986) 149—160
Elsevier Science Publishers B.V., Amsterdam — Printed in The Netherlands

SOME APPLICATIONS OF THE PARTIAL LEAST-SQUARES METHOD

SERGIO CLEMENTI*, GABRIELE CRUCIANI and GIANLUCA CURTI
Dipartimento di Chimica, Università di Perugia 06100 Perugia (Italy)
(Received 28th May 1986)

SUMMARY

The philosophy of the applications of the partial least-squares method in chemistry is outlined. The method is compared with multiple regression and illustrated by means of examples in various fields of chemistry.

The basic design of the PLS (partial least-squares in latent variables) method was developed by H. Wold for studying systems under indirect observation where a causal relationship could exist [1—3]. Its recent application in chemistry, where it is used as an improved alternative to earlier methods such as multiple regression (MR) and principal-components regression (PCR), is mainly due to the work of S. Wold [4—8], Kowalski [9—12] and Martens [13—16] and their co-workers. In particular, S. Wold and his co-workers have developed the method called SIMCA [17], based on disjoint principal-components modelling, which constitutes the first two levels of pattern recognition [18]. The two higher levels, involving the establishment of a causal relationship between two blocks of data, require the use of the PLS algorithm, which is included in the chemometric package for microcomputers called SIMCA/MACUP, which was used for all calculations of the examples reported below.

Multivariate statistics appears to be the most promising field of chemometrics. Application of these methods, made possible to many scientists by easy access to microcomputers, is required to handle the large amount of data easily collected, by newer instruments, on the same sample.

The geometrical representation of a sample on which P analytical variables have been measured is that of a point in a P-dimensional space, where each orthogonal axis represents one of the measured variables. When P variables are measured on N samples (objects) the data set is represented by N points in the P-space. The methods of multivariate statistics [19] then seek similarities among the points. Two main similarity criteria have been developed: the euclidean distance and the mathematical models. However, the methods based on euclidean distance are mainly aimed at classifying samples, i.e., to pattern recognition (supervised learning), or to cluster analysis (unsupervised learning or pattern cognition). Methods based on mathematical models are

0003-2670/86/$03.50

more powerful because they permit, besides classification, interpretation of results and prediction of unmeasured values. The most popular and well known such approach is multiple regression analysis (MR), where a dependent variable y is described in terms of explanatory variables x. However, the regression models rely on assumptions that often render them inappropriate for applications in chemistry (vide infra).

When the problem is to evaluate the relative importance of individual variables in establishing the data structure, i.e., the extraction of chemical information contained in a data set, the most appropriate statistical approach is principal components analysis (PCA). This method, which has the same mathematical form as multiple regression, is aimed at finding the simplest mathematical model that can describe the data set satisfactorily, giving to each variable the same initial importance in the evaluation. However, PCA is not aimed at finding any cause/effect relationship. This latter problem can be solved by the PLS method which does not require any preliminary assumption on the relevance of individual variables, because it relies on PCA. In the latent variable analysis, the aim is to find possible relationships between one or more dependent variables and a number of potentially explanatory variables. The question is whether it is possible to describe the elements of the Y matrix as a simple function of the elements of the X matrix. In the past, this problem has been handled by computing PC models for each of the two matrices followed by establishment of any linear relationship between the principal components of these two blocks. Instead of this two-step procedure, called principal components regression (PCR), it is possible to perform the analysis in a single stage, accomplishing the two steps simultaneously, by using an appropriate algorithm.

The statistical results obtained by the PLS method permit: (a) the detection of which variables in the X block actually govern the dependent variable(s); (b) the prediction of the response for unmeasured samples; (c) the classification of samples in different categories in cases where classification is relevant and possible. The PLS algorithm has been described in detail [4, 6, 8], thus only a brief summary is reported here.

In the case when there is only one dependent variable, the method extracts the principal components of the independent variables block under the constraint to maximize the relationship with the dependent variable values:

$$x_{ki} = x_i + \Sigma\, b_{ai}\, t_{ka} + e_{ki} \tag{1}$$

When many dependent variables are available (PLS2), the analysis results in a description of the X matrix by one PC-like model (Eqn. 1), a description of the Y matrix by another PC-like model and predictive relations between the latent variables t and u:

$$y_{kj} = y_j + \Sigma\, c_{aj}\, u_{ka} + f_{kj} \tag{2}$$

$$u_{ka} = d_a\, t_{ka} + h_{ka} \tag{3}$$

The algorithm is iterative for each dimension as in PCA. It consists in finding the latent variables of the X matrix (t_k) from initial values of u_k and the X elements, and then recomputing the latent variables of the Y matrix (u_k) from the Y elements and the t_k values until the process converges. In other words, the two models (Eqns. 1 and 2) are calculated so that, simultaneously, the residuals e_{ki} and f_{kj} are minimized, and maximally correlated vector pairs $\mathbf{u}_a$ and $\mathbf{t}_a$ are obtained.

COMPARISON BETWEEN PLS AND MULTIPLE REGRESSION

Both PCA and PLS are bilinear "least-squares" methods, which have some practical advantages over the analogous "maximum-likelihood" methods, such as factor analysis, linear structural relationship and linear discriminant analysis.

The main difference between the least-squares and maximum-likelihood approaches is that the latter assumes that the data are a sample from a postulated distribution; this assumption can also be used in least-squares modelling, but it is not necessary. Furthermore, the scope of the least-squares approach is to predict future observation, and to describe the data points well, whereas the main objective of maximum-likelihood methods is to find the structure of the data, usually with interest concentrated on either the object or the variable parameters [20]. Both methods, being bilinears models, permit presentation of results in a few illustrative plots, handling of missing data, and finding outliers, if any.

Multiple regression, because of its linearity, can be seen as both a least-squares and a maximum-likelihood method and is commonly used in chemistry to predict response variables from a set of causal variables

$$y_k = b_0 + \Sigma b_i x_{ki} + e_{ki} \tag{4}$$

Traditionally the regression coefficients b_i are interpreted as the influence of the ith variable x on the dependent variable y. However, MR has a number of weak points that render it rarely applicable to problems in chemistry. First, the number of objects should be at least three times greater than the number of variables, otherwise the risk of spurious correlations is large. In contrast, in PCA and PLS modelling, the ratio between variables and objects is not important, provided that there are at least five elements for each row or column. The second weak point is that MR is based on the causal assumption that each variable is precise and relevant to the problem. In other words, the model dimensionality is fixed beforehand; each variable taken into account must contribute to the problem thus increasing the number of dimensions. Finally, to obtain good estimates of the regression coefficients, the x variables should be almost orthogonal to each other. If correlations between the independent variables do exist (multicollinearity), multiple regression results become numerically, as well as statistically, unreliable [21]. To correct for the instability caused by collinearity and to make

possible the inversion of matrices with singularity problems [22], two different approaches have been used: ridge regression and principal components regression (PCR), but both these methods have further drawbacks [20]. Ridge regression is quite lengthy in calculations and one never knows how to choose the constant that should be added to the ridge of the covariance matrix. The problem with PCR is that the small components in the **X** matrix are discarded even if they contain information relevant to the **Y** matrix.

The pitfalls of multiple regression and the merits of PLS may be illustrated with a simple example on the dependence of the quality of Italian white wines on their contents of alcohols and esters. The data set consists of a number of wine samples on which three variables are measured: a sensory score (the "quality", y variable) and two analytical determinations, e.g., total alcohols and total esters. Geometrically, the data set is represented by a number of points in a three-dimensional space (Fig. 1). If the causal variables are both relevant and independent of each other, there is no problem: multiple regression will find the plane of best fit. But if the amounts of alcohols and esters are highly correlated, then the points will line up along a line in the space. The causal relationship therefore requires one dimension only to explain a unique effect: the increase in quality depends on the increase in esters and the simultaneous decrease in alcohols. Nevertheless, multiple regression will find the best plane fitting the points, just because the "independent" variables considered are two. Consequently, the stability of the model (and the reliability of the regression coefficients believed to measure some chemical properties) gets lost, but inexperienced operators will not be aware of it if they do not compute the standard deviations of the coefficients.

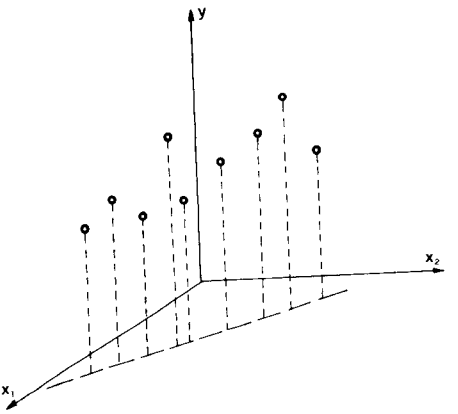

Fig. 1. Three-dimensional illustration of the dependence of wine quality on the alcohol and ester contents, in the hypothesis of a high correlation between the two causal variables.

Principal components regression, which first detects the relationship between alcohols and esters and then plots this principal component against the sensory data would have solved the problem with the correct dimensionality. The PLS method, finding the latent variable under the constraint of maximizing its relationship with the y vector, would give the same result. However, in general, the number of potentially causal variables constituting the **X** block is much larger than two, and there is no reason to suppose that the principal components of the **X** block have to be strictly related to y. Accordingly, the merits of PLS, where the latent variable is found involving y in the one-step computation, appear to be much greater.

To summarize, it should be pointed out that in multiple regression the x variables are known to be relevant to the problem and their collinearity gives meaningless results. In contrast, in PLS the relevance of individual variables results from the analysis and their correlations are used to find the numerical solution. It is interesting to note that PLS converges towards multiple regression when the number of components increases [22]. Finally, PLS is sensitive to groupings as is multiple regression. However, results from the latter method are not usually presented as plots, so that groupings, if any, are not detected: as a consequence, quite often these results appear to be falsely excellent, just because the dramatic decrease of the degrees of freedom arising from the groupings is not taken into account.

EXAMPLES

QSAR and toxicology

Traditionally, QSAR (quantitative structure/activity relationships) was where the power of the PLS method was most needed, and where the first applications appeared [23—25]. Establishing quantitative relationship between biological activities and structural descriptors has long been the goal in drug design [7, 26, 27], although the results were often unsatisfactory [28, 29] because of the extensive use of unreliable tools such as multiple regression. In all these cases, there are two main aims: (a) finding the structural features responsible for the activity, and (b) predicting the activity of new compounds before they are available. In general, the variation in chemical structure is described in terms of substituents around a common skeleton, these being expressed as substituents parameters such as sigma, pi, molecular refractivity, steric constants, etc. The application of the PLS method usually provides answers to the problems mentioned, much better than the classification approach, because of the asymmetric structure of most biological data [30].

A relevant example in this area is the relationship between a battery of 5 measures of mutagenicity of 7 chlorinated aliphatic hydrocarbons and 11 structural descriptors, including molecular parameters, physical properties and computed charges or electronegativities [22]. The model required three significant latent variables, the first of which consists mainly of the

traditional global variables related to size and lipophilicity. Another example of this kind [31] is a study of the anaesthetic activity and toxicity of 22 halogenated ethyl methyl ethers, described by an ensemble of 41 structural parameters, mainly calculated by the (PEOE) method based on partial equalization of orbital electronegativity [32] which gives atomic charges and electrophilicity parameters. Once more the dominant factors appear to be nonspecific "chemical bulk" descriptors. These types of descriptors, however, represent new ways of quantifying structures. Preliminary studies used traditional Hansch descriptors for electronic, steric and lipophilic effects in the X block [26]. The β-adrenergic activity of phenetylamines was studied by this approach [7, 25].

A study aimed at comparing different statistical tools and different ensembles of structural descriptors was undertaken on the activity and toxicity of a number of 9-anilinoacridines with varying substituents at three positions [29]. Each substituent was first represented by an arrow of nine traditional variables (sigmas, pi, molecular refractivity, Verloop parameters) so that each molecule is described by a vector of 27 elements. The results showed that the mathematical model gave slightly better predictions than the traditional Hansch approach, besides providing a simpler straight interpretation of the structural features relevant to the biological properties. In the same study, the first two principal components scores for each substituent, obtained by applying PCA on the matrix of traditional descriptors, were also used as possible descriptors, and compared with the electronic distributions and residual electronegativities for each atom, obtained by the PEOE approach [32]. In both cases, although fairly good models were obtained, these new descriptors did not prove to be clearly superior to the traditional ones, especially in view of the work needed to compute them [29].

Toxicity modelling with predictions by pattern recognition methods is a very attractive field and a review article has recently appeared [33]. A PLS analysis of genotoxicity data on chemical carcinogens and non-carcinogens was recently undertaken [34]. The scope of the study was modelling carcinogenicity by means of short-term genotoxicity descriptors and identifying relevant tests for carcinogenicity predictions. The data base contained 17 non-carcinogen and 25 carcinogen compounds in animal studies. The X block was made up by 1/0 responses to ten selected genotoxicity end-points (bacteria, yeasts, in vivo, etc.). The final model, requiring three latent variables, explained over 75% of the y variance and 95% of samples were correctly assigned to their own class. The analysis also allowed the relevance of individual end-points to be studied. The most important appeared to be the test on Salmonella, the cytogenetic analysis and the gene mutation test, whereas low or no relevance could be attributed to any other test, including in vivo tests.

Toxicity data for a number of substituted triazines have been described by a PLS model in terms of some of their physical properties [35]. The num-

erical result was almost as good as that obtained by modelling with traditional structural descriptors. However, this latter approach is always preferable, because it permits predictions of biological properties on the basis of well established constants, prior to synthesizing the compounds and measuring their physical properties. The present superiority of traditional structural descriptors was also established by principal components analysis of new biological data [36] and antitumor tests [27, 37].

A recent application of PLS in the QSAR area deals with the chemistry of peptides. Activity data on a family of 15 pentapeptides were modelled by means of appropriate coding scales (derived from PCA) describing each amino acid. The resulting model, requiring two latent variables, was used to predict the activities of another set of pentapeptides, which was experimentally investigated later. The plot of predicted versus observed activity values showed good agreement [38].

These successful results open interesting possibilities of quantifying parts of microbiology and biochemistry by means of semi-empirical multivariate analogy models.

Prediction of product properties

The same type of ensemble of structural descriptors can also be used to model any kind of property, within homogeneous series, which depends on structure modification. Quite a good example of such an approach was recently reported on modelling fastnesses of a series of azo dyes [39]. The five properties under investigation were light, washing (at two temperatures), alkali and perspiration fastnesses. The 65 samples were described by electronic (sigma), steric (Charton's ν), lipophilic (Hansch's π) and molecular refractivity values of the substituents at four different sites. The model required two latent variables, the first of which described the relation between light, alkali and perspiration fastnesses in terms of structural features, which are favoured by the presence of a halogen or a methoxy group at site 1, a nitro group at site 2 and a short alkyl chain at site 4. But the second latent variable showed that washing fastness depended on a long chain at site 4. Consequently, the model made it possible to elucidate the structural features relevant to the property under investigation, and to predict the molecules having the best compromise between light and washing fastness, thus indicating how to enhance technological properties. A second such study was done on azo dyes with a different skeleton, leading to similar results [40]. These same compounds were also modelled by their ^{13}C n.m.r. spectra in another investigation [41]. In this case, the results showed that n.m.r. data can be used successfully to predict dye fastness quickly and cheaply.

In general, the PLS method appears to be extremely suitable for prediction of product quality. Predictor variables from spectral sources have already been used to model quality-control variables of industrial products [12].

Food chemistry

Another field where the application of PLS methods has proved beneficial is food chemistry. The PLS methods, being appropriate tools for detecting relationships between two blocks of data, can be used to handle various relevant problems in this area. Relationships between sensory data and chemical indices can be established, and many problems of multivariate calibration can be properly solved.

Much work has been done in this area by Martens and his co-workers [13–16]. His exciting suggestions to judge the quality of foods on the basis of simple measurements like near-infrared reflectance spectra deserve special mention. The procedure works, provided that the sensory data have been described by a PLS analysis based on the chemical constituents of foods and these, in turn, have been described by their near-infrared spectra [42]. Even more interesting was the estimation in vivo of the composition of pig meat by a computer tomography analysis of a few sacrificed animals and an appropriate PLS analysis of the pixels intensities [43].

Multivariate calibration based on near-i.r. reflectance data was also used to detect protein and water concentrations in grain samples [6].

In this laboratory the PLS method has been applied to relate sensory data to chemical composition, or to analytical indices of starting materials, or to technological parameters in the preparation of foods. The first such example relates to the quality of a selection of 47 Italian white wines [44]. The descriptor variables were 40 sets of data including head-space gas chromatographic measurements of esters, alcohols, acids and carbonyl compounds, and some traditional standard items (pH, SO_2, ash, etc.). The response variables were the total scores attributed by a panel to each sample and the partial scores given to colour, odour and taste. The results showed that a single latent variable, after exclusion of three outliers, could explain 76% of the total score variance, with very few variables contributing significantly to the linear combination of the X block. The quality was mainly due to increasing amount of esters (hexyl acetate, isoamyl acetate, 2-phenetyl acetate, ethyl caprylate, ethyl caprate, ethyl caproate and their corresponding acids, ethyl laurate) and to the decrease of alcohols (3-methyl-1-butanol and 2-phenetyl alcohol). When the three separated sensory scores were used, a similar model was obtained, and showed that the colour score was almost irrelevant to the model.

Two typical Italian cheeses, Provolone and Parmigiano-Reggiano, were also studied. The study on Provolone [45] related sensory properties (pungent character and milk aroma) to the flavour given by the content in volatile compounds found in the head-space. It was possible to show that the pungent character is directly linked to 2-pentanone, butyric acid and caproic acid and that milk aroma decreases as pungency increases. These sensory properties and chemical contents were shown to increase with ripening, but were not affected significantly by storage or cheese size. In a subsequent study, the age of Parmesan cheese samples was related to their free amino-

acid composition [46]. During the first year of maturation, the amount of almost all amino-acids increased, whereas during the second year the relative amount of three amino-acids only was modified (GLN, ARG, ORN). The PLS method therefore can establish if an unknown sample is really a "reference" Parmesan cheese and can allow estimates of its age on the basis of its amino-acid composition. The PLS method was also used to assess the reliability of the procedure for determining the amount of roasted hazelnuts in sweet creams or spreads, based on the electrophoretic pattern of their protein fraction [47].

Applications in environmental chemistry and geochemistry

The multivariate calibration problem is obviously general and so the methods have proved useful in studying the chemistry of the environment. For example, the fluorescence spectra of samples of Baltic sea water were used to measure the content of humic acid and lignin sulfonate after a PLS modelling, with six latent variables, for a training set containing the intensities at 27 digitized frequencies [48].

The PLS method can also be used to detect relationships between chemical composition of water samples and meteorological parameters (humidity, pressure, wind, rain, etc.). Such a study confirmed that the sea water in the Trieste gulf is cleaner when the Bora blows [49]. In another case, the height above sea level of the sampling sites on a slippery slope of the Perugia hill could be related to the chloride, nitrate and sulphate in the phreatic water [50].

In the geochemistry area, the intrinsic information content of trace elements determination in the volcanic rocks of the Aeolian archipelago was studied [51]. The PLS method provided a good classification between individual islands, and showed by a four latent-variables model, that up to 67% of the information was common to the major elements and trace elements blocks. However, a small but significant amount of information appeared to be specific to each block, thus confirming the usefulness of collecting data on trace elements.

Geochemistry is a field where chemometric methods have had significant impact, and in which chemometricians can test their methods. An example of this idea is given by the development of selective partial least-squares techniques (SELPLS). In this approach, recognition of the most dominant first-order genetic process is used to define a subset of variables comprising a subspace in which a correction can be done, with the aim of enhancing more subtle data patterns. This subspace is modelled by a selective two-block PLS configuration (SELPLS), allowing prediction of the systematic effects ascribed to the recognised process. The subtraction of the predicted values results in a corrected data matrix free of these effects [52]. Iteration of the SELPLS correction may further serve to bring out successively more masked data patterns. This approach should be valuable for detecting any kind of geochemical anomaly.

Newer developments

Although the PLS method has proved to be extremely useful for handling data sets in various branches of chemistry, its potential can be improved by newer developments. An example of such possible improvements is the need for a tool to handle multiway data arrays. Sensory data, geographical data and environmental data always have such structures. The problem was first reported as a subconstrained N-way decomposition and illustrated with geological examples [53]. More recently, a PLS analysis generalized to multiway data arrays has been presented [54]. The decomposition of such arrays is developed as products of a score vector times a loading array. The resulting methods are equivalent to the method of unfolding a multiway array to a two-way matrix followed by ordinary analysis. A solution to the parallel problem of a multiblock PLS has also been suggested [12].

A second area of PLS applications is that of optimization studies. The present state of the art in this area requires the use of multiple regression to construct response surfaces and subsequent illustrative isoresponse plots [55]. The variables relevant to the response can be selected either by fractional factorials or by the PLS method. However, because of the usual drawbacks of multicollinearity, the experiments needed for such studies must be collected according to a rigorously orthogonal experimental design; a simple factorial design does not give enough degrees of freedom to obtain a numerical solution, so that a central composite design is preferable [55]. Nevertheless, while a certain number of variables can easily be controlled to program a suitable design, other types of variables (e.g., the analytical indices of raw materials in a chemical process) cannot be controlled, thus preventing the calculation of a response surface. In order to overcome this problem, the possibility of using PLS instead of multiple regression in computing the response values for defining the surface is presently under investigation [56].

The Italian Ministry of Education is thanked for a research grant on chemometrics to S.C.; Dr. G. Giulietti and Mr. D. Chiocchini are also thanked for invaluable help and advice.

REFERENCES

1 H. Wold, Nonlinear estimation by iterative least squares procedures, in F. N. David (Ed.), Research Papers in Statistics: Festschrift for J. Neyman, Wiley, New York, 1966.

2 H. Wold, Causal-predictive analysis when the problems explored are complex and prior knowledge is scarce: An example of partial least squares, International Conference of the Psychometric Society, June 1978, Uppsala, Sweden.

3 H. Wold, in K. G. Joreskog and H. Wold (Eds.), Systems under Indirect Observation, North-Holland, Amsterdam, 1982, Vol. 2, p. 1.

4 S. Wold, A. Ruhe, H. Wold and W. J. Dunn, J. Sci. Stat. Comput., 5 (1984) 735.

5 M. Sjostrom, S. Wold, W. Lindberg, J. A. Persson and H. Martens, Anal. Chim. Acta, 150 (1983) 61.

6 S. Wold, C. Albano, W. J. Dunn, K. Esbensen, S. Hellberg, E. Johansson, M. Sjostrom, in H. Martens and H. Russwurm Jr. (Eds.), Food Research and Data Analysis, Applied Science, London, 1983, p. 147.
7 S. Wold, W. J. Dunn and S. Hellberg, in G. Jolles and K. R. H. Wooldridge (Eds.), Drug Design: Fact or Fantasy?, Academic Press, London, 1984, p. 95.
8 S. Wold, C. Albano, W. J. Dunn, U. Edlund, K. Esbensen, P. Geladi, S. Hellberg, E. Johansson, W. Lindberg, M. Sjostrom, in B. R. Kowalski (Ed.), Chemometrics, Reidel, Dordrecht, 1984, p. 17.
9 R. W. Gerlach, B. R. Kowalski and H. Wold, Anal. Chim. Acta, 112 (1979) 417.
10 B. R. Kowalski, R. W. Gerlach and H. Wold, in K. G. Joreskog and H. Wold (Eds.), Systems under Indirect Observation, Part II, North-Holland, Amsterdam, 1982.
11 I. E. Frank, J. H. Kalivas and B. R. Kowalski, Anal. Chem., 55 (1983) 1500.
12 I. E. Frank, J. Feikema, N. Constantine and B. R. Kowalski, J. Chem. Inf. Comput. Sci., 24 (1984) 20.
13 H. Martens, in H. Martens and H. Russwurm (Eds.), Food Research and Data Analysis, Applied Science, London, 1983, p. 5.
14 H. Wold, H. Martens and H. Wold, in A. Ruhe and B. Kagstrom (Eds.), Matrix Pencils, Springer, Heidelberg, 1983, p. 286.
15 H. Martens and T. Naes, Trends Anal. Chem., 3 (1984) 204, 266.
16 H. Martens, Ph.D. Thesis, Technical University of Norway, Trondheim, 1985.
17 S. Wold and M. Sjostrom, in B. R. Kowalski (Ed.), Chemometrics: Theory and Application, ACS Symposium Series No. 52, American Chemical Society, Washington, DC, 1977, p. 243.
18 C. Albano, W. J. Dunn, U. Edlund, E. Johansson, B. Norden, M. Sjostrom and S. Wold, Anal. Chim. Acta, 103 (1978) 429.
19 K. V. Mardia, J. T. Kent and J. M. Bibby, Multivariate Analysis, Academic Press, New York, 1979.
20 E. Johansson, Ph.D. Thesis, Umea University, Sweden, 1984.
21 N. R. Draper and H. Smith, Applied Regression Analysis, Wiley, New York, 1981.
22 W. J. Dunn, S. Wold, U. Edlund, S. Hellberg and J. Gasteiger, Quant. Struct. Act. Relat., 3 (1984) 131.
23 W. J. Dunn and S. Wold, J. Med. Chem., 21 (1978) 922.
24 W. J. Dunn and S. Wold, J. Chem. Inf. Comput. Sci., 23 (1983) 6.
25 S. Hellberg, S. Wold and W. J. Dunn, in X. Hoskuldson (Ed.), Proc. Conference on Applied Statistics, Copenhagen, 1982.
26 C. Hansch and A. J. Leo, Substituent Constants for Correlation Analysis in Chemistry and Biology, Wiley, New York, 1978.
27 S. Clementi, in G. Jolles and K. R. H. Wooldridge (Eds.), Drug Design: Fact or Fantasy?, Academic Press, London, 1984, p. 73.
28 T. Fujita, in G. Jolles and K. R. H. Wooldridge (Eds.), Drug Design: Fact or Fantasy?, Academic Press, London, 1984, p. 19.
29 S. Clementi, G. Coata, M. Marsili, C. Ebert, L. Lassiani, P. Linda, S. Hellberg, S. Wold, and W. J. Dunn, Paper presented at VII ICCCRE, Garmisch, 1985.
30 W. J. Dunn and S. Wold, J. Med. Chem., 23 (1980) 595; Biorg. Chem., 9 (1980) 505.
31 S. Hellberg, S. Wold, W. J. Dunn, J. Gasteiger and M. G. Hutchings, Quant. Struct. Act. Relat., 4 (1985) 1.
32 J. Gasteiger and M. Marsili, Tetrahedron, 36 (1980) 3219.
33 S. Wold, W. J. Dunn and S. Hellberg, Environ. Health Perspec., 61 (1985) 257.
34 M. L. Tosato, D. Cesareo, N. Loprieno and S. Clementi, Unpublished work.
35 D. Cesareo, L. Passerini, M. L. Tosato and S. Clementi, Unpublished work.
36 M. Codarin, P. Linda, C. Ebert, L. Lassiani, F. Rubessa, S. Alunni, S. Clementi, M. Sjostrom, S. Wold and W. J. Dunn, in QSAR in Design of Bioactive Compounds, J. R. Prous, Barcelona, 1984, p. 347.
37 C. Ebert, L. Lassiani, P. Linda, C. Nisi, S. Alunni and S. Clementi, Quant. Struct. Act. Relat., 3 (1984) 143.

38 S. Hellberg, M. Sjostrom and S. Wold, Acta Chem. Scand., Ser. B., in press.
39 R. Carpignano, P. Savarino, E. Barni, S. Clementi and G. Giulietti, Dyes and Pigments, 6 (1985) 189.
40 R. Carpignano, P. Savarino, E. Barni, G. DiModica and S. S. Papa, J. Soc. Dyes Colour, 101 (1985) 270.
41 R. Carpignano, P. Savarino, E. Barni, G. Viscardi, S. Clementi and G. Giulietti, Anal. Chim. Acta, 191 (1986) 445.
42 H. Martens, S. A. Jensen and P. Geladi, Proc. Nordic Symposium on Applied Statistics, Stokkard Forlag Pub., 1983, p. 205.
43 H. Martens, O. Vangen and E. Sandberg, Proc. Nordic Symposium on Applied Statistics, Stokkard Forlag Pub., 1983, p. 235.
44 M. Bertuccioli, S. Clementi and G. Giulietti, Vini d'Italia, 3 (1984) 27.
45 M. Bertuccioli, G. Montedoro and S. Clementi, in G. Charalambous (Ed.), The Shelf Life of Foods and Beverages, Elsevier, Amsterdam, 1986, p. 335.
46 P. Resmini, L. Pellegrino, M. Bertuccioli and S. Clementi, Unpublished work.
47 W. Garrone, M. Antonucci, U. Bona and S. Clementi, Unpublished work.
48 W. Lindberg, J. A. Persson and S. Wold, Anal. Chem., 56 (1983) 643.
49 S. Clementi, G. Giulietti and M. Princi, Unpublished work.
50 S. Clementi, E. Zinato and S. Arzilli, Unpublished work.
51 M. L. Bisani, D. Faraone, S. Clementi, K. Esbensen and S. Wold, Anal. Chim. Acta, 150 (1983) 61.
52 K. Esbensen, E. Johansson, S. Wold and K. M. Drake, in A. Hoskuldsson and D. Edwards (Eds.), Proc. Symposium on Applied Statistics, DTH, Copenhagen, 1983.
53 K. Esbensen and S. Wold, Proc. of Symposium on Applied Statistics, Stavanger, 1983, p. 11.
54 S. Wold, P. Geladi, K. Esbensen and J. Öhman, Proceedings of Symposium on Applied Statistics, Copenhagen, 1986.
55 G. E. P. Box, W. J. Hunter and J. S. Hunter, Statistics for experimenters, Wiley, New York, 1978.
56 R. Carlsson, B. Skagerberg, S. Wold, S. Clementi and G. Cruciani, Unpublished work.

Analytica Chimica Acta, 191 (1986) 161—168
Elsevier Science Publishers B.V., Amsterdam — Printed in The Netherlands

EXPERTISE – AN EXPERT SYSTEM FOR INFRARED SPECTRA EVALUATION

T. BLAFFERT

Philips GmbH Forschungslaboratorium Hamburg, Vogt-Kölln-Str. 30, D-2000 Hamburg 54 (Federal Republic of Germany)

(Received 29th May 1986)

SUMMARY

A system for the automated elucidation of chemical structures by the interpretation of infrared spectra is described. "Rules" for the finding of substructure features in an unknown spectrum are obtained by a pattern recognition procedure. A structure generation algorithm links particular substructures, called "superatoms", together. Fuzzy set operators are used to consider inaccuracies in peak positions and intensities.

The role of computers in the elucidation of chemical structures has become increasingly important, because digitized data from analytical instruments are directly available and the performance of interpretation programs has improved. Although software systems are currently far from replacing experienced chemists, carefully designed recognition procedures and structure-generation algorithms can often elucidate the correct chemical structure. Because of its high information content, infrared (i.r.) spectroscopy is particularly interesting for the application of advanced methods. Much attention has been given to the application of pattern-recognition methods [1].

The DENDRAL system offered an important approach to modelling the work of a human operator in mass spectrometry [2]. A computer program for an expert type of analysis of infrared spectra was reported by Woodruff and Smith [3]. Both systems run automated analysis of unknown spectra, but the acquisition of the interpretation knowledge is done more or less manually.

An ideal system for interpretation of spectra, as outlined by Clerc [4], would include some preprocessing, the identification of substructures by spectral features, the generation of tentative structures from these substructures, the prediction or calculation of spectra from the structure, comparison of this predicted spectrum with the unknown, and modification of the tentative structures. Because infrared spectra are practically impossible to predict, only substructure correlation and tentative structure generation can be done. Comparison with spectra in a reference library is also possible, but this is limited by compounds not present in the library.

0003-2670/86/$03.50

The expert system described here for infrared spectra evaluation (EXPERTISE) follows this approach, but in contrast to earlier work [2, 3] it avoids the manual knowledge acquisition by incorporating an additional pattern-recognition procedure, which forms the "rules" for the expert system.

CONCEPT OF THE INTERPRETATION SYSTEM

The concept of EXPERTISE follows the general scheme of knowledge-based systems. This means that a distinct knowledge base exists, which is updated from the knowledge-acquisition component, and used by the component for knowledge application or problem solving (Fig. 1). The knowledge base is further divided into structure and substructure knowledge, where the structural knowledge consists of a spectra library and the associated structural formulae of the compounds. Substructure knowledge means spectral features and formulae of substructures plus some relational information. In the system described, knowledge acquisition means systematic generation of substructures and learning their spectral features. The information for these steps is taken from the spectra library, which is built from known spectra.

Searching for reference spectra, searching for spectral features of substructures, and generating complete chemical structures from a list of recog-

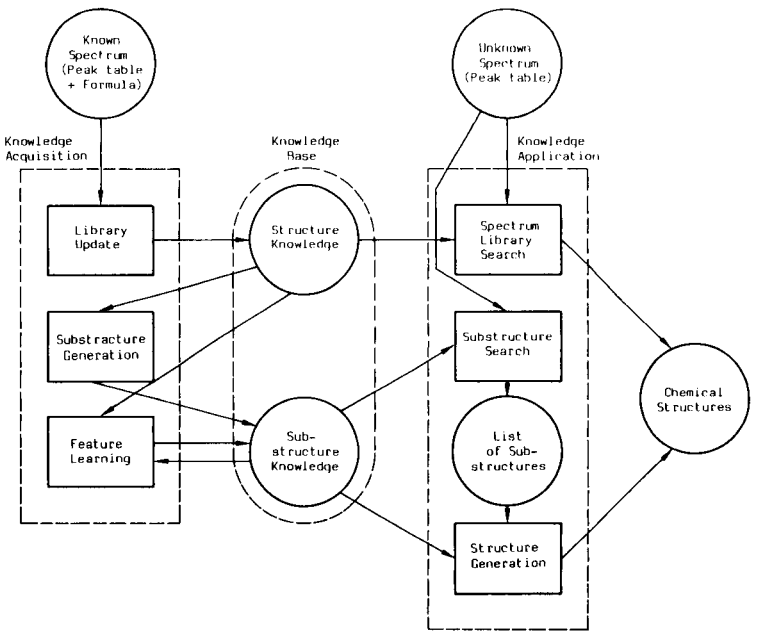

Fig. 1. Overview of the structure of the EXPERTISE system for infrared spectra evaluation. Data structures are represented by circles, operations on the data are indicated by boxes.

nized substructures is the application of the acquired knowledge. Searching for reference compounds in a spectra library is a very common method for the interpretation of an infrared spectrum, so it has been included in an interpretation system for completeness. Because the method has been described earlier [5], attention will be paid only to the substructure analysis here. It must be noted for the following discussion that the substructure learning and recognition algorithms use peak tables rather than full spectra. If only peak position and height are considered, these peak tables define a set of points in a position/intensity plane, which is necessary for the theoretical description of the learning and recognition process.

Knowledge acquisition

Features of substructures are computed from a collection of spectra with this substructure, the training set. For this purpose, substructures are systematically generated from structures stored in the structure knowledge base, and then stored in the substructure knowledge base together with a back-pointer to the structures. This is done for all structures, thus for all substructures the peak tables of the training set are immediately available. It may be noted that the knowledge about the chemical structure determines the training set rather than the judgement of an expert.

The occurrence of peaks in a certain wavenumber/absorbance range are the spectral features of substructures. This range can be viewed as an interval in a wavenumber/absorbance plane, which has to be found by the learning algorithm. A simple search for intervals, where there is at least one peak of each compound in the training set, finds (or "learns") these intervals (Fig. 2). Some additional constraints select the relevant ones from all possible intervals, e.g., the intervals with the smallest area are selected. The set of such intervals obtained for one substructure is defined as the substructure feature

$$S = \{I_i, i = 1 \ldots n\} \quad (1)$$

This non-statistical procedure guarantees that the substructures of all compounds in the training set are recognized in the substructure search, something that is not always true for statistical algorithms. There is also a chemical reason for defining a feature interval by the simultaneous existence of peaks in the training set, if a substructure exists it will definitely lead to certain molecular vibrations and particular absorption peaks. This learning approach is derived from knowledge about the origin of infrared absorption peaks.

Knowledge base

The systematic generation of substructures in the knowledge acquisition leads to the net relation in Fig. 3, where nodes differing in one additional or missing atom are connected. A successive node always contains a larger number of atoms, and is a specialized extension of its predecessor. For instance, $-CH_3$ is more specialized than $-CH_2-$, and $-NH_2$ is more generalized than $-C-NH_2$.

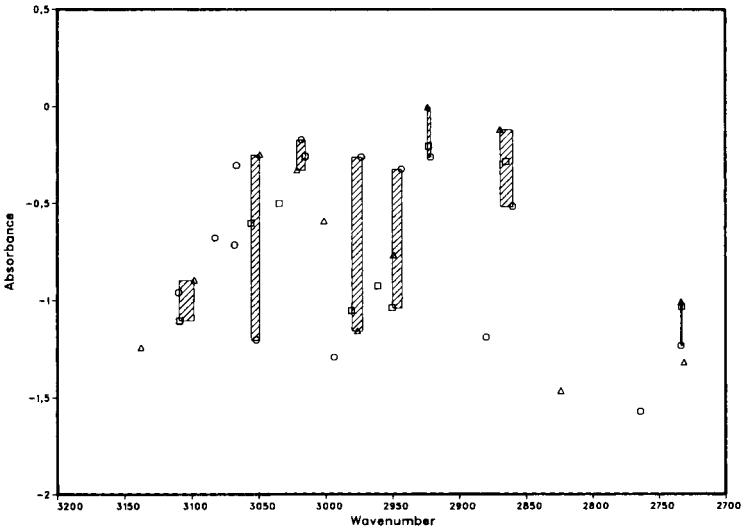

Fig. 2. Feature intervals found with a training set of 3 aromatic compounds.

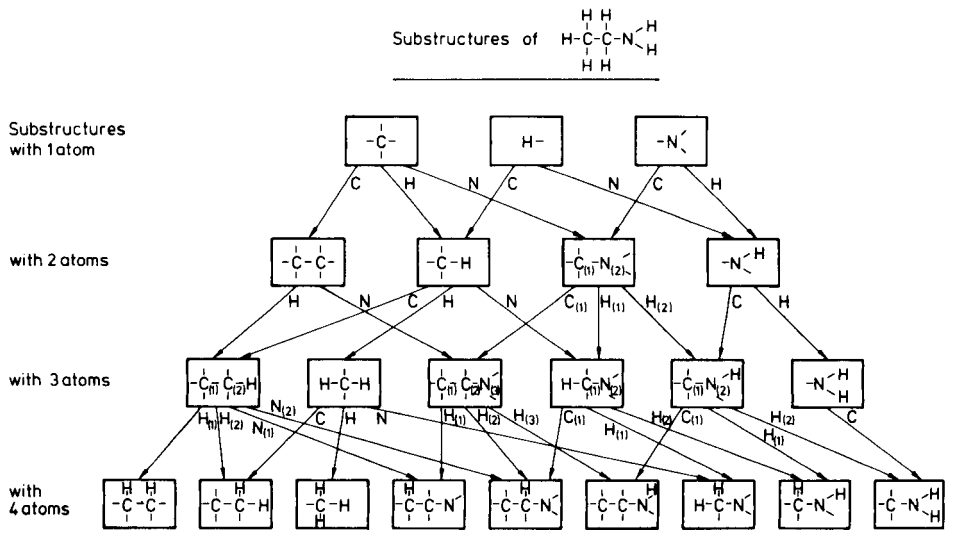

Fig. 3. Net organization of the substructure knowledge base.

An important property of the EXPERTISE learning algorithm is that this specialization/generalization relation can also be seen in the spectral features. To show this, a "specialized" relation in features has to be defined. This is defined as

$$S_1 \text{ is more specialized than } S_2, \Leftrightarrow \forall I_2 \in S_2 \; \exists I_1 \text{ with } I_1 \in I_2 \qquad (2)$$

This means that for all intervals I_2 in the more generalized substructure feature S_2, there must exist at least one interval I_1 in the more specialized substructure feature S_1, which is contained in I_2. In other words, all peaks of a generalized substructure must occur in the specialized substructure, but the wavenumber/absorbance range of their occurrence can be larger. This definition is also meaningful in spectroscopic terms, because the additional atoms in specialized substructures define the environment of the vibrating bonds more accurately and reduce the wavenumber and absorbance range for peak positions and intensities.

Interestingly, the EXPERTISE learning approach generates substructure features, where the specialized relation holds for specialized substructures. This can be derived from the fact that the training set of a specialized substructure is a subset of the training set of the generalized substructure.

SUBSTRUCTURE SEARCH

In the substructure search, the absorption peaks of an unknown spectrum are compared with the substructural features stored in the substructure knowledge base. The comparison is done by simple superposition of the peaks with the feature intervals, where a substructure is recognized if there is at least one peak in each interval. This can be formulated by introducing a containment c_i of peaks in a peak table $P = [p_j, j = 1 \ldots m]$ in a substructure interval I_i.

$$\begin{aligned} c_i &= p_1 \in I_i \vee p_2 \in I_i \vee \ldots \vee p_m \in I_i \\ z &= c_1 \wedge c_2 \wedge \ldots \wedge c_n \end{aligned} \tag{3}$$

The boolean variable z denotes the membership of the substructure with the intervals I_i to the set of substructures in the unknown spectrum.

Inaccuracies in measurement or in peak finding can produce peak positions or intensities just outside the feature intervals; this will lead, from Eqn. 3, to erroneous exclusion of a substructure. This problem can be overcome by the introduction of fuzzy sets [6]. Similarly to the earlier method [5], the sharp feature intervals I_i in Fig. 2 are fuzzified by a characteristic function $F_{I_i}(x)$, which is 1 (full membership) inside the interval, and decreases continuously to 0 (no membership) outside the interval (Fig. 4).

The formal definition of the substructure membership in Eqn. 3 can also be used in fuzzy set terminology, but the boolean operators $\vee$ and $\wedge$ have to be replaced by a minimum and maximum operator. The variables c_i and z become real values in the interval [0,1]:

$$\begin{aligned} c_i &= \max\left[f_{I_i}(p1), f_{I_i}(p2), \ldots, f_{I_i}(p_m)\right] \\ z &= \min\left(c_1, c_2, \ldots c_n\right) \end{aligned} \tag{4}$$

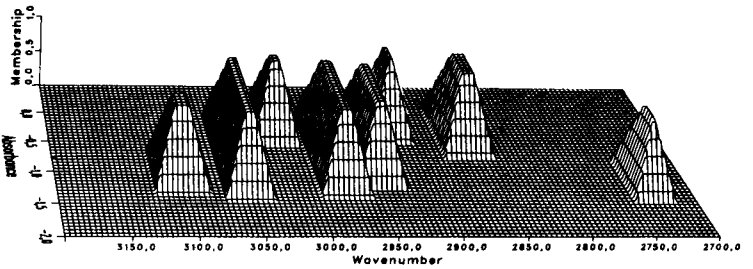

Fig. 4. Fuzzified feature intervals of Fig. 2.

For the calculation of membership values z, the nodes in the substructure net are inspected by a "depth-first" search. Exhaustive search can be avoided, and thus the search accelerated, if the search is stopped at nodes with a membership value z smaller than a threshold t. The chosen membership criterion (Eqns. 4) guarantees that all successive nodes also have a membership value less than t if the substructure features are more specialized. But this specialization of features in more specialized substructures is a result of the feature-learning method outlined above and additionally checked in a consistency routine.

STRUCTURE GENERATION

For the complete elucidation of the total structure, the problem remains to connect the recognized substructures. In contrast to the CONGEN structure generator of the DENDRAL system [2], which starts with a known sum formula and generates all plausible structural isomers, the approach described starts with known substructures and links them together under plausible constraints. This additive approach has the important advantage that the sum formula need not be known at the beginning.

For the additive structure generation, particular substructures, here called superatoms, superelements, and superbonds, have to be defined. The linking procedure follows immediately from this definition. The approach is illustrated in Fig. 5. First, bonds and elements are treated as individual items, which are connected by an abstract link. In Fig. 5(a) bonds are marked by boxes, elements are marked by circles, and the connections are simple lines. Then bonds are considered, which connect non-terminal elements, i.e., elements with more than one bond connected to them; These bonds divide the structure into several superelements, which are encircled by full lines in Fig. 5(b). Bonds plus neighbouring elements plus their remaining bonds define a superbond, marked by dashed lines. If the superelements are denoted by A, B, and C, and the superbonds are denoted by a and b, the resulting superstructures can be drawn as in Fig. 5(c). This process can be repeated to create superelements, bonds and atoms of a second or higher order.

For the inverse process, the generation of superstructures from super-

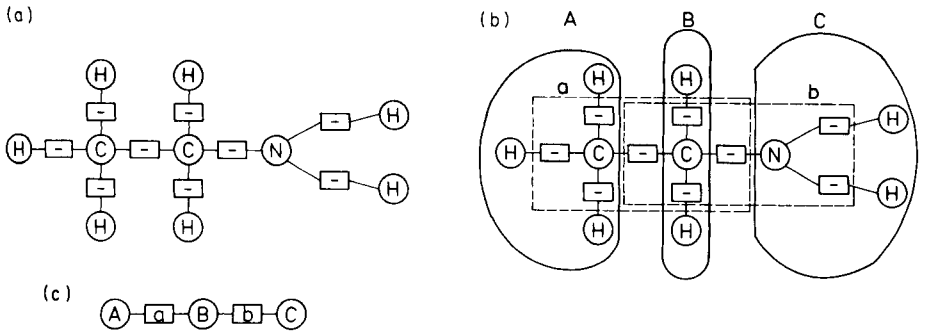

Fig. 5. Splitting of the chemical structure (a) into superbonds and superelements (b) and representation as superstructure (c). For details, see text.

elements and superbonds, the superatoms have to be defined. Superatoms are superelements plus all attached superbonds (Fig. 6). Superatoms can be linked together by satisfying their open superbonds with identical open superbonds of other superatoms. This linking can be done until there are no more open superbonds in the generated superstructure. The chemical structure is then simply obtained by inserting the chemical substructure formulae associated with the superelements and the bond type associated with the superbond into the superstructure.

Generally, more than one structure can be generated from the recognized substructures. In principle, all structures are generated by the system, although some constraints reduce this to a useful subset. For example, the repetitive use of substructures leads to endless chains, so that each superatom with more than one bond must be used only once. It has also to be considered that some superbonds are asymmetric, e.g., superbond b in Fig. 5. Another problem is to exclude superatoms from the structure-generation process if they have no bond with a corresponding superatom. Also structures are rejected as possible solutions if they do not contain all the superatoms found in the substructure search.

A general assumption of the described approach to structure generation is the exclusion of ring closures, which would cause tremendous problems in the linking of substructures. Ring structures can be included if a ring is treated as a superatom.

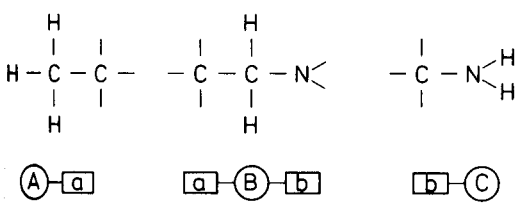

Fig. 6. Superatoms of the structure in Fig. 5.

RESULTS

The performance of the feature learning and recognition system was tested with a set of about 900 substructures generated from 100 acyclic compounds. All substructures of compounds from the training set were correctly recognized, which is a consequence of the feature-learning algorithm. For substructures of test compounds which were not included in the training set, the recognition rate was 95%. About 15% of the substructures found by the search were erroneous substructures, which were not actually present in the compounds. This shows the tendency of the system to find more substructures than are actually present in the unknown compound, but not to miss any. The speed of the substructure search was increased by a factor of 2–5 with the pruned search.

The structure generation was tested with 20 compounds (acyclic); twelve of them were correctly identified, but for the other eight, the system found a larger chemical structure. This is mainly due to the additional substructures found in the substructure search, which mostly produce additional $-CH_2$ groups.

The author thanks Pye-Unicam, Cambridge, for providing the library of reference spectra, and Mr. v. d. Bogaert from Philips Research Laboratories, Eindhoven, for his comments and important suggestions during the development of the EXPERTISE system.

REFERENCES

1 K. Varmuza, Pattern Recognition in Chemistry, Springer Verlag, Heidelberg, 1980, p. 157.
2 B. Buchanan and E. Feigenbaum, Artificial Intelligence, 11 (1978) 5.
3 H. B. Woodruff and G. M. Smith, Anal. Chem., 52 (1980) 2321.
4 J. T. Clerc, Pure Appl. Chem., 50 (1978) 103.
5 T. Blaffert, Anal. Chim. Acta, 161 (1984) 135.
6 L. A. Zadeh, Inf. Control, 6 (1965) 338.

Analytica Chimica Acta, 191 (1986) 169—180
Elsevier Science Publishers B.V., Amsterdam — Printed in The Netherlands

EVALUATION OF ENERGY-DISPERSIVE X-RAY SPECTRA WITH THE AID OF EXPERT SYSTEMS

K. JANSSENS and P. VAN ESPEN*

Department of Chemistry, University of Antwerp (UIA), Universiteitplein 1, B-2610 Wilrijk-Antwerpen (Belgium)

(Received 20th June 1986)

SUMMARY

Two recently developed Expert systems in the field of x-ray fluorescence are discussed. The first deals with the qualitative interpretation of x-ray spectra; it is characterized by a large knowledge base and a relatively small data base, both of which are of uniform structure. The second contains knowledge on quantitative spectrum evaluation and so has a much larger data base; its knowledge base is much smaller (at present), but contains several different types of rules.

X-ray fluorescence spectrometry (x.r.f.) is a fast simple technique. The sample is excited with x-rays, and the fluorescence x-rays are detected with an Si(Li) solid-state detector, resulting in an energy-dispersive x-ray spectrum (Fig. 1). It is also possible to obtain x-ray spectra by bombarding the sample with electrons (as in electron microprobe analysis) or with accelerated particles (as in particle-induced x-ray emission spectrometry). The technique is widely used for simultaneous multi-element determinations in a variety of materials and measurements are easily automated. Four steps are involved: (a) measurement of the sample (data acquisition), (b) qualitative examination of the obtained spectra in order to establish which elements are present, (c) evaluation of the spectrum to obtain the intensities of the characteristic peaks, and (d) calculation of concentrations on the basis of the peak intensities for each element.

Each of these steps is well understood by itself and can (at present) be semi-automated. Programmable x-ray fluorescence apparatus is available commercially, quantitative spectrum processing can be done with non-linear least-squares fitting techniques [1, 5] while several calibration models have been proposed (e.g., thin-film method [2], use of influence coefficients [3], fundamental parameter method [4]) and implemented as computer programs. The qualitative interpretation of x-ray spectra still needs to be done almost entirely by hand, and operator interaction is usually required in the other steps to obtain reliable results. In order to achieve a fully automated (and unsupervised) procedure, many fairly small and straightforward decisions need to be taken during each of these steps. For example,

0003-2670/86/$03.50

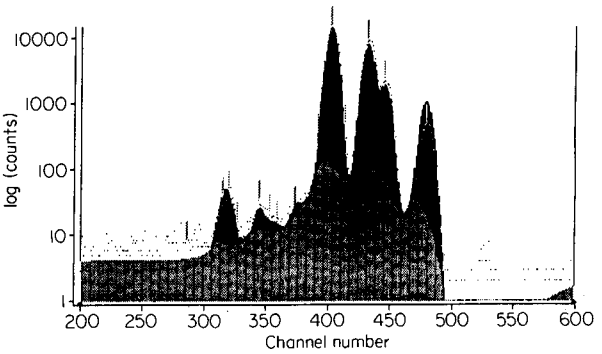

Fig. 1. Part of an energy-dispersive x-ray spectrum of a brass sample: (...) original spectrum; (black) fit prior to absorption correction; (grey) background.

the measuring conditions (voltage, counting time, etc.) and subsequent quantitative spectrum processing have to be adapted to the sample type; the optimal calibration model needs to be used with the best available standards. It was decided to use Expert system methodology to implement a system which can make such decisions as required.

Computer programs can be considered as data transformers. From an initial state of input data, a final state (of output data) is reached by successive transformations. Both Expert systems and conventional programs have these characteristics, the main difference being the way in which decisions are made. In conventional software, decisions regarding the execution of a transformation and the transformations themselves are intermingled throughout the program. This implies that the original programmer must anticipate all possible situations that the program can encounter in any combination. For complex problems, this often leads to very complicated and nearly incomprehensible programs. Also, maintenance and updating or extension of this software will be very difficult if not impossible to accomplish. In an Expert system, however, there is a clear distinction between the actions the program can take and the decisions to perform these actions. In most expert systems, these decision/action couples are represented in the form of IF/THEN rules, having the general form:

IF:	(condition-1)	THEN:	(action-1)
	(condition-2)		(action-2)
	.		.
	.		.
	.		.
	(condition-n)		(action-m)

The IF/THEN juxtaposition has proven to be an efficient and simple way of representing domain-specific knowledge. The collection of all the IF/THEN rules is called the knowledge base of the system. Other important parts of the Expert system are the data base (i.e., the collection of all variables used by the program in order to represent and solve the problem), the inference

engine (which controls the interaction between the knowledge base and the data base) and the user interface. This interface, though not essential, is very important, because it permits the user to communicate with the system, often in almost normal language. In most systems, extension or modification of the knowledge base is also handled by the user interface.

The experiences of the authors in using Expert systems in two parts of the x.r.f. procedure are reported below. First, the energy-dispersive x-ray interpretation system (EDXIS) will be discussed. This system attempts to interpret x-ray spectra automatically in terms of the chemical elements present in the sample. The second Expert system is called Axess (i.e., AXIL Expert system shell), which supervises the least-squares spectrum evaluation done with Axil software [1, 5].

AUTOMATED QUALITATIVE INTERPRETATION OF X-RAY SPECTRA BY EDXIS

Principles

Because of the relatively low resolving power of the Si(Li)-detectors used for the measurement of x-ray spectra, there is considerable interference and peak overlap between the characteristic lines of the different elements (Fig. 1). Thus the qualitative interpretation of the spectrum often poses problems and these problems have not been solved by conventional programming techniques. The order of assigning the elements often plays a crucial role. Conventional software is also unable to incorporate efficiently the large amount of knowledge required for proper interpretation. These disadvantages can be overcome by the use of an Expert system.

The Expert system EDXIS consists of two parts: a preprocessor program and the actual expert system (Fig. 2). The details of its implementation can be found elsewhere [6]. The preprocessor program is a conventional Fortran program which converts the spectral data to a form more suitable for the Expert system. Each spectrum is considered as an array of peaks, while each peak is characterized by its location in the spectrum (i.e., the energy of the peak maximum), its height, intensity and width. In order to obtain accurate peak descriptions, the program suppresses the noise in the spectrum and subtracts the continuous background beneath the characteristic peaks [5] (Fig. 1). For each peak, the preprocessor also generates a list of all possible chemical elements which could be responsible for its presence. This is done by comparing the energy of the peak maximum with characteristic line entries in an x-ray library and selecting all elements which have peak energies within 200 eV of the measured peak.

The Expert system itself was implemented in Pascal. The implementation of the basic skeleton of the system, involving construction of the inference engine and the data base, took about 2 weeks. However, building a minimal knowledge base, which presently holds about 200 rules, took 3 months. Initially, each rule was implemented directly in Pascal. After some time, a more sophisticated user interface was added to the system, which allows the

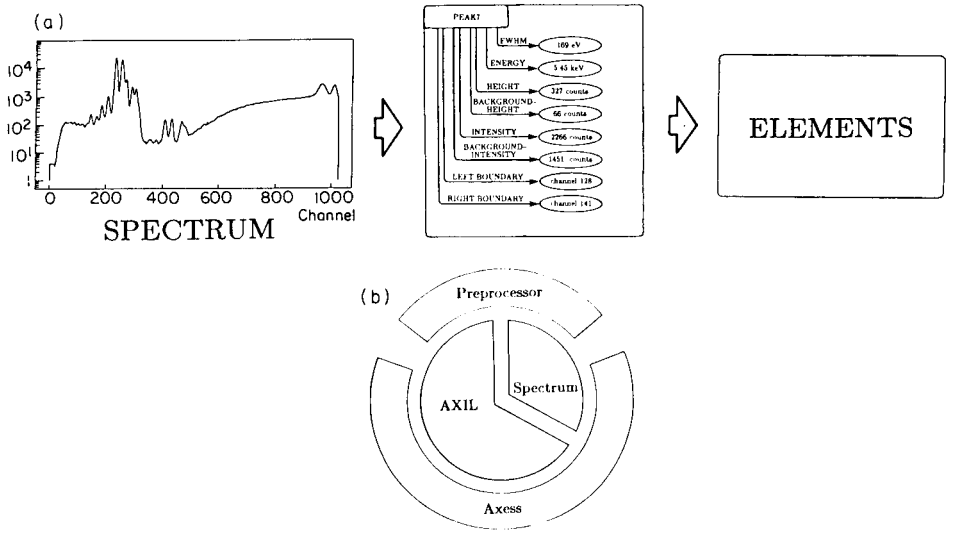

Fig. 2. Structure of the EDXIS and the Axess Expert System. (a) The spectrum is preprocessed to give the relevant characteristics of the peaks in peak frames; from these, EDXIS outputs the elements present. (b) The Axess Expert system.

rules to be entered in formalized English by means of a rule editor. Another part of the user interface makes it possible to trace the reasoning process the system has followed during an interpretation. An example of a rule (and its Pascal equivalent) used by the EDXIS to infer the presence of lead in a spectrum is shown in Table 1.

Structure

The data base of the system consists of static and dynamic parts. The static part holds all the information generated by the preprocessor on the spectrum to be interpreted. These data are read by the Expert system at start-up. The dynamic part is fairly small and consists of an array of certainty factors (CF) corresponding to all chemical elements from sodium up to uranium. These certainty factors can acquire four different values: "absent", "possible", "plausible" (if there is a high probability that the element is present) and "present", if the element is sure to be present.

By means of the rule editor, rules of the type represented in Table 1 can be entered into the knowledge base. The equivalent of this rule in Pascal is also indicated. As can be seen from this example, if the IF part of each rule consists of a number of calls to data base querying functions (e.g. PRESENT (e, de)), which searches the static part of the data base for peaks having an energy between (e — de) and (e + de). If such a peak is found, this function returns the logical value TRUE, else it returns FALSE. Thus, when evaluating the IF part of a rule, certain items from the data base are retrieved and combined in a particular way. Similarly, the THEN part of each rule involves

TABLE 1

Example of a rule used by the EDXIS in English and Pascal forms

English version

```
Rule    : Pb0
If      : no Pb was previously found [P(Pb) < 0.75];
          a peak at (2.35 +/— 0.08) keV is present;
          a peak at (10.55 +/— 0.10) keV is present;
          a peak at (12.62 +/— 0.10) keV is present;
          the intensity ratio of the peaks at (2.35 +/— 0.08) keV and (10.55 +/— 0.10)
          keV lies between (PbMa_La — PbD1) and (PbMa_La + PbD2);
          the intensity ratio of the peaks at (12.62 +/— 0.10) keV and (10.55 +/— 0.10)
          keV lies between (PbLb_La — PbD2) and (PbLb_La + PbD2).
Then    : there is evidence that Pb is present [P(Pb) = 0.75].
```

Pascal version

```
[global] function check_Pb0: boolean;
begin    if (
                 not stored (82) and
                 present (2.35, 0.08) and
                 present (10.55, 0.10) and
                 present (12.62, 0.10) and
                 q_ok(2.35, 0.08, 10.55, 0.10, PbMa_La — Pbd1, PbMa_La + Pbd1) and
                 q_ok (12.62, 0.10, 10.55, 0.10, PbLb_La — Pbd2, PbLb_La + Pbd2)
          )
         then check_Pb0 : = true
         else check_Pb0 : = false;
end;
[global] procedure act_Pb0;
begin    store(82, 'Pb');
end;
```

changes in the certainty factors of one or more chemical elements. For instance, in the above rule, the certainty factor of lead it set to "plausible", by means of the function Store(z).

An Expert system constructs deduction processes by combining the information contained in its data base with the rules from its knowledge base. The functioning of the inference engine which controls this interaction is cyclic. During each cycle, the system advances one step along a line of thought, i.e., during each cycle, one or several new facts are deduced. This cyclic behaviour is continued until a state is reached for which no more new facts can be deduced. Each cycle consists of three parts: first, the IF parts of all the rules in the knowledge base are evaluated. The rules that evaluate to TRUE form the conflict set. Secondly, one rule is selected from this set. In the final phase, the THEN part of that rule is executed, involving a change in the data base or an action to be taken. Since during each cycle only one rule can be executed, the conflict resolution, i.e., the selection of one rule from the knowledge base, is very important.

The EDXIS uses the following multiple strategy to do this: first, rules are

selected on the basis of their priority. When entered into the knowledge base, it is possible to give higher priorities to some rules than to others. Thus, only the subset of rules having the highest priority level is retained. Secondly, rules that use the most recently changed data base item in their IF part are selected. And finally, if the conflict set still contains more than one rule, one of these is selected at random.

Application

To illustrate the functioning of the Expert system and its ability to adapt its procedure to the particular interpretation problem encountered, the interpretation of the spectra depicted in Fig. 3 will be discussed. In both spectra, the same group of peaks is present between channels 130 and 200. When conventional software (typically the energy-window technique) is used to interpret these spectra, the following results are obtained: spectrum A shows Si, S, Cr, Mn, Fe, Co and Ni while spectrum B shows Si, Cl, Cr, Mn, Fe, Co and Ni. The EDXIS obtains different results. The preprocessor suggests Si, Cr, Pm, Eu, Mn, Fe, Co, Ni and Si for spectrum A, and Si, Cr, Pm, Eu, Mn,

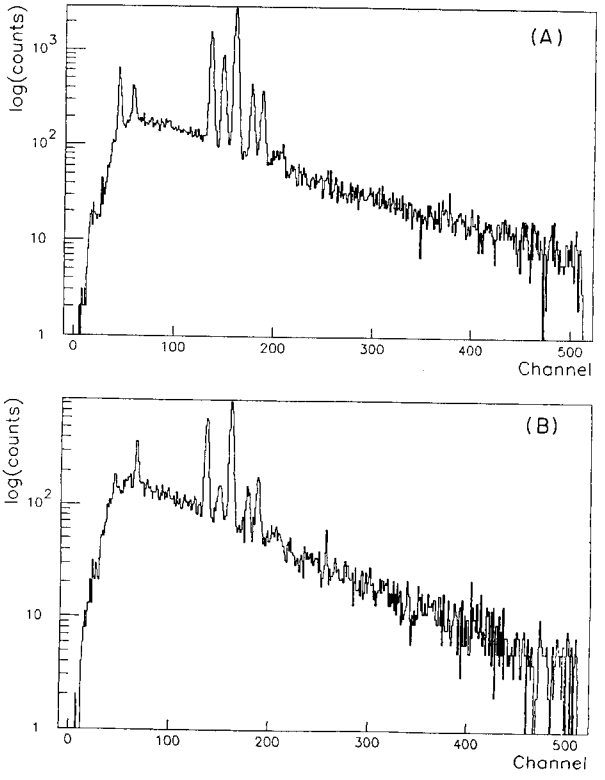

Fig. 3. Electron-induced x-ray spectra: (A) Cr-Mn-Fe-Ni; (B) Cr-Fe-Ni particles, both sampled in an industrial indoor environment.

Fe, Co, Ni and Cl for spectrum B. The final results of the Expert system are Si, Cr, Mn, Fe and Ni for spectrum A and Si, Cl, Cr, Fe and Ni for spectrum B.

The reasoning constructed by the system for interpreting spectrum A can be summarized as follows. In the first cycle, by means of the rule check_Fe0, Fe acquires the "stored" status. In the second cycle, CF[Ni] is set to the "stored" status by the rule check_Ni0. In the third cycle, Eu is removed because no M line (at 1.15 keV) was detected. In the fourth cycle the rule check_Cr_Mn_Fe1 becomes applicable; from the facts that Fe has a "plausible" status (i.e., that the K_α/K_β ratio is approximately correct) and that this is not the case for Mn or Cr, this rule deduces that underneath the Cr-K_β peak there is a significant contribution of Mn-K_α, which distorts the K_α/K_β ratio of Cr. By comparing the intensities of the four peaks between 3.2 and 5.0 keV, the hypothesis that Cr, Mn and Fe are present together is proven. Thus, Cr, Mn and Fe acquire the "present" status. In the fifth cycle, because Fe and Ni acquired the "stored" status during the first two cycles (implying correct K_α/K_β ratios for both elements), while this was not the case for Co, no Co contributions can be present under the Fe-K_β and Ni-K_α peaks. Thus, the CF[Co] is set to "absent", while Ni like Fe acquires the "present" status.

Inspection of the spectrum B, however, shows that the peak corresponding to Cr-K_β (or Mn-K_α) is less intense than the corresponding peak in spectrum A. The expert system handles this slightly different situation by constructing the following reasoning process. During the first 3 cycles, the elements Ni, Cr and Fe successively acquire the "stored" status, implying that the K_α/K_β ratios for these elements are approximately correct. In the fourth cycle, similarly as for spectrum A, the rule check_Fe_Co_Ni sets the status of Co to "absent", while Fe and Ni acquire a "present" status. In the fifth cycle, however, instead of the rule check_Cr_Mn_Fe1, the rule check_Cr_Mn_Fe2 is applicable, and it is concluded that Mn cannot be present when the K_α/K_β ratios of Cr and Fe are correct. Thus, for spectrum B, the Expert system predicts the presence of Cr, Fe and Ni, rejecting both Mn and Co.

Both predictions were confirmed by fitting spectra A and B with the AXIL software.

AXESS, THE AXIL EXPERT SYSTEM SHELL

Principle

In x-ray fluorescence, the aim of quantitative spectrum processing is the accurate measurement of net peak intensities of the characteristic lines of interest in the spectrum. However, because of considerable peak overlap in most x-ray spectra, this can only be accomplished by means of sophisticated deconvolution algorithms. An example of a software package for such deconvolution is called AXIL [1, 5]. For the program to perform a fit, a relatively

large number of control parameters and input flags describing the measuring process, the approximate composition of the sample, etc. need to be specified. The information needed includes the approximate absorption of the fluorescence x-rays in the sample and on their way to the detector, the type of excitation mode used, the characteristic lines/elements that need to be fitted, the background model to be used, etc.

Although the non-linear fit algorithm itself is very suitable, the values of these parameters needs to be approximately correct for each individual spectrum in order to obtain an optimal fit. In general, a considerable amount of experience in x.r.f. and in operating the program is needed before reliable results can be obtained with a minimum of computational effort. In order to channel this experience into an automated system the implementation of an Expert system shell around the AXIL program was started. The principal function of this system is the automatic optimization of the input of the fit-procedure for each individual spectrum Thus, the system will also be able to serve as a troubleshooter when bad-fit results are obtained, suggesting possible causes for the misfit to the AXIL user. In the long run, it is also intended to function as a tutoring system for analysts unfamiliar with quantitative x-ray spectra processing.

The implementation of this system was only recently started. It was decided to develop the system on an IBM-PC AT, on which the latest version of AXIL also runs. The C programming language was chosen as the major developing tool because of its speed and versatility. In its present state, the Axess system consists of three main parts (Fig. 2b): the expert system itself (with its data and knowledge bases and inference engine) together with two subsystems: the AXIL-fit program and the same preprocessor as in EDXIS. The system is based on the generate-and-test principle which has been extensively used in the DENDRAL project [7]. Initially, the Expert system uses the rules in its knowledge base to optimize the fitting parameters as much as possible, after which the AXIL-fit program is executed. If the fit obtained is not satisfactory, the system tries to find a solution to this problem, e.g. by asking the user for more information or by extracting more data from the spectrum by means of the preprocessor program. These requests for additional information originate from the THEN parts of the appropriate rules. On the basis of the new information, the fit model will be adjusted, after which a second fit is attempted. This process is repeated until a satisfactory result is obtained or until the system has exhausted all its knowledge and information resources.

Structure

Similarly to EDXIS, the data base of Axess can be divided into static and dynamic parts. The static data base, which is extensive, contains all the internal variables used by the AXIL program, while the dynamic part contains miscellaneous variables which usually correspond to one of the fitting parameters of the program. At the present stage, certainty factors or fuzzy set variables have not yet been implemented.

Rules can be entered into the knowledge base using a rule-translator utility. Examples of two of these rules are represented in Table 2. Each rule is characterized by a name, a priority level, the variables it uses in its IF part, the variables which are changed in the THEN part, a number of STATIC conditions, a number of VARIABLE conditions and a number of actions. Rules concerned with the same general aspect of the fitting process are organized in different modules. Each module can also have a priority level and can be active or inactive. If a module is not active, the rules in it are not used by the system. The activity of a module can be controlled by special rules, called meta rules, because they are rules concerned with the use of other rules.

As Axess, in contrast to EDXIS, contains various types of rules and variables, a much more sophisticated inference engine was implemented. Instead of evaluating all rules in the knowledge base, the inference engine searches only the active modules. In these modules, only the rules which have static conditions evaluating to TRUE are searched. Conflict resolution is done on the basis of successive reduction strategies. Rules are selected on the basis of: (a) the priority level of the module they are in; (b) their own priority level; (c) whether or not they use the most recently changed data-base item; (d) the number of conditions in their IF part; (e) the number of variable con-

TABLE 2

Example of two rules used by the Axess system. (The symbols surrounding the words in the first column of output have been deleted for clarity.)

module	control
priority	15
rule	window1
priority	15
if	(window.endwin − window.begwin) ⩽ 0;
then	AskFor("the beginning of the fit window", window.begwin);
	AskFor("the end of the fit window", window.endwin);
...	
End	
module	background
priority	10
rule	background1
priority	15
changes	backtype;
	bordlin;
	bordexp;
static	(window.endwin − window.begwin) < 200;
then	backtype = LINEAR;
	b_ordlin = 2;
	b_ordexp = 0;
...	
End	

ditions in their IF part; and (f) the number of actions in their THEN part. In EDXIS, only (b) and (c) were implemented.

Example

A brief example of the functioning of this Expert system will illustrate the querying of the system for information from the user and by means of the preprocessor program. The example involves adjustment of the fitting model because of considerable absorption of the zinc K_β radiation by copper in a brass sample. When an attempt is made to fit the spectrum of Fig. 1 with AXIL software, with the K_α/K_β lines for Cu and Zn included in the fitting model and with K_α/K_β ratios evaluated from measurements on pure zinc and copper samples, the Zn-K_β peak is over-estimated. In general, the K_β component of a K_α/K_β pair can be overestimated because of spectral interference at the K_α peak or absorption of the K_β radiation. The former case occurs when the spectrum of Fig. 1 is fitted with Zn lines only, i.e., when the characteristic lines of copper are not included in the model. However, absorbance of the Zn-K_β radiation would occur only if the spectrum were taken from a thick sample, so that the absorption can be attributed to the copper matrix. In order to be able to fit spectra in which K_α/K_β ratios are distorted because of other reasons as mentioned above, the AXIL software also permits the splitting of the K_α-K_β group into a K_α and a K_β group; thus, the K_α/K_β ratio can acquire any value. In order to discover the cause of this misfit, the Expert system needs to move through the decision tree shown in Fig. 4. For this purpose, each node in this tree is represented as an IF/THEN rule, which can be entered into the system rule base. Examples of these rules are given in Table 3. Because, in this example, the Cu-K_α and K_β lines are already included in the fitting model, the system moves to the nodes concerned with the absorption of the K_β radiation of zinc. After checking that the sample type is THICK, and that no radiation absorption correction was previously included, it decides to approximate the sample composition by means of the rule "KaKbTooLow3". A subsequent fit, including the correction for absorption, corresponds more closely to physical reality. Clearly, the spectrum can be fitted with a fixed (though corrected) K_α/K_β ratio and splitting of this ratio becomes unnecessary.

Conclusion

The development of Expert systems for analytical purposes requires considerable effort in the construction of the knowledge base. The domain-specific knowledge to be incorporated into the system must be made explicit and translated into a (large) number of rules; individual rules are simple and easy to comprehend.

Compared to the building of the knowledge base, the implementation of an inference engine is relatively easy. To obtain an efficient Expert system, which can be used for practical purposes in the laboratory, the use of programming languages like C, Pascal, Modula-2, etc. is recommended. When

these general programming languages are used, it is possible to adjust the inference engine to the particular problems which will be dealt with by the Expert system. In general, the integration of conventional software with Expert systems is not straightforward.

TABLE 3

Some of the rules used by the Axess system while generating the decision tree shown in Fig. 4.

```
rule        KaKbTooLow1
  priority  13
  uses      bf_opt;
            ratio_type;
            crit_elem;
  if        bf_opt == BAD_KAKB;
            ratio_type == TOO_LOW;
            Element(crit_elem + 1) == NOT_INCLUDED;
  then      IncludeElement(crit_elem + 1);
rule        KaKbTooLow2
  priority  13
  uses      bf_opt;
            ratio_type;
            crit_elem;
            sample_type;
            sample_composition;
  changes   sample_composition;
  if        bf_opt == BAD_KAKB;
            ratio_type == TOO_LOW;
            Element(crit_elem + 1) == INCLUDED;
            sample_type == THICK;
            sample_composition == UNKNOWN;
  then      ApproxSampleComp();
            sample_composition = KNOWN;
rule        KaKbTooLow3
  priority  13
  uses      bf_opt;
            ratio_type;
            crit_elem;
            sample_type;
  if        bf_opt == BAD_KAKB;
            ratio_type == TOO_LOW;
            Element(crit_elem + 1) == INCLUDED;
            sample_type != THICK;
  then      SplitGroup(crit_elem,KA_KB);
End
```

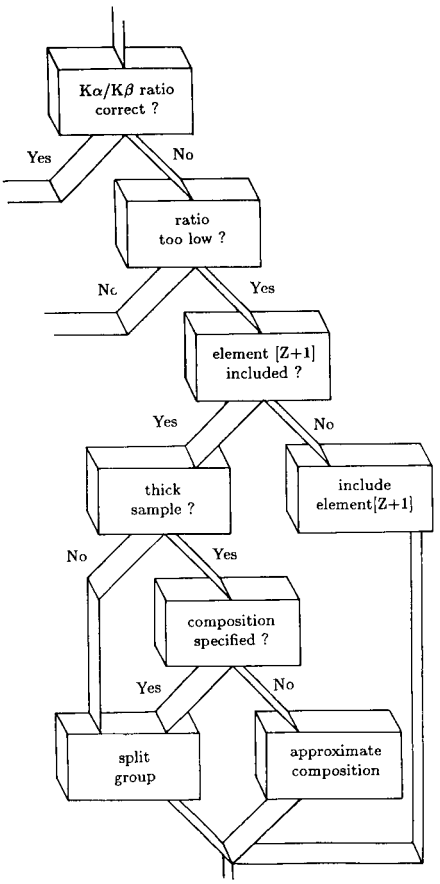

Fig. 4. Decision tree generated by the Axess system during the fit of the spectrum depicted in Fig. 1.

REFERENCES

1 P. Van Espen, H. Nullens and F. Adams, Nucl. Instrum. Methods, 142 (1977) 243.
2 P. Van Espen and F. Adams, X-Ray Spectrom., 10 (1981) 64.
3 S. D. Rasbury and K. F. J. Heinrich, Anal. Chem., 46 (1974) 81.
4 J. W. Criss, L. S. Birks and J. V. Gilfrich, Anal. Chem., 50 (1978) 33.
5 K. Janssens, J. Nobels and P. Van Espen, Chem. Lab., 1 (1986) 109.
6 K. Janssens and P. Van Espen, Anal. Chim. Acta, 184 (1986) 117.
7 B. Buchanan, E. A. Feigenbaum and J. Lederberg, Applications of Artificial Intelligence for Chemical Inference, McGraw-Hill, New York, 1980.

Analytica Chimica Acta, 191 (1986) 181—192
Elsevier Science Publishers B.V., Amsterdam — Printed in The Netherlands

THE INCLUSION OF DOUBLE-CHANNEL ULTRAVIOLET SPECTROPHOTOMETRY IN AN EXPERT SYSTEM FOR PHARMACEUTICAL ANALYSIS

J. SMEYERS-VERBEKE, M. R. DETAEVERNIER and D. L. MASSART*

Vrije Universiteit Brussel, Farmaceutisch Instituut, Laarbeeklaan 103, B-1090 Brussels (Belgium)

(Received 11 July 1986)

SUMMARY

Different criteria are compared for the selection of optimal wavelengths in the u.v. spectrophotometry of pharmaceutical samples. The effect of over-determination on the precision and accuracy of the results is evaluated. It is concluded that for the commercial samples of tablets containing two active substances investigated, good results are obtained when the classical approach (measurement at λ_{max}) is applied and that no improvement is observed when over-determination is used. Rules are derived to include the two-component u.v. spectrophotometry in an expert system for pharmaceutical analysis.

In an earlier paper [1], the expert systems approach to pharmaceutical analysis was introduced. This paper related the development of rules that decide whether a substance can be determined by u.v. spectrophotometry and how it should be dissolved. That first paper was restricted to the analysis of tablets, to about half of the pharmacological groups and to one-channel spectrophotometry. Since then, the system has been developed to include solutions and most pharmacological groups, as will be reported elsewhere. The present paper reports on the derivation of rules to select conditions when two active substances are present. It is necessary to decide if two-channel u.v. spectrophotometry is needed and which wavelengths should be used for the measurements.

THEORY

The Beer-Lambert Law is $A = kC$, where A represents the absorbance, k the absorptivity and C the concentration (provided that the optical path-length is 1 cm). This can be expanded for the analysis of an n-component mixture to:

$$A_1 = k_{11}C_1 + \ldots + k_{1n}C_n$$

$$A_p = k_{p1}C_1 + \ldots + k_{pn}C_n$$

0003-2670/86/$03.50

A_i represents the absorbance of the mixture at wavelength i, C_j the concentration of the component j, and k_{ij} the absorptivity of component j at wavelength i. In matrix notation, this becomes $\mathbf{A} = \mathbf{KC}$, where $\mathbf{A}$ is the vector of the absorbances measured at p wavelengths, $\mathbf{C}$ is the concentration vector for n components and $\mathbf{K}$ is the absorptivity matrix consisting of p rows and n columns (components).

For the analysis of an n-component mixture, at least n independent measurements are required ($p = n$). A so-called exactly-determined system is then obtained and the concentrations of the n components in the mixture can be calculated if the absorptivities are known: $\mathbf{C} = \mathbf{K}^{-1}\mathbf{A}$. When $p > n$, an over-determined system is obtained and $\mathbf{K}$ is no longer a square matrix. Therefore the generalized inverse of $\mathbf{K}(= (\mathbf{K}'\mathbf{K})^{-1}\mathbf{K}')$ is needed for the calculation of the concentrations:

$$\mathbf{C} = (\mathbf{K}'\mathbf{K})^{-1}\mathbf{K}'\mathbf{A} \tag{1}$$

with $\mathbf{K}'$ the transpose of $\mathbf{K}$ and $(\mathbf{K}'\mathbf{K})^{-1}$ the inverse of $\mathbf{K}'\mathbf{K}$. This corresponds to the least-squares solution that minimizes the sum of squares of the differences between the observed and calculated absorbances.

Criteria for selecting optimal wavelengths

For exactly-determined systems, different criteria for the selection of optimal wavelengths have been proposed. Classically, the absorption maxima of the pure components are used. This selection, however, is not necessarily optimal except when overlap of the absorption spectra is small.

The sensitivity, H, of a multicomponent system, defined by Kaiser [2] as the absolute value of the determinant of the absorptivity matrix, is a parameter that can be used for comparing different sets of wavelengths. Because maximum sensitivity is obtained for a determinant with large diagonal elements and low off-diagonal elements, maximization of the determinant corresponds to optimization of the sensitivity.

A generalization of the sensitivity concept to the over-determined situation was proposed by Junker and Bergmann [3]: $H = \mathrm{sqr}|\mathbf{K}'\mathbf{K}|$. This equals the sensitivity as defined by Kaiser for $p = n$. An optimization procedure that would consist in comparing H for all combinations of wavelengths would require an appreciable number of calculations. To obtain the optimal combination of 4 out of 25 possible wavelengths, one needs to calculate and compare 12 650 determinants. Junker and Bergmann [3] developed an optimization procedure that requires fewer calculations. Starting with p wavelengths, the sensitivity of the p possible combinations of $(p - 1)$ wavelengths is calculated. The combination with the highest sensitivity is retained and the wavelength that is not included in this combination is dropped. The procedure is then repeated by considering the $(p - 1)$ combinations of $(p - 2)$ wavelengths. Again the set with the highest sensitivity is retained and one wavelength dropped as a consequence. This procedure is repeated until a predetermined number of wavelengths ($\geqslant n$) remains. In this way, one greatly reduces the number of determinants to be calculated. For the above-mentioned

example, one needs to calculate 315 determinants (i.e., a reduction by a factor 40).

Another approach is to minimize the so-called condition of the **K** matrix. A set of equations is ill-conditioned if small errors in the measurements y lead to large errors in the analytical result x. If **K** is known exactly, the relationship between the relative errors in the analytical result and the relative error in the measurement is given by

$$(\|\Delta x\|)/(\|x\|) \leqslant \text{cond } (\mathbf{K})\ (\|\Delta y\|/\|y\|)$$

where $\|\ \|$ represents the norm of the vector (e.g., $\|x\| = [\Sigma_{i=1,n}(x_i)^2]^{1/2}$. Maximal precision is thus obtained for a minimal condition of the matrix **K**:

$$\text{cond } (\mathbf{K}) = \|\mathbf{K}\|\ \|\mathbf{K}^{-1}\| \tag{2}$$

For a nonsingular symmetric matrix, $\|\mathbf{K}\|$ equals the largest eigenvalue of $\mathbf{K}[\lambda(\mathbf{K})_{max}]$, $\|\mathbf{K}^{-1}\|$ equals the reciprocal of the smallest eigenvalue of $\mathbf{K}[\lambda(\mathbf{K})_{min}]$. Equation 2 then becomes

$$\text{cond } (\mathbf{K}) = \lambda(\mathbf{K})_{max}/\lambda(\mathbf{K})_{min} \tag{3}$$

For an asymmetric or rectangular matrix **K**,

$$\|\mathbf{K}\|\ \|\mathbf{K}^{-1}\| = [\lambda(\mathbf{K}^T\mathbf{K})_{max}/\lambda(\mathbf{K}^T\mathbf{K})_{min}]^{1/2} \tag{4}$$

This is a generalization of Eqn. 3 because for a symmetric matrix **K**

$$\lambda(\mathbf{K}^T\mathbf{K}) = [\lambda(\mathbf{K})]^2 \tag{5}$$

Fully-selective measurements with equal sensitivity result in a **K** matrix with condition 1. Less selective measurements give rise to condition numbers >1.

Optimizing the precision by minimizing the condition of **K** is even more time-consuming than optimizing the determinant and fast procedures have not been reported previously. The method proposed here is similar to that used by Junker and Bergmann for optimizing the determinant. Starting with p wavelengths, the conditions for the p possible combinations of $(p-1)$ wavelengths are calculated with Eqn. 4. Of these combinations that with the smallest condition is retained. This means that one wavelength is dropped from consideration, namely, the one that has the largest (i.e., the worst) influence on the condition of the system. The procedure is then repeated by considering the $(p-1)$ combinations of the $(p-2)$ remaining wavelengths. Again, the set with the smallest condition is retained. The procedure is repeated until a predetermined number of wavelengths ($\geqslant n$) remains.

EXPERIMENTAL

Mixtures containing paracetamol and salicylamide in different ratios were prepared in 0.1 M sodium hydroxide. Standard solutions of paracetamol and salicylamide, respectively, were prepared in 0.1 M sodium hydroxide to determine the absorptivities ($E^{1\%}_{1\,cm}$) of paracetamol and salicylamide at different wavelengths. Blank solutions were of 0.1 M sodium hydroxide.

The spectra of the pure compounds and of the mixture were recorded in the 230—370-nm region by means of a LAMBDA 3 u.v.-visible spectrophotometer and a model 561 recorder (both from Perkin-Elmer). Each time a mixture spectrum was measured, the two standard spectra were also recorded. Automatic correction for the blank was done after storage of the spectrum of the blank solution in the memory of the spectrophotometer.

From the spectra of each of the pure compounds, the absorptivities were calculated between 230 and 370 every 5 nm and at the absorption maxima of both components (256, and 240 and 327 nm, the absorption maxima of, respectively, paracetamol and salicylamide in 0.1 M sodium hydroxide). In this way, p equals 31 and consequently **K** is a 31 × 2 matrix. From the spectrum of the mixture, the absorbance at the 31 wavelengths were obtained.

Computations for the optimization procedure were done by a program specially written in BASIC for the Apple-2 computer. For each combination of wavelengths, the condition (Eqn. 3) as well as the concentration of both components in the mixture (Eqn. 1) are computed.

A program for the optimization of the determinant as described by Junker and Bergmann [3] was also developed in order to compare the performances of both optimization criteria. Concentrations reported are calculated as (calculated/true) × 100. The relative % error is given by [(|true − calculated|)/true] × 100.

RESULTS AND DISCUSSION

The spectra of paracetamol and salicylamide are given in Fig. 1. Table 1 shows the first step of the optimization. Because a minimum for the condition is obtained when the measurement at 245 nm is dropped, this wavelength is no longer considered in the next step. Table 2 summarizes the complete optimization procedure. The procedure is repeated until two wavelengths remain; these are 260 and 327 nm.

The performance of this combination of wavelengths is compared in Table 3 with other combinations, namely, combinations of the absorption maxima of the pure components (256, 327 and 256, 240 nm), and combination of

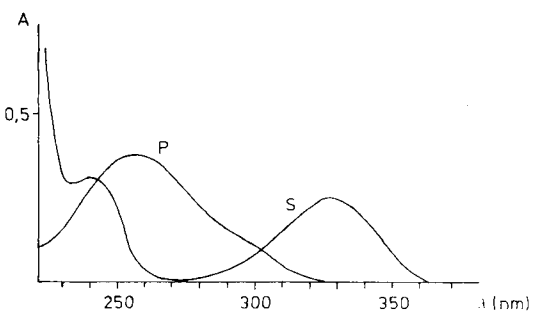

Fig. 1. Spectra of salicylamide and paracetamol.

TABLE 1

First step in the optimization of the condition

Wavelength dropped	Cond (K)	Wavelength dropped	Cond (K)	Wavelength dropped	Cond (K)
230	1.822	280	1.802	327	1.888
235	1.783	285	1.801	330	1.887
240	1.746	290	1.799	335	1.871
245	1.709	295	1.798	340	1.849
250	1.713	300	1.800	345	1.830
255	1.765	305	1.809	350	1.817
256	1.775	310	1.825	355	1.812
260	1.802	315	1.849	360	1.810
265	1.808	320	1.874	365	1.810
270	1.806	325	1.887	370	1.809
275	1.804				

TABLE 2

Summary of the complete optimization procedure

p	Wavelength dropped	Cond (K) of remaining system	p	Wavelength dropped	Cond (K) of remaining system
31	245	1.709	16	365	1.085
30	250	1.603	15	360	1.085
29	240	1.529	14	285	1.085
28	255	1.443	13	315	1.065
27	256	1.383	12	355	1.065
26	235	1.296	11	350	1.070
25	275	1.274	10	280	1.077
24	230	1.225	9	340	1.057
23	270	1.180	8	345	1.065
22	300	1.158	7	335	1.144
21	295	1.138	6	265	1.225
20	305	1.117	5	325	1.083
19	290	1.105	4	320	1.166
18	310	1.085	3	330	1.621
17	370	1.085			

the two wavelengths selected by optimizing the determinant according to Junker and Bergmann (230, 260 nm). Because several authors have advocated over-determination to obtain better precision [4, 5], over-determined systems are also included in the comparison. These are a combination of four wavelengths, selected by minimizing the condition as described earlier (265, 320, 327, 330 nm) and a set containing all 31 wavelengths. Mixtures containing different concentration ratios of paracetamol and salicylamide were examined. The comparison shows that the measurement obtained by the smallest

TABLE 3

Results of different combinations of wavelengths to evaluate the concentration of paracetamol (P) and salicylamide (S) in mixtures containing both components in different ratios. The spectra are considered between 230 and 370 nm

P/S ratio	$p = 2$								$p = 4$		$p = 31$	
	λ_{max}				COND (K)		H		COND (K)		230—370	
	256/327		240/256		260/327		230/260		260/320/327/330			
	P	S	P	S	P	S	P	S	P	S	P	S
1/1	99.0	99.7	98.5	102.9	98.8	99.7	98.7	100.9	98.8	99.5	98.3	100.6
	100.0	100.0	99.7	102.5	99.3	100.0	99.0	104.8	99.4	99.7	99.4	101.1
	100.2	100.7	100.2	100.5	99.2	100.7	98.9	105.6	99.1	100.6	99.0	101.6
MRE[a]	0.40	0.33	0.67	1.97	0.90	0.33	1.13	3.77	0.90	0.47	1.10	1.10
1/4	97.8	100.7	98.4	99.5	100.8	100.7	101.3	98.7	100.9	100.3	95.9	100.3
	97.9	99.4	97.8	99.6	97.8	99.4	97.7	99.7	97.9	98.9	97.2	99.3
	96.9	100.1	97.1	99.9	96.6	100.1	96.2	102.1	96.5	100.4	95.2	100.7
MRE[a]	2.47	0.47	2.13	0.33	2.33	0.47	2.47	1.57	2.17	0.60	3.90	0.57
4/1	100.7	100.7	100.6	101.2	100.7	100.7	100.6	105.0	100.7	99.8	100.3	100.6
	99.7	98.4	99.7	98.1	99.9	98.4	99.9	102.6	99.9	98.8	99.8	98.5
	99.6	99.9	99.6	99.1	99.5	99.9	99.4	105.4	99.5	99.2	99.4	99.2
MRE[a]	0.47	0.80	0.43	1.33	0.43	0.80	0.43	4.33	0.43	0.73	0.37	0.97

[a]Mean relative error.

condition criterion (260/327 nm) yields relative % errors similar to those obtained for measurements at the absorption maxima of the components (256/327 nm). Moreover, there seems to be no need to use over-determination; neither for $p = 4$ nor for $p = 31$ was any improvement in the results observed.

When the spectra of paracetamol and salicylamide are inspected, it might be concluded that the situation chosen is a favorable one because of the presence of an absorption peak for salicylamide around 327 nm where the interference of paracetamol is small. Therefore a situation with more overlapping spectra was investigated by ignoring the second absorption peak. The same data were used but only part of the spectra (between 230 and 285 nm) was taken into account. Again several combinations of wavelengths were compared: (a) the absorption maxima of the pure components (240 and 256 nm); (b) the two wavelengths selected by minimizing the condition (230 and 265 nm); (c) the two wavelengths selected by optimizing the determinant (230 and 260 nm); (d) the four wavelengths selected by optimizing the condition (230, 235, 265 and 275 nm); and (e) the 13 wavelengths between 230 and 285 nm.

The comparison is summarized in Table 4. For all concentration ratios examined, the classical approach, measurement at the absorption maxima, gives good results and no improvement is observed for the wavelength combination obtained by minimizing the condition nor for the over-determined situations studied.

To investigate whether the conclusions obtained on this example can be generalized, 18 commercial samples of tablets containing two active substances

TABLE 4

Results of different combinations of wavelengths to evaluate the concentration of paracetamol (P) and salicylamide (S) in mixtures containing both components in different ratios. The spectra are considered between 230 and 285 nm

P/S ratio	$p = 2$						$p = 4$		$p = 13$	
	λ_{max} 240/256		H 230/260		COND (K) 230/265		COND (K) 230/235/265/275		230/285	
	P	S	P	S	P	S	P	S	P	S
1/1	98.5	102.9	98.7	100.9	97.0	101.9	97.0	102.2	97.7	102.3
	99.7	102.5	99.1	104.8	97.7	105.7	97.6	104.1	98.6	103.6
	100.2	100.5	98.9	105.6	97.7	106.4	97.6	104.2	98.7	102.8
MRE[a]	0.67	1.97	1.10	3.77	2.53	4.67	2.60	3.50	1.67	2.90
1/4	98.4	99.5	101.3	98.7	95.4	99.6	93.5	100.7	96.2	100.3
	97.8	99.6	97.7	99.7	95.4	100.1	94.0	100.1	96.4	100.1
	97.1	99.9	96.2	102.1	94.1	102.5	92.6	101.8	94.9	101.2
MRE[a]	2.23	0.33	2.47	1.23	5.03	1.00	6.63	0.87	4.17	0.53
4/1	100.6	101.2	100.1	105.0	100.2	106.0	100.3	102.0	100.1	102.9
	99.7	98.1	99.9	102.6	99.8	102.9	99.7	98.5	99.8	98.2
	99.6	99.1	99.4	105.4	99.2	106.0	99.3	98.7	99.4	99.0
MRE[a]	0.43	1.33	0.27	4.33	0.40	4.97	0.43	1.60	0.30	1.90

[a]Mean relative error.

TABLE 5

Application to commercial samples

Sample	Substances	Solvent[a]	R^b	Cond (K)			λ_{max}		
				λ	SM[c]	CS[d]	λ	SM[c]	CS[d]
					Conc. (%)			Conc. (%)	
Aldactazine	Altizide	M	1.4	240/270	102.7	101.5	235/270	102.7	101.3
	Spironolactone				102.2	98.8		100.5	99.0
Moduretic	Hydrochlorothiazide	H-M	10	269/355	98.6	97.8	269/362	98.4	97.6
	Amiloride • HCl				95.3	104.4		99.2	106.6
Postadoxine	Pyridoxine • HCl	H	2.5	230/280	99.1	94.4	230/290	99.4	94.8
	Meclozine • HCl				99.3	103.0		100.9	105.0
Cibalgine	Propylphenazone	N-M	7.0	239/272	100.1	99.6	239/272	100.1	99.6
	Allobarbital				100.4	102.2		100.4	102.2
Parafon	Paracetamol	M	3.0	255/282	100.8	101.9	247/282	98.8	100.4
	Chloroxazone				97.5	99.8		98.3	100.6
Dismenol	Carzenide	M	2.7	233/268	98.2	96.0	233/268	98.2	96.0
	Aminophenazone				101.2	94.5		101.2	94.5
Tomanol	Phenylbutazone	H-M	1.2	235/275	100.5	97.6	240/265	98.8	97.4
					100.7	98.5		101.3	97.7
Trenteron	Bamiphylline • HCl	H-M	1.1	245/280	98.9	104.7	230/275	102.2	102.3
	Metamizol • Na				102.2	102.8		99.0	101.2
Parmentier	Phenazone	M	2.1	242/280	102.8	101.3	242/272	101.8	100.5
	Caffeine				100.6	100.4		104.6	101.6
Hydromet	Hydrochlorothiazide	M	3.3	255/290	97.5	99.9	269/281	102.5	100.6
	Methyldopa				101.6	101.6		99.6	101.3
Mucorhinyl	Phenylephrine • HCl	H	1.1	235/280	102.0	108.8	263/272	97.6	112.5
	Chloropheniramine • Mal				99.2	102.8		102.5	97.2
Betapyr	Thiamine • HCl	H	1.1	250/290	102.0	105.6	245/290	103.0	106.2
	Pyridoxine • HCl				100.8	105.0		99.7	102.5
Neutraphylline-Papaverine	Papaverine • HCl	H-M	1.0	240/270	102.3	94.6	251/268	102.0	97.4
	Diprophylline				102.5	97.5		102.5	96.8
Rhinopront	Phenylephrine • HCl	H	1.9	250/280	102.5	107.0	262/271	99.8	106.9
	Carbinoxamine • Mal				96.5	104.2		96.7	95.9

Monotrean	**Papaverine**	H	1.7	275/360	105.8	102.8	307/345	102.7	105.6
	Kinine • HCl				103.0	99.5		100.8	97.3
Hibitane	Chlorohexidine • HCl	M	1.3	255/295	99.2	101.7	256/292	100.9	101.8
	Benzocaïne				100.3	96.2		102.0	96.4
Uractazide	Hydrochlorothiazide	M	1.5	240/269	100.8	100.8	236/269	100.7	100.7
	Spironolactone				95.6	98.8		96.8	103.0
Actifed	Tryprolidine • HCl	H	1.3	256/300	100.1	99.7	256/288	100.5	101.3
	Pseudoephedrine • HCl				101.9	101.6		101.4	100.1

[a]M, methanol; H, 0.1 M HCl; H-M, 0.2 M HCl in methanol; N-M, 0.1 M NaOH in methanol. [b]For explanation, see text. [c]Standard mixture. [d]Commercial sample.

were investigated. Both the sample as such and a sample consisting of a mixture of the two active substances in the right proportions were analysed. Because it is intended to include the selection procedure in an expert system for the analysis of pharmaceutical substances, some rules of thumb need to be derived. One rule (or set of rules) is needed to decide whether or not to apply multicomponent spectrophotometry and another to decide whether to apply the simple procedure, consisting in measurement at some absorption maxima, or rather to go to the much more time-consuming condition criterion method described above. The rule applied here is to select the simple method when there is a pair of λ_{max} values separated by at least 10 nm and for which $R < 10$; R is the quotient of dose times absorptivity for the substance with higher absorbance divided by the same product for the substance with lower absorbance. Only binary mixtures of active substances satisfying this rule are included in the investigation (about 50% of all samples).

The results are shown in Table 5. The results obtained for the wavelength combinations obtained by the minimum condition criterion are also reported. The mean result for all samples in the artificial mixtures is 100.49 and the standard deviation is 1.85; the mean result for all commercial samples is 100.61 and the standard deviation is 3.86. One concludes that there is no significant difference between the means and that the means are not significantly different from 100.0%. The variances, however, are significantly different. The additional variance in the commercial samples could have two causes: the variance of the concentration in the industrial product and the additional steps in the analytical procedure such as dissolution of the tablet, filtration, etc. The additional step in the analysis of commercial samples has, however, only a very limited influence on the accuracy of the results. The errors as a whole are randomly distributed and due to imprecision not to inaccuracy. A two-sample map (Fig. 2) does not show a clear difference between the + + and — — results on the one hand and the +— and —+ results. This again is an indication that the deviations from 100% are due to random and not to systematic errors.

The rules

In summary, the following rules were derived in addition to those already included in the first article about expert systems for u.v. spectrophotometry of active substances in tablets [1] (to promote readability, the rules are given in plain english and not in Prolog).

(1) Two active substances in a tablet are "easy to measure" by two-channel spectrophotometry if their spectra contain a pair of absorption maxima separated by at least 10 nm and for which $R \leqslant 10$ and if each active substance separately is measurable by one-channel spectrophotometry (according to the rules derived earlier).

(2) If two active substances are "easy to measure", then they are measured at the λ_{max} values obeying the conditions given above; priority is given to the λ_{max} values for which the lowest R value is obtained.

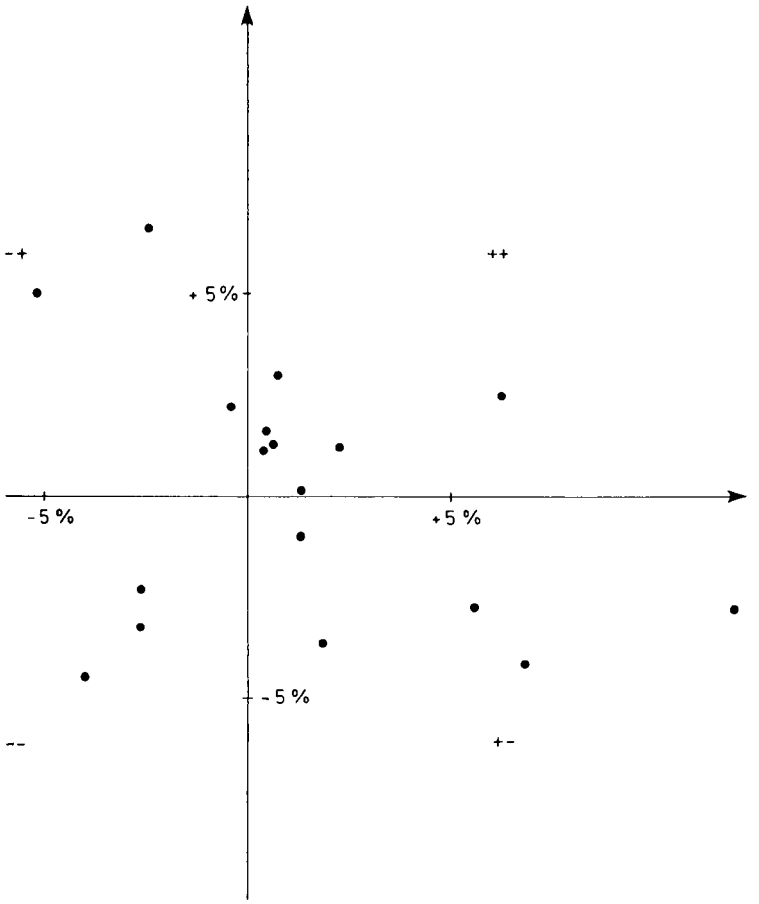

Fig. 2. Two-sample map of the results obtained on the commercial samples. Each dot is one of the 18 samples analysed. The horizontal axis gives the deviation from 100% of the first component and the vertical axis the deviation of the second one.

(3) Two active substances in a tablet are "difficult to measure" by two-channel spectrophotometry if there are no λ_{max} values separated by at least 10 nm for which also $R \leqslant 10$ and if each active substance separately is measurable by one-channel spectrophotometry. The condition selection procedure is then applied (or if one prefers, one resorts to liquid chromatography).

(4) Two substances "cannot be measured" by two-channel spectrophotometry if one or both of these substances cannot be measured separately by one-channel spectrophotometry (in all probability, a rule will be added that in such a case chromatography must be considered).

Further directions

It was the intention of this research to investigate when simple two-channel spectrophotometry at the absorption maxima is possible. Further work will

concentrate on exactly what to do in "difficult-to-measure" situations and, more particularly, when it is worthwhile to make the rather extensive calculations necessary for the selection procedure based on conditions. Another point to be investigated is the small interference that can occur when excipients such as phthalates are present. A solution could be to apply calibration methods based on principal components models, because this so-called soft modelling approach should permit elimination of small, systematic errors.

The final aim is to include these rules into a larger expert system which also provides guidance to the selection of alternative methods such as high-performance liquid chromatography (h.p.l.c.). As a first contribution, preliminary material about the selection of h.p.l.c. detectors has been reported [6]. More general rules for the selection of such detectors have since been derived, and rules for the selection of the initial elution mode (reversed or normal phase) will be described at a later date.

Finally, there is the problem of which software solution to choose. Preliminary results indicate that writing one's own expert systems in Prolog (which was done here) or Lisp is possible but extremely time-consuming. More promising results have been obtained with a knowledge engineering system called KES [7, 8].

The authors thank Lotto and FGWO for financial assistance.

REFERENCES

1 M. R. Detaevernier, Y. Michotte, L. Buydens, M. P. Derde, M. Desmet, L. Kaufman, G. Musch, J. Smeyers-Verbeke, A. Thielemans, L. Dryon and D. L. Massart, J. Pharm. Biomed. Anal., 4 (1986) 297.
2 H. Kaiser, Fresenius Z. Anal. Chem., 260 (1972) 252.
3 A. Junker and G. Bergmann, Fresenius Z. Anal. Chem., 278 (1976) 191.
4 J. H. Kalivas, Anal. Chem., 55 (1983) 565.
5 M. Otto and W. Wegscheider, Anal. Chem., 57 (1985) 63.
6 G. Musch, M. Desmet and D. L. Massart, J. Chromatogr., 348 (1985) 97.
7 J. A. Reggia, Knowledge-based decision support systems: development through KMS, Univ. MN, Comput. Sci. Dept., TR 1121, 1985.
8 L. Buydens, M. R. Detaevernier, D. Tombeur and D. L. Massart, Chemometrics Intelligent Lab. Systems, 1 (1986) 99.

Analytica Chimica Acta, 191 (1986) 193—204
Elsevier Science Publishers B.V., Amsterdam — Printed in The Netherlands

A FUZZY METHOD FOR COMPONENT IDENTIFICATION AND MIXTURE EVALUATION IN THE ULTRAVIOLET SPECTRAL RANGE

MATTHIAS OTTO* and HANS BANDEMER

Department of Chemistry and Department of Mathematics, Bergakademie Freiberg, Leipziger Strasse, DDR-9200 Freiberg (German Democratic Republic)

(Received 28th May 1986)

SUMMARY

A fuzzy theory approach is proposed for interpreting component spectra that takes into account the imprecise character of both reference and sample spectra. The method enables more decisions to be made than is possible in least-squares comparison of spectra. The method can be used to quantify components under overlapping bands as needed in multicomponent spectrophotometry and for component resolution in chromatography with u.v. detection. The method is particularly suitable for problems in the u.v. range because it can deal with continuous spectra where factor and principal components methods fail.

For identification and quantification of components in a multicomponent sample, spectroscopic methods such as mass spectrometry and infrared spectrometry (i.r.) have been widely used. With the invention of rapid-scanning photodiode-array detectors, the basic equipment is now available to extend library searching to the ultraviolet (u.v.) and visible spectral range on-line with chromatographic separations. Contemporary approaches to spectral library search in u.v. spectroscopy after liquid chromatography [1] are based on comparing the sample spectrum with the candidate reference spectrum by means of adding up a distance measure at every wavelength position, e.g., the euclidian distance. These methods do not account for possible modification of spectra caused by solvent conditions, or their imprecise nature arising from measurement noise or variation in the chromatographic conditions. In addition, the reference spectra used are rarely recorded under the same conditions as applied in the actual chromatographic run, the reference spectra must be taken as blurred (fuzzy) and so cannot be compared properly by classical statistical methods.

A first step to consider the imprecision of spectra was reported by Blaffert [2] for identification of components with use of i.r. spectroscopy. He based his method on comparing fuzzed line positions of the sample spectrum with crisp reference spectra stored in the library. An extension to line intensities was also indicated. To solve the envisaged problem of comparing u.v./visible spectra, however, a method is needed that enables both reference and sample spectra to be considered as being fuzzed.

0003-2670/86/$03.50

The first aim of the present work is to present a new approach for matching blurred sample spectra to blurred reference spectra by using a fuzzy criterion that is derived explicitly for the problem considered. The second aim is to extend the search method to cases of unresolved component spectra. Latest developments for component resolution are based on multivariate data analysis, such as factor analysis [3, 4] and principal components analysis [5], also with the partial least-squares (PLS) approach [6].

Such methods are aimed at self-modelling resolution of the components to produce normalized component spectra that can be used for identification purposes. Apart from recent successes in overcoming the limitations of the methods with respect to noisy data and to the number of components that can be resolved, some shortcomings of contemporary approaches should be noted. First, the methods are based on multivariate data-evaluation techniques that can be applied only if matrices of data rather than vectors are generated, e.g., either in spectroscopy/chromatography [3, 4, 6] or by combining multivariate calibration techniques with spectroscopy [7—9] or chromatography [10]; because multivariate calibration can be laborious, a method that works even with data vectors would be applicable more generally. Secondly, in the case of continuous spectra, e.g., in u.v./visible spectroscopy, data analysis based on eigenvalue decomposition (factor or principal components analysis) will fail, as the number of eigenvalues would tend to infinity and eigenfunctions would have to be solved rather than eigenvalue problems. Thirdly, quantification of concentrations of the resolved components is possible only if the normalized spectra are related to pure component spectra. Thus, a library of reference spectra should be included into the data-treatment scheme.

A combination of curve resolution and of matching the resolved spectra to a library of reference spectra has been demonstrated recently by Delaney and Mauro [11] for i.r. component identification. The pure component spectra are found by self-modelling curve resolution based on principal components analysis under the constraints of positive concentrations and component spectra, and by determining the similarity between the sample and reference spectra with a least-squares criterion as the objective function. This approach seems to be the most successful one available for identification and quantification of components. It does not take into account, however, the uncertainty of spectra as found in the u.v./visible range. Quantification of component concentrations based on Kalman filtering suffers from the same shortcomings because it recursively approximates the concentration-weighted pure component spectra to the sample spectrum in a least-squares sense [12].

Here, the fuzzy identification method is extended to quantification of unresolved components by using a library of reference spectra. This method can be applied to multicomponent determinations based on a single sample spectrum as well as to spectrometric/chromatographic combinations by measurements at single retention positions.

THEORY

Comparison of fuzzy spectra

In order to account for the uncertainty of spectra, fuzzy theory is applied [13]. The concepts of fuzzy theory appropriate to chemical analysis have recently been described [2, 14] and a general outline of fuzzy theory in analytical chemistry is available [15].

In fuzzy theory the spectra can be considered as blurred curves taken as fuzzy sets over the actual spectra. Characterization of these fuzzy sets is done by defining a membership function renormed to the interval [0, 1] as follows: $m(., x)$: $\mathbf{Y} \rightarrow [0, 1]$, where $\mathbf{Y}$ is the absorbance set and x is a point on the feature (wavelength) axis X. The membership function used throughout this work is of the type

$$m(z) = [1 - z^2]^+ \tag{1}$$

where $[v]^+ = \max(0, v)$, i.e., only the positive part of the function is considered.

The membership function is best described here by using the so-called LR representation (left/right) of the fuzzy sets over the spectra as outlined by Dubois and Prade [13]. In the LR representation, the sample spectrum $a(x)$ at x can be written as

$$m_a(y; x) = \begin{cases} \mathrm{L}\,[(a(x) - y)/\alpha_0(x)] & \text{for } y \leqslant a(x) \\ \mathrm{R}\,[(y - a(x))/\beta_0(x)] & \text{for } y \geqslant a(x) \end{cases} \tag{2}$$

where the specified $\alpha_0(x) > 0$ and $\beta_0(x) > 0$ represent the left and right spreads of the domain of influence, respectively, and y is the absorbance (Fig. 1).

Likewise, the fuzzed reference spectrum is expressed by

$$m_b(y; x) = \begin{cases} \mathrm{L}\,[(b(x) - y)/\alpha(x)] & \text{for } y \leqslant b(x) \\ \mathrm{R}\,[(y - b(x))/\beta(x)] & \text{for } y \geqslant b(x) \end{cases} \tag{3}$$

with given $\alpha(x) > 0$ and $\beta(x) > 0$.

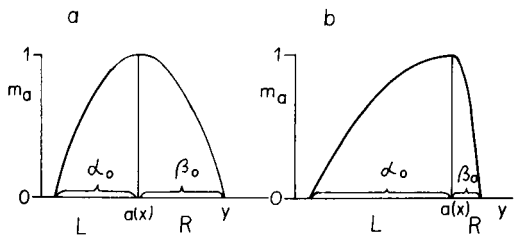

Fig. 1. Membership functions for characterizing fuzzy numbers in LR representation: (a) symmetric membership function according to Eqn. 1; (b) asymmetric membership function.

The arguments of L and R can be directly inserted into Eqn. 1 for z giving the membership values along the absorbance axis Y. The difference between sample and reference spectrum can be characterized by a new membership function derived from fuzzy subtraction of the sample from the reference spectrum:

$$m_{a-b}(y;x) = \begin{cases} \mathrm{L}\,[(a(x) - b(x) - y)/(\alpha_0(x) + \beta(x))] \\ \mathrm{R}\,[(y - (a(x) - b(x))]/(\beta_0(x) + \alpha(x))) \end{cases} \tag{4}$$

This offers the advantage of characterizing the difference between the spectra by also considering the membership function of the resulting residual values.

A suitable criterion N for estimating the deviation from the (crisp) zero function is proposed:

$$N = \int_{x_1}^{x_h} \int_{0}^{y_h(x)} y m_{a-b}(y;x)\mathrm{d}y\mathrm{d}x - \int_{x_1}^{x_h} \int_{y_1(x)}^{0} y m_{a-b}(y;x)\mathrm{d}y\mathrm{d}x \tag{5}$$

Thus, the criterion N is formed by integrating the product of y and its membership value m_{a-b} over the whole spectral range (with $x_1 - x$ low and $x_h - x$ high) and over the whole absorbance range Y.

The best fit of spectra is obtained if N is at a minimum. In addition, a parameter for the quality of the obtained comparison can be calculated by defining a degree of similarity, say, m_c,

$$m_c = [1 - N/N_{\max}]^+ \tag{6}$$

where $N_{\max}$ is the criterion N computed for the case where no attempt has been made to match the reference spectrum to the sample spectrum and the plus suffix denotes truncation of the argument to zero when $(1 - N/N_{\max}) < 0$. $N_{\max}$ is computed from the pure sample spectrum by

$$N_{\max} = \int_{x_1}^{x_h} \int_{0}^{y_h(x)} y m_a(y;x)\mathrm{d}y\mathrm{d}x - \int_{x_1}^{x_h} \int_{y_1(x)}^{0} y m_a(y;x)\mathrm{d}y\mathrm{d}x \tag{7}$$

With this definition, m_c approaches 1 as the spectra compared become identical.

To make the sample and reference spectra comparable, they must be normalized somehow. The methods used are based on normalization to the area under the spectrum [1] or to the maximum intensity [11]. Another possibility is to move the reference spectrum along the sample spectrum until the objective function achieves an optimal value. This technique was used throughout this work. From comparison with maximum normalized spectra, however, no distinct difference was found between the methods so that, in the case of large libraries, the fastest normalization procedure should be chosen.

Optimal matching of spectra is done computationally by stepping the reference spectrum with a weighting factor, c, as long as maximum coincidence is obtained, e.g., by stepping with the simplex technique. The actual membership function is then calculated, according to Eqn. 4 as follows:

$$m_{a-cb}(y;x) = \begin{cases} \mathrm{L}\,[(a(x) - cb(x) - y)/(\alpha_0(x) + c\beta(x))] \\ \mathrm{R}\,[(y - (a(x) - cb(x)))]\,/(\beta_0(x) + c\alpha(x))] \end{cases} \quad (8)$$

The degree of m_c (Eqn. 6) considered as a function on c, $m_c(c)$, becomes a membership function of a fuzzy set over the set of all possible c values. As the product cb can be also regarded as concentration-weighted spectra following Beer's law, the extension of the method to mixture analysis is straightforward as described below.

Mixture analysis

Beer's law can be expressed in the context of the fuzzy method for every wavelength position x by

$$a(x) = \sum_{j=1}^{r} c_j b_j(x) \quad (9)$$

where r is the number of components in the mixture. The membership function for the spectrum composed of the linear combination of the concentration-weighted spectra is then

$$m_{\sum c_j b_j(x)}(y;x) = \begin{cases} \mathrm{L}\,[(\sum c_j b_j(x) - y)/(\sum c_j \alpha_j(x))] \\ \mathrm{R}\,[(y - \sum c_j b_j(x))/(\sum c_j \beta_j(x))] \end{cases} \quad (10)$$

This reveals a membership function for the difference between the sample and reference spectrum $m_d[d = a(x) - \Sigma c_j b_j(x)]$:

$$m_d(y;x) = \begin{cases} \mathrm{L}\,[(a(x) - \sum c_j b_j(x) - y)/(\alpha_0(x) + \sum c_j \beta_j(x))] \\ \mathrm{R}\,[(y - a(x) - \sum c_j b_j(x))/(\beta_0(x) + \sum c_j \alpha_j(x))] \end{cases} \quad (11)$$

The criterion N and the m_c value for characterizing the quality of coincidence is computed with Eqns. 5 and 6 in the described manner. Now $m_c(c)$ defines a fuzzy set over the set of all possible weighting vectors $c = (c_1, \ldots c_r)$.

The special problem in the case of mixture analysis is to find a combination of c_j's such that the objective function N achieves a minimum value. This can be done by any multivariate optimization technique that is able to locate an optimum on a unimodal hypersurface. Here, the well known modified simplex method of Nelder and Mead [16] was used.

EXPERIMENTAL

Apparatus and computations

Digitized u.v. spectra were obtained with a microprocessor-controlled double-beam scanning spectrophotometer M40 (VEB Carl Zeiss, Jena). Data processing was done with a SM4/20 model digital computer (Tesla) programmed in FORTRAN. A BASIC version of the program is available for running on a Commodore 64 minicomputer connected to a model 1541 floppy disk.

Ordinary least-squares estimates of concentrations were computed from the known molar absorptivities (pure spectra) according to the well known least-squares equation:

$$\mathbf{c} = (\mathbf{b}^T\mathbf{b})^{-1}\mathbf{b}^T\mathbf{a} \qquad (12)$$

where **c** is the vector of the concentrations sought, **a** the absorbance vector of the sample, **b** the matrix of absorptivities, and T means the transpose of the matrix. Equation 12 was solved by means of the Cholesky algorithm [17].

Procedures

Spectra were recorded with solutions of pharmaceutical substances (commercial quality) at concentrations of 20 μg ml^{-1} in 0.5-cm quartz cuvettes between 230 and 290 nm. The absorbances were digitized every 5 nm. Mixtures of the substances were prepared from aqueous 0.1% (w/v) stock solutions of the individual components.

RESULTS AND DISCUSSION

Component identification

The fuzzy approach of comparing spectra was applied to compounds typically found in pain-relieving tablets, i.e., phenacetin, papaverine, propyphenazone, caffeine, phenobarbital, barbital and codeine phosphate. Comparison of spectra recorded under identical experimental conditions (aqueous solutions) are shown in Table 1 for phenacetin and phenobarbital as the candidate spectra. The fuzzy criterion recognizes the identical spectra with values near 1. The fuzziness of both the sample and reference spectra was set to 0.01 absorbance for both the left (α) and right (β) spreads, i.e., about 1.7% uncertainty with respect to the maximum absorbance of 0.6. The rank for identifying the spectra is the same for the fuzzy and the least-squares criterion. However, the fuzzy measure (double spread) gives a clearer picture in retrieving phenobarbital among the similar spectra of codeine phosphate and barbital (Table 1, cf. Fig. 2). This conclusion is drawn from the fact that the values of the least-squares criterion for codeine phosphate (0.203) and barbital (0.387) approach those obtained if noisy spectra are compared (see below). In the second column of Table 1 the m_c values (Eqn. 6) were computed by normalizing to the pure sample spectrum $a(x)$ with spreads of 0.01. When the sample is compared with the reference spectrum, a fuzzy subtraction is performed (cf. Eqn. 8) the resulting spreads of the residual values are larger than those for the original spectrum. This offers the possibility of sharpening the result of comparison by normalizing the pure sample spectra to the double-spread width (i.e., 0.02 absorbance) as shown in Table 1 (third column).

The addition of random gaussian noise to the sample spectrum is considered in Table 2 for phenacetin as the candidate component. The fuzzy criterion is relatively robust against noise addition. The least-squares criterion

TABLE 1

Identification of phenacetin and phenobarbital by comparisons based on a least-squares (LS) and a fuzzy criterion

Compounds	Criterion		
	Fuzzy[a]		LS[b]
	Single spread	Double spread	
A. Phenacetin vs.			
Phenacetin	0.958	0.979	0
Papaverine	0.661	0.755	1.133
Propyphenazone	0.149	0.573	1.981
Caffeine	0.001	0.253	3.459
B. Phenobarbital vs.			
Phenobarbital	0.823	0.976	0
Codeine phosphate	0.359	0.540	0.387
Barbital	0.206	0.779	0.203

[a]Equation 6; see text for full explanation. [b]$[(a(x) - cb(x))^2]^{1/2}$.

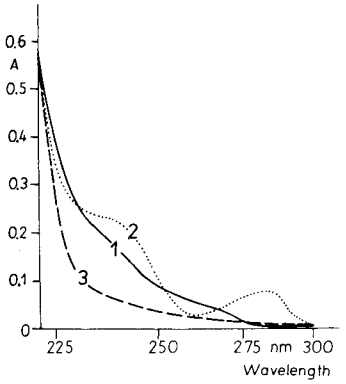

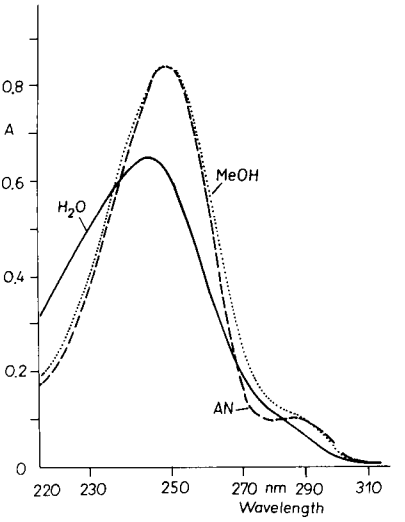

Fig. 2. U.v. spectra: (1) phenobarbital; (2) codeine phosphate; (3) barbital. Concentrations, 20 μg ml^{-1}; 10-mm cuvettes.

Fig. 3. Solvent effects on u.v. absorption spectra of phenacetin (20 μg ml^{-1}) in water, methanol (MeOH) and acetonitrile (AN) (5-mm cuvettes).

TABLE 2

Influence of noise on the recognition of phenacetin[a]

Matched compound	Criterion[b]					
	Fuzzy			Least-squares		
	1%	5%	10%	1%	5%	10%
Phenacetin	0.956	0.949	0.879	0.022	0.128	0.229
Papaverine	0.658	0.667	0.639	1.140	1.186	1.102
Propyphenazone	0.146	0.167	0.146	1.986	1.954	1.963
Caffeine	0	0	0	3.463	3.334	3.446

[a]Noise (1, 5 and 10% relative) was superimposed as normally-distributed random noise related to the actual absorbance reading. [b]For explanation, see footnotes to Table 1.

is affected by noise to such an extent that at 10% relative noise its value is 0.229, which is of the same order of magnitude as the values used for differentiating between the similar compounds phenobarbital and barbital (cf. Table 1, last column). Thus, with the least-squares criterion there would be difficulties in recognizing the correct spectrum when similar but noisy spectra are to be compared.

As a second effect, the influence of systematic deviations of the sample spectrum from the reference spectrum was evaluated. Systematic deviations caused by solvent effects are shown in Fig. 3 for phenacetin dissolved in water, methanol or acetonitrile. In order to approach experimental conditions as applied in liquid chromatography, the spectrum of phenacetin was recorded in a methanol/water (1/9, v/v) mixture and matched to spectra that were obtained in differently composed methanol/water solutions. Table 3 gives the results of comparison of spectra for increasing methanol contents from 10% to 40% (v/v). The least-squares criterion is affected in a way similar to that observed with superimposed noise (cf. Table 2); at 40% methanol, the least-squares criterion (0.330) is similar to that obtained in differentiating between substituted and unsubstituted barbitals (cf. Table 1). Thus, the solvent effect also makes recognition of spectra difficult when the least-squares criterion is used.

The fuzzy method enables the performance of the criterion to be tuned according to the solvent effect expected. Varying the amount of fuzziness (the spreads) for the spectra from 10^{-5} (nearly crisp) to 0.05 (about 8% of maximum absorbance) causes the criterion to change between 10% and 40% methanol content from $\Delta m_c = 0.138$ to 0.025, respectively (Table 3, columns 2—5). The results also show that the fuzzier the input data (higher spreads), the lower the final m_c value (i.e., the degree of similarity that can be achieved). The degree of similarity can be improved if additional knowledge can be incorporated in the specification of the fuzziness. In the present example, comparison of the spectra at different methanol contents showed

TABLE 3

Identification of phenacetin dissolved in methanol/water (1/9, v/v) with varying solvent conditions

Methanol content (%)	Criterion[a]						
	Fuzzy[b]						LS
	Symmetric membership function				Asymmetric membership function		
	10^{-5}	0.010	0.025	0.050	0.025	0.050	
10	0.999	0.957	0.892	0.786	0.950	0.929	0
20	0.912	0.906	0.868	0.772	0.914	0.898	0.20
30	0.880	0.858	0.833	0.761	0.889	0.892	0.29
40	0.862	0.859	0.832	0.761	0.879	0.873	0.33

[a]For explanation, see footnotes to Table 1. [b]The given spreads (10^{-5} to 0.050) refer to the left spreads (α_0, α); the right spreads β_0, β were set at 0.010 absorbance.

that between 235 nm and 290 nm higher methanol contents increased the absorbances. Thus it seems logical to use an asymmetric membership function, that assigns a broader domain for effects to absorbances higher than the reference spectrum (Fig. 1b). The result of comparison of spectra with an asymmetric membership function is shown in Table 3 (columns 6 and 7). The possibility of matching the correct spectra is increased compared to a symmetric function with the same spreads (0.025 or 0.050, Table 3) as used for the asymmetric part of the membership function.

Analysis of mixtures

The method of component resolution is demonstrated here for mixtures of u.v.-absorbing species by referring to the pure component spectra. In the first example, a simulated two-component mixture of caffeine and propyphenazone at equal concentrations of 0.5 (arbitrary units) was used. The resulting plot of the fuzzy criterion $m_c(c)$ vs. component concentrations is shown in Fig. 4 for spectra fuzzed with spreads for α and β of 0.01 each. The search was made in the concentration space between 0.1 and 0.9 concentration units for each component. The concentrations were found correctly at 0.5 concentration units with a maximum $m_c(c)$ value of 0.953 (cf. Table 4).

When the amount of fuzziness was changed from the nearly crisp case (spreads of 10^{-5}) to relatively broad fuzziness (absorbance spreads of 0.1), the $m_c(c)$ values changed linearly from 0.999 to 0.527, respectively, at equal component concentrations, i.e., the fuzzier the input spectra, the less precise concentrations can be retrieved. At α, β values greater than 0.075, however, the exact concentrations can no longer be located, as can be seen from a data window of the $m_c(c)$ table for α, β values of 0.1 absorbance (Table 4).

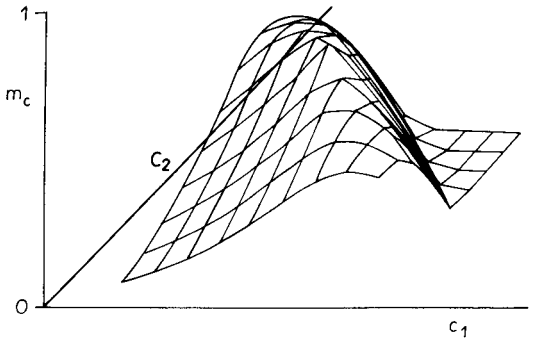

Fig. 4. Plot of the fuzzy criterion $m_c(c)$ (Eqn. 6) for evaluating the composition of a mixture composed of caffeine and propyphenazone.

TABLE 4

Component location in a mixture of caffeine (c_1) and propyphenazone (c_2) for spectra with different levels of fuzziness

$m_c(c)$ values for c_1 = 0.4, 0.5, 0.6							
c_2	Spreads of 0.010			c_2	Spreads of 0.100		
	0.4	0.5	0.6		0.4	0.5	0.6
0.4	0.640	0.802	0.909	0.4	0.518	0.548	0.520
0.5	0.818	0.953	0.799	0.5	0.548	0.527	0.434
0.6	0.909	0.780	0.560	0.6	0.520	0.457	0.326

Noise superimposed on the sample spectrum has the same effect on estimating the concentrations as the effect observed in the library retrieval experiments: varying superimposed random noise between 1%, 5% and 10% (relative) produced $m_c(c)$ values of 0.952, 0.929 and 0.887, respectively. Simultaneously, the $m_c(c)$ values for concentrations around the optimum value increased.

The robustness of the fuzzy method for mixture analysis was evaluated from experiments with a 3-component system and the results were compared to those obtained with a least-squares algorithm. The mixtures contained caffeine, propyphenazone and phenacetin. Triplicate results for a sample of a typical tablet composition are given in Table 5. The fuzzy estimates for caffeine and phenacetin had relative prediction errors less than 3%. Propyphenazone was quantified with an average relative prediction error of 14%. Such high errors can be attributed to the non-additivity of spectra as found in other experiments [18]. It should also be noted that the pure spectra used in the data processing were stored in the library for several months before this work in order to approximate the conditions of actual retrieval techniques. The least-squares estimates (Table 5) were worse than the fuzzy

TABLE 5

Comparison of fuzzy and ordinary least-squares (LS) estimates in the analysis of a mixture of caffeine, propyphenazone and phenacetin based on their pure component spectra

Sample	Method	Concentrations found[a] (μg ml^{-1})			Mean prediction error[b] (%)
		Caffeine	Propyphenazone	Phenacetin	
1	Fuzzy	5.89	13.90	8.97	11.78
	LS	9.29	7.76	11.82	37.53
2	Fuzzy	6.12	13.70	8.94	10.56
	LS	9.16	7.89	11.75	36.33
3	Fuzzy	6.19	13.35	9.15	8.49
	LS	8.97	8.38	11.46	32.74
Average prediction error[c] (%)					
	Fuzzy	2.4	13.9	1.05	
	LS	52.4	33.3	29.8	

[a]Actual concentrations: 6 μg ml^{-1} caffeine, 12 μg ml^{-1} propyphenazone, 9 μg ml^{-1} phenacetin. [b]Mean prediction error, $100[\Sigma_j \Sigma_i (c_{ij} - c_{ij,\text{act.}})^2 / \Sigma_j \Sigma_i c_{ij,\text{act.}}^2]^{1/2}$. [c]Prediction error for one component, $100[\Sigma (c_i - c_{i,\text{act.}})^2 / \Sigma c_{i,\text{act.}}]^{1/2}$.

estimates, giving average prediction errors for the single components between 30 and 52%. In general, the ordinary LS method gave mean prediction errors (averaged over all three components) that were about three times as high as are those obtained with the fuzzy method (Table 5). If still worse coincidence between the pure component spectra and the concentration-weighted mixture spectrum occurred, the LS method could even give negative concentrations whereas the fuzzy method is robust enough to achieve concentration values which are interpretable from a physical point of view.

Conclusion

The fuzzy method proposed for component identification is advantageous for several reasons. First, noisy and/or similar spectra are better recognized with use of the fuzzy criterion than with the least-squares criterion. Secondly, additional knowledge about the uncertainty of data can be incorporated into the membership function for characterizing the spectra. The results of spectra identification can thus be sharpened. Thirdly, a measure reflecting the quality of fit is easily derived, i.e., the membership function for the degree of similarity (Eqn. 6). Such estimates of possibility can be obtained without any of the assumptions that would be necessary for deducing statistically-based confidence statements.

The concept of the method for quantitative analysis of mixtures is general enough to be useful for resolution of overlapping chromatographic peaks or spectroscopic bands and can be extended to spectrochromatograms where the component spectra are deconvoluted and quantified pointwise along the retention axis.

REFERENCES

1 A. F. Fell, B. J. Clark and H. P. Scott, J. Chromatogr., 316 (1984) 423.
2 T. Blaffert, Anal. Chim. Acta, 161 (1984) 135.
3 M. A. Sharaf and B. R. Kowalski, Anal. Chem., 54 (1982) 1291.
4 B. G. M. Vandeginste, W. Derks and G. Kateman, Anal. Chim. Acta, 173 (1985) 253
5 A. Meister, Anal. Chim. Acta, 161 (1984) 149.
6 W. Lindberg, J. Ohman and S. Wold, Anal. Chem., 58 (1986) 299.
7 M. Otto and W. Wegscheider, Anal. Chem., 57 (1985) 63.
8 B. H. Saxberg and B. R. Kowalski, Anal. Chem., 51 (1979) 1031.
9 H. Martens and T. Naes, Trends Anal. Chem., 3 (1984) 204.
10 M. Otto and W. Wegscheider, Anal. Chim. Acta, 171 (1985) 13.
11 M. F. Delaney and D. M. Mauro, Anal. Chim. Acta, 172 (1985) 193.
12 H. N. J. Poulisse, Anal. Chim. Acta, 112 (1979) 361.
13 D. Dubois and H. Prade, Fuzzy Sets and Systems: Theory and Application, Academic Press, New York, 1980.
14 M. Otto and H. Bandemer, Anal. Chim. Acta, 184 (1986) 21.
15 H. Bandemer and M. Otto, Mikrochim. Acta (Wien), in press.
16 J. A. Nelder and R. Mead, Comput. J., 7 (1965) 308.
17 J. Stoehr, Einführung in die Numerische Mathematik I, Springer, Berlin-Heidelberg, 1976.
18 M. Otto and K. Sporreiter, Mikrochim. Acta (Wien), (III) (1985) 167.

Analytica Chimica Acta, 191 (1986) 205—218
Elsevier Science Publishers B.V., Amsterdam — Printed in The Netherlands

MULTIVARIATE ANALYSIS OF TIME-RESOLVED MASS SPECTRAL DATA

W. WINDIG*, T. CHAKRAVARTY, J. M. RICHARDS and H. L. C. MEUZELAAR
Biomaterials Profiling Center, University of Utah, Salt Lake City, UT 84108 (U.S.A.)
(Received 29th May 1986)

SUMMARY

Multivariate analysis of time-resolved pyrolysis/mass spectrometric data is described. The approach is based on the variance diagram (VARDIA), a recently developed technique that quantifies the clustering of variables in two-dimensional factor analysis (sub)-spaces in a rotational scanning procedure. A maximum in the VARDIA plot indicates a correlated behavior of the mass variables, indicating a common origin. This common origin is generally caused by a change in the concentration of a chemical component. With this information the "factor spectrum" and the scores of the component can be retrieved. For time-resolved serial data, consideration of the clustering behavior of the variables as a function of time is more appropriate than a rotational scanning procedure. Adaptation of the VARDIA for serial data, such as time-resolved data, is described. This approach has the advantage that all the factors can be used. It will be shown that the resolution of the obtained curve can be higher than the total ion current curve as a function of time. Examples will be given for time-resolved data of coal, rubber and wood samples.

Recently Windig and Meuzelaar [1] described a method for nonsupervised deconvolution of complex mass spectral data, the so-called variance diagram (VARDIA) technique. The VARDIA technique quantifies the clustering of mass variables in two-dimensional factor or discriminant (sub)spaces through a rotational scanning procedure. If a clustering of mass variables occurs, this indicates a common origin of these variables, which is generally a chemical component. This technique has been applied successfully to mass spectral and conventional data from samples such as biopolymer mixtures [1], lignites [1], paper pulps [2], peats [3], jet fuels [4] and bacteria [5]. Application of the VARDIA technique to time-resolved mass spectral data from various complex samples has demonstrated its applicability to serial data [6].

This paper will show some further applications of the VARDIA technique to time-resolved data and will present a new form of the VARDIA plot. For mixture data in general the VARDIA technique uses polar plots in two-dimensional (sub)spaces. For serial data it may be more convenient to plot the VARDIA as a function of time using the factor (or discriminant) scores of the mass spectral data over all significant dimensions of the factor space. This approach has the advantage that all the dimensions of the factor space

can be used rather than only two at a time. Examples of this VARDIA technique for serial data (VARDIA-S) will be given for a coal sample, a rubber sample and a wood sample. Comparisons with the VARDIA technique will be made to evaluate the relative advantages and disadvantages of both methods.

EXPERIMENTAL

Sample preparation

Coal sample. About 4 mg of a -60 mesh sample of high volatile subbituminous Pittsburgh coal was weighed accurately and suspended in 0.5 ml of methanol. After hand-grinding the particles to produce a finer and more uniform suspension, an additional 0.5 ml of methanol was added to produce a 4 mg ml^{-1} suspension. A 5-μl aliquot of the suspension (20 μg of coal, dry weight) was applied to the ferromagnetic wire used in Curie-point pyrolysis (Curie-point temperature, 610°C).

Rubber sample. A small rubber sample (ca. 10 mg) was cut from a sheet of uncured silica-filled neoprene/ethylenepropylenediene monomer (EPDM) copolymer rubber compound, finely divided by hand with a scalpel and ground under liquid nitrogen in a freezer mill (Spex Industries) to give a fine powder. Approximately 3 mg of this powder was weighed, suspended in toluene (HPLC grade) to form a 4 mg ml^{-1} suspension and ground by hand to insure homogeneity of the suspension. A 3-μl drop of the rubber suspension (12 μg of rubber) was coated onto the ferromagnetic filament as above.

Wood. The wood sample was obtained by scraping a piece of Douglas fir wood with a scalpel. A 10-mg sample of the fine wood scraping was put into a platinum crucible and placed in a Mettler I thermogravimetry (TG) system

Mass spectrometry

Coal sample. Time-resolved pyrolysis/mass spectrometry (m.s.) was done in an Extranuclear Model 5000-1 Curie-point system interfaced with an IBM 9000 microcomputer. Pyrolysis conditions were as follows: Curie-point temperature 610°C, temperature-rise time 5.4 s and total heating time 10 s. The m.s. was done at 12-eV (set value) electron energy by scanning the mass range m/z 50—200 at a rate of 5 spectra per second during 8 s after an initial delay of 0.5 s. The 41 resulting spectra were stored in the IBM 9000 system.

Rubber sample. The system used was the same as above. Experimental conditions were as follows: Curie-point temperature 610°C, temperature-rise time 5—5.5 s, total heating time 10 s, electron energy 12 eV (set value), mass range scanned m/z 27—91 and scan speed 823.3 amu s^{-1} (12.67 scans/s) after an initial delay of 1.0 s. The resulting 76 spectra were stored in the IBM 9000 system.

Wood. The wood sample was analyzed with a combined thermogravimetry/m.s. system. The oven of a Mettler I thermogravimetry system was adapted so that helium could be passed at a flow rate of 6 ml min^{-1} in order

to transport the pyrolyzate to a HP 5930A mass spectrometer. The transfer line from the furnace directly into the ion source was a 2-m fused silica capillary column (inner diameter 20 μm) permitting a flow rate of approximately 0.1 ml min^{-1}. The rest of the gas flow was split off to atmosphere. The temperature of the transfer line was set at 150°C. Thermogravimetric conditions were: temperature program 15°C min^{-1} for 45 min (final temperature approximately 650°C) and total sample weight 10 mg. Conditions for m.s. were: electron energy 15 eV, mass range scanned *m/z* 35—220, and scanning speed 10.6 scans/min. All (approximately 500) spectra obtained were stored for subsequent data analysis.

Multivariate data analysis

Factor and discriminant analysis. The data sets were subjected to multivariate analysis using the factor and discriminant routines of the SIGMA program. The SIGMA (system for interactive graphics-oriented multivariate analysis) program is a highly user-friendly software package for the IBM 9000 developed in this laboratory.

The factor (principal component) analysis routine produces independent linear combinations of the original variables according to

$$F_j = a_{1j}Z_1 + a_{2j}Z_2 + \cdots a_{nj}Z_n \quad (1)$$

where F_j is factor j and a_{ij} is the loading (correlation coefficient) of variable Z_i with F_j [7, 8].

This generally results in a substantial data reduction, because of correlated behavior of the mass variables. In order to compare the linear combinations with the original data, the loadings are multiplied by the corresponding standard deviation for each mass variable. The values obtained can be represented in the form of bar plots (factor spectra [9]). The factor scores represent the relative contributions of the original spectra to the factors. The scores are standardized, i.e., the average value is 0.0 and the standard deviation is 1.0. The relation between the original data set, the factors and the scores (S) is

$$\mathbf{D} = S\,\mathbf{F}^{\mathrm{T}} \quad (2)$$

where **D** is the (standardized) data set, size $c \times n$, where c is the number of spectral cases and n is the number of variables. The matrix **F** is the loading matrix, size $n \times l$, where l is the number of factors. If the transformation matrix **T** is found to get scores at a certain rotation, the matrix **F** needs to be transformed by $\mathbf{T}^{-1}$ in order to preserve this relation [8]:

$$\mathbf{D} = (S\,\mathbf{T})(\mathbf{T}^{-1}\,\mathbf{F}^{\mathrm{T}}) \quad (3)$$

Variance diagram. Extraction of chemical information from pyrolysis/m.s. data meets with several problems. First, the spectrum obtained from a complex mixture is not necessarily the exact sum of the spectra of the individual components in the mixture, as intermolecular reactions may occur [10].

Second, appropriate reference spectra of individual mixture components are often not available. For these reasons, supervised methods such as target rotation [8] cannot be used.

Methods that do not require reference spectra, such as "pure mass" (i.e., mass value methods [11—13]), rely on assumptions that are not fulfilled for pyrolysis/m.s. data [1]. Therefore, Windig and Meuzelaar [1] developed the variance diagram (VARDIA) technique to obtain unsupervised mixture analysis of pyrolysis/m.s. data. The variance diagram calculates the correlated behavior of the mass variables with the following equation:

$$\mathrm{Var}(W = \beta)_\gamma = \sum_{i=1}^{n} a_i^2 \text{ for } a_i \geqslant (\alpha_{i1}^2 + \alpha_{i2}^2)^{1/2} \cos(\beta/2) \tag{4}$$

where $a_i = \alpha_{i1} \cos\gamma + \alpha_{i2} \sin\gamma$ and $\mathrm{Var}(W = \beta)_\gamma$ is the variance in the direction in the space at an angle of γ degrees with the first factor (or discriminant function), using a window W of β degrees. Furthermore, a_i is the loading of mass variable i on the rotated function, n is the total number of mass variables and α_{ij} are the loadings of the mass variables in the unrotated factor j. Expressed in terms that are easier to visualize, Eqn. 4 accomplishes the following task: in a two-dimensional system the sum of the squares of the lengths of all mass axes present in a window of β degrees (generally 10° or 20°) is calculated while the window "scans" the whole two-dimensional space, in discrete steps (generally 10°).

RESULTS AND DISCUSSION

Coal sample

Time-resolved pyrolysis/m.s. analysis of the coal sample resulted in a total ion current (TIC) curve with two clear maxima (Fig. 1). The time-integrated spectrum of this sample is given in Fig. 2. It shows that the phenols are the most abundant homologous ion series in the spectrum of fresh whole coal. Other major components dominating the spectra are benzenes, naphthalenes, short-chain aliphatic hydrocarbons, and acids [14—16]. Factor analysis was performed using the 100 variables with the highest variance, resulting in four factors with an eigenvalue >1, describing 97% of the total variance. As the eigenvalues clearly leveled off after the first two factors describing 94% of the total variance, it was concluded that the intrinsic dimensionality of this data set was 2. As this data set is used to demonstrate the VARDIA-S technique, only 2 factors are used in order to emphasize the principles.

The plot of the scores in the $F1$—$F2$ space is given in Fig. 3. The VARDIA plot (Fig. 4) of the first two factors shows a clear maximum at an angle of 350° (counter clockwise) with respect to the first factor ($F1+$) and a small maximum at an angle of 60° with respect to $F1+$. In this representation of the VARDIA plot, the "component axes" are the two outer boundaries of the maxima, indicated in the figure. This is due to the fact that the mass

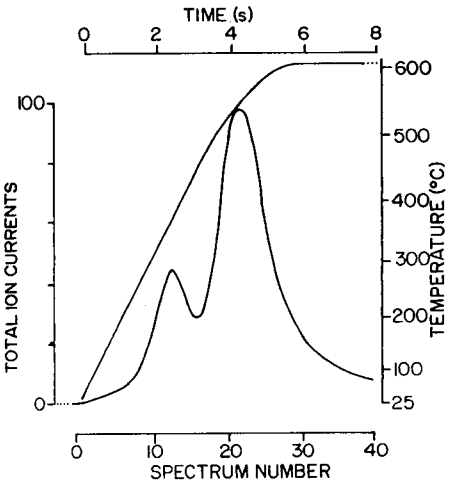

Fig. 1. Total ion current (TIC) profile of the spectra obtained from the time-resolved pyrolysis/m.s. analysis of the coal sample together with the temperature/time profile of the pyrolysis wire. The two maxima clearly show the presence of at least two processes.

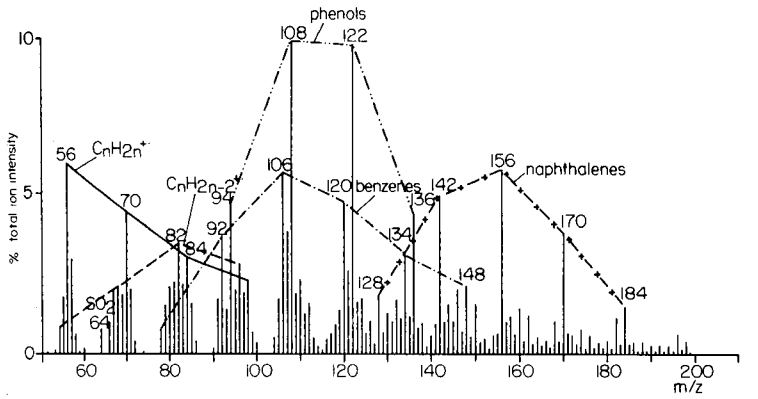

Fig. 2. Time-integrated pyrolysis mass spectrum of the coal sample. Several component classes are present, as indicated in the spectrum by their typical ion series.

variables are all bracketed by the component axes. The outer boundaries thus represent "pure masses" for the components (or at least the best approximation of a pure mass). The time-resolved curves of the two components can be calculated by projecting the scores on the two "component axes" given by the VARDIA. The resulting curves (Fig. 5) show a clear deconvolution into two components. The factor spectra of the two components were calculated, using the inverse of the matrix used to calculate the scores. The mathematically extracted spectrum of the first time-resolved component is given in Fig. 6. Comparison of this mathematically extracted

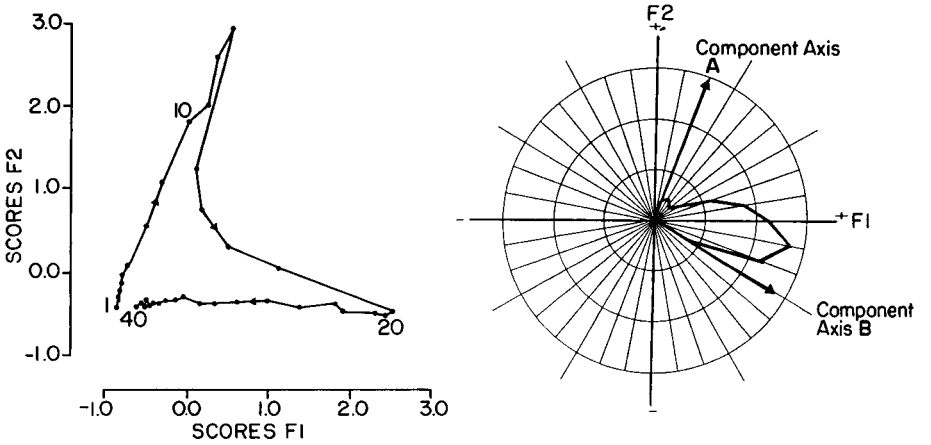

Fig. 3. Scatter plot of the scores of the first two factors obtained from the coal data set. The two processes shown in the TIC curve (Fig. 1) are clearly present. The numbers indicate the spectrum number. The scores are interconnected as a function of time.

Fig. 4. The VARDIA plot in the space described by the first two factors, $F1$ and $F2$. The presence of two processes is clear again from this plot. The component axes are indicated by two vectors which bracket all the mass variables. The component axis A describes the first process in time, production of the relatively volatile components, axis B describes the second process, production of the less volatile components.

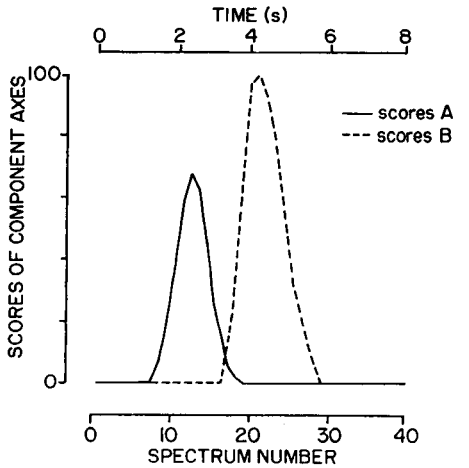

Fig. 5. Projection of the scores on the component axes A and B in Fig. 4 results in the scores of the two time-resolved curves. The two obtained curves were scaled according to their standard deviations, as calculated by the VARDIA technique.

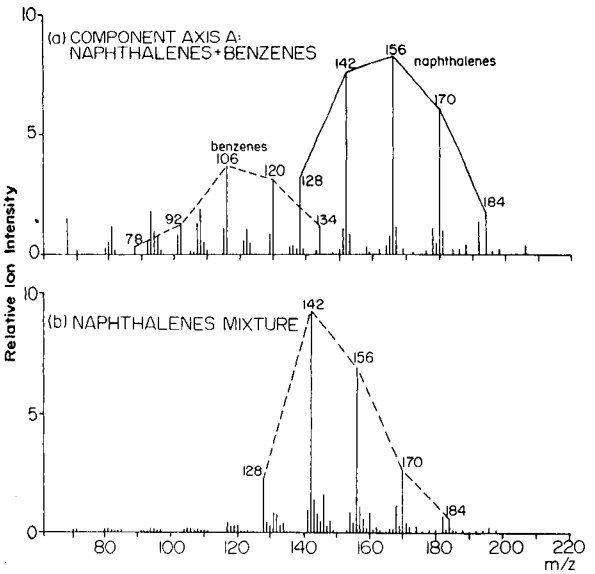

Fig. 6. The mathematically extracted spectrum of the first process (a) has a dominant naphthalenes series, as can be deduced from the model spectrum (b). The model spectrum sample was prepared from a highly naphthalenic petroleum product. Other relatively volatile components such as benzenes are also present. Less volatile components such as lignins are clearly absent.

spectrum with the integrated spectrum in Fig. 2 shows that volatile components such as naphthalenes (Fig. 6b) are clearly present. Less volatile components such as phenols are absent. It is possible to extract more components from this data set using more factors.

Although the VARDIA technique as described above is a powerful tool to find the component axes (scores), presentation of the occurrence of these component axes as a function of time gives a more appropriate representation of the data. This is possible by calculating the variance not in 10° rotational steps in a 2-dimensional subspace but in the directions of the sequential spectra in n-dimensional factor space.

Normally, the calculated average spectrum of a data set is used as the reference point (the "origin") in n-dimensional space for rotational procedures such as graphical rotation and the VARDIA technique. This is done because the interest is generally in the relatively minor differences between spectra rather than in the absolute intensities of the signals. In the case of time-resolved spectra, however, the absolute contribution of each spectrum to the data set is of interest. Thus the "permanent" background spectrum seen by the mass spectrometer is a more appropriate reference point. Thus for the time-resolved VARDIA method, the variance as calculated by Eqn. 4, in the direction of the sample spectra with a background spectrum as the reference point can be used. In contrast to the variance values calculated by Eqn. 2, which only considers two dimensional (sub)-

spaces, the variance in the directions of the sample spectra can be calculated in an n-dimensional space containing all significant factors. The equation describing this procedure is

$$\mathrm{Var}_t = \sum_{i=1}^{m} a_{i,t}^2 \text{ for } a_{i,t} \geqslant \sum_{j=1}^{n} \alpha_{i,j}^2 L \tag{5}$$

$$\text{where } a_{i,t} = \sum_{j=1}^{n} \left[\left(S_{t,j} - S_{tr,j} \right) \Big/ \left(\sum_{j=1}^{n} \left(S_{t,j} - S_{tr,j} \right)^2 \right] \alpha_{i,j}$$

Here m is the number of variables, n the number of factors, $a_{i,t}$ the loading of mass variable i from spectrum t on the rotated function, $\alpha_{i,j}$ the loading of mass variables i on the original factor j, $S_{t,j}$ the score on factor j of spectrum t, $S_{tr,j}$ the score on factor j of reference spectrum, and L the cosine of the angle between the mass-axis and the rotation under consideration.

This procedure subtracts the scores of the reference spectrum from the n scores of each spectrum, normalizes the new scores (i.e., the sum of the squares of the n scores of each spectrum are made equal to 1.0), calculates linear combinations of factors for each spectrum, selects all mass axes that are within a certain angle (angle = $\cos^{-1} L$) of the rotated functions, and finally sums the squares of the selected loadings of each factor to give the variance as defined by the equation.

Thus, only mass variables which have a projected direction in n-dimensional factor space making a relatively small angle (15–20 degrees) with the direction of the selected linear combination of factors are included in this adapted variance calculation. A high variance value indicates a relatively high loading of included mass variables on the selected linear combination of factors, thus indicating which mass variables are responsible for the observed correlated behavior.

Initial application of this technique showed that the results improved considerably after smoothing the scores with the following triangular window:

$$S_{t,j}^* = 1/4\, S_{(t-1),j} + 1/2\, S_{t,j} + 1/4\, S_{(t+1),j} \tag{6}$$

where $S_{t,j}^*$ is the smoothed score. Because the time-resolved VARDIA uses a subspace of the original factor space, the question may arise if the overlap between the two spaces is sufficiently high to regard the subspace as representative of the original space. In order to check this, the % variance covered by the serial subspace was calculated from

$$\mathrm{Vars} = \sum_{i=1}^{m} \left[\max \left(a_{i,1}, a_{i,2} \cdots a_{i,k} \right) \right]^2 \times 100\% \tag{7}$$

where k is the number of spectra. The maximum of a loading $a_{i,j}$ ($j = 1, k$) for all linear combinations in the direction of the spectra in the factor

subspace may be considered as the "length" of that mass variable in the subspace (the standardized length of each mass variable in the original factor space is 1.0). Because communality 7 is the square of the length of a variable, the above formula calculates the sum of all the communalities from which the relative variance can be calculated by dividing this sum by the number of variables involved.

The application of the VARDIA-S technique to the coal data set results in the curve shown in Fig. 7. Although in this example the VARDIA-S curve shows the same information as the TIC curve (Fig. 1), the next examples will show that a considerable improvement in resolution can be obtained with the VARDIA-S technique.

Rubber sample

The major components of the rubber compound are neoprene, EPDM, sulfur cross-linking agents, and a silica filler. Neoprene compounds degrade at a lower temperature than EPDM [17]. Analysis of a similar silica-filled neoprene/EPDM rubber compound showed that the pyrolysis proceeds in four stages: (1) volatilization of excess elemental sulfur and low-molecular-weight fractions, (2) degradation of the neoprene portion, (3) degradation of the EPDM segments, and (4) charring of the remaining material [6]. Thus it is reasonable to expect that this rubber compound will exhibit similar pyrolysis behavior.

The TIC from the rubber analysis (Fig. 8) shows two large maxima as well as a small shoulder preceeding the first maximum, and a tail after the second major peak. A time-integrated spectrum is shown in Fig. 9. Peaks character-

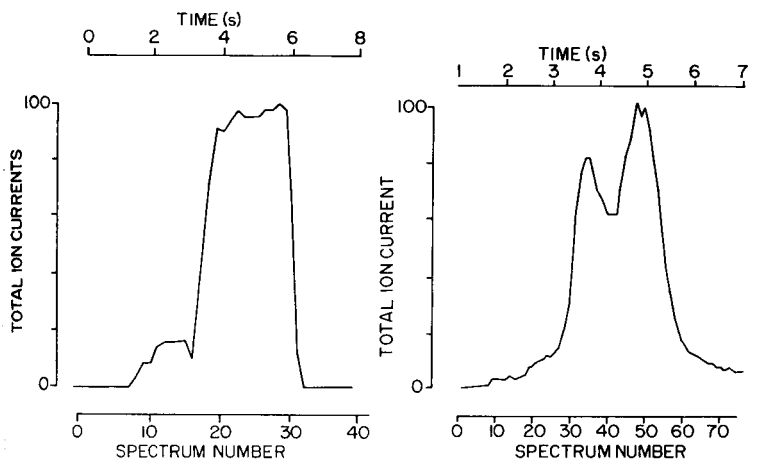

Fig. 7. The VARDIA-S curve clearly shows the presence of the two processes. The overlap between the original space and the VARDIA-S space is 99.7%.

Fig. 8. TIC curve obtained on pyrolysis of a rubber sample.

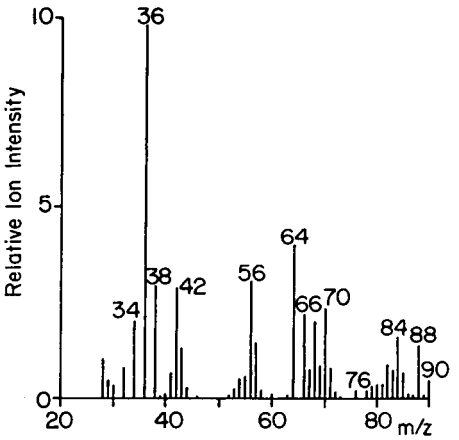

Fig. 9. The time-integrated spectrum of the rubber sample.

istic of neoprene [m/z 36/38 (HCl^+), 53 ($C_4H_5^+$), and 88/90 (monomer)], EPDM [m/z 42 ($C_3H_6^+$), 56 ($C_4H_8^+$), 70 ($C_5H_{10}^+$), and 84 ($C_6H_{12}^+$)], and organic and elemental sulfur [m/z 32 (S), 34 (H_2S), 64 (S_2 or SO_2), 66/68 (HSSH), and 76 (CS_2)] are present. Multivariate analysis of these data found 8 factors with an eigenvalue greater than 1.0. These 8 factors account for 88% of the variance in the data. The eigenvalues of these factors level off after the fourth factor (representing 77% of the variance); therefore, only the first four factors were used in subsequent data analyses.

A VARDIA of the $F2/F3$ subspace (not shown) showed three distinct maxima representing three different processes occurring during pyrolysis. A VARDIA of the $F3/F4$ subspace (not shown) contained four maxima, indicative of the above-described four stages of pyrolysis for this sample. Figure 10 is a curve from the VARDIA-S analysis of these data. This curve resolves the first three processes, but the fourth is still seen as a shoulder on the maximum representing the EPDM depolymerization step. Comparison with the TIC curve (Fig. 8) shows the clearly improved resolution achieved by the VARDIA-S curve. The component spectrum corresponding to the second maximum in the VARDIA-S and a neoprene model spectrum are shown in Fig. 11.

Wood sample

The time-resolved data set for a wood sample has been studied before with the VARDIA technique [4, 5]. For the study, the 155 spectra recorded between 300°C and 500°C were used. Prior to multivariate analysis, sequences of five spectra were averaged in order to reduce noise and the size of the data matrix. Three significant factors (describing 97% of the total variance) resulted in three maxima using the VARDIA technique, which allowed a complete deconvolution into three processes. From this study [5], it was concluded that the first process was dominated by hemicellulose pyrolysis,

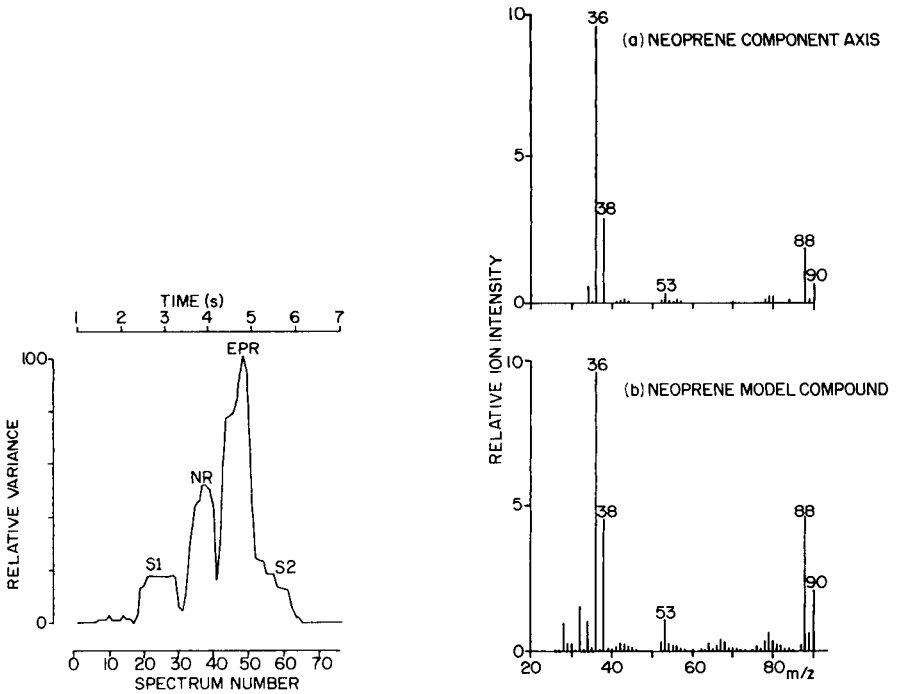

Fig. 10. The VARDIA-S curve (describing 93.9% of the variance in the original space). The deconvoluted processes are identified as volatilization of low-molecular-weight sulfur compounds (S1), degradation of the neoprene component (NR), degradation of the EPDM (EPR) and release of sulfur compounds as the matrix chars (S2).

Fig. 11. Comparison of the mathematically extracted spectrum of the neoprene component (a) with a neoprene model spectrum (b).

the second by cellulose pyrolysis and the third by lignin pyrolysis. The pyrolysis of lignin, however, does not take place only in the third pyrolysis step process. It appeared that there were three separate lignin pyrolysis processes, of which the first two were highly correlated with the hemicellulose and cellulose pyrolysis steps [6]. These findings were in agreement with a time-resolved m.s. study on biomass samples by Evans et al. [18].

The TIC curve of the time-resolved wood data set [5] did not show clearly resolved processes. The time-integrated spectrum of this data set is shown in Fig. 12. The VARDIA-S technique resulted in the curve given in Fig. 13(a), which clearly shows three processes with a resolution not found in the TIC curve. Although the maxima of the hemicellulose and lignin components appear minor, their significance is obvious after subtracting 25% of the first factor, as shown in Fig. 13(b). The overlap of curve (a) with the original space is 92.4%, the overlap of (b) with the original space is 90.9%. The process indicated as secondary pyrolysis has been discussed [4].

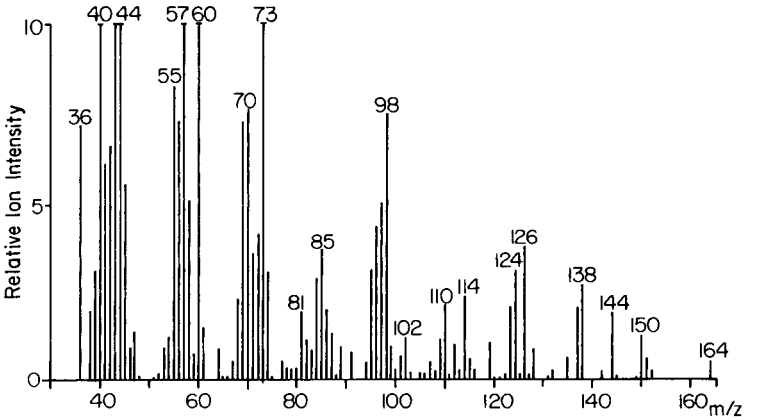

Fig. 12. The time-integrated spectrum of the wood sample. Contributions of the three major wood components are clearly present: hemicellulose (*m/z* 85 and 114), cellulose (*m/z* 98, 102, 110, 126 and 144) and lignin (*m/z* 124, 138, 150 and 164).

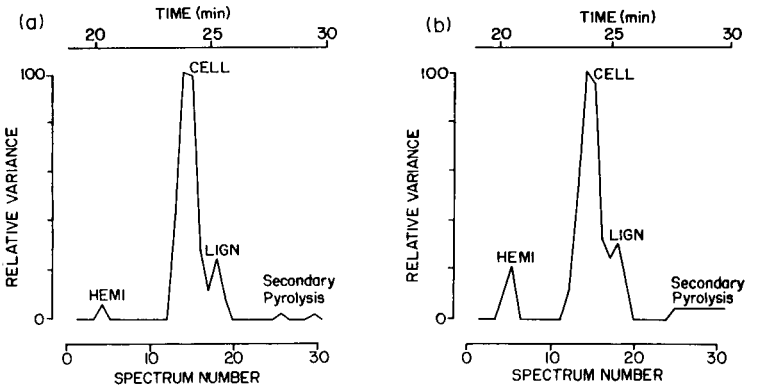

Fig. 13. VARDIA-S curves: (a) obtained from the first three factors of the data set of time-resolved analysis of wood; (b) after subtraction of 25% of the first factor.

The mathematically extracted spectrum of describing the main lignin pyrolysis process and a model spectrum of lignin are presented in Fig. 14.

CONCLUSIONS

The examples given show that the VARDIA-S method is a useful addition to the VARDIA method. Because all factors can be used simultaneously, the VARDIA-S method provides a rapid way to determine the intrinsic dimensionality of time-series data in terms of (classes of) chemical components or processes. From other data sets, it was learned that the steps in which the factor space is scanned in the VARDIA-S technique (as measured by the scores of the spectra) may give a lower resolution than the 10° steps of the regular VARDIA technique. In order to improve this, the angle between two

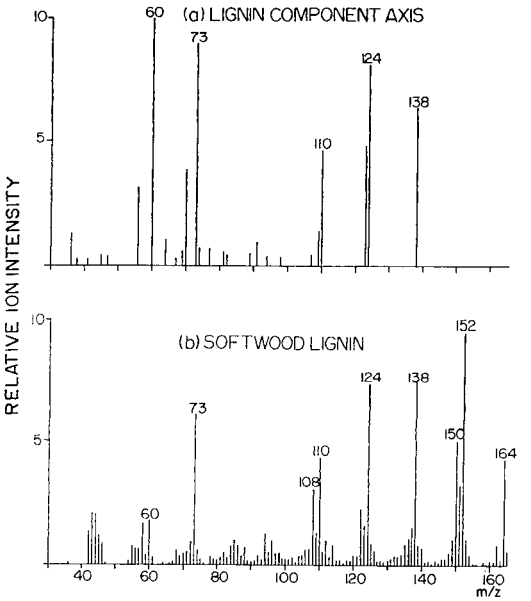

Fig. 14. The mathematically extracted spectrum of the wood data set shows typical lignin peaks at *m/z* 110, 124 and 138 (a). The softwood lignin spectrum (b) shows additional lignin peaks at *m/z* 150, 152 and 164. The absence of the latter peaks in (a) is due to the complex behavior of lignin.

sequential score directions can be calculated. If this angle is larger than 10°, an interpolation can be applied in order to insert a few steps between these scores. Another possibility is to calculate a least-squares curve through the scores and use this curve to scan the space in steps of 10°.

It has to be noted that there are data sets which can be deconvoluted by the VARDIA technique but cannot be deconvoluted by the VARDIA-S method. This is the case if time-resolved curves reach their maxima at the same point in time, but their shape is different.

In principle, the VARDIA-S technique should be very useful as a monitoring tool, e.g., for quality assurance, process control or environmental monitoring, since the VARDIA-S curve indicates changes much more clearly than the regular TIC. A high, noisy background signal will not produce maxima in the VARDIA-S curve because there is no correlated behavior of mass variables in this case. However, if a systematic signal change occurs, even a minor one, the VARDIA-S technique will detect this change clearly as soon as a few peaks show a correlated behavior. Furthermore, the linear combination of factors associated with a maximum in the VARDIA-S curve can be used to calculate the spectrum of the component or process responsible for the observed change.

Henk Stolk is acknowledged for analyzing the wood samples, Koli Taghizadeh is thanked for assistance in analyzing the rubber. Van Nguyen and

Apostolos Dedes are acknowledged for software development assistance. The research reported was supported in part by Army Research Office contract no. DAAG29-84-K-0009. Additional support was provided by Hercules Inc. for the analysis of the rubber sample.

REFERENCES

1 W. Windig and H. L. C. Meuzelaar, Anal. Chem., 56 (1984) 2297.
2 W. Windig, H. L. C. Meuzelaar, F. Shafizadeh and R. G. Kelsey, J. Anal. Appl. Pyrol., 6 (1984) 233.
3 G. Halma, D. van Dam, J. Haverkamp, W. Windig and H. L. C. Meuzelaar, J. Anal. Appl. Pyrol., 7 (1984) 167.
4 W. Windig, W. H. McClennen, H. Stolk and H. L. C. Meuzelaar, Opt. Eng., 25 (1986) 117.
5 H. L. C. Meuzelaar, W. Windig, A. M. Harper, S. M. Huff, W. H. McClennen and J. M. Richards, Science, 226 (1984) 268.
6 W. Windig, E. Yaleah, J. M. Richards and H. L. C. Meuzelaar, unpublished work.
7 H. H. Harman, Modern Factor Analysis, The University of Chicago Press, Chicago, 1976.
8 E. R. Malinowski and D. G. Howery, Factor Analysis in Chemistry, Wiley, New York, 1980.
9 W. Windig, P. G. Kistemaker and J. Haverkamp, J. Anal. Appl. Pyrol., 3 (1981) 199.
10 D. Van de Meent, J. W. de Leeuw, P. A. Schenck, W. Windig and J. Haverkamp, J. Anal. Appl. Pyrol., 4 (1982) 133.
11 F. J. Knorr and J. H. Futrell, Anal. Chem., 51 (1979) 1236.
12 E. R. Malinowski, Anal. Chim. Acta, 134 (1982) 129.
13 O. S. Borgen and B. R. Kowalski, Anal. Chim. Acta, 174 (1985) 1.
14 H. L. C. Meuzelaar, A. M. Harper and P. H. Given, Utah Geol. Mineral. Surv. Bull., 118 (1982) 192.
15 W. H. Wiser, Proceedings of the Conference on Scientific Problems Relevant to Coal Utilization, DOE Symposium Series, 1977.
16 P. H. Given, Fuel, 39 (1960) 147.
17 J. J. Maurer, in E. A. Turi (Ed.), Thermal Characterization of Polymeric Materials, Academic Press, New York, 1981, p. 571.
18 R. J. Evans, T. A. Milne and M. N. Soltys, J. Anal. Appl. Pyrol., 9 (1986) 207.

Analytica Chimica Acta, 191 (1986) 219—226
Elsevier Science Publishers B.V., Amsterdam — Printed in The Netherlands

X-RAY FLUORESCENCE RAW INTENSITIES VS. CONCENTRATION DATA FOR MULTIVARIATE CLASSIFICATION OF HUNGARIAN COAL

ALESSANDRA RACHETTI and WOLFHARD WEGSCHEIDER*

Institute for Analytical Chemistry, Micro- and Radiochemistry, Technical University, A-8010-Graz (Austria)

JÁNOS BORSZÉKI

Institute for Analytical Chemistry, University of Chemical Engineering, Veszprem (Hungary)

(Received 19th June 1986)

SUMMARY

A set of coal samples was examined by routine methods of coal analysis (density, calorific value, sulfur content, etc.) and by trace element determinations on the coal ash. Both data sets gave satisfactory clustering of samples from similar geological zones. X-ray fluorescence spectra were evaluated in order to identify the significant data-reduction steps in the sequence raw spectra/net intensities/trace element concentrations that is commonly used in x-ray spectrometry. The deconvolution yielding net intensities from spectra was identified as the most significant step. This was explained by the decorrelation effect of geochemically dissimilar elements.

The increasing availability of simultaneous multi-element methods [1], such as energy-dispersive x-ray fluorescence spectrometry (x.r.f.), inductively-coupled plasma/atomic emission spectrometry (i.c.p./a.e.s.) or mass spectrometry following plasma excitation has led to a significant need to evaluate and interpret the measured data in order to link them to the original problem. Pattern recognition methods have been found useful for this purpose ever since the "classical" data set on obsidians was examined [2]. Results have been published for diverse applications, such as rain samples [3], ambient particulate matter [4] and paper sheets [5]. Multivariate classification of coal samples has been examined to study fouling characteristics [6] or the origin of coals [7]. Trace element data have been used along with diffraction data to predict the fouling characteristics, while infrared data in the low-frequency range served to indicate the origin of the coal. When the i.r. data were supplemented by information on elemental content, the prediction of sintering strength proved feasible [7].

In this paper, a single coal deposit in Hungary is studied to identify different geological zones by using routine data on various physical and geochemical parameters and comparing the results to those obtained from

0003-2670/86/$03.50

a single multi-element determination of inorganic constituents by energy-dispersive x.r.f. This method is attractive for trace element determinations, as recently developed calibration procedures based on fundamental x-ray physical parameters [8] obviate the need for extensive sample preparation and matched standardization, often the bottleneck of applications of multi-element methods at trace levels. For practical reasons, it is of great interest to keep the data reduction sequence ordinarily consisting of a deconvolution procedure and the mentioned fundamental-parameters calculations as simple as possible, because both steps involve recursive algorithms in multi-dimensional spaces of energy channels and elements, respectively. It will be shown that these steps are not essential to the usefulness of x-ray data for classification purposes. Finally, a reduced set of parameters is suggested for economic considerations.

EXPERIMENTAL

Equipment and samples

The x.r.f. measurements were made on an energy-dispersive system (Philips EDAX Exam VI) equipped with an x-ray generator (PW 1140) and a secondary target turret with zirconium, titanium and samarium. A Data General NOVA-3 computer controlled the spectrometer functions and stored the spectral data which were subsequently transmitted to a VAX-750 for computing net intensities and concentration data. All computations related to x-ray spectrometry can be done on the NOVA, albeit with less convenience for the user.

Thirty coal samples were taken from a vertical height of about 30 m about 455—485 m below ground (Fig. 1) and were subjected to standard methods of characterization [8]. Coal ash samples corresponding to the coal samples were finely ground, homogenized and poured into a SOMAR spectral cup covered with a 6-μm mylar foil. The analysis of coal itself was discussed earlier [9]; it included not only the determination of most inorganic constituents but also the estimation of the organic matter in coal, which is, of course, highly correlated with heat of combustion [10].

Data-reduction procedures

In the x.r.f. spectrum, the elemental information is represented by counts accumulated in the channels of the multichannel analyzer. Because of the limited resolution of the Si(Li) detector, peaks often overlap and there is considerable spectral background so that summation over a narrow energy range gives only a rough estimate of the presence of an element. In general, deconvolution is used but its performance is critically dependent on peak-shape information to decompose the primary spectra into separate peaks or peak clusters. As the exact position of the peaks can vary slightly because of instability of the electronic circuitry, a non-linear least-squares algorithm of the Marquardt-type [11] is used.

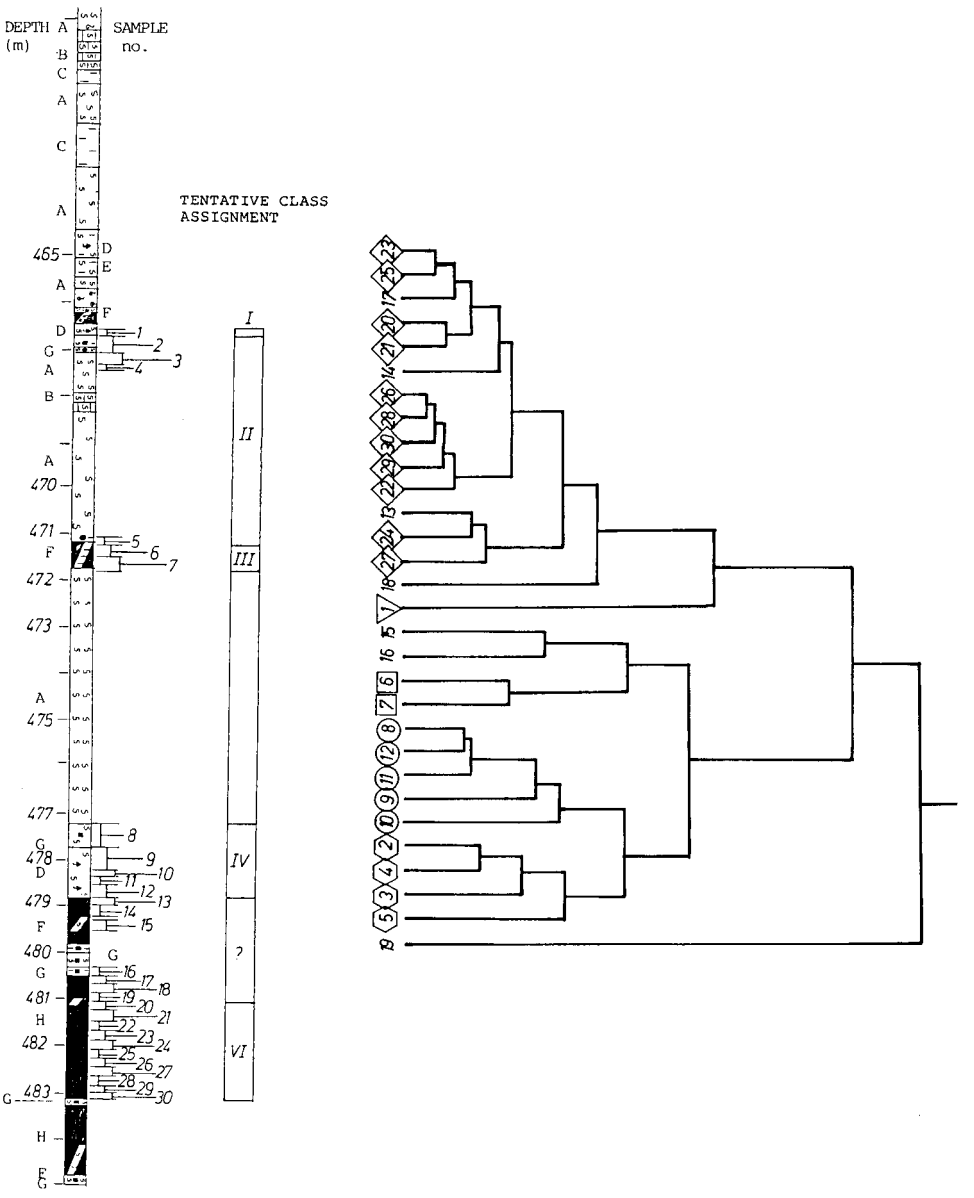

Fig. 1. Vertical cross-section of coal deposits. Layers: A, marl; B, calcareous marl; C, clay; D, argillaceous marl colored with organic material; E, argillaceous marl; F, brown coal with some marl; G, argillaceous marl with some brown coal; H, brown coal.

Fig. 2. Clustering on routine data.

From the extracted net intensities, the elemental concentrations are calculated from the fundamental parameters expression for relating intensity to concentration:

$$C = (I/t\,K)\left\{[1 - \exp(\mu\,\rho\,d)]/(\mu\,\rho\,d)\right\}[1/(E + 1)]$$

where the concentration C of each element is modelled as a function of the net intensity I, the measuring time t, a calibration factor K, the mass absorption coefficient μ, the density ρ, the sample thickness d and an enhancement correction factor E [9]. From this data reduction process, one can obtain three data sets: gross intensities, net intensities and elemental concentrations for each sample in addition to the routine data set.

The classification of the coal-ash samples was done on each of these data sets by hierarchical clustering, SIMCA, k-nearest-neighbor classification and Bayesian probabilistic classification. An eigenvector projection served to visualize the data. The most relevant features were selected from the original features according to variance and Fisher weighting. All the computer programs are contained in the ARTHUR package [12].

RESULTS AND DISCUSSION

Description of deposit

Figure 1 shows the vertical structure of the sampling region from the Hungarian coal deposit of Várpolta. From 465 to 485 m depth, the deposit consists of layers of clay, different types of marl and brown coal more or less stratified by other material. The first four samples were taken at ca. 467-m depth in a region consisting mainly of argillaceous marl with small amounts of brown coal. The next three samples came from ca. 471 m deep in a layer of marly brown coal of poor quality. Samples 8—12 were taken at 477—479 m in a region where mainly argillaceous marl contains small amounts of combustible organic material. From 479—481 m there was a very inhomogeneous stratum (samples 13–19), whereas at 481 m the samples were mainly of good-quality brown coal.

Data sets

Summary of raw data (routine and trace elements). Multivariate classification was attempted on all four data sets, but data sets B, C and D corresponded to different processing stages of identical x.r.f. data and only data A were independent (see Table 1). The elements mentioned could all be recorded under one set of excitation conditions with zirconium as secondary target. In order to establish if there was supplementary information in other elements (e.g., Na, Mg, Al, Si, S, P, Cl, Y, Zr, Nb and Mo), two additional excitation conditions with titanium or samarium as secondary targets were examined. The results were found to be invariant and so only the spectrum excited with zirconium was retained for further investigations.

Comparison with data from i.c.p./a.e.s. On a few samples the elemental

TABLE 1

Summary of data sets

Data set	Features
A	Physical/geological data (routine measurements): sample depth, density, gross heat of combustion, net heat of combustion, ash content, % hydrogen found, % sulfur found, water content, calorific value (ash-free).
B	Gross intensities at energy of characteristic lines of elements[a]
C	Net intensities for elements[a]
D	Element concentration in ash ($\mu g\ g^{-1}$)[a]

[a]The elements considered were K, Ca, Ti, V, Cr, Mn, Fe, Co, Ni, Cu, Zn, Ga, Rb, Sr, Pb.

contents were quantified by i.c.p./a.e.s. after a decomposition step [13]. These data showed fair agreement with the x.r.f. data (see Table 2), but problems were encountered in the plasma method for elements that were not liberated completely in the decomposition step (Cr) and in the x.r.f. method for elements with characteristic peaks which could not be satisfactorily deconvoluted (Mn) because of the presence of a large amount of iron.

Classifications

Initial classification according to geochemistry and routine data. To establish if there was any detectable structure in the geochemical routine data (data set A), a hierarchical clustering of the samples based on the euclidian distance was done (Fig. 2). Five fairly well separated clusters could be detected and were used for preclassification of all the four data sets. Samples 14–19 did not show a clear similarity. Alternative algorithms, e.g., *KNN*

TABLE 2

Comparison of i.c.p./a.e.s. and x.r.f. data for samples 1, 6 and 7

Metal	Element concentration[a]					
	Sample 1		Sample 6		Sample 7	
	X.r.f.	I.c.p.	X.r.f.	I.c.p.	X.r.f.	I.c.p.
Ca	26.7	30	1.76	1.76	2.29	3.2
V	103	85	224	250	390	417
Cr	95	67	380	160	112	150
Mn	51	62	5	72	—	70
Fe	2.06	1.98	4.94	3.3	4.66	4.45
Ni	76	75	110	95	154	150
Cu	12	26	64	60	70	74
Zn	56	65	194	135	77	70

[a]Data in $\mu g\ g^{-1}$ except for Ca and Fe (%).

and Bayesian probabilistic classification, proved the consistency of these initial class assignments. The classification provided for these samples could therefore be taken as a sensitive test case both for the information content of data sets A—C, and for studying variations in performance among the different algorithms.

Data on projections. Figure 3 shows the eigenvector plots of the rotated data. Sample 19 appears to be an outlier with respect to routine data, but no peculiarities were noted from the x.r.f. data. Inspection of the routine data showed an atypical sulfur value of 11.7% while the mean sulfur content of all other samples was 1.6 with a standard deviation of 0.9%. The first two eigenvectors spanned nearly the same fraction (ca. 85%) of total variance for the routine data (Fig. 3A) as for the x-ray gross intensities (Fig. 3B).

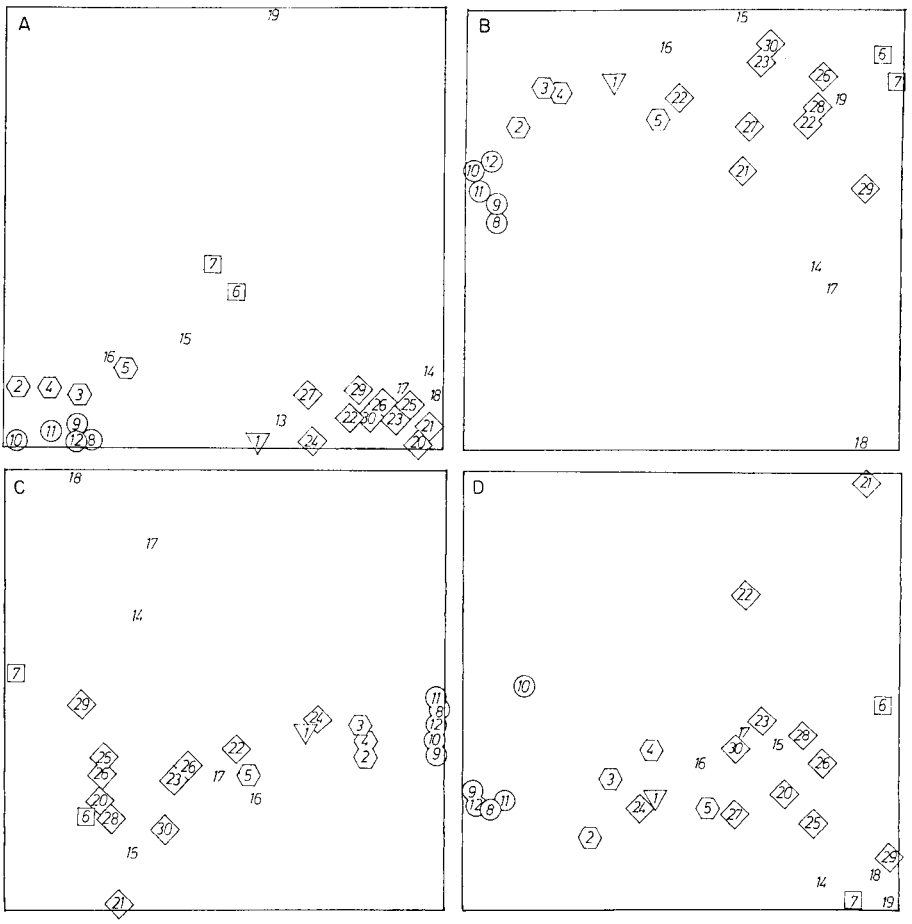

Fig. 3. Eigenvector plots of rotated data: (A) routine data; (B) x-ray gross intensities; (C) x-ray net intensities; (D) trace element concentrations. The symbols denote the class membership assigned from hierarchical clustering (Fig. 2).

This means that the greater number of features in the x-ray data set compared to the routine data set (15 vs. 9) did not reveal any more structure. This picture changed dramatically after deconvolution: the first two eigenvectors then spanned only 62% of the total variance, thus reducing the total correlation among features significantly (Fig. 3C). As this correlation in raw intensities must be caused by overlapping peaks, the explanation can be suggested that neighboring elements in the periodic table (which are overlapping elements in x-ray spectra) carry a lot of independent geochemical information because of their membership in different groups of the periodic system. Deconvolution makes this information accessible and the data become much more structured. Additionally, some of the trace elements show a very low signal/background ratio. As the background is more or less evenly spread over the energy range, the use of gross intensities obscures the variation of individual elements. The next step in data reduction, the conversion of net intensities to concentrations by fundamental parameters calculations enhances this structuring process even further, bringing the information in the first two dimensions from 62 to 52% (Fig. 3D). As all elements are involved in the corrections for any one element, geochemically similar constituents contribute (on average) correction factors similar to those from geochemically dissimilar constituents; thus, the augmentation of structure is not nearly as large as the one achieved by deconvolution. To explain 95% of total variance, nine eigenvectors are involved as opposed to three eigenvectors from routine data for a similar amount of variance.

Data on classifications

The reclassification of samples generally confirmed their initial assignment. SIMCA suggested a separate class for sample 1, as had been visually decided on the basis of hierarchical clustering of routine data. For trace element data, class 3 consisting of samples 6 and 7 were included in class 6 by *KNN* and hierarchical clustering, but treated as separate class by the SIMCA and Bayes methods. The reclassification of the tentative class 5 was done for all x-ray data, either by assigning samples 13 -19 to class 6 or by using a separate class. As expected, SIMCA again gave the strongest clues for defining a separate class.

The routine data that proved most useful for the purpose of the described classification were the sampling depth below ground, the heat of combustion and the hydrogen content. Fortunately, the number of elements selected is not critical for methods of multi-element analysis. When the set was constrained to those elements excited efficiently by the zirconium secondary target, the relevant set contained the elements Ca, Mn, Sr, Pb and V.

Conclusions

Both the routine data and the trace element data are useful to distinguish between the various geological formations of the coal deposit. The analysis

of coal ash could easily be replaced by an analysis of the coal itself if the ash is not readily available.

Trace element data are satisfactory alternatives to the routine data acquired with many different methods. The non-linear transformation involved in the calculation of concentrations from x-ray net intensities has much less influence on the data structure than spectral deconvolution. More structure is detected in the concentration data than in either the spectra or the routine data.

This work was supported in part by the Fonds zur Foerderung der wissenschaftlichen Forschung, Vienna, project P5200.

REFERENCES

1 B. Sansoni (Ed.), Instrumentelle Multielementanalyse, Verlag Chemie, Weinheim, 1985.
2 B. R. Kowalski and T. F. Schatzki, Anal. Chem., 44 (1972) 2176.
3 E. J. Knudsen, D. L. Duewer, G. D. Christian and T. V. Larson, in B. R. Kowalski (Ed.), Chemometrics, Theory and Application, ACS Symposium Series 52, Washington DC, 1977.
4 P. D. Gaarenstom, S. P. Perone and J. L. Moyers, Environ. Sci. Technol., 11 (1977) 795.
5 P. J. Simon, B. C. Giessen and T. R. Copeland, Anal. Chem., 49 (1977) 2285.
6 M. R. Detaevernier, G. Platbrood, M. P. Derde and D. L. Massart, J. Inst. Energy, March (1985) 24.
7 G. Platbrood and H. Barten, Anal. Chem., 57 (1985) 2504.
8 C. Karr, Jr. (Ed.), Analytical Methods for Coal and Coal Products, Academic Press, New York, 1978.
9 A. Rachetti and W. Wegscheider, Anal. Chim. Acta, 188 (1986) 37.
10 H. D. Pandey, R. Haque and R. Ramaswamy, Adv. X-Ray Anal., 24 (1980) 323.
11 E. Marageter, W. Wegscheider and K. Mueller, Nucl. Instrum. Methods, B1 (1984) 137.
12 D. L. Duewer, J. R. Koskinen and B. R. Kowalski, ARTHUR package, Laboratory for Chemometrics, Department of Chemistry, University of Washington, Seattle, WA 98195.
13 G. Knapp, Int. J. Environ. Anal. Chem., 22 (1985) 71.

Analytica Chimica Acta, 191 (1986) 227—241
Elsevier Science Publishers B.V., Amsterdam — Printed in The Netherlands

FOURIER TRANSFORM-BASED DECONVOLUTION TECHNIQUES FOR RESOLUTION OF OVERLAPPING BANDS IN X-RAY PHOTOELECTRON AND FOURIER-TRANSFORM INFRARED SPECTRA OF BISPHENOL-A-POLYCARBONATE/DIMETHYL SILOXANE BLOCK COPOLYMERS

ERIC R. MITTLEFEHLDT and JOSEPH A. GARDELLA, Jr.*

Department of Chemistry, State University of New York at Buffalo, Buffalo, NY 14214 (U.S.A.)

LAWRENCE SALVATI, Jr.

Perkin-Elmer Physical Electronics Division, 5 Progress Street, Edison, NJ 08820 (U.S.A.)

(Received 26th May 1986)

SUMMARY

A series of bisphenol-A-polycarbonate/poly(dimethylsiloxane) (BPAC/DMS) block copolymers is studied by x-ray photoelectron (x.p.s.) and Fourier-transform infrared (F.t.i.r.) spectroscopies. Previous quantitative results, obtained without resolution enhancement, provided calibration of the signal-processing techniques used. A Van Cittert technique for x.p.s. is evaluated for the deconvolution of the carbon 1*s* core photoelectron spectrum, and self-deconvolution by Fourier methods is evaluated for the overlapping Si-CH_3 and aromatic C—O stretch bands at 1261 and 1228 cm^{-1}, respectively, in the i.r. spectrum. These features can be utilized in quantitative analysis of the surface and bulk of the BPAC/DMS copolymers. The ability of deconvolution techniques to narrow the bands artificially so as to resolve complex spectral envelopes, while retaining the quantitative data is discussed. The studies illustrate the ability of modern signal processing techniques to extract exact complex data from spectroscopic results, and allow quantitative evaluation without standards for complex polymer systems.

The surface composition and morphology of block copolymers of bisphenol-A-polycarbonate and poly(dimethylsiloxane) by x-ray photoelectron spectroscopy (x.p.s.) was recently investigated [1]. The extraction of quantitative information concerning microphase segregation at the surface of these systems stimulated interest in the application of mathematical techniques to enhance spectral data. In work presented by Schmitt et al. [1, 2], quantitative x.p.s. information was extracted with a least-squares curve-fitting routine applied to resolve the functional group concentration, and therefore determine the surface polymer concentrations. Several difficulties arise with this approach. Because such routines require manual input of virtually all important parameters, as well as degrees of freedom for each individual parameter, the fitted result is highly dependent on the degree of good chemical intuition exercised in choosing the number, intensities, and

0003-2670/86/$03.50

full width at half maximum (FWHMs) of the peaks involved in the fit. Often, the same data can be successfully fitted by almost completely different parameters. Furthermore, because no "goodness of fit" criterion is used in this package, the difference between two reasonably good fits is often impossible to perceive. Even when the sum of the squared residuals is used as a measure of goodness of fit, it can be difficult to insure that this sum will be zero. The result of extracting quantitative information from fitted spectra for which this sum is not zero should be obvious. Finally, even if the analyst is guided by sound chemical sense and has used an appropriate method of ensuring a fit for which the sum of the squared residuals is zero, the resulting line shape will still fail to represent the true chemical response of the system without proper attention to factors that act to broaden the spectral features under consideration. While x.p.s. was successful without band narrowing, the severity of band overlap is a source of particular concern in Fourier-transform infrared (F.t.i.r.) spectra of these polymers. In F.t.i.r., band overlap makes quantitation practically impossible for this system, and limits the ability to discuss quantitative results accessible with F.t.i.r. at different depths.

The goal of this work is to formulate procedures that accurately and reproducibly enhance the line shapes present in both the x-ray photoelectron and F.t.i.r. spectra of the block copolymers mentioned. It will become clear that this depends on improving present knowledge of the broadening functions and on clarification of the criteria used to evaluate the quality of the enhanced result.

THEORY

The utilization of new computer technology has brought into common use several techniques, the purpose of which has been to enhance various forms of spectral information by removing intrinsic interferences arising from the instrumental method used in obtaining the original chemical data. Before the criteria needed for their proper utilization are discussed, three deconvolution methods will be briefly described with respect to their nature and mathematical foundations.

An excellent discussion of the subject has been given by Jansson [3]. The nature of deconvolution is best understood by first understanding the nature of convolution, which is essentially the process by which one function is smeared or blurred by another. A simple example of this is the discrete case in which a sliding average of a series of numbers is obtained by operating on an original series. Thus for a given series 1 4 2 7 5 9 3 1 6 4 9 2 7 3 4 5 1 1 9, one might compute a five-point sliding average by replacing each value in the series with the mean value of the original value and two values on either side of it. Ignoring, at present, the loss of two values at either end of the series, the result obtained is 3.8 5.4 5.2 5.0 4.8 4.6 4.6 4.4 5.6 5.0 5.0 4.2 4.0 4.6 4.0. In this operation, the original series is effectively smoothed; this is what is

done in traditional smoothing routines. Edwards and Willson [4] have provided an excellent discussion of smoothing as well as criteria for choosing the optimum number of points to be used in such routines. Whittaker and Robinson [5] have addressed the problem of data loss by suggesting ways of artificially extending the original series of values so that all the original values are retained on smoothing. The distinction between smoothing and deconvolution is the same as that between any two inverse operations.

In an effort to illustrate more rigorously how the computation of a sliding average relates to convolution, the smoothing procedure is formulated as follows:

$$h_n = \sum_{i=n-2}^{n+2} (1/5) f_n \tag{1}$$

where h_n represents the smoothed data, and f_n represents the original series. If both h and f are considered to be discrete functions, Eqn. 1 represents the convolution of f with a third discrete function, g, where g assumes a non-zero value only between $n - 2$ and $n + 2$. Equation 1 is expanded in matrix form (Table 1) to illustrate the utility of matrix algebra in the convolution of discrete functions: $\mathbf{h} = \mathbf{g} \times \mathbf{f} = g(X)f$. After the indicated matrix multiplication, the absence of the first and last two values in the result shown earlier takes on greater meaning. The four values are ignored because g experiences end-effects that, while critical to the formulation of the matrix representation of g, produce anomalous results in h. As a result, these values are lost.

If sufficient information about the blurring function is available, one can proceed in a similar fashion to remove its effect. The deconvolution of h to obtain the original series is accomplished by inverting the matrix formulation of g and subsequently taking the matrix product $\mathbf{g}^{-1} \times \mathbf{h}$. The original series is returned (Table 2).

While discrete functions both lend themselves well to matrix algebra and accurately model the form in which most conventional chemical data are digitally collected and stored, all the above discussion can be extended to continuous functions of greater complexity. In the continuous case, the convolution of $f(x)$ with $g(x)$ is represented by the integral

$$h(x) = \int_{-\infty}^{+\infty} f(x)g(x)\,dx$$

which can be expressed in the simpler form $h = f(X)g$. In much the same way that matrix algebra aids in the computations for the discrete case, several aspects of working in Fourier space help to simplify computations for the continuous case. In Fourier space, the transformations of $h(x)$, $f(x)$, and $g(x)$ enjoy the simplicity of the relationship [6] $H(\omega) = F(\omega)G(\omega)$, where $H(\omega)$, $F(\omega)$, and $G(\omega)$ are the Fourier transforms of $h(x)$, $f(x)$, and $g(x)$, respectively:

TABLE 1

Convolution matrix

g																		f	h
.2	.2	.2	0	0	0	0	0	0	0	0	0	0	0	0	0	0	.2	.2	1	3.4
.2	.2	.2	.2	0	0	0	0	0	0	0	0	0	0	0	0	0	0	.2	4	4.6
.2	.2	.2	.2	.2	0	0	0	0	0	0	0	0	0	0	0	0	0	0	2	3.8
0	.2	.2	.2	.2	.2	0	0	0	0	0	0	0	0	0	0	0	0	0	7	5.4
0	0	.2	.2	.2	.2	.2	0	0	0	0	0	0	0	0	0	0	0	0	5	5.2
0	0	0	.2	.2	.2	.2	.2	0	0	0	0	0	0	0	0	0	0	0	9	5.0
0	0	0	0	.2	.2	.2	.2	.2	0	0	0	0	0	0	0	0	0	0	3	4.8
0	0	0	0	0	.2	.2	.2	.2	.2	0	0	0	0	0	0	0	0	0	1	4.6
0	0	0	0	0	0	.2	.2	.2	.2	.2	0	0	0	0	0	0	0	0	6	4.6
0	0	0	0	0	0	0	.2	.2	.2	.2	.2	0	0	0	0	0	0	0	X 4	= 4.4
0	0	0	0	0	0	0	0	.2	.2	.2	.2	.2	0	0	0	0	0	0	9	5.6
0	0	0	0	0	0	0	0	0	.2	.2	.2	.2	.2	0	0	0	0	0	2	5.0
0	0	0	0	0	0	0	0	0	0	.2	.2	.2	.2	.2	0	0	0	0	7	5.0
0	0	0	0	0	0	0	0	0	0	0	.2	.2	.2	.2	.2	0	0	0	3	4.2
0	0	0	0	0	0	0	0	0	0	0	0	.2	.2	.2	.2	.2	0	0	4	4.0
0	0	0	0	0	0	0	0	0	0	0	0	0	.2	.2	.2	.2	.2	0	5	4.6
0	0	0	0	0	0	0	0	0	0	0	0	0	0	.2	.2	.2	.2	.2	1	4.0
.2	0	0	0	0	0	0	0	0	0	0	0	0	0	0	.2	.2	.2	.2	1	3.4
.2	.2	0	0	0	0	0	0	0	0	0	0	0	0	0	0	.2	.2	.2	9	3.2

TABLE 2

Deconvolution matrix

g^{-1}																		f	h
−1	−1	4	−1	−1	−1	−1	4	−1	−1	−1	−1	4	−1	−1	−1	−1	4	−1	3.4	1
−1	−1	−1	4	−1	−1	−1	−1	4	−1	−1	−1	−1	4	−1	−1	−1	−1	4	4.6	4
4	−1	−1	−1	4	−1	−1	−1	−1	4	−1	−1	−1	−1	4	−1	−1	−1	−1	3.8	2
−1	4	−1	−1	−1	4	−1	−1	−1	−1	4	−1	−1	−1	−1	4	−1	−1	−1	5.4	7
−1	−1	4	−1	−1	−1	4	−1	−1	−1	−1	4	−1	−1	−1	−1	4	−1	−1	5.2	5
−1	−1	−1	4	−1	−1	−1	4	−1	−1	−1	−1	4	−1	−1	−1	−1	4	−1	5.0	9
−1	−1	−1	−1	4	−1	−1	−1	4	−1	−1	−1	−1	4	−1	−1	−1	−1	4	4.8	3
4	−1	−1	−1	−1	4	−1	−1	−1	4	−1	−1	−1	−1	4	−1	−1	−1	−1	4.6	1
−1	4	−1	−1	−1	−1	4	−1	−1	−1	4	−1	−1	−1	−1	4	−1	−1	−1	X 4.6	= 6
−1	−1	4	−1	−1	−1	−1	4	−1	−1	−1	4	−1	−1	−1	−1	4	−1	−1	4.4	4
−1	−1	−1	4	−1	−1	−1	−1	4	−1	−1	−1	4	−1	−1	−1	−1	4	−1	5.6	9
−1	−1	−1	−1	4	−1	−1	−1	−1	4	−1	−1	−1	4	−1	−1	−1	−1	4	5.0	2
4	−1	−1	−1	−1	4	−1	−1	−1	−1	4	−1	−1	−1	4	−1	−1	−1	−1	5.0	7
−1	4	−1	−1	−1	−1	4	−1	−1	−1	−1	4	−1	−1	−1	4	−1	−1	−1	4.2	3
−1	−1	4	−1	−1	−1	−1	4	−1	−1	−1	−1	4	−1	−1	−1	4	−1	−1	4.0	4
−1	−1	−1	4	−1	−1	−1	−1	4	−1	−1	−1	−1	4	−1	−1	−1	4	−1	4.6	5
−1	−1	−1	−1	4	−1	−1	−1	−1	4	−1	−1	−1	−1	4	−1	−1	−1	4	4.0	1
4	−1	−1	−1	−1	4	−1	−1	−1	−1	4	−1	−1	−1	−1	4	−1	−1	−1	3.4	1
−1	4	−1	−1	−1	−1	4	−1	−1	−1	−1	4	−1	−1	−1	−1	4	−1	−1	3.2	9

$$H(\omega) = (2\pi)^{-1/2} \int_{-\infty}^{+\infty} h(x) \exp(-j\omega x)\, dx$$

$$F(\omega) = (2\pi)^{-1/2} \int_{-\infty}^{+\infty} f(x) \exp(-j\omega x)\, dx$$

$$G(\omega) = (2\pi)^{-1/2} \int_{-\infty}^{+\infty} g(x) \exp(-j\omega x)\, dx$$

In Fourier space, the two functions that were convolved with each other are now factors of a product that can be easily transformed back to its original state. Furthermore, deconvolution in Fourier space is reduced to a simple arithmetic operation.

Unfortunately, however, deconvolution is rarely as simple as suggested by the ease of the calculations described above. The problem lies in the fact that the functions responsible for blurring the information of interest are rarely known precisely. The blurring effect is often the result of a function that represents the convolution of several other functions. Accordingly, several methods have been advanced for the purpose of approximate deconvolution [3, 7, 8].

If $i(x)$ represents the instrumentally obtained spectral data, $s(x)$ the convolution of all important broadening functions, and $o(x)$ the true chemical response function, then [3]:

$$i(x) = \int_{-\infty}^{+\infty} s(x - x')o(x')\, dx'$$

and in the discrete case, $i_n = \sum_{-\infty}^{+\infty} s_{n-m} o_m$. Even without specific knowledge about $s(x)$, $i(x)$ can be considered an approximation to the true chemical response. From this point of view, one might suggest that blurring $i(x)$ could lead to formulation of a better approximation to the true chemical response function. This is the basis of the traditional Van Cittert approach [7]. The first approximation, $o^\circ(x)$ is $o^\circ(x) = i(x)$. Next, $i(x)$ is blurred: $i(x) \geqslant i^\circ(x)$. The difference $i(x) - i^\circ(x)$ is the error introduced by blurring the data. Adding this error to the initial estimate of the chemical response function gives a new estimate of the response, $o^1(x)$:

$$o^1(x) = o^\circ(x) + [i(x) - i^\circ(x)]$$

If $i(x)$ is carefully blurred, the resulting $[i(x) - i^\circ(x)]$ will be such that $o^1(x)$ approximates the true chemical response better than $o^\circ(x)$. By repeatedly performing this routine with each new approximation to the chemical response function, successively better estimates of the true response are obtained:

$$o^{(n+1)}(x) = o^{(n)}(x) + [i(x) - i^{(n)}(x)]$$

Upon convergence, i.e., $o^{(n+1)}(x) \approx o^{(n)}(x)$, this iterative approach is expected to yield the true chemical response function. Unfortunately, depending on the choice of blurring function, the method may or may not converge, and can seldom be expected to provide a unique result. For this reason, users of this method must be guided by a strong chemical sense in order to avoid blurring that results in divergence. Furthermore, without proper constraint of the process, it is possible to over-deconvolve the data and thereby degrade or destroy its quantitative content.

In keeping with the aim of enhancing instrumentally obtained spectral data without degrading it, careful consideration of the effects that broaden spectral bands is needed. In order to illustrate this, both x.p.s. and F.t.i.r. can serve as examples.

In x.p.s., the true chemical response function assumes the form of an energy profile that, by virtue of the unique binding energies of core level electrons for various elements in different chemical environments, can be used to characterize surfaces both qualitatively and quantitatively. The sample surface is bombarded with x-rays of sufficient energy to dislodge core-level electrons. These electrons leave the surface with a kinetic energy related to their binding energies [11]: $E_B = h\nu + E_K$, where E_B is the binding energy, $h\nu$ is the energy of the incident photon, and E_K is the kinetic energy of the electrons leaving the surface. The intensity of the profile is then a function of the number of electrons having a particular binding energy.

With an instrument providing perfect resolution and no line broadening, the spectrum should appear as a series of Dirac functions of varying intensity, but several factors act to distort this ideal spectrum. These factors can be grouped into two broad categories; one includes all those factors inherent in the phenomenon observed, and the other includes all those factors attributable to the method of observation.

In x.p.s., factors that inherently broaden spectral features include natural broadening and broadening caused by inelastic scattering. Natural broadening arises from the Heisenberg uncertainty involved in attempting simultaneous measurements of energy and time with absolute accuracy. Natural broadening gives Lorentzian character to the features of the spectrum. Broadening caused by inelastic scattering results from the fact that some electrons lose part of their kinetic energy through inelastic collisions with other electrons leaving the surface at the same time. This means electrons emerging from the surface are not necessarily electrons that had the same binding energy; they may have been electrons of different binding energies that either lost or gained kinetic energy in collisions with other electrons on their way from the surface. While it is obviously impossible to correct for natural line broadening, correction for inelastic scattering by spectral subtraction has been successful [10].

Factors attributable to the method of observation include source broadening, detector broadening, and surface changing. Source broadening is due to the convolution of the Lorenztian-shaped x-ray emission lines with the natural line width. Senemaud [11] described the source broadening effects for Mg K_α radiation. Lastly, broadening caused by surface charging predominantly affects the line shape in the analysis of nonconducting materials and results directly from the fact that the sample surface is constantly losing electrons. If the sample is an insulating polymer, for example, the surface region becomes electron-deficient relative to the sample bulk and electrons leaving the surface are subject to potential fields of varying magnitude on their way from the surface. While methods exist for minimizing these effects mechanically, it is reasonable to assume that deconvolution can also be used to remove such effects. By applying a Van Cittert iterative method, knowledge about the specific effects mentioned above can be combined in establishing appropriate blurring functions.

In F.t.i.r., a slightly different approach to deconvolution is pursued. Fourier self-deconvolution utilizes the unique property of Fourier transforms discussed earlier. An interferogram is collected in the domain of x (cm) and transformed to give, in the domain of ν (wavenumbers), an emission spectrum. If $i(x)$ is the data collected as an interferogram, and $E(\nu)$ is the data transformed into an emission spectrum, these two functions are Fourier pairs:

$$E(\nu) = \int_{-\infty}^{\infty} i(x) \exp(i2\pi\nu x)\, dx \text{ and } i(x) = \int_{-\infty}^{\infty} E(\nu)\exp(-i2\pi\nu x)\, d\nu$$

Furthermore, if $E^0(\nu)$ is considered to be the intrinsic line shape, $i^0(x)$ can be considered [12] the deconvolved spectrum under the conditions given by

$$i^\circ(x) = [A(x)/E^0(\nu)^{-1}]\, i(x)$$

where $A(x)$ is an apodization function, and $E^0(\nu)^{-1}$ represents the inverse Fourier transform of the intrinsic line shape. In practice, $E^0(\nu)$ is approximated [12] by a Lorentzian line shape of the character

$$E^0(\nu) = (\sigma/\pi)/(\sigma^2 + \nu^2)$$

For the work presented here, $A(x)$ was chosen to be a Bessel function of the type [13]:

$$A(x) = B(x)\, [1 - (x/L)^2]^2$$

where $B(x)$ is a boxcar function, such that $B(x) = 1$ for $|x| \leqslant L$ and $B(x) = 0$ for $|x| > L$, and where L and $-L$ replace the limits for the integral that is used to calculate the $E(\nu)$ from $i(x)$.

While it is true that several functions can and have been evaluated as choices for $A(x)$, Kauppinen et al. [13] have shown that the Bessel function yields

the best results. Two criteria are imposed. First, for S/N ratios of any particular magnitude, the factor by which the resolution of the spectrum can be enhanced is estimated by

$$K = \log_{10}(S/N) = 2\sigma/\Delta_{(1/2)}$$

where 2σ is the half bandwidth of the intrinsic line shape, and $\Delta_{(1/2)}$ is the half bandwidth of $A(x)$. Meeting these two criteria insures that L in $A(x)$ corresponds to the maximum $A(x)$. This minimizes the unwanted amplification of noise that otherwise results.

It is important to realize that, in the Fourier self-deconvolution approach utilized in F.t.i.r., unlike the iterative Van Cittert method used in x.p.s., virtually no knowledge is assumed in terms of the nature of the broadening functions. $E^0(\nu)$ is merely assumed to be Lorentzian and of a character that will support the analyst's choice of K.

Certainly, the second approach has merit, but it is actually the nature of the method (F.t.i.r.) that provides the simplicity of the approach. In F.t.i.r., many of the instrumental broadening effects present in x.p.s., or even in traditional dispersive i.r., do not play significant roles. In fact, most of the broadening present in F.t.i.r. spectra is the direct result of inherent and not instrumental factors. Furthermore, because natural line broadening and collision broadening both lead to line shapes that are Lorentzian in character, it would seem reasonable to assume such a shape for $E^0(\nu)$.

With a fundamental understanding of the basic approaches utilized in both x.p.s. and F.t.i.r., the application of these methods to real data seems appropriate. The problem, as previously indicated, would seem to revolve less around the validity of what has been presented than around the practical point at which poor approximations result in quantitative degradation of spectral data. In each case, approximations to the true chemical response function are necessary. If these approximations are poor, the results obtained from the application of these methods will result in over-enhancement to the extent that what remains still fails to represent the true data. The present goal is to demonstrate for a specific example the extent to which deconvolution can be performed before the quantitative character of the data is degraded. Once this has been achieved, the results will be compared to those reported from maximum entropy methods [8]. It is important to realize, however, that the above discussion is limited in that, with the exception of the Van Cittert technique, exact solutions are obtained with knowledge about the blurring functions that is normally not available.

EXPERIMENTAL

X-ray photoelectron spectroscopy

The data presented below were obtained from a Perkin-Elmer PHI-5100 instrument operated at a resolution of 0.100 eV/step and a pass energy of 17.90 eV. The take-off angle was 45° and the Mg K_α source was operated

at 300 W, 15.0 kV and 20 mA. Base pressure was maintained at 5.0×10^{-9} torr. The region of interest for this work was the carbon 1*s* region of bis-phenol-A-polycarbonate (BPAC) cast on thin copper films (Fig. 1). Deconvolution, smoothing, and curve-fitting were all accomplished with routines available on the Perkin-Elmer 7300 computer. While the exact routine used in deconvolving the spectra is not available, it is a Van Cittert iterative method available with the standard data-processing package.

Fourier-transform infrared spectroscopy

Transmission studies were performed on block copolymers of varying composition: 25/75 dimethylsiloxane (DMS)/bis-phenol-A-polycarbonate (BPAC), 50/50 DMS/BPAC, and 35/65 DMS/BPAC [1]. All i.r. results were obtained on a Nicolet 7199 Fourier-transform infrared spectrometer operated at 2 cm^{-1} resolution with an MCT detector. The transmission results were obtained by casting 1% solutions of the copolymers in chloroform directly onto sodium chloride plates. All deconvolutions of the results were done in the region between 1316 and 1127 cm^{-1} with software obtained from Nicolet (Application Note 8311).

RESULTS AND DISCUSSION

X-ray photoelectron spectroscopy

Table 3 shows the values for the peak position, peak intensity, full width at half-maximum percent Gaussian, and peak area for all four peaks in the

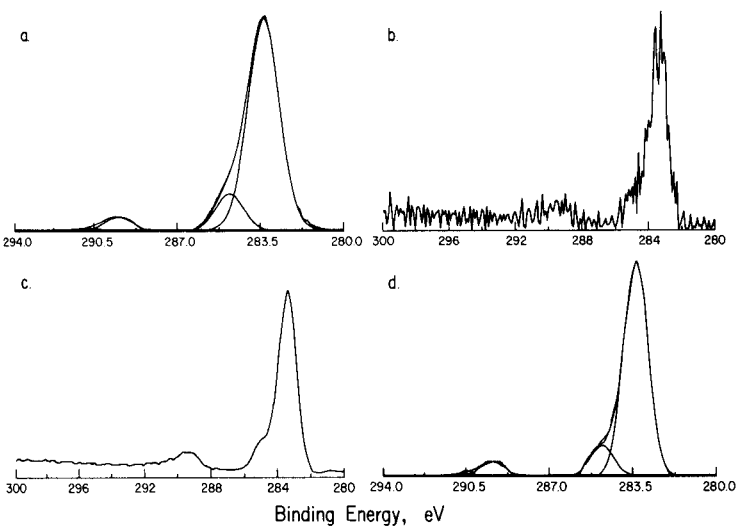

Fig. 1. The carbon 1*s* region of BPAC: (a) curve fit of original data; (b) original data deconvolved with 30 iterations; (c) deconvolved result after smoothing with 11, 5, 5 point routines; (d) curve fit for smoothed result.

TABLE 3

Deconvoluted results from x.p.s. in the carbon 1*s* region

Peak	Iterations	Peak position	Peak intensity	FWHM[a]	Percent Gaussian	Peak area
I	0	283.38	21899	1.55	90	37710
	5	283.39	22044	1.55	88	38368
	10	283.37	30298	1.18	100	38018
	15	283.35	30922	1.15	100	37845
	20	283.37	42300	1.01	100	45473
	30	283.35	31004	1.22	100	40245
	40	283.39	30950	1.21	100	39864
	50	283.40	30957	1.29	100	42509
	100	283.38	30950	1.23	100	40446
II	0	284.81	3800	1.45	100	5865
	5	284.86	3900	1.35	100	5604
	10	284.86	4622	1.37	100	6740
	15	284.65	4809	1.44	100	7371
	20	284.89	4540	1.03	100	5002
	30	284.80	4508	1.25	100	5974
	40	284.80	4500	1.19	100	5700
	50	284.98	4044	0.91	100	3939
	100	284.87	4150	1.19	100	5257
III	0	289.52	1479	1.40	100	2205
	5	289.49	1450	1.45	90	2344
	10	289.38	2098	1.37	100	3060
	15	289.40	2203	1.44	100	3376
	20	289.38	3570	1.27	100	4831
	30	289.40	2191	1.24	100	2892
	40	289.40	2150	1.27	100	2907
	50	289.39	2099	1.14	100	2547
	100	289.35	2270	1.11	100	2682
IV	0	290.64	350	1.25	100	466
	5	290.50	350	1.25	100	467
	10	290.49	609	1.24	100	805
	15	290.50	359	1.09	100	417
	20	291.15	750	1.50	100	1198
	30	290.49	814	1.21	100	1045
	40	290.58	550	1.19	97	707
	50	290.49	522	1.09	100	605
	100	290.51	613	1.11	100	725
Ratio III:II:I[b]	0					0.76:2.02:13
	5					0.79:1.90:13
	10					1.05:2.30:13
	15					1.16:2.53:13
	20					1.38:1.43:13
	30					0.93:1.93:13
	40					0.95:1.86:13
	50					0.78:1.20:13
	100					0.86:1.69:13

[a]The best results are underlined. [b]See text for detail.

carbon 1*s* region. Several comments can be made. Because the peak position is never altered by more than ±0.3%, it can be said that the deconvolutions done here are shift-invariant. Because improving resolution is of primary concern, the optimum number of iterations should be reflected by a minimization of the FWHM. Furthermore, because retention of the quantitative characteristics of the data is also crucial, the optimum number of iterations should also result in peak areas that correspond to those known from previous work [1]. For the carbon 1*s* region of bis-phenol-A-polycarbonate, a peak-area ratio of 1:2:13 for peaks III:II:I should be maintained.

When these parameters are handled separately, the best value for the FWHM occurs as indicated by underlining in Table 3. For the peak-area ratios the best agreement with known results occurs after 30 iterations (bottom of Table 3). Although none of the peaks has minimum FWHM after 30 iterations, the values obtained after 30 iterations are considerably reduced from those obtained prior to any deconvolution. The percent reduction in FWHM for the various peaks after 30 iterations is: peak I 21.3%; peak II 13.8%; peak III 11.4%; peak IV 3.2%. And the percent reduction at minimum FWHM is: peak I 34.8%; peak II 37.2%; peak III 20.7%; peak IV 12.8%.

Some workers [14] have measured the enhancement of resolution through deconvolution solely by the reduction in FWHM and claimed the maximum improvement to be of the order of 30%. Proponents of the method of maximum entropy also calculate this degree of enhancement to be maximized at 30% [8]. While peaks I and II do show an enhancement of this magnitude at their minimum FWHMs, the quality of the quantitative data suffers when only this parameter is chosen as the criterion of improvement. It is therefore reasonable to assume that other factors must be considered.

A noticeable feature of the data is that the best fits of the data yield peaks that are almost exclusively Gaussian in nature. Considering that the chemical response function should be comprised of bands that are Lorentzian in nature, it is clear that the deconvolution routines available have failed to remove several of the effects that broaden the bands so much that they become Gaussian. This suggests that the blurring applied to the data in the iterative Van Cittert procedure used (see above) was not the best choice. The goal for future work will be to improve the blurring in an effort to obtain a deconvolved response that yields line shapes closer to what is characteristic of the true chemical response function, but retains the quantitative peak areas known to be 1:2:13 for peaks III:II:I.

Attempts to improve the quality of deconvolution results will include consideration of charging effects, and more exact formulations of the broadening caused by source and detector. This can be done, but only to an extent comparable to the resolution of the instrument used in obtaining the original data; beyond that point, enhancement becomes pure conjecture.

Variations in the ratios shown above indicate a trend toward better agreement with the known result followed by a marked degradation in results after 50 iterations. While more data are obtainable, it seems probable that no

single number of iterations will ever consistently yield the best results. This, however, is unnecessary if a narrow region can be discovered where the results vary by only ±10%. Unfortunately, the necessity to smooth the data after deconvolution but prior to curve fitting has probably introduced the variations in the presented results beyond the degree to which such a region can presently be identified with confidence.

Fourier-transform infrared spectroscopy

The ratioed absorbance spectra for each block copolymer are shown in Fig. 2a. In each case, the region between 1316 and 1127 cm^{-1} appears to be comprised of only three poorly resolved peaks. Upon deconvolution, with a half bandwidth of 9.6 cm^{-1} (as chosen for the narrow C—O stretch at 1164 cm^{-1}) and an exponential weighting factor (K) of 3.0 (Fig. 2b), the first peak is resolved to reveal several features; two of these yield important information about the composition of the block copolymer. By ratioing the intensities of the aromatic C—O stretch at 1228 cm^{-1} and Si—CH_3 stretch at 1261 cm^{-1}, the change in the composition of the block copolymer can be charted. The BPAC/DMS mass ratios of 75:25, 50:50 and 35:65 correspond to BPAC/DMS mole ratios of 0.88, 0.29 and 0.16, respectively. Figure 3 shows the linear relationship (variance 2.3×10^{-4}) between the ratioed peak intensities and molar ratios where the slope of the line is the ratio of the molar absorptivities.

In essence, the information obtained through the application of deconvolution provides a means by which the bulk composition of the block copolymers can be identified. This would be a hopeless task if only the poorly resolved results depicted in Fig. 2a were available.

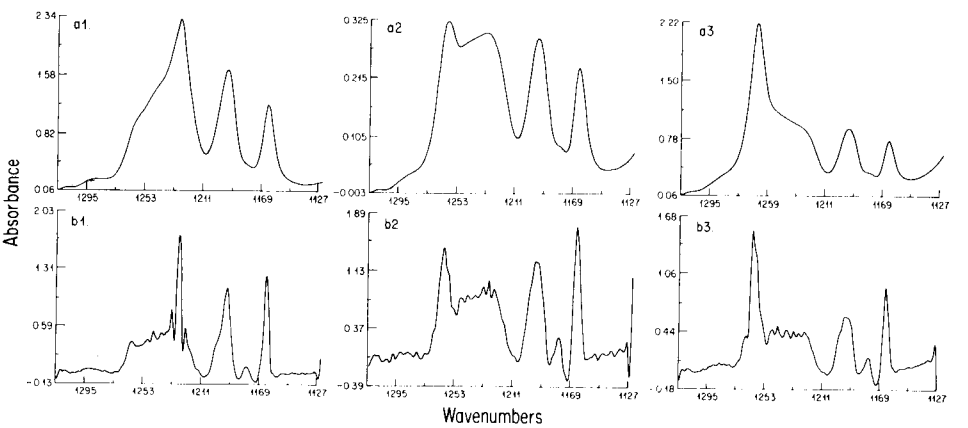

Fig. 2. F.t.i.r. absorbance spectra of BPAC/DMS copolymers. Original spectra: (a1) 75/25 BPAC/DMS; (a2) 50/50 BPAC/DMS; (a3) 35/65 BPAC/DMS. Spectra deconvolved with a half bandwidth of 9.6 cm^{-1} and K = 3.0: (b1) 75/25 BPAC/DMS; (b2) 50/50 BPAC/DMS; (b3) 35/65 BPAC/DMS.

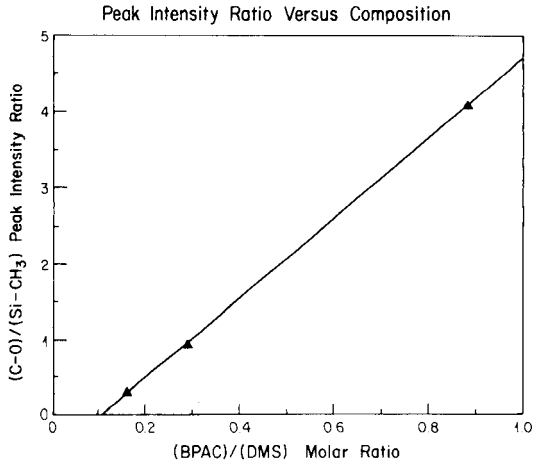

Fig. 3. Linear relationship between (C—O)/Si—CH_3) peak intensity ratio and molar ratio.

The software used in the deconvolution of the infrared data involves self-deconvolution utilizing a Bessel apodization function. As indicated by the results above, significant enhancement of the data is achieved. The particular package used retains the integrated band areas, and thus insures that quantitative information is not destroyed. In the case of Fourier-transform self-deconvolution, over-deconvolution is indicated by the appearance of increasingly large side lobes (Fig. 4).

Improvement of the method for Fourier-transform self-deconvolution rests primarily on the choice of apodization function. By using a $sinc^2$ function, resolution enhancement deteriorates but side lobes are better suppressed (Nicolet Application Note 8311). The development of new apodization functions is essential. Again, any resolution enhancement in Fourier self-deconvolution will be limited by the resolution limits of the instrument used to collect the data.

Conclusion

Three important considerations in any deconvolution routine must be the resolution of the instrument used to obtain the original data, the operations performed on the original data between deconvolution and quantitation, and the criteria used to judge the quality of the end result.

If deconvolution is ever to assume its proper place as a technique for quantitative enhancement of spectral data, closer attention will have to be paid to the form of the broadening functions that affect the true chemical response function. Careful consideration of these broadening functions will insure better results because the blurring functions will be better formulated and more computationally facile.

Further work in the development of more specific apodization functions should aid both in the application of deconvolution techniques to i.r. spectra, and the future application of Fourier self-deconvolution techniques in the deconvolution of x-ray photoelectron spectra.

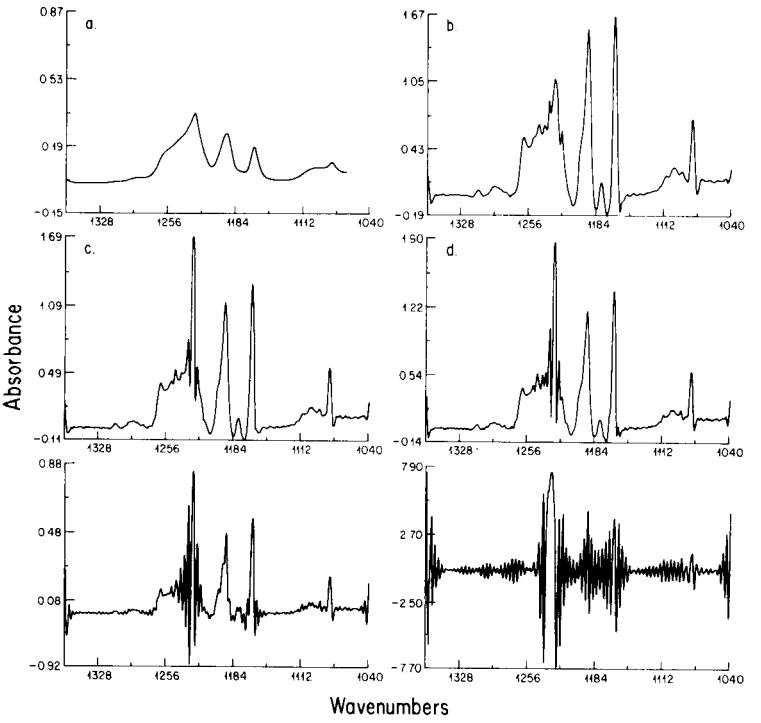

Fig. 4. Deconvolution results illustrating the effects of over-deconvolution. (a) Original absorbance spectrum of 75/25 BPAC/DMS; (b) spectrum (a) deconvolved with a half bandwidth of 10.77 cm^{-1} and K = 2.5; (c) spectrum (a) deconvolved with a half bandwidth of 10.00 cm^{-1} and K = 3.0; (d) spectrum (a) deconvolved with a half bandwidth of 10.00 cm^{-1} and K = 3.5; (e) spectrum (a) deconvolved with a half bandwidth of 10.00 cm^{-1} and K = 15; (f) spectrum (a) deconvolved with a half bandwidth of 15.00 cm^{-1} and K = 15.

The authors thank Dr. Robert Osteryoung at the State University of New York at Buffalo for use of the F.t.i.r. spectrometer. Support for this project was provided by the National Science Foundation Grant DMR 8812781 from the Polymers Program.

REFERENCES

1 R. L. Schmitt, J. A. Gardella, Jr., J. H. Magill, L. Salvati, Jr. and R. L. Chin, Macromolecules, 18 (1985) 2675.
2 R. L. Schmitt, J. A. Gardella, Jr. and L. Salvati, Jr., Macromolecules, 19 (1986) 648.
3 P. A. Jansson, Deconvolution With Applications in Spectroscopy, Academic Press, Orlando, Fl., 1984, pp. 4, 28, 102.
4 T. H. Edwards and P. D. Willson, Appl. Spectrosc., 28 (1974) 541.
5 E. Whittaker and G. Robinson, The Calculus of Observations, 4th edn., Blackie, Glasgow, 1954, Chap. 11.
6 R. Bracewell, The Fourier Transform and Its Applications, 2nd edn., McGraw-Hill, New York, 1978, Chap. 6.

7 P. H. Van Cittert, Z. Phys., 69 (1931) 95.
8 R. P. Vasquez, J. D. Klein, J. J. Barton, and F. J. Grunthaner, J. Electron Spectrosc. Relat. Phenom., 23 (1981) 63.
9 D. Briggs and M. P. Seah, Practical Surface Analysis by Auger and X-ray Photoelectron Spectroscopy, Wiley, New York, 1983, Chapter 1.
10 D. A. Shirley, Phys. Rev., B 5 (1972) 4709.
11 C. Senemaud, Doctoral Thesis, University of Paris, 1968.
12 J. K. Kauppinen, D. J. Moffatt, H. H. Mantsch and D. G. Cameron, Appl. Spectrosc. 35(3) (1981) 271.
13 J. K. Kauppinen, D. J. Moffatt, D. G. Cameron and H. H. Mantsch, Appl. Opt., 20(10) (1981) 1866.
14 H. H. Madden and J. E. Houston, J. Appl. Phys., 47 (1976) 3071.

Analytica Chimica Acta, 191 (1986) 243—259
Elsevier Science Publishers B.V., Amsterdam — Printed in The Netherlands

AUTOMATED OPTIMIZATION IN HIGH-PERFORMANCE LIQUID CHROMATOGRAPHY

J. C. BERRIDGE

Pfizer Central Research, Sandwich, Kent CT13 9NJ (Great Britain)

(Received 29th May 1986)

SUMMARY

The development and optimization of liquid chromatographic (l.c.) separations has traditionally required an ill-defined mix of experience, intuition and guesswork. Even today, as systematic optimization schemes for separation become available, many workers in chromatography remain dedicated to the trial-and-error approach. Chemometric principles are, however, being more frequently applied to all aspects of l.c., especially in the area of rational and automated separation optimization. In this review of automated optimization, the definition of the separation problem, the description of the attainment of a solution and the experimental methods for obtaining that solution are considered.

The current "state of the art" in high-performance liquid chromatography (h.p.l.c.) is such that a completely unknown sample can be given to a suitably configured chromatograph and the system can then be left to its own devices to produce an optimum separation for this sample. Such capabilities are relatively recent and their origins and success are surely a consequence of the converging developments in chromatography, chemometrics and computing. There is still, however, a considerable reluctance to invoke formal optimization schemes in liquid chromatography, the majority of chromatographers preferring to rely on the tried and tested "trial-and-error" methods rather than apply a systematic technique. This is somewhat surprising because, without a logical approach, development and optimization of h.p.l.c. will continue to be a difficult and frustrating operation. As well as needing decisions on the mode of chromatography to be used and the selection of hardware, the actual optimization is complicated by the interdependence of many of the variables being considered (Fig. 1) [1]. The ultimate goal of fully automated method development, i.e., the situation where the instrument is able to choose automatically the chromatographic mode as well as develop the separation, is still some way off. Nevertheless, there are rational, systematic approaches, many of which can be automated, for efficient optimization of h.p.l.c. separations [2—5].

The basic problem

As can be seen from Fig. 1, the optimization of an h.p.l.c. separation is likely to be complicated as a consequence of the large number of variables

0003-2670/86/$03.50

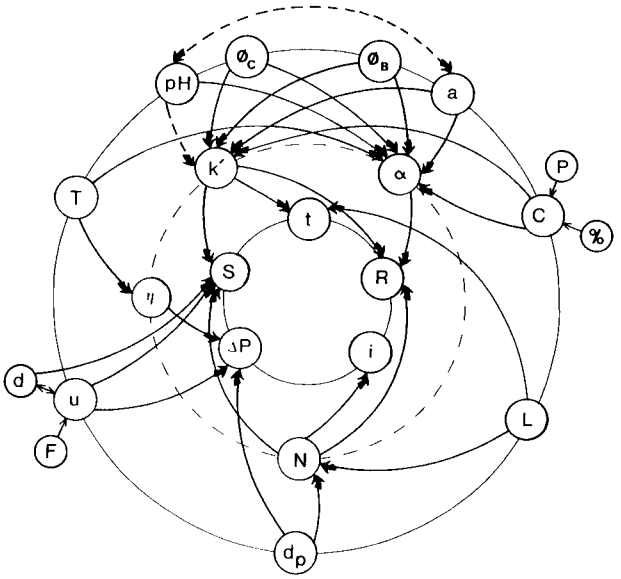

Fig. 1. Dependent variables of liquid chromatography (after ref. 1). Primary variables: ϕ_B, modifying solvent; ϕ_C, ternary modifier (or ion-interaction reagent); pH, mobile phase pH; T, separation temperature; u, reduced velocity (dependent on flow rate (F) and column diameter (d)); d_p, particle diameter; L, column length; C, column stationary phase selectivity (dependent on support loading (%) and polarity (P)); a, activity of support (may be due to residual silanols and thus may depend on pH). Secondary variables: α, selectivity; k', capacity factor; η, mobile phase viscosity; N, plate count. Optimization criteria variables: i, number of peaks; R, resolution; t, separation time; S, sensitivity; P, pressure drop.

which can be introduced. In common with all good experimental techniques, it is first essential to decide on just what is to be optimized — speed, resolution, number of components, etc. This is most effectively covered by the selection of an appropriate optimization criterion. Secondly, the variables which are to be considered must be selected. These may include separation temperature and flow rate as well as several components of the mobile phase. At present, there is no easy solution to this aspect, other than to rely on chromatographic expertise. This expertise is likely to become more computer-based in the future as Expert Systems become more readily available. Finally, a suitable design must be selected which is compatible with the first two decisions that were made and which is best suited to the amount of information which can be extracted from each experiment conducted. Indeed it is this latter aspect, the information obtainable from each separation, that is quite likely to govern the choice of method employed. This is surely the area to which the discipline of chemometrics can make the greatest contributions. Equipment capabilities must not be neglected but instrument limitations are very much less of a problem today.

OPTIMIZATION CRITERIA AND METHODS

Criteria

For effective h.p.l.c. optimization, and certainly for all automated applications, an appropriate optimization criterion is a pre-requisite. Almost any aspect of a separation is usually amenable to optimization. For many years, attention was directed towards solving basic hardware problems, particularly column design and packings [2, 6—11], but by and large these are no longer a limiting factor. Even so, there is still work continuing on improvement of the kinetic aspects of chromatography [9, 10—13] although one philosophy (the "abt" concept [10]) is regarded by some as being controversial and has not benefited from full exploitation. The current main interest is in optimizing the choice of column support and the mobile-phase composition to achieve the desired separation.

It is not easy, unfortunately, to be absolute about a definition for an optimized separation. It is generally the case that most chromatographers require the optimum combination of speed of elution and resolution of the maximum number of solutes. Even this statement is far from providing a definition because it does not quantify "optimum". The way that the problem is approached practically is to establish a mathematical expression that incorporates terms which can accommodate the particular needs of the separation or optimization scheme being considered. The objective of the expression is to provide a single number which describes in at least a semi-quantitative way, the quality of any given separation.

There is a large number of optimization functions and a selection is reproduced in Table 1. It is not necessarily true that complexity is essential for successful automated optimization: it has been argued [31] that none of the published criteria is unconditionally useful in directing automated optimization. Furthermore, evaluation of more involved criteria can lead to the conclusion [30] that simpler equations are actually just as good and may even be better. There is little doubt that more effective optimization criteria are still required. Nevertheless, the criteria listed have all been successfully demonstrated to be useful in separation optimization.

What is emerging from the use of the current range of criteria is that a successful criterion accommodates the need to consider peak separation (usually expressed as resolution), the number of peaks present in a given chromatogram and a time-based factor. Ideally the peaks should be evenly spaced throughout the chromatogram and it may be desirable to weight specific terms in the response function to accommodate particular needs of the separation problem. These points were recognized in the optimization criterion proposed by Berridge [20] but still two major requirements have to be solved. The first is that all criteria produce local optima when peak cross-overs occur and, secondly, there is no way currently available of automatically optimizing the separation of selected peaks from an interfering matrix.

TABLE 1

Evaluation functions for chromatographic quality

Function	Variables	Optimization method	R
Peak separation $P = f/g$			1
Total overlap $\phi = \Sigma \exp(-2R_i)$			1
$P_{inf} = t^{-1} \Sigma_i \log_2 S_i$			1
$CRF = \Sigma_i \ln(P_i)$	G.l.c.	Simplex search	1
$COF = \Sigma_i a_i \ln(R_i/R_d) + b(t_m - t_n)$	Quaternary mobile phase	Simplex design and model	1
$CRF = \Sigma_i \ln(P_i/P_0) + a(t_m - t_i)$	Gradient parameters and flow	Simplex search	1
$CRF = \Sigma_i R_i + n^a - b\lvert T_m - T_n\rvert - c(t_0 - t_1)$	Ternary mobile phase, temperature, flow, pH	Simplex search	2
$CRF = \lvert t_m - t_m^*\rvert/t_m + \lvert R_s - R_s^*\rvert/R_s$	Binary mobile phase	Numerical solution	2
$CRF = t^{-1}\Pi F_i/(g_i + 2n_i)$	Modifier, buffer, pH	Simplex search	2
$CRF = \Sigma_i \ln(f_i/g_i) - 100(M - n)$	Modifier, pH	Simplex search	2
$F_{obj} = \Sigma_i[10(1.5 - R_i)]^2$	Ternary mobile phase	Simplex search	24, 2
$R_s = \Pi R_i$	Ternary mobile phase	Iterative mixture design	2
$r^* = \Pi_{i=0} R_s/[\Sigma_{i=0} R_s/(n-1)]^{n-1}$	Ternary and quaternary mobile phase	Iterative mixture design	2
$CEF = \Sigma_i A_i + (n-1)^{-1} \Sigma_j B_j P_j$			2
$S = \Sigma_{a<b}(t_b - t_a)/(t_a + t_b)$	pH	Window diagram	2
$CRF = \Sigma[(\Sigma f/g) - cf(1) - \lvert cf(2)\rvert]k^{-1} + n^{1.5}$	Ternary mobile phase		3

However, the availability of multi-wavelength and rapid-scanning detectors has brought with it the opportunity to add an additional dimension to the information produced in a chromatographic separation. The use of absorbance ratios [32, 33] and peak deconvolution methods [34—39], perhaps combined into the optimization function [30], should mean that more efficient and more highly automated procedures become available.

Choice of methods

In the period since 1975, when the first applications of chemometrics to liquid chromatography were reported [40, 41], there has been a steady growth of methods for chromatographic optimization. All have their uses in particular situations but none so far emerges as the clear leader because each has its own advantages and disadvantages and some are easier to implement than others. The methods currently available can be classified conveniently according to the amount of information each requires for implementation and the assumptions each makes during the optimization process.

The first method, the "brute-force" approach simply involves a stepwise search of the variable space available. Chemometrics hardly enters into this method, as no detailed thought goes into the selection of the best experimental design. The second classification includes directed search methods. These have grown in popularity and familiarity almost certainly as a direct

consequence of the increasing application of the sequential simplex procedure [42, 43] to all branches of analytical chemistry [44, 45]. As more has become known about the kinetics and thermodynamics of chromatography, it has been possible to formulate equations describing retention behaviour. These form the basis of regression methods, the third classification. Regression methods should be more efficient than searching methods but they do require a substantially increased amount of information both prior to and during the optimization process. The equations formulated may prove not to have been a good description of the retention behaviour, leading to a false conclusion and this is taken into account in the fourth main classification in which the regression equations are gradually refined to take into account the increasing amount of information that is being gained during the optimization procedure.

Mapping

Mapping methods are generally unintelligent and many have not considered the philosophy of chemometrics. For example, it is possible just to conduct a stepwise search of all the available factor space and evaluate each chromatogram manually, or with an optimization criterion, to select the optimum separation. This was one of the first approaches to separation optimization. With the introduction of pre-programmable, automated chromatographs, it became possible to set up a series of conditions which could be used to examine samples. Known as "programmed runs" [46] or, in a more rational sequence, as sequential isocratic step chromatography (SIS) [47] these methods are still as relevant now as when they were first introduced. SIS is a very effective technique for quickly scouting solvent strengths in reversed-phase chromatography. Six separations are done with 20% decrements of organic modifier (acetonitrile is recommended), each experiment covering approximately a k' range of 10.

The major drawback with simple mapping methods is their gross inefficiency. To obtain a detailed map (e.g., 1% increments) of a three-solvent system takes some 5000 experiments. The experimental design is set before any experimentation is conducted and little information is available before all experiments are completed. On the positive side, such schemes are extremely simple to set up and automate. Additionally, it is unnecessary to know anything about the absolute qualities of the separations achieved because the "best" separation can simply be selected by inspection at the end of the sequence. There is, however, a completely automated system (PESOS, Perkin-Elmer solvent optimization system [48]) that uses a chromatographic response function to assess separation quality and takes advantages of computer colour graphics to display a map of optimum separation conditions. Despite these drawbacks of the brute-force methods, a detailed mapping of the factor space remains the only method presently available which can be relied on to provide an optimum separation, if one exists for the variables provided, and not get stuck on a local optimum. In practice, most other methods will compare favourably with this method in considerably fewer experiments.

Directed search methods

While brute-force mapping methods, if conducted in sufficiently small steps, can be relied on to cover the optimum separation conditions, they can be very time-consuming. By applying some degree of feedback to the controlling algorithm, the efficiency of experimentation should increase. This concept of adaptation during the optimization process provided the basis for Optim 1, one of the first commercially available automated optimization h.p.l.c. systems [49, 50], suitable for both isocratic and gradient separations. One of its drawbacks is, however, that it considers essentially a single variable at a time. For h.p.l.c., independence of variables is the exception and, in accordance with good chemometric principles, it is highly desirable to vary all factors simultaneously. Thus the Optim systems use a step-search approach to define an appropriate solvent strength of a binary mobile phase. The size of the step is progressively reduced as the maximum of the optimization criterion is reached. When the optimum binary composition has been located, an equivalent solvent strength for a binary mobile phase using a different selectivity modifier is calculated. The chromatogram with this mobile phase is compared with those obtained previously. If improvement is observed, this binary combination will then be explored until the maximum value of the response function is found. Finally, ternary mobile phases may be used, prepared from simple proportional mixing (usually 1:1) of the two binary phases. This univariate approach fails to capitalize on the selectivity effects available from a full search of the factor space available.

Where the Optim approach may prove to be more successful is in the optimization of gradient separations [50], particularly for reversed-phase h.p.l.c. Here the philosophy is first to locate the starting solvent strength which produces the first detected peaks over a reasonable capacity factor range. The slope of a linear gradient is then modified to produce the best separation as defined by the optimization criterion. This optimum gradient is then compared with a similar gradient using an alternative modifier, its slope also being adjusted until the response function is maximized. Finally, a ternary gradient may be investigated, its composition being calculated in a manner similar to that used in the isocratic optimization. A nice refinement is that if the slope of the gradient is less than a specified minimum, the optimization reverts back to an isocratic sequence. This approach has much in common with the approaches to gradient optimization proposed by Dolan et al. [51] and Jandera and co-workers [52, 53] although it again does not take into account the full selectivity effects available with multi-solvent gradients.

If a directed search method is going to be used successfully in h.p.l.c., then it needs to be one that is able to consider the simultaneous optimization of all the desired variables. The sequential simplex procedure [42—45] is one of the most widely used multifactor optimization algorithms used in analytical chemistry. The advantages of the simplex procedure are that it is ideally suited to the simultaneous optimization of many interdependent variables and that the calculations required are relatively simple. There are many

variants of the basic simplex procedure [54—56], each designed to try to improve the rate of convergence on the optimum but it is the basic and modified simplex procedures (Fig. 2) that are most usually found in optimization of h.p.l.c. separations. A detailed description of the procedure is not appropriate here; suffice it to say that the simplex procedure can be thought of as a hill-climbing method. A geometric figure, the simplex (which is defined by having one more point than the number of variables being optimized), is advanced towards the optimum region by successive replacement of the worst experimental point by its reflection through (usually) the centroid of the remaining points. In the basic procedure, the simplex size is kept constant but, in the modified procedure, the simplex size is expanded towards favourable directions and contracted away from less favourable directions.

For such an attractive method, there must obviously be some disadvantages and these stem mainly from the requirement to use a chromatographic response function to guide the procedure towards the optimum separation. It was the basic simplex procedure that first found use in the systematic optimization of mobile-phase composition in liquid chromatography [41] but, right from the start, it was recognized that the simplex method would always be limited by its inability to distinguish between local and global optima. Early applications of the simplex procedure to h.p.l.c. optimization were

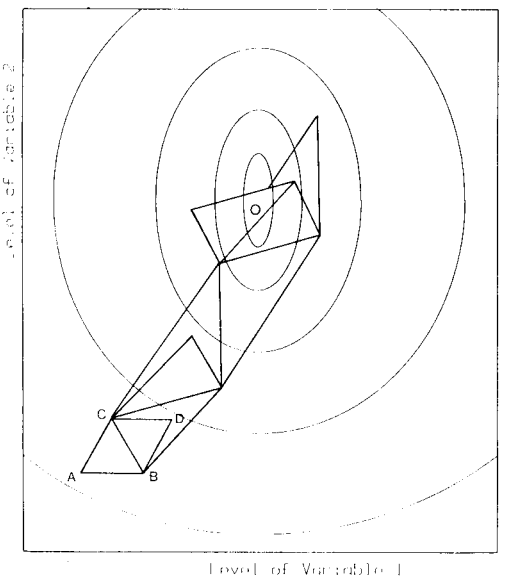

Fig. 2. Modified Simplex procedure. This initial simplex is ABC: point A is rejected and its coordinates reflected through BC to point D. The optimum region is at O.

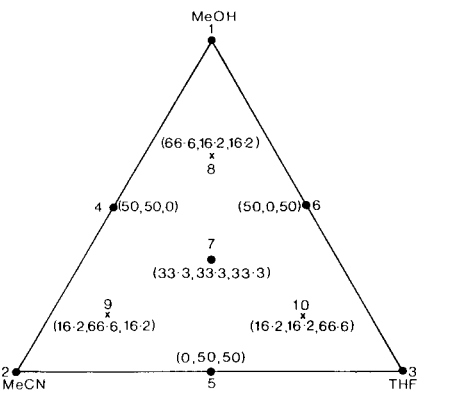

Fig. 3. Simplex lattice design. Experiments 1—7 are used to evaluate polynomial coefficients; experiments 8—10 can be used (optionally) to estimate goodness of fit of model.

restricted, by the hardware available, to manual implementation. Now that microcomputer-controlled chromatographs are available, the simplex procedure has been shown to be well suited to the totally automated optimization of normal [57] and reversed-phase separations, both isocratic and gradient [20, 51—57]. The number of experiments required to locate an optimum depends on the particular situation and the chromatographic mode being used, but is generally in the range 15—30, a considerable improvement on unguided methods. At least two manufacturers offer complete systems (TAMED, Laboratory Data Control, and SUMMIT, Bruker Spectrospin) which use the simplex algorithm for automated separation optimization. Table 2 lists the major applications of the procedure to h.p.l.c. separation development. Because the simplex procedure is a general optimization method, it has also been used for other purposes in h.p.l.c., for example in fitting peak profiles and in peak deconvolution.

Regression methods

In moving from mapping and searching methods to regression methods, there is a dramatic change in the amount of information required both before and during experimentation. The efficient use of regression methods requires that some model be used which approximates chromatographic behaviour and also that each individual component can be identified, or at least recognized, in every chromatogram. Factorial designs are an example of chemometrics at work in the efficient design of an experimental sequence and factorial designs have indeed been used for separation optimization [68—71]. The more frequently used protocol for h.p.l.c. is a simplex statistical design (no connection with the sequential simplex method) sometimes referred to as a mixture design (Fig. 3), in fact a restricted factorial design [72]. This design is particularly appropriate for taking advantage of the "solvent selectivity triangle" classification of modifiers in liquid chromatography. Snyder [73] developed a rational classification of solvents based on their proton-donor, proton-acceptor and dipole/dipole interaction properties. This classification suggests that the maximum range of selectivities in reversed-phase chromatography, for example, will be provided by mixtures of methanol, acetonitrile and tetrahydrofuran with water as the solvent strength adjuster. Because the total composition of any mobile phase must be 100%, this is an ideal situation for a three-variable simplex design which can require as few as seven experiments prior to data analysis. Thus the vertices of the mixture design triangle are set to isoeluotropic (equal solvent strength) binary mobile phases. The sides of the triangle then represent isoeluotropic ternary mixtures with quaternary mixes being in the centre. The starting solvent strengths are defined by an initial gradient run (water/methanol for reversed-phase chromatography). The most successful method of data analysis is to prepare an overlapping resolution map [18] which will define those areas where all peaks are separated with at least a minimum resolution. Should it not be possible to identify all peaks in all chromatograms then it is still possible to use mixture designs by using a chromatographic response function.

TABLE 2

H.p.l.c. optimization using the simplex procedure

Application	Variables	Ref.
Separation of phospholipids[a]	Mobile-phase composition	60
Ion-exchange separation of inorganic cations	Binary mobile-phase composition	41
Separation of PTH-amino acids[a]	4 gradient parameters and flow rate	19
Separation of nucleotides	Buffer concentration, pH, organic modifier level	61
Separation of steroids[a]	Temperature, flow rate, binary gradient shape	62
Separation of alkaloids[a]	Quaternary mobile phase composition and flow rate	25
Separation of dinitrophenyl-hydrazone derivatives[a]	Flow rate, binary gradient parameters	63
Separation of nitroaromatics and flavones[a]	Binary mobile-phase composition	64
Separation of flavones[a]	Binary mobile-phase and temperature	65
Separation of carotenoids[b]	Ternary mobile-phase composition	24
Separation of sulphonamides[b]	Ternary mobile-phase composition	66
Fully automated examples		
Isocratic separation of pyridines[a]	Binary mobile-phase composition and flow rate	20
Gradient separation of anti-oxidants[a]	3 gradient parameters	20
Isocratic separation of substituted aromatics[a]	Ternary mobile-phase composition	20
Isocratic separation of imidazoles and furans[a]	Ternary mobile-phase composition	67
Isocratic separation of aromatics[b]	Ternary mobile-phase composition	20
Ion-pair separations of organic acids[a]	Ternary mobile-phase, (ion-pair reagent, pH), flow rate and temperature	58
Rapid isocratic separation of sulphonamides[a]	Ternary mobile-phase composition	59
Isocratic separation of PTH-amino acids[a]	pH and organic-modifier content	23

[a]Reversed phase. [b]Normal phase.

Neither method will define the global optimum but local optima caused by total peak overlap will be avoided. Many literature examples attest to the value of this approach [74—85] but, whilst it did form the basis for one commercial automated system (the Sentinel system from Du Pont), there is not at present a commercially available system which uses regression methods for fully automated separation optimization.

This method, whilst being one of the more attractive systematic procedures available, does suffer from the drawback that, by defining the three limiting isoeluotropic binary mobile phases, the range of compositions available does

not reflect the full variability attainable with four solvents. While the three binary mixes may give approximately equal retention times, it is actually hoped that, upon mixing, retention times and orders will be substantially altered. Without the freedom to adjust the component governing solvent strength (water for reversed-phase chromatography), the full range of retention times may not be accessible. This limitation has been recognized in modifications of the triangular mixture design approach [3, 86] and a commercial system for off-line optimization was described in 1985 which could accommodate full four-solvent utilization for both isocratic and gradient separations (CHEOPS, Gilson Instruments).

The mixture design approach with a single (cyanopropyl) column and a reduced set of solvents is also used in the simplified scheme proposed by de Smet et al. [87]. Following an examination of 100 basic drugs by a variety of chromatographic systems, it was concluded that a single column, using a cyanopropyl-bonded silica, together with just two mobile phases could be used to separate the majority of basic compounds [88, 89]. The selection of the preferred h.p.l.c. systems was made on the basis of relative discriminating power. Thus, for the selected column, normal-phase separations would use a mobile phase based on n-hexane (or n-heptane)/dichloromethane/acetonitrile/propylamine (50:50:25:0.1) while reversed-phase separations would use acetonitrile/water/propylamine (90:10:0.01). Where solvent-strength adjustments were required, the amount of hexane or water, respectively, would be adjusted. This simplified scheme has been demonstrated to be valid in widely differing circumstances but, for extension to neutral and acidic substances, it has been necessary to extend the experimental design so that it now more closely follows the regression method of Glajch et al. [79], although with a restricted set of variables [87]. The results of de Smet et al. are not, however, in full agreement with proposals of Glajch et al. in which a mixture design scheme is applied with three columns (octadecyl-, phenyl- and cyanopropyl-bonded phases) to select the best combination of column and mobile phase. However, experience suggests that even this approach does not fully encompass the selectivity possibilities readily obtainable and it needs to be extended to include the effects of pH and ion-interaction reagents (Fig. 4) [90], combining simplex lattice and factorial designs, and perhaps adding an iterative method if necessary.

Kirkland and Glajch [76] have also demonstrated that the overlapping resolution mapping approach can be applied to the optimization of reversed-phase gradient separations. To do this successfully requires an understanding of what actually constitutes a gradient separation [91] because both solvent strength and selectivity can be varied during gradient chromatography. The simple rational optimization of multi-solvent gradient separations still, unfortunately, remains elusive.

Another optimization method which involves fitting chromatographic data to a suitable model followed by plotting some measure of the degrees of separation achieved is referred to as "window diagrams". Window diagrams

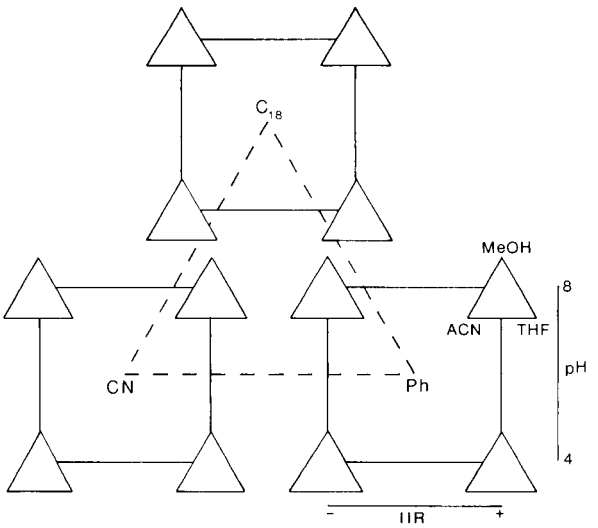

Fig. 4. Experimental design for optimization of type of column support, mobile-phase modifiers, mobile-phase pH and presence of ion-interaction reagent in reversed-phase liquid chromatography.

were first used in gas chromatography for the selection of mixed stationary phases [40] but, being a general optimization method, were later applied to h.p.l.c. Window diagrams are most easily used with a single variable, for example in the optimization of pH [93], and it has been reported that such applications can be fully automated [94]. Two-variable optimizations have been reported [92] but the realization of the window diagram (perhaps better referred to as a minimum resolution or selectivity map) is very much more complex. A great advantage of window diagrams is that it is necessary to conduct only as many experiments as are required to fit the results to the proposed model; this may be as few as four experiments. Additionally, the resulting window diagrams will reveal the global optimum as well as local optima, any one of which might be selected should secondary criteria (e.g., time or a particular retention order) be considered. However, the successful exploitation of window diagrams in h.p.l.c. has been somewhat limited by the difficulties in devising a method for considering more than two variables simultaneously. Table 3 lists the major applications of window diagrams in optimization of h.p.l.c. separations. Window diagrams, as an optimization method, have also been compared with the sequential simplex method [109].

Iterative regression methods

The overlapping resolution mapping method and window diagrams are both efficient in terms of the amount of experimentation needed but both require that the model being fitted is an accurate representation of chromatographic behaviour. Unfortunately, not all solutes can be relied on to

TABLE 3

Window diagram and minimum α plot (map) applications in h.p.l.c.

Application	Variables	Ref.
Separation of benzoic acids[a]	Mobile-phase pH	93, 94
Separation of cinnamic acids[a]	Mobile-phase pH	95
Separations of barbiturates, aromatic bases and phenothiazines[b]	Mobile-phase polarity	96
Separation of acids and bases[a]	pH and ion-pair concentration	97
Separation of aromatic acids[a]	Mobile-phase pH	29
Ion-pair separation of 2,6-disubstituted anilines[a]	Ion-pair and methanol concentrations	98
Ion-pair separation of phencyclidine mixtures[a]	Methanol content	99
Separation of dibasic acids, bases and peptides[a]	pH and methanol content	69, 100
Separation of organic acids[a]	Mobile-phase pH	101
Separation of aromatics[a]	Methanol content	102
Separation of PTH-amino acids[a]	Temperature, acetonitrile content	103
Separation of 9 phenols[a]	THF content	104
Separation of sulphonamides[a]	Ternary mobile-phase compositions	92
Separation of aromatic acids[a]	Temperature, pH, methanol content	105
Ion-chromatography of anions	pH, buffer strength	106
Separation of components in cough/cold formulation[a]	Mixed ion-pair modifiers	107
Separation of complex hydroxyl aromatics[a]	Ternary mobile-phase compositions	108

[a]Reversed phase. [b]Normal phase.

behave in an ideal manner. The iterative regression method [26, 27, 33, 38, 110] avoids this difficulty by revising the regression model during experimentation as more data become available. The initial phases of experimentation mirror those of the regression methods in that a gradient is used to define the required solvent strength and then isoeluotropic solvents are calculated. The mixture design triangle is then, as it were, opened out and laid on its sides to form a linear figure, each part of which describes a ternary mix. Experiments are conducted at each of the binary mobile phases and it is then assumed that retention behaviour can be described by a linear relationship across the ternary compositions. By using a suitable optimization criterion (a resolution product, see Table 1) an optimum composition is then predicted. An experiment is conducted at a position slightly offset from this point to establish the agreement between prediction and reality and, if necessary, the linear relation is modified to two linear portions. The separation quality is then re-calculated across the compositions and the procedure is repeated until the linear segments that are progressively built up sufficiently closely model the real situation. If it should be necessary to extend the procedure to quaternary mobile phases, this can be done by considering triangular planes [111] but the computation times tend to be rather extended.

The combination of a chromatographic response function, a statistical design and an iterative component therefore produces a relatively simple way of optimizing reversed-phase separations. The method is most easily applied to binary and ternary solvent mixes (pH can be included as one of the variables [112] but can be extended to the optimization of tertiary mobile phases [111] and ion-pair separations [113]. A requirement for iterative regression methods is that peaks be identified in successive chromatograms. The same group responsible for the development of the optimization method have also been vigorously exploiting the capabilities of diode-array detection for (initially) manual and fully automated on-line tracking of solutes [110]. The iterative regression method then becomes a very attractive scheme and a commercial system capable of at least semi-automated optimization is expected to become available in the near future.

Expert systems and artificial intelligence

Amongst the most exciting new developments in optimization of h.p.l.c. separations are the Expert Systems [114—116]. As a concept, Expert Systems are deceptively simple, comprising essentially a data base of knowledge and sets of rules to process and act on the knowledge (Fig. 5). It is the selection of the knowledge and the formulation of the rules that is proving difficult and which is occupying most of the current research effort. Nevertheless, very encouraging progress is being made. The dividing line between an Expert System and a chromatography employing "artificial" intelligence may be

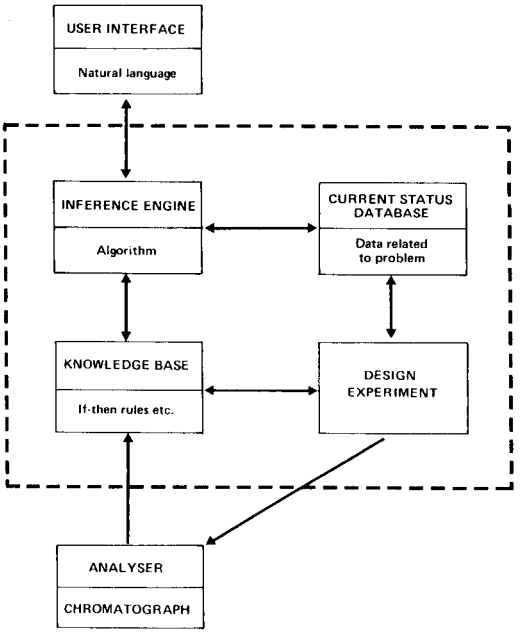

Fig. 5. Representation of Expert System for automated separation development.

somewhat indistinct but the latter more usually utilizes the application of regression equations to minimal experimental data [21, 117—119]. Once again, the design of experimentation becomes all important. It is already possible to combine physicochemical parameters (pK_a, log P etc.) with minimal experimentally derived data to obtain good predictions of chromatographic retention times [118, 120, 121]. Alternatively, "training sets" of compounds can be used to provide data from which retention of new compounds can be predicted. What remains is to derive an a priori method of predicting the all-important resolution that is attainable between solutes. This is still elusive, although progress on pragmatic methods is encouraging [1].

Optimization of post-chromatographic separations

Much current chemometrics research is directed towards the extraction of extra information after the chromatographic separation. Even with a single-channel detection system, it is possible to examine elution profiles for the existence of hidden peaks [57] but the real potential is only just coming to light with the availability of rapid-scanning u.v., fluorescence, infrared and electrochemical detectors [122]. It is beyond the scope of this paper to consider the possibilities of peak deconvolution techniques for resolution enhancement [36—39, 123]. Attractive though deconvolution methods are, they need considerable computing power combined with at least a partial separation or some knowledge of the expected elution profile or components present. As yet, the chromatographic column cannot be completely dispensed with.

Towards fully automated method development

All the schemes discussed, with perhaps the exception of Expert Systems, are suited only to the optimization of separations once fundamental decisions have been made about the selection of chromatographic mode and suitable hardware has been acquired. Expert Systems offer the chance for those fundamental decisions to be taken with a degree of automation and artificial intelligence. Only when such decisions are taken by computer will it be possible to claim automated method development. The execution of the subsequent separations may require further experimental manipulations that are presently outside the capabilities of standard chromatographs. Robotic systems coupled to chromatographs [124—128] are now available which will be able to conduct all the necessary experimentation. The combination of robotics with Expert Systems will surely realize the goal of totally automated method development.

REFERENCES

1 J. P. Bounine, G. Guiochon and H. Colin, J. Chromatogr., 298 (1984) 1.
2 G. Guiochon, in Cs. Horvath (Ed.), High Performance Liquid Chromatography, Advances and Perspectives, Vol. 2, Academic Press, New York, 1980.

3 G. D'Agostino, L. Castagnetta, F. Mitchell and M. J' O'Hare, J. Chromatogr., 338 (1985) 1.
4 H. J. G. Debets, J. Liq. Chromatogr., 8 (1985) 2725.
5 J. C. Berridge, Techniques for the Automated Optimisation of HPLC Separations, Wiley, Chichester, 1985.
6 L. R. Snyder, J. Chromatogr. Sci., 10 (1972) 200.
7 L. R. Snyder, J. Chromatogr. Sci., 10 (1972) 369.
8 J. H. Knox, J. Chromatogr. Sci., 15 (1977) 352.
9 R. E. Kaiser, J. High Res. Chromatogr. Chromatogr. Commun., 2 (1979) 679.
10 R. E. Kaiser and E. Oelrich, Optimization in HPLC, Hüthig, Heidelberg, 1981.
11 I. Halasz and G. Görlitz, Angew. Chem., Int. Ed. Engl., 21 (1982) 213.
12 F. Erni, J. Chromatogr., 282 (1983) 371.
13 I. Atamna, E. Grushka, H. Colin and G. Guiochon, Chromatographia, 19 (1984) 48.
14 R. E. Kaiser, Gas Chromatographie, Geest and Portig, Leipzig, 1960.
15 J. C. Giddings, Anal. Chem., 32 (1960) 1707.
16 D. L. Massart and R. Smits, Anal. Chem., 46 (1974) 283.
17 S. L. Morgan and S. N. Deming, J. Chromatogr., 112 (1975) 267.
18 J. L. Glajch, J. J. Kirkland, K. M. Squire and J. M. Minor, J. Chromatogr., 199 (1980) 57.
19 M. W. Watson and P. W. Carr, Anal. Chem., 51 (1979) 1835.
20 J. C. Berridge, J. Chromatogr., 244 (1982) 1.
21 K. Jinno and K. Kawasaki, J. Chromatogr., 298 (1984) 326.
22 W. Wegscheider, E. P. Lankmayr and K. W. Budna, Chromatographia, 15 (1982) 498.
23 J. H. Nickel and S. N. Deming, Liq. Chromatogr. Mag., 1 (1983) 414.
24 A. S. Kester and R. E. Thompson, J. Chromatogr., 310 (1984) 372.
25 D. L. Dunn and R. E. Thompson, J. Chromatogr., 264 (1983) 264.
26 P. J. Schoenmakers, A. C. J. H. Drouen, H. A. H. Billiet and L. de Galan, Chromatographia, 15 (1982) 688.
27 A. C. J. H. Drouen, H. A. H. Billiet, P. J. Schoenmakers and L. de Galan, Chromatographia, 16 (1982) 48.
28 J. Vajda and L. Leisztner, in H. Kalasz (Ed.), New Approaches in Liquid Chromatography, Analytical Symposium Series, Vol. 16, Elsevier, Amsterdam, 1983, p. 103.
29 P. Jones and C. A. Wellington, J. Chromatogr., 213 (1981) 357.
30 H. J. G. Debets, A. W. Wijnsma, D. A. Doornbos and H. C. Smit, Anal. Chim. Acta, 171 (1985) 33.
31 J. W. Weyland, C. H. P. Bruins, H. J. G. Debets, B. L. Bajema and D. A. Doornbos, Anal. Chim. Acta, 153 (1983) 93.
32 P. C. White, J. Chromatogr., 200 (1980) 271.
33 A. C. J. H. Drouen, H. A. H. Billiet and L. de Galan, Anal. Chem., 56 (1984) 971.
34 J. M. Halket, J. High Res. Chromatogr. Chromatogr. Commun., 2 (1979) 197.
35 M. McCue and E. R. Malinowski, J. Chromatogr. Sci., 21 (1983) 229.
36 A. Lorber, Anal. Chim. Acta, 164 (1984) 293.
37 D. W. Osten and B. R. Kowalski, Anal. Chem., 56 (1984) 991.
38 A. C. J. H. Drouen, H. A. H. Billiet and L. de Galan, Anal. Chem., 57 (1985) 962.
39 B. Vandeginste, R. Essers, T. Bosman and G. Kateman, Anal. Chem., 57 (1985) 971.
40 R. J. Laub and J. H. Purnell, J. Chromatogr., 112 (1975) 71.
41 R. Smits, C. Vanroelen and D. L. Massart, Fresenius Z. Anal. Chem., 273 (1975) 1.
42 S. N. Deming and S. L. Morgan, Anal. Chem., 45 (1973) 278A.
43 D. E. Long, Anal. Chim. Acta, 46 (1969) 193.
44 S. N. Deming and L. R. Parker, Crit. Rev. Anal. Chem., 7 (1978) 187.
45 S. N. Deming and S. L. Morgan, Anal. Chim. Acta, 150 (1983) 183.
46 L. Sybrandt and E. Montoya, Am. Lab., 9(8) (1977) 79.
47 V. V. Berry, J. Chromatogr., 199 (1980) 219.
48 R. D. Conlon, Int. Instrum. Res., Sept. 1985, 74.

49 M. P. T. Bradley and D. Gillen, Spectra-Physics Chromatogr. Rev., 10(2) (1983) 2.
50 M. P. T. Bradley and D. Gillen, Spectra-Physics Chromatogr. Rev., 11(1) (1984) 10.
51 J. W. Dolan, J. R. Gant and L. R. Snyder, J. Chromatogr., 165 (1979) 31.
52 P. Jandera, M. Janderova and J. Churacek, J. Chromatogr., 192 (1980) 19.
53 P. Jandera and J. Churacek, Adv. Chromatogr., 19 (1981) 125.
54 M. W. Routh, P. A. Swartz and M. B. Denton, Anal. Chem., 49 (1977) 1422.
55 P. B. Ryan, R. L. Barr and H. D. Todd, Anal. Chem., 52 (1980) 1460.
56 E. R. Aberg and A. G. T. Gustavsson, Anal. Chim. Acta, 144 (1982) 39.
57 J. C. Berridge, Chromatographia, 16 (1982) 173.
58 J. C. Berridge, Analyst, 109 (1984) 291.
59 J. C. Berridge and E. G. Morrissey, J. Chromatogr., 316 (1984) 69.
60 M. L. Raney and W. C. Purdy, Anal. Chim. Acta, 93 (1977) 211.
61 V. Svoboda, J. Chromatogr., 201 (1980) 241.
62 D. M. Fast, P. H. Culbreth and E. J. Sampson, Clin. Chem., 28 (1982) 444.
63 L. G. Sabate, A. M. Diaz, X. M. Thomas and M. M. Gassiot, J. Chromatogr. Sci., 21 (1983) 439.
64 J. Rafel and J. Cema, Afinidad, 41 (1984) 30.
65 J. Rafel, J. Chromatogr., 282 (1983) 287.
66 M. de Smet, L. Dryon and D. L. Massart, J. Pharm. Belg., 40 (1985) 100.
67 J. C. Berridge, Proc. Anal. Div. Chem. Soc., 19 (1982) 472.
68 R. C. Kong, B. Sachok and S. N. Deming, J. Chromatogr., 199 (1980) 307.
69 M. Otto and W. Wegscheider, J. Chromatogr., 258 (1983) 11.
70 W. Lindberg, E. Johansson and K. Johansson, J. Chromatogr., 211 (1981) 201.
71 M. L. Cotton and G. R. B. Down, J. Chromatogr., 259 (1983) 17.
72 R. D. Snee, Chemtech., 9 (1979) 702.
73 L. R. Snyder, J. Chromatogr. Sci., 16 (1983) 223.
74 R. Leher, Ind. Res. Dev., 25 (1983) 116.
75 P. E. Antle, Chromatographia, 15 (1982) 277.
76 J. J. Kirkland and J. L. Glajch, J. Chromatogr., 255 (1983) 27.
77 J. L. Glajch, J. C. Gluckman, J. G. Charikofsky, J. M. Minor and J. J. Kirkland, J. Chromatogr., 318 (1985) 25.
78 G. M. Landers and J. A. Olsen, J. Chromatogr., 291 (1984) 51.
79 J. L. Glajch, J. J. Kirkland and L. R. Snyder, J. Chromatogr., 238 (1982) 269.
80 I. S. Lurie, A. C. Allen and H. J. Issaq, J. Liq. Chromatogr., 7 (1984) 463.
81 V. W. Wachter, B. Sczepanik, G. Gottmann and G. Cordes, Pharm. Ind., 45 (1983) 1000.
82 A. P. Goldberg, E. L. Nowakaoska, P. E. Antle and L. R. Snyder, J. Chromatogr., 316 (1984) 241.
83 J. E. Haky, A. M. Young, E. A. Domonkos and R. L. Leeds, J. Liq. Chromatogr., 7 (1984) 2127.
84 T. Tsuneyoshi, A. Kawamoto and J. Koezuka, Clin. Chem., 30 (1984) 1889.
85 J. W. Weyland, H. Rolink and D. A. Doornbos, J. Chromatogr., 247 (1982) 221.
86 G. D'Agostino, F. Mitchell, L. Castagnetta and M. J. O'Hare, J. Chromatogr., 305 (1984) 13.
87 M. de Smet, G. Hoogewijs, M. Puttemans and D. L. Massart, Anal. Chem., 56 (1984) 2662.
88 D. L. Massart and G. Hoogewijs, Pure Appl. Chem., 55 (1983) 1861.
89 M. R. Dataevernier, G. Hoogewijs and D. L. Massart, J. Pharm. Biomed. Anal., 1 (1983) 321, 331.
90 J. C. Berridge, A. Wright and A. F. Fell, Paper presented at 3rd Int. Symp. Drug Anal., Brussels, 1986.
91 J. L. Glajch and J. J. Kirkland, Anal. Chem., 54 (1982) 2593.
92 J. W. Weyland, C. H. P. Bruins and D. A. Doornbos, J. Chromatogr. Sci., 22 (1984) 31.
93 S. N. Deming and M. L. H. Turoff, Anal. Chem., 50 (1978) 546.

94 J. H. Nickel and S. N. Deming, Am. Lab., 16 (1984) 69.
95 W. P. Price, R. Edens, D. L. Hendrix and S. N. Deming, Anal. Biochem., 93 (1979) 233.
96 J. P. Thomas, A. Brun and J. P. Bounine, J. Chromatogr., 172 (1979) 107.
97 B. Sachok, R. C. Kong and S. N. Deming, J. Chromatogr., 199 (1980) 317.
98 B. Sachok, J. Stranahan and S. N. Deming, Anal. Chem., 53 (1981) 70.
99 L. A. Jones, R. W. Beaver and T. L. Schmoeger, Anal. Chem., 54 (1982) 182.
100 M. Otto and W. Wegscheider, J. Liq. Chromatogr., 6 (1983) 685.
101 C. Calcagno and M. Forina, Farmaco Ed. Prat., 38 (1983) 49.
102 H. J. Issaq, G. M. Muschik and G. M. Janini, J. Liq. Chromatogr., 6 (1983) 259.
103 C. M. Noyes, J. Chromatogr., 266 (1983) 451.
104 A. J. Hsu, R. J. Laub and S. J. Madden, J. Liq. Chromatogr., 7 (1984) 615.
105 B. Patel, J. H. Purnell and C. A. Wellington, J. High Res. Chromatogr. Chromatogr. Commun., 7 (1984) 375.
106 D. R. Jenke, Anal. Chem., 56 (1984) 85, 2674.
107 S. J. Coustanzo, J. Chromatogr., 314 (1984) 402.
108 H. A. Cooper and R. J. Hurtubise, J. Chromatogr., 328 (1985) 81.
109 F. H. Walters and S. N. Deming, Anal. Chim. Acta, 167 (1983) 361.
110 L. de Galan, Anal. Proc., 22 (1985) 328.
111 A. C. J. H. Drouen, H. A. H. Billiet and L. de Galan, J. Chromatogr., 352 (1986) 127.
112 P. R. Haddad, A. C. J. H. Drouen, H. A. H. Billiet and L. de Galan, J. Chromatogr., 282 (1983) 71.
113 H. A. H. Billiet, A. C. J. H. Drouen and L. de Galan, J. Chromatogr., 316 (1984) 231.
114 E. A. Feigenbaum, in D. Michie (Ed.), Expert Systems in the Microelectronic Age, Edinburgh University Press, Edinburgh, 1979.
115 J. Karnicky, Anal. Chem., 56 (1984) 1312A.
116 G. Musch, M. de Smet and D. L. Massart, J. Chromatogr., 348 (1985) 97.
117 L. Peichang and L. Xiaoming, J. Chromatogr., 292 (1984) 169.
118 K. Jinno and K. Kawasaki, J. Chromatogr., 316 (1984) 1.
119 P. Jandera, J. Chromatogr., 352 (1986) 91, 111.
120 M. N. Hasan and P. C. Jurs, Anal. Chem., 55 (1983) 263.
121 D. E. Martive and R. E. Boehm, J. Phys. Chem., 87 (1983) 1045.
122 A. F. Fell, Anal. Proc., 17 (1980) 512; Lab. Pract., 34(3) (1985) 11.
123 G. T. Carter, R. E. Schiesswohl, H. Burke and R. Young, J. Pharm. Sci., 71 (1982) 971.
124 C. H. Lochmüller, K. R. Lung and K. R. Cousins, Anal. Lett., 18 (1985) 439.
125 R. K. Brown, P. R. Volk and J. N. Little, Polym. Mater. Sci. Eng., 52 (1985) 284.
126 C. H. Lochmüller, K. R. Lung and M. R. Cushman, J. Chromatogr. Sci., 23 (1985) 429.
127 J. Van Antwerp and R. F. Venteicher, in J. R. Strimaitis and G. L. Hawk (Eds.), Advances in Laboratory Automation Robotics, Zymark Corp., Hopkinton, 1985, p. 75.
128 K. J. Halloran and H. M. Franze, in J. R. Strimaitis and G. L. Hawk (Eds.), Advances in Laboratory Automation Robotics, Zymark Corp., Hopkinton, 1985, p. 575.

Analytica Chimica Acta, 191 (1986) 261—273
Elsevier Science Publishers B.V., Amsterdam — Printed in The Netherlands

EVALUATION OF THE NUMBER OF COMPONENTS IN MULTI-COMPONENT LIQUID CHROMATOGRAMS OF PLANT EXTRACTS

FRANCESCO DONDI*, YASSIN DUALE KAHIE[a], GAETANO LODI, MAURIZIO REMELLI, PIERLUIGI RESCHIGLIAN and CORRADO BIGHI

Analytical Chemistry Laboratory, Department of Chemistry, University of Ferrara, Via L. Borsari 46, I-44100 Ferrara (Italy)

(Received 26th May 1986)

SUMMARY

Optimization of the chromatographic separation of flavonoid compounds in camomile extracts by the simplex method and by the Monte Carlo method is described. Evaluation of the number of peaks at unit resolution (R_s = 1) is used as the criterion of separation quality. The Davis-Giddings theory is applied in calculating the number of components and the results are validated by numerical simulations. Peak-purity checks for three identified compounds in commercial sample extracts are reported. Capacity factor patterns for 18 flavonoid and phenolic compounds over an extended range of methanol/aqueous buffer (pH 2.8) mobile phases are described.

Complex mixture separation together with identification and quantitation of selected components are required in many analytical methods for quality control. In the great majority of cases of biological, environmental and industrial interest, the number of components in the sample is unknown and there may be as many as several hundred. In common gradient-elution techniques by reversed-phase high-performance liquid chromatography (h.p.l.c.) with standard columns (5—10 μm), typical available peak capacities [1] are about 50—100. Because uncontrolled peak overlapping always occurs and because part of the chromatographic space may not be completely available for sample separation, complete resolution can be difficult to achieve. The resulting chromatograms of such complex mixtures often have a complex appearance and no quantitative measure of the extent of separation or of individual peak purity is available.

Recently, the many different aspects of such complex analytical problems have been widely studied. Experimental optimization methods of complex analytical procedures have been suggested [2—5], overlapping problems in multicomponent chromatograms have been described theoretically [1, 6—10], and an index of chromatographic performance, the extent of separation

---

[a]Present address: Analytical Chemistry, Faculty of Industrial Chemistry, Somali National University, P.O. Box 1081, Mogadishu, Somalia.

0003-2670/86/$03.50

γ, has been suggested [9]: $\gamma = p/m$, where p is the number of separated peaks and m is the number of single components in the sample mixture. Experimental methods for evaluating component number m have been suggested and checked [6, 7, 9—12].

The best approach to a complex mixture separation will thus be to estimate this component number m, to attain the best extent of separation and to describe the peak overlapping pattern and purity of selected component peaks. The characterization of the flavonoid compound fraction in camomile extracts provides a concrete example of such a multistep analytical procedure.

EXPERIMENTAL

Equipment and reagents

A Spectra-Physics SP-8700 solvent delivery system equipped with a Rheodyne injection valve (10-μl sample loop), a variable-wavelength u.v.-visible detector (200—700 nm) (Chromatronix model 770) and a Mega Series recorder integrator (C. Erba) was used for gradient-elution chromatography of camomile flavonoid extracts. Capacity factors (k') were evaluated on 18 standard phenolic and flavonoid compounds with a Spectra-Physics 3500 liquid chromatograph equipped with a Rheodyne injection valve (10-μl sample loop), a Varian fixed-wavelength detector (254 nm) and a Speedomax recorder (Leeds and Northrup).

The following standard compounds were considered: apigenin, luteolin (flavones); galangin, morin, quercetagetin, quercetin (flavonols); eriodictyol, naringenin (flavanones); apigenin 7-glucoside, luteolin 7-glucoside, quercitrin, rutin, apiin (glycosides); caffeic acid, cinnamic acid, gallic acid (phenolic acids); coumarin, herniarin, umbelliferone (coumarins). The phenolic and flavonoid standards used were Sarsyntex (standard grade); they were dissolved in methanol (HPLC grade) to give 10—100 μg ml^{-1} solutions.

A 30 cm × 3.9 mm, 10-μm C_{18} μBondapak column (Waters) and a 5-μm Bakerbond C_{18} column (Baker) were used. A 2 cm × 3.9 mm precolumn was filled with a 37—50-μm C_{18}/Corasil phase (Waters). Solvents were methanol (HPLC grade; Rudi-Pont) and aqueous 80 mM citric acid/8 mM disodium hydrogenphosphate (pH 2.8) solution (buffer). Water distilled and prepurified by a Norganic system (Millipore) was used. Solvent mixtures were filtered on a 0.2-μm Millipore filter and degassed with pure helium.

Sample handling and gradient-elution conditions

Dry camomile flavonoid extracts (from *Matricaria chamomilla*) were kindly supplied by Indena (Italy). Glycolic extract was a commercial product (Gazan, Italy). These extracts (500 mg) dissolved in 10 ml of water acidified with 1 M HCl to pH 2—3 were extracted with three 30-ml portions of ethyl acetate (reagent grade). The organic phase was extracted with two 50-ml portions of distilled water. The aqueous phase was discarded and the organic phase was filtered on anhydrous sodium sulfate and evaporated to dryness under reduced

pressure (25—30 mmHg, 40—50°C). The residue was redissolved in 2 ml of ethyl acetate/methanol (1:1). The resulting solution, filtered on Sep-Pak C_{18} cartridges (Millipore), was the sample used for flavonoid gradient-elution chromatography.

The conditions for gradient-elution chromatography were as follows: flow rate ranging from 0.25 to 2 ml min^{-1}; gradient elution with two solvents (solvent A, 95% aqueous buffer/5% methanol; solvent B, 95% methanol/5% aqueous buffer); and two linear solvent-strength gradient duration times computed from [13—15]

$$t_1 = (\Phi_2 - \Phi_1)\, t_m\, (S'/b) \text{ and } t_2 = (\Phi_3 - \Phi_2)\, t_m\, (S''/b)$$

where $\Phi_1 = 0.05$, $\Phi_2 = 0.5$, $\Phi_3 = 0.95$, and t_m is the retention time of an unretained compound. The gradient steepness parameter, b, was considered to be equal to 0.2 or 0.1 when, respectively, a 10-μm or 5-μm column packing was used. Optimum S' and S'' values near 10 and 2, respectively, were considered; t_1 and t_2 are, respectively, the gradient duration time in order to go from 100% solvent A to 50%A/50%B and from 50%A/50%B to 100%B.

Measurement of chromatographic features

Capacity factors, $k' = (t_R - t_m)/t_m$, were measured under isocratic conditions at flow rates of 1 ml min^{-1}. The retention time t_R was measured at the maximum of the elution peak and the retention time t_m of an unretained compound at the maximum of the first signal after the injection of an aqueous 1% KNO_3 solution.

Peak capacities, n_c, under specific gradient-elution conditions were evaluated by injecting three standards falling within the initial, middle and final parts of the useful chromatographic space, i.e., that portion of the chromatogram randomly covered by sample peaks. A χ^2 test was used to verify the random character sequence of peaks within the chromatographic space (see below). Because the differences observed did not exceed 5% between these three peaks, a mean width at the baseline, X_0, was computed. Thus the unit resolution convention ($R_s = 1$) was followed [1], and n_c was computed from

$$n_c = (X_f - X_i)/X_0 \qquad (1)$$

where X_f and X_i are, respectively, the last and first peak positions on the useful part of the chromatogram.

The number of peaks p in the chromatogram was evaluated as follows. The baseline is traced between the first and the last part of the chromatogram. Systematic drift was never in fact observed when the three standard compounds used for n_c computation were eluted under any of the gradient-elution conditions tested. The sequence of maxima (A_i) and minima (V_i) was identified and the heights were measured. The critical noise level value was fixed at 0.003 absorbance; all maxima beneath this level were disregarded so as to avoid peak counting arising from uncontrolled bubble signals. The filter (3% of the standard full scale used) thus set automatically, filtered out

any minor component peaks. From the above A_i, V_i sequence, $x = A_i/A_{i+1}$ and $y = A_{i+1}/V_i$ values were computed when $A_i > A_{i+1}$. For $A_{i+1} > A_i$, the reverse of these x, y quantities were considered. Then a critical value of $(A/V)_C$ ratio was calculated from

$$(A/V)_C = 4.89425 - 1.36146x + 0.168858x^2 - 0.0061x^3 \quad (2)$$

This equation is the least-squares fit of the above quantities (A_2/V vs. A_1/A_2) measured on the envelopes of two gaussian peaks of different areas, but resolved at $R_s = 1$. These envelopes were described by Snyder and Saunders [16]. If y was greater than $(A/V)_C$, the peaks i and i + 1 were considered as being resolved at $R_s \geqslant 1$ and the number of peaks (p) was increased by one. If this was not the case, the next maximum A_{i+2} was taken and the minimum between V_i and V_{i+1} was considered in order to compute the new peak/peak and peak/valley values. The $(A/V)_C$ ratio (Eqn. 2) was again calculated for a new peak separation search. The final peak count p was increased by one in order to complete the cycle.

Computations

The contour plot of Fig. 1 was obtained by fitting the set of experimental p data (Y_e points) to the S'/b, S''/b values (X_1, X_2 points, Table 1) by a bivariate least-squares polynomial program PSII [17], by computing a grid of calculated Y_c points on the X_1, X_2 region and then using these as input points to a general-purpose contouring program (GPCP; California Computer Products, Anaheim, CA). All these computations were done on a CDC CY76 (Cineca-Casalecchio, Bologna). The Instrumentune-up program [4] (Apple IIe version) was used for the simplex optimization (Table 2). The program for

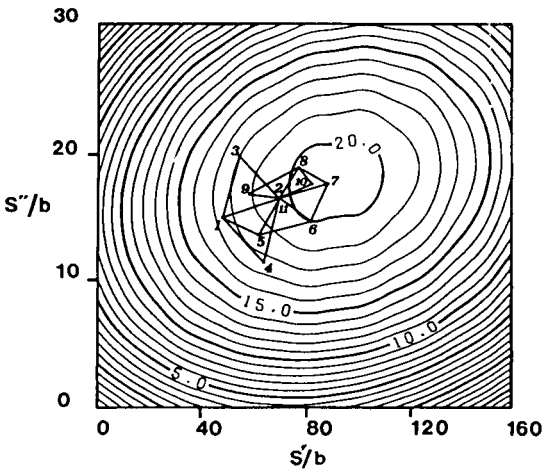

Fig. 1. Peak number contour plot vs. gradient parameters (from the equations for t_1 and t_2) and simplex grid (10-μm C_{18} column).

TABLE 1

Results of random (Monte Carlo) search of the optimum gradient program

Test no.	X_1 S'/b	X_2 S''/b	No. of peaks		
			Y_e (Expected)	Y_c (Calculated)	Residue ($Y_e - Y_c$)
1	50.0	15.0	18	17.5	0.5
2	59.7	15.3	20	18.6	1.4
3	52.6	16.0	18	17.9	0.1
4	52.3	16.2	19	18.9	0.1
5	68.4	16.8	21	19.5	1.5
6	86.9	16.2	21	20.1	0.9
7	75.4	16.1	21	19.8	1.2
8	95.6	17.8	19	20.3	−1.3
9	80.0	25.0	17	17.1	−0.1
10	50.0	20.0	17	17.0	0.0
11	64.0	11.5	17	17.4	−0.4
12	100.0	10.0	17	16.6	0.4
13	140.0	15.0	15	15.6	−0.6
14	110.0	22.0	17	19.1	−2.1
15	150.0	25.0	15	13.4	1.6
16	20.0	20.0	12	11.4	0.6
17	20.0	5.0	6	6.1	−0.1
18	10.0	10.0	7	8.3	−1.3
19	69.5	16.3	20	19.5	0.5
20	55.0	19.8	17	17.7	−0.7
21	64.5	11.5	18	17.5	0.5
22	62.0	13.6	19	18.3	0.7
23	81.0	14.9	19	19.7	−0.7
24	88.0	17.6	19	20.3	−1.3
25	76.8	19.0	19	19.8	−0.8
26	57.5	16.7	18	18.5	−0.5
27	81.0	17.6	20	20.1	−0.1

TABLE 2

Simplex optimization of gradient program

Test no.	S'/b	S''/b	No. of peaks	Test no.	S'/b	S''/b	No. of peaks
1	50.0	15.0	18	7	88.0	17.6	19
2	69.5	16.3	20	8	76.8	19.0	19
3	55.0	19.9	17	9	57.5	16.7	18
4	64.5	11.5	18	10	81.0	17.6	20
5	62.0	13.6	19	11	69.5	16.3	20
6	81.0	14.9	19				

TABLE 3

Peak counts on synthetic chromatograms[a]
(Number of components, m = 50. Peak capacities, n_c = 30—80, $\ln p = \ln \bar{m}_i - \bar{m}_s/n_c$)

No. of noisy minor peaks	$\bar{m}_i$ from intercept	$\bar{m}_s$ from slope
0	46.1 ± 4.1	41.2 ± 7.0
100	44.9 ± 5.3	39.0 ± 6.1
250	58.3 ± 7.0	51.9 ± 6.3
500	45.2 ± 5.8	51.2 ± 6.3

[a]The reported errors are limits of confidence at 95% probability.

computing p as described was run on a Commodore 64. Computer simulation of p evaluations on synthetic chromatograms were done on an Olivetti M24 personal computer. All these programs were written in Basic. The synthetic chromatograms were generated by a procedure similar to that of Giddings and Davis [10]; 50 components were randomly distributed on the chromatogram with 11 peak capacities varying from 30 to 80. The peak heights were randomly distributed between 1 and 10 and a 2—10-fold number of minor components, with random peak position and random peak height between 0 and 0.03, were added to the same chromatogram (Table 3).

The χ^2 test on the random character of peak sequence in the chromatogram was done by dividing the chromatographic space into ten parts, counting the number of peaks in each region and then following the usual procedure for χ^2 calculation [18].

CHOICE OF METHODS

The optimal chromatographic separation requires the highest possible performance index γ, as described by Martin and Guiochon [9]. Chromatographic separation (peak-generating process) can be considered complete when the column produces as many peaks as there are components [9]. The extent of separation is then complete, and γ attains its maximum value of unity, with $p = m$.

A classical experimental optimization procedure [2] was tested first. The four necessary steps [2] are: (1) choice of procedure; (2) choice of utility function (the dependent variable to be optimized); (3) definition of type and range of experimental variables within which to seek the optimal conditions; and (4) definition of the method for identifying the optimum conditions. The obvious choice of procedure is a linear gradient elution. The literature on liquid chromatography of flavonoids [19—26] suggests aqueous acid or buffer (pH 2—3)/ methanol as the mobile phase and a C_{18} stationary phase. To define the gradient elution program (type and range of variables), 18 standard compounds (see Experimental) were examined first. The best utility

function to be optimized was γ or p (which is equivalent because the number of components in the sample, m, is here unknown). This quantity (p under the given resolution) is better than other utility functions such as the CRF or COF [27, 28] for separation of unknown complex mixtures. This is so because no previous knowledge of the number of components is needed to count p and because it is immediately useful in the Davis-Giddings evaluation of component numbers.

The peak number p enables the chromatogram to be divided into distinct peaks or bands, each of which may relate to several components. The $R_s = 1$ criterion used cannot ensure that the Davis-Giddings definition of a "peak" is respected. In the context of the Davis-Giddings model, a peak is "a detected cluster of one or more components, in which the first and the last components in the cluster are separated by components adjacent to the cluster by a resolution greater than or equal to $R_s = 1$ and in which each member of the cluster is separated from adjacent members of the cluster by a resolution less than $R_s = 1$" [6, 7]. This is a theoretical concept which in practice can never be met completely because only the maxima which appear on a peak or band can be acted upon. Significant errors can arise [7, 10, 12]. The bias introduced in counting p was shown to be unacceptable under bad separation conditions [10, 12], i.e., for very low γ values; away from the highest γ values, this bias has great weight while it is less important around a good optimum.

There are many possibilities in choosing the number of experimental variables in gradient analysis [13—15]. In a multi-stage solvent program, with different slopes and different intermediate solvent-composition points, both slopes and intermediate points can be chosen as independent variables, but the problem can then become very complicated. Accordingly, a two-step gradient with fixed starting, intermediate and final points was chosen. The problem of optimization then involves a two-dimensional search on a (X_1, X_2) plane, with $X_1 = S'/b$ and $X_2 = S''/b$ as the independent experimental variables. Each (X_1, X_2) point defines a particular gradient program (from the definitions of t_1 and t_2). The optimum search field ranged between 0 and about three times the best trial values drawn from the preliminary study.

The optimization methods tested were a simplex method [3, 4] and a Monte Carlo (random) sampling method of experimental variables. With the Monte Carlo data, a least-squares contour map was traced. The accuracy of the simplex displacements towards the true maximum was thus checked for future, less expensive, applications of this method to closely related problems.

Once the optimum experimental conditons had been estimated, evaluation of the number of components by the Davis-Giddings extrapolation procedure was considered. The two fundamental approaches for this purpose use the same basic equation [1]:

$$\ln p = \ln \bar{m} - \bar{m}/n_c \qquad (3)$$

The quantity $\bar{m}$ is the statistical analog of the component number m. For

large m values, the relative differences between m and $\bar{m}$ become small and the evaluation of m through $\bar{m}$ is increasingly reliable. The first procedure is based on the production of many chromatographic separations with different peak capacities n_c, which can be obtained by changing the column efficiency (e.g., changing the flow rate, column length or column packing dimensions [15]). This may be termed the multi-chromatogram procedure. A second (single-chromatogram) procedure was recently suggested [10]. Briefly, this consists of measuring the number of times that adjacent maxima interdistances exceed a fixed distance X_0 which, in turn, defines n_c according to Eqn. 1. Because there is a free choice in the X_0 value, many peak counts under different n_c conditions are possible on the same chromatogram. This single-chromatogram procedure was validated by Davis and Giddings by simulation and variance analysis [10]; it appears to be unbiassed under normal component peak amplitude and noise conditions, provided that the component number exceeds 100. There was some doubt about the suitability of this procedure for the present study in which the number of components was probably much less than 100. A third (few-chromatogram) procedure was thus devised; three (instead of about ten) chromatograms were used twice, i.e., the peaks were counted at $R_s = 1$ and then the number of maxima were also counted. This last quantity corresponds to a peak count on a two-fold peak capacity n_c, with $R_s = 0.5$ [1, 10, 11].

All extrapolation methods for component numbers suffer from sources of uncontrolled error stemming from the incompleteness of the statistical peak-overlapping theory [1], and from its present inability to take into account important chromatogram attributes such as the differences in the amplitude of component peaks [6—12]. For this reason, the results of the Davis-Giddings evaluation of component number m were validated. This was done by a numerical simulation procedure for evaluating component number on a synthetic chromatogram which was fairly similar in component number, noise and component amplitude distribution to the experimental chromatogram. This procedure is analogous to that followed by other authors [7, 10—12], and was necessary because the earlier cases involved $m > 100$ whereas $m \approx 50$ in the present work.

The final step was the identification of some components of the flavonoid extracts. Four mixtures with 3—4 standard components were separately injected under the same gradient conditions and the peak maxima were compared. Because retention times may shift slightly as a result of slight changes in experimental conditions, dubious cases were checked by adding standard mixtures to the sample and noting the increments of peak heights. A spectral identification was also attempted by running the analysis on both the sample mixture and a standard mixture and using the detector at wavelengths of 260, 280, 340 and 380 nm. The absorbance vs. wavelength plot was used to check peak purity and confirm the identity of selected standard compounds.

These experiments were done in order to evaluate the relevance of peak overlapping. Sure identification would require the use of selective detectors and/or different chromatographic systems for all the considered compounds.

RESULTS AND DISCUSSION

The log k' plots vs. Φ_B% (methanol, v/v%, in buffer) for selected compounds (Fig. 2) show two different behaviours. Some compounds exhibit k' values between 1 and 10 with under 50% methanol concentration, with a slope of the log k' vs. Φ_B% plot of 0.1 (luteolin 7-glucoside, quercitrin, apigenin 7-glucoside and morin). The solvent strength, S [13—15] is 10 in this case. Similar behaviour is exhibited by quercetin, naringenin, eriodictyol, rutin, apiin, umbelliferone, coumarin, herniarin and caffeic, gallic and cinnamic acids. Other compounds exhibit k' values between 1 and 10 above 50% methanol. The slope of the log k' vs. Φ_B% plot is lower (0.02) and the solvent strength is 2 in these cases (e.g., luteolin, apigenin in Fig. 2 and also galangin and quercetagetin). In order to elute all these compounds with optimum resolution [13—15], the steepness of the gradient must differ above and below 50% methanol. Thus a two-step gradient was chosen (see definitions of t_1 and t_2) and the range of action was between 5% and 50% and 95% methanol (see Experimental). The search for optimization was in the range $0 < S' < 30$ and $0 < S'' < 6$.

Complete experimental optimization was done with the 10-μm C_{18} column. The results of the Monte Carlo search and bivariate least-squares fitting are reported in Table 1. Figure 1 shows the least-squares contour plot obtained from the data in Table 1. The results of the simplex search are reported in Table 2 and the simplex grid is superimposed on the contour plot of Fig. 1. The contour plot shows a well behaved and extensive maximum region around the (90, 18) point, which is slightly displaced with respect to the original trial values (50, 15), and with respect to the final simplex points (70, 16). However, the difference between the simplex and the true maximum is not significant (about 1 peak), and the simplex method is therefore a strong contender for quick optimization of separations of closely related sample mixtures. The optimum gradient program can easily be computed: $t_1 = 41.5\ t_m$, $t_2 = 8.1\ t_m$ for a 10-μm C_{18} column; these quantities must be doubled for a 5-μm C_{18} column.

Figure 3 shows the results of the Davis-Giddings multi-chromatogram procedure for two flavonoid extracts. Figure 4 shows the results of the few-chromatogram procedure. For all these chromatograms, the χ^2 test on the random character of the peak sequence was respected, except for one point in Fig. 3A. It can be observed that the m values drawn from both slope and intercept are practically equal and the Davis-Giddings equation is respected. Importantly, the multi- and few-chromatogram procedures give the same results, but this finding does not necessarily mean that the measured quantity $\bar{m}$ is an unbiased estimate of the true component number, because of insufficient data. The fact that the present peak counting follows an equation similar to Eqn. 3 simply means that the counting follows Poisson-type statistics [10, 11].

Table 3 summarizes the validation results of the multi-chromatogram procedure for synthetic clean and noisy chromatograms. The calculation of

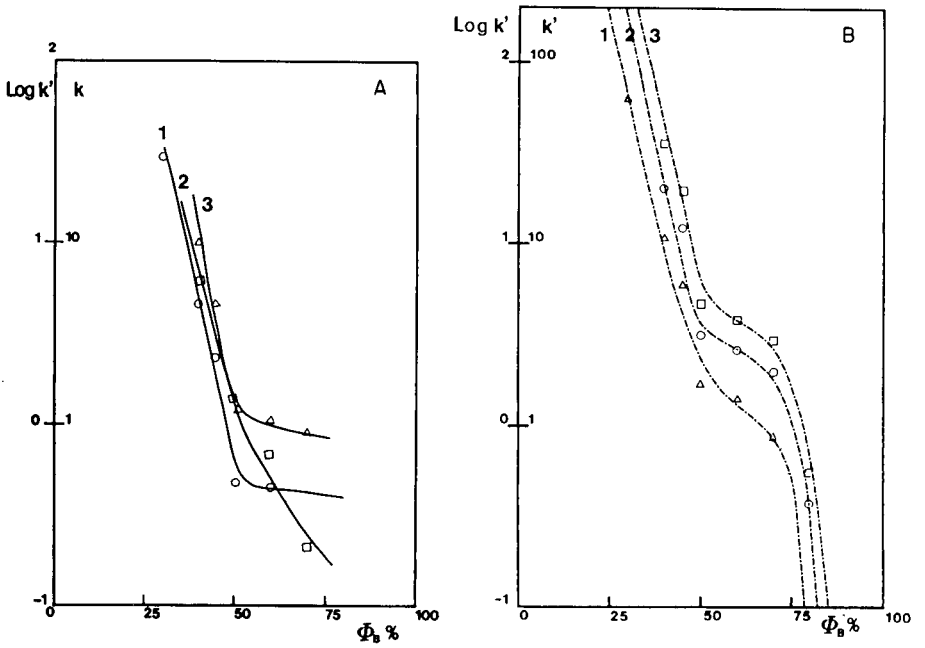

Fig. 2. Retention vs. methanol (v/v%; Φ_B%) in the mobile phase. For *A*: (1) luteolin 7-glucoside; (2) quercitrin; (3) apigenin 7-glucoside. For B: (1) morin; (2) luteolin; (3) apigenin.

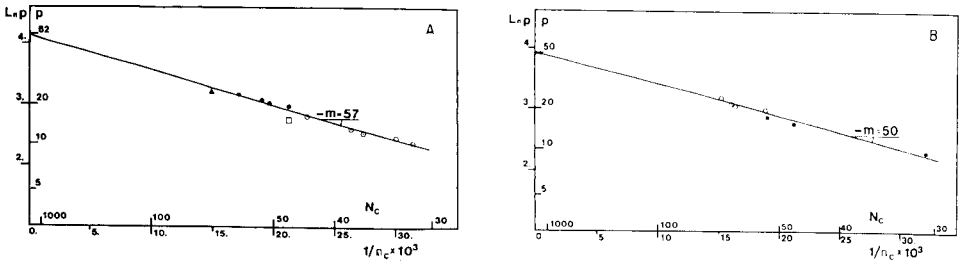

Fig. 3. Davis-Giddings plots for the multi-chromatogram procedure. (A) Gazan sample with a 10-μm C_{18} column: (⊙) non-optimized gradients; (●) optimized gradients; (□) non-optimized gradient which did not pass the χ^2 test; (▲) two columns in series. (B) Indena sample with optimized gradients and different flow rates: (●) 10-μm C_{18} column; (⊙) 5-μm C_{18} column.

the number of components can be biassed by up to ±20%, which is of the same order of magnitude as that observed elsewhere [10]. Figure 5 shows the frequency of peak heights on the experimental chromatograms. It can be seen that this frequency is exponential in type, as observed for similar plant extracts [8], and the lower peaks appear about five times more frequently

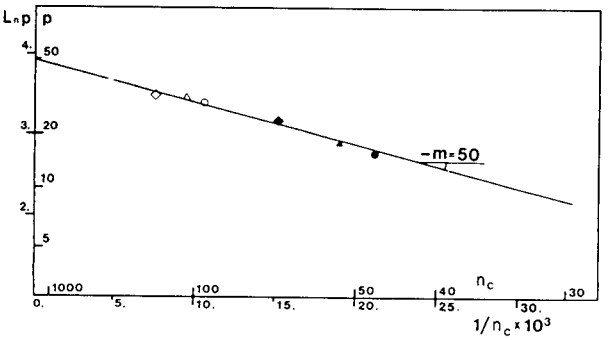

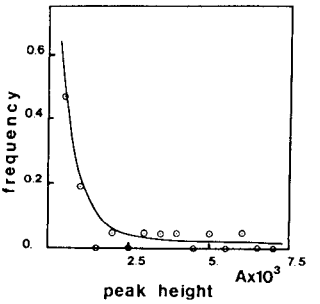

Fig. 4. Davis-Giddings plot based on the few-chromatogram procedure for the Indena sample on a 5-μm C_{18} column: (◇△○) number of maxima (R_s = 0.5); (◆▲●) number of peaks (R_s = 1).

Fig. 5. Peak heights vs. frequency for the Indena sample.

than higher ones. Even if these peak-height statistics differ somewhat from the single-component amplitude statistics [8, 10, 11], the simulated cases can be considered as significant and the evaluation of component number on real samples (50—60) can be considered as a reasonable estimate of the real major component number for the sample.

An example of chromatographic separation attained under optimum conditions is presented in Fig. 6. The values of the chromatographic parameters, n_c = 75; p = 25; m = 50, $\gamma = p/m$ = 0.5; $\alpha = m/n_c$ = 0.67, express the type and validity of the separation.

The results of a peak-purity check on three selected standard compounds are reported in Fig. 7. Only quercetagetin is confirmed as a pure peak. Caffeic acid and quercitrin, the presence of which was confirmed from retention times, are either multiplet peaks or different compounds.

By using the statistical peak-overlapping theory [1], it is possible to evaluate some statistical features of the separation presented in Fig. 6. The expected numbers of singlet (i.e., pure), doublet and triplet peaks are 12, 6 and 3, respectively. Among the 25 peaks, there is a 30% probability that one randomly chosen will be a singlet. Thus the finding that only one (quercetagetin) of the three examined cases (Fig. 7) was a pure peak is coherent with the theory.

Finally, it may be noted that, with respect to the available peak capacity (75), the number of expected singlet peaks (12), was very close (0.17) to the maximum (0.18) predicted by the theory. However, in order to increase the extent of separation more significantly (e.g., from 0.5 to 0.75), a much greater peak capacity (about 180) must be used (see Eqn. 18 [1]). In this case, the number of expected singlet peaks would only be 18 (over 50 components) and the separation would still not be complete. Thus total success

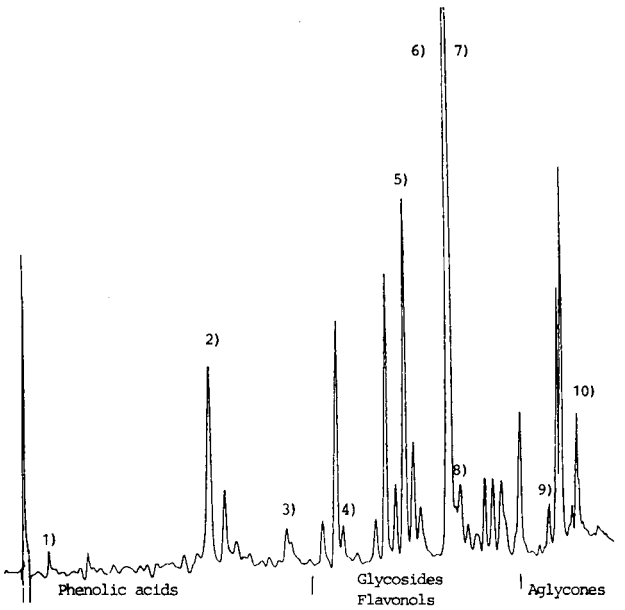

Fig. 6. Example of optimum separation on a 5-μm C_{18} column. Identified compounds: (1) gallic acid; (2) caffeic acid; (3) umbelliferone; (4) quercetagetin; (5) luteolin 7-Gl; (6) apigenin 7-Gl; (7) herniarin; (8) quercitrin; (9) luteolin; (10) apigenin.

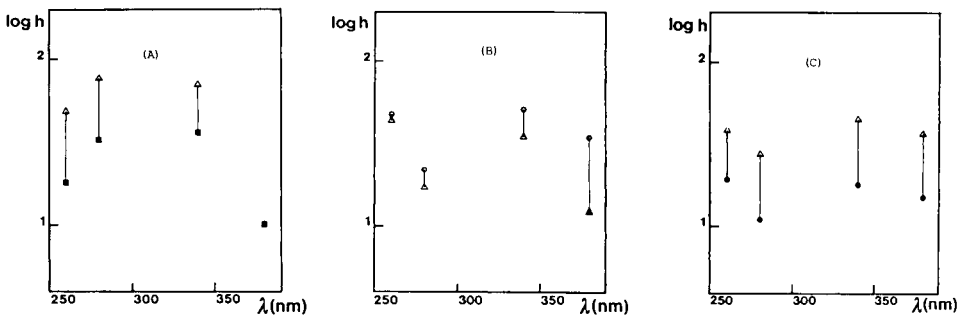

Fig. 7. Peak-purity check. Comparison between identified peak height in the sample chromatogram (lower points) and standard compound peak height (upper points) vs. detector wavelength. (A) Caffeic acid; (B) quercitrin; (C) quercetagetin.

in the characterization of complex mixtures of natural products (component number determination, identification and quantitation) cannot be achieved only by increasing column efficiency; efficient gradient programs and different chromatographic systems are also needed. The use of more selective detectors and advanced numerical handling of the data are also important.

This work was supported by the Italian Education Department (MPI), Italian Foreign Co-operation Department (MAE) and Somali National University.

REFERENCES

1 J. M. Davis and J. C. Giddings, Anal. Chem., 55 (1983) 418.
2 D. L. Massart, A. Dijkstra, L. Kaufman, Evaluation and Optimization of Laboratory Methods and Analytical Procedures, Elsevier, Amsterdam, 1978, Chap. 14.2.
3 S. M. Deming, J. G. Bower and K. D. Bower, in J. C. Giddings, E. Grushka, J. Cazes and P. R. Brovn (Eds.), Advan. Chromatogr., Vol. 24, M. Dekker, 1980, p. 35.
4 S. L. Morgan, S. N. Deming, INSTRUMENTUNE-up Program, Elsevier Scientific Software, Amsterdam, 1984.
5 J. C. Berridge, Techniques for Automated Optimization of HPLC Separations, Wiley, Chichester, 1985.
6 J. C. Giddings, J. M. Davis and M. R. Schure, in S. Ahuja (Ed.), ACS Symposium on Ultra-High Resolution Chromatography, American Chemical Society, Washington, DC, 1983.
7 J. C. Giddings and J. M. Davis, J. Chromatogr., 289 (1984) 277.
8 L. J. Nagels, W. L. Creten and P. M. Vanpeperstraete, Anal. Chem., 55 (1983) 216.
9 M. Martin and G. Guiochon, Anal. Chem., 57 (1985) 289.
10 J. C. Giddings and J. M. Davis, Anal. Chem., 57 (1985) 2168.
11 J. M. Davis and J. C. Giddings, Anal. Chem., 57 (1985) 2178.
12 D. P. Herman, M. F. Gonnord and G. Guiochon, Anal. Chem., 56 (1984) 995.
13 L. R. Snyder, J. W. Dolan and J. R. Gant, J. Chromatogr., 165 (1979) 3.
14 J. W. Dolan, J. R. Gant and L. R. Snyder, J. Chromatogr., 165 (1979) 31.
15 L. R. Snyder, J. J. Kirkland, Introduction to Modern Liquid Chromatography, 2nd eqn., Wiley, New York, 1979, Chap. 2.
16 L. R. Snyder and D. L. Saunders, J. Chromatogr. Sci., 7 (1969) 195.
17 T. Pomentale "PSII, Bivariate Least Square Polynomials Program", Data Handling Division, CERN, Geneva, 1980.
18 H. Cramer, Mathematical Methods of Statistics, Princeton University Press, Princeton, NJ, 1946, p. 416.
19 J. B. Harborne and T. J. Mabry, The Flavonoids: Advances in Research, Chapman & Hall, London, 1982.
20 R. Schuster, Chromatographia, 13 (1980) 379.
21 G. J. Niemann, Z. Naturforsch., Teil C, 32 (1977) 1015; 35 (1980) 514.
22 N. W. Preston and C. F. Timberlake, J. Chromatogr., 214 (1981) 222.
23 J. B. Harborne and M. Boardley, J. Chromatogr., 299 (1984) 377.
24 J. Sachse, J. Chromatogr., 298 (1984) 175.
25 L. J. Nagels and W. L. Creten, Anal. Chim. Acta, 169 (1985) 299.
26 L. J. Nagels, W. L. Creten and L. Van Haverbeke, Anal. Chim. Acta, 173 (1985) 185.
27 J. L. Glajch, J. J. Kirkland and M. R. Squire, J. Chromatogr., 299 (1980) 57.
28 M. W. Watson, P. W. Carr, Anal. Chem., 51 (1979) 1835.

Analytica Chimica Acta, 191 (1986) 275—281
Elsevier Science Publishers B.V., Amsterdam — Printed in The Netherlands

COMPUTER-AIDED EVALUATION OF LIQUID-CHROMATOGRAPHIC PROFILES FOR ANTHOCYANINS IN *Vaccinium myrtillus* FRUITS

E. M. MARTINELLI*, A. BAJ and E. BOMBARDELLI

Inverni della Beffa S.p.A., Research and Development Laboratories, Via Ripamonti 99, 20141 Milan (Italy)

(Received 13th May 1986)

SUMMARY

The anthocyanin constituents of thirty samples of *Vaccinium myrtillus* fruits of various origin were examined by high-performance liquid chromatography. The data, characterized by 15 peaks for each chromatogram, were subjected to principal component analysis in order to reveal differences in the chromatograms. The vector space generated by eigenvector projection produced a clear separation between a group composed of Norwegian and Swedish berries and a group of berries of Italian or Romanian origin. Cyanidin glycosides are slightly better represented in all the samples of the first group, while delphinidin glycosides are better represented in the latter.

Vaccinium myrtillus is the well known shrub bilberry, which is widespread in hilly areas. The berries are a rich source of anthocyanins, which are the active components in the purified extracts used in the therapy of various microcirculation diseases. Fifteen anthocyanins (i.e., 3-*O*-arabinosides, 3-*O*-glucosides and 3-*O*-galactosides of cyanidin, delphinidin, peonidin, petunidin and malvidin), the structures of which are shown in Table 1, constitute the pigment of bilberry. A high-performance liquid chromatographic (h.p.l.c.) method for determining the anthocyanins in *V. myrtillus* was recently described [1], and has been used extensively here for the routine analysis of berries, purified extracts and medicinal preparations.

The present paper deals with the possibility of characterizing *V. myrtillus* extracts of fruits of different origin through the examination of their h.p.l.c. profiles. Information retrieval from very similar patterns such as these liquid chromatograms is very difficult, but suitable computerized handling of the data enables subtle differences in the h.p.l.c. profiles to be detected and related to the origin of the plants.

EXPERIMENTAL

Reagents, chemicals and instrumentation

The *V. myrtillus* fruits were obtained from Indena (Milan). Acetonitrile and methanol were h.p.l.c. grade (Merck). Formic acid (98% purity) and

0003-2670/86/$03.50

TABLE 1

Structures of *V. myrtillus* anthocyanins

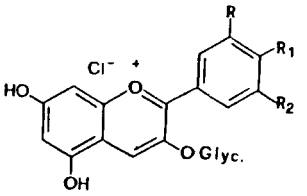

(Glyc = arabinoside, glucoside or galactoside)

Compound	R	R_1	R_2
Delphinidin 3-*O*-glycoside	OH	OH	OH
Cyanidin 3-*O*-glycoside	OH	OH	H
Petunidin 3-*O*-glycoside	OH	OH	OCH_3
Peonidin 3-*O*-glycoside	OCH_3	OH	H
Malvidin 3-*O*-glycoside	OCH_3	OH	OCH_3

hydrochloric acid (37% in water) were from Eurobase (Milan).

The instrumentation included two Model 510 solvent delivery systems, a Model 680 solvent programmer (Water Associates), a Model 7010 injector (Rheodyne), a Model LC-55 variable-wavelength ultraviolet-visible absorbance detector (Perkin-Elmer) and a Model 3390A reporting integrator (Hewlett-Packard).

Sample solutions and h.p.l.c. procedure

About 30 g of frozen *V. myrtillus* fruits was shaken for 5 h with 100 ml of methanol. The extraction was repeated four times. The combined extracts (500 ml) were concentrated to low volume at reduced pressure with the bath temperature not exceeding 50°C. The residue was diluted to 100 ml with methanol containing 2% (v/v) of concentrated hydrochloric acid. An aliquot (5 ml) was transferred to a 25-ml volumetric flask and diluted to volume with a mixture of water and phosphoric acid (90:10 v/v). Aliquots of 20 μl were injected.

Separation of the fifteen anthocyanins was achieved with a column (22 cm × 4.6 mm i.d.) packed with Aquapore RP-300, 10 μm (Brownlee Labs., Santa Clara, CA) connected with a guard column (3 cm × 2.1 mm i.d.) packed with the same material. The mobile phase was a mixture of solvent A (water/formic acid, 90:10, v/v) and solvent B (methanol/acetonitrile/water/formic acid, 22.5:22.5:45:10, v/v). Solvent B was increased from 0 to 30% in 40 min in a concave gradient (curve 7 of Waters Model 680 solvent programmer). The flow rate was 1 ml min^{-1} and the monitoring wavelength was 535 nm.

Data handling

Eigenanalysis [2—4] was done with a 64K Apple-II personal computer equipped with a dual floppy-disk drive and Watanabe Wx4671 plotter. The software, written in BASIC Applesoft, was implemented in five subsequent procedures: preprocessing of stored data matrix (normalization, autoscaling, data about the mean), covariance matrix calculation, eigenvalues and eigenvectors evaluation through the Jacobi rotation method [5], and projection on principal selected eigenvectors.

RESULTS AND DISCUSSION

Thirty samples of *V. myrtillus* fruits of different origin (mainly from Italy and Sweden, some from Norway, Romania, France and Poland) were examined by h.p.l.c. The chosen detector wavelength (535 nm) enabled only the anthocyanin fraction to be visualized in the h.p.l.c. profiles; the anthocyanins were represented by fifteen well-separated peaks which were attributed on the basis of a previous study [1].

Some typical chromatograms are reported in Fig. 1. Visual inspection of the h.p.l.c. profiles did not allow differences attributable to the origin of the fruits to be clearly distinguished with any certainty. For this reason, the capability of the eigenvector projection method [3, 4] was tested in an attempt to reveal a possible correlation between the origin of the fruits and subtle, significant differences of the anthocyanin composition. For this purpose, each chromatogram was converted to a quantitative data vector by measuring the area of the fifteen peaks. Preprocessing of the data involved only normalization to a sum of 100 over all 15 peaks; no other information about the class assignment of the sample was used to enhance possible class separation at the data-preprocessing stage [4]. To ascertain the reproducibility of the data vectors, replicated analyses of the same lot of *V. myrtillus* fruits were done on different days. The results are reported in Table 2.

Thirty *V. myrtillus* samples gave a 30 × 15 data matrix, which was initially processed to obtain a data matrix centred about the mean according to the formula $x'_{ij} = x_{ij} - \mu_i$, where x'_{ij} is the centred ith component (peak) of the jth object (the chromatogram) and μ_i the mean.

Through the calculated covariance matrix, a set of variables (eigenvectors or factors) is produced by the computer program, and it is possible to consider fewer than those contained in the original set (15 peaks) as principal components with a minimal loss of information. The eigenvectors describe the factor space and the associated eigenvalues the importance in terms of variance (Table 3). When the points of the 30-sample data set are projected down on the plane conserving most of the variance, the eigenvector projection corresponding to the first two eigenvalues is obtained (Fig. 2). The eigenvector score plot of eigenvector 1 vs. eigenvector 2 shows that eigenvector 1 clearly separates berries from Norway and Sweden (North regions) from those of Italy, Poland and Romania. The berries from France (unfor-

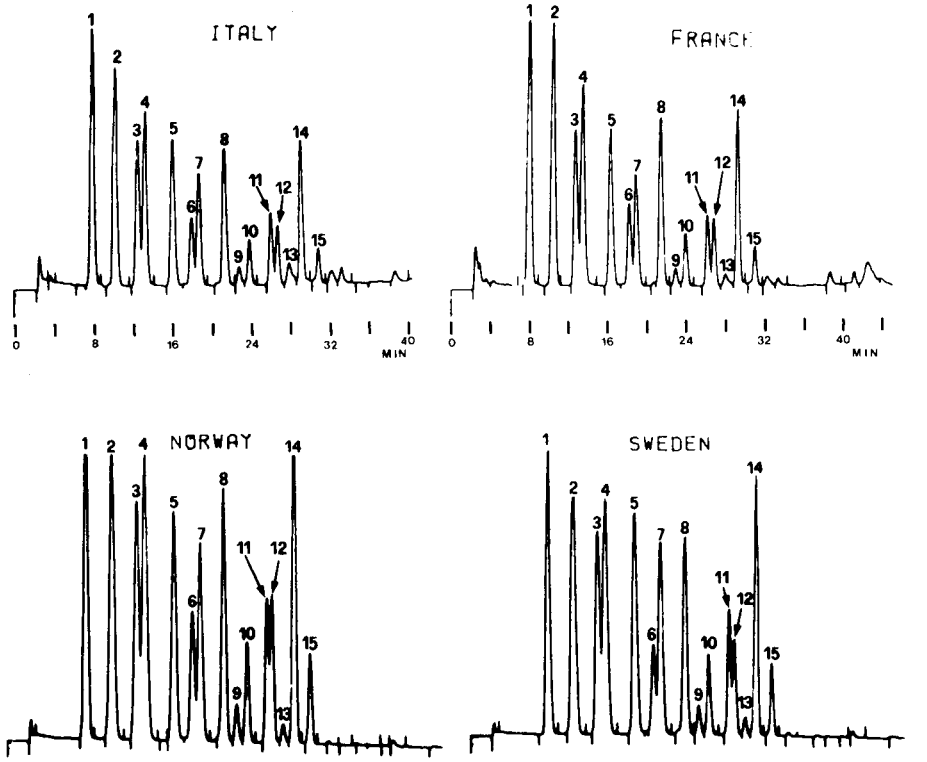

Fig. 1. Typical liquid chromatograms of *V. myrtillus* fruits of different origin. Peaks (1) delphinidin 3-*O*-galactoside; (2) delphinidin 3-*O*-glucoside; (3) cyanidin 3-*O*-galactoside; (4) delphinidin 3-*O*-arabinoside; (5) cyanidin 3-*O*-glucoside; (6) petunidin 3-*O*-galactoside; (7) cyanidin 3-*O*-arabinoside; (8) petunidin 3-*O*-glucoside; (9) peonidin 3-*O*-galactoside; (10) petunidin 3-*O*-arabinoside; (11) peonidin 3-*O*-glucoside; (12) malvidin 3-*O*-galactoside; (13) peonidin 3-*O*-arabinoside; (14) malvidin 3-*O*-glucoside; (15) malvidin 3-*O*-arabinoside.

TABLE 2

Analytical precision of normalized peak areas obtained on the same lot of *V. myrtillus* fruits of French origin

Peak no.	$\bar{x} \pm$ SD ($n = 6$)	RSD (%)	Peak no.	$\bar{x} \pm$ SD ($n = 6$)	RSD (%)
1	13.79 ± 0.0041	0.03	9	1.03 ± 0.0004	0.04
2	13.38 ± 0.0023	0.02	10	2.85 ± 0.0005	0.02
3	9.08 ± 0.0016	0.02	11	4.06 ± 0.0009	0.02
4	11.67 ± 0.0024	0.02	12	3.41 ± 0.0007	0.02
5	9.58 ± 0.0011	0.01	13	1.04 ± 0.0032	0.31
6	4.32 ± 0.0007	0.02	14	8.17 ± 0.0024	0.03
7	7.29 ± 0.0013	0.02	15	2.08 ± 0.0012	0.06
8	8.73 ± 0.0018	0.02			

TABLE 3

Eigenvector analysis variances of h.p.l.c. profiles of *V. myrtillus*

Eigenvector	Eigenvalue		Variance (%)	
	Ce[a]	Au[b]	Ce[a]	Au[b]
1	271.7	192.2	63.0	44.2
2	69.9	85.3	16.2	19.6
3	43.9	65.0	10.2	14.9
Others	45.6	92.5	10.6	21.3

[a]Data centred about the mean. [b]Autoscaled data.

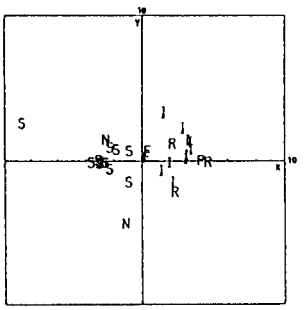

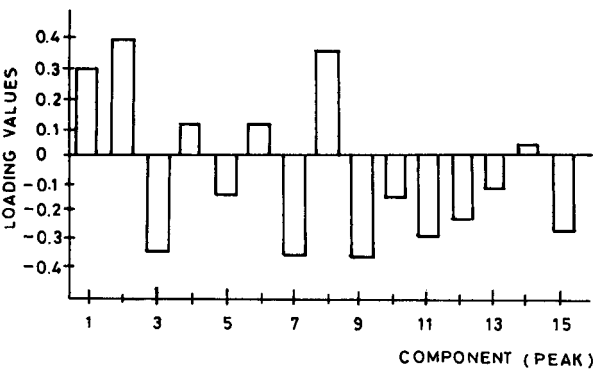

Fig. 2. Eigenvector projection of *V. myrtillus* profiles: (x) Eigenvector 1; (y) eigenvector 2 (data centred about the mean). (I) Italian; (R) Romanian; (P) Polish; (F) French; (S) Swedish; (N) Norwegian.

Fig. 3. Loadings of eigenvector 1 (data centred about the mean).

tunately, only two supplies were available) both lie in an intermediate zone. From observation of the loadings for eigenvector 1, visualized in Fig. 3, the major determinants of the differences of the anthocyanin composition of the berries are the delphinidin glycosides (measured by the associated loadings 1, 2, 4) which are relatively more abundant (as percent area) in the berries from the Italian, Romanian and Polish regions. In contrast, cyanidin and peonidin glycosides (loadings 3, 5, 7 and 9, 11, 13, respectively) are relatively more abundant constituents in Swedish and Norwegian berries. This can also be inferred from examination of the data reported in Table 4.

It is important to note that the above results were obtained with data which had not been scaled at the preprocessing level to the same variance; thus large peaks tend to dominate the patterns. When the data are scaled [4], about the same importance is given to all peaks irrespective of their intensity. Accordingly, the starting data matrix was subjected to auto-

TABLE 4

H.p.l.c. of *V. myrtillus* anthocyanins from berries of different origin

Peak no.	Peak area (%)[a]		Peak no.	Peak area (%)[a]	
	I, R, P	N, S		I, R, P	N, S
1	14.11 ± 0.60	12.39 ± 0.71	9	0.86 ± 0.10	1.22 ± 0.20
2	15.21 ± 0.78	11.85 ± 1.52	10	2.92 ± 0.17	2.98 ± 0.28
3	7.56 ± 0.69	10.12 ± 1.11	11	3.30 ± 0.31	4.19 ± 0.24
4	12.27 ± 0.74	11.25 ± 1.51	12	3.18 ± 0.47	3.66 ± 0.65
5	8.75 ± 0.55	9.93 ± 1.04	13	0.56 ± 0.20	0.63 ± 0.12
6	4.67 ± 0.56	4.23 ± 0.38	14	8.60 ± 1.25	8.59 ± 0.94
7	6.26 ± 0.64	8.43 ± 1.03	15	2.19 ± 0.19	2.35 ± 0.38
8	9.56 ± 0.37	8.12 ± 0.98			

[a]Mean ± SD. I, Italian; R, Romanian; P, Polish; S, Swedish; N, Norwegian.

scaling [6] according to the formula $x'_{ij} = (x_{ij} - \mu_i)/\sigma_i$, where x'_{ij} is the autoscaled ith component of the jth object, μ_i the mean and σ_i the standard deviation of the ith component in all objects. The resulting data matrix was re-processed as before (correlation matrix calculation, etc.). After autoscaling, the eigenvector projection produced the data set shown in Fig. 4.

The results obtained are substantially in agreement with those achieved before without autoscaling of the data peaks. In addition, the loadings of the eigenvector 1 (Fig. 5) retain the sign of the previous data processing (Fig. 3), confirming the previous trends of the individual anthocyanins in contributing to the separation of the two groups.

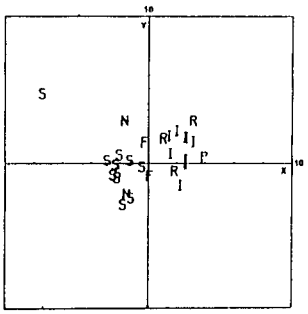

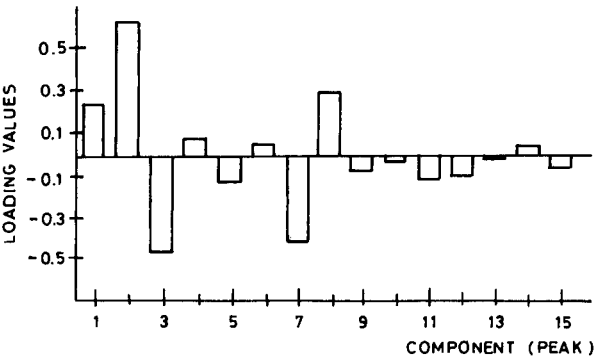

Fig. 4. Eigenvector projection of *V. myrtillus* profiles: (x) eigenvector 1; (y) eigenvector 2 (autoscaled data). I—N as for Fig. 2.

Fig. 5. Loadings of eigenvector 1 (autoscaled data).

Conclusions

It has been shown that eigenvector projection can be used advantageously to characterize complex plant extracts by considering some important selected constituents. In this case, the data handling of the chromatographic peaks of a whole class of pharmacologically active constituents (i.e., the anthocyanins) present in different raw materials, makes it possible to choose the most suitable starting product to guarantee the preparation of constant purified extracts.

The authors thank Mr. G. Chen for the h.p.l.c. data.

REFERENCES

1 A. Baj, E. Bombardelli, B. Gabetta and E. M. Martinelli, J. Chromatogr., 279 (1983) 365.
2 E. R. Malinowski and D. G. Howery (Eds.), Factor Analysis in Chemistry, Wiley-Interscience, New York, 1980.
3 B. R. Kowalski and C. F. Bender, J. Am. Chem. Soc., 95 (1973) 686.
4 S. Wold and E. Johansson, Anal. Chim. Acta, 133 (1981) 251.
5 G. Beech (Ed.), Fortran IV in Chemistry, Wiley, London, 1975, p. 50.
6 B. R. Kowalski, in C. L. Wilkins and C. E. Klopfenstein (Eds.), Computers in Chemical and Biochemical Research, Vol. II, Academic Press, New York, 1974, p. 2.

Analytica Chimica Acta, 191 (1986) 283—297
Elsevier Science Publishers B.V., Amsterdam — Printed in The Netherlands

THE PREOPT PACKAGE FOR PRE-OPTIMIZATION OF GRADIENT ELUTIONS IN HIGH-PERFORMANCE LIQUID CHROMATOGRAPHY

R. CELA*, C. G. BARROSO, C. VISERAS and J. A. PÉREZ-BUSTAMANTE
Analytical Chemistry Department, Faculty of Sciences, University of Cádiz (Spain)
(Received 28th May 1986)

SUMMARY

A theoretical model is described for quick pre-optimization of binary multistep gradient elutions in liquid chromatography. This model utilizes experimental retention-time data under isocratic elution conditions for different proportions of organic modifier in the mobile phase, and simulates the position of the peaks in the chromatogram by calculation of the average velocity of the peaks through the column. Optimization is done for multistep gradients by means of the simplex algorithm. The results must then be confirmed experimentally. Results are given demonstrating the power and validity of the model in the resolution of complex mixtures. The whole process done on a microcomputer with the PREOPT package usually takes about 30 min, without requiring user participation or chromatographic instrumentation.

The growing sophistication of liquid chromatographic instrumentation places a large number of instrumental variables at the disposal of the chromatographer. The initial and final composition of the solvents, gradient shape (if used) and duration, temperature and flow of the mobile phase can be varied at will. Each advance in instrumentation makes it easier to get an "acceptable" separation, but complicates the location of the truly optimum experimental conditions; chromatographic theory does not allow precise predictions of how a given change in the operative conditions will affect separations.

Extensive research has been done on the development of theoretical or empirical models and procedures which can be applied to obtain efficient optimization of isocratic elutions [1—5]. Gradient separations have attracted less attention [6—12]. The automation of optimization processes has been discussed [13—19]. At present, the optimization of gradient elutions is not wholly satisfactory. Very few papers tackle the problem of gradient optimization, although the prospects of the technique seem good [20]. There are basically two approaches: (a) analytical approximations (i.e., the physicochemical principles underlying the method are identified and an exact or approximate equation to describe the process is developed; (b) black-box (empirical) approximations, in which the chromatographic method is considered from a purely experimental point of view so that the effects of factor variations on the response, and the variations of such factors, are tested more

0003-2670/86/$03.50

or less simultaneously. For the analytical-type approximations [7—9], the formulae proposed become extremely complicated if the gradient shapes considered are not linear. Something similar occurs if the range of percent modifier in the mobile phase is large, or when the relation $\ln k' = f(B)$ is not linear. In such cases, previous experimental work is necessary and may be considerable if the reliability of the adjustments obtained is properly verified. Moreover, these methods are not valid for procedures which include steps in the gradient (composite gradients); this limits their application in the case of the separation of very complex mixtures, where optimization is in fact more necessary.

Black-box approximations, which commonly use the simplex method [6, 10, 11, 13, 17, 18], permit the development of totally automated optimization procedures. However, the nature of the simplex approximation [21—23], makes it impossible to guarantee obtaining a global optimum when the response surface is multimodal, as in chromatographic separations. In such cases, optimization requires repeating the simplex search from different points of the response surface. This means that many experiments must be done. Totally automated instrumental systems could run optimizations overnight but this does not solve the other problems and also requires considerable investment (autosampler, control system, etc.).

The efficiency of the simplex method for the location of the optimum depends on the objective function used (i.e., in the way the quality of the chromatogram is converted to numerical terms). Various papers [24—27] demonstrate that this question has not yet been solved satisfactorily.

The number of necessary experiments depends on the number of variables considered in the simplex. Usually, the variables are taken as the slope of the gradient, the flow rate, and the initial and final modifier percentages in the mobile phase. If more variables (e.g., the number of steps in the gradient or changes in the gradient slope during elution) are considered, a simplex with more dimensions must be used, which complicates not only interpretation of the results but also increases the number of convergence possibilities beyond the global optimum, so that the number of experiments needed increases enormously. Nevertheless, overlooking such possibilities in practice means ignoring some of the facilities available in the instrumentation, which may be especially useful for the resolution of complex mixtures.

The idea of pre-optimization is not frequent in the literature dealing with this subject, although it could be placed in an intermediate position between analytical and empirical optimizations and is directly related to computerized simulation techniques. A computerized optimization technique based on a simulation model must be capable of dealing with the following aspects. First, computer simulation of chromatographic gradient separations is needed to avoid extra experimental work; these simulations should be achieved with the same or lesser margin of error as the theoretical models for such separations. Secondly, all gradient possibilities (simple and composite gradients) should be accessible during the optimization process. Thirdly, the

optimization should be done by means of computer-simulated chromatograms, which would obviously be quicker and cheaper. And the final situation should be sufficiently close to the real optimum, so that it may be put into practice with only a few testing and fine-tuning experiments. Obviously, these four aims particularly the last one, will not be easily achieved, given that errors are cumulative during iteration, but the general idea is of interest for a pre-optimization plan capable of providing conditions sufficiently close to the real optimum so that a much shorter and simplified experimental optimization process can be started from it. Given a pre-optimized set of conditions, it would be feasible to start several simplexes in different zones of the response surface, and thus check the validity of the optimum obtained.

The PREOPT package offers a new procedure which can simulate any gradient profile in stepwise fashion and can account for the differences arising from comparison of the "programmed" and the "real" gradient profiles. A theoretical model which takes into account the average velocity of the peaks through the column for each step of a programmed gradient, serves to simulate the retention time of each species in the mixture to be separated. The PREOPT package works on a microcomputer, and avoids the need for experimental work other than obtaining primary data from isocratic elutions. The search for the optimum is given by means of the simplex algorithm, and several objective functions are available.

THEORY

Any model which will fit the above-mentioned needs must be based on the possibility of simulating gradient curves close to those which are formed in actual chromatographic systems, and on the possibility of predicting the retention times under these gradient conditions.

Balke and Patel [28, 29] have shown that it is possible to simulate any step gradient and to take into account the difference between the "programmed" and "real" gradients, by using residence time distribution techniques, so that if the mixing of liquids is not altered, the response to one entry stage of tracer concentration (not affecting the properties of the fluid mixture) can be superimposed for different flow and fluid speeds. In practice, gradient programmers run through a series of small steps, where the proportion of one of the solvents increases stepwise; the steps are as low as possible and keep close to the shape of the required gradient [30]. Thus a gradient can be simulated by a series of steps and, to a first approximation, if the increase in modifier percent is produced with sufficient speed, the elution process of one species in the column during the gradient can be regarded as a series of small isocratic elution stages, each one with a greater proportion of modifier percent. Obviously, this is an ideal situation, given that the advance of the species through the column is not immediately affected by variations in modifier concentrations. Even if this variation were

practically instantaneous, the "new" mobile phase would have to reach the site of the band in the column, which would meanwhile continue advancing through the column maintaining equilibrium with a mobile phase of lower modifier concentration. This may be regarded as the delay time of the gradient, or the time taken by the system to react to a change in concentration in the mobile phase plus an error arising from the time that the band advances with the "old" mobile phase. An attempt to represent this effect is shown in Fig. 1. Line (a) corresponds to the programmed theoretical gradient (in this case, a linear gradient). According to the model described, if there is no delay time, the gradient can be broken up into a series of steps, as shown by line (b). Line (c) corresponds to the shape of the "real" gradient which should be obtained under these conditions, from which it can be seen how the initial increase in concentration of the modifier is not detected immediately, so that the real delay time is less than that calculated by extrapolation of the two branches (point t_d) from which the steps making up the linear gradient should be superimposed (line d).

If it is assumed that the band is at the top of the column at the beginning of the gradient, the situation shown in Fig. 1 indicates that for a certain time (t_d) the peak will advance through the column in conditions of isocratic elution, with a solvent composition identical to that established at the beginning of the gradient and will then advance through successive steps until it leaves the column. The fact that there is a transition zone at the end of the delay time minimizes the error caused by the time that the peak advances with the old phase; this error is also minimized because transition zones are always obtained even when the steps are purposely programmed. This means that only the delay time need be considered as an additional factor in the model which, in any case, is easily computed by addition to the predicted theoretical time for the first step. Obviously, the exact experimental measurement of this delay time is of major importance. Obviously too, this delay time will be valid only for the instrumental system used, and all experiments must be done with one system.

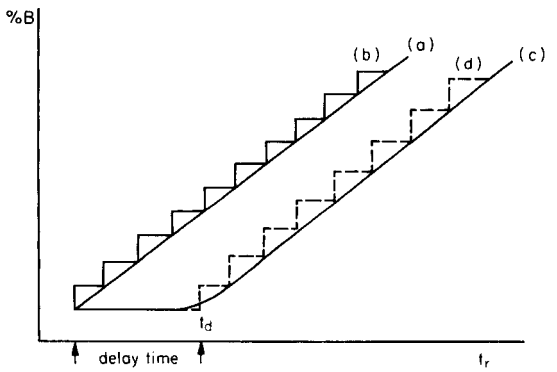

Fig. 1. Profiles of a linear gradient according to the step model: (a) theoretical (programmed) gradient; (b) programmed gradient broken into steps; (c) real gradient obtained; (d) real gradient broken into steps taking into account the system delay time.

With regard to the second condition, i.e., the possibility of predicting retention times under these gradient conditions, if a linear relationship of ln $k' = f(B)$ is approximately obtained, the step model implies the following approximations. If the retention data for a species in isocratic elution corresponding to several proportions of modifier are available, the linear velocity of the band through the column can be defined as $V = L/t_{ir}$ (cm min^{-1}), where L is the length of the column (cm) and t_{ir} is the isocratic retention time (min).

If it is accepted that a gradient program can be broken up into a series of isocratic steps, then it must also be accepted that the band will move inside the column with an average velocity which will be proportional to the modifier percent at each moment; and if the modifier concentration varies in a series of steps, the bands will also advance through a series of discrete steps. Thus, for a multistep gradient elution, the retention time of the species considered could be calculated from the following expression:

$$t_{gr} = (t_d + t_1)V_1 + \sum_{2}^{n} t_i V_i + \{L - [(t_d + t_1)V_1 + \sum_{2}^{n} t_i V_i]\} / V_{L+1}$$

where t_i is the time of each completed step i, without the band having left the column, V_i is the average linear velocity of the band during step i, V_{L+1} is the average linear velocity of the band during the step in which the peak leaves the column, n is the number of steps minus one necessary for the appearance of the peak at the end of the column, and t_d is the delay time of the instrumental system used.

EXPERIMENTAL

Equipment

All experiments were done with Millipore/Waters chromatographic equipment consisting of the following units: model 680 automated gradient controller, models M6000A and M45 pumps, model UK6 universal injector, model 490 programmable multiwavelength detector, an E-5000 Omniscribe strip-chart recorder and a model 840 data and chromatography control station. A Sigma-15 integrator (Perkin-Elmer) was also used. HPLC-grade solvents and standards were used in all cases.

The program package was implemented on a DEC PC-350 computer (part of the Waters model 840), running PRO/BASIC V.1.2, with a DEC LA-50 printer.

Program package

The PREOPT package consists of a set of eight programs written in PRO/BASIC V.1.2 and eight data files, six of which are used by the different programs of the package and two are included for initial training of the user. Four main options are available: (1) INSTRUCTIONS, which include basic

warnings, norms and advice for the correct use of the package; (2) STORAGE OF PRIMARY DATA, which permits the storage on a file, named by the user, of the primary retention-time data for the bands in the mixture to be separated; (3) INITIALIZATION AND RUN, which is the centre of the package, where the simplex search for the optimum is performed, and where the different routines of the available objective functions are found; and (4) UTILITIES, which includes routines for the direct manipulation and operation of the gradients by the user.

The simplified flow charts of the last three modules are shown in Fig. 2. The package is designed for the following tasks.

First, data and parameter selection are input (number of peaks, retention times in the isocratic mode as a function of the percent modifier, delay time, column length, dead volume). Two modes of simplex algorithm are available: the modified simplex method (MSM) of Nelder and Mead [31], and the weighted centroid method of Ryan et al. [32]. In each run, the user may choose an objective function from the six offered by the package for evaluating the quality of the chromatograms obtained. Because at present no objective function is generally accepted for such purposes [25—27], it is necessary to offer a selection so that the user can choose the most appropriate one for the specific problem or the one that seems most reliable. In the package, the user can select one of the following objective functions: (1) chromatographic response function (CRF) [6]; (2) chromatographic response function (CRFM) [10, 11, 17, 18]; (3) chromatographic optimization function (COF) [33]; (4) a modified chromatographic optimization function (COFM), which will be described elsewhere; (5) amount of information criterion (CCI) and (6) amount of information criterion with variable peak-width (CCIM). Details of the CCI and CCIM will be reported elsewhere. Finally, the user selects the desired time to end the gradient (DTTEG), i.e., the slope of the first gradient tested. This datum is also used by the package for constructing the initial simplex (according to the model of Spendley et al. [34, 35]), unless the user prefers to design his own initial simplex. The DTTEG is a very important parameter, given that the objective functions included in the PREOPT package do not use total elution-time weighting factors.

In the subsequent procedure, basic parameters (velocity of the species to be separated in the column) are calculated as a function of the selected variable (% organic modifier usually), and the initial simplex conditions (number of steps, height between steps, time for each step, advances calculation, etc.) are established. The retention times are calculated for each species under the conditions of the pre-established gradient, from the formulation of the step model, and the chromatogram corresponding to the calculated situation is simulated. This chromatogram is evaluated in terms of the selected objective function. The simplex advances by repeating these steps until convergence or an optimum is obtained.

All these operations are fully automated with the logical exception of the

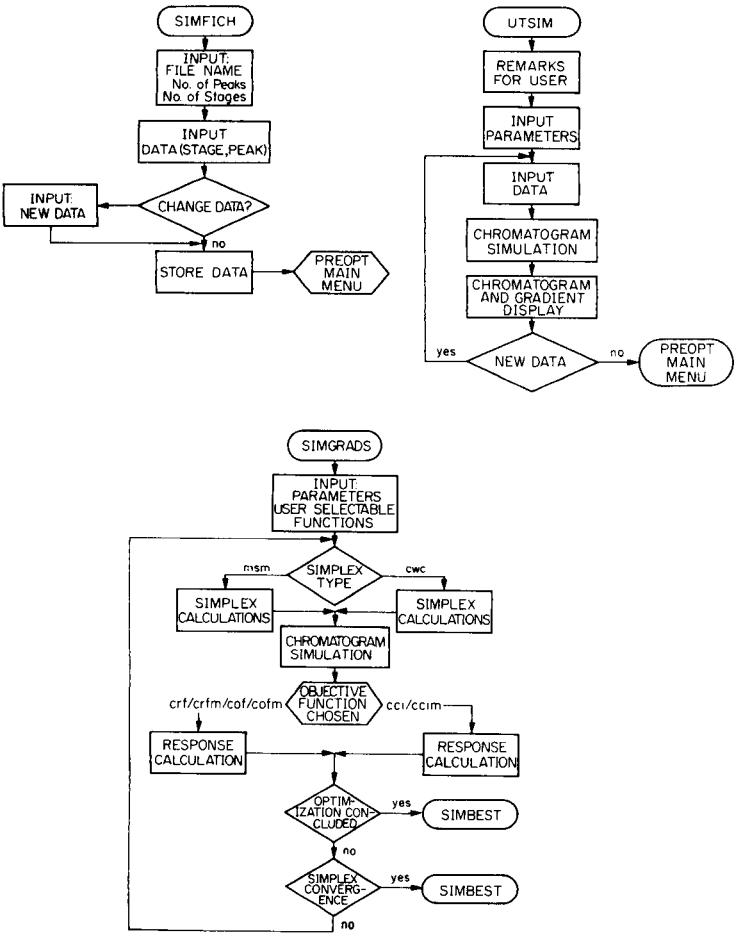

Fig. 2. Simplified flow charts of the main modules of the PREOPT package.

input stage. Alternatively, the operator may choose to use his own gradients and obtain the results manually. In any case, the simulated chromatograms, the results and operation conditions are displayed both on screen and on the printer in order to allow further study of the optimization process.

RESULTS AND DISCUSSION

Preliminary validation of the PREOPT model by means of literature data

As a first test, the results given by the step model were compared with those given by theoretical models for gradient elution [8, 9]. For this purpose, the retention time data for uracil published by Hartwick et al. [8], were used; for uracil, Hartwick et al. obtained $k'_0 = 1.61$, and $A = 0.0871$ ($-A$ is the slope of the ln k' vs. % organic modifier plot). The experimental values and those predicted by means of Hartwick's equation for three

gradient slopes 0.5, 1.33 and 2.5 (which are equivalent to 0--10% methanol gradients in 20, 7.5 and 4 min, respectively) are given in the first two rows of Table 1; these data are taken from Hartwick et al. [8] with indication of the corresponding relative errors (%). For the equation of Snyder et al., [9], given that the solvent is methanol, $S = 3.0$ and for the three considered gradients the values of b are 0.035, 0.08 and 0.17, respectively, taking into account that $t_0 = 2.34$ min [8]. Substitution of these data into the equation of Snyder et al. gives the data in the third row of Table 1. As can be seen, the errors involved in predicting retention times are somewhat higher than those obtained using Hartwick's formula. Hartwick et al. explicitly considered the delay time, which was not considered in the model of Snyder et al. In both cases, as the gradient slope increases, so does the error, especially in Snyder's model where parameter b moves away from its optimum value. In fact, gradient III implies that the peak is eluted after the gradient is complete, so that good agreement between the experimental and predicted data cannot be expected. The fourth row in Table 1 shows the data obtained for the step model, assuming an 11-step process between 0 and 10% methanol (1% increase between steps), with prefixed times and with average band velocities obtained from Hartwick's study for $t_0 = 2.34$ min and a delay time of 3.26 min (data from Hartwick), the size of each step being respectively 1.82, 0.68 and 0.36 min for the three gradients. The errors are of the same order as those obtained by applying Hartwick's formula and therefore, in principle, the validity of the method seems to be demonstrated. A similar calculation assuming 6-step gradients gave respectively 6.11, 5.93 and 5.73 min for the retention time of uracil in the three gradients considered. Thus, the results obtained for the step model do not seem to be altered if the number of steps is varied (within reasonable limits) provided that the relation $\ln k' = f(B)$ is linear, as in this case.

Table 2 shows another comparison between the results obtained by means of the step model and the formula of Hartwick et al. for other species studied by these authors [8]. The results are of the same order of magnitude regardless of the species or the gradient slope considered.

Once the validity of the step model had been established, a series of simulation experiments (pre-optimization by the PREOPT package) was done from the data of Hartwick et al. [8]. The chromatograms corresponding to the "optima" for the six different objective functions included in the package by means of six PREOPT experiments based on the MSM simplex are shown in Fig. 3. If the peak-height differences are disregarded (the PREOPT model assumes that all the components to be separated exhibit peaks of the same area which widen as their retention times increase), it is clear that the chromatograms obtained by PREOPT coincide reasonably well with the experimental chromatograms. However, it is also clear that the different objective functions do not give a single optimum, thus confirming the necessity to include several possibilities in a package such as PREOPT.

TABLE 1

Experimental and predicted values of t_r(min) according to different models for the elution of uracil, using different gradients with methanol

Method	Retention time (min)		
	Gradient I	Gradient II	Gradient III
Experimental [8]	6.21	6.14	6.51
Hartwick et al. [8]	6.00 (Δ% = 3.4)	5.99 (Δ% = 2.4)	5.99 (Δ% = 8.0)
Snyder et al. [9]	5.88 (Δ% = 5.3)	5.59 (Δ% = 8.9)	5.26 (Δ% = 19.2)
Step model	6.10 (Δ% = 1.8)	5.90 (Δ% = 3.9)	5.72 (Δ% = 12.1)

These results also indicate the impossibility of achieving a global optimum giving perfect separation of the nine peaks considered with a 0—10% methanol gradient. The optimization considered here involves only the variation of gradient conditions while other variables that can affect the quality of separation are not taken into account. However, from a practical point of view, when the user is concerned with optimization of a separation, having selected a particular column/mobile phase system from prior experience, it can be useful to examine the possibilities of separation without having to resort to experimentation. If application of the PREOPT model indicates that the separation is not possible by gradient modification, then the many other conditions of chromatography (flow rate, temperature, modifier nature, column) must be given attention.

Optimization of separations of phenolic acids and aldehydes

Once the validity of the PREOPT model had been demonstrated as described above, experiments were conducted to optimize real separations of complex mixtures. The first experiment was done with a mixture of the 14 benzaldehyde derivatives listed in Table 3. The primary data were the retention times for the 14 species obtained in isocratic elution in the 20—50% methanol range, using a μBondapak C18 column (30 cm long). The delay time measured for the system was 6.8 min (average of six determinations). The optimization was done with 7-step gradients. Two of the chromatograms obtained with the considered simulation model are compared in Fig. 4 with those obtained experimentally; the coincidence of retention times is good. Certain improvements were introduced for chromatogram (b) compared with chromatogram (a), leading to sharper separation of the 8—10, 11—12 and 13—14 peaks. The retention times reported in Table 3 show good agreement for the peaks considered with both gradients.

In this particular case, the PREOPT system gave warning that a satisfactory separation of the 14 species would not be feasible under the conditions selected; consequently, it was decided to include two further steps and to use a 10—50% methanol gradient. Under these modified conditions, the optimum obtained corresponds to the chromatograms in Fig. 5 which show

TABLE 2

Comparison between the results obtained by the formula of Hartwick et al. and the step model for the species studied by Hartwick et al. [8][a]

Compound	Gradient I (slope = 0.5)			Gradient II (slope = 1.33)			Gradient III (slope = 2.5)		
	Exp.	Hartwick	Step model	Exp.	Hartwick	Step model	Exp.	Hartwick	Step model
Cytosine	4.63	4.54 (−1.9)	4.61 (−0.4)	4.55	4.54 (0.2)	4.59 (0.8)	4.81	4.54 (−5.6)	4.55 (−5.4)
Uric acid	6.69	6.56 (−1.9)	6.58 (−1.6)	6.69	6.50 (−2.8)	6.26 (−6.4)	6.93	6.44 (−7.1)	5.95 (−14.1)
Tyrosine	7.82	7.49 (−4.2)	7.53 (−3.7)	7.48	7.36 (−1.6)	7.15 (−4.4)	7.58	7.20 (−5.0)	6.76 (−10.8)
Hypoxanthine	10.15	9.45 (−6.9)	9.41 (−7.3)	8.94	8.91 (−0.3)	8.45 (−5.4)	8.56	8.40 (−1.9)	7.67 (−10.4)
Uridine	11.33	10.77 (−4.9)	10.65 (−6.0)	9.50	9.69 (2.0)	9.05 (−4.7)	8.81	8.83 (0.2)	8.67 (−1.6)
Xanthine	11.33	10.77 (−4.9)	10.70 (−5.5)	9.74	9.86 (1.2)	9.32 (−4.3)	9.10	9.08 (−0.2)	8.35 (−8.2)
Inosine	17.18	17.50 (1.8)	16.99 (−1.1)	12.57	13.07 (3.9)	12.30 (−2.1)	10.61	10.74 (1.2)	10.69 (0.7)
Guanosine	18.29	18.71 (2.3)	18.16 (−0.7)	13.18	13.64 (3.5)	12.95 (−1.7)	11.00	11.06 (0.5)	11.39 (3.5)

[a]Relative errors, in parentheses, are expressed as percentage.

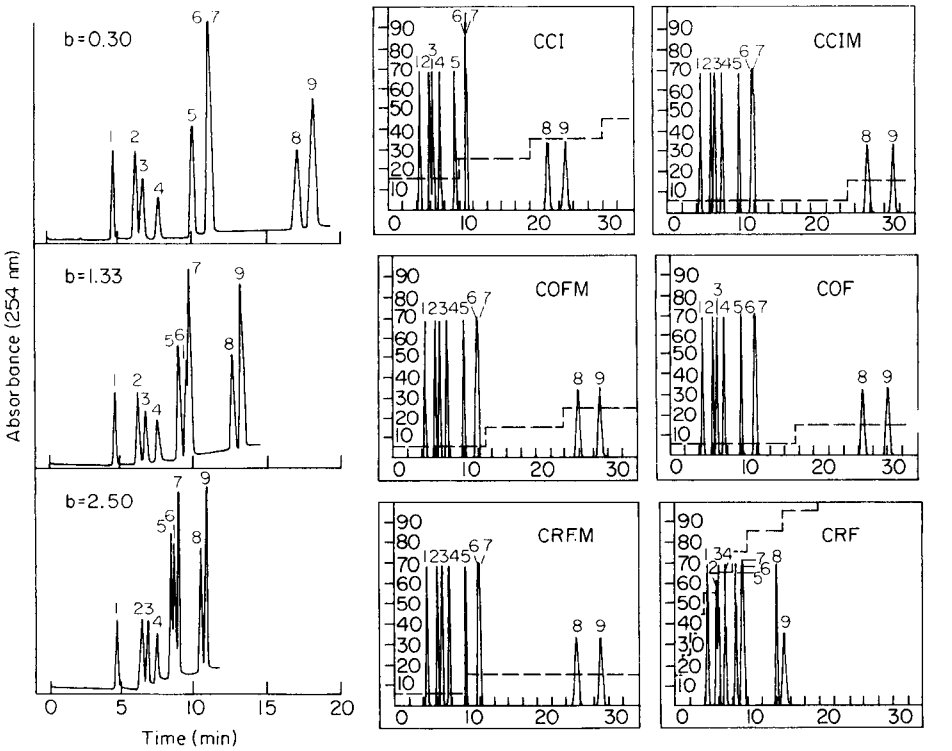

Fig. 3. Comparison between the experimental chromatograms of Hartwick et al. [8] (on the left) and those obtained through six PREOPT runs using different objective functions in the pre-optimization process.

TABLE 3

Results for phenolic aldehydes on a μBondapak column with different gradients[a]

Peak	Benzaldhyde derivative	Gradient (a)			Gradient (b)		
		t_r (PREOPT)	t_r (exp)	Error (%)	t_r (PREOPT)	t_r (exp)	Error (%)
1	3,5-Dihydroxy	6.8	6.3	7.3	6.8	6.31	7.2
2	2,5-Dimethoxy	8.5	8.35	1.7	8.5	7.48	6.1
3	4-Hydroxy	8.9	8.75	1.7	8.9	8.39	5.7
4	3-Hydroxy	8.9	8.75	1.7	8.96	8.39	5.7
5	4-Hydroxy-3-methoxy	10.7	10.11	5.5	10.96	10.21	6.8
6	3-Hydroxy-4-methoxy	11.1	—[b]	—	11.57	—[b]	—
7	4-Hydroxy-3,5-dimethoxy	12.2	12.04	1.3	12.76	12.37	3.0
8	2-Hydroxy-3-methoxy	14.2	14.11	0.6	16.29	15.73	3.4
9	3,4-Dimethoxy	16.0	15.71	1.8	20.88	19.18	8.1
10	2-Hydroxy	13.9	—[b]	—	15.19	15.20	0.1
11	3,4,5-Trimethoxy	18.2	18.30	0.5	24.85	24.57	1.1
12	2-Methoxy	18.0	17.27	4.0	23.24	21.66	6.8
13	2,4-Dimethoxy	21.3	21.08	1.0	32.01	29.61	7.5
14	3,5-Dimethoxy	21.4	21.90	2.0	34.41	31.52	8.4

[a]All retention times are given in minutes. [b]Peak not well detected in the chromatogram.

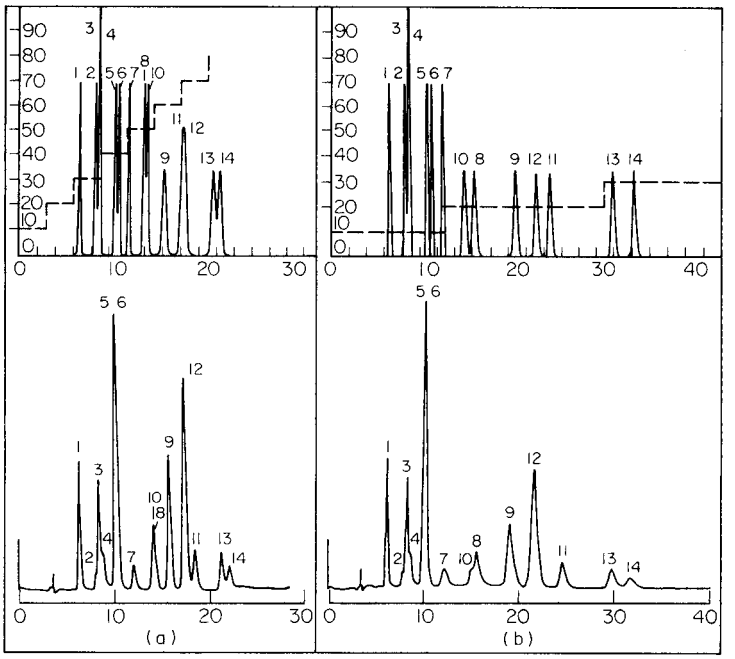

Fig. 4. Simulated experimental chromatograms obtained through the pre-optimization for the 14 phenolic aldehydes on a μBondapak column with different gradients.

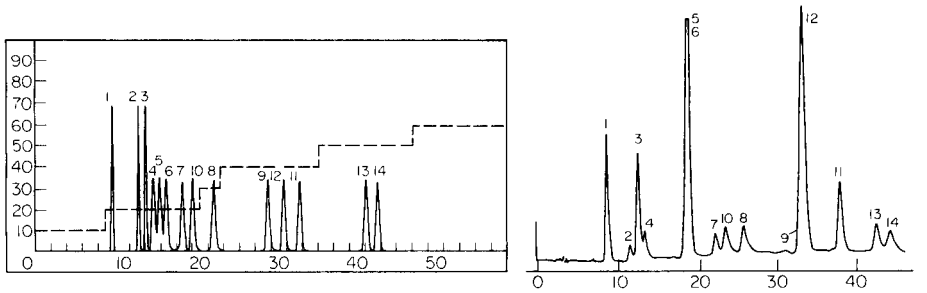

Fig. 5. Simulated and experimental chromatograms obtained through the pre-optimization for the 14 phenolic aldehydes with a 9-step gradient in the 10—50% methanol range.

that the separation of the species with short retention times has been considerably improved (cf. Fig. 4); but peaks 5 and 6 and peaks 9 and 12 overlap. It was concluded that a good separation of all the 14 species was impossible with this column and gradients in the range of modifier considered. Further experiments were therefore done with a more efficient column (Novapak C18, 15 cm long, 5-μm particle size). The chromatograms in Fig. 6 correspond to the optimum proposed by the PREOPT for this new column, using a 5-step gradient in the 5—45% methanol range. In this case, the peaks of all the 14 species are separated, which demonstrates the possibility of

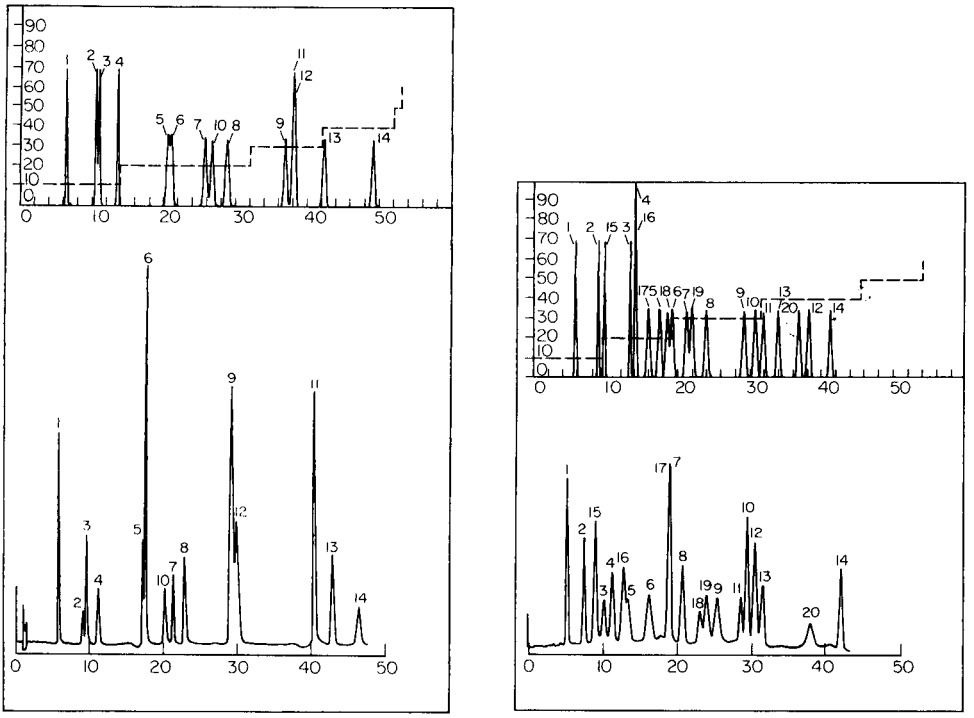

Fig. 6. Simulated and experimental chromatograms obtained through the pre-optimization for the 14 phenolic aldehydes on a Novapak C18 column.

Fig. 7. Simulated and experimental chromatograms obtained through the pre-optimization for 20 phenolic compounds on a μBondapak C18 column. See text for detail.

resolving complex mixtures by means of the PREOPT package and so avoiding the need for lengthy experimental optimization.

Similar experiments were done with other mixtures of phenolic compounds (Figs. 7—9). The chromatograms in Fig. 7 correspond to the optimum obtained for the resolution of a mixture of 20 phenolic compounds (gallic acid, 3,4-dihydroxybenzoic acid, gentisic acid, *p*-hydroxybenzoic acid, *m*-hydroxybenzoic acid, vanillic acid, caffeic acid, syringic acid, *p*-coumaric acid, ferulic acid, veratric acid, *o*-coumaric acid, sinapic acid, 3,4,5-trimethoxycinnamic acid, 3,5-dihydroxybenzaldehyde, vanillin, *p*-hydroxybenzaldehyde, syringaldehyde, *o*-vanillin and 3,5-dimethoxybenzaldehyde), all identified in sherry wines, on a μBondapak C18 column and gradients with five steps in the 10—50% methanol range. Figure 8 corresponds to the optimum for this same mixture of phenolic compounds with a Novapak C18 column and gradients with five steps in the same range of percent modifier. Finally, Fig. 9 shows the optimum for the separation of a mixture of 22 phenolic acids (those mentioned above plus 2,4,6-trihydroxybenzoic acid, α-resorcylic, β-resorcylic and γ-resorcylic acids, 2,6-

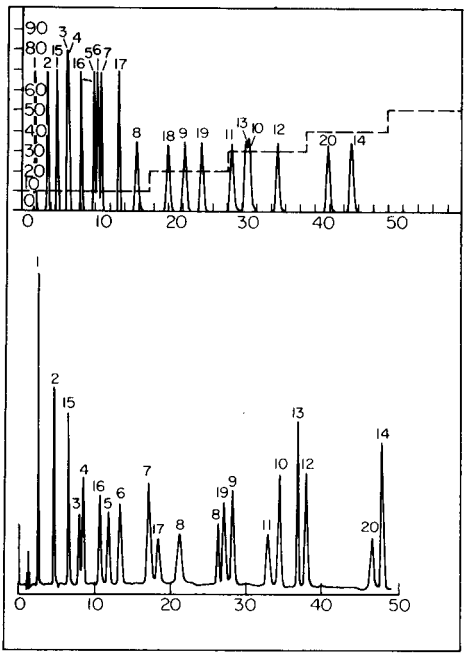

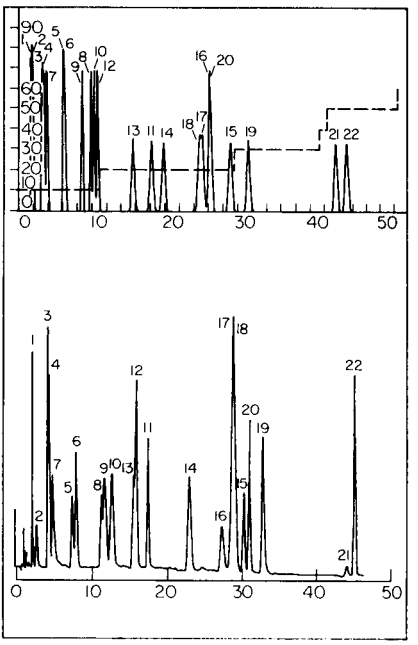

Fig. 8. Simulated and experimental chromatograms obtained through the pre-optimization for 20 phenolic compounds on a Novapak C18 column.

Fig. 9. Simulated and experimental chromatograms obtained through the pre-optimization for 22 phenolic acids on a Novapak C18 column.

dimethoxybenzoic acid, 2,4-dimethoxybenzoic acid, 3,5-dimethoxybenzoic acid and *m*-coumaric acid), on a Novapak C18 column and gradients with five steps in the 10—50% methanol range. Agreement between the experimental chromatograms and those predicted by the PREOPT is good, except for small differences in the retention times of a few peaks including some reversal. These cases correspond to substances for which the $\ln k' = f(B)$ plot was far from linear. Thus, in general, it will be necessary to run some fine-tuning chromatographic experiments to obtain a truly satisfactory overall separation. These results compare favourably with previously reported separations for these mixtures [36].

REFERENCES

1 J. C. Berridge, Trends Anal. Chem., 3 (1984) 5.
2 L. de Galan, Trends Anal. Chem., 4 (1985) 3.
3 G. D'Agostino, L. Castagnetta, F. Mitchell and M. J. O'Hare, J. Chromatogr., 338 (1985) 1.
4 S. N. Deming, J. G. Bower and K. D. Bower, Adv. Chromatogr., 24 (1984) 35.
5 H. J. Issaq, Adv. Chromatogr., 24 (1984) 55.
6 M. W. Watson and P. W. Carr, Anal. Chem., 51 (1979) 1835.

7 M. A. Stadalius, H. S. Gold and L. R. Snyder, J. Chromatogr., 296 (1984) 31.
8 R. A. Hartwick, C. M. Grill and P. R. Brown, Anal. Chem., 51 (1979) 34.
9 L. R. Snyder, J. R. Gant and J. W. Doland, J. Chromatogr., 165 (1979) 3; 165 (1979) 31.
10 J. C. Berridge, Microproc. Microsystems, 7 (1983) 19.
11 J. C. Berridge, Anal. Proc., 19 (1982) 472.
12 H. J. Issaq, K. L. McNitt and N. Goldbager, J. Liq. Chromatogr., 7 (1984) 2535.
13 J. C. Berridge, Techniques for the Automated Optimization of HPLC Separations, Wiley, Chichester, 1985.
14 J. H. Nickel and S. N. Deming, Am. Lab., 16 (1984) 69.
15 K. Jinno and K. Kawasaki, J. Chromatogr., 298 (1984) 326.
16 H. Ostermann, Labor Praxis, 8 (1984) 304.
17 J. C. Berridge and E. G. Morrisey, J. Chromatogr., 316 (1984) 69.
18 J. C. Berridge, Analyst, 109 (1984) 291.
19 Lu Peichang and Lu Xiaoming, J. Chromatogr., 292 (1984) 169.
20 J. L. Glajch and J. J. Kirkland, Anal. Chem., 54 (1982) 2593.
21 S. L. Morgan and S. N. Deming, Anal. Chem., 46 (1974) 1170.
22 S. N. Deming and L. R. Parker, CRC Crit. Rev. Anal. Chem., 7 (1978) 187.
23 R. Cela and J. A. Perez-Bustamante, Quim. Anal., 3 (1984) 87.
24 W. Wegscheider, E. P. Lankmayr and K. W. Budna, Chromatographia, 15 (1982) 498.
25 W. Wegscheider, E. P. Lankmayr and M. Otto, Anal. Chim. Acta, 150 (1983) 87.
26 H. J. G. Debets, B. L. Bajema and D. A. Doornbos, Anal. Chim. Acta, 151 (1983) 131.
27 J. W. Weyland, C. H. P. Bruins, H. J. G. Debets, B. L. Bajema and D. A. Doornbos, Anal. Chim. Acta, 153 (1983) 93.
28 S. T. Balke and R. D. Patel, J. Liq. Chromatogr., 3 (1980) 741.
29 S. T. Balke, Quantitative column liquid chromatography, a Survey of Chemometric Methods, Elsevier, Amsterdam, 1984, pp. 119—129.
30 M. Bogdan and P. K. Warme, Comp. Appl. Lab., 2 (1984) 21.
31 J. A. Nelder and R. Mead, Comput. J., 7 (1965) 308.
32 P. B. Ryan, R. L. Barr and H. D. Todd, Anal. Chem., 52 (1980) 1460.
33 J. L. Glajch, J. J. Kirkland, K. M. Squire and J. M. Minor, J. Chromatogr., 199 (1980) 57.
34 W. Spendley, G. H. Hext and F. R. Himsworth, Technometrics, 4 (1962) 441.
35 L. A. Yarbro and S. N. Deming, Anal. Chim. Acta, 73 (1974) 391.
36 C. G. Barroso, R. Cela and J. A. Perez-Bustamante, Chromatographia, 17 (1983) 249.

Analytica Chimica Acta, 191 (1986) 299—307
Elsevier Science Publishers B.V., Amsterdam — Printed in The Netherlands

EFFECT OF AMMONIA IN THE ION-CHROMATOGRAPHIC DETERMINATION OF TRACE ANIONS AND OPTIMIZATION OF ANALYTICAL CONDITIONS

M. L. BALCONI and F. SIGON*

ENEL (Italian Electricity Board), Research and Development Division, Thermal and Nuclear Research Centre, via Rubattino 54, Milano (Italy)

(Received 14th June 1986)

SUMMARY

The ion-chromatographic determination of traces of anions in the fluids of a thermal power plant is examined with an on-line automated system. Ammonia in the sample affects the analytical response for the Dionex AS4-A and AS2 anion-separation columns, because of the variable efficiency of the preconcentration. This effect can be corrected for, without sample pretreatment, by evaluating the response surface of the systems. The use of the more sensitive AS4-A column requires the chloride peak to be shifted away from the "water dip" in the chromatograms. Simplex optimization of the eluent enabled this to be done for samples without ammonia. Real utilization of AS4-A columns is however inhibited if samples contain organic acids because their peaks are not well resolved from that of chloride under the conditions adopted.

Ion chromatography, which was first suggested in 1975 [1] is one of the best techniques for the determination of soluble constituents in water. Its most important feature is the possibility of determining very low concentrations of dissolved ions, simply and quickly, even at ng l^{-1} levels. Potential applications of the technique to nuclear and thermal power plants have been reported [2—4]. It became clear that, to obtain useful and correct analytical data, the instrument itself had to be placed on-line in order to avoid contamination and to obtain greater productivity. So far, two commercial on-line ion chromatography systems have been developed: the Iontrac (GE-EPRI) and the Dionex 8000 [3, 4]. The Italian ENEL started to develop a low-cost on-line system named ENELIC [2].

In the determination of trace anions, mainly chloride, special care is needed to evaluate the effect of sample pH on the preconcentration efficiency and on the relative positions of the "water dip" (caused by dilution of eluent with water formed during the suppression) and the chloride peak. This second phenomenon causes difficulties in the integration of the chloride peak with the most efficient and sensitive Dionex anion columns, the AS4-A ones. In normal laboratory routine work, the analyst can correct for these effects but with automatic systems, greater care is needed to prevent errors arising from these uncontrolled factors.

0003-2670/86/$03.50

A general problem is caused by different concentrations of ammonia (usually in the range 0—1500 $\mu g\ l^{-1}$) in the samples, because thermal and nuclear power plant fluids are conditioned with ammonia and hydrazine to reduce corrosion phenomena. One solution to this problem is to eliminate the free base by ion-exchange, i.e., by on-line insertion of a cation-exchange column [2—4]. The effect is thus completely corrected but it is then necessary to monitor the ion-exchange efficiency. Another way to solve this problem would be to calibrate the analytical system with standards containing an average ammonia concentration; but this approach produced higher uncertainty in the analytical results and does not solve the problem of integration of the chloride peak when the AS4-A columns are used.

These problems made it necessary to study the analytical system to define the effect of ammonia on the anion determinations in order to correct the results. Accordingly, the response surface of the system was examined for the chloride ion in the presence of ammonia, with the AS4-A and the AS2 Dionex anion columns. Moreover, in an attempt to remove the chloride peak from the "water dip", the analytical conditions, mainly the eluent composition, were optimized by use of the simplex technique. This optimization was done for the AS4-A column only, because with the AS2 column, the chloride peak is sufficiently separated from the "water dip".

EXPERIMENTAL

Reagent and equipment

For the determination of chloride, a Dionex model 2120i ion chromatograph with a single piston sampling pump was used with a Hewlett-Packard model 3390A reporting integrator. The analytical columns used were the AS4-A and the AS2 Dionex anion columns. Conductimetric detection was done after the chemical suppression of the eluting phase; a Dionex-AFS fiber suppressor was used.

All the reagents were analytical grade or Aristar. The ultrapure dilution water was obtained from a Millipore Milli-Q system.

Procedures

Response surface. The response surface was evaluated for the AS4-A and the AS2 analytical columns. The operating conditions are reported in Table 1. Because of the low concentrations investigated, a preconcentration step was necessary and because of the lower sensitivity of the AS2 column compared to the AS4-A, different preconcentration times were needed to achieve appreciable signals.

The solutions analyzed had different concentrations of chloride and ammonia in the ranges 0—10 $\mu g\ l^{-1}$ and 0—1.500 $\mu g\ l^{-1}$, respectively. The reagents used to prepare the samples were sodium chloride and liquid ammonia solution (d = 0.88). The concentrations of the different samples were defined by means of a factorial design. Peak heights were measured

TABLE 1

Operating conditions for the experiments with the AS4-A and the AS2 Dionex anion columns[a]

Dionex anion column	Preconcn. time (min)	Eluent	Eluent flow (ml min^{-1})
AS4-A	5	0.75 mM $NaHCO_3$ 2 mM Na_2CO_3	2
AS2	10	2 mM NaOH 3 mM Na_2CO_3	3

[a]In both cases, a TAC preconcentration column was used and the sample flow was 2.5 ml min^{-1}. The suppressor column was a Dionex-AFS. The regenerating solution was 0.0125 M sulfuric acid at 2.5 ml min^{-1}. The full-scale signal of the conductimeter was 10 μS.

because they were more precise than the areas. The experimental data were processed by the linear regression technique in order to evaluate model parameters [5, 6].

Simplex optimization. The simplex optimization was used for the data from the AS4-A analytical columns. The operating conditions are reported in Table 1. The variable-size simplex algorithm, proposed by Nelder and Mead [7] as modified by Spendley et al. [8] with regard to the "massive contraction" rule, was used with two factors. Because the optimization was done with the aim of establishing the best eluent composition based on carbonate, hydrogencarbonate and hydroxide as eluting ions, the two factors were the molar concentrations of sodium hydroxide and sodium hydrogencarbonate in the eluent.

The response function R that had to be maximized was $R = [t_r(Cl^-) - 1.3][10 - t_r(SO_4^{2-})]^{0.25}$ where $t_r(Cl^-)$ is the chloride retention time and $t_r(SO_4^{2-})$ the sulfate retention time (both in minutes). This function was used in order to remove the chloride peak from the "water dip", while the sulfate retention time was kept at $\leqslant 10$ min. However, greater importance was attached to removing the chloride peak from the "water dip" than to any increase of the sulfate retention time.

The two factors could be varied in the range of concentration from 0 to 8 mM with an initial step size of 2.5 mM. The initial simplex was calculated with the so-called "tilted simplex algorithm" [8], which produced an equilateral triangle as the factors were measured in the same unit. The coordinates of the starting vertex were set at a concentration of 5 mM for both factors. In order to keep the system under statistical control, each experiment was repeated three times and the variance and the mean value of the three measurements were calculated. The different means were compared according to the results of the F-test on the variances previously carried out. Further, to correct for possible system response drift, a control standard (the starting vertex) was used between every two points of the simplex; every standard was

tested in triplicate and each new mean value was compared to the previous one. If the means were statistically different, a correction factor was calculated as the ratio between the means. The results of the simplex were then corrected by multiplying them by the appropriate correction factor. All the statistical evaluations were done at the 95% probability level.

RESULTS AND DISCUSSION

The AS4-A columns were chosen because the range of concentrations that had to be investigated was at the $\mu g\ l^{-1}$ level and the AS4-A columns are the most efficient and sensitive available. However, integration of the chloride peak is difficult because of the variable position of the "water dip" correlated to the sample pH variability. The chloride peak is well resolved from the "water dip" on the less sensitive AS2 columns. For these reasons, these analytical systems were investigated with regard to the response surface during the optimization of the eluent for the AS4-A column.

To investigate the response surface of the chloride system, the composition of the samples analyzed was varied in factorial designs; some extra data obtained outside the plan were also used. Although the final design appeared to be unrotatable and not well balanced, the larger number of data allowed more information to be obtained. The data are reported in Table 2.

The effect of ammonia on the chloride peak causes a shift of the peak maximum and a decrease of the peak height depending on the ammonia concentration in the sample. To investigate this effect, the analytical data were fitted to the following model:

$$t_r(Cl^-) = (a + kb)C_{NH_3} + bC^0_{Cl^-} + bC^{dil.}_{Cl^-} + c$$

where concentrations C are in $\mu g\ l^{-1}$. The physical sense of c, a and b could be interpreted, respectively, as the intrinsic retention time of chloride $t^0_r(Cl^-)$, the effect of ammonia on $t^0_r(Cl^-)$, and the effect of nonlinearity on $t_r(Cl^-)$. The true chloride concentration had to be taken into account; this can be expressed as $C_{Cl^-} = C^0_{Cl^-} + C^{dil.}_{Cl^-} + kC_{NH_3}$, where $C^0_{Cl^-}$ is the amount of chloride added, $C^{dil.}_{Cl^-}$ is the chloride content of the dilution water used and kC_{NH_3} is the amount of chloride added with the ammonia. Therefore the model will be

$$t_r(Cl^-) = (a + kb)C_{NH_3} + bC^0_{Cl^-} + bC^{dil.}_{Cl^-} + c$$

Evaluation of the data showed that the intrinsic retention time for chloride was 1.635 min for the AS4-A column and 2.265 min for the AS2 column, and that ammonia caused a positive shift of about 5% at a concentration of 1000 $\mu g\ l^{-1}$ with both columns. The nonlinearity caused a positive shift of about 1.5% for the AS4-A column and a negative shifting of about 3% for the AS2 column, both at 10 $\mu g\ l^{-1}$ chloride. In our practice, only the effect of ammonia is really recognized because of the high ammonia concentration and the low chloride content in the samples analyzed.

TABLE 2

Effect of ammonia on the determination of trace chloride. Data obtained for the chromatographic system with the Dionex AS4-A or AS-2 column and the standard eluent composition[a]

Chloride added ($\mu g\ l^{-1}$)	Ammonia ($\mu g\ l^{-1}$)	Replicates (n)	Peak height (mV)		t_r (min)	
			Mean	S.d.	Mean	S.d.
The AS4-A column						
0	0	3	8.458	0.677	1.64	0.01
0	0	2	53.569	3.492	1.65	0.01
0	0	2	87.427	39.556	1.60	0.01
0	0	2	53.829	1.744	1.64	0.02
0	0	2	33.785	7.413	1.62	0.01
3	0	4	1167.123	4.062	1.65	0.02
6	0	3	2261.633	104.473	1.65	0.01
9	0	3	3289.950	194.671	1.66	0.04
0	500	4	86.552	5.674	1.71	0.01
3	500	4	844.171	16.167	1.70	0.02
4.5	500	3	1330.569	39.480	1.67	0.01
4.5	500	3	1562.427	284.762	1.67	0.02
4.5	500	4	1274.044	110.030	1.66	0.02
6	500	4	2147.750	102.504	1.73	0.01
0	1000	4	252.252	69.255	1.72	0.02
3	1000	3	1009.178	40.703	1.72	0.01
6	1000	3	2078.867	91.744	1.74	0.01
9	1000	3	2818.417	94.036	1.74	0.01
The AS2 column						
0	0	2	208.962	18.204	2.25	0
0	0	2	197.997	11.127	2.27	0.04
10	0	2	1188.612	59.661	2.20	0.04
10	0	2	1247.142	59.490	2.20	0.02
0	750	2	112.392	19.443	2.33	0.01
0	750	3	40.950	12.822	2.41	0.05
0	750	2	97.122	4.785	2.33	—
10	750	2	410.952	61.950	2.21	0
10	750	2	691.731	429.292	2.36	0
0	1500	1	80.091		2.43	—
0	1500	1	158.268		—	—
0	1500	1	58.416		2.35	—
10	1500	2	289.971	13.677	2.38	0.01
10	1500	2	169.482	3.966	2.42	0.08
10	1500	1	219.360		2.36	—
10	1500	2	175.650	33.393	2.36	0.01

[a]The experimental points (0, 0) refer to dilution water blanks sampled over the experimental period.

The same approach was used to investigate the variation of the chloride peak height (H). In this case, the model tested was $H_{Cl^-} = dC_{Cl^-} + eC_{NH_3}C_{Cl^-}$. This model is valid if the response to chloride is linear in the range investigated. When the chloride content is expressed as in the previous case, the model becomes

$$H_{Cl^-} = dC^0_{Cl^-} + (kd + eC^{dil.}_{Cl^-})C_{NH_3} + ke(C_{NH_3})^2 + eC^0_{Cl^-}C_{NH_3} + dC^{dil.}_{Cl^-}$$

where d is the slope of the analytical response of the chromatographic system to chloride (peak height) and e is the effect of ammonia on the analytical response.

Evaluation of the data showed that the ammonia reduced the response to chloride, as expected. Typically, there is 1 mg l^{-1} ammonia in the power plant fluids, other than in the effluents from the condensate treatment system where ammonia is absent, thus there would be a 13% or 61% decrease in the response to chloride with the systems based on the AS4-A or AS2 column, respectively. Because of the low concentration of chloride in the dilution water used, the chloride contents in the samples without analyte addition can be considered statistically the same. The values of the parameters a–e are reported in Table 3.

During this investigation, the simplex technique was used to optimize the eluent for the AS4-A column. A graphical representation of the simplex evolution is shown in Fig. 1. The surface over which the response function was statistically the same at the 95% probability level had the vertices 15, 18, 21, 22, 23, 24. The simplex stopped at the 24th experiment because the vertices in the last simplex (15, 24, 23, 25) had the same response and the 25th vertex had the same coordinates as the 18th. Table 4 lists the eluent compositions related to the vertices with maximum response. It can be seen that the influence of the eluent composition is greater on sulfate than on chloride, as already reported [9], but it is difficult to identify a parameter that could lead to the choice of the best eluent. Because of the presence of a

TABLE 3

Parameters calculated by linear regression to establish the response surface of the chromatographic systems based on the AS4-A and AS2 analytical columns

Column used	Parameters				
	a[a] (min/μg l^{-1} NH_3)	b[b] (min/μg l^{-1} Cl^-)	c[c] (min)	d[d] (mV/μg l^{-1} Cl^-)	e[e] (mV/μg l^{-1} Cl^-/ μg l^{-1} NH_3)
AS4-A	8.3510×10^{-5}	2.5243×10^{-3}	1.6352	3.3870×10^{2}	-4.4168×10^{-2}
AS2	1.1851×10^{-4}	-6.6306×10^{-3}	2.2653	9.7897×10^{1}	-5.9923×10^{-2}

[a]Effect of ammonia on $t^0_r(Cl^-)$. [b]Effect of nonlinearity on $t^0_r(Cl^-)$. [c]$t^0_r(Cl^-)$. [d]Slope of response to chloride based on peak heights. [e]Effect of ammonia on response slope.

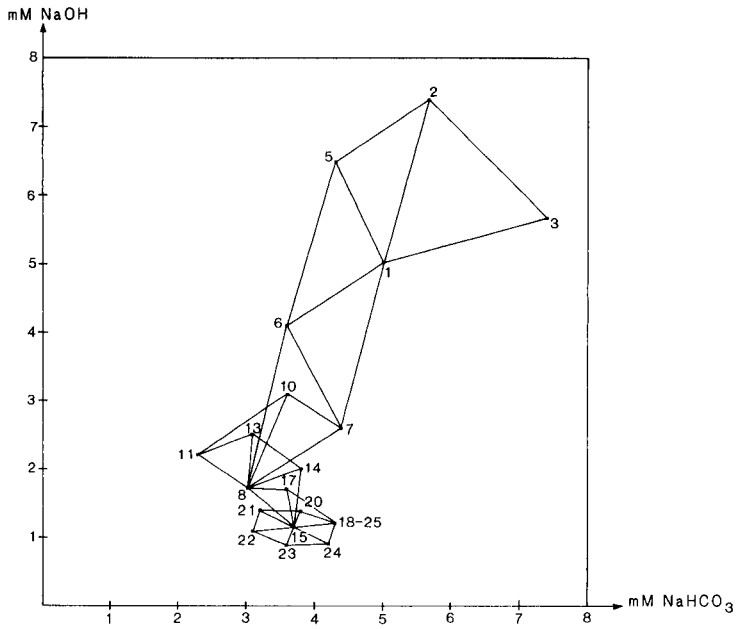

Fig. 1. Graphical representation of the simplex optimization for the AS4-A analytical column. The missing points are rejected vertices.

plateau with the same maximum response, the eluent composition corresponding to the 23rd vertex was selected here as the best.

During these experiments, the correction factor had to be changed only once. The correction factor calculated as described above allows a linear correction. In preliminary tests, the presence of possible memory effects and significant non-linear behaviour of the response with time were evaluated. When the eluents were changed and the trend of the response factor was monitored, no memory effect was observed. When analyses were repeated every 30 min for a few days, with two changes of eluents, only a slight linear drift was found.

Figure 2 shows different chromatograms obtained with the Dionex standard eluent and the eluent chosen by the simplex optimization. At retention times close to that of chloride, several unidentified peaks (probably organic acids) are eluted when ammonia is present. The organic acids are, in fact, efficiently preconcentrated because of the high pH of the sample. It was therefore not possible to prepare standards matching the real samples, because of lack of information about the nature and amount of the organic acids, the latter being quite variable. Thus, although it has proved possible to remove the chloride peak from the "water dip", the presence of organic acids in the same chromatographic region as chloride does not allow reliable use of the AS4-A columns for automatic on-line analysis of the steam-water cycle of power plants where such acids are present.

TABLE 4

Simplex optimization for the AS4-A column, with eluent composition and calculated parameters related to the vertices with, statistically, the maximum response

Vertex no.	Eluent		Ionic strength	pH	Activity		Ratio	t_r	
	OH^-	HCO_3^{2-}			HCO_3^-	CO_3^{2-}	HCO_3^-/CO_3^{2-}	Cl^- (min)	SO_4^{2-} (min)
	(10^{-3} M)		(10^{-3} M)		(10^{-3} M)				
15	1.15	3.68	5.92	9.77	2.39	0.78	3.06	1.99	7.66
18	1.20	4.29	6.64	9.70	2.88	0.81	3.56	1.91	7.06
21	1.39	3.17	5.85	9.98	1.73	0.93	1.86	1.90	6.76
22	1.10	3.07	5.19	9.85	1.89	0.75	2.52	1.99	7.74
23	0.86	3.58	5.26	9.62	2.55	0.60	4.25	2.12	8.80
24	0.91	4.19	5.97	9.56	3.05	0.63	4.84	1.99	7.85

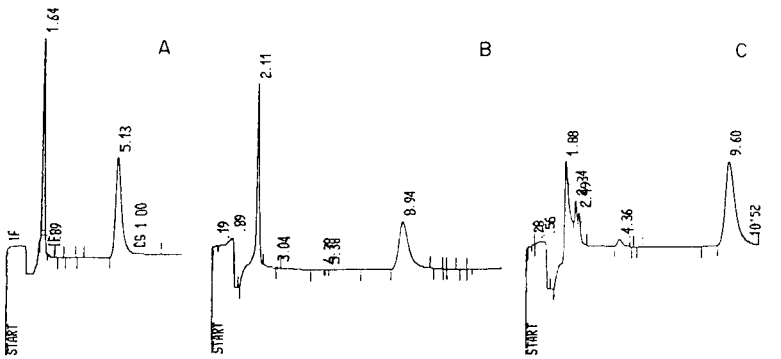

Fig. 2. Chromatographic separation of chloride and sulfate (10 $\mu g\ l^{-1}$ added) obtained with the AS4-A analytical column: (A) standard eluent; (B) simplex-optimized eluent; (C) simplex-optimized eluent, in the presence of ammonia (1000 $\mu g\ l^{-1}$). In C, unidentified peaks (probably organic acids) are seen in the same region as the chloride peak.

Conclusions

The presence of ammonia at variable and high concentrations in the samples causes problems in the automatic determination of trace amounts of chloride by ion chromatography. The response surface appears quite simple for use in automatic correction of the analytical data obtained from chromatographic systems based on the AS4-A and the AS2 columns.

The application of the simplex technique to optimize the eluent composition for the AS4-A columns, in order to achieve better integration of the chloride peak, was successful only for samples without ammonia. The presence of ammonia changes the characteristics of the chromatogram if organic acids are present in the samples. For automatic operation without sample pretreatment, the use of Dionex AS2 analytical columns is recommended because chloride is then eluted well away from the "water dip" and away from the organic acid peaks. Their disadvantage is that they provide less sensitivity than the AS4-A columns.

The authors thank Mrs. F. Tulli for experimental assistance.

REFERENCES

1 H. Small, T. Stevens and W. Bauman, Anal. Chem., 47 (1975) 1801.
2 M. L. Balconi, R. Pascali and F. Sigon, Anal. Chim. Acta, 179 (1986) 419.
3 M. Cútler, EPRI Condensate Polishing Workshop Proceedings, October, 1985, Richmond, VA.
4 M. N. Robles and J. L. Simpson, EPRI NP-4121, Project 1447-1, Interim Report, September, 1985.
5 Owen L. Davies, The Design and Analysis of Industrial Experiments. Longmans, London, 1956.
6 G. Buzzi Ferraris, Analisi ed Identificazione di Modelli, CLUP, Milan, 1981.
7 J. A. Nelder and R. Mead, Comput. J., 7 (1965) 308.
8 W. Spendley, G. R. Hext and F. R. Himsworth, Technometrics, 4 (1962) 441.
9 D. R. Jenke and G. K. Pagenkopf, J. Chromatogr., 269 (1983) 202.

Analytica Chimica Acta, 191 (1986) 309—317
Elsevier Science Publishers B.V., Amsterdam — Printed in The Netherlands

SOURCE ALLOCATION OF ORGANIC AIR POLLUTANTS BY APPLICATION OF FUZZY C-VARIETIES PATTERN RECOGNITION

K. E. THRANE*
Norwegian Institute for Air Research, N-2001 Lillestrøm (Norway)
R. W. GUNDERSON
Utah State University, Logan, Utah (U.S.A.)
(Received 27th March 1986)

SUMMARY

Data for polynuclear aromatic hydrocarbons (PAH) from 44 air samples are processed by unsupervised clustering techniques in order to resolve the contributions from two sources (domestic heating and motor vehicles). The fuzzy c-varieties (FCV) clustering algorithms are applied. The cluster configuration which best describes the characteristic properties of the samples is selected by computation of validity discriminant coefficients. The FCV method permits the data samples to belong partially to different clusters, and source apportionments are estimated by multiplying the membership values by the PAH concentrations of the individual samples. The results are compared to those obtained by other methods of dispersion or receptor modelling in the same areas. The FCV method is valuable for estimating contributions from two types of emission sources.

Numerous air-quality studies have shown that polynuclear aromatic hydrocarbons (PAH) are one of the most important groups of pollutants in urban and residential areas. Such hydrocarbons are produced by incomplete combustion of organic material, the main sources being car engines and domestic heating (wood, oil, coke, etc.). Industrial sources may also contribute. Some PAH compounds are carcinogens, so that identification of sources and reduction of emissions are considered most important. However, estimation of the relative influence of different types of combustion source in an airshed has proved to be difficult. The problems involved are well known [1—8]. Different methods for source allocation of combustion products in air have been presented. Although several workers have stated that the relative amounts of the individual compounds vary depending on the source of the emission, and that the composition of PAH in an air sample may carry information about its origin, cluster analysis appears not to have been used previously to study apportionment of PAH from the two most important source types. Some studies have involved clustering techniques to estimate the contribution of PAH from an industrial source where the PAH are released by an electrolytic process [9—11].

This paper demonstrates the application of unsupervised pattern recognition and cluster analysis in order to distinguish between the contributions of

0003-2670/86/$03.50

PAH from heating and traffic. The relative contributions from the two sources, are estimated from the cluster analysis, and compared with results obtained by independent methods.

THE CLUSTERING METHOD

The fuzzy c-varieties (FCV) clustering method was applied. The FCV algorithms were first published by Bezdek et al. [12]. Since then, they have been used in many cluster applications. In air pollution studies, the method was first used to estimate the contribution of PAH from aluminum industries relative to other sources in the regions near the factories, and proved to be a useful tool [9—11]. The FCV program can be applied to unsupervised pattern recognition, i.e., it automatically searches for patterns in the data and clusters the data according to these patterns. The program should therefore be most useful when pre-specified structures are difficult to obtain, as in air pollution studies of combustion products.

There is a basic difference between the FCV and most of the better-known methods for cluster analysis. Traditional methods require that every sample is assigned to only one of the clusters, whereas the FCV technique permits data samples to possess partial memberships in different clusters. In most cases, ambient air samples contain a mixture of pollutants from a number of sources so that the FCV technique is well suited to such samples. If the samples can be clustered according to the origin of the pollutants, the contribution from each source can be calculated from the membership values and the concentrations of PAH in each sample.

Briefly, the FCV program is as follows. The measurement matrix $\mathbf{X} = (x_1, \ldots, x_n)$ consists of n samples x_k, each with d variables $x_k = (x_{k1} \ldots x_{kd})$, and c ($c \geqslant 2$) is the number of clusters sought. The membership value of object x_k with respect to cluster i ($i = 1, 2, \ldots, c$) is u_{ik}. The membership values are subject to the conditions $0 \leqslant u_{ik} \leqslant 1$ and $\Sigma_{i=1}^{c} u_{ik} = 1$. The computation consists of looping through the two equations

$$u_{ik} = 1 / \sum_{j=1}^{c} (\|\bar{\mathbf{x}}_k - \bar{\mathbf{v}}_i\| / \|\bar{\mathbf{x}}_k - \bar{\mathbf{v}}_j\|)^{1/(m-1)} \tag{1}$$

$$\bar{\mathbf{v}}_i = \sum_{k=1}^{n} (u_{ik})^m \bar{\mathbf{x}}_k / \sum_{k=1}^{n} u_{ik}^m \tag{2}$$

where $\bar{\mathbf{v}}_i$ is the cluster centre vector for cluster i and m is a fixed weighting exponent. The iteration proceeds until a pre-specified minimum change criterion is met for either the membership values or the cluster center vectors. Usually one chooses $m = 2$, but by increasing m, less weight is attached to the importance of small membership values. This means that the higher the value of m, the "fuzzier" the algorithms become. The choice $m = 1$ means that each sample is a member of only one cluster (hard clustering).

One of the advantages of fuzzy clustering is the possibility of using the fuzziness of a given configuration as an indicator of its quality. This can be achieved by computing the cluster validity coefficient (CVC) of the clusters, which is a pairwise measure of the separation, for increasing values of m [10]. The CVC is the maximum value of the ratio of the distance between the two cluster centres to the weighted scatter of the two clusters. The algorithms are given in [10]. This means that the greater the coefficient, the better the separation between data clusters. The membership weighted values in the definition of the cluster validity coefficient are also raised to the power of m. By introducing successively increasing values of m, the effect of samples with poor membership is increasingly filtered out. An indication of the cluster quality can therefore be obtained by comparing the values of the cluster discriminant from computations where m is increased stepwise. If there is little change in the values of CVC, the conclusion is that most of the data have shared membership values close to either zero or unity, which means a good quality. A marked increase in the values as m increases would be taken as an indication of substantial sharing between classes. Such a configuration would be considered of poor quality and rejected. Examples of good and poor quality of cluster configurations and the effect on the cluster validity coefficient when m is increased are illustrated in Fig. 1.

MONITORING STATIONS AND METHODS

Locations and data collection

The PAH data used for the cluster analysis were obtained from three different air pollution studies. The samples had been collected at four stations in South Norway (see Table 1) exposed to PAH mainly from domestic heating and car traffic. The relative contribution from the two source types varied from one station to another (Table 1); it was assumed that other sources were of minor importance in the areas near the sampling stations. One station was located in Elverum (population 10 000) where some wood is used for domestic heating, but oil and electricity are also used. These samples were collected in order to obtain information about the influence of residential wood combustion on the air quality in an inland town where the winter season is cold and inversions occur frequently in winter. The second station was situated in Aurskog (population 500) where wood is mostly used for domestic heating. This is a residential, sparsely built-up area and the only traffic is private cars. This site was chosen to obtain a "fingerprint" of the PAH in air emitted mainly from residential wood burning. The meteorological conditions in this area are quite similar to those in Elverum. Two stations were located in the same neighbourhood in Oslo (population 450 000). One was set up in a street with dense traffic during daytime (St. Olavsgate) and the other one in Nordahl Brunsgate, on top of a roof and facing a backyard. All samples were collected during January and February but not simultaneously (Table 1).

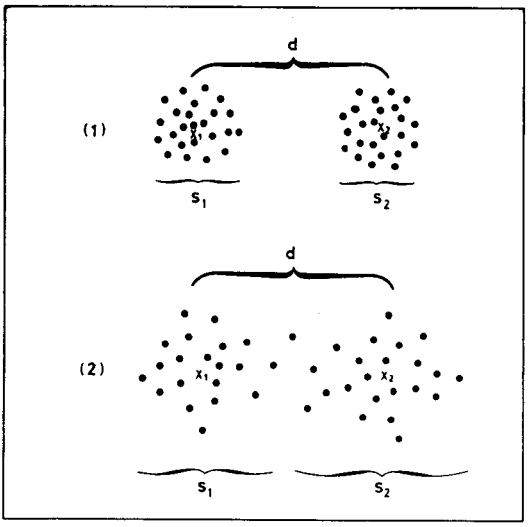

Fig. 1. Two examples illustrating cluster configurations of good and poor quality. Example 1 shows two well separated clusters. On increasing the weighting exponent m, few samples will be ignored; the changes of the CVC are minor. In example 2, there are samples with shared or low memberships that will be filtered out with increasing m, and the scatter S_1 and S_2 will decrease; this will result in a marked increase in the CVC.

TABLE 1

Number of samples (n) collected at each station and information on the main contributors of PAH

Station	n	PAH exposure
Elverum[a]	15	Mainly domestic heating, but also motor vehicles
Aurskog[b]	14	Mainly domestic heating by wood burning
Nordahl Brunsgate[c]	7	Domestic heating and motor vehicles
St. Olavsgate[c]	8	Mainly motor vehicles, but also domestic heating

[a]120 km north-east of Oslo, collected in 1983. [b]45 km due east of Oslo, collected in 1984. [c]Downtown Oslo, collected in 1985 (see text).

Some of the studies included inorganic components such as lead and other metals, sulfur dioxide and nitrogen oxides, and the isotopic carbon ratio $^{14}C/^{12}C$. Meteorological observations such as ambient air temperature, wind speed and wind directions were obtained from nearby weather stations.

In all the studies, the same methods for sampling and quantitation were applied; to obtain data of good quality, the methods had been carefully selected and tested [13]. Sampling time was 24 h. Particulate PAH were collected on glass-fibre filters while the volatile portion was trapped on polyurethane foam plugs. Individual PAH components were quantified by high-resolution glass-capillary gas chromatography, integration of chromatographic peaks and standard calibration techniques.

Input data

The selection of PAH compounds (Table 2) was based on the quality of the chemical data (i.e., consistency and minimum risk of interferences, degradations and losses) and on the importance of the individual PAH for source identification. For example, cyclopenta(cd)pyrene and coronene are associated with traffic while the main source of retene (1-methyl-7-isopropyl-phenanthrene) is wood combustion [14]. The data were standardized by centering each column of features to the mean of the column and then normalizing to the standard deviation of the column.

RESULTS AND DISCUSSION

Clustering of PAH samples

The FCV algorithm was used to partition the data into $c = 2$, $c = 3$ and $c = 4$ classes. The quality of the cluster configurations was determined by computing the cluster validity discriminant coefficient (CVC) for increasing weighting exponents (m). The CVC values (Table 3) were computed for successively increasing values of the membership weighting exponent (m). When the data were partitioned into two clusters ($c = 2$), only minor changes of the CVC were observed with increasing values of m, i.e., increasing m has little effect on the class models, which means that the configuration is of acceptable quality. Subclustering was tested for samples with a membership value >0.5 in cluster 1; the CVC increased slightly as m increased. When the data were partitioned into three clusters ($c = 3$), the discriminant values indicate good separation between clusters 1 and 2, but not between cluster 3 and the other two; thus partitioning into three clusters was not satisfactory. The CVC also increased markedly with increasing m when the computation was tested for four clusters; this configuration is therefore also of poor quality.

On the basis of these results, partitioning of the data into two clusters followed by subclustering is considered superior to the other configurations. The memberships of the samples in the different clusters were therefore studied for these configurations. With $c = 2$, all the samples from Aurskog (mainly wood combustion) were assigned to one cluster. The samples from Elverum and from the Oslo stations were assigned to the other, i.e., samples exposed to pollution from both traffic and domestic heating were clustered together. The subclustering, however, separated street samples exposed mainly

TABLE 2

The PAH compounds included in the cluster analysis

No.	Compound	No.	Compound	No.	Compound	No.	Compound
1	Biphenyl	5	Fluoranthene	9	Cyclopenta(cd)pyrene	13	Benzo(a)pyrene
2	Fluorene	6	Pyrene	10	Benzo(a)anthracene	14	Indeno(1,2,3-cd)py
3	Phenanthrene	7	Retene	11	Chrysene/triphenylene	15	Benzo(ghi)perylen
4	Anthracene	8	Benzo(b)fluorene	12	Benzo(e)pyrene	16	Coronene

TABLE 3

Results for cluster validity coefficients with different weighting exponents (m)

Clusters		Validity coefficient			
		$m = 2$	$m = 4$	$m = 6$	$m = 8$
2 clusters,	1 and 2	3.26	6.18	6.92	6.97
2 subclusters of 1		2.90	7.18	10.1	11.7
3 clusters,	1 and 2	6.33	12.7	12.5	11.8
	1 and 3	2.99	8.12	12.4	16.7
	2 and 3	5.37	12.5	18.9	23.4
4 clusters,	1 and 2	20	123	145	151
	1 and 3	6.13	36.3	83.4	384
	1 and 4	9.26	59.2	130	382
	2 and 3	4.8	13.6	22.3	28.9
	2 and 4	7.11	19.1	31	43.3
	3 and 4	2.39	8.04	15.9	28.2

to car traffic from the samples collected in Nordahl Brunsgate and Elverum where the main source was domestic heating.

For $c = 3$, most samples exposed mainly to traffic were assigned to one cluster, but their membership values were low. This indicates that the centre (prototype) of this cluster was not similar to the typical PAH pattern in air samples from traffic exhaust. The second and third clusters consisted of samples from Aurskog, and from Elverum and Nordahl Brunsgate, respectively. Cluster analysis evaluated for $c = 4$ gave almost the same result as for three clusters; the only difference was that the cluster containing the samples from St. Olavsgate was broken into two clusters. Two samples from this street station formed one cluster where the membership values for all the other samples were close to zero. The other samples from St. Olavsgate were assigned to the other cluster, but their membership values were low. The samples from Aurskog on the one hand and from Elverum and Nordahl Brunsgate on the other were grouped into the two remaining clusters.

These results show that $c = 2$ and subclustering is the best way of separating the contribution from the two source types in this particular data set. It should, however, be noted that the street samples contained pollutants from both types of source, although most of the PAH came from car exhaust. The above discussion suggests that a more representative set of samples for the traffic exposure would have made the clustering less fuzzy and the interpretation of the clustering results easier. Also it would have been a great advantage if all the samples had come from the same area or sampling station.

Source apportionment

The relative contribution of PAH from the two sources, domestic heating and motor vehicles, was estimated by multiplying the membership values for

each sample in the clusters by the total PAH concentration measured in the sample. The sum of the weighted PAH estimates for each station was divided by the total measured PAH concentration at the site. The results are given in Table 4 together with results obtained by several independent methods in the same areas. Information on the fuel consumptions was available in Elverum and in Oslo and the relative emissions of PAH in the two areas were estimated on the basis of these data and emission factors [15, 16]. Lahmann et al. [5] have used the ratio between two of the more stable PAH, indeno-(1,2,3-cd)pyrene and benzo(ghi)perylene (IP/BghiPe) to obtain a first impression of the relative contribution from the two types of source. This ratio should be 0.35—0.39 for PAH emitted from car exhaust only and 0.90 for PAH from domestic heating by coal and oil combustion [5]. Although the conditions in Norway are quite different from those in West Germany, the ratios were calculated for our samples. The relative contribution of particulate carbon in air from wood combustion was determined in 7 samples from Elverum by the isotopic ratio $^{14}C/^{12}C$; the average result is given.

Comparison of the results in Table 4 shows that there is satisfactory agreement between three of the estimated results in Elverum. The result obtained by using the IP/PghiPe ratio is obviously too high. The average ratio in air samples collected at this station was 1.15. Lahmann et al. [5] also found that the ratio exceeded 0.90 in winter and suggested that the types of fuel used and sources other than heating and traffic influenced the PAH profiles as well as the ratio of the two compounds. There is good agreement between the estimated results for Aurskog given the probable uncertainties in the initial data. The calculations based on consumption and emission factors were made for the entire Oslo area [16]; as expected, the relative contribution from domestic heating at the street station was less than the influence from heating averaged over the Oslo area (Table 4). At Nordahl Brunsgate, the ratio IP/BghiPe yielded a result that was only 10% lower than the one obtained by cluster analysis. This ratio at St. Olavsgate was 0.35, indicating no PAH from heating although this station did receive pollutants from

TABLE 4

Relative contribution of PAH from domestic heating at four monitoring stations

Station	Relative contribution (%)			
	A[a]	B[b]	C[c]	D[d]
Elverum	88	95	>100	90
Aurskog	97		100	
Nordahl Brunsgate	60	35—55	50	
St. Olavsgate	30		0	

[a]Estimated by FCV. [b]Estimates based on consumption of fuel and emission factors [15, 16]. [c]Estimated from the ratio indeno(1,2,3-cd)pyrene/benzo(ghi)perylene [5]. [d]Contribution of wood carbon estimated by the ratio $^{14}C/^{12}C$.

domestic heating; accordingly, the contribution from heating obtained by this ratio seems to be too low.

Lead is a good tracer for motor vehicles, and the concentrations of this pollutant were measured in Elverum and Oslo. The results from a regression analysis for lead and total PAH showed little correlation in Elverum (correlation coefficient $r = 0.57$); r was 0.83 and 0.82 in Nordahl Brunsgate and St. Olavsgate, respectively. The average ratios between lead and total PAH indicated that the contribution of PAH from traffic relative to the total contribution in Elverum was about 25% of the relative contribution in Oslo; the relative contributions from traffic at the two Oslo stations could not be distinguished by using these ratios [16].

CONCLUSIONS

The control of hazardous pollutants in urban air depends on a good understanding of the origins and fate of the compounds. Reliable source identification is therefore essential, and several dispersion and receptor models have been developed. Dispersion models rely on information about emission rates, stack parameters and meteorological conditions, and are commonly used when such information is available. In many cases, emission data are difficult to obtain and receptor models based on air quality measurements have become alternatives for source allocation. In the case of organic pollutants, source allocation has proved to be particularly difficult. The main aim of this study was to find a practical solution to this problem.

The results show that the FCV algorithms can be useful in a receptor model which identifies the major combustion sources of PAH in air and estimates their contributions to air pollution. These investigations demonstrate that this method leads to valid results.

The FCV algorithms have several advantages over other methods. First, the computation can be done on the basis of the monitoring data only, without knowledge of emission inventories. Secondly, FCV can be used for unsupervised pattern recognition. In this mode, the compositions of the variables in air samples exposed to the individual sources need not be known prior to data processing. Unsupervised pattern recognition is therefore useful when the composition of the pollutants emitted by a source is unknown and when the individual compounds are unstable during transport from the source to the sampler. In air pollution studies of PAH, these problems are acute, because the PAH composition varies from one source to another within the same source type, depending on the combustion conditions, and decomposition of PAH can occur on exposure to light and air. Provided that there is a difference in the compositions (patterns) of air pollutants from the sources and that some of the samples selected for the cluster analysis contain pollutants typical for these sources, the FCV program can find these patterns and divide the data samples into clusters. These clusters can be traced back to the appropriate sources from knowledge of position of the source, meteorological conditions, topography of the environment or the concentration of tracer

elements [9, 11]. Thirdly, when the FCV technique yields clusters that can be associated with sources, the prototype (centre) of each cluster will indicate a composition that is typical for the source related to that cluster. Thus information on the PAH composition in air samples from the various sources can be obtained and the largest emitters of the most hazardous PAH components can be identified. The FCV algorithms are powerful tools in the difficult studies of organic air pollutants, and their use can supplement, support and in some cases replace other methods.

The authors are grateful to Mr. S. Larssen and Mr. J. Schjoldager for making the data available for this study.

REFERENCES

1 J. M. Daisey, M. A. Leyko and T. J. Kneip, in P. W. Jones and P. Leber (Eds.), Polynuclear Aromatic Hydrocarbons, Ann Arbor Science Publishers, Ann Arbor, 1979, p. 201.
2 P. S. Pedersen, J. Ingwersen, T. Nielsen and E. Larsen, Environ. Sci. Technol., 14 (1980) 71.
3 J. M. Daisey, in Receptor Models Applied to Contemporary Pollution Problems, Air Pollution Control, Pittsburg, 1982, p. 348.
4 S. K. Friedlander, in Proceedings of the 2nd International Conference on Carbonaceous Particles in the Atmosphere, Linz, Sept., 1983, Paper No. 2, Institut für Analytische Chemie, Wien, 1983.
5 E. Lahmann, B. Seifert, L. Zhao and D. Bake, Staub-Reinhalt. Luft, 44 (1984) 149.
6 J. R. Cretney, H. K. Lee, G. J. Wright, W. H. Swallow and M. C. Taylor, Environ. Sci. Technol., 19 (1985) 397.
7 A. Greenberg, F. Darack, R. Harkov, P. Lioy and J. Daisey, Atmos. Environ., 19 (1985) 1325.
8 P. Masclet, G. Mouvier and K. Nikolaou, Atmos. Environ., 20 (1986) 439.
9 K. E. Thrane and L. Wikström, in M. Cook and A. J. Dennis (Eds.), Polynuclear Aromatic Hydrocarbons: Mechanisms, Methods and Metabolism, Columbus, Ohio, 1984, p. 1299.
10 R. W. Gunderson and K. E. Thrane, in J. J. Breen and P. E. Robinson (Eds.), Environmental Applications of Chemometrics, ACS symposium series 292, Washington, DC, 1985, p. 130.
11 K. E. Thrane, Atmos. Environ., (1987) in press.
12 J. C. Bezdek, C. Coray, R. W. Gunderson and J. D. Watson, SIAM J. Appl. Math., 40 (1981) 339, 358.
13 K. E. Thrane, A. Mikalsen and H. Stray, Int. J. Environ. Anal. Chem., 23 (1985) 111.
14 T. Ramdahl, Nature, 306 (1983) 580.
15 M. Møller, T. Ramdahl, I. Alfheim and J. Schjoldager, Environ. Int., 11 (1985) 189.
16 B. Sivertsen, The Relative Contribution of Air Pollutants from Various Sources to Man and Environment, Final Report — MIL 4. Norw. Inst. Air Research OR 41/85, Lillestrøm, 1985.

Analytica Chimica Acta, 191 (1986) 319—330
Elsevier Science Publishers B.V., Amsterdam — Printed in The Netherlands

ANALYSE TOPOLOGIQUE DU COMPORTEMENT D'ESTERS ALIPHATIQUES SATURÉS ET INSATURÉS EN CHROMATOGRAPHIE GAZ-LIQUIDE

J. R. CHRETIEN* et K. SZYMONIAK

Laboratoire de Chimie Analytique Industrielle et Chimiométrie, Université d'Orléans, B.P. 6759, 45067 Orléans Cédex 2 (France)
Institut de Topologie et de Dynamique des Systèmes, associé au C.N.R.S., Université Paris VII, 1, rue Guy de la Brosse, 75005 Paris (France)

(Reçu le 28 mai 1986)

SUMMARY

(*Topological analysis of the gas-liquid chromatographic behaviour of saturated and unsaturated aliphatic esters.*)

Topological analysis is applied to the Kovats retention indices for a collection of aliphatic esters on six stationary phases. Three subclasses are treated separately: (1) 100 saturated esters; (2) 45 esters unsaturated in the acidic part and 53 saturated but topologically similar esters; (3) 24 esters unsaturated in the alcohol moiety and 6 saturated but topologically similar esters. A detailed study is reported for the correlation of structural effects with numerical data for the specific solute/stationary phase interactions at the level of carbon atoms and ethylenic double bonds. The roles of the carboxylic ester nucleus, the branching and lengthening of the chain and the presence of ethylenic double bonds is elucidated. The selectivity of trifluoropropyl- and phenyl-bonded stationary phases is clarified.

RÉSUMÉ

L'analyse topologique a été appliquée aux indices de rétention, d'une population d'esters aliphatiques analysés sur six phases stationnaires. Trois sous-populations de composés ont été traitées séparément: la première comporte 100 esters saturés, la deuxième 45 esters insaturés dans la partie acide et 53 esters saturés isotopologues, et la troisième 24 esters insaturés dans la partie alcool et 6 esters saturés isotopologues. Une analyse très fine des effets de structure avec quantification des interactions spécifiques soluté-phase stationnaire, au niveau des atomes de carbone et des doubles liaisons éthyléniques a été effectuée. Le rôle du foyer ester carboxylique, des ramifications, de l'allongement de chaîne et de la présence de doubles liaisons éthyléniques a été déterminé. La spécificité de deux phases stationnaires particulières QF1 et 100% PHENYL est dégagée.

L'avantage des techniques chromatographiques est la possibilité d'obtenir relativement facilement des séries de données, pour une même série de composés, en variant les conditions expérimentales et notamment la nature de la phase stationnaire. Mais l'exploitation du contenu informationnel de

0003-2670/86/$03.50

ces matrices de données de rétention chromatographiques, aussi bien en phase gazeuse qu'en phase liquide, pose le problème de disposer de méthodes chimiométriques adaptées et performantes pour atteindre l'objectif souhaité. Ainsi, pour éclairer les mécanismes de rétention et les interactions soluté/phase stationnaire nous avons développé l'analyse topologique [1, 2] aussi bien pour l'étude d'hydrocarbures [2—5] que d'esters [6]. Mais alors que les alcènes analysés en chromatographie gaz-solide sur résines échangeuses d'ions substitués par divers ions métalliques [4, 5] ou d'esters moyennement encombrés [6] montrent la prépondérance des effets stériques sur les effets polaires, par contre l'étude de nouveaux esters, très encombrés au voisinage du groupe carbonyle, a montré la prépondérance des effets électroniques sur les effets stériques [7, 8].

Aussi, dans le cadre d'une étude portant sur le développement des méthodes chimiométriques [2, 9—11] dans un but physico-chimique et analytique, nous avons recherché à développer la complémentarité des méthodes d'analyse factorielle et d'analyse topologique pour cerner l'intérêt et les limites maximales de possibilité d'utilisation de ces méthodes. En prenant les esters comme population modèle, ainsi que cela a été souvent fait en chimie organique physique, pour des études du type relation linéaire d'énergie libre (LFER) [12], par exemple, ou pour des études chromatographiques, nous avons entrepris de dégager la complémentarité entre méthode de classification ascendante hiérarchique (CAH) [13] analyse factorielle des correspondances (AFC) ou en composante principale (ACP) [14] et analyse topologique.

Le présent article aborde le dernier point, l'analyse topologique de la même population de 169 esters aliphatiques saturés [15] et insaturés [16] sur 6 phases stationnaires en vue de quantifier les interactions spécifiques, entre certaines sous-populations de ces solutés et certaines phases stationnaires, qui avaient été détectées par CAH, AFC ou ACP et d'obtenir l'analyse la plus fine possible de ces effets de structure.

PARTIE EXPERIMENTALE

Nous avons utilisé les données de rétention en chromatographie en phase gazeuse d'Ashes et Haken [15, 16] pour une population de 169 esters aliphatiques comportant 100 esters saturés et 69 esters insaturés. Les indices de Kovats de ces esters ont été déterminés sur six phases stationnaires (Tableau 1) en utilisant des colonnes (3.66 m de long, 5 mm de diamètre intérieur), remplie avec 10% de celaton silanisé (67—72 mesh) lavé à l'acide.

La méthode DARC-PELCO (perturbation d'un environnement limité concentrique et ordonné) a été développée par Dubois et al. [17]. C'est une méthode de recherche de corrélation entre la structure d'un composé et la propriété qui lui est associée. Ces corrélations de topologie/information permettent d'estimer les effets de substitution de sites localisés dans un environnement limité concentrique ordonné (ELCO) limité à deux couches

TABLEAU 1

Caractéristiques des phases stationnaires utilisées

Symbole utilisé	Dénomination commerciale	Substitution des méthyles
SE3	SE-30	
DC5	DC-530	6% aminoalkyl
PHE	100% phenyl	100% phenyl
QF1	QF1	50% trifluoropropyle
SIL	SILAR-5CP	50% phenyl + 50% cyanoethyle
XF1	XF1-1150	50% cyanoethyle

concentriques d'atomes. Les principes de cette méthode ont été présentés par ailleurs pour ses applications chromatographiques qui ont été développées dans un but analytique ou physico-chimique [1—6]. Cette méthode a été appliquée également avec succès en pharmacochimie [18] et en spectroscopie [19].

L'information relative à un ELCO est générée successivement par l'adjonction progressive à l'environnement antérieur des sites topologiques et chromatiques. Pour exprimer l'information $I(X)$ relative à un composé X, on utilise la relation

$$I(X) = I(X_0) + \int_{X_0}^{X} \vec{I}\, \mathrm{d}\, \vec{\tau}$$

où X_0 est le composé de référence, composé dont l'environnement du foyer est constitué d'atomes d'hydrogène, $\mathrm{d}\tau$ est la différentielle topologique. Elle exprime un modification structurale à laquelle est associée une variation d'information d I, $\vec{I}$ est le vecteur d'information ayant les composantes $p(s_1)$, $p(s_2)$, . . . $p(s_n)$ qui expriment les perturbations liées à l'introduction progressive des sites s_1, s_2, . . . s_n.

La Fig. 1 montre la variation progressive de l'environnement pour un ensemble de dix esters aliphatiques R—COO—R′ dérivés du formiate de méthyle, pris comme foyer. A chaque composé est associé un graphe dont les noeuds correspondent aux sites topologiques. La superposition des graphes donne la trace de la série (Fig. 1a). Deux directions de développement apparaissent: DD_1 et DD_2 qui correspondent respectivement à la description de la partie alcool (R′) et de la partie acide (R) de l'ester. Chaque site (s_i) est localisé dans l'ELCO (E^1, E^2 . . .) et identifié par A_i et B_{ij} (Fig. 1b).

Ce système permet d'exprimer d'une manière précise et univoque la structure des molécules et de relier une grandeur physique quelconque à cette structure. Les valeurs des sites calculées à partir de l'ensemble des individus de la population sont pondérées à l'aide d'un programme de régression multiple. Les corrélations de topologie/information ainsi obtenues peuvent être

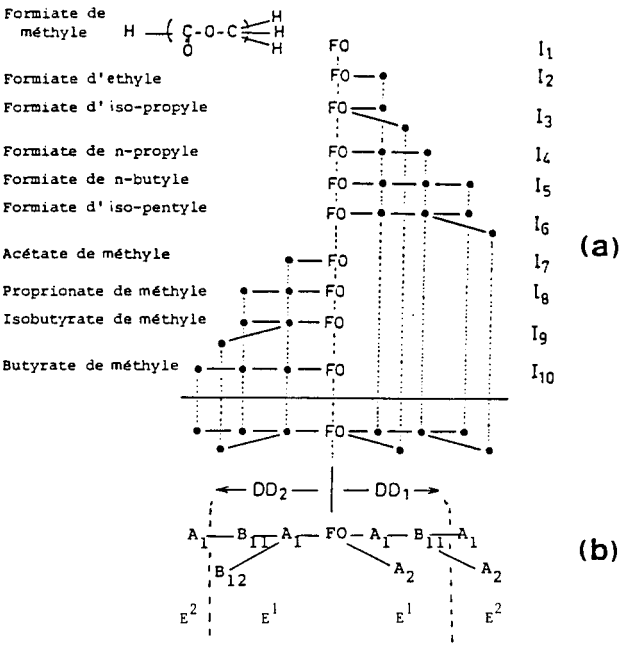

Fig. 1. (a) Trace d'une série: superposition des graphes élémentaires d'une série de 10 esters aliphatiques dérivés du formiate de méthyle, pris comme foyer. (b) Organisation de l'ELCO autour du foyer, pour cette série.

exploitées dans un but physico-chimique ou analytique, elles permettent de prévoir, dans ce dernier cas, le comportement de composés nouveaux.

RESULTATS ET DISCUSSION

Parmi la population de 169 esters aliphatiques nous distinguerons trois ensembles: le premier comporte 100 esters saturés; le deuxième 45 esters insaturés dans la partie acide et 53 esters saturés isotopologues, et le troisième ensemble comporte 24 esters insaturés dans la partie alcool et 6 esters saturés isotopologues. A chacun de ces ensembles correspond une empreinte ou trace. La trace de l'ensemble des 100 esters saturés est présentée à la Fig. 2.

Les contributions à l'information de tous les sites topologiques calculés pour les six phases stationnaires indiquées au Tableau 1, sont présentées sous la forme d'incréments dans le diagramme de topologie/information de la Fig. 3. La première valeur supérieure indique la contribution τI des sites sur la phase stationnaire SE-30. Les valeurs situées au-dessous indiquent les contributions supplémentaires $\tau(\Delta I)$ qui expriment les interactions spécifiques, par rapport à la phase SE-30 prise comme référence, des autres phases stationnaires à savoir, successivement et de haut en bas: PHE, QF1, SIL, XF1

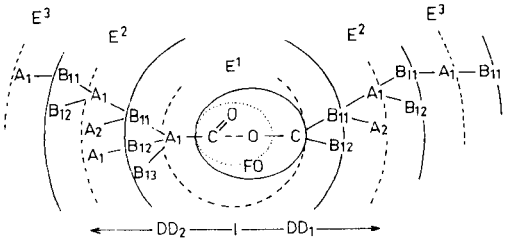

Fig. 2. Trace de l'ensemble des 100 esters saturés.

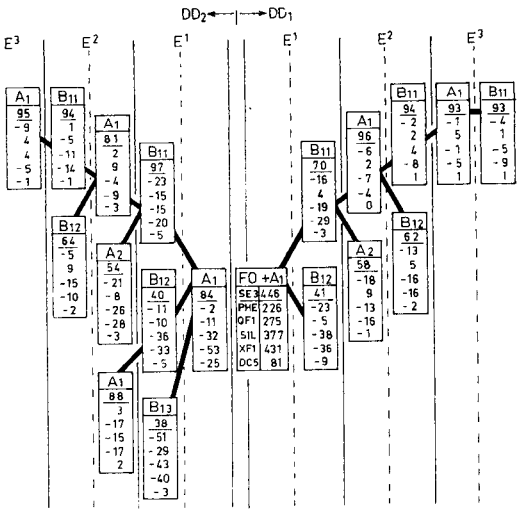

Fig. 3. Diagramme de topologie/information: interactions spécifiques calculées pour 100 esters saturés sur les différentes phases stationnaires. La première valeur encadrée est une contribution τI de site sur SE-30 et les valeurs situées au-dessous sont les contributions supplémentaires $\tau(\Delta I)$ sur les diverses phases indiquées (PHE, QF1, SIL, XF1, DC5).

et DC5. L'examen de cette figure montre que la contribution du foyer FO s'accroît linéairement avec l'augmentation de la polarité des phases stationnaires exprimées par le paramètre de polarité de McReynolds $\Sigma_1^5 \Delta I$ [20]. La corrélation correspondante est FO = 0,19 ($\Sigma_1^5 \Delta I$) + 393 avec un coefficient de corrélation $r = 0.98$.

Pour les phases stationnaires les plus polaires (XF1, SIL), les contributions du foyer sont de 800 environ, tandis que pour les phases peu polaires (SE3, DC5) elles sont de l'ordre de 400—500 (Tableau 2). Par contre, les contributions des sites adjacents au foyer diminuent avec l'augmentation de la polarité des phases stationnaires. La diminution des valeurs des sites est plus importante pour A_1 (E^1, DD_2) du côté acide (—32 sur SIL, —53 sur XF1) que pour le site B_{11} (E^1, DD_1) du côté alcool (—29 sur XF1, —19 sur SIL) toujours en prenant le comportement sur la phase SE-30 comme base de référence. Par contre, les sites B_{12} (E^1, DD_1) et B_{12} (E^1, DD_2) ont des

TABLEAU 2

Contribution du foyer ester carboxylique et paramètre de polarité de McReynolds pour six phases stationnaires, exprimées en indices de Kovats

Phase stationnaire	SE3	DC5	PHE	GF1	SIL	XF1
Contribution du foyer	446	527	672	719	823	877
Polarité generale des phases	219	781	1552	1483	2432	2438

valeurs très similaires: −36, −33 sur XF1, et −38, −36 sur SIL. La ramification autour du foyer des esters accélère l'élution.

Tous ces effets sont illustrés à la Fig. 4. Nous constatons que les esters ramifiés ont un comportement particulier vis-à-vis de QF1. Pour les sites correspondant aux ramifications, aussi bien dans la partie alcool (DD_1) que dans la partie acide (DD_2), soit pour les sites B_{12} (E^1), A_2 (E^1), B_{12} (E_2) et B_{13} (E^1, DD_2) toutes les contributions sur la phase QF1 sont supérieures aux contributions sur les phases XF1, SIL et PHE de 20 à 30. Les contributions des sites plus éloignés du foyer qui prennent en compte l'allongement de chaîne deviennent pratiquement constantes à partir du deuxième environnement (E^2), c'est-à-dire pour le carbone γ dans la partie alcool et le carbone δ dans la partie acide. Elles sont de l'ordre de 90 par groupe méthylénique (Fig. 4). La nature des phases stationnaires ne joue qu'un rôle très faible pour ces sites.

Le deuxième ensemble de composés considéré est constitué de 45 esters

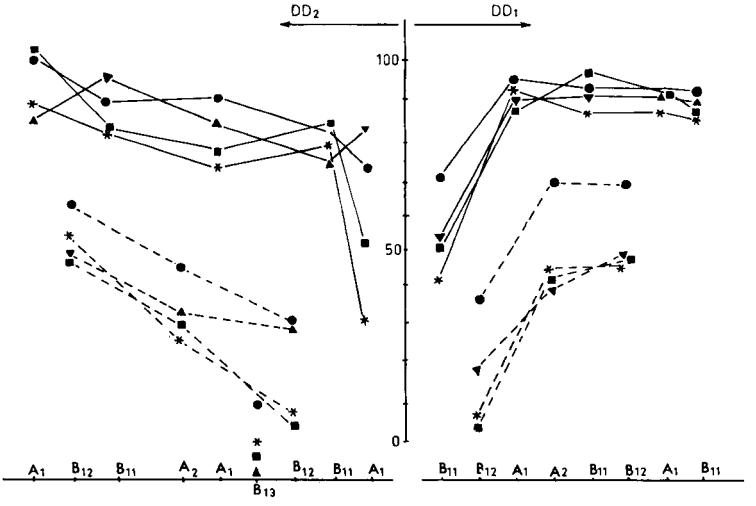

Fig. 4. Illustration graphique des contributions des sites topologiques τI des esters saturés calculées pour les phases stationnaires: (●) QF1; (▲) PHE; (■) SIL; (*) XF1. (- - - -) Ramification; (——) allongement.

aliphatiques insaturés dans la partie acide (DD_2) et de 53 esters saturés isotopologiques dont la présence permet de calculer les contributions des doubles liaisons éthyléniques. Sa trace est donnée à la Fig. 5. Les contributions des sites topologiques du côté acide, calculées pour les mêmes phases stationnaires que précédemment, sont présentées sous la forme d'incréments τ (ΔI), à la Fig. 6. Par rapport à la phase SE-30, les contributions de tous les sites, sauf le site A_1 (E^2, DD_2), diminuent sur les autres phases stationnaires. Par contre, les contributions τ (ΔI) du site A_1 (E^2, DD_2) sont positives pour la plupart, les valeurs les plus élevées sont observées sur QF1 (26) et sur SIL (19).

Les contributions topologiques τI calculées pour les phases QF1, PHE, SIL et XF1 sont données à la Fig. 7. Le graphique montre la particularité de QF1 pour les esters ramifiés. La contribution de B_{12} (E^1, DD_2) sur QF1 est de 58, elle est supérieure à celle sur SIL et QF1 de 25 environ. Pour le site A_2 (E^2, DD_2), plus éloigné du foyer, la contribution descend à 38, alors que nous n'avons pas observé de diminution dans les autres cas.

Les différences $\delta(\tau I)$ entre les contributions des sites topologiques des esters insaturés et saturés sont présentées à la Fig. 8: $\delta(\tau I) = \tau I_{insat} - \tau I_{sat}$. La grandeur $\delta(\tau I)$ indique donc les variations de grandeur de rétention apportée par la double liaison éthylénique dans les esters. L'examen de ces grandeurs montre une augmentation des contributions des sites A_1 (E^2, DD_2) et B_{12} (E^1, DD_2) par rapport aux esters saturés. Ainsi pour A_1 (E^2, DD_2) les écarts δ (τI) sont: de 53 sur SIL, de 46 sur XF1, de 47 sur QF1 et de 7 sur PHE. L'augmentation de contribution du site B_{12} (E^1, DD_2) pour toutes les phases stationnaires, par rapport à la phase SE-30 est de l'ordre de 20—30. Ce phénomène est interprétable en terme d'effets électroniques et stériques. La présence des sites A_1 (E^2, DD_2), A_2 (E^2, DD_2) et B_{12} (E^1, DD_2) renforce la conjugaison et facilite les interactions avec la phase stationnaire, ce qui retarde l'élution. Le rôle des effets stériques est moins important ici que pour les esters saturés en raison de l'hybridation sp^2 et de la planéité du motif structural. L'augmentation de la contribution des sites adjacents à la

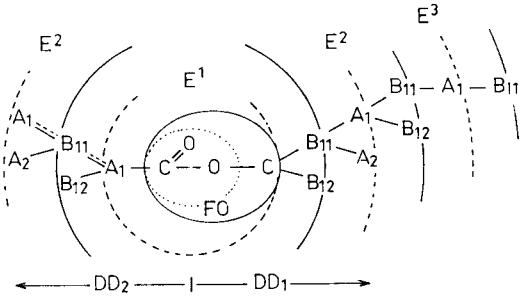

Fig. 5. Trace de l'ensemble des 45 esters insaturés dans la partie acide et des 53 esters saturés isotopologiques.

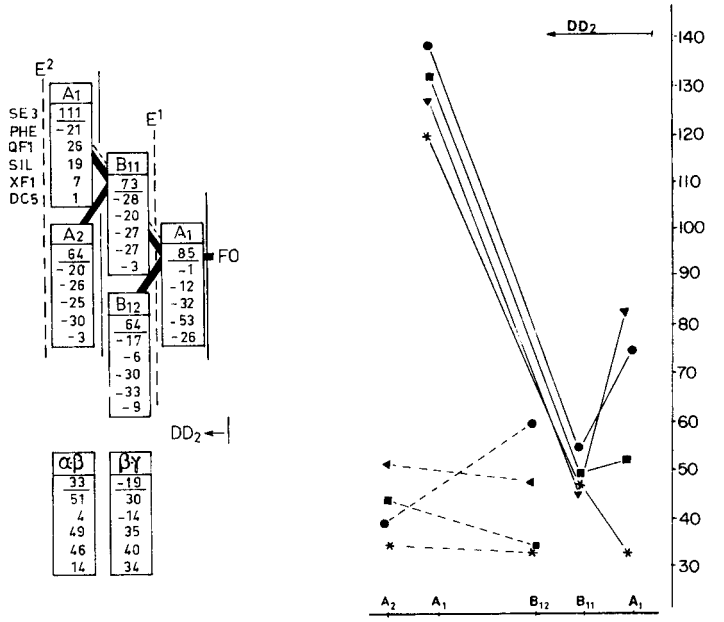

Fig. 6. Diagramme de topologie/information: interactions spécifiques calculées pour l'ensemble de 45 esters insaturés et 53 esters saturés isotopologiques pour la deuxième direction de développement (DD_2). La première valeur encadrée est la contribution τI des sites et des doubles liaisons α—β et β—γ sur SE-30. Les valeurs situées au-dessous sont les contributions supplémentaires $\tau(\Delta I)$ sur les diverses phases stationnaires indiquées.

Fig. 7. Diagramme de topologie/information: illustration graphique des contributions des sites topologiques pour la deuxième direction de développement (DD_2) des esters insaturés, calculés pour les phases stationnaires: (●) QF1; (▲) PHE; (■) SIL; (*) XF1. (- - - -) Ramification; (——) allongement.

double liaison a été observée déjà dans le cas des alcènes [2]. Par contre, pour le site B_{11} (E^1, DD_2) on remarque une diminution des contributions par rapport aux contributions des esters saturés. Les écarts δ (τI) sont tous négatifs et varient de —22 sur DC5 à —36 sur XF1.

L'examen du troisième ensemble, constitué des esters insaturés dans la partie alcool (DD_1) permet de comparer les contributions des doubles liaisons présentes dans la partie acide et alcool. Elles sont indiquées au Tableau 3 et sur les schémas de la Fig. 9. Toutes les contributions des doubles liaisons α—β dans la partie acide des esters insaturés sont plus fortes que les contributions des liaisons β—γ et γ—δ dans la partie acide ou alcool. Ceci s'explique par la conjugaison de la double liaison α—β avec le groupe carbonyle qui favorise l'interaction avec la phase stationnaire. Elles sont de l'ordre de 80 pour PHE, SIL, XF1. Les contributions des doubles liaisons non conjuguées sont inférieures aux contributions des liaisons α—β de 50 environ. Elles ont même des valeurs négatives pour les phases QF1 (de —18 à —33) et SE-30 (de —5 à —19). Pour la phase PHE les contributions de toutes

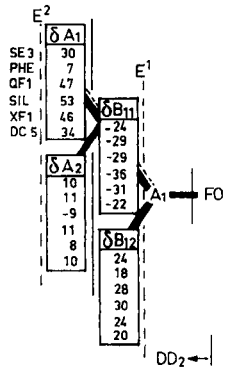

Fig. 8. Différences entre les contributions des sites topologiques des esters insaturés et saturés: $\delta(\tau I) = \tau I_{insat} - \tau I_{sat}$. La figure présente la deuxième direction de développement (DD_2) où les incréments sont significatifs.

TABLEAU 3

Contribution des doubles liaisons éthyléniques et paramètre de polarité de McReynolds pour six phases stationnaires[a]

Double liaison	XF1	SIL	QF1	PHE	DC5	SE3
Acide C=C α—β	79	82	37	84	47	33
Acide C=C β—γ	21	16	—33	11	15	—19
Alcool C=C β—γ						
cis	20	28	—27	29	2	—5
trans	19	23	—22	39	7	—3
Alcool C=C γ—δ						
cis	6	13	—18	31	1	—5
trans	25	25	—25	28	—4	—11
Polarité	2438	2432	1485	1552	781	219

[a]Tableau 1.

les doubles liaisons sont supérieures aux autres phases. Une formation de complexe à transfert de charge entre le noyau aromatique de la phase stationnaire et la double liaison C=C des esters insaturés est envisageable. Pour la double liaison γ—δ les contributions *trans* sont en général plus fortes que les contributions *cis*, 19 sur XF1 par exemple. La comparaison des contributions des doubles liaisons avec le paramètre de polarité de McReynolds des phases stationnaires montre leur relative indépendance (Fig. 9). Par contre, la nature de la phase stationnaire peut jouer un rôle prépondérant

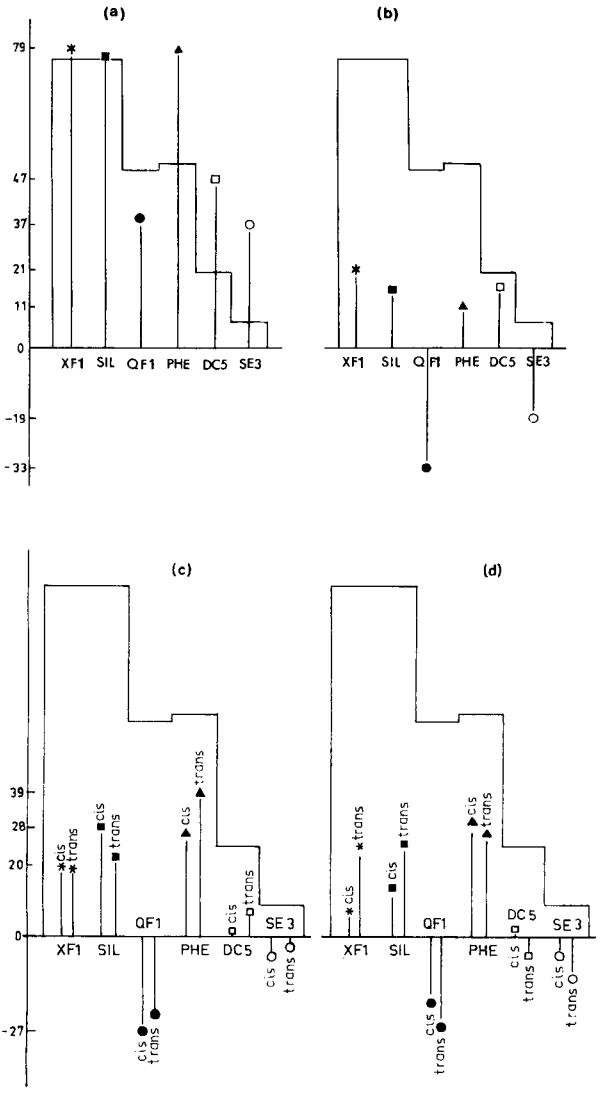

Fig. 9. Contributions des doubles liaisons superposées avec les variations de la polarité des phases stationnaires exprimées par le paramètre de McReynolds: (a) partie acide, doubles liaisons α—β; (b) partie acide, doubles liaisons β—γ; (c) partie alcool, doubles liaisons *cis* et *trans* β—γ; (d) partie alcool, doubles liaisons *cis* et *trans* γ—δ.

dans les contributions des doubles liaisons. C'est, en particulier, le cas de QF1 pour les doubles liaisons β—γ et γ—δ (Fig. 9b—d) ou PHE pour la liaison conjuguée α—β (Fig. 9a).

CONCLUSION

L'analyse factorielle et la classification ascendante hierarchique appliquée par ailleurs à la même population d'esters ont démontré la spécificité des phases QF1 et PHE vis-à-vis de la double liaison éthylénique, aussi bien dans la partie acide que dans la partie alcool, ou vis-à-vis des ramifications.

L'analyse topologique présentée ici permet une analyse fine des effets de structure, elle offre une quantification de ces effets au niveau des sites topologiques. Ainsi nous pouvons dégager les points suivants ayant trait successivement à la contribution du foyer ester, des ramifications, de l'allongement de chaine et des doubles liaisons éthyléniques. La contribution du foyer croît linéairement (r = 0,98) avec la polarité des phases stationnaires exprimée avec le facteur de polarité de McReynolds. Les contributions des sites adjacents au foyer diminuent avec l'augmentation de la polarité des phases (de —53 sur XF1 par rapport au comportement sur SE-30 pour le site A_1 (E^1, DD_2), par exemple). La ramification autour du foyer accélère l'élution. Cependant, sur QF1, les contributions des sites responsables de la ramification sont supérieures de 20 par rapport aux autres phases stationnaires. La ramification autour des doubles liaisons du côté acide retarde l'élution par rapport aux esters saturés. Les contributions des sites sont supérieures de 20 à 30 pour B_{12} (E^1, DD_2) et de 10, environ, pour A_2 (E^2, DD_2), par rapport aux autres phases stationnaires.

Les contributions à l'allongement de chaîne se stabilisent à partir du deuxième environnement (E^2), et sont de l'ordre de 90 par groupe méthylénique, indépendemment de la nature de la phase stationnaire. Les contributions de la double liaison α—β sont plus fortes de 50 environ que les contributions des liaisons β—γ et γ—δ. Pour les phases QF1 et SE 30 les contributions des doubles liaisons β—γ et γ—δ sont négatives. Pour la phase PHE les contributions des doubles liaisons sont le plus souvent supérieures à celles observées sur les autres phases stationnaires. Pour la double liaison γ—δ les contributions *trans* sont, en général, plus fortes que les contributions *cis* (de 5 à 19).

BIBLIOGRAPHIE

1 J. R. Chrétien et J. E. Dubois, J. Chromatogr., 126 (1976) 171.
2 J. R. Chrétien et J. E. Dubois, Anal. Chem., 49 (1977) 747.
3 J. E. Dubois, J. R. Chrétien, L. Sojak et J. A. Rijks, J. Chromatogr., 194 (1980) 121.
4 J. R. Chrétien, J. E. Dubois, R. F. Hirch et R. J. Gaydosh, J. Chromatogr., 207 (1981) 115.
5 J. R. Chrétien, K. Szymoniak, J. E. Dubois, R. F. Hirch et R. J. Gaydosh, J. Chromatogr., 294 (1984) 1.
6 J. R. Chrétien et J. E. Dubois, J. Chromatogr., 158 (1978) 43.
7 J. K. Haken, J. R. Chrétien et C. Lion, J. Chromatogr., 217 (1981) 125.
8 J. R. Chrétien, K. Szymoniak, C. Lion et J. K. Haken, J. Chromatogr., 324 (1985) 355.
9 R. F. Hirsch, R. J. Gaydosh et J. R. Chrétien, Anal. Chem., 52 (1980) 723.
10 B. Walczak, M. Dreux, J. R. Chrétien, K. Szymoniak, M. Lafosse, L. Morin-Allory et J. P. Doucet, J. Chromatogr., 353 (1986) 109.

11 B. Walczak, J. R. Chrétien, M. Dreux, L. Morin-Allory, M. Lafosse, K. Szymoniak et F. Membrey, J. Chromatogr., 353 (1986) 123.
12 J. Shorter, Correlation Analysis in Organic Chemistry: an Introduction to Linear Free-Energy Relationships, Clarendon Press, Oxford, 1973.
13 K. Szymoniak et J. R. Chrétien, à paraître.
14 K. Szymoniak et J. R. Chrétien, à paraître.
15 J. R. Ashes et J. K. Haken, J. Chromatogr., 101 (1974) 103.
16 J. R. Ashes et J. K. Haken, J. Chromatogr., 111 (1975) 171.
17 J. E. Dubois, D. Laurent et A. Aranda, J. Chim. Phys., 11—12 (1973) 1608.
18 C. Mercier, Y. Sobel et J. E. Dubois, Eur. J. Med. Chem., 16 (1981) 473.
19 J. E. Dubois et J. P. Doucet, Org. Magn. Reson., 11 (1978) 87.
20 W. O. McReynolds, J. Chromatogr. Sci., 8 (1970) 685.

Analytica Chimica Acta, 191 (1986) 331—350
Elsevier Science Publishers B.V., Amsterdam — Printed in The Netherlands

STATISTICAL EVALUATION OF THE GROUP STRUCTURES OF FIVE VENETIAN WINES FROM CHEMICAL MEASUREMENTS

I. MORET, G. CAPODAGLIO and G. SCARPONI*
Cattedra di Chimica Analitica, Universita' di Venezia, Venezia (Italy)
M. ROMANAZZI
Laboratorio di Statistica, Universita' di Venezia, Venezia (Italy)
(Received 26th May 1986)

SUMMARY

Exploratory statistical methods are used to elucidate the group structures pertaining to a chemical data set obtained from 184 samples of five typical white wines from the Venetian Region: Soave Classico, Prosecco di Conegliano-Valdobbiadene, Verduzzo del Piave, Tocai di Lison, Tocai delle Grave del Friuli. Analytical data included 19 classical parameters and 9 aroma components. Correlation matrices showed that the same three sets of intercorrelated variables were present in all the groups, and that aroma components were nearly uncorrelated with classical parameters. Principal components analysis allowed a subspace of reduced dimensionality to be derived for each group. However, because of similar pattern of the correlation matrices, a high degree of similarity was also observed among the subspaces. An efficient differentiation of the groups was obtained by canonical variates analysis. The most important chemical parameters were potassium, ash content, total nitrogen, *cis*-3-hexen-1-ol and 1-hexanol. Classification of samples by the Euclidean distances from the centroids in the canonical space gave on average 94% correct results.

Some Venetian white wines have already been studied chemometrically with the aim of characterizing them and classifying samples of unknown origin from chemical information [1—8]. Some inorganic ions, a few higher alcohols and other classical parameters were determined and used as the chemical data. Fisher's linear discriminant functions and nearest-neighbor rules were applied to derive classification rules. Some preliminary work dealing with the use of aroma components and the application of the SIMCA (soft independent modelling of class analogy) method, were also published [7, 8].

In the work described here, samples from two more vintage years (1982 and 1983) were analysed both for classical and aroma parameters, and a new type of wine (Tocai delle Grave del Friuli) was included in the study. Thus, the data set is far more extensive than the previous ones, which should make it possible to give a synthetic description of the data by means of a small number of "factors" accounting for a high proportion of data variability, to explore the group structures in the data so as to establish potentially dis-

0003-2670/86/$03.50

criminant parameters, and to evaluate the importance of aroma parameters with respect to the classical ones, not only in data description but in characterization of the wines.

Because wines belonging to different vintages are included in the data set, attention will be given to the evaluation of year-to-year variations in the chemical measurements. As regards the statistical methods, an exploratory approach is adopted, i.e., the relevant information is drawn from the data without introduction of probabilistic models.

EXPERIMENTAL

Wine samples

The following 5 Venetian white wines were considered (the abbreviations used in the later text are given in parentheses): Soave Classico (Soave, S), Prosecco di Conegliano-Valdobbiadene (Prosecco, P), Verduzzo del Piave (Verduzzo, V), Tocai di Lison Classico (Tocai L., TL), Tocai delle Grave del Friuli (Tocai G., TG).

Samples from vintages of 1982 and 1983 (see Table 1) were collected in the production zones, from lots which were guaranteed to be typical by the Italian D.O.C. (Denominazione di Origine Controllata; Certified Brand of Origin) brand. The permitted grape varieties (all *Vitis Vinifera*) are: (i) for Soave [9], Garganega (70% minimum) and Trebbiano di Soave plus Trebbiano Toscano (30% maximum); (ii) for Prosecco [10], Prosecco (90% minimum) and Verdiso (10% maximum), but a maximum of 15% of the given mixture can be replaced by Pinot Bianco and/or Pinot Grigio and/or Chardonnay; (iii) for Verduzzo [11], Verduzzo Trevigiano and/or Verduzzo Friulano; (iv) for Tocai L. [12], Tocai Friulano (95% minimum) plus white grape (5% maximum); and (v) for Tocai G. [13], Tocai Friulano (90% minimum), Pinot Bianco and/or Pinot Grigio and/or Verduzzo Friulano (10% maximum). It should be noted that Tocai L. and Tocai G. only differ for production area.

Samples (collected in 750-ml bottles and stored at 3—4°C) were analysed for the following species and properties (abbreviations and concentration units are given in parentheses): sodium (mg l^{-1}); potassium (mg l^{-1}); calcium (mg l^{-1}); magnesium (mg l^{-1}); chloride (mg l^{-1}); pH; titratable acidity (TA, g l^{-1}, expressed as tartaric acid); phosphorus (given as mg l^{-1} P_2O_5); ash content (AC, g l^{-1}); alkalinity of the ash (ALA, meq l^{-1}); lithium (μg l^{-1}); total nitrogen (TN, mg l^{-1}); theoretical sugar-free dry extract (DE, g l^{-1}); absorbance measured at 420 nm (A); total phenols (TP, mg l^{-1}, expressed as (+)catechin); 1-propanol (POL, mg l^{-1}); 2-methyl-1-propanol (MPOL, mg l^{-1}); 2-methyl-1-butanol plus 3-methyl-1-butanol (MBOL, mg l^{-1}); higher alcohols (HOLS = POL + MPOL + MBOL, mg l^{-1}); 2-methyl-propanoic acid (MPA, mg l^{-1}); butanoic acid (BA, mg l^{-1}); 3-methylbutanoic acid (MBA, mg l^{-1}); hexanoic acid (HA, mg l^{-1}); octanoic acid (OA, mg l^{-1}), decanoic acid (DA, mg l^{-1}); 1-hexanol (HOL, mg l^{-1}); *trans*-3-hexen-1-ol (THOL, mg l^{-1}); *cis*-3-hexen-1-ol (CHOL, mg l^{-1}).

TABLE 1

Number of wine samples by type of wine and vintage year

Vintage year	Type of wine					Total
	Soave	Prosecco	Verduzzo	Tocai L.	Tocai G.	
1979[a]	—	19	—	—	—	19
1980[a]	8	14	—	10	—	32
1981[b]	10	—	18	11	—	39
1982[b]	11	12	16	10	18	67
1983[b]	—	12	—	—	15	27
Total	29	57	34	31	33	184

[a]Samples analysed for classical parameters only. [b]Samples analysed for classical and aroma parameters.

In the following sections, the first 19 determinations (i.e., from Na to HOLS) will be referred to as classical parameters, while the latter 9 (i.e., from MPA to CHOL) will be referred to as aroma parameters.

Classical determinations

Sodium, potassium and lithium were determined by flame emission spectrometry and calcium and magnesium by atomic absorption spectrometry. Phosphorus (according to Schneyder), chloride (according to Volhard), total nitrogen (according to Kjeldahl), theoretical sugar-free dry extract, absorbance (measured at 420 nm), total phenols (according to Folin-Ciocalteau), pH, titratable acidity, ash content and alkalinity of the ash were determined by classical procedures [14, 15]. A Perkin-Elmer 5000 atomic absorption spectrometer, a Perkin-Elmer 320 u.v.-visible spectrophotometer, and a Beckman 5000 pH-meter, were used.

1-Propanol, 2-methyl-1-propanol and 2-methyl-1-butanol/3-methyl-1-butanol were determined by gas chromatography after wine distillation with 2-pentanol as internal standard [5]. A gas chromatograph (Model 5790, flame ionization detector), an Ultra 2 cross-linked capillary column, and a Model 3390A integrator (all Hewlett-Packard) were used. Repeatabilities, expressed as relative standard deviations (RSD) from 5 measurements, were always less than 5%.

Determination of aroma compounds

The volatile aroma components were isolated by continuous liquid-liquid extraction with a pentane/dichloromethane mixture (2 + 1, v/v). 1-Heptanol, as internal standard, was added before the extraction. The aroma extracts were concentrated to 1 ml in a Vigreux column (45°C) and quantified by capillary gas chromatography [7, 16]. The above-mentioned gas chromatograph and integrator were used with a fused silica capillary column (50 m × 0.2 mm i.d.) coated with Carbowax 20 M. The compounds

were identified by comparing their retention times on dissimilar columns with those of authentic compounds; they had also been identified previously through comparison with reference compounds before and after fractionation of aroma extract on silica gel 60 [17]. Calibration factors (obtained by comparing the ratios of the component peak heights to the internal standard peak height, before and after addition of known quantities of the detected compounds) were used for quantification. Repeatability of the instrument response, obtained from 5 injections of the same solution (expressed as RSD of the ratioed peak heights) was better than 3%. Repeatability of calibration factors was between 5 and 10% for alcohols and between 10 and 25% for acids (RSD from 14 extractions). Repeatabilities of the ratios of the component peak height to the internal standard peak height, obtained from extractions of the same sample contained in different bottles, were between 2 and 5% for alcohols, and between 3 and 10% for acids.

In each case, before analyses of new samples, stability of measurements over time was checked by re-analysing some of the earlier samples. In this way, differences caused by possible analytical bias, were prevented.

Data set

The whole data set, obtained by joining data collected in this work with those obtained previously in this laboratory, can be divided in two subsets (see Tables 1 and 2). The first subset (which includes 51 samples of the wines Soave, Prosecco and Tocai L., vintages of 1979 and 1980), contains only measurements of the 19 classical parameters. The second subset (i.e., 133 samples of the wines Soave, Prosecco, Verduzzo, Tocai L. and Tocai G., vintages of 1981—1983) contains measurements of all 28 parameters. The vintages examined for the 5 wines are neither the same nor of the same number; moreover, vintage of 1982 is over-represented compared with the others (67 observations out of 184). As complete data are available only for vintages from 1981, the results of statistical analyses on the second subset suffer less from the different-vintage effect than those obtained with only the classical parameters, for which data from 1979 to 1983 are available. The number of observations on the classical parameters is higher than that for the aroma components.

These characteristics, which will be important in the evaluation of the results discussed below, suggested the choice of a descriptive-exploratory approach, different from that adopted in previous papers in which less extensive data sets were considered.

Statistical methods

The multivariate statistical methods used were principal components analysis (PCA), Krzanowski's method for evaluating the between-groups similarity of principal components, and the canonical variates technique.

Principal components analysis. This procedure [18, 19] was mainly used to achieve a reduction of dimensionality, i.e., to fit a k-dimensional subspace

to the original p-variate ($p \gg k$) observations. The analysis was applied separately to the correlation matrices of the 5 wines by the PRINCOMP routine of the IMSL library [20]. Correlation matrices were used instead of covariance matrices, because of the lack of homogeneity both in the measurement units and in the variances of parameters.

The statistics used to summarize the most important results were: (i) the proportion of the total variation explained by the first k principal components; (ii) the linear correlations between principal components and original variables; and (iii) the squared multiple correlation coefficients obtained from linear regression of each parameter on the first k principal components.

Krzanowski's method. The principal components obtained for the 5 wines were compared by the procedure suggested by Krzanowski [21]. An outline of the method for the general G groups problem is as follows. $\mathbf{L}_g$ is defined as $p \times k_g$ matrix; the columns are the first k_g characteristic vectors of the group g correlation matrix. D_g is defined as the vector subspace spanned by the column vectors of $\mathbf{L}_g$ ($g = 1, \ldots, G$). The configuration of subspaces $D_1, \ldots, D_G$ in the p-dimensional space can vary between two extreme situations; (i) a "maximum similarity" configuration, i.e., the subspaces are coincident; and (ii) a "maximum dissimilarity" configuration, i.e., the subspaces are orthogonal. To evaluate how much a given configuration differs from the maximum similarity one, a subspace D must be sought such that the sum $V = \sum_{g=1}^{G} \cos^2 \delta_g$ is a maximum, where δ_g is the angle formed by a vector $\mathbf{y}$ of D with its projection on D_g. An orthonormal basis for D is given by the vectors $\mathbf{y}_1, \ldots, \mathbf{y}_q$ corresponding to the characteristic roots $\alpha_1, \ldots, \alpha_q$ of the matrix $\mathbf{H} = \sum_{g=1}^{G} \mathbf{L}_g \mathbf{L}_g^t$ and $q = \min(k_1, \ldots, k_G)$. The comparison of the subspaces $D_1, \ldots, D_G$ is based on $\alpha_1, \ldots, \alpha_q$ and $\mathbf{y}_1, \ldots, \mathbf{y}_q$. It can be shown that $\alpha_i = \sum_{g=1}^{G} \cos^2 \delta_{gi}$, where δ_{gi} is the angle formed by $\mathbf{y}_i$ with its projection on D_g. It follows that $0 \leqslant \alpha_i \leqslant G$; $\alpha_i = 0$ when $\mathbf{y}_i$ is orthogonal to $D_1, \ldots, D_G$ and $\alpha_i = G$ when the projections of $\mathbf{y}_i$ on $D_1, \ldots, D_G$ coincide with the vector $\mathbf{y}_i$ itself. The vectors $\mathbf{y}_1, \ldots, \mathbf{y}_q$ are referred to the original axes, so that they can be compared with the characteristic vectors of the correlation matrices and can be interpreted as the "average directions" that agree most closely with all G sets of characteristic vectors.

Canonical variates analysis. The use of PCA as a dimension-reducing technique, preliminary to the examination of clustering effects in the data, is recognized to be fallible [22, 23]. Canonical variates analysis (CVA) is a different method, particularly designed for this purpose and unaffected by these criticisms [24].

First, $\mathbf{W}$, $\mathbf{B}$ and $\mathbf{T}$ are defined as the "within-groups", the "between-groups" and the overall sums of squares and cross-products matrices, respec-

tively, after correction for the mean. CVA looks for linear combinations of original measurements such that the ratio of between-groups variance to total variance is maximized. If $\mu_1 \geqslant \mu_2 \geqslant \ldots \geqslant \mu_q$ and $\mathbf{c}_1, \ldots, \mathbf{c}_q$ denote the characteristic roots and vectors of the matrix $\mathbf{T}^{-1}\mathbf{B}$, the vector of canonical variates $\mathbf{v} = (v_1, \ldots, v_q)^t$ of an observation $\mathbf{x} = (x_1, \ldots, x_p)^t$ is given by the transformation $\mathbf{v} = \mathbf{C}^t\mathbf{x}$, where the columns of the $p \times q$ matrix $\mathbf{C}$ are the characteristic vectors $\mathbf{c}_1, \ldots, \mathbf{c}_q$ and $q = \text{rank}\,(\mathbf{T}^{-1}\mathbf{B}) \leqslant \min(p, G-1)$. The characteristic roots and vectors of the matrix $\mathbf{T}^{-1}\mathbf{B}$ were computed by the ODFISH routine of the IMSL library [20]; the $\mathbf{c}_i$ vector were normalized by $\mathbf{c}_i^t\mathbf{S}_w\mathbf{c}_i = 1$, $i = 1, \ldots, q$, where $\mathbf{S}_w$ is the pooled within-groups covariance matrix of the observations.

The evaluation of each canonical variate can be based on the corresponding characteristic root μ_i, because this value is the ratio of the between-groups variance to the total variance for the same variate. Thus, one can consider only the first k canonical variates for which these ratios appear high enough. As in PCA, linear correlations between canonical variates and original measurements may give an interpretation of the group structure, whereas scatter plots of data points on the first 2—3 canonical variates will be helpful for examining the degree and nature of the separation of groups. In the study of these plots, the Euclidean distance will be used for assessing interpoint distances, as the pooled within-groups covariance matrix of the canonical variates is the identity matrix.

RESULTS AND DISCUSSION

Univariate distributions

Table 2 gives the means and the minimum and maximum values for all the variables with standard deviations and relative standard deviations (RSD). Comparison of the RSD indicates that the scatter about the mean of aroma parameters is generally higher than that of classical parameters. Major variations are observed for Na, Cl, A and TP among the classical parameters, and for DA, THOL and BA among the aroma parameters.

To evaluate the importance of each parameter in differentiating the groups, the ratio of between-groups variance to total variance was computed for all the variables (Table 3). It is clear from the results that parameters CHOL, HOL, TN and K have the highest values of this ratio (0.73, 0.47, 0.37 and 0.34, respectively). In particular, the concentration of CHOL increases significantly in the order Soave < Prosecco < Verduzzo < Tocai G. < Tocai L., so that it appears very effective in separating wine samples of different types (Fig. 1). The concentrations of K and TN in the Soave samples are notably different from those in the other wines, and HOL separates both Soave and Tocai L. from the other groups. Of the variables with overlapping distributions in the 5 groups, TA and Mg for classical parameters and BA for aroma parameters should be noted (Fig. 1).

Several variables show a tendency to spread as the concentration increases

(this feature is well documented, e.g., for CHOL and K, in the box plots in Fig. 1) and some have asymmetric and/or leptokurtic distributions. These results, although some high values of the skewness and kurtosis may be due to extreme observations or outliers, suggest that some caution is needed before Gaussian models are adopted to describe the variable distributions.

The effect of the different vintage years

Variability from vintage year to vintage year (i.e., the vintage effect) is a well known characteristic of wine. The main problems are to evaluate the effect accurately and to ascertain whether the vintage effect should be regarded as a random fluctuation affecting all wines and all variables, or as being relatively unimportant for a set of variables and/or some wines. The small number of vintages do not allow a definitive answer to these problems yet some observations are of interest.

Table 4 reports, for selected variables, the means and the ranges observed by type of wine and vintage year; the ratio of the variance produced by the different vintages to the total variance is also given for each type of wine. If one considers variables K and TN, the means obtained in different vintages show remarkable changes; in some cases, the range of observations, not merely the mean, is modified (compare, e.g., Soave 1980 and 1981 for K, or Soave 1981 and 1982 for TN). However, the separating effect of the parameters (i.e., the different concentration values detected for Soave compared to those of the other wines) is confirmed in each vintage year as in the overall comparison. Similar considerations can be made for AC and ALA. Conversely, for Li and P, the variability from the vintage effect completely obscures differences among types of wine, making these parameters of little utility, if any, in wines differentiation (compare, e.g., Prosecco 1980 and 1982 or Tocai L. 1980 and 1981 for Li, and Tocai G. 1982 and 1983 for P). In contrast, pH, Mg and TA are affected very little by the vintage effect; however, in this case, differences among wines are insignificant (except perhaps for pH). As regards the aroma components, the evaluation of variability of the different vintages would require a greater number of years than that available.

In conclusion, the vintage effect is important in the examined data set, particularly for some parameters. In worst cases, this effect is likely to prevent any possibility of characterizing a wine through data obtained for previous vintages.

Correlation matrices

Three groups of intercorrelated variables can be clearly distinguished in the correlation matrix of each type of wine. Both the variables involved and the similar structure of the matrices, although not surprising from an enological viewpoint, must be stressed in relation to application of PCA. The first group of variables includes the alcohols HOLS, MPOL and MBOL, with the highest correlation observed between HOLS and MBOL (>0.80

TABLE 2

Minimum and maximum values, means, standard deviations (SD) and RSD of chemical

Chemical parameter	Unit	Minimum—Maximum				
		S	P	V	TL	TG
		Classical parameters (1979—1983 vintages)				
Na	mg l^{-1} X 10^{-1}	0.3—3.3	0.2—4.1	0.8—7.3	0.3—5.4	1.0—5
K	mg l^{-1} X 10^{-2}	1.9—6.6	2.8—11.4	4.9—10.9	4.0—10.6	4.9—1
Ca	mg l^{-1} X 10^{-1}	5.1—13.0	8.2—18.1	5.7—14.0	5.0—13.1	5.7—1
Mg	mg l^{-1} X 10^{-1}	5.3—10.8	5.8—12.2	5.2—9.6	6.0—10.5	5.4—1
Cl	mg l^{-1} X 10^{-1}	0.7—2.5	1.1—5.3	1.4—8.4	1.4—7.7	0.8—8
pH		3.0—3.4	2.9—3.6	3.2—3.7	3.0—3.6	3.1—3
TA	g l^{-1}	4.8—7.9	4.1—10.4	4.5—7.7	4.5—8.6	4.6—7
P	mg l^{-1} X 10^{-2}	0.9—2.7	0.9—3.4	0.7—2.7	1.4—4.1	0.4—3
AC	g l^{-1}	1.0—1.9	1.0—3.1	1.3—2.8	1.4—2.8	1.3—3
ALA	meq l^{-1} X 10^{-1}	1.1—1.9	1.2—3.2	1.2—2.6	1.2—2.8	1.3—3
Li	μg l^{-1} X 10^{-1}	0.6—2.4	0.3—1.4	0.8—2.6	0.3—1.9	0.6—1
TN	mg l^{-1} X 10^{-2}	0.8—4.0	0.5—2.5	0.9—2.7	0.5—3.6	0.2—2
DE	g l^{-1} X 10^{-1}	1.5—2.3	1.4—2.6	1.5—2.1	1.5—2.4	1.5—2
A	X 10	0.6—2.1	0.5—3.4	0.6—2.7	0.6—3.3	0.3—1
TP	mg l^{-1} X 10^{-2}	1.4—5.0	1.4—13.0	1.9—5.0	1.4—4.3	1.2—4
POL	mg l^{-1} X 10^{-1}	0.5—3.8	1.2—4.5	1.8—5.5	1.2—4.2	0.9—6
MPOL	mg l^{-1} X 10^{-1}	1.5—8.4	1.6—10.3	3.7—13.7	4.7—12.0	3.2—1
MBOL	mg l^{-1} X 10^{-2}	1.1—4.2	1.1—3.5	1.8—3.1	1.9—4.3	1.7—4
HOLS	mg l^{-1} X 10^{-2}	1.7—5.2	1.6—4.6	2.7—4.8	2.8—4.8	2.5—5
		Aroma parameters (1981—1983 vintages)				
MPA	mg l^{-1}	0.5—3.5	0.6—1.8	0.5—3.0	1.2—4.5	0.8—
BA	mg l^{-1}	0.5—1.8	0.4—2.1	0.2—3.2	0.5—3.6	0.6—
MBA	mg l^{-1}	0.3—2.1	0.4—1.4	0.3—2.0	0.4—3.1	0.5—
HA	mg l^{-1}	0.7—6.4	1.3—5.3	0.9—3.2	1.2—3.4	0.9—
OA	mg l^{-1}	1.0—8.8	1.9—10.2	1.2—4.7	1.2—4.8	1.3—
DA	mg l^{-1}	0.2—2.8	0.3—3.8	0.1—1.3	0.3—1.8	0.1—
HOL	mg l^{-1}	0.6—2.9	0.9—3.7	1.6—3.7	2.0—5.7	1.4—
THOL	mg l^{-1} X 10	0.2—1.4	0.3—1.2	0.2—2.9	0.4—2.0	0.1—
CHOL	mg l^{-1} X 10	0.1—0.8	0.5—1.7	0.2—2.6	1.5—7.1	1.2—

for all the wines). In constrast, POL shows negligible correlations with the variables of this group. The other two sets of intercorrelated variables are: (i) AC, ALA, K and pH within the inorganic parameters, and (ii) HA, OA and DA within the aroma parameters. In the latter set, correlations >0.85 are observed between HA and OA for all the wines.

In general, variables not included in the previous three sets show very low correlations; in particular, the lack of any important linear relationships between classical and aroma parameters should be noted. Exceptions are observed only in the correlation matrix of Soave, in which high correlations are also present between variables not included in the three groups quoted above; e.g., corr(HOLS, MPA) = 0.81, corr(HOLS, MBA) = 0.84, corr(MBOL, MBA) = 0.87, corr(MPA, MBA) = 0.94, corr(BA, HA) = 0.85.

neters, by type of wine

				SD					RSD				
P	V	TL	TG	S	P	V	TL	TG	S	P	V	TL	TG
1.4	2.7	2.0	2.2	0.8	0.9	1.3	1.0	1.0	0.48	0.63	0.47	0.48	0.44
7.1	7.7	7.4	7.9	1.2	1.8	1.5	1.6	1.8	0.27	0.25	0.19	0.21	0.22
11.0	9.6	9.0	10.1	1.8	1.9	1.9	1.9	2.1	0.21	0.17	0.19	0.21	0.21
7.9	7.4	8.1	7.3	1.5	1.3	1.2	1.2	1.3	0.19	0.17	0.16	0.14	0.18
2.3	3.3	2.7	2.3	0.6	0.9	1.6	1.4	1.9	0.43	0.39	0.49	0.50	0.84
3.3	3.4	3.4	3.4	0.1	0.1	0.1	0.1	0.2	0.03	0.04	0.03	0.04	0.04
5.9	6.0	6.0	6.0	0.6	1.3	0.6	0.9	0.6	0.11	0.21	0.11	0.15	0.10
1.8	1.6	2.5	2.2	0.4	0.5	0.5	0.6	0.9	0.21	0.29	0.31	0.23	0.42
1.9	2.0	2.0	2.0	0.2	0.4	0.3	0.3	0.4	0.16	0.21	0.16	0.16	0.20
2.2	2.1	2.0	2.0	0.2	0.4	0.3	0.3	0.5	0.13	0.21	0.16	0.16	0.26
0.8	1.3	1.1	1.1	0.4	0.3	0.3	0.4	0.3	0.39	0.37	0.25	0.36	0.24
1.3	1.5	1.4	1.5	0.8	0.4	0.4	0.6	0.6	0.29	0.33	0.28	0.45	0.43
1.8	1.9	1.9	2.0	0.2	0.2	0.1	0.2	0.3	0.10	0.14	0.08	0.10	0.14
1.2	1.2	1.3	1.0	0.4	0.6	0.5	0.6	0.4	0.36	0.48	0.42	0.44	0.38
4.0	3.4	2.7	2.3	0.8	2.0	0.9	0.6	0.8	0.32	0.51	0.26	0.23	0.37
2.5	3.1	2.5	3.1	0.8	0.7	0.8	0.6	1.3	0.38	0.27	0.27	0.23	0.42
6.1	7.7	8.0	8.4	1.7	2.0	2.0	1.8	2.8	0.29	0.32	0.26	0.23	0.33
2.1	2.5	2.8	2.8	0.6	0.5	0.3	0.5	0.6	0.27	0.25	0.13	0.16	0.22
3.0	3.6	3.8	4.0	0.7	0.7	0.5	0.5	0.8	0.24	0.22	0.13	0.13	0.20
1.2	1.5	2.2	2.1	0.6	0.3	0.6	0.8	0.8	0.57	0.28	0.38	0.36	0.38
1.0	1.2	1.1	1.1	0.3	0.4	0.7	0.7	0.4	0.34	0.42	0.61	0.63	0.39
0.8	0.9	1.3	1.2	0.4	0.2	0.3	0.6	0.3	0.52	0.27	0.37	0.43	0.26
2.6	1.6	2.0	2.4	1.3	0.9	0.5	0.5	0.9	0.52	0.36	0.33	0.25	0.40
4.4	2.5	3.0	3.5	2.1	2.0	0.9	0.9	1.5	0.55	0.44	0.35	0.31	0.42
1.3	0.7	0.9	0.9	0.7	0.8	0.3	0.4	0.6	0.77	0.60	0.46	0.45	0.61
2.4	2.5	3.6	2.6	0.5	0.8	0.6	1.0	0.6	0.46	0.35	0.23	0.29	0.24
0.7	0.9	1.0	0.7	0.3	0.3	0.7	0.5	0.4	0.42	0.48	0.78	0.46	0.53
1.1	1.6	4.2	3.0	0.2	0.3	0.5	1.3	1.0	0.64	0.27	0.33	0.32	0.33

Principal components analysis

Results of PCA are reported in Table 5 with reference to classical parameters only, aroma parameters only, and all the parameters. First, it can be seen that the approximation of the multidimensional space of observations through the subspace spanned by only the first two characteristic vectors of the correlation matrix, leads to a very high loss of information. The "unexplained" proportion of the total variation would be more than 0.50 and 0.30 for the set of classical and aroma parameters, respectively. To achieve values of more than 0.70 for the "explained" proportion of the total variation, $\geqslant 5$ or 3 components are needed for the classical and aroma parameters, respectively, and $\geqslant 5$—6 for all the parameters. In each case, the best fit is obtained for Soave.

TABLE 3

Ratios of between-groups variance to total variance for 1981—1983 vintages

Classical parameters	Variance ratio[a]	Aroma parameters	Variance ratio
Na	0.23 (0.21)	MPA	0.29
K	0.40 (0.34)	BA	0.02
Ca	0.10 (0.19)	MBA	0.25
Mg	0.03 (0.05)	HA	0.16
Cl	0.17 (0.17)	OA	0.17
pH	0.23 (0.23)	DA	0.13
TA	0.10 (0.00)	HOL	0.47
P	0.16 (0.19)	THOL	0.08
AC	0.36 (0.27)	CHOL	0.73
ALA	0.22 (0.22)		
Li	0.12 (0.19)		
TN	0.43 (0.37)		
DE	0.11 (0.08)		
A	0.09 (0.05)		
TP	0.15 (0.22)		
POL	0.09 (0.14)		
MPOL	0.21 (0.21)		
MBOL	0.17 (0.23)		
HOLS	0.23 (0.29)		

[a]Results for 1979—1983 vintages are given in parentheses.

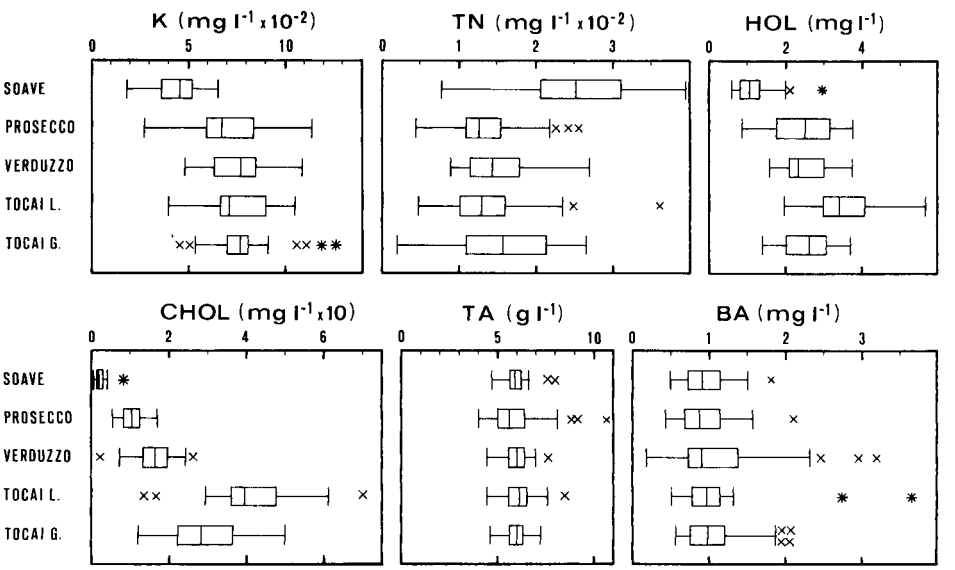

Fig. 1. Box plots [25, 26] for selected parameters.

Linear correlations between the principal components and the variables reveal much the same pattern in all the 5 groups. For PCA applied to classical parameters, the first component is highly correlated with AC, ALA, K and to a lesser degree, Mg and DE (see Fig. 2); the second component is mainly correlated with HOLS, MBOL and MPOL. With the aroma parameters, the first component has higher correlations with HA, OA and DA. Overall, the first two principal components have the highest linear correlations with the intercorrelated variables previously recognized and discussed. PCA based on all the variables seems to agree with the latter observations.

Squared multiple correlations are very high for almost all the variables, provided that an adequate number of components is considered (Table 6). This confirms that the selected components ensure a reasonable fit, not only overall but also with respect to each variable. An exception is CHOL; when the multiple linear regression of CHOL on the first three principal components is considered, the squared multiple correlation is lower than those for other parameters. These results are confirmed by PCA done with all the variables. Thus, if the original measurements are replaced by the first few principal components, the information provided by CHOL (the importance of which was stressed above) is lost to some extent.

Between-groups comparison of principal components

The above PCA results suggest the hypothesis that the subspaces spanned by the first few characteristic vectors are similar, i.e., they are almost coincident hyperplanes. This problem was worked out by Krzanowski's procedure. Results obtained with classical and aroma parameters separately (Table 7) show that the first two characteristic roots of the **H** matrix are very near the maximum allowable value (here 5, which should be reached if the hyperplanes were coincident). However, increasing dissimilarities are shown by the third and fourth characteristic roots which appear far apart from the maximum. These findings support the idea that the subspaces have a common bidimensional subspace, apart from slight differences which may be due to sampling variability. The angles formed by the directions corresponding to the characteristic vectors of the **H** matrix with their projections on the subspaces of the 5 wines, present interesting features. As can be seen in Table 7, the range of angles obtained in the first and second directions is much too small for the classical parameters than for the aroma parameters.

In summary, PCA makes it possible to derive, for each group, a subspace of reduced dimensionality, giving a reasonable fit of data scattering both overall and for each variable. The 5 subspaces have a common bidimensional subspace corresponding to correlation structures present, with similar characteristics, in all the groups. However, although the aim of a short summary of the data has been reached, it is doubtful that all the information contained in the group-separating parameters has been retained (cf. discussion about CHOL). A better exploitation of data may be obtained by CVA.

TABLE 4

Means, minimum and maximum values for a selected number of chemical parameters by type of wine and vintage year

Chemical parameter[a]	Year	Mean (minimum—maximum)				
		Soave	Prosecco	Verduzzo	Tocai L.	Tocai G.
K	1979		7.4 (5.7—9.5)			
	1980	3.8 (2.2—5.2)	8.7 (5.6—11.4)		7.0 (4.0—10.6)	
	1981	5.4 (4.5—6.6)		8.4 (4.9—10.9)	8.4 (5.8—10.4)	
	1982	3.9 (1.9—5.7)	6.3 (3.0—8.1)	6.9 (5.6—10.3)	6.7 (4.3—7.5)	8.3 (5.7—12.6)
	1983		5.6 (2.8—6.9)			7.4 (4.9—9.1)
Overall[b]		4.4 (1.9—6.6)	7.1 (2.8—11.4)	7.7 (4.9—10.9)	7.4 (4.0—10.6)	7.9 (4.9—12.6)
Variance ratio[c]		0.37	0.40	0.25	0.22	0.07
pH	1979		3.3 (3.0—3.6)			
	1980	3.2 (3.0—3.4)	3.3 (3.1—3.5)		3.3 (3.1—3.5)	
	1981	3.2 (3.1—3.4)		3.4 (3.2—3.6)	3.3 (3.0—3.6)	
	1982	3.2 (3.0—3.4)	3.3 (2.9—3.6)	3.4 (3.2—3.7)	3.4 (3.1—3.6)	3.5 (3.3—3.8)
	1983		3.3 (3.1—3.5)			3.3 (3.1—3.4)
Overall		3.2 (3.0—3.4)	3.3 (2.9—3.6)	3.4 (3.2—3.7)	3.4 (3.0—3.6)	3.4 (3.1—3.8)
Variance ratio		0.08	0.03	0.01	0.03	0.30
P	1979		1.6 (1.0—2.5)			
	1980	1.6 (1.4—2.0)	2.3 (1.6—3.4)		2.7 (1.7—4.1)	
	1981	2.1 (1.4—2.7)		1.7 (0.9—2.6)	2.6 (1.9—3.1)	
	1982	1.6 (0.9—2.1)	2.0 (0.9—3.0)	1.5 (0.7—2.7)	2.0 (1.4—3.1)	2.8 (2.0—3.8)
	1983		1.5 (1.0—2.3)			1.4 (0.4—2.8)
Overall		1.8 (0.9—2.7)	1.8 (0.9—3.4)	1.6 (0.7—2.7)	2.5 (1.4—4.1)	2.2 (0.4—3.8)
Variance ratio		0.37	0.29	0.03	0.26	0.59
Li	1979		0.7 (0.5—1.4)			
	1980	1.1 (0.7—1.4)	0.5 (0.3—0.8)		0.7 (0.3—1.0)	
	1981	1.2 (0.6—2.4)		1.3 (1.0—2.6)	1.4 (0.9—1.9)	
	1982	0.9 (0.7—1.5)	1.0 (0.8—1.3)	1.3 (0.8—1.7)	1.3 (0.8—1.6)	1.1 (0.6—1.6)
	1983		1.1 (0.9—1.4)			1.0 (0.6—1.5)
Overall		1.1 (0.6—2.4)	0.8 (0.3—1.4)	1.3 (0.8—2.6)	1.1 (0.3—1.9)	1.1 (0.6—1.6)
Variance ratio		0.08	0.65	0.00	0.57	0.03

TN	1979		1.2 (0.7—1.6)			
	1980	2.5 (0.8—3.5)	1.6 (0.5—2.5)		1.7 (0.8—3.6)	
	1981	3.2 (2.7—4.0)		1.6 (0.9—2.7)	1.3 (0.6—2.4)	
	1982	2.1 (1.4—2.5)	1.2 (0.7—1.7)	1.3 (0.9—1.8)	1.2 (0.5—2.0)	1.5 (0.5—2.5)
	1983		1.3 (0.7—2.2)			1.6 (0.2—2.7)
Overall		2.6 (0.8—4.0)	1.3 (0.5—2.5)	1.5 (0.9—2.7)	1.4 (0.5—3.6)	1.5 (0.2—2.7)
Variance ratio		0.36	0.15	0.09	0.12	0.00
HOL	1981	1.0 (0.6—2.0)		2.4 (1.6—3.5)	3.8 (2.2—5.7)	
	1982	1.3 (0.8—2.9)	2.3 (1.2—3.3)	2.6 (1.6—3.7)	3.3 (2.0—4.5)	2.6 (1.4—3.7)
	1983		2.5 (0.9—3.7)			2.6 (1.5—3.5)
Overall		1.2 (0.6—2.9)	2.4 (0.9—3.7)	2.5 (1.6—3.7)	3.6 (2.0—5.7)	2.6 (1.4—3.7)
Variance ratio		0.09	0.01	0.03	0.06	0.00
CHOL	1981	0.2 (0.1—0.8)		1.6 (0.2—2.2)	4.4 (3.0—7.1)	
	1982	0.3 (0.1—0.4)	1.0 (0.7—1.7)	1.7 (0.7—2.6)	3.9 (1.5—5.8)	3.4 (1.3—5.0)
	1983		1.1 (0.5—1.7)			2.5 (1.2—3.6)
Overall		0.3 (0.1—0.8)	1.1 (0.5—1.7)	1.6 (0.2—2.6)	4.2 (1.5—7.1)	3.0 (1.2—5.0)
Variance ratio		0.01	0.03	0.02	0.04	0.25

[a]Concentration units as in Table 2. [b]Overall: results for all the available vintages. [c]Variance ratio: ratio of between-groups (years) variance to total variance.

TABLE 5

Characteristic roots of the correlation matrices and "explained" proportion of total variation, by type of wine (only the first seven roots are given)

Component no.	Characteristic roots (cumulative proportion of total variation, %)				
	Soave	Prosecco	Verduzzo	Tocai L.	Tocai G.
Classical parameters (1979—1983 vintages)					
1	6.4 (34)	6.3 (33)	6.1 (32)	4.2 (22)	6.4 (34)
2	3.2 (50)	2.5 (47)	2.9 (47)	3.6 (41)	2.6 (47)
3	2.2 (62)	1.9 (57)	2.2 (59)	2.6 (55)	2.3 (60)
4	1.7 (71)	1.6 (65)	1.5 (67)	2.0 (65)	1.9 (70)
5	1.2 (77)	1.4 (73)	1.4 (74)	1.6 (74)	1.2 (76)
6	0.9 (82)	1.1 (78)	1.1 (80)	1.0 (79)	1.0 (82)
7	0.9 (87)	0.8 (82)	0.9 (85)	1.0 (85)	0.9 (86)
Aroma parameters (1981—1983 vintages)					
1	4.1 (46)	3.9 (43)	3.4 (38)	3.0 (33)	3.8 (43)
2	2.5 (73)	2.0 (65)	2.0 (60)	1.8 (53)	1.6 (60)
3	1.2 (86)	1.4 (80)	1.3 (75)	1.7 (72)	1.3 (75)
4	0.6 (93)	0.8 (89)	0.8 (84)	1.1 (84)	0.8 (84)
5	0.3 (97)	0.4 (93)	0.6 (91)	0.6 (90)	0.6 (90)
6	0.2 (99)	0.3 (97)	0.4 (95)	0.5 (96)	0.5 (95)
7	0.1 (99)	0.2 (99)	0.3 (99)	0.3 (99)	0.2 (98)
Classical and aroma parameters (1981—1983 vintages)					
1	9.1 (33)	6.9 (25)	6.8 (24)	6.7 (24)	7.6 (27)
2	6.3 (55)	4.5 (41)	3.9 (38)	4.7 (41)	3.9 (41)
3	2.9 (66)	3.6 (54)	2.8 (48)	3.4 (53)	2.8 (51)
4	2.7 (75)	2.7 (63)	2.6 (57)	2.8 (63)	2.6 (61)
5	1.4 (80)	2.6 (72)	2.0 (64)	2.6 (72)	1.8 (67)
6	1.3 (85)	1.6 (78)	1.8 (71)	2.2 (80)	1.8 (73)
7	0.9 (88)	1.4 (83)	1.5 (76)	1.5 (85)	1.3 (78)

Canonical variates analysis

The tendency of the observations to form well separated clusters, each corresponding to a different type of wine, was examined by evaluating the Euclidean distance of the wine samples from the group centroids in the space of the original measurements (standardized to overall zero mean and unit variance) [28]. Samples were then classified with the group corresponding to the smallest distance. The results (Table 8) show that percentages of correct classifications are generally high, with the exception of Tocai G. samples for which there was some overlapping with the Verduzzo and Prosecco clusters (64% correct classification).

Table 9 gives the main results of CVA on the data set including classical and aroma measurements both separately and together. The analysis based on all the parameters gave 4 canonical variates; the first three have high canonical correlation coefficients whereas the fourth is less important. Both the characteristic roots of the $T^{-1}B$ matrix and the canonical correlation coefficients indicate that use of all the parameters is more effective for dis-

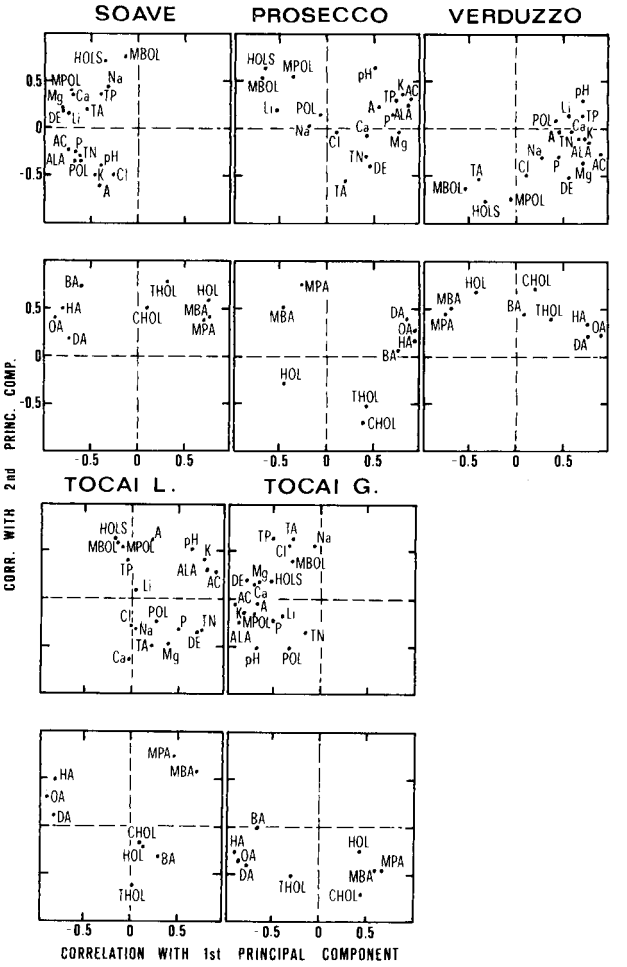

Fig. 2. Correlation plots [27].

crimination than use of either group of parameters separately. The parameters having the highest linear correlation coefficients with the first canonical variate are CHOL (0.82), K (0.67), HOL (0.64), AC (0.63), MPA (0.52), TN (—0.50), HOLS (0.50); TN has also a correlation value of 0.50 with the third canonical variate. No variables have correlations higher than 0.50 with the second and third canonical variates. These results agree with previous findings from the study of single-variable distributions.

Figure 3 shows the scatter plot of the wine samples in the space of the first three canonical variates, obtained with all the parameters. Observations for the Soave and Prosecco wines occupy regions that are well separated from those for all the other wines. Data points relative to the Verduzzo, Tocai L. and Tocai G. wines appear in contiguous, partly joined regions; some overlapping is seen between Tocai L. and Tocai G.

TABLE 6

Squared multiple correlations (R^2) of original variables with the first 5 or 3 principal components for classical and aroma parameters, respectively, by type of wine

Chemical parameter	R^2					Chemical parameter	R^2				
	S	P	V	TL	TG		S	P	V	TL	TG
Classical parameters (1979—1983 vintages)						*Aroma parameters (1981—1983 vintages)*					
Na	0.69	0.57	0.69	0.67	0.72	MPA	0.93	0.83	0.83	0.92	0.78
K	0.70	0.85	0.83	0.85	0.85	BA	0.90	0.59	0.61	0.22	0.60
Ca	0.81	0.57	0.67	0.62	0.65	MBA	0.95	0.61	0.88	0.91	0.73
Mg	0.82	0.69	0.78	0.51	0.53	HA	0.90	0.94	0.73	0.89	0.90
Cl	0.52	0.50	0.33	0.58	0.70	OA	0.98	0.96	0.88	0.97	0.92
pH	0.59	0.90	0.80	0.91	0.95	DA	0.71	0.91	0.76	0.80	0.84
TA	0.86	0.79	0.87	0.86	0.91	HOL	0.93	0.88	0.69	0.48	0.66
P	0.57	0.68	0.76	0.63	0.65	THOL	0.75	0.86	0.76	0.60	0.58
AC	0.81	0.90	0.86	0.94	0.93	CHOL	0.74	0.62	0.60	0.69	0.77
ALA	0.87	0.83	0.75	0.73	0.88						
Li	0.77	0.55	0.68	0.78	0.37						
TN	0.73	0.72	0.80	0.82	0.77						
DE	0.80	0.64	0.85	0.81	0.81						
A	0.75	0.66	0.63	0.62	0.48						
TP	0.83	0.72	0.65	0.56	0.86						
POL	0.74	0.73	0.65	0.68	0.73						
MPOL	0.84	0.75	0.75	0.71	0.86						
MBOL	0.95	0.83	0.81	0.78	0.86						
HOLS	0.98	0.93	0.96	0.95	0.92						

TABLE 7

Test for similarity of principal components. Angles between the Krzanowski's directions and their projections on the subspaces of the 5 wines

Projection on the subspace of	Angles (degrees)			
	1st dir.	2nd dir.	3rd dir.	4th dir.
	Classical parameters (1979—1983 vintages)			
Soave	16	25	31	43
Prosecco	20	26	24	35
Verduzzo	15	22	27	59
Tocai L.	19	22	25	75
Tocai G.	11	24	46	36
Sum of squared cosines	4.6	4.2	3.7	2.2
	Aroma parameters (1981—1983 vintages)			
Soave	21	8	20	
Prosecco	12	24	11	
Verduzzo	6	18	66	
Tocai L.	29	15	31	
Tocai G.	6	17	31	
Sum of squared cosines	4.6	4.6	3.5	

TABLE 8

Classification of samples by their Euclidean distances from the group centroids in the space of original measurements

Actual group	No. of samples	Predicted group					Correct rate (%)
		S	P	V	TL	TG	
Classical parameters (1979—1983 vintages)							
Soave	29	27	0	0	1	1	93
Prosecco	57	3	43	3	4	4	75
Verduzzo	34	2	1	27	2	2	79
Tocai L.	31	1	2	2	22	4	71
Tocai G.	33	4	0	6	4	19	58
Classical and aroma parameters (1981—1983 vintages)							
Soave	21	19	0	1	0	1	91
Prosecco	24	2	20	1	0	1	83
Verduzzo	34	1	3	27	3	3	79
Tocai L.	21	0	0	2	18	1	86
Tocai G.	33	1	4	6	1	21	64

TABLE 9

Characteristic roots of matrices $T^{-1}B$ (μ), $W^{-1}B$ (λ), and canonical correlation coefficients (ρ) for 1981—1983 vintages

Canonical variate	Classical parameters[a]			Aroma parameters			All parameters		
	μ	λ	ρ	μ	λ	ρ	μ	λ	ρ
1	0.73 (0.71)	2.8 (2.4)	0.86 (0.84)	0.75	3.0	0.87	0.85	5.7	0.92
2	0.58 (0.62)	1.4 (1.6)	0.76 (0.79)	0.28	0.4	0.53	0.70	2.3	0.84
3	0.41 (0.37)	0.7 (0.6)	0.64 (0.61)	0.27	0.4	0.52	0.66	1.9	0.81
4	0.36 (0.23)	0.6 (0.3)	0.60 (0.48)	0.03	0.0	0.17	0.46	0.9	0.68

[a]Results for 1979—1983 vintages are in parentheses.

Classification of samples by their Euclidean distances from the group centroids in the (hyper)space of canonical variates confirmed previous remarks (Table 10). Furthermore, the first canonical variate, which is highly correlated with CHOL, K, HOL and AC (see above), correctly classifies a high proportion of observations for all wines except Tocai G.; correct classifications for Soave and Prosecco samples are higher than 80%. Use of the first two canonical variates improves the poorer classifications, and the first three canonical variates provide better classification of Tocai L. but Tocai L. and Tocai G. are still not well separated. The addition of the fourth canonical variate further reduces the number of erroneous classifications. The overall correct classification rate is 94% finally. The difficulty in separating the Tocai wines is not surprising, because they differ in the production area but not in the grape variety.

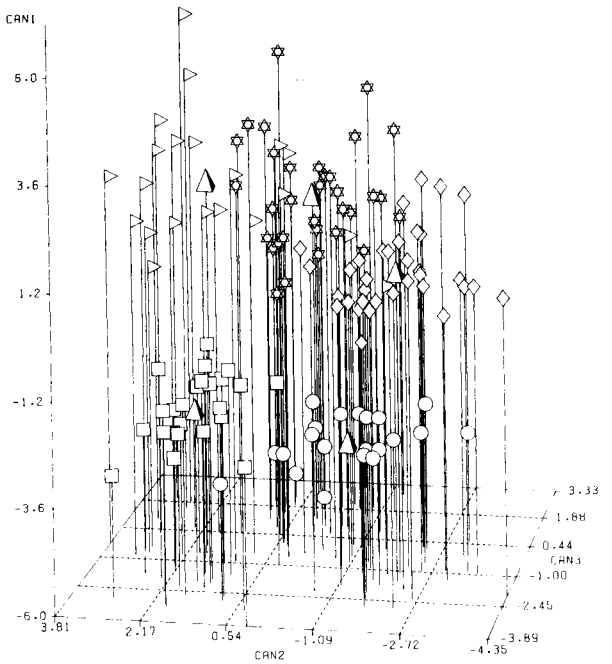

Fig. 3. Scatter plot of wine samples on the first three canonical variates (classical and aroma parameters; 1981—1983 vintages); (○) Soave; (□) Prosecco; (◇) Verduzzo; (▷) Tocai L.; (☆) Tocai G.; (△) group centroid. (Obtained with the 3D routine of the SAS package, version 5, 1985; SAS Institute, Cary, NC.)

Again, the use of aroma and classical parameters remarkably improves the classifications. For example, percentages of correct classifications obtained with the first two canonical variates derived from classical, aroma and all parameters were 62, 73, and 87%, respectively, mainly because of the variables CHOL and HOL.

In summary, differences in the distributions of some variables among the 5 wines give rise, in the canonical space, to a group structure, which is better defined for Soave and Prosecco than for the other wines, particularly Tocai G. The analytical parameters which are better correlated with the canonical variables, and so more informative about specific characteristics of wines, are K, AC, TN, CHOL and HOL; the contribution of the last 2 parameters is very important.

Conclusions

The main aim was to find group structures in the data. Several results indicate a clear-cut separation of samples belonging to the 5 wines considered. This is mainly due to between-groups differences in the concentration values of a few classical and aroma parameters. In contrast, the linear relationships of the variables do not provide noteworthy differentiations

TABLE 10

Classification of samples by their Euclidean distances from the group centroids in the canonical space (classical and aroma parameters; 1981—1983 vintages)

Actual group	No. of samples	Predicted group											
		1st canon. variate					Correct rate (%)	First 2 canon. variates					Correct rate (%)
		S	P	V	TL	TG		S	P	V	TL	TG	
Soave	21	21	0	0	0	0	100	21	0	0	0	0	100
Prosecco	24	2	21	1	0	0	88	0	24	0	0	0	100
Verduzzo	34	0	0	22	4	8	65	0	0	32	0	2	94
Tocai L.	21	0	0	3	12	6	57	0	0	1	16	4	76
Tocai G.	33	0	0	14	14	5	15	0	1	4	6	22	67
		First 3 canon. variates						All canon. variates					
		S	P	V	TL	TG		S	P	V	TL	TG	
Soave	21	20	1	0	0	0	95	20	1	0	0	0	95
Prosecco	24	0	24	0	0	0	100	0	24	0	0	0	100
Verduzzo	34	0	0	32	0	2	94	0	0	33	0	1	97
Tocai L.	21	0	0	2	16	3	76	0	0	2	19	0	90
Tocai G.	33	0	0	2	4	27	82	0	0	2	2	29	88

between the groups; from this point of view, the selected chemical measurements suggest an underlying similarity of the groups.

Among the open questions, the vintage effect is important. The data available allowed quantitative evaluation of the variability arising from different vintages, but the remaining unsolved problems include the need for parameters showing little variation across the years, and the control of the stability of group structures with time. However, information derived from the data, and the hypotheses suggested in this work, should be valuable in further investigations of the subject, in particular to overcome the exploratory approach adopted here. The present results could be developed with a 5-group discriminant model for use in wine description and in assigning samples of unknown origin.

The authors gratefully acknowledge Prof. P. Cescon for encouragement and helpful discussion.

REFERENCES

1 I. Moret, G. Scarponi, G. Capodaglio, S. Zanin, G. Camaiani and A. Toniolo, Am. J. Enol. Vitic., 31 (1980) 245.
2 G. Scarponi, I. Moret and G. Capodaglio, Riv. Vitic. Enol., 34 (1981) 254.
3 G. Scarponi, I. Moret, G. Capodaglio and P. Cescon, J. Agric. Food Chem., 30 (1982) 1135.
4 I. Moret, F. Di Leo, V. Giromini and G. Scarponi, J. Agric. Food Chem., 32 (1984) 329.

5 I. Moret, G. Scarponi and P. Cescon, Ras. Chim., 35 (1983) 319.
6 I. Moret, G. Scarponi, G. Capodaglio, V. Giromini and P. Cescon, Ann. Chim., 74 (1984) 73.
7 I. Moret, G. Scarponi and P. Cescon, J. Sci. Food Agric., 35 (1984) 1004.
8 I. Moret, G. Scarponi, G. Capodaglio and P. Cescon, Riv. Vitic. Enol., 38 (1985) 254.
9 Gazz. Uff. Repubb. Ital., 1968, No. 269, p. 6349; 1976, No. 227, p. 6399.
10 Gazz. Uff. Repubb. Ital., 1969, No. 141, p. 3349; 1986, Ser. Gen., No. 51, p. 6.
11 Gazz. Uff. Repubb. Ital., 1971, No. 242, p. 5946.
12 Gazz. Uff. Repubb. Ital., 1971, No. 220, p. 5478.
13 Gazz. Uff. Repubb. Ital., 1970, No. 244, p. 6351.
14 M. A. Amerine and C. S. Ough, Methods for Analysis of Musts and Wines, Wiley, New York, 1980.
15 Off. Int. Vigne Vin (O.I.V.), Recueil des Methodes Internationales d'Analyses des Vins, O.I.V., Paris, 1978.
16 F. Drawert, W. Heimann, R. Emberger and R. Tressl, Chromatogr., 2 (1969) 57.
17 P. Schreier, F. Drawert and M. Schmid, J. Sci. Food Agric., 29 (1978) 729.
18 C. R. Rao, Sankhya, Ser. A, 26 (1964) 329.
19 K. V. Mardia, J. T. Kent and J. M. Bibby, Multivariate Analysis, Academic Press, New York, 1979.
20 IMSL Library Reference Manual, 1980 edn., IMSL, Houston.
21 W. J. Krzanowski, J. Am. Statist. Assoc., 74 (1979) 703; 76 (1981) 1022.
22 W. C. Chang, Appl. Statist., 32 (1983) 267.
23 R. Gnanadesikan and J. Kettenring, Biometrics, 28 (1972) 81.
24 G. A. F. Seber, Multivariate Observations, Wiley, New York, 1984.
25 D. C. Hoaglin, F. Mosteller and J. W. Tukey, Understanding Robust and Exploratory Data Analysis, Wiley, New York, 1983.
26 J. W. Tukey, Exploratory Data Analysis, Addison-Wesley, Reading, MA, 1970.
27 P. Bertier and J. M. Bouroche, Analyse des Donnees Multidimensionnelles, Presses Universitaires de France, Paris, 1975.
28 K. Varmuza, Pattern Recognition in Chemistry, Springer-Verlag, Berlin, 1980, pp. 18–30.

Analytica Chimica Acta, 191 (1986) 351—358
Elsevier Science Publishers B.V., Amsterdam — Printed in The Netherlands

USE OF A LIMITED-MEMORY FILTER TO ELIMINATE UNPREDICTABLE CHANGES IN ANALYTICAL MEASUREMENTS

C. B. M. DIDDEN

DSM Research, Physical and Analytical Chemistry Department, P.O. Box 18, 6160 MD Geleen (The Netherlands)

(Received 7th April 1986)

SUMMARY

A limited-memory filter is described for analytical measurements which are affected by unpredictable changes. The filter is capable of reducing the effects of those changes. Applications in multicomponent determinations, control charts and spectra smoothing are discussed. For the last application, a less abrupt type of limited-memory filtering, called fading-memory filtering, is described.

With the increasing availability and decreasing cost of digital hardware, a growing need has been felt for the development of sophisticated mathematical tools which are capable of extracting more, and more precise, information from measurements. In this paper, attention is focussed on the development of a limited-memory filter. The application of limited-memory filtering in multicomponent determinations will be discussed, as well as applications in control charts and in data smoothing. For the last application, a fading-memory filter, another type of Kalman filtering, is also described.

Multicomponent determinations are often done by processing the data of a recorded spectrum (e.g., u.v., infrared) by means of a mathematical technique, e.g., Kalman filtering [1—3] or the general standard-additions method [4—6]. These techniques will give only the best possible estimates of the concentrations, because the recorded spectra will always be affected by measurement noise. Besides the measurement noise the spectral signals are measured with respect to a ground level, e.g., a nonzero baseline. The baseline may not be constant and may be a straight line, a sinusoid, etc. If the baseline is known, its subtraction from the measured spectrum gives the unaffected spectrum. However, the level of the baseline is often not known in advance and a correction has to be estimated. Usable methods for background correction have been given by Poulisse and Engelen [3], Bond and Grabaric [7] and Goehner [8]. A disadvantage of these methods is the assumption that the background is described by a model with constant parameters.

If earlier experiments have shown that an instrument suffers from, say, linear drift, problems arise if the parameters (e.g., slope) describing the

0003-2670/86/$03.50

drift change abruptly during the measurements or even worse the instrument just cuts out. From the equations for multicomponent analysis [3, 4], it follows that all information obtained before and after the failure is retained in the estimates of the concentrations. However, if such a sudden change occurs then the information from the past is no longer relevant and will lead to biased estimates. Therefore in such situations, the equations have to be adapted so that all earlier information is forgotten. In the literature on automatic control much attention has been given to this subject [9—12]. Poulisse and Jansen [13] and Hartley [14] were the first to report applications in analytical chemistry, but their attention was focussed on memory effects in analytical runs. In this paper, a method which is termed limited-memory filtering is discussed. The method was first described by Jazwinski [9], although earlier O'Donell [11] had given the equations for the one-dimensional parameter case.

THEORY

The composition of a sample, consisting of n components, is determined with a suitable analytical procedure. The contribution of each component to the measured signal y is weighted by known coefficients $h_i, i = 1, 2, \ldots, n$:

$$y = h_1 x_1 + h_2 x_2 + \ldots + h_n x_n + v \tag{1}$$

where x_i, $i = 1, 2, \ldots, n$ is the unknown concentration of the ith component and v is measurement noise. This equation adequately describes many analytical situations, e.g., for an absorption spectrum, the h_i values are known molar absorptivities, and y is the absorbance. To evaluate the concentrations x_i, several measurements are required:

$$y(\lambda_k) = h_1(\lambda_k)\, x_1 + h_2(\lambda_k)\, x_2 + \ldots h_n(\lambda_k)\, x_n + v(\lambda_k)$$
$$(k = 1, 2, 3, \ldots, m) \tag{2}$$

In the case of an absorption spectrum, λ_k is the wavelength at the kth measurement. In general, the number of measurements has to be larger than the number of unknown concentrations (i.e., $m > n$).

Analytical measurements are often influenced by background effects. If this background is a linear function of the measurement index k, e.g., for an absorption spectrum the wavelength λ_k, Poulisse and Engelen [3] extended Eqn. 2 to the form:

$$y(\lambda_k) = h_1(\lambda_k)\, x_1 + \ldots + h_n(\lambda_k)\, x_n + \lambda_k\, a + b + v(\lambda_k) \tag{3}$$

where a and b are constant parameters describing the linear background disturbance. In this case, the number of measurements should exceed the number of components by two ($m > n + 2$). Rewriting Eqn. 3 in matrix notation yields

$$y(\lambda_k) = \mathbf{h}^{\mathrm{T}}(\lambda_k)\mathbf{x} + v(\lambda_k) \tag{4}$$

with $\mathbf{h}^T(\lambda_k) = (h_1(\lambda_k), \ldots, h_n(\lambda_k), \lambda_k, 1)$ and $\mathbf{x}^T = (x_1, \ldots, x_n, a, b)$.

Poulisse and Engelen [3] derived a Kalman filter which estimates the concentrations corrected for the background disturbance:

$$\hat{\mathbf{x}}(k/k) = \hat{\mathbf{x}}(k-1/k-1) + k(k)\,[y(k) - \mathbf{h}^T(k)\,\hat{\mathbf{x}}(k-1/k-1)] \tag{5}$$

$$\mathbf{k}(k) = \mathbf{P}(k-1/k-1)\,\mathbf{h}(k)\,[\mathbf{h}^T(k)\,\mathbf{P}(k-1/k-1)\,\mathbf{h}(k) + R(k)]^{-1} \tag{6}$$

$$\mathbf{P}(k/k) = [\mathbf{I} - k(k)\,\mathbf{h}^T(k)]\,\mathbf{P}(k-1/k-1) \tag{7}$$

with $\epsilon\{v(k)v(l)\} = R(k)\delta_{k,l}$, $\epsilon\{v(k)\} = 0$, $\delta_{k,l} = \begin{cases} = 0 \;\forall\; k \neq l \\ = 1 \;\forall\; k = l \end{cases}$

$\mathbf{I}$ = unity matrix $(n + 2 \times n + 2)$ and $k = \lambda_k$

Here $\hat{\mathbf{x}}(k/k)$ is the estimate of $\mathbf{x}$ after k measurements have been processed and the matrix $\mathbf{P}(k/k)$ is the error covariance matrix of the difference between $\mathbf{x}$ and its estimate $\hat{\mathbf{x}}(k/k)$ [15]. In a probabilistic sense, the estimate $\hat{\mathbf{x}}(k/k)$ must be interpreted as the mean of the conditional probability function of $\mathbf{x}$ given the measurement sequence $y(1), \ldots, y(k)$, e.g.,

$$\hat{\mathbf{x}}(k/k) = \epsilon[\mathbf{x}|y(1), \ldots, y(k)] \tag{8}$$

and the error covariance matrix,

$$\mathbf{P}(k/k) = \epsilon\{[\mathbf{x} - \hat{\mathbf{x}}(k/k)]\;[\mathbf{x} - \hat{\mathbf{x}}(k/k)]^T\,|y(1), \ldots, y(k)\} \tag{9}$$

Equation 8 shows that the estimate of $\mathbf{x}$ after k measurements, $\hat{\mathbf{x}}(k/k)$ depends on the entire sequence of measurements $y(1), \ldots, y(k)$. However, if during measurements y_{m-i} to y_{m-l} an event occurs which influences the measurements but which is not modelled in the state-space description (cf. Eqn. 4), then Eqn. 8 shows that the estimate $\hat{\mathbf{x}}(k/k)$ will also be influenced. Such an event will often cause divergence of the estimate $\hat{\mathbf{x}}(k/k)$. Although the measurements y_m to y_k would be useful for calculating an estimate of $\mathbf{x}$, the estimate is ruined by the measurements y_{m-i} to y_{m-l}.

To obtain an estimate of $\mathbf{x}$ based on the measurements y_m to y_k, i.e., to evaluate the mean of the conditional probability function of $\mathbf{x}$ based on y_m to y_k, the relevant equation is

$$\hat{\mathbf{x}}(k/N) = \epsilon[\mathbf{x}|y(m), \ldots, y(k)] \tag{10}$$

where $N = k - m$ is the memory window, with its error covariance matrix,

$$\mathbf{P}(k/N) = \epsilon\{[\mathbf{x} - \hat{\mathbf{x}}(k/N)]\;[\mathbf{x} - \hat{\mathbf{x}}(k/N)]^T\,|y(m), \ldots, y(k)\} \tag{11}$$

Jazwinski [9] derived the limited memory filter as a solution to this problem, assuming white noise on the measurements. The calculation of the limited memory estimate, $\hat{\mathbf{x}}(k/N)$ is based on the Kalman filter estimate at an earlier measurement y_m, $\hat{\mathbf{x}}(m/m)$ and at the latest measurement y_k, $\hat{\mathbf{x}}(k/k)$:

$$\hat{\mathbf{x}}(k/N) = \mathbf{P}(k/N)\;[\mathbf{P}(k/k)^{-1}\;\hat{\mathbf{x}}(k/k) - \mathbf{P}(m/m)^{-1}\;\hat{\mathbf{x}}(m/m)] \tag{12}$$

with error covariance matrix

$$\mathbf{P}(k/N)^{-1} = \mathbf{P}(k/k)^{-1} + \mathbf{P}(m/m)^{-1} \tag{13}$$

In Eqns. 12 and 13, $\hat{\mathbf{x}}(k/k)$ and $\hat{\mathbf{x}}(m/m)$ are the estimates of $\mathbf{x}$ and $\mathbf{P}(k/k)$ and $\mathbf{P}(m/m)$ are the error covariance matrices associated with those estimates as produced by the Kalman filter equations (Eqns. 5—7). In practice, this means that two identical Kalman filters, running simultaneously with different measurements, e.g., $y(k)$ and $y(m)$, have to be combined with the aid of Eqns. 12 and 13 to give a limited-memory estimate. Figure 1 shows a computational scheme of a limited-memory filter.

A computational disadvantage of Eqns. 12 and 13 for the limited-memory filter is the necessity of performing three matrix inversions. This disadvantage can partly be overcome [15, 16] by computing the inverses of the error covariance matrices given by the Kalman filters recursively with

$$\mathbf{P}(k/k)^{-1} = \mathbf{P}(k-1/k-1)^{-1} + \mathbf{h}(k)\,\mathbf{h}^{\mathrm{T}}(k)/R(k) \tag{14}$$

The choice of starting values has been discussed by Poulisse [1].

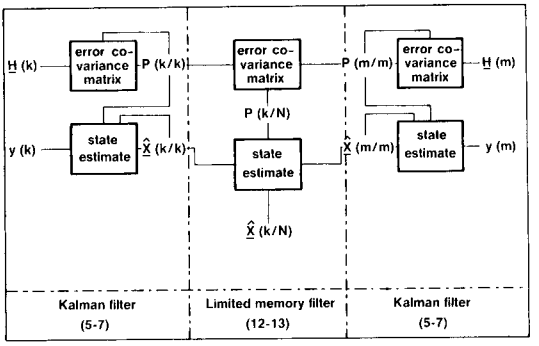

Fig. 1. Computational scheme of a limited-memory filter.

APPLICATIONS

Multicomponent determinations

The first application of a limited-memory filter here is to a two-component spectrum affected by a linear background. The type of simulation used was described earlier [2]. A spectrum can be simulated by

$$y(k) = h_1(k)\,x_1 + h_2(k)\,x_2 + k\,a + b + v(k) \tag{15}$$

where $k = \lambda_k = 1600$—$1645\ \mathrm{cm}^{-1}$ (45 measurements) and x_1 (= 1.5) and x_2 (= 3.0) are the concentrations of two components; a is the slope and b the constant of the linear background effect, $v(k)$ is the simulated measurement noise with variance $\epsilon\{v(k)\,v(k)\} = R\forall_k$, $h_1(k)$ and $h_2(k)$ are the molar absorptivities generated by

$$h_1(k) = 0.4 \exp\left[-(k-1631)^2/72\right] + 0.1 \exp\left[-(k-1610)^2/200\right] \tag{16}$$

$$h_2(k) = 0.8 \exp\left[-(k-1616)^2/200\right] + 0.1 \exp\left[-(k-1640)^2/200\right] \tag{17}$$

A spectrum generated with the above equations can be processed by Eqns. 3—5. The following failure was simulated:

drift: $a = 0.008$, $b = 0.02$, $k < 1626$ cm^{-1}

cut out: $y(k) = 0.0$, $k = 1626, 1627$ cm^{-1}

drift: $a = 0.007$, $b = 0.01$, $k > 1627$ cm^{-1}.

This means that the instrument cuts out at $k = 1626, 1627$ cm^{-1} and the drift changes abruptly at 1628 cm^{-1}. Figure 2 shows the simulated spectrum with and without the background effects, with the measurement noise variance set at $R = 10^{-6}$. Figure 3 shows the estimates obtained with a Kalman filter and with a limited-memory filter, with a memory window $N = 15$.

The usefulness of the limited-memory filter in this kind of situation is clearly demonstrated in Table 1. The estimates obtained with the standard Kalman filter diverge from their true values (1.5 and 3.0) whereas the estimates of the limited-memory filter converge to their true values after the filter has forgotten the 'different' past. This happens at $\lambda = 1642$ cm^{-1} because the last failure occurred at 1627 cm^{-1} and the filter remembers only the measurements between 1628 cm^{-1} and 1642 cm^{-1}. Table 1 also contains the results of experiments with different variances of the measurement noise.

Control charts

The second application is the detection of a sudden change in the calibration factor of an analytical method [18, 19]. In this example, the calibration factor changes from 0.205 to 0.210, and the standard deviation of the analytical method is 0.005. Figure 4 shows the course of the measurements on a control chart. The chart contains a total of 200 measurements and the calibration factor changes at the 100th measurement. Also shown are the limited-memory estimate of the calibration factor and its 99% error bounds. As can be seen, the control chart does not detect the change in the

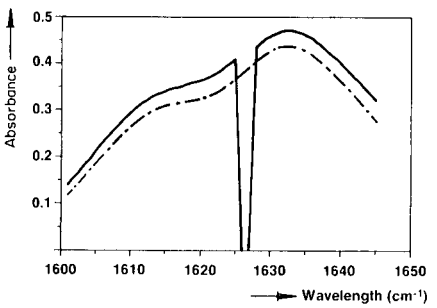

Fig. 2. Simulated spectra with a noise variance of $R = 10^{-6}$. The dotted line is the undisturbed spectrum, whereas the straight line is the disturbed spectrum.

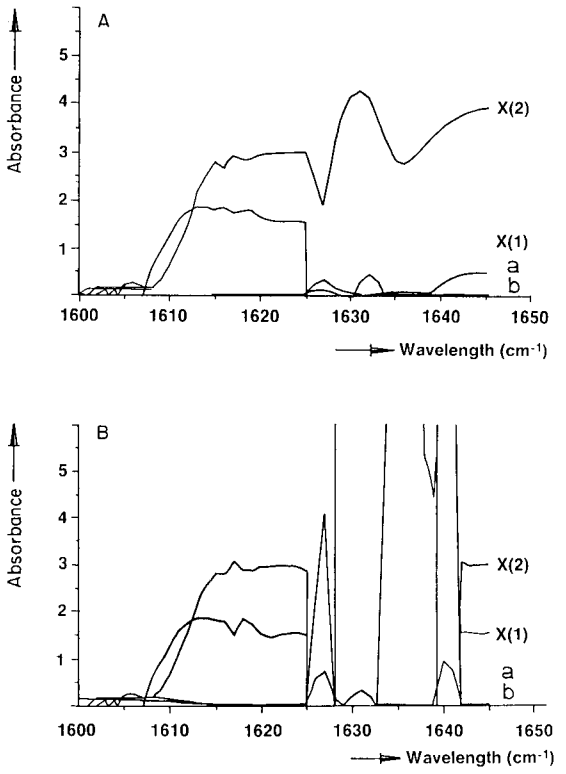

Fig. 3. Estimates given by: (A) the Kalman filter; (B) the limited-memory filter.

calibration factor. The limited-memory estimate shows a significant difference from the original calibration factor (0.205), with the 99% error limit of the filter intersecting the level of the original calibration factor at measurement 114. In the case of a Gaussian distribution, one can state with 99.7% certainty that the calibration factor has changed.

Smoothing of data

The third application is the smoothing of noisy data. As the smoothing model, a third-order Chebyshev polynomial is used in the limited-memory filter equations (Eqns. 5—7, 12 and 13). Figure 5A shows the result of the smoothing operation of this filter on simulated noisy data. Figure 5B shows the results of using the well-known Savitzky-Golay filter [20] on the same data set with the same width of the window. Figure 5C shows the results of smoothing with a filter that is closely related to the limited-memory filter, the fading-memory filter developed by Sörenson and Sachs [21]. Whereas the limited-memory filter abruptly cuts out the past, the fading-memory filter weights the past measurements in an exponential way. The fading-memory equations are

TABLE 1

Results of Kalman and limited-memory (LM) filtering on spectra with different noise variances

Noise	Filter	Concn. 1	Error in estimate	Concn. 2	Error in estimate
10^{-8}	Kalman	0.48	0.001	3.90	0.002
10^{-8}	LM	1.51	0.008	3.00	0.006
10^{-6}	Kalman	0.48	0.006	3.90	0.02
10^{-6}	LM	1.51	0.07	2.99	0.06
2.5×10^{-5}	Kalman	0.51	0.03	3.80	0.08
2.5×10^{-5}	LM	1.28	0.36	2.49	0.31

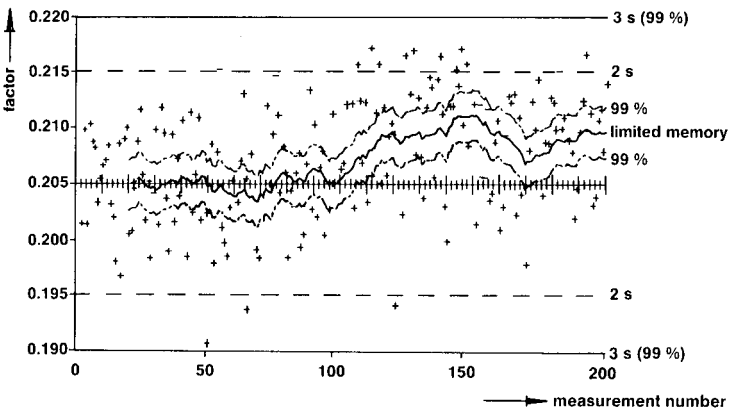

Fig. 4. General and limited-memory control charts.

$$\hat{\mathbf{x}}(k/k) = \hat{\mathbf{x}}(k-1/k-1) + \mathbf{k}(k)\,[y(k) - \mathbf{h}^{\mathrm{T}}(k)\,\hat{\mathbf{x}}(k-1/k-1)] \tag{18}$$

$$\mathbf{P}(k/k-1) = \mathrm{e}^{\alpha}\,\mathbf{P}(k-1/k-1) \quad (\text{for } 0 \leqslant \alpha \leqslant \infty) \tag{19}$$

$$\mathbf{k}(k) = \mathbf{P}(k/k-1)\,\mathbf{h}(k)\,[\mathbf{h}^{\mathrm{T}}(k)\,\mathbf{P}(k/k-1)\,\mathbf{h}(k) + R(k)]^{-1} \tag{20}$$

$$\mathbf{P}(k/k) = [\mathbf{I} - \mathbf{k}(k)\,\mathbf{h}^{\mathrm{T}}(k)]\,\mathbf{P}(k/k-1) \tag{21}$$

In Eqn. 19, α is the so-called fading factor. When $\alpha = 0$, the fading-memory filter becomes similar to the standard Kalman filter; and when α is infinite, it becomes a limited-memory filter with a memory width of one measurement. Figure 5 shows that the fading-memory filter gives a smoother picture because of its fading character. The fading-memory filter was used earlier by Jansen and Bonants [22], who called it a low-pass noise filter. Comparison of their equations shows that this filter is the scalar version of the fading-memory filter described by Sörensen and Sachs [21].

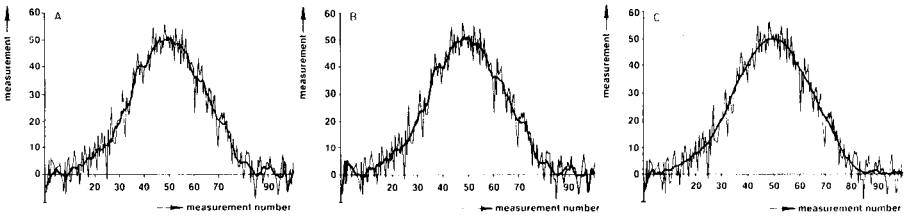

Fig. 5. Data smoothing with different filters: (A) limited-memory filter of width $N = 10$; (B) Savilzky-Golay filter of width $N = 10$; (C) fading-memory filter with factor $\alpha = 0.8$.

Discussion

With the aid of the limited-memory filter, the true concentrations can still be estimated recursively even when model changes occur, which normally causes the calculations to diverge [17]. As shown, application of a limited-memory filter is not restricted to any specific area of analytical chemistry.

Three applications of a totally different nature are given. Although the applications may appear rather simple, it should be recalled that the strength of the limited-memory filter is its vector nature which follows from the state-space description of the system under investigation. The simple Eqns. 10 and 11 can be used even in the most difficult situations. If, for example, a calibration factor has a sinusoidal and quadratic drift, failures can still be detected with these equations.

The author thanks Dr. H. Poulisse, Shell, for helpful discussions on this subject and P. Hendriks, DSM, for reading the manuscript critically.

REFERENCES

1 H. N. J. Poulisse, Anal. Chim. Acta, 112 (1979) 361.
2 C. B. M. Didden and H. N. J. Poulisse, Anal. Lett., A13 (1980) 921.
3 H. N. J. Poulisse and P. L. M. Engelen, Anal. Lett., A13 (1980) 1921.
4 B. E. H. Saxberg and B. R. Kowalski, Anal. Chem., 51 (1979) 1031.
5 J. H. Kalivas and B. R. Kowalski, Anal. Chem., 54 (1982) 560.
6 R. W. Gerlach and B. R. Kowalski, Anal. Chim. Acta, 134 (1982) 119.
7 A. M. Bond and B. S. Grabaric, Anal. Chem., 51 (1979) 337.
8 R. P. Goehner, Anal. Chem., 50 (1978) 1223.
9 A. H. Jazwinski, IEEE Trans. Autom. Control, AC-13 (1968) 553.
10 B. Friedland and S. M. Grabonsky, IEEE Trans. Autom. Control, AC-27 (1982) 237.
11 J. J. O'Donell, IEEE Trans. Autom. Control, AC-9 (1964) 105.
12 G. J. Bierman, IEEE Trans. Inf. Theory, IT-21 (1975) 690.
13 H. N. J. Poulisse and R. T. P. Jansen, Anal. Chim. Acta, 151 (1983) 433.
14 P. E. Hartley, Anal. Chem., 54 (1982) 56.
15 B. D. O. Anderson and J. B. Moore, Optimal Filtering, Prentice Hall, Englewood Cliffs, 1979.
16 A. Gelb, Applied Optimal Estimation, MIT Press, Cambridge, MA, 1977.
17 J. B. Geyle and H. D. Bennett, Anal. Chem., 50 (1978) 2085.
18 J. Segen and A. C. Sanderson, IEEE Trans. Inf. Theory, IT-26 (1980) 249.
19 A. S. Willsky, Automatica, 12 (1976) 601.
20 A. Savitzky and M. Golay, Anal. Chem., 36 (1964) 1627.
21 H. W. Sörensen and J. E. Sachs, Inf. Sci., 3 (1971) 101.
22 R. T. P. Jansen and P. Bonants, Anal. Clin. Biochem., 20 (1983) 174.

Analytica Chimica Acta, 191 (1986) 359—368
Elsevier Science Publishers B.V., Amsterdam — Printed in The Netherlands

ERRORS IN PARAMETERS EXTRACTED FROM $A \exp(-kt) + Z$ DATA AND EFFECTS OF NOT WEIGHTING THE DATA

A. H. KALANTAR

Department of Chemistry, University of Alberta, Edmonton, Alberta T6G 2G2 (Canada)

(Received 7 April 1986)

SUMMARY

Earlier work is extended by providing relative standard deviations (σ) for the background (Z) and the pre-exponential factor (A) via analysis of 2400 simulated decays for various decade ranges, Z/A and kinds of error using weighted non-linear least squares (WNLLS), the method yielding the lowest relative standard deviation of the rate constant. These σ enable experimenters to make more objective and quantitative assessments of the relative worth of extending, for example, the time over which data are collected to get more precise parameters. Effects of ignoring relative weights in the analyses are also examined. Their omission yields σ derived from the fit that are unreliable. Moreover, the σ^2 calculated from the sets of parameters extracted from many simulated decays are sometimes more than doubled. Efficiency [= σ^2 (weighted)/σ^2 (not weighted)] is then halved: this amounts to ignoring half the data that has required time, effort and resources to collect.

Data following the single exponential with a constant but unknown background are widespread in the physical and natural sciences. So common are the examples of such first-order processes that several studies [1—6] have focussed on how best to extract the rate (k), pre-exponential factor (A) and background (Z) from such data accurately (without bias) and with the highest possible precision (lowest standard deviation, greatest efficiency). Several methods have been compared particularly for minimizing the error in k. Other studies [7, 8] have used only an iterative non-linear least-squares (NLLS) method [7, 9], seeking the errors propagated in A and Z [7] or in k [8] for a growth function. Recently [6], the dependence of the error in only k was evaluated for a broad range of experimental conditions. Here the errors in A and Z are also evaluated for these same conditions for the same method (WNLLS, weighted NLLS) that yields k most efficiently. These are provided because these parameters are also needed [1, 4, 7] and to enable the experimentalist to consider the relative worth of attempting to optimize various experimental conditions.

The other goal of this work concerns the dependence of the errors of the parameters extracted from data upon whether or not these data are weighted when processed. The precision of the parameters is sometimes appreciably enhanced if weighting is done. This has been found for a few cases of double

0003-2670/86/$03.50

exponential decays [10], for the model of interest here using Guggenheim's [11] method [6] (both for Poisson (P) errors) and for simply $A \exp(-kt)$ [12]. Another study involving the growth function and equal (E) or constant (C) relative errors found some anomalous effects [8]. Moreover, treated data are commonly assumed to be equally valid (whether explicitly stated or by default when ignoring weights altogether). For these reasons (earlier observations and implicit omission of weighting), a systematic examination of the effects of ignoring weights on precision is of potential value. Should precisions depend strongly on whether weighting is included or not, this fact would set the stage for reducing the standard deviations of the parameters or, equivalently, getting the parameters more efficiently (i.e., with less experimental work) by weighting these fewer data. But if precision is not so dependent, weighting would not be necessary. As we will see, both situations exist, depending on the particular case (Z/A, range, etc.).

Importance of efficiency

Consider the situation where two methods of analysis provide the same estimate of a parameter but with different standard deviations (σ) or variances (σ^2). The methods could be WNLLS and Guggenheim's or Guggenheim's with and without weighting. Efficiency is the ratio of variances $(\sigma_m/\sigma_n)^2$, where $\sigma_m < \sigma_n$ [13]. When the efficiency is 0.2 (or 20%), $\sigma_n = \sigma_m 5^{1/2}$. To reduce σ_n to σ_m it is possible either to switch from method n to method m or to collect 400% more data and process them with the less efficient method n. This choice makes it clear that 4/5 of the data merely compensate for using the less efficient method. Using method m here would yield the lower σ_m with only 20% of the total experimental effort envisioned above. Thus efficiency, which relates relative standard deviations, is more directly and, for the experimentalist, more importantly related to how much work has to be done to get the desired parameters at a given level of uncertainty. In a very real sense, using an inefficient method amounts to ignoring a sizeable portion of the data [6, 14].

SIMULATIONS AND EVALUATION

The relative efficiencies and the relative standard deviations of A, k and Z are obtained from the parameters extracted from many simulated sets of data. The 'data' are simulated by adding random numbers (the variances of which reflect E, P or C errors) to decays following $y = A \exp(-kt) + Z$ exactly. The conditions and various cases, which mimic a broad range of experimental situations, will be apparent from the tabulated results and deliberately match those detailed earlier [6], to which reference should be made.

As noted [6], WNLLS [7, 9] yields k most efficiently. Hence this iterative method was used to extract the parameters until none changed by more than 0.01% compared to the previous iteration. This procedure involves the

variance/covariance matrix and so yields estimates of the σ derived from each fit: these individual σ are referred to as predicted standard deviations of the parameters. The σ could also be calculated from the entire set of extracted parameters: these are called the observed standard deviations of the parameters. Because 2400 sets of parameters were extracted for each case, the standard errors of the σ_k, σ_A and σ_Z are ca. 1.44% [14]. As before [5, 6], the results are expressed in terms of error factors. Thus EFA (for the error factor of A) is (σ_A/A)/(noise level at the first datum) and similarly for EFK. Because Z can be zero, the ratio σ_Z/(noise level at the first datum) is reported as $\sigma(Z)$. The relative efficiencies were calculated from the observed σ obtained by evaluating each of 1200 simulated decays using both WNLLS and NLLS. In all, about 3×10^5 simulated decays were examined.

While most of the results were obtained for low levels of added 'noise' (the standard deviation of the first datum is $\sim 10^{-3}$% to 1%), some higher noise levels were used to check for bias in the extracted parameters. In such cases, the experimentalist must also iterate the weights, using the fit of the previous iteration [15]. Using the data for relative weights (as $1/y_i$ or $1/y_i^2$) for all iterations contributes to convergence failures (especially for inaccurate y_i near zero) and to the absurdity that proper weighting yields larger parameter errors than if weighting is ignored [8].

RESULTS AND DISCUSSION

Errors in the parameters

Table 1 presents EFA, EFK and $\sigma(Z)$ for all three kinds of error structures examined. Thus the last EFK and $\sigma(Z)$ entries for P noise are 6.56 and 1.45. To understand exactly what these mean, let us suppose the noise level is 2% at the first datum. Then the standard deviation of the first datum is $0.02\ [(A + Z)^2]^{1/2}$ or 0.08 for $A = 1$ and $0.02\ [4(3.01)]^{1/2}$ for the last datum. EFK = 6.56 means that (any) k extracted from a properly weighted 2-decade decay having 24 uniformly spaced data will have a standard deviation which is 13.1 (±0.19)% of k [5, 6]. Similarly $\sigma(Z) = 1.45$ means that the standard deviation of Z is 0.029.

The tabulated EFA, EFK and $\sigma(A)$ show many regularities. As Z/A increases, the C and P results approach those for E noise and the E results are linear in $(Z + A)$. Reporting the results to three significant figures enables these to be checked. Finally comparison of these EFK values with those (also for 24 data) presented earlier (Tables III, IVa and V [6]) confirms that the standard errors are indeed ca. 1.4% [14].

As a whole, Table 1 provides the necessary quantitative information to allow the experimenter to establish what level of errors in the data can be tolerated for a given parameter precision. It also enables him to judge the relative worth of trying, for example, to extend the range over which the data are recorded. For instance, going from a half to one decade reduces the error greatly, but going still further may not be worth the extra time in-

TABLE 1

Relative errors[a] in parameters of $A\ \exp(-kt) + Z$ observed[b,c] for $\geqslant 2400$ sets of 24 simulated data evaluated by weighted non-linear least squares, for different error structures, Z/A and decade ranges

		E noise			P noise			C noise		
Z/A	Dec.	EFA	EFK	$\sigma(Z)$	EFA	EFK	$\sigma(Z)$	EFA	EFK	$\sigma(Z)$
0	0.5	3.59	6.64	3.96	2.52	5.08	2.84	1.74	3.83	2.05
	1	0.963	2.82	1.08	0.530	1.69	0.532	0.402	1.01	0.265
	1.5	0.733	2.04	0.589	0.557	1.01	0.179	0.454	0.480	0.0573
	2	0.754	1.80	0.415-	0.614	0.765	0.0764	0.466	0.294	0.0149
0.1	0.5	3.92	7.32	4.30	2.87	5.74	3.23	2.16	4.64	2.52
	1	1.06	3.09	1.20	0.647	2.08	0.692	0.473	1.37	0.398
	1.5	0.809	2.25	0.638	0.632	1.36	0.291	0.546	0.810	0.135-
	2	0.844	2.00	0.458	0.708	1.14	0.178	0.604	0.642	0.0697
0.5	0.5	5.35	9.98	5.86	4.42	8.60	4.93	3.63	7.31	4.12
	1	1.43	4.22	1.64	1.08	3.56	1.22	0.834	2.64	0.884
	1.5	1.11	3.09	0.882	0.929	2.34	0.585-	0.836	1.76	0.385
	2	1.15	2.73	0.629	1.02	2.05-	0.392	0.936	1.50	0.248
1	0.5	7.24	13.3	7.89	6.18	11.8	6.84	5.42	10.7	6.08
	1	1.95-	5.66	2.20	1.58	4.83	1.79	1.28	4.09	1.43
	1.5	1.46	4.11	1.17	1.30	3.43	0.905-	1.20	2.83	0.689
	2	1.51	3.63	0.828	1.39	2.96	0.629	1.32	2.44	0.455-
3	0.5	14.3	26.5	15.6	13.4	25.2	14.8	12.8	24.2	14.1
	1	3.97	11.4	4.46	3.54	10.6	4.03	3.20	9.86	3.69
	1.5	2.96	8.31	2.37	2.83	7.54	2.10	2.65	6.99	1.86
	2	3.06	7.42	1.67	2.94	6.56	1.45	2.83	6.18	1.31

[a]EFA in the percent error in A, per 1% noise at the first datum, and similarly for EFK. Therefore, the product of EFA and the noise level (expressed as a percent) yields the percentage error in A. $\sigma(Z)$ is σ_Z/the noise level. [b]The standard errors of the EFA, EFK and $\sigma(Z)$ are $\leqslant 1.44\%$ [14]. [c]A minus sign after a final five means these would round down.

volved or be affected by other non-first-order processes that begin to manifest themselves, etc. The same sharp drop in parameter error with increasing decade range has been shown for E noise (Fig. 6, [7]). One can also determine the optimal number of decades over which to record a fixed number of data. To minimize EFA, this is <1.6 decades, dropping to 0.9 decades for $Z = 0$ and C noise. (For k it is >3 decades, a result that is useless because if one followed the process for >3 decades, one would know Z well enough to avoid having to deal with the $A\ \exp(-kt) + Z$ model at all: see below.)

The correlations of the parameters show several regular patterns. The linear correlation coefficient for k with Z falls from 1 to 0.75 as the decade range increases for all 3 kinds of noise. The coefficient for A with k increases from -1 to $+0.2$, 0.6 and 0.8 for E, P and C noise, respectively, as the decade range increases. For P and C noise, this correlation coefficient decreases

as Z/A increases for $\geqslant 1$ decade. Because this correlation coefficient can be zero, the errors in A and k can be linearly independent of one another (unlike the case for k with Z). This happens in the 1—1.5 decade range, which is approximately optimal for minimizing EFA. For P and C noise, the generally negative correlation of A with Z also becomes positive at higher decade ranges and lower Z/A. This is in accord with an earlier study [7] in which it was shown that this correlation changes with decade range for $Z/A = -1$ (that study involved a specific growth case and E noise).

The EFA values refer here to evaluating A at the first datum, taken at $t = 0$. If A must be extracted for earlier times, the EFA will be greater because of extrapolations beyond the data range.

Comparison with the A *exp(—*kt*) case*

In the introduction it was noted that part of the reason for this study is related to some findings [12] for the simple $A \exp(-kt)$ case. If either $Z = 0$ or if there is no error associated with the constant background, then it is appropriate to consider relationships between this simpler 2-parameter model and the 3-parameter model here. Table 2 shows that the optimal decade ranges are different for these two models, that the error factors are rather larger if the 3-parameter model is used even if Z is known (the 3-parameter model is less efficient than the 2-parameter model [6]), and that the error factors in both models approach one another as the decade range spanned by the data increases.

TABLE 2

Effect of 2-(A, k) and 3-(A, k, Z)-parameter WNLLS models on EFA and EFK values for 24 decay data following $A \exp(-kt)$

	E noise		P noise		C noise	
Dec.	*Ak*	*AkZ*	*Ak*	*AkZ*	*Ak*	*AkZ*
	EFA					
0.5	0.499[a]	3.59[b]	0.448	2.52	0.396	1.74
1	0.594	0.963	0.499	0.530	0.396	0.402
1.5	0.676	0.733	0.548	0.557	0.396	0.454
2	0.743	0.754	0.594	0.614	0.396	0.466
3	0.836	0.842	0.676	0.694	0.396	0.450
4	0.894	0.902	0.743	0.745-	0.396	0.436
	EFK					
0.5	1.07	6.64	0.79	5.08	0.589	3.83
1	0.954	2.82	0.534	1.69	0.295	1.01
1.5	1.04	2.04	0.479	1.01	0.196	0.480
2	1.16	1.80	0.477	0.765	0.147	0.294
3	1.36	1.71	0.522	0.617	0.0982	0.156
4	1.52	1.78	0.580	0.603	0.0736	0.103

[a]These EFA and EFK values are exact for low noise levels. [b]See footnotes to Table 1.

Effects of ignoring weights on EFK, EFA and σ(Z)

It is clear that the default of ignoring weights is correct for the E case. Changes in EFA, EFK and $\sigma(Z)$ are also small for cases approximating the E case. These include large Z/A or a small decade range, that is, any situation where the relative errors (and hence weighting) among the data are rather similar.

Otherwise, the errors in the parameters rise sharply for P and especially C noise when the errors among the data differ appreciably. This is the case for small Z/A and for data sets that span larger decade ranges. The larger errors in the parameters are expressed by the efficiencies (as percentages):

efficiency(%) = 100 variance using WNLLS/variance using NLLS

These are presented in Table 3. Taking the ratio also makes these results relatively independent of the number of data, unlike those in the first two tables. If the unweighted analog of Table 1 is evaluated separately (that is, without paired analyses on the same simulated sets of data) and divided into Table 1 and squared, some efficiencies range to ca. 105% because of the errors propagated in squaring the ratio. As noted, each simulated set of data was instead analyzed twice, with both WNLLS and NLLS, thereby partially cancelling errors. Because the largest efficiency found was <101% and because of the consistency of Table 3, it seems unlikely that the standard errors of these efficiencies exceed 2%. Some simulations were done at very high noise levels to check on bias. Where this occurred (ca. 20% C noise), it occurred to virtually the same extent for both WNLLS and NLLS. Thus the efficiencies seem valid even at higher noise levels because the means, though slightly biased, are the same, irrespective of weighting. (Efficiencies are defined only if the means are equal [13].)

Some comments on agreement with Dawson's study [8] are appropriate. There a growth curve $[Z - A \exp(-kt)]$ was considered with $Z/A = -1$ to -2. E and C noise were used and most evaluations involved no weighting, 8 or 35 data and $\leqslant 50$ simulations per case beginning at varying times after $t = 0$. Because these conditions do not correspond to the cases examined here, quantitative comparison is not feasible. Qualitatively, however, there is general agreement. Any differences arise because of the broader decade and Z/A ranges considered here (and for the weighted cases, where the biased weights invalidate many of those results).

To the extent that relatively little error may be associated with the background, it is clear that there can be appreciable losses in efficiency if weights are ignored, particularly for C noise. This is crucial, as discussed in the introduction, because ignoring weights amounts to discarding the data which have taken much time and effort to collect [6, 14]. Obviously, the correct relative errors are not usually known. Table 3 shows the varying, and sometimes very serious, consequences if the error structure is not known or not used. These results make it clear that there are some cases where it pays to establish the relative errors, via replicate measurements or by analyzing

TABLE 3

Efficiencies (%) of determining constants (A, k, Z) of $A \exp(-kt) + Z$ if weights are ignored for different error structures, Z/A and decade ranges

Z/A	Dec.	Efficiencies (%)[a]						
		E noise	P noise			C noise		
		AkZ	A	k	Z	A	k	Z
0	0.5	100	93[a,b]	93	93	67	69	68
	1	100	92	72	69	93	37	28
	1.5	100	98	55	44	78	17	8
	2	100	91	42	26	57	8	1.6
0.1	0.5	100	93	93	93	76	77	76
	1	100	94	86	84	93	50	45
	1.5	100	99	75	74	89	36	29
	2	100	94	70	73	81	34	26
0.5	0.5	100	97	97	97	92	91	91
	1	100	99	96	96	97	81	82
	1.5	100	100	92	94	97	74	77
	2	100	98	89	93	95	72	78
1	0.5	100	99	99	99	95	95	95
	1	100	100	98	98	98	89	90
	1.5	100	98	98	98	100	88	90
	2	100	99	96	98	98	90	93
3	0.5	100	100	100	100	100	100	100
	1	100	100	99	99	99	98	98
	1.5	100	100	100	100	100	97	98
	2	100	100	99	99	100	99	99

[a]The efficiencies are calculated from the variances for non-linear least-squares using correct weights, divided by the variances for analyses on the same simulated sets (24 data), ignoring weights. [b]Based on the 1200 paired repetitions, the reproducibility and the self-consistency, the standard deviations of these efficiencies are about 2%.

residuals. The handsome dividends resulting from such efforts are either that errors in the parameters are much smaller or that these same parameters can be extracted from far fewer data without any reduction in precision.

There are other effects of not using the appropriate relative weights. The correlations of the parameters, found by means of WNLLS, with those found by NLLS, mirror the efficiencies: the correlations are low when the efficiencies are low. In other words, the parameters are unreliable or have large uncertainties. These product moment correlation coefficients dip to 0.95 for A, 0.66 for k and 0.52 for Z for P noise and to 0.75 for A, to 0.30 for k and 0.14 for Z for C noise, reaching these minima for $Z = 0$ and 2-decade delays. [Correlations among the parameters (A with k, etc.) are virtually identical to those obtained if the relative weights are correct.]

Of these other effects caused by ignoring weights, the most striking, and

the most important, involves the predicted σ. Unlike the case when WNLLS was used, they are not equal to the observed σ_A, σ_k or σ_Z. The errors predicted on the basis of the fit were sometimes <50% of the observed σ. For P noise, the inequalities are largest for EFA for >1 decade (irrespective of Z/A) and run to 20—40% differences for $\sigma(Z)$ and EFK when Z/A is small, for 1.5 and 2 decades. The relative differences are about twice as large for C noise. The observed EFK are always larger than the predicted EFK whereas the observed EFA are (much) larger only for $\geqslant$1.5 decades and range to 10% smaller than the predicted EFA for $\leqslant$1 decade. Obviously this finding means that estimates of the standard deviations of the parameters based on fits without regard to the appropriate relative weights may be in considerable error, thus misleading one about the precision of the experimental results and making tests of significance unreliable.

CONCLUSIONS

This study had two foci: extending earlier work [6—8] by providing EFA and $\sigma(Z)$ as well as EFK and evaluating effects on these when the data are not weighted. Confidence in the tabulated results is enhanced by their consistency, derived from the very large number of simulated sets of data analyzed.

Table 1 follows from the use of WNLLS and is based on the fact that this least-squares procedure was found to be most efficient for extracting k [6]. It was found that weighted treatment of the data yields unbiased parameters (except at very high C noise levels) and it has been shown how one can both optimize the decade range for A and minimize the correlation between A and either k or Z. Table 1 shows how greatly the errors in the parameters are reduced if the decay can be followed beyond merely 0.50 decades or 1.66 half-lives. Table 2, apart from confirming the low Z/A results of Table 1, shows that the errors in the parameters can also be greatly reduced (if Z is known) if the more efficient 2-parameter WNLLS treatment is used rather than the corresponding WNLLS method yielding 3 parameters.

While Tables 1 and 2 show the lower limits for EFA, EFK and $\sigma(Z)$ quantitatively, achieving some of these is sometimes barred by experimental constraints, such as the decade range over which the data can be collected without complicating effects. Hence any reduction in the errors of the parameters may come only from improving the data or increasing the number of experiments. Table 3, however, indicates that a third route may exist for those who do not weight their data.

The second part of this study shows that ignoring weights can markedly reduce efficiencies for some experimental cases of interest. Some of these efficiency decreases are so great that awareness of their magnitude will practically force the experimenter to seriously consider designing and executing studies to evaluate relative weights appropriate to his case. Such considerations must be made in the context of the ease of making further

replicate measurements compared to getting at the error structure underlying the data. At least, Table 3 shows where these considerations are important and provides, via the experimentally meaningful efficiencies, the numbers to permit objectivity. It is also clear that the precisions of the parameters could be confidently calculated from the fits only when the data are weighted. Thus the second part of this study is of particular value. Weighting is important to: (i) the precision achievable in the parameters extracted, (ii) the reliability of the reported precisions, and (iii) the efficiency with which the parameters are found.

Limitations

It is clear that this case (24 uniformly spaced data starting at $t = 0$ and having uncorrelated noise), and thus these results, will not be directly applicable for many situations. The variances are roughly inversely proportional to the number of degrees of freedom. Table 3 applies for any number of data greater than about 10. Simple first-order autoregression (common if the measuring circuit is too slow) can be removed [16]. Some effects of gradually more closely spaced data have been found but they are small if weighting is used [17]. Thus these results should still allow sufficiently reasonable estimates to be made about relative values of EFA, EFK and $\sigma(Z)$ to warn the investigator of high error/low efficiency cases. Then, of course, simulations can be done for the particular situation (kind of noise, achievable decade range, etc.). Moreover, EFA can be evaluated for an A at some specific distance beyond the data range. Effects of using the wrong weights, of the sensitivity of the results to the required initial guesses or to large errors, outliers or non-normality could also be checked, as deemed appropriate. Thus the results tabulated here provide a standard enabling one to judge how best to proceed to improve evaluation of $A \exp(-kt) + Z$ decay data and provide warnings about several effects.

The cooperation of Computing Services at this University is gratefully acknowledged as are R. E. D. McClung for WNLLS and J. Leduc for its conversion to APL. Partial support was provided by the Natural Sciences and Engineering Research Council of Canada.

REFERENCES

1 L. M. Schwartz, Anal. Chem., 53 (1981) 206.
2 J. R. Bacon and J. N. Demas, Anal. Chem., 55 (1983) 653.
3 A. H. Kalantar, Nucl. Instrum. Methods, 215 (1983) 437.
4 R. J. Woods, S. Scypinski, L. J. Cline Love and H. A. Ashworth, Anal. Chem., 56 (1984) 1395.
5 G. H. McKinnon, C. J. Backhouse and A. H. Kalantar, Int. J. Chem. Kinet., 16 (1984) 1427.
6 G. H. McKinnon, C. J. Backhouse and A. H. Kalantar, Int. J. Chem. Kinet., 17 (1985) 655.
7 G. E. Mieling and H. L. Pardue, Anal. Chem., 50 (1978) 1611.
8 R. M. Dawson, Anal. Biochem., 131 (1983) 483.

9 N. Draper and H. Smith, Applied Regression Analysis, 2nd edn., Wiley, New York, 1982, Chap. 10.
10 A. H. Kalantar, Nucl. Instrum. Methods, 201 (1982) 403.
11 E. A. Guggenheim, Philos. Mag., 2 (1926) 538.
12 A. H. Kalantar, J. Phys. Chem., 90 (1986) 6301.
13 R. R. Sokal and F. J. Rohlf, Biometry, 2nd edn., Freeman, New York, 1981, p. 311.
14 A. J. Lyon, Dealing With Data, Pergamon, Oxford, 1970, section 26.
15 A. H. Kalantar, Nucl. Instrum. Methods, 211 (1983) 555.
16 J. J. Thomas, An Introduction to Statistical Analysis for Economists, Weidenfeld and Nicolson, London, 1973, Chap. 11.
17 A. H. Kalantar, Chem. Eng. J., 32 (1987), in press.

Analytica Chimica Acta, 191 (1986) 369—376
Elsevier Science Publishers B.V., Amsterdam — Printed in The Netherlands

MONITORING THE PRECISION OF ROUTINE ANALYSES BY USING DUPLICATE DETERMINATIONS

PENTTI MINKKINEN

Department of Chemical Technology, Lappeenranta University of Technology, P.O. Box 20, SF-53851 Lappeenranta (Finland)

(Received 26th May 1986)

SUMMARY

To ensure the reliability of results, analytical laboratories require a continuous quality-control program which must take account of both systematic and random errors. Analyses of reference materials can be used to estimate systematic errors but estimates of random errors (precision) tend to be optimistic, mainly because reference materials cannot be put through the whole analytical process (e.g., primary sampling is often a major source of error). Estimates of precision must be based on routine samples. If duplicate determinations are done on routine samples, the precision can be estimated reliably. Within the optimum concentration range of analytical methods (usually starting from 5—10 times the detection limit), the relative standard deviation (s_r) can be regarded as being almost constant or independent of concentration. The precision can then be estimated by first calculating the s_r value of each pair of results. Individually, these are not reliable estimates of the true s_r, but they can be regarded as independent measurements of the same s_r and so can be pooled to obtain a more reliable estimate of precision with the number of duplicates as the degrees of freedom. The applicability of the method is tested on soil, rock and ore samples.

Chemical analyses are used in many fields of science and technology, generally to make decisions. If wrong action is taken because the analytical laboratory produces erroneous results, the consequences can be costly or even dangerous. Analytical laboratories should, therefore, devote significant time to internal quality control, otherwise they cannot guarantee the reliability of their results. The quality control program should be designed so that the levels of both random and systematic errors can be monitored.

Quality criteria of analytical results

The accuracy of a method refers to the difference (bias) between the mean, $\bar{x}$, of the set of results and the value μ, which is accepted as the true or correct value for the quantity measured. The term accuracy is also used as the difference between an individual value x_i and μ (in which case it represents the total error of the result). Bias refers to the systematic error of the method, i.e., to the error component, which is constant within a set of measurements. Precision means the reproducibility of measurements within a set,

0003-2670/86/$03.50

i.e., to the random scatter of results about the central value. The standard deviation and the relative standard deviation are the best estimates of this scatter and are generally used as the measure of the precision. In this paper, the precision of a method, $P_{0.95}$, is defined as the maximum relative random error at the 95% confidence level:

$$P_{0.95} = t_\nu(0.05)\, s_r, \tag{1}$$

where $t_\nu(0.05)$ is the 5% value of the t-distribution with ν degrees of freedom and $s_r = (s/\bar{x})\ 100\%$ is the relative standard deviation, $s = [\sum_i (x_i - \bar{x})^2/(n-1)]^{1/2}$ being the standard deviation. One of the main difficulties in the monitoring of the error components of analytical methods is that both the systematic errors and the random errors depend on the concentration of the analyte as well as on the type of sample matrix. The method described here is designed to overcome these problems.

Monitoring of systematic and random errors

The following methods can be used to evaluate systematic errors: blank determinations, analysis of reference samples, comparisons between different laboratories, and comparison of results with those obtained by independent analytical methods. The first two of these should be used routinely; the other two methods are usually too expensive for daily use.

The precision (random error) of routine analyses cannot be estimated reliably by using reference samples because the results tend to be too optimistic. There are three main reasons for this. First, reference samples cannot be put through the complete analytical process; at least some of the sampling steps are necessarily omitted. Secondly, reference materials are by their nature carefully prepared and homogenized, whereas routine samples often are not. Thirdly, the standard deviation of analytical methods depends on concentration as well as on the type of sample. As a single analytical method can be used to analyse many types of samples covering a large concentration range, values obtained just by using a few reference samples are not necessarily generally applicable, when the reliability of routine data is evaluated. For these reasons, it is imperative that the data used to evaluate the precision of routine analyses is based on routine samples.

ESTIMATION OF PRECISION BY USING DUPLICATE MEASUREMENTS

Precision of routine analyses can be estimated by conducting duplicate determinations on randomly selected routine samples. If the precision of the complete analytical process is to be checked, then duplicate primary samples must be taken. If only the performance of the laboratory is of interest, then duplicate determinations are done from the laboratory samples. The use of duplicate samples for monitoring precision has been suggested by Garrett [1] and Thompson and Howarth [2, 3]. Garrett used a logarithmic transformation to eliminate the dependence of standard deviation on concentration.

The logarithmic precision values obtained after this transformation are difficult to interpret, however. Thompson and Howarth based their work on the empirical observation that the dependence of the standard deviation on concentration can usually be approximated by a simple linear equation:

$$\sigma_c = \sigma_0 + kc, \tag{2}$$

where σ_c is the (absolute) standard deviation, σ_0 the standard deviation at zero concentration (i.e., the noise of the blank), k is a proportionality constant, and c the concentration.

Thompson and Howarth presented three different methods for estimating σ_0 and k experimentally by using the differences and mean values of each duplicate as estimators of σ_c and of the concentration c, consecutively. Quite a large number of duplicates must be run, however, to give a stable solution, especially if the samples routinely analysed cover a wide concentration range.

Estimation of precision based on relative differences between duplicate measurements

The method presented here is based on empirical modelling of the relative standard deviation instead of the absolute standard deviation by using the relative differences of each duplicate as estimators of the relative standard deviation. Originally, the method was based on the observation that the relative standard deviation of trace analytical methods could be regarded as practically constant (independent of concentration), if the relatively narrow concentration range from the detection limit up to 5—10 times the detection limit was excluded [4]. The method can also be derived by using Thompson and Howarth's equation (Eqn. 2) as the starting point.

If there is a linear relationship between the concentration and the standard deviation, then the relative standard deviation is by definition (concentration c = mean):

$$\sigma_r = (\sigma_c/c)\ 100\% = [(\sigma_0/c) + k]\ 100\% \tag{3}$$

This represents a hyperbolic function (Fig. 1), which rises quickly near the detection limit and approaches the constant value of $k \times 100\%$ at higher concentrations. This means that at the optimum concentration range of analytical methods, the relative standard deviation can be regarded as practically constant, i.e., independent of concentration. Equation 3 then reduces to

$$\sigma_r = k \times 100\% \quad (\text{for } c \gg c_{dl}) \tag{4}$$

where c_{dl} is the detection limit.

When Eqn. 4 is valid, the random error of an analytical method can be characterized by a single value, the relative standard deviation, which can easily be estimated from the differences of the duplicate measurements. If n duplicates are run and the results of each pair are x_{i1} and x_{i2}, then the relative standard deviations can be calculated separately for each duplicate:

$$s_{ri} = (s_i/\bar{x}_i)\ 100\% = [(x_{i1} - \bar{x}_i)^2 + (x_{i2} - \bar{x}_i)^2/\bar{x}_i^2]^{1/2}\ 100\%, \tag{5}$$

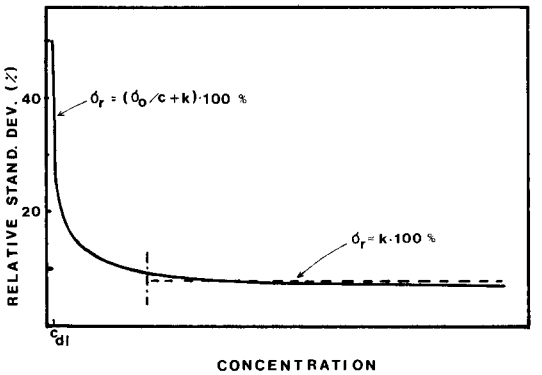

Fig. 1. Variation of the relative standard deviation, σ_r, with concentration can often be approximated with a hyperbolic function and, consequently, over a wide concentration range, generally the optimum range of analytical methods, σ_r is practically constant.

where $\bar{x}_i = (x_{i1} + x_{i2})/2$ is the mean of the duplicates i. By using the expression $d_i = (x_{i1} - x_{i2})$ for the differences (d_i), and the expression $d_{ri} = (d_i/\bar{x}_i) \times 100\%$ for the relative differences (d_{ri}) of the duplicates, and by taking into account that $|x_{i1} - \bar{x}_i| = |x_{i2} - \bar{x}_i| = |d_i|/2$, Eqn. 5 can be rewritten as $s_{ri} = |d_{ri}|/2^{1/2}$. Each s_{ri} has only one degree of freedom and, therefore, these values are not reliable estimates of the true relative standard deviation, σ_r. However, if Eqn. 4 is justified, then each s_{ri} can be regarded as an independent estimate of the same parent relative standard deviation, σ_r (with $\sigma_r = \sigma_{r1} = \sigma_{r2} = \ldots = \sigma_{rn}$) and the individual estimates can be pooled to obtain a more reliable estimate, s_r, of the relative standard deviation, which in this case has n degrees of freedom:

$$s_r = (\sum_i s_{ri}^2/n)^{1/2} = [\sum_i d_{ri}^2/(2n)]^{1/2} \quad (6)$$

To check if Eqn. 4 is valid so that Eqn. 6 can be used, it is advisable to arrange the data in ascending or descending order of concentration. A quick check can then be made by scrutiny of the individual d_{ri} values. Statistical tests can also be used to test the validity of the basic assumptions if judged necessary. If the concentration range near the detection limit is of interest, then Eqn. 6 cannot be used. In this case the variation of the relative standard deviation with concentration can be modelled, e.g., by fitting Eqn. 3 through points ($\bar{x}_i$, s_{ri}).

If the detection limit is defined as the concentration which gives a signal twice the standard deviation of the measurement noise (σ_0) at zero concentration, then $\sigma_r = (0.5 + k)\ 100\%$, when $c = c_{dl}$. The lowest limit at which Eqn. 4 is acceptable varies with the value of k. For $k = 0.1$ and $c = 20\ c_{dl}$, $\sigma_r = 12\%$, the limiting value of σ_r being 10%. For a more precise procedure with $k = 0.01$, $\sigma_r = 1.2\%$, when $c = 200\ c_{dl}$. For many analytical procedures, however, the

relative standard deviation reaches an approximately constant value more quickly than predicted by Eqn. 3 and so Eqn. 4 can often be extended to cover a wider concentration range than expected. For example, the data used in the following examples 1 and 2 are consistent with Eqn. 4 starting from concentrations only about five times the detection limit. When the method based on Eqn. 4 is used to monitor the precision of a particular analytical procedure, one must, however, check if the equation is justified over the whole concentration range for which the procedure is used.

PRACTICAL EXAMPLES ON THE USE OF THE RELATIVE DIFFERENCES METHOD IN ANALYTICAL QUALITY CONTROL

The analysis of relative differences of duplicate measurements has been successfully applied in geochemical and industrial laboratories to monitor the precision of routine analyses. The first example is given in Table 1, where the results of 31 duplicates are recorded. Duplicates were prepared from laboratory samples and were analysed for lead by atomic absorption spectrometry (a.a.s.) after dissolution in a hydrochloric/nitric acid mixture. Sample 17 was rejected from calculations after application of Grubbs' outlier test [5]. To check the validity of the basic assumption on the constant relative standard deviation, the data were arranged in ascending order of concentration and the relative standard deviation was estimated separately for three subgroups of ten duplicates. Each subgroup gave practically the same result. If there were any doubt about homogeneity of the relative standard deviation estimates, this could be checked, e.g., by applying Bartlett's test [6]. The estimate for the relative standard deviation for the whole concentration range was 7.75%, which gives a precision estimate $P_{0.95}$ = 16%. This is quite adequate for this type of analysis.

Table 2 presents the results of a set of 60 duplicates, which were run to check an a.a.s. method for determining molybdenum in molybdenite ore samples. Estimates of the relative standard deviation were calculated for five subgroups each covering a part of the concentration range of three orders of magnitude. Bartlett's test applied on these is far from significant. The relative standard deviation, s_r = 6.66%, calculated for the whole set can, therefore, be accepted as the best estimate of σ_r for the whole range of concentrations from 45 mg kg^{-1} to 4.1%. Figure 2 shows the frequency distribution of the relative differences of the 60 duplicates. The distribution is symmetric and agrees closely with the normal distribution shown in the figure. This confirms that the $P_{0.95}$ value (13% for this method) can be used as symmetric confidence limits of the random errors characteristic of this method.

For the third example, the results were taken from a paper by Rice [7]. Potassium was determined by flame photometry in international and other reference rocks and minerals; run 2 was done about two months after run 1. The subgroups of five duplicates do not differ significantly from each other. The $P_{0.95}$ confidence limits for the random error are 0.87% and 0.97% for the

TABLE 1

Precision of routine determinations of lead in soil and rock samples by flame a.a.s.

Sample no.	Results of duplicates (mg kg^{-1})			d_i	d_{ri} (%)
	x_{i1}	x_{i2}	$\bar{x}_i$		
1	60	63	61.5	−3	−4.88
2	60	65	62.5	−5	−8.00
3	72	72	72.0	0	0
4	80	99	89.5	−19	−21.23
5	100	92	96.0	8	8.33
6	104	100	102.5	4	3:92
7	130	115	122.5	15	12.24
8	140	151	145.5	−11	−7.56
9	200	208	204.0	−8	−3.92
10	480	550	515.0	−70	−13.59 s_r = 7.18%
11	600	807	703.5	−207	−29.42
12	800	800	800.0	0	0
13	820	855	837.5	−35	−4.18
14	920	836	878.0	84	9.57
15	2880	2990	2935	−110	−3.75
16	4000	4140	4070	−140	−3.44
17	3840	6000	4920	−2160	(−43.90) [a]
18	6000	6470	6235	−470	−7.54
19	6720	6600	6660	120	1.80
20	7200	6150	6675	1050	15.73
21	8120	6950	7535	1170	15.53 s_r = 8.80%
22	7320	8120	7720	−800	−10.36
23	8240	7550	7895	690	8.74
24	8560	8300	8450	220	2.60
25	8880	8490	8685	390	4.49
26	10240	9650	9945	590	5.93
27	11120	11000	11060	120	1.08
28	14300	14400	14350	−100	−0.70
29	13250	16600	14925	−3350	−22.45
30	14880	15100	14990	−220	−1.47
31	17700	15000	16350	2700	16.51 s_r = 7.16%
				$\bar{d}_r = -1.20\ s_r = 7.75\%$	
				$P_{0.95} = t_{30}(0.05)\ s_r$	
				$= 2.042 \times 7.75\% = 16\%$	

[a] The result was rejected as an outlier after using Grubb's test.

subgroups and 0.74% for the whole set. Because the samples in this study were reference materials, the obtained estimates of precision should also be regarded as reference values rather than representative of routine work. This example shows that the suggested method can also be used to monitor the performance of analytical methods having good precision (low value of k).

TABLE 2

Precision of a flame a.a.s. method used for molybdenite ore analysis. Precision was checked by running 60 duplicates

Concentration range (mg kg^{-1})	n	s_r (%)
45 . . . 355	12	6.82
365 . . . 535	12	8.44
575 . . . 1410	12	4.44
1500 . . . 4525	12	7.13
4600 . . . 41000	12	5.80
45 . . . 41000	60	6.66

Bartlett's test = 5.03 < χ^2 (0.05) = 9.49

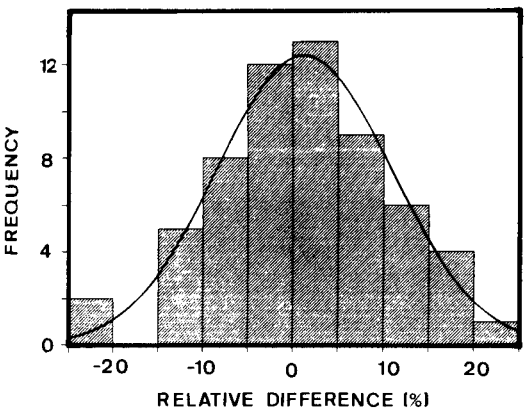

Fig. 2. Distribution of relative differences of 60 duplicate molybdenum determinations with a normal distribution (solid line) fitted to the same data.

Conclusions

Duplicate determinations done regularly on randomly selected duplicate samples provide an effective means of gathering reliable information on the precision of routine analytical work. When the precision of measurements is in statistical control, it is also easier to detect and control systematic errors. With a continuous quality control program in use, new data can be easily compared with old data and, if the quality of results starts to deteriorate, corrective actions can be taken immediately. With reliable data available on the performance of laboratory procedures, it is easier to select optimal methods for given analytical problems.

TABLE 3

Precision of a precise flame photometric method for potassium checked with reference materials [7]

Sample	Results of duplicates (%)			d_i	d_{ri} (%)
	x_{i_1}	x_{i_2}	$\bar{x}_i$		
NSWMD-1	0.0556	0.0554	0.05550	0.0002	0.36
NSWMD-2	0.0721	0.0720	0.07205	0.0001	0.14
NSWMD-3	0.2991	0.3012	0.30015	−0.0021	−0.70
T-1	1.011	1.009	1.0100	0.002	0.20
BCR-1	1.426	1.418	1.4220	0.008	0.56 s_r = 0.32%
AGV-1	2.458	2.459	2.4585	−0.001	−0.04
G-2	3.738	3.713	3.7255	0.025	0.67
GSP-1	4.610	4.579	4.5945	0.031	0.67
NSWMD-9	7.61	7.58	7.595	0.03	0.39
NSWMD-10	9.84	9.80	9.820	0.04	0.41 s_r = 0.35%
					$\bar{d}_r$ = 0.27 s_r = 0.33%
					$P_{0.95}$ = 0.74%

Financial support from Suomen Kulttuurirahasto (The Cultural Foundation of Finland) is gratefully acknowledged.

REFERENCES

1 R. G. Garrett, Econ. Geol., 64 (1969) 568; 68 (1973) 281.
2 M. Thompson and R. J. Howarth, Analyst, 98 (1973) 153; 101 (1976) 690.
3 R. J. Howarth and M. Thompson, Analyst, 101 (1976) 699.
4 P. Minkkinen, Precision Determination from Geochemical Duplicate Analyses, United Nations-MTA Int. Rep. B-45/11, Ankara, 1974; P. Minkkinen, Kemia-Kemi, 3 (1976) 12.
5 F. E. Grubbs, Technometrics, 11 (1969) 1.
6 J. R. Green and D. Margerison, Statistical Treatment of Experimental Data, Elsevier, Amsterdam, 1978, p. 168.
7 T. D. Rice, Talanta, 23 (1976) 359.

Analytica Chimica Acta, 191 (1986) 377—384
Elsevier Science Publishers B.V., Amsterdam — Printed in The Netherlands

SIMPLEX OPTIMIZATION PROCEDURE FOR EVALUATING EQUIVALENCE POINTS IN SIGMOIDAL AND SEGMENTED TITRATION CURVES

DOMENICO PEROSA, FRANCO MAGNO*, GINO BONTEMPELLI and PAOLO PASTORE

Department of Inorganic, Organometallic and Analytical Chemistry, University of Padova, via Marzolo 1, 35131 Padova (Italy)

(Received 5th February 1986)

SUMMARY

The use of the simplex procedure as a non-linear least-squares curve-fitting method is proposed for evaluation of equivalence points in sigmoidal and segmented titration curves. The application of this procedure to theoretical curves affected by different amounts of random noise indicates its effectiveness and accuracy for locating the correct end-point in titrations characterized by very low reaction constants. The relevant results are compared with those obtained by other regression methods as well as by the first-derivative and Gran approaches.

The widespread application of titration techniques has prompted numerous studies [1—3] dealing with the proper location of end-points in both sigmoidal and segmented titration curves. The reliability of this location may be doubtful when the product of the equilibrium constant for the titration reaction and the analyte concentration is low. When this product is low, acid/base titrations show inflection points (characterized by the maximum slope in the curve) which do not coincide with the equivalence points, while titrations exhibiting a linear dependence of the recorded signal on the analyte concentration give smooth curves in which linear portions are difficult to detect. In many cases, the titration of a very weak acid must be done under experimental conditions (i.e., reaction mixtures from which the quantitative recovery of the analyte is impossible) such that it cannot be replaced by the more accurate titration of its conjugated base with acid.

Suitable algorithms, i.e., multiparametric curve-fitting procedures, have been used extensively either to evaluate the best slope and intercept of linear segments [4] or to simulate the titration reactions themselves [1, 5, 6]. However, the modified simplex procedure [7] does not seem to have been applied to this problem even though its potentialities are well known [8, 9].

Because no algorithm can be considered in principle superior to any other for general purposes and because the simplex procedure is very easily used even by untrained operators, this sequential method was selected for application

0003-2670/86/$03.50

to the sigmoidal and segmented curves found in acid/base potentiometric and spectrophotometric titrations, respectively, chosen as typical examples. This paper reports the results obtained for both these cases.

DIGITAL SIMULATION MODELS

Sigmoidal titration curves

Titration curves were generated by a numerical computation method following well-established procedures [10]. Two different approaches were adopted. In the first, the potential range spanned in the titration was suitably divided in equal intervals and the corresponding volumes of titrant were easily calculated. In the second approach, a recursive computation method was used; i.e., the potential values corresponding to any incremental volume were calculated. The latter, more involved, way of generating titration curves was adopted in order better to reproduce the general experimental procedure in which the volume data are experimental settings [2]. Appropriate noise, the amounts of which reflected the actual precision obtained with commercially available instrumentation, was added both to volume and potential data. In particular, the uncertainty in the volume delivery was accounted for by applying the equation given by Radiometer for its ABU-80 autoburette (total volume 10 ml)

$$V = V_R \pm 2.5 \times 10^{-3} \pm 2 \times 10^{-3} V_R \quad (1)$$

where V is the modified volume data and V_R the volume readings; the constant error (2.5×10^{-3} ml) and relative error ($2 \times 10^{-3} V_R$ ml), given by Radiometer, were used in these simulations as the standard deviations of two independent Randu-Gauss subroutines (Scientific Subroutines Package, 1980; Digital Co., Marlboro, MA). In this way, variable noise consistent with the mentioned specifications was provided. The modified volumes so obtained were inserted in the appropriate relationship to derive the relevant potential values which were modified in their turn by adding, once again by a Randu-Gauss subroutine, a random potential noise with an average value of zero and a standard deviation of 0.5 mV.

Only weak monoprotic acids, characterized by pK_a values greater than 7.5, were considered in the calculations because the difference between the point of maximum slope (apparent end-point) and the equivalence point is appreciable only for very low values of the K_aC/K_w quantity, where K_a is the acidity constant, K_w the ionic product of water and C the analytical concentration of the acid.

Segmented titration curves

As typical examples, spectrophotometric titration curves for reactions of the type $A + B \rightleftharpoons P$, characterized by the absorption of light by the reaction product alone, were generated by calculating the absorbance during the titration as a function of the added titrant. In all cases, the product of the molar

absorptivity of the P species and its concentration was chosen in such a way that absorbance values less than one were obtained at the end of the titration; the uncertainty in the absorbance could then be considered independent of the absorbance [11].

In this case also, the generated quantity was modified by adding appropriate noise which took into account that absorbance and volume readings can be simultaneous sources of error. For this purpose, the volumes used to generate the titration curves were fuzzed according to Eqn. 1 and the absorbances thus obtained were further modified by adding random noise generated again by a Randu-Gauss subroutine. The latter noise was characterized by an average value of zero and a standard deviation of either 0.002 or 0.004 in the absorbance, i.e., uncertainties which are four and eight times, respectively, the values given by Perkin-Elmer for its Lambda-5 u.v.-visible spectrophotometer.

MULTIPARAMETRIC CURVE-FITTING PROCEDURES

The simplex optimization method, modified according to Nelder and Mead [12] was used as a non-linear multiparametric curve-fitting procedure. In acid/base titrations, the unknown parameters were the acid concentration, the acidity constant and the titration-cell constant ($E^* + E_{ref} + E_j$, where E^* is the "standard potential" of the indicator electrode, E_{ref} the potential of the reference electrode and E_j the junction potential). In the spectrophotometric tests, these parameters were the analyte concentration, the molar absorptivity and the equilibrium constant of the titration reaction. The convergence was made either on potentials or volumes in the first case, and in the latter case only on the absorbance values. In both cases, the data points (50) were treated with a constant-weight ($w = 1$) least-squares approach.

Very roughly estimated values of the unknown parameters can be accepted by this curve-fitting procedure which converges easily without requiring any transformation to normalize the factor (parameter) domains. A very satisfactory fit could be achieved, as indicated by the very low value of the standard deviation of the fitting calculated at the end of the sequential process. Because the simplex method used here does not furnish directly the uncertainties relative to the optimized parameters as standard deviations, they were calculated by the inverse matrix of the second derivatives of the parameters obtained at the convergence point by a finite difference approach [13]. Finally, in order to compare accuracy, computation time and stability of the simplex procedure with those relevant to other multiparametric curve-fitting methods, a previously described Gauss-Newton method [14] which is particularly suitable for acid/base titrations was also tested, as well as a general function minimization program [13].

The programs, available on request, were written in Fortran-IV and run on a MINC-11/23 minicomputer (Digital Equipment Corp.) under the RT-11 operating system. The general function minimization program was the

MINUIT algorithm available on a Digital Vax model 780 computer from the CERN Computer Centre Program Library [13].

A Tektronix 4662 digital plotter was used for drawing all diagrams.

RESULTS

Sigmoidal titration curves

Table 1 reports typical errors made when the forward first-derivative approach $[(E|V_{j+1}| - E|V_j|)/(V_{j+1} - V_j)$, where $E|V_j|$ and V_j are the coordinates of the jth data point] is used to evaluate the end-points in theoretical (free of noise) acid-base potentiometric titration curves. This Table also shows the results obtained by Gran's method [15] applied to the points located before and after the equivalence point. As can be seen, when the acid concentration or the acidity constant is decreased, the differential method gives increasing negative errors which are only slightly reduced by using the Gran approach. It is worth noting that these errors are basically parametric in the K_aC/K_w value. In contrast, the application of the simplex procedure even to flat titration curves with no sharp indication of the end-point, typified in Fig. 1, allows one to obtain concentration values practically coincident with the theoretical ones. This satisfactory result comes from the fact that the response surface relevant to this procedure, shown in Fig. 2, exhibits a very narrow range of uncertainty for the unknown concentration. Table 2 compares the results found by the simplex fitting method for some typical titration curves affected by noise with those obtained by a Gauss-Newton approach [14]. Similar accuracy is achieved with both methods but the simplex procedure requires a longer computation time, typical of a general optimization approach.

Segmented titration curves

When no definite break is present in segmented titration curves, the end-point can be located by resorting to extrapolation procedures [4] if linear

TABLE 1

Errors (%) found in simulated potentiometric titrations using either the first-derivative or the Gran method for evaluating the end-point

Log (K_aC/K_w)[a]	Mean error (%)	
	First-derivative method	Gran's method
3.50	−0.32	0.00
3.00	−0.32	−0.25
2.50	−1.00	−0.70
2.00	−4.32	−2.50

[a]Used to generate the titration curves.

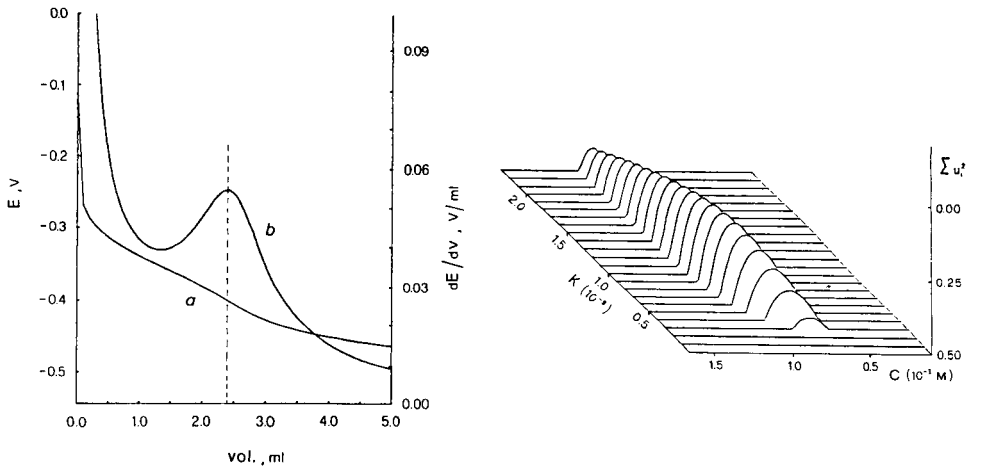

Fig. 1. Typical flat potentiometric titration curve (a) and its associated first-derivative curve (b) calculated for $pK_a = 10.0$, $C = 1.0 \times 10^{-2}$ M with an initial volume of 25 ml and a titrant concentration of 1.0×10^{-1} M. The dashed line shows that the apparent end-point (2.392 ml) does precede the equivalence point (2.500 ml).

Fig. 2. Surface error as a function of C and pK_a for a potentiometric titration curve simulated for $C = 1.0 \times 10^{-3}$ M and $pK_a = 9.0$. Error evaluated as the sum of the squared residuals. Note that the error increases in the negative z direction and that all values beyond 0.5 are considered equal to 0.5 for the sake of clarity.

portions, even though over small ranges, can be identified before and after the equivalence point. When smooth curves without linear portions are obtained, these extrapolation methods become unfeasible. It was found that these difficulties can easily be overcome by using the simplex procedure which allows the experimental data to be fitted by either a simulation (physicochemical) or a mathematical model. The simulation model used here was simply derived from the relationships which hold for spectrophotometric titrations and could be profitably applied to any kind of curve. The mathematical model was the following general function devised to make possible a smooth transition between two straight lines with different slopes [16], in this case the two linear regions present before and after the equivalence point:

$$y = y_0 + a_1(x - x_0) + a_2(x - x_0) \tanh [(x - x_0)/\gamma] \quad (2)$$

(x_0 and y_0 are the coordinates of the inconspicuous or invisible intersection point and a_1, a_2 and γ are appropriate parameters). Of course, in the present application the variables x and y are the volume and absorbance values, respectively.

Table 3 compares the results obtained at two different levels of noise with the simplex method (with either the physicochemical or the mathematical model) for titration curves characterized by very low KC products. The

TABLE 2

Comparison between the results found with the simplex method and a suitable Gauss-Newton procedure [14] in the fitting of theoretical curves generated with random noise both on potential (σ = 0.5 mV) and on volume (see Eqn. 1)

Values used to generate reference curves	Simplex[a]			Simplex[b]			Gauss-Newton[b]		
	Found[c]	Rel. error (%)	Time[d] (s)	Found[c]	Rel. error (%)	Time[d] (s)	Found[c]	Rel. error (%)	Time[d] (s)
E^* = 242 mV	241.94	−0.02		241.86	−0.06		241.99	0.00	
$K_a = 10^{-8}$ M	1.01×10^{-8}	1.00	179	1.01×10^{-8}	1.00	112	1.01×10^{-8}	1.00	19
$C = 10^{-2}$ M	10^{-2}	0.00		10^{-2}	0.00		10^{-2}	0.00	
E^* = 242 mV	242.34	0.14		241.40	−0.25		241.52	−0.20	
$K_a = 3.16 \times 10^{-11}$ M	3.29×10^{-11}	4.11	241	3.18×10^{-11}	0.63	254	3.18×10^{-11}	0.63	22
$C = 10^{-3}$ M	9.65×10^{-4}	−3.50		1.028×10^{-3}	2.80		1.028×10^{-3}	2.80	
E^* = 242 mV	242.32	0.13		241.50	−0.21		241.63	−0.15	
$K_a = 3.16 \times 10^{-12}$ M	3.29×10^{-12}	4.11	242	3.20×10^{-12}	1.27	211	3.20×10^{-12}	1.27	22
$C = 10^{-2}$ M	9.65×10^{-3}	−3.50		1.021×10^{-2}	2.10		1.021×10^{-2}	2.10	
E^* = 242 mV	242.34	0.14		241.40	−0.25		241.55	−0.19	
$K_a = 3.16 \times 10^{-13}$ M	3.28×10^{-13}	3.80	256	3.18×10^{-13}	0.63	265	3.18×10^{-13}	0.63	22
$C = 10^{-1}$ M	9.66×10^{-2}	−3.40		1.028×10^{-1}	2.80		1.028×10^{-1}	2.80	

[a] Algorithm written to minimize the squared residuals of potential values; it includes hence a Newton-Raphson subroutine. [b] Algorithm written to minimize the squared residuals of volume values. [c] Optimized values found with relative error. [d] Execution time.

TABLE 3

Results found with the simplex method based on the physicochemical model and the mathematical model in the fitting of segmented titration curves generated with two different noise levels (σ)

Values used[a]			σ = 0.002		σ = 0.004	
K_a (M^{-1})	C (M)	KC	Conc. found (M)	Rel. error (%)	Conc. found (M)	Rel. error (%)
Physicochemical model						
10^4	10^{-3}	10	9.850×10^{-4}	−1.5	9.700×10^{-4}	−3.0
5×10^3	10^{-3}	5	9.750×10^{-4}	−2.5	9.480×10^{-4}	−5.2
10^3	2×10^{-3}	2	1.922×10^{-3}	−3.9	1.826×10^{-3}	−8.7
10^3	10^{-3}	1	1.199×10^{-3}	19.9		
Mathematical model						
10^5	2×10^{-3}	200	1.982×10^{-3}	−0.9	1.978×10^{-3}	−1.1
10^5	10^{-3}	100	9.840×10^{-4}	−1.6	9.800×10^{-4}	−2.0
10^5	5×10^{-4}	50	4.845×10^{-4}	−3.1	4.810×10^{-4}	−3.8
10^5	2×10^{-4}	20	1.846×10^{-4}	−7.7	1.800×10^{-4}	−10.0

[a] Values for generating the reference curves.

accuracy is quite good and appears to depend on the precision of the input absorbance data.

It must be noted that the use of the mathematical model leads to accurate results only for KC products higher than 50. For lower values, progressively increasing errors are found (ca. −3% for KC = 20) because of the inadequate extent of the linear portions present in these cases. Consequently, a satisfactorily accurate end-point evaluation (within 4%) can be achieved by the mathematical model only for KC values (about 50) of about one order of magnitude higher than those required by the physicochemical approach (about 5).

Conclusions

The simplex procedure has been shown to be a valuable tool for measuring unknown concentrations from potentiometric and spectrophotometric titrations involving systems for which the derivative or extrapolation methods do not yield satisfactory results. Through suitable data analysis, it becomes possible to avoid particular experimental devices such as the determination of a very weak acid by titration of its conjugated base or the addition of suitable amounts of indicators in spectrophotometric titrations. It might be profitably applied in automatic apparatus for improving the results provided by these devices under the unfavourable conditions mentioned above. The simplex algorithm, even run on a microcomputer, is able to provide good results with an accuracy depending only on the amount of noise characterizing the measurements.

This work was supported by the Italian National Research Council (C.N.R.) and by the Ministry of Public Education.

REFERENCES

1 S. R. Goode, Anal. Chem., 49 (1977) 1408 and references therein.
2 L. M. Schwartz and R. I. Gelb, Anal. Chem., 56 (1984) 1487.
3 D. Midgley and C. McCallum, Talanta, 27 (1984) 409.
4 J. G. McCullough and L. Meites, Anal. Chem., 47 (1975) 1081.
5 G. Arena, E. Rizzarelli, S. Sammartano and C. Rigano, Talanta, 26 (1979) 1.
6 W. E. Gordon, J. Phys. Chem., 83 (1979) 1365; Anal. Chem., 54 (1982) 1595.
7 D. Betteridge, A. P. Wade and A. G. Howard, Talanta, 32 (1985) 709, 723.
8 Y. C. Martin and J. J. Hackbarth in B. R. Kowalski (Ed.), Chemometrics: Theory and Application, Anal. Chem. Symposium Series, 52 (1977) 153.
9 S. N. Deming and S. L. Morgan, Anal. Chem., 45 (1973) 278A.
10 K. J. Johnson, Numerical Methods in Chemistry, M. Dekker, New York, 1980.
11 H. A. Strobel, Chemical Instrumentation, Addison-Wesley, London, 1972.
12 R. O'Neill, in P. Griffiths and I. D. Hill (Eds.), Applied Statistics Algorithms, Ellis Horwood, Chichester, 1985.
13 F. James, Function Minimization, Proceedings of the 1972 CERN Computing and Data Processing School, Pertisan-A, September 1972.
14 C. Rigano, M. Grasso and S. Sammartano, Ann. Chim. (Rome), 74 (1984) 537.
15 F. J. C. Rossotti and H. Rossotti, J. Chem. Ed., 42 (1965) 375.
16 P. Moritz, in G. Svehla (Ed.), Comprehensive Analytical Chemistry, Vol. XI, Elsevier, Amsterdam, 1981, p. 114.

Analytica Chimica Acta, 191 (1986) 385—398
Elsevier Science Publishers B.V., Amsterdam — Printed in The Netherlands

THE CALCULATION OF EQUILIBRIUM CONCENTRATIONS IN LARGE MULTIMETAL/MULTILIGAND SYSTEMS

ALESSANDRO DE ROBERTIS, CONCETTA DE STEFANO and SILVIO SAMMARTANO*

Istituto di Chimica Analitica dell'Università, Via dei Verdi, 98100 Messina (Italy)

CARMELO RIGANO

Dipartimento di Matematica dell'Università, viale A. Doria, 95125 Catania (Italy)

(Received 26th May 1986)

SUMMARY

An algorithm for computing equilibrium concentrations by the "equilibrium constant" method is described. The main features of this algorithm are: (a) a damping procedure in conjunction with the Newton-Raphson technique that avoids divergence in dealing with very complicated (simultaneous presence of simple, mixed, protonated, polynuclear and hydroxypolynuclear species) and/or very large systems; (2) the use of devices to decrease core requirements, calculation time, and ill-conditioned problems; and (3) the calculation of errors in free and species concentrations from the uncertainties in analytical concentrations and in formation constants. Four systems are used for testing computer programs on calculation of equilibrium concentrations.

The problem of finding species concentrations in a multicomponent system is of great importance in many fields. Geochemists and marine chemists are interested in studying the real composition of sea, estuarine, lake, river, interstitial and, in general, ground waters. Biochemists, bio-inorganic chemists and analytical biochemists are interested in the speciation of fluids such as blood plasma and urine. Analytical chemists are interested in general speciation problems and in implementing titrations, etc. Environmental chemists are interested in all natural-fluid compositions. Other chemists are often concerned with the composition of multiphase/multicomponent systems in kinetic, complex formation, synthesis and other studies.

Many papers have been published on the problems of computing the concentrations of all species in a multicomponent system [1—34]. Two methods have been commonly adopted, i.e., the "equilibrium constant" and "free energy minimization" methods [7, 8]. With regard to numerical approaches for the solution of equations defining the system under study, the algorithms may or may not involve matrix inversion. The commonest algorithm that involves matrix inversion is the Newton-Raphson one [35, 36]. The reported algorithms and computer programs can deal with very different systems, such as simple acid/base, up to systems comprising several

0003-2670/86/$03.50

components and several phases. The possibility of simulating titration curves, of scanning analytical and/or free concentrations and of plotting distribution diagrams, is considered in some programs. The various computer programs have been designed for work with large, medium, mini and personal computers and have been written in different languages (generally, Fortran, Basic and Algol). Interesting applications of programs for computing concentrations in analytical, geological and biological problems have been reported [23, 37—41].

Topics of current interest in this laboratory are titration procedures for the determination of formation constants and formation enthalpies of weak, polynuclear and mixed complexes by potentiometry and calorimetry [42—51] and the speciation of biological fluids [52], thus it was thought worthwhile to investigate further the problem of computing equilibrium concentrations, with the aim of examining in detail all related features.

In this first contribution, a general algorithm is described for calculating concentrations in multicomponent systems. The reliability of the algorithm in handling four systems is tested.

THE ALGORITHM

For a system containing N components and M species, the mass-balance equations are

$$C_k = c_k + \sum_i p_{ik}\, \beta_i \prod_j c_j^{p_{ij}} \tag{1}$$

$$C_k = c_k + \sum_i p_{ik}\, x_i \tag{1'}$$

where C_k and c_k are the analytical and free concentrations of the kth component, respectively, x_i is the concentration of the ith species, β_i is the formation constant of the ith species, p_{ik} (or p_{ij}) is the stoichiometric coefficient of the kth component in the ith species, and the indices are defined as $k = 1 \ldots N$, $i = 1 \ldots M$ and $j = 1 \ldots N$. If C_k, p_{ik} and β_i are known, Eqn. 1 represents a set of N nonlinear equations to be solved simultaneously in order to find N c_k values. The problem is then to solve the set of equations

$$f_k(c) = c_k + \sum_i p_{ik}\, \beta_i \prod_j c_j^{p_{ij}} - C_k = 0 \tag{2}$$

subject to the constraint $c_k > 0$.

The Newton-Raphson technique allows c_k values to be calculated by the iterative procedure

$$\mathbf{c}^{(n+1)} = \mathbf{c}^{(n)} - \mathbf{G}^{-1}\,\mathbf{e} \tag{3}$$

where $\mathbf{c} = (c_1 \ldots c_k \ldots c_N)$, $\mathbf{G} = [\partial f_k(c)/\partial c_j] = (g_{kj})$ and $\mathbf{e} = (e_1 \ldots e_k \ldots e_N)$ ($e_k = C_{k,\mathrm{calcd}} - C_k$); at a certain stage n, the calculated analytical concentration is taken from Eqn. 1:

$$C^{(n)}_{k,\text{calcd}} = c^{(n)}_k + [\sum_i p_{ik}\,\beta_i \prod_j c_j^{p_{ij}}]^{(n)} \tag{4}$$

This technique offers the important advantage that few iterations are generally needed to reach convergence, but two main difficulties: (a) when G is singular or near-singular, inversion is impossible; (b) the iteration is often very unstable and, at some stage, the correction $\mathbf{G}^{-1}$ e may lead to divergence. These difficulties must always be kept in mind when the Newton-Raphson technique is used, but are particularly severe in dealing with highly nonlinear equations and when $N > 5$.

In order to overcome difficulty (a), scaling was applied to matrix G and to vector e according to the equations $g^*_{kj} = g_{kj}(g_{kk}\ g_{jj})^{-1/2}$ and $e^*_k = e_k g^{-1/2}_{kk}$ where g^*_{kj} and e^*_k are the elements of the scaled matrix and vector, respectively. In order to improve the stability of the iterations, it proved best to use the following procedure. If in a certain stage n, the ratio $R^{(n)}_k = C_k / C^{(n)}_{k,\text{calcd}}$ for the kth component lies outside the range $\rho^{-1} < R^{(n)}_k < \rho$ (ρ is a limit chosen in the range $1 < \rho < 10$), then the free concentration of the kth component is damped by the equation

$$c^{(n)}_{k,\text{damped}} = c^{(n)}_k (R^q_k)^{(n)} \tag{5}$$

where $q = |p_{ik}|^{-1}_{\max}$ (i.e., q is the reciprocal of the largest stoichiometric coefficient of the species containing the kth component). This procedure is applied to the component for which $\ln|R_k|$ assumes the maximum value, and is repeated until R_k for all components satisfies the condition $\rho^{-1} < R^{(n)}_k < \rho$. Then a new Newton-Raphson iteration step is performed. For the solution of the system outlined in Eqn. 2, the compact Gauss method was chosen (modified Gauss elimination method, more easily programmable on computers) [53].

Another important factor for the efficiency of the Newton-Raphson procedure is the choice of initial estimates, here $c^{(0)}_k$. This choice is not critical when the above damping procedure is used but, for speed of calculations, it is advisable to adopt some devices. According to the available knowledge of the system under study, users may choose estimates as follows: $c^{(0)}_k = 10^{-7}$, $c^{(0)}_k = C_k$ or $c^{(0)}_k = 10^{-\log(c_k)}$, with $-\log(c_k)$ supplied by the user. When several points for a titration curve or for a distribution diagram are to be calculated, the estimates of second and third points are the output of the first and second points, respectively. For the fourth and subsequent points, the empirical extrapolation equation (valid for a continuous monotonic function) is

$$c^{(0)}_{k,p} = c_{k,p-1} + [(c_{k,p-1} - c_{k,p-2})/(x_{p-1} - x_{p-2})]^2 \times [(x_{p-2} - x_{p-3})/(c_{k,p-2} - c_{k,p-3})]\ (x_p - x_{p-1}) \tag{6}$$

where p ($\geqslant 4$) is the index of the point and x_p is the titrant volume for simulating a titration curve or $-\log(c_N)$ for calculating distribution diagrams. For constant increments, Eqn. 6 reduces to

$$c_{k,p}^{(0)} = c_{k,p-1} + [(c_{k,p-1} - c_{k,p-2})^2/(c_{k,p-2} - c_{k,p-3})] \tag{7}$$

Other devices for reducing calculation time and core requirements must be taken into account. Unfortunately, very often the reduction of core requirements leads to increasing calculation time. An interesting example regarding this problem is the storage of stoichiometric coefficients (a very sparse two-dimensional array). Some reported algorithms [24, 31] reduce drastically the space required, but increase significantly the execution time. In the preliminary versions of ES4EC (see Results and Discussion), the calculation time was reduced as much as possible. However, probably the best way is to reduce storage when $N > 20$ and $M > 100$ but to reduce calculation time when $N < 20$ and $M < 100$.

In practice, in all cases in which species concentrations are to be calculated, it is necessary to give not only the free concentrations of components and the concentration of species but also the errors in these quantities arising from the uncertainties in the analytical concentrations and in the formation constants. Thus, given the error propagation law, it is necessary to calculate

$$\sigma_{c_j}^2 = \sum_i (\partial c_j/\partial \beta_i)^2 \, \sigma_{\beta i}^2 + \sum_r (\partial c_j/\partial C_r)^2 \, \sigma_{C_r}^2 \tag{8}$$

$$\sigma_{x_i}^2 = \sum_l (\partial x_i/\partial \beta_l)^2 \, \sigma_{\beta l}^2 + \sum_r (\partial x_i/\partial C_r)^2 \, \sigma_{C_r}^2 \tag{9}$$

where $r = 1 \ldots N$ and $l = 1 \ldots M$. The partial derivatives in Eqns. 8 and 9 can be obtained by deriving Eqns. 1 and 1′ with respect to β_i and C_j:

$$\partial C_j/\partial \beta_i = (\partial c_j/\partial \beta_i) + \sum_r (\partial c_r/\partial \beta_i) \sum_k (p_{ir} \, p_{ik} \, x_i/c_r) + p_{ij} \, x_i/\beta_i \tag{10}$$

$$\partial C_j/\partial C_r = (\partial c_j/\partial C_r) + \sum_k (\partial c_k/\partial C_r) \sum_i (p_{ir} \, p_{ik} \, x_i/c_k) \tag{11}$$

Because $\partial C_j/\partial \beta_i = 0$ [54] and $\partial C_j/\partial C_r = \delta_{jr}$ ($\delta_{jr} = 0$ for $j \neq r$ but $= 1$ for $j = r$; δ, Kronecker delta), Eqns. 10 and 11 represent $(M + N)$ sets of N linear equations

$$\mathbf{A}\,\mathbf{x} = \mathbf{b} \; (M \text{ systems, one for each } i) \tag{10′}$$

where $\mathbf{A} = (a_{jk})$ with $a_{jk} = \sum_l (p_{lj} \, p_{lk} \, x_l/c_k) + \delta_{jk}$, $\mathbf{x} = (\kappa_j)$ with $\kappa_j = \partial c_j/\partial \beta_i$, and $\mathbf{b} = (b_j)$ with $b_j = -p_{ij} \, x_i/\beta_i$;

$$\mathbf{B}\,\mathbf{y} = \mathbf{d} \; (N \text{ systems, one for each } r) \tag{11′}$$

where $\mathbf{B} = (b_{jk})$ with $b_{jk} = \sum_i (p_{ij} \, p_{ik} \, x_i/c_k) + \delta_{jk}$, $\mathbf{y} = (y_j)$ with $y_j = \partial c_j/\partial C_r$, and $\mathbf{d} = (\delta_{jr})$.

Once the partial derivatives of free concentrations of components have been obtained with respect to β_i and C_r, the analogous derivatives of species concentrations can be obtained from the equations

$$\partial x_i/\partial \beta_l = (\delta_{il} \, x_i/\beta_l) + \sum_i [p_{ij} \, x_i/c_j(\partial c_j/\partial \beta_l)] \tag{12}$$

$$\partial x_i/\partial C_r = \sum_j [p_{ij}\, x_i/c_j\, (\partial c_j/\partial C_r)] \qquad (13)$$

The values of $\partial c_j/\partial \beta_i$ obtained from Eqns. 10 or 10′, $\partial c_j/\partial C_r$ from Eqns. 11 or 11′, $\partial x_i/\partial \beta_l$ with Eqn. 12, and $\partial x_i/\partial C_r$ from Eqn. 13 allow $\sigma^2_{c_j}$ and $\sigma^2_{x_i}$ to be calculated from Eqns. 8 and 9, respectively. The procedure adopted does not take into account covariance terms in Eqns. 8 and 9; this is correct for dealing with data collected from various sources and obtained by means of different techniques, but is hardly to be recommended for simulating titration curves by using a homogeneous set of formation constants obtained in the same laboratory by the same technique [55, 56].

RESULTS AND DISCUSSION

A series of computer programs all dealing with the computation of equilibrium concentrations, ES4EC (equilibria in solution, problem 4, equilibrium concentrations), was written or will be written, in different languages and with different features. [In this paper, the computer programs ES4EC1 and ES4EC2 are briefly discussed in order to evaluate the performance of the proposed algorithm; more details will be given in subsequent papers but copies of the ES4EC1 and ES4EC2 listings (not definitive), are available on request.] A first edition, ES4EC1, was written in Fortran, on the basis of the described algorithm. The flow diagram of the program ES4EC1 is reported in Fig. 1. This edition can deal with systems containing 20 components and 80 species of any kind in one homogeneous phase; it can simulate titration curves and calculate a series of points for distribution diagrams [the free concentration of the last component (—log c_N) is scanned in a certain range]; it can calculate errors in free concentrations of components and species. A second program, ES4EC2, was written in Basic, and shows the same characteristics as ES4EC1. The ES4EC1 program was run in a Honeywell Level 6 (System 43) computer [program size, 17 kbytes; data size, 50 kbytes (double precision, 64-bit)] and the ES4EC2 program was run in an IBM AT personal computer (512 kb, double precision, 64-bit).

In order to evaluate the reliability of the proposed algorithm and of the ES4EC1 and ES4EC2 programs, four systems showing some interesting difficulties were selected.

System I. This had two components (Al^{3+} and H^+) and 10 species: $\log \beta[AlH_{-1}] = -4.4$, $\log \beta[AlH_{-2}] = -9.3$, $\log \beta[AlH_{-3}] = -15.0$, $\log \beta[AlH_{-4}] = -23.0$, $\log \beta[Al_2H_{-2}] = -7.7$; $\log \beta[Al_3H_{-4}] = -13.9$, $\log \beta[Al_4H_{-8}] = -28.2$, $\log \beta\ [Al_7H_{-16}] = -54.7$, $\log \beta[Al_{13}H_{-32}] = -100.0$ and $\log \beta[H_{-1}] = \log K_w = -14.0$. The conditions tested were $C_{Al} = 3.7 \times 10^{-5}$, 10^{-6} and 10^{-1} mol dm^{-3} at several pH values.

Formation constants of system I were taken from various sources. Though the considered constants do not represent the best set to explain the hydrolysis of aluminium, the proposed system shows an interesting variety of mono- and polynuclear species, so that various problems can be encoun-

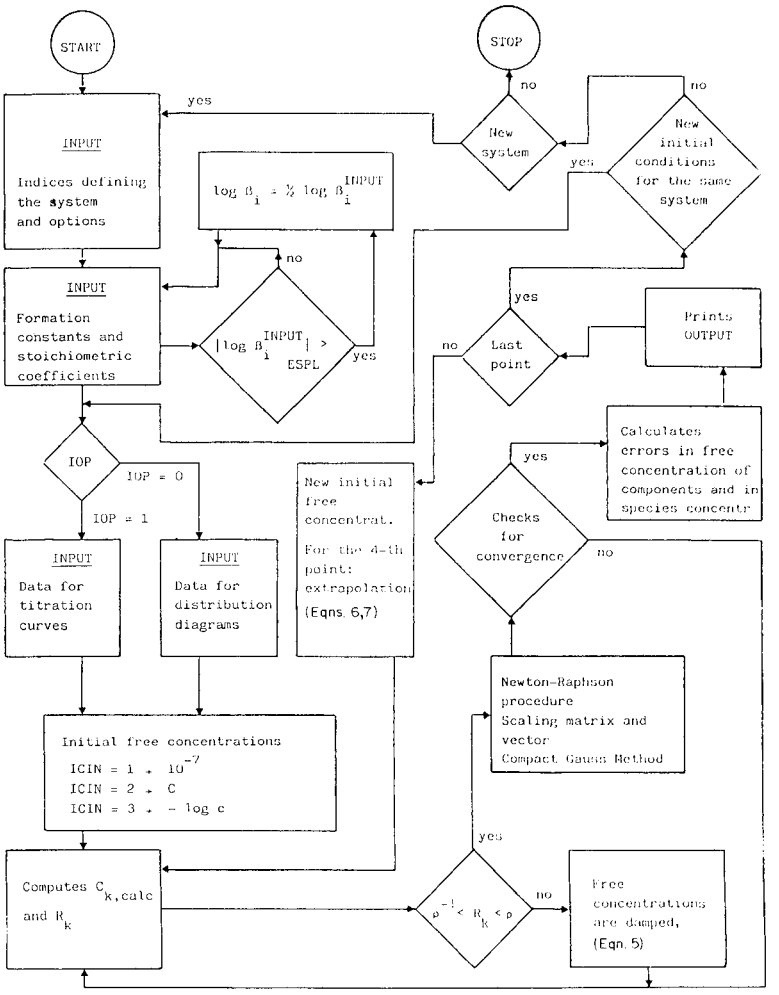

Fig. 1. Flow diagram of the ES4EC1 program.

tered if the algorithm used is not robust. In particular, the presence of species for which $\beta < 10^{-50}$ can lead to underflow problems. In the ES4EC program, formation constants $>10^{\mathrm{ESPL}}$ or $<10^{-\mathrm{ESPL}}$ (ESPL is an input value, depending on the machine used) are decreased by the following procedure: (1) if $|\log \beta_i^{\mathrm{INPUT}}| > \mathrm{ESPL}$, the formation constant is kept in memory as $\log \beta_i = \frac{1}{2} \log \beta_i^{\mathrm{INPUT}}$, and an index $IB_i = 2$ is recorded (otherwise $IB_i = 1$); (2) the species concentrations are calculated from the equation

$$\log X_i = IB_i \log \beta_i + \sum_j p_{ij} \log c_j$$

System II. This had five components [K^+, Cu^{2+}, Ni^{2+}, cit^{3-} (citrate), H^+] and 18 species: $\log \beta[H(cit)] = 5.99$, $\log \beta[H_2(cit)] = 10.42$, $\log \beta[H_3(cit)] = 13.41$, $\log \beta[K(cit)] = 0.74$, $\log \beta[K(cit)H] = 6.15$, $\log \beta[K(cit)H_2] = 10.26$, $\log \beta[Cu_2(cit)_2] = 15.28$, $\log \beta[Cu_2(cit)_2H_{-1}] = 11.90$, $\log \beta[Cu_2(cit)_2H_{-2}] = 6.66$, $\log \beta[Cu(cit)H] = 10.01$, $\log \beta[Cu_2(cit)H_{-1}] = 5.37$, $\log \beta[Ni(cit)] = 5.56$, $\log \beta[Ni(cit)H] = 9.59$, $\log \beta[Ni(cit)_2] = 8.85$, $\log \beta[Ni(cit)_2H] = 14.34$, $\log \beta[Ni_2(cit)_2H_{-2}] = -3.90$, $\log \beta[CuNi(cit)H_{-2}] = 2.37$, and $\log \beta[H_{-1}] = \log K_w = -13.97$. The conditions tested were $C_K = 0.75$, $C_{Cu} = 0.003$, $C_{Ni} = 0.003$, $C_{cit} = 0.008$ mol dm^{-3} at several pH values.

System II, taken from earlier work [48] is an interesting example of studies of complicated equilibria with the formation of polynuclear and mixed species.

System III. The fourteen components were Na^+, K^+, Ca^{2+}, ac^- (acetate), mal^{2-} (malonate), $male^{2-}$ (maleate), $succ^{2-}$ (succinate), $mala^{2-}$ (malate), $tart^{2-}$ (tartrate), pht^{2-} (phthalate), oda^{2-} (oxydiacetate), gly^- (glycinate), his^- (histidine), H^+ and there were 75 species (see Table 1). The conditions tested were $C_{Na} = C_K = 110$, $C_{Ca} = 10$, $C_{ac} = 1$, $C_{oda} = 0.1$, $C_L = 0.5$ mmol dm^{-3} (L = other ligands) at several pH values.

This rather large system is an example of a multicomponent solution in which several weak species are formed. The formation constants for this system were taken from earlier work [44—47, 49—51].

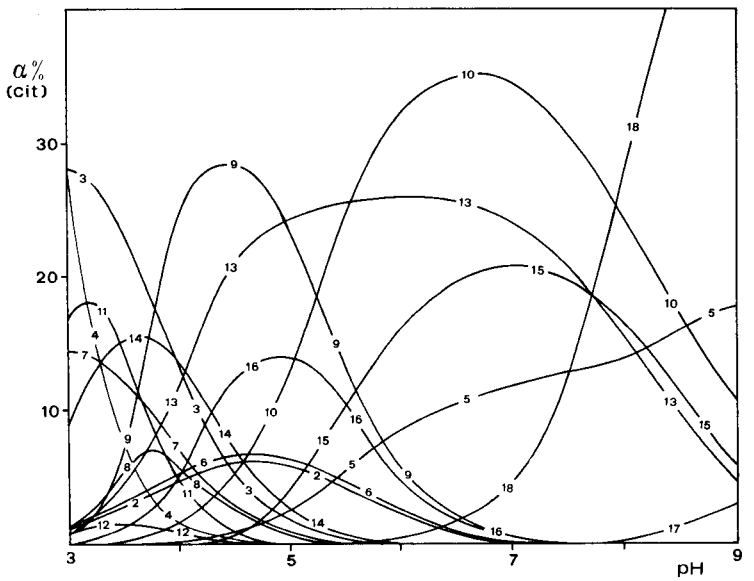

Fig. 2. Distribution of species vs. pH for the system IIa. Percentage refer to citrate. For the analytical conditions, see Table 3, and for the indices of species, see footnote (b) of Table 4.

TABLE 1

Log β values for the complexes formed in System III[a]

Species	Metal	Ligands									
		ac	mal	male	succ	mala	tart	pht	oda	gly	his
[HL]	—	4.571	5.36	6.02	5.26	4.74	4.01	5.09	3.97	9.55	9.06
[H_2L]	—	—	8.06	7.79	9.31	8.02	6.87	7.91	6.79	11.95	15.07
[H_3L]	—	—	—	—	—	—	—	—	—	—	16.82
[ML]	Na	−0.27	0.57	0.83	0.47	0.3	0.58	0.73	0.34	—	—
	K	−0.47	0.68	0.84	0.48	0.38	0.5	0.83	0.25	9.10	—
	Ca	0.57	1.64	1.76	1.45	1.95	2.10	1.71	3.46	1.05	0.95
[MLH]	Na	—	5.15	5.99	5.26	4.7	4.05	4.96	3.50	—	—
	K	—	5.31	6.00	5.28	4.5	4.0	5.16	3.50	9.08	—
	Ca	—	5.90	6.67	5.96	5.72	5.02	5.70	6.38	9.85	9.35
[MLH_2]	Ca	—	—	—	—	—	—	—	—	—	15.4

[a]Log β[NaH_{-1}] = −13.94; log β[CaH_{-1}] = −12.92; log β[H_{-1}] = log K_w = −13.84.

System IV. This concerned the hydrolysis of six metals, M_1—M_6 and H^+, i.e., 7 components and 35 species (see Table 2). The conditions tested were C_M = 1 mmol dm^{-3} (for all metals) at several pH values.

This system is an artificial example, for which the hydrolysis of six metal ions, simultaneously present in a solution and forming several species with a high degree of polymerization and hydrolysis was simulated. This system showed the same difficulties as System I, increased by the presence of more than one metal ion.

The ES4EC1 program was tested with all the above systems, and no divergence difficulties were encountered. The ES4EC2 program was tested with Systems II and III, and again no divergence problems were observed. The execution time for both programs (and machines) was very reasonable for all systems, as reported in Table 3. Moreover, it must be considered that all systems were tested by also calculating errors in the concentrations, and this increases the calculation time considerably. [For the systems here proposed, the ratio τ_e/τ (τ = execution time; τ_e = execution time when calculating errors) varies from 9 (System IIIa) to 2 (System IIb), according to the complexity of the system.] For clarity, only total iterations and functions evaluations, are reported in Table 3, but it should be noted that the first three points require generally a higher number of iterations (2—5 times) with respect to the mean value, and this indicates that the adopted extrapolation method (to find initial free concentrations, see Eqns. 6 and 7) allows a significant time-saving. For the damping procedure (see equations for $R_k^{(n)}$ and $C_{k,\mathrm{damped}}^{(n)}$), the values ρ = 4 (ES4EC1) and ρ = 2 (ES4EC2) were chosen for all systems. The choice of the factor ρ is not critical (ρ = 2—4 is a good choice in all these cases) but can have some influence on the number of function evaluations, in particular when initial estimates of free concentra-

TABLE 2

Equilibrium constants for the hydrolysis of metal ions in System IV[a]

Species	M_1	M_2	M_3	M_4	M_5	M_6
$[MH_{-1}]$	−3.00	−3.40	−7.71	—	−4.97	−2.19
$[M_2H_{-2}]$	−4.83	−4.80	—	−10.83	−7.70	−2.95
$[MH_{-2}]$	−8.29	−7.10	−17.12	−15.54	−9.30	−5.67
$[MH_{-3}]$	−20.0	−16.6	−28.06	−28.52	−15.0	−12.5
$[MH_{-4}]$	−32.2	—	—	—	−23.0	−21.6
$[M_3H_{-4}]$	—	−6.88	−23.88	−24.31	−13.94	−6.30
$[M_4H_{-4}]$	—	—	−20.88	—	—	—
$[M_4H_{-6}]$	−16.17	—	—	—	—	—
$[M_6H_{-8}]$	—	—	−43.61	—	—	—
$[M_2H_{-1}]$	—	—	−6.36	—	—	—

[a]Log $\beta[H_{-1}]$ = log K_w = −13.85.

TABLE 3

Some characteristics and execution times for the proposed test systems
(In all cases errors in free and species concentrations are calculated)

Program	System[a]	IOP[b]	No. of points	Total no. of iterations	Total no. of function evaluations	Time[c] (s)
ES4EC1	Ia	0	12	18 (1.5)[d]	142 (11.8)[d]	30 (6)
	Ib	0	12	13 (1.1)	125 (10.4)	30 (6)
	Ic	0	12	26 (2.2)	173 (14.4)	30 (7)
ES4EC1	IIa	0	41	85 (2.1)	176 (4.3)	151 (26)
	IIb	1	10	50 (5.0)	120 (12.0)	45 (12)
ES4EC2	IIa	0	41	85 (2.1)	174 (4.2)	249 (150)
ES4EC1[e]	IIIa	0	20	32 (1.6)	105 (5.3)	341 (200)
	IIIb	1	10	70 (7.0)	162 (16.2)	226 (150)
ES4EC1	IVa	0	14	48 (3.4)	156 (11.1)	79 (23)
	IVb	1	21	82 (3.9)	252 (12.0)	140 (50)

[a]Ia: $C_{Al} = 3.7 \times 10^{-5}$. Ib: $C_{Al} = 10^{-6}$. Ic: $C_{Al} = 10^{-1}$ mol dm^{-3}. pH 1—12 (constant increment). IIa: pH 3—9 (constant increment). IIb: titrant $C_{OH} = 0.75$ mol dm^{-3}, $V_0 = 100$ cm^3; 10 additions of 0.4 cm^3; pH 2.7—9.9. IIIa: pH 1—10.5 (constant increment). IIIb: titrant $C_{OH} = 0.1$ mol dm^{-3}; $V_0 = 100$ cm^3; 9 additions of 1.3 cm^3; pH 2.9—11.3. IVa: pH 3.5—10 (constant increment). IVb: titrant $C_{OH} = 0.25$ mol dm^{-3}; $V_0 = 100$ cm^3; 20 additions of 0.5 cm^3; pH 2—9.2.

Bad initial estimates of free concentrations were used, in order to check the convergence ability of the algorithm.

[b]0, distribution diagrams; 1, titration curves. [c]Including printer time (ES4EC1) or disk recording (ES4EC2); in parentheses, net time. [d]Mean values for each point. [e]Same results for ES4EC2 (execution time increased as in the case of System II).

TABLE 4

Some calculation details for System IIb[a]

V (cm^3)	I[b]	2	3	4	5	6	7	8	9	10
0.4	0.127	2.652	2.578	7.832	2.659					
	11.31	4.50	2.73	2.40	7.22	4.47	3.02	5.69	6.41	8.99
0.8	0.129	2.754	2.627	7.320	2.884					
	11.09	4.21	2.67	2.56	6.71	4.18	2.96	4.87	5.37	7.72
1.2	0.131	2.913	2.703	6.825	3.123					
	10.85	3.96	2.65	2.78	6.22	3.93	2.94	4.20	4.45	6.57
1.6	0.133	3.145	2.802	6.378	3.364					
	10.61	3.75	2.69	3.06	5.77	3.72	2.98	3.77	3.78	5.66
2.0	0.134	3.464	2.927	5.968	3.609					
	10.36	3.59	2.77	3.39	5.36	3.56	3.06	3.58	3.36	4.99
2.4	0.136	3.904	3.103	5.541	3.894					
	10.08	3.45	2.91	3.81	4.94	3.42	3.21	3.61	3.10	4.44
2.8	0.137	4.551	3.398	5.028	4.294					
	9.68	3.33	3.20	4.50	4.43	3.31	3.49	3.88	2.96	3.91
3.2	0.139	5.502	3.983	4.298	5.041					
	8.93	3.35	3.96	6.01	3.70	3.33	4.26	4.72	3.06	3.26
3.6	0.141	7.918	4.611	3.670	6.822					
	7.15	4.50	6.89	10.73	3.07	4.48	7.20	7.90	4.45	2.87
4.0	0.143	11.644	6.407	3.420	9.946					
	4.02	7.38	12.89	19.85	2.82	7.36	13.20	14.85	8.28	3.58

[a] See text for formation constants and Table 3 for concentrations. [b] First row: $-\log c_k$, $k = 1 \ldots$ (1) [OH]; (2) [H(cit)]; (3) [H_2(cit)]; (4) [H_3(cit)], (5) [K(cit)]; (6) [K(cit)H]; (7) [K(cit)H_2] (13) [Ni(cit)]; (14) [Ni(cit)H]; (15) [Ni(cit)$_2$]; (16) [Ni(cit)$_2$H]; (17) [Ni_2(cit)$_2H_{-2}$]; (18 [d] See ref. 9. (For the program EQUIL, $n_{it} = n_{fe}$.)

tions are not very good. In Table 4, some detail of System IIb calculations are reported and Fig. 2 shows a distribution diagram (System IIa).

Comparisons with the well known COMICS [5] and EQUIL [9] computer programs were also made. These two computer programs were chosen because they use two very different calculation methods, have been widely used in several laboratories, and are the progenitors of two families of other programs written for both general and specific problems (see e.g., [28]). Moreover, the comparisons can be extended to other computer programs through the testing results of Leggett [22] and Garcia and Madariaga [33]. For the comparison between ES4EC1 and COMICS, six test systems proposed by Leggett [22] were also used. In Table 5, some details of the comparisons between ES4EC1 and other computer programs are reported.

All the programs gave the same results within 0.01%. In the case of System I, both EQUIL and COMICS failed. For System II, COMICS failed

11	12	13	14	15	16	17	18	n_{it}^{c}	n_{fe}^{c}	n_{it}^{c} (EQUIL[d])
								12	37	22
3.13	5.11	4.85	3.48	9.39	6.56	19.40	13.21			
								5	7	6
2.95	4.58	4.39	3.24	8.42	5.81	18.03	11.89			
								5	7	6
2.85	4.16	3.97	3.06	7.50	5.14	16.71	10.65			
								3	5	5
2.88	3.93	3.62	2.95	6.71	4.58	15.53	9.61			
								3	5	5
3.03	3.92	3.33	2.91	6.01	4.13	14.47	8.74			
								3	5	7
3.33	4.08	3.08	2.95	5.33	3.74	13.40	7.93			
								3	5	13
3.86	4.47	2.87	3.13	4.60	3.41	12.16	7.05			
								4	6	12
5.03	5.29	2.72	3.73	3.73	3.28	10.38	5.83			
								7	9	10
8.40	7.31	2.72	5.51	3.10	4.43	6.82	3.86			
								7	11	8
15.00	11.39	4.27	10.18	4.40	8.85	3.66	2.63			
							Total	52	97	94

]qn. 1′); (1) K^+; (2) Cu^{2+}; (3) Ni^{2+}; (4) cit^{3-}; (5) H^+. Second row: $-\log X_i$, $i = 1 \ldots 18$ (Eqn. 1′);) $[Cu_2(cit)_2]$; (9) $[Cu_2(cit)_2H_{-1}]$; (10) $[Cu_2(cit)_2H_{-2}]$; (11) [Cu(cit)H]; (12) $[Cu(cit)H_{-1}]$; Ni(cit)$_2$H$_{-2}$] (charges omitted). [c] n_{it}, number of iterations; n_{fe}, number of function evaluations.

at pH $\geqslant$ 8. ES4EC1 was always faster than the other two programs. [It should be observed that the EQUIL program (Newton-Raphson technique) is more efficient for dealing with a few mass-balance equations whilst the COMICS program is more efficient for dealing with large systems with uncomplicated equilibria (such as System III)]. On average, ES4EC1 is five times faster than COMICS and three times faster than EQUIL (see Table 5). By considering the results of Leggett [22] and Garcia and Madariaga [33], ES4EC1 is probably faster than the majority of other programs in this field.

Future developments of this work may be considered. First of all, it is necessary to find an algorithm for the comparison of execution times among various machines. In fact, comparisons of various computer programs need an objective method for avoiding dependence on the computer used; then several computer programs could be compared, even in different laboratories. Although test routines are available, for the present problem it would

TABLE 5

Comparisons for execution times among different computer programs for the calculation of equilibrium concentrations

System	Calculation times (s)		
	ES4EC1[a]	EQUIL[b]	COMICS[b]
Ia[c]	4	failed	failed
IIa	11	—	85
IIb	6	15	—
IIIa	22	—	73
IIIb	43	141	—
IVa	10	—	failed
IVb	19	42	—
I'[d]	9	—	59
II'	7	—	13
III'	9	—	25
IV'	8	—	82
V'	10	—	57
VI'	7	—	10
I'—VI'[e]	—	100	307

Other computer programs	Leggett results [22]	Garcia and Madariaga results [33]
COMICS	100[f]	100[f]
COMPLEX [19]	53	—
EQUIL	33	—
COMPLEX-80 [32]	—	110
HALTAFALL [4]	—	103
SOLGASWATER [27]	—	104

[a]Net time, without calculating errors. [b]These computer programs were run in double-precision arithmetic. [c]Systems I—IV: see text and Table 3. [d]Systems I'—VI': see Leggett [22]. [e]Average results of Leggett [22] for systems I'—VI'; arbitrary times: τ (EQUIL) = 100. [f]Average results of Leggett [22] and Garcia and Madariaga [33] (in both cases, six relatively simple systems were tested).

be better to build up specific algorithms that take into account the features of the problem under study.

Further developments of the ES4EC program will be: (a) the use of formation constants at various ionic strengths and the simulation of titration curves at variable ionic strength; (b) the possibility of plotting results in a graphical form; (c) the possibility of dealing with more than one phase; (d) an analysis of various factors to be considered in the calculations relative to different systems e.g., hints must be given for choosing initial estimates and ρ values on the basis of the type of system; (e) the possibility of solving specific problems with a high degree of efficiency. Some of these developments are already under way in this laboratory. Results on these investiga-

tions, together with definitive versions of the program ES4EC, will soon be reported.

We thank CNR (Rome) and the Ministero della Pubblica Istruzione for financial support.

REFERENCES

1 W. B. White, S. M. Johnson and G. B. Dantzig, J. Chem. Phys., 28 (1958) 751.
2 J. W. Swinnerton and W. W. Miller, J. Chem. Educ., 36 (1959) 485.
3 A. J. Bard and D. M. King, J. Chem. Educ., 42 (1965) 127.
4 N. Ingri, W. Kakolowicz, L. G. Sillen and B. Warnqvist, Talanta, 14 (1967) 1261; B. Elgquist, Talanta, 16 (1969) 1502; R. Ekelund, L. G. Sillen and O. Wahlberg, Acta Chem. Scand., 24 (1970) 3073.
5 D. D. Perrin and I. G. Sayce, Talanta, 14 (1967) 833.
6 E. S. Johansen, Acta Chem. Scand., 21 (1967) 2273.
7 S. Gordon, Complex Chemical Equilibrium Calculations, NASA Spec. Publ. 239, 1970.
8 F. Van Zeggeren and H. S. Storey, The Computation of Chemical Equilibria, Cambridge University Press, Cambridge, 1970.
9 Ting Po I and G. H. Nancollas, Anal. Chem., 44 (1972) 1940.
10 I. K. Karpof and L. A. Kaz'min, Geochem. Int., 9 (1972) 252.
11 M. Bos and H. Q. J. Meershoek, Anal. Chim. Acta, 61 (1972) 185.
12 F. Marel and J. Morgan, Environ. Sci. Technol., 6 (1972) 58.
13 R. E. McDuff and F. M. M. Morel, Description and Use of the Chemical Equilibrium Program REDEQL2, W. M. Keck Laboratory of Environmental Engineering Science, California Institute of Technology, Pasadena, CA, 1973.
14 H. S. Dunsmore and D. Midgley, Anal. Chim. Acta, 72 (1974) 121.
15 A. H. Truesdell and B. F. Jones, J. Res. U. S. Geol. Surv., 2 (1974) 233.
16 D. A. Crerar, Geochim. Cosmochim. Acta, 39 (1975) 1375.
17 L. J. Walters, Jr., and T. J. Walery, Comput. Geosci., 1 (1975) 57.
18 L. N. Plummer, D. L. Paskhurst and D. R. Kosiur, MIX2: A Computer Program for Modeling Chemical Reactions in Natural Waters, U. S. Geol. Survey, Water-Resources Investigations, Reston, VA, 1975, pp. 75—161.
19 G. Ginzburg, Talanta, 23 (1976) 149.
20 R. Maggiore, S. Musumeci and S. Sammartano, Talanta, 23 (1976) 43.
21 D. J. M. Park, J. Chem. Phys., 65 (1976) 3085.
22 D. J. Leggett, Talanta, 24 (1977) 535.
23 P. M. May, P. W. Linder and D. R. Williams, J. Chem. Soc. Dalton Trans., (1977) 588.
24 G. Arena, C. Rigano and S. Sammartano, Ann. Chim. (Rome), 68 (1978) 693.
25 J. J. Fardy and R. N. Sylva, SIAS. A Computer Program for the Generalized Calculation of Speciation in Mixed Metal-Ligand Aqueous Systems, AAEC/E445, Lucas Heights, Australia, 1978.
26 J. W. Ball, E. A. Jenne and D. K. Nordstrom, in E. A. Jenne (Ed.), Chemical Modeling in Aqueous Systems, ACS Symp. Ser. No. 93, Am. Chem. Soc., Washington, D.C., 1979.
27 G. Eriksson, Anal. Chim. Acta, 112 (1979) 375.
28 D. K. Nordstrom et al., in E. A. Jenne (Ed.), Chemical Modeling in Aqueous Systems, ACS Symp. Ser. No. 93, Am. Chem. Soc., Washington, D.C., 1979; D. K. Nordstrom and J. W. Ball, in C. J. M. Kramer and J. C. Duinker (Eds.), Complexation of Trace Metals in Natural Waters, M. Nijhoff and W. Junk, The Hague, 1984.
29 L. Avery, J. Chem. Phys., 76 (1982) 3242.

30 D. D. Clark and S. M. Schuster, Computers and Chem., 7 (1983) 25.
31 V. S. Tripathi, Talanta, 30 (1983) 65.
32 J. M. Madariaga and A. Garcia, Comput. and Chem., 8 (1984) 187.
33 A. Garcia and J. M. Madariaga, Comput. Chem., 8 (1984) 193.
34 J. Kostrowicki and A. Liwo, Comput. Chem., 8 (1984) 91.
35 F. B. Hildebrand, Introduction to Numerical Analysis, McGraw-Hill, New York, 1956.
36 L. C. W. Dixon, Nonlinear Optimization, The English Universities Press, London, 1972.
37 D. D. Perrin, Nature, 206 (1965) 170.
38 P. S. Hallman, D. D. Perrin and A. E. Watt, Biochem, J., 121 (1971) 549.
39 D. Dyrssen, D. Jagner and F. Wengelin, Computer Calculation of Ionic Equilibria and Titration Procedures, Almqvist, Stockholm, 1968.
40 T. Anfalt and D. Jagner, Anal. Chim. Acta, 47 (1969) 57; 57 (1971) 165.
41 E. A. Jenne (Ed.), Chemical Modeling in Aqueous Systems, ACS Symp. Ser. No. 93, Am. Chem. Soc., Washington, D.C., 1979.
42 C. Rigano, E. Rizzarelli and S. Sammartano, Thermochim. Acta, 33 (1979) 211.
43 G. Arena, E. Rizzarelli, S. Sammartano and C. Rigano, Talanta, 26 (1979) 1.
44 P. G. Daniele, A. De Robertis, S. Sammartano and C. Rigano, Ann. Chim. (Rome), 73 (1983) 619.
45 P. G. Daniele, C. Rigano and S. Sammartano, Thermochim. Acta, 62 (1983) 101.
46 P. G. Daniele, A. De Robertis, S. Sammartano and C. Rigano, Thermochim. Acta, 72 (1984) 305.
47 A. De Robertis, C. Rigano and S. Sammartano, Thermochim. Acta, 74 (1984) 343.
48 P. G. Daniele, G. Ostacoli, C. Rigano and S. Sammartano, Transition Met. Chem., 9 (1984) 385.
49 A. De Robertis, C. De Stefano, R. Scarcella and C. Rigano, Thermochim. Acta, 80 (1984) 197.
50 A. De Robertis, C. De Stefano, S. Sammartano, R. Scarcellá and C. Rigano, J. Chem. Res., 42(S) (1985) 629 (M).
51 P. G. Daniele, A. De Robertis, C. De Stefano, S. Sammartano and C. Rigano, J. Chem. Soc. Dalton Trans., (1985) 2356.
52 P. Amico, G. Arena, P. G. Daniele, G. Ostacoli, E. Rizzarelli and S. Sammartano, in K. J. Irgolic and A. E. Martell (Eds.), Environmental Inorganic Chemistry, VCH Publ., Deerfield Beach, FL, U.S.A., 1985.
53 I. S. Berezin and N. P. Zhidkov, Computing Methods, Pergamon, Oxford, 1965.
54 I. Nagypal, I. Paka and L. Zekani, Talanta, 25 (1978) 549.
55 W. E. Wentworth, J. Chem. Educ., 42 (1965) 96, 162.
56 M. Micheloni, A. Sabatini and A. Vacca, Inorg. Chim. Acta, 25 (1977) 41.

Analytica Chimica Acta, 191 (1986) 399—411
Elsevier Science Publishers B.V., Amsterdam — Printed in The Netherlands

A CRITICAL COMPARISON OF COMPUTER PROGRAMS FOR THE POTENTIOMETRIC DETERMINATION OF STABILITY CONSTANTS

E. CASASSAS*, R. TAULER and M. FILELLA

Departament de Quimica Analitica, Universitat de Barcelona Diagonal 647, 08028 Barcelona (Spain)

(Received 26th May 1986)

SUMMARY

The performance of five of the best-known computer programs LETAGROP, SCOGS, MINIQUAD, SUPERQUAD and ESTA, is critically discussed. All these programs are based on least-squares refinement procedures but differ in some important aspects: (a) the definition of the residuals function; (b) the minimization procedure; (c) the statistical and weighting scheme; (d) the species selection procedure; and (e) the ability to refine some titration parameters. Each of these aspects is evaluated and the programs are compared on this basis.

For the last twenty-five years the study of solution chemistry, a fundamental of analytical chemistry, has been strongly reinforced by the development of powerful computer programs for the evaluation of potentiometric titration data [1—5].

The mass-balance equations for a system of NR reactants and N species can be written in a general way:

$$T_i = c_i + \sum_j q_{ij} B_j \prod_k c_k q_{kj} = c_i + \sum_j q_{ij} C_j$$

where T_i and c_i are the total analytical and free concentration of the reactant i, q_{ij} is the stoichiometric coefficient of the species j for the reactant i, B_j is the stability constant of the species j, and C_j refers to the concentration of the species j. The experimental known quantities in a potentiometric titration are: (a) the initial analytical concentrations of the reactants in the solution; (b) the added volumes of the titrant solution of known concentration; and (c) the free concentration of one (or more) reactants in the solution, which implies previous calibration of the potentiometric cell.

There are NR mass-balance equations at each potentiometric point. For NP titration points, there will be $NR \times NP$ mass-balance equations. As one or more free concentrations (NE) are measured potentiometrically, and N stability constants should be estimated, there is a total of $(NR - NE) \times NP + N$ parameters to be evaluated. Usually not all the stability constants of one system should be evaluated with the same data, and often the simpler equilibria are studied previously.

0003-2670/86/$03.50

There are three kinds of quantities or parameters in the mass-balance equations: (a) those which are common to all the titration points (stability constants); (b) those which are only common to each titration (initial concentration of the reactants, initial volume, electrode-calibration parameters, titrant concentration) from which the analytical concentrations at each titration point will be calculated; and (c) those particular to each titration point (unknown free concentrations).

In order to estimate the unknown parameters (e.g., the stability constants), the least-squares method [6] is used. In this procedure, the simultaneous optimization of the unknown parameters, $x_1\ x_2\ \ldots, x_N$ is achieved through minimization of the error square sum:

$$U = \sum_i w_i\,(f_{oi} - f_i\,(x_1, x_2, \ldots, x_N)^2 = \sum_i w_i\,(f_{oi} - f_{ci})^2$$

where f_{oi} are the observed quantities and $f_i(x_1, x_2, \ldots, x_N) = f_{ci}$ are the corresponding calculated values, by means of a functional relationship which is assumed to be known; w_i are the weights of each observation i. In a general way, f_{ci} is considered a non-linear function of the parameters to be estimated, therefore the least-squares solution at the minimum of U gives the equation (in matrix notation):

$$\mathbf{B}\,s = \mathbf{A}\,\mathbf{W}\,\mathbf{v} \qquad (1)$$

where v is the residuals vector with the elements $v_i = f_{io} - f_{ci}$, W is the diagonal matrix of the weights, A is the design matrix with elements a_{ij} which are the partial derivatives $\mathrm{d}f_{ci}/\mathrm{d}x_j$, s is the vector correction or shift of the parameters, and **B** = **AWA** (Gauss-Newton procedure) or **B** = **AWA** − **C** (in the Newton-Raphson procedure [7]), **C** being the matrix with elements containing the second derivatives of f_{ic}, $c_{ij} = v_i[\mathrm{d}^2 fc_i/(\mathrm{d}x_j \mathrm{d}x_k)]$. With an iterative process, convergence towards the minimum is obtained, and the values of the optimized parameters are calculated.

In the present paper, the performance of five of the best-known computer programs, SCOGS [8], LETAGROP [9–11], MINIQUAD [12], SUPERQUAD [13] and ESTA [14], for the evaluation of stability constants from potentiometric data is discussed and critically compared.

ERROR-SQUARE FUNCTION AND WEIGHTING

The first difference between the programs is the way in which the residuals function is defined. In potentiometry, there is controversy about which function (f_{oi}) should be used to define the residuals (v_i) or, put another way, which quantity should be taken as the dependent variable (response) and which one as the independent (predictor) variable (this controversy is not present in other experimental techniques such as spectrophotometry, where the observed absorbance has always been taken as the dependent variable). Two main approaches have been considered (see Table 1):

TABLE 1

Main features of the programs compared

Programs	Defined residuals	Method	Derivatives	Weighting
LETAGROP [9—11] (1962—68)	T_H; e.m.f.	Pit-mapping (Newton-Raphson)	Numerical	No
SCOGS [8] (1968)	Titrant volume	Gauss-Newton	Numerical	No
MINIQUAD [12] (1976)	All T_i	Gauss-Newton	Analytical	No
SUPERQUAD [13] (1985)	E.m.f.	Marquardt (Fletcher)	Analytical	Yes
ESTA [14] (1984)	T_H; e.m.f.	Marquardt	Analytical	Yes

in the first, the added volumes of titrant, or the analytical concentration of the titrating reactant (which is a linear function of the added titrant volume) is the dependent variable (SCOGS, MINIQUAD, LETAGROP with val = 1, and task OBJT in ESTA). In the second approach, the observed e.m.f. reading is taken as the dependent variable (LETAGROP with val = 4, SUPERQUAD and task OBJE in ESTA).

The use of the measured pH to calculate the free hydrogen-ion concentration (an exponential function of pH), which is then used to derive the calculated volumes of titrant (SCOGS), or to calculate the total concentration of hydrogen ion, has been considered not strictly rigorous by several authors [5], although it has practical and mathematical advantages. There is a related controversy about which quantities are better measured experimentally, either the analytical concentrations or the calibration parameters of the indicator electrode. When the dependent variable is defined in terms of the analytical concentrations as in MINIQUAD, it is assumed that the observed e.m.f. readings are exact; this means that calibration of the electrode is taken as free from error. In contrast, those procedures which define the residuals in terms of the e.m.f. readings consider the analytical concentrations free from error. Clearly, both procedures are partly incorrect, because both kinds of parameters will carry an undefined error even with the best set-up. This error, although random, becomes systematic for the titration points corresponding to each group of data or titration curve.

When the residuals are defined in terms of the analytical concentrations (as in MINIQUAD, LETAGROP (val 1) or ESTA (task OBJT)), a calibration error in the calculated standard potential causes a systematic error in the measured pH. This leads to larger residuals of total hydrogen concentration at lower pH than at high pH values. Moreover, the curves with lower total concentrations will participate less than those with higher concentrations in the residuals function defined in terms of all the total concentrations, as in MINIQUAD.

When the residuals are defined in terms of the measured e.m.f. (as in SUPERQUAD, LETAGROP (val 4) or ESTA (task OBJE)), the two problems

mentioned above do not appear, but it should be noted that e.m.f. readings are extremely sensitive to small systematic errors in the unbuffered parts of the titration curve, i.e., the end-points. The buffer capacity produced by the complexation equilibria in solutions with low concentrations of metal ion is smaller than in the presence of higher metal concentrations, and the unavoidable systematic errors in the analytical concentrations will yield larger deviations in the calculated e.m.f. values in the titration curves of lower metal-ion concentration. Therefore, these curves will contribute more to the error sum, the situation being the reverse of the one when the residuals are defined in terms of analytical concentrations.

From the above discussion, it can be concluded that weighting is necessary in both cases, and consequently a rigorous least-squares method [15] should be used, because the variance of the different residuals is not equal. The weights of each measured quantity are defined as $w_i = s_o^2/s_{y_i}^2$, where s_o^2 is the variance of one observation with weight 1, which in practice is taken as unity. From this equation, it follows that observations with small variances have high weight.

In contrast to this conclusion, it has been claimed [16] that when residuals are defined in terms of analytical concentrations, the results are not affected by weighting. This fact can be explained on the following grounds: (1) the high accuracy obtained in pH measurements using careful calibration and experimental conditions makes the error in the measured e.m.f. values rather small (in contrast to the accuracy attainable in the determination of the analytical hydrogen-ion concentration); (2) because the pH ranges under which the equilibria are studied (usually going from weakly acidic to weakly alkaline pH) are not very different for all the titration curves, the residuals are little affected by small imprecisions in electrode calibration; (3) when the model does not imply polynuclear complexes, the same species are formed in diluted and in concentrated metal-ion solutions, and therefore the relative overweighting of the latter gives a more accurate estimate of the stability constants. This is not the case, in our experience, when unit weights are applied to residuals defined in terms of e.m.f. readings (LETAGROP, val = 4), because as was pointed out above, gross deviations can be obtained in unbuffered ranges, and the fit is forced to the diluted curves, where small systematic errors have greater influence. In conclusion, when unit weights are applied, more reliable results are obtained for residuals defined in terms of total concentrations or added volumes than for residuals defined in terms of e.m.f. readings.

For use of the rigorous least-squares procedure, the variances in the measured quantities should be previously estimated. Among the programs considered, only SUPERQUAD and ESTA use such an approach. Briefly, the procedure used by SUPERQUAD is as follows. The problems with the reliability of the e.m.f. readings appear in the unbuffered parts of the titrations. The formula for calculation of the variance in one observation is

$$s^2 = s_E^2 + (dE/dV)^2 \, s_V^2$$

where s_E^2 is the estimated variance in the e.m.f. readings, s_V^2 is the estimated variance in the volume additions, and dE/dV is the slope of the titration curve which will be high in unbuffered parts of the titration curve (end-points). The weight is calculated for each experimental point from $w_i = 1/(s^2)_i$. For two electrodes,

$$s^2 = s_{E_a}^2 + s_{E_b}^2 + (dE_a/dV)(dE_b/dV)(dV)^2$$

For the calculation of the derivatives, SUPERQUAD uses a five-point cubic interpolation [13] or an analytical formula from the calculated titration curve.

Weights are calculated by ESTA by means of a similar error propagation formula

$$w_i = 1/(\sum_i (d(f_{oi} - f_{ci})/dx_j)^2 dx_j^2)$$

where the summation extends over e.m.f. readings and added titrant volumes. The variances associated with the total analytical concentrations can be calculated from the variances of all the experimental quantities by using the variance propagation rules. These experimental quantities include the number of moles of the reactants, the added volume, the concentration (titre) of the titrant, the experimental e.m.f., the standard potential and the initial volume of the solution. However, only in the case of ESTA is it possible to evaluate the influence of weights in the residuals defined in terms of total concentrations. As indicated above, MINIQUAD gives equal weights to all the titration input data.

NON-LINEAR LEAST-SQUARES ALGORITHMS

Only SCOGS uses the Gauss-Newton method in the simple way expressed by Eqn. 1, which sometimes leads to overshifting in the refinement of the parameters. The main problem with Eqn. 1 is the inversion of matrix **B**. When **B** is ill-conditioned, the values calculated for s oscillate across a narrow valley [5] because of the poor Taylor first-order-series approximation, particularly when the starting values of the parameters are far from the minimum, resulting in overshoot. To avoid this, several procedures have been proposed: (a) linear scaling of the shifts (old MINIQUAD [12]); (b) the Fletcher-Marquardt method [17] in MINIQUAD-75 and SUPERQUAD; the Levenberg-Marquardt method [18] in ESTA; and (c) an axial iteration method followed by a change of axes along which the variation of the constants is made, in LETAGROP [9—11]. Among these possibilities, the two versions of the Marquardt method give faster and more reliable results, whatever the initial values of the refined parameters.

The evaluation of the **A** and **B** matrices requires the calculation of the partial derivatives of the dependent variable with respect to the parameters to be estimated. This derivation is an important step when the speed of the programs is compared. In MINIQUAD, SUPERQUAD and ESTA, the deriva-

TABLE 2

Comparison of execution times of the programs[a] in the copper(II)/ammonia system

Program	Execution time (s)	
	1[b]	2[c]
SCOGS	40	102
LETAGROP (T_H)	49	257
LETAGROP (e.m.f.)	221	819
MINIQUAD	6	17
SUPERQUAD	9	18
ESTA OBJT $w = 1$	26	31
$w \neq 1$	12	33
ESTA OBJE $w = 1$	30	24
$w \neq 1$	16	35

[a]The times were obtained with a IBM 370/3083XE1 computer. They should only be considered comparatively.
[b]The initial proposed values for the constants were $\log \beta_{110} = 4.11$, $\log \beta_{120} = 7.62$, $\log \beta_{130} = 10.36$ and $\log \beta_{140} = 12.51$.
[c]The initial proposed values for the constants were $\log \beta_{110} = 3.0$, $\log \beta_{120} = 8.0$, $\log \beta_{130} = 11.0$ and $\log \beta_{140} = 15.0$.

tives are calculated from an analytical formula, while the other programs use numerical differentiation, a procedure that is not only less precise but also longer. The times needed for the calculations with the different programs in the copper/ammonia system are given in Table 2.

The analytical derivatives in MINIQUAD are calculated easily because the dependent variables (the total analytical concentrations) are a linear function of the parameters to be evaluated (the stability constants). In SUPERQUAD, the dependent variables (e.m.f.) are not explicit functions of the parameters to be evaluated, and implicit differentiation is required. It should be noted that in either MINIQUAD-75 and SUPERQUAD unknown free concentrations are also considered parameters to be refined by least-squares, while the other programs work at two different levels, one for the evaluation of stability constants by a least-squares procedure, and the other for solving the mass-balance equations for the free concentrations using each set of previously refined constants. The success of the MINIQUAD program compared to the others (LETAGROP, SCOGS) comes largely from intelligent exploitation of the matrix handling by the program [16]. The choice of total concentrations in the residuals function leads to simplified building of the design matrix. For SUPERQUAD, obtaining a suitable analytical formula for the calculation of the derivatives represented a big challenge because of the difficulties involved in its indirect deduction; however, with the use of implicit differentiation [19] and again with efficient application of matrix algebra, it was possible to calculate in a precise way the values of the derivatives needed, resulting in very short execution times.

STANDARD DEVIATIONS AND PARAMETER CORRELATION

The possibility of estimating the precision of the refined parameters is one of the major advantages of least-squares procedures. These estimates are directly obtained from the matrix $\mathbf{T} = s_o^2\,\mathbf{B}^{-1}$, where s_o^2 is the variance of unit weight which, being rarely available, is estimated from the standard deviation of the residuals $s_o^2 = U/(NP - N)$. The variances of the parameters are obtained from the diagonal elements of the matrix $\mathbf{B}^{-1}$, s_{ii}, and the covariances from the off-diagonal elements s_{ij}. From these values, it is possible to calculate a confidence contour $x \pm t(NP - N, \alpha)\ (s_o^2 B^{-1})^{1/2}$, where $t(NP - N, \alpha)$ is the appropriate percentage point of the t distribution at the significance level desired, with $NP - N$ degrees of freedom. The contour so determined will be a proper confidence contour only in the linear case and for a gaussian distribution of residuals. The use of the above expressions sometimes results in very small values of the confidence contours, and Anderegg [20] has discussed their reliability. For instance, in the study of a protonation or of simple binary complex equilibria, it is not unusual to obtain standard deviations affecting the third or even the fourth figure of the decimal logarithm of the constant, which implies a precision higher than the accuracy reasonably attainable in pH determination. Even if all other sources of error had been completely eliminated, the calibration and response of the electrode (assymetry potential, time drift) would still account for a systematic error of more than 0.002 in pH. Therefore, great caution is needed in reporting values for stability constants and their deviations. Usually only the first two significant decimal figures are likely to be reliable, as deduced from the analysis of variance applied to the different titration curves (see below).

The values of the correlation parameters are comprised between 0 and 1, and provide a measure of the linear dependence of one parameter on another, the remaining parameters being held constant. Values close to one indicate that the experimental data do not separately define the parameters. It is possible to obtain a very good fit to the data even when one parameter is erroneously estimated because the error affecting it can be compensated by an appropriate change in another parameter. Correlation of parameters is present when successive constants are refined together and one (or more) of them is not sufficiently defined by the available data, or when the corresponding species is already completely formed before the titration starts. Correlation frequently appears in the case of simultaneous refinement of titration group parameters and stability constants, and is a common situation in spectrophotometric work when molar absorptivities and stability constants are refined simultaneously. It is therefore important, to ensure the reliability of the given values of the constants, that the programs give the correlation parameters as MINIQUAD, SUPERQUAD and ESTA do.

STATISTICAL ANALYSIS OF THE RESULTS AND SYSTEMATIC ERRORS

Provided that observational errors are normally distributed, the distribution of the obtained residuals after the least-squares estimation of the parameters for the right model should also be normal. The main cause of deviation from normality is the presence of systematic errors introduced by an erroneous model selection or by the input experimental data (from limitations of the operator, the apparatus or the procedure), which produces inaccurate estimated parameters. Sources of systematic errors in potentiometric determinations include: (a) electrode calibration, (b) preparation and standardization of solutions, (c) use of contaminated reagents (particularly carbonated alkaline solutions), (d) temperature changes, (e) water quality, (f) changes in ionic strength that affect activities, (g) liquid junction potentials, and (h) imperfect selectivity of the indicator electrode.

In practice, for regression analysis, a detailed examination of the residuals plot is informative [15]. For this purpose, MINIQUAD and SUPERQUAD supply very useful residuals plots. Directly from these plots, it is possible to detect anomalous titration points, large deviations in unbuffered parts of the titrations, and lack of agreement between different titration curves. In a completely gaussian distribution of the residuals, these should be distributed randomly, without alternate sequences of positive and negative deviations. Additionally, MINIQUAD and SUPERQUAD give the value of the χ^2 statistic [12, 13] which also helps in the detection of systematic errors. Obviously, the best way to remove causes of systematic errors is careful experimental work, but even the best set-up may not eliminate all such errors.

When only one titration curve is examined, good fits and precision with a normal or quasi-normal residuals distribution are easily obtained. But from several titration curves which have been produced and examined independently, values of the stability constants will be obtained which differ by an amount probably higher than the predicted accuracy (e.g., three times the standard deviation). When the curves are examined together, a worse fit results and the residuals show some systematic trends. These facts suggest that the data coming from each titration curve belong to different statistical populations with different uncertainties in the group parameters. For instance, in potentiometric work with a glass electrode and an alkali solution as titrant, there are three group parameters which are critical: these are the initial acid concentration, the standard potential and the titrant concentration. And of course if the usual Gran procedure is used to calibrate the cell and to estimate the initial free acid concentration, these parameters are correlated. Braibanti et al. [21] suggested that the unavoidable systematic errors in each series of experiments (titration curves) when many series are being treated should be considered as a random population. First, all the titration data should be taken together, then each titration should be examined alone, and the averages of the estimated parameters and the averaged standard deviations should be calculated. An example of such an analysis for the copper(II)/ammonia system [22] is shown in Table 3.

TABLE 3

Analysis of variance between different titration curves in the potentiometric determination of the stability constants in the Cu(II)/NH_3 system[a]

Titration	s	χ^2	$\overline{\log \beta_{110}}$[b]	$\overline{\log \beta_{120}}$	$\overline{\log \beta_{130}}$	$\overline{\log \beta_{140}}$
1	1.48	9.14	4.044(26)	7.570(15)	10.266(28)	12.467(22)
2	1.22	14.6	4.114(09)	7.483(08)	10.326(11)	11.938(25)
3	2.10	7.47	4.115(13)	7.461(12)	10.346(15)	11.712(61)
4	1.27	23.9	4.097(05)	7.561(05)	10.331(08)	12.363(12)
5	1.19	12.7	4.082(04)	7.566(04)	10.296(06)	12.323(06)
6	1.91	8.82	4.118(09)	7.661(08)	10.346(13)	12.580(11)
7	1.10	10.5	4.143(21)	7.516(16)	10.400(21)	12.440(20)
All	4.14	27.2	4.099(09)	7.559(08)	10.315(11)	12.346(13)
$\overline{\log \beta_{pqr}}$[c]			4.102(12)	7.545(25)	10.330(16)	12.260(119)

[a]The results correspond to numerical analysis using SUPERQUAD; s (sigma) and χ^2 refer respectively to the standard deviation and χ^2 statistic of the weighted residuals (see [13]). [b]$\overline{\log \beta_{pqr}(k)}$ is the mean value from all the points in the kth titration; standard deviations appear in parentheses. [c]$\overline{\log \beta_{pqr}} = \Sigma \overline{\log \beta_{pqr}(k)}/m$ where m is the number of titrations.

QUALITY OF THE FIT AND MODEL SELECTION

When a particular model (set of the proposed species with their formation constants) has been fitted to the observed data, and the stability constants calculated, it is important to be able to judge the adequacy of the postulated model. Some kind of measure is needed to estimate the quality of the fit. In this sense, the value of the error function itself is not satisfactory; the standard deviation of the residuals is much more useful. In SCOGS, this can be related to the estimated errors in burette volume additions. In MINIQUAD, the comparison is less immediate because the variance in the values of all the total concentrations should be estimated; alternatively, the criterion has been used that a fit is acceptable when the value of the standard deviations of residuals is <1% of any of the total analytical concentrations (values between 0.1% and 1% accord with the precision usually obtained in such chemical procedures). In LETAGROP, the value of SIGY is a measure of the standard deviation of residuals. When residuals are defined in terms of analytical hydrogen concentration, SIGY gives the standard deviation of the total acid concentration in the millimolar scale. Values <1 are obtained usually for an acceptable fit. When the residuals are defined in terms of e.m.f. readings, it has been proposed that values of SIGY below 3 mV are acceptable for a reasonably good fit. It should be noted that as the e.m.f. readings are unweighted, a small number of large deviations (e.g., end-points), can distort greatly the measure of the fit. In SUPERQUAD, a magnitude with a more clear statistical meaning has been defined, σ, which is the ratio of the root mean square residual to the estimated standard deviation in the observations, or weighted standard deviation of residuals [13].

The value of σ is also called the sample standard deviation and is highly dependent on the chosen s_E and s_V values. When s_E and s_V have been correctly estimated [s_E is usually assumed to be the instrumental precision of the potentiometer (0.1 or 0.2 mV) and s_V is regarded as the precision in the burette readings which depends on the instrument used (usually 0.02–0.002 ml)], the value of sigma should be about one. Although this approach is clearly the most attractive of those so far proposed, there remains the difficulty of obtaining good estimates of the errors in observation, i.e., s_V and s_E. These values depend on the actual experimental conditions and on the quality of the instruments (as well as practical expertise). In a model-selection process models which have $\sigma \leqslant 3$ can be accepted. In ESTA, the value of the variance of the residuals is also given; from this, the standard deviation can be calculated and compared with the probable errors associated with the magnitudes considered in the residuals function.

The statistical F-test can be used to compare variances if a prior estimate is available. However, as accurate prior estimates are difficult to achieve, other methods have been proposed, e.g., the R ratio test [23]. For this purpose, MINIQUAD, SUPERQUAD and ESTA give the calculated values of R, which can be compared with the value of

$$R_{\text{lim}} = [\sum_i (w_i e_i^2)/(w_i f_{oi}^2)]^{1/2}$$

calculated by using the error propagation rules and the estimated errors associated with the dependent variables. A satisfactory fit is obtained when $R < R_{\text{lim}}$. When two or more models give R values smaller than R_{lim}, the R-factor ratio test can be applied to see if one of the hypothetical models can be rejected.

Experience suggests that, when such a situation arises (several models with a reasonable fit), it is difficult to select one of them by statistical means alone. The main reason for the ambiguity usually lies in the available data, which do not allow the proposed models to be distinguished. Typical examples encountered in the potentiometric method are model selection in systems involving monomer/dimer species [24] or, in general, involving equilibria which cause analogous changes in the measured quantities. In these cases, other methods (e.g., different kinds of spectroscopy) can be used successfully. Sometimes, too, there are experimental limitations like those arising when it is impossible to work at enough different reactant ratios and concentrations to identify models involving species with different stoichiometries and with the same number of released protons (an example of this is found in studies of metal/amine complexation [24–26]).

Various attempts have been made to implement methods for automatic model selection. SCOGS and ESTA do not have any automatic model selection for different species and each model must be tested independently by the user. In the automatic methods, a critical point is how to deal with negative constants appearing during the refinement. MINIQUAD allows the parameters to assume negative values during the linear minimization, but rejects

the negative values at the end of each iteration cycle. This procedure is considered dangerous, because the negative values can be partly due to incidental mathematical artifacts. In MINIQUAD, after an initial model has been examined, other combinations of its species can be tested by changing the refinable parameters. Because many of the data from the previous model have been stored, they can be used in the initial steps in the treatment of the new model, which results in a big saving of time and enables several models to be tested in a short time. In LETAGROP, new species are added to an initial model and the new model is tested, being accepted when the fit improves and the new constants (not negative) have values higher than a preselected multiple (usually 2 or 3) of their standard deviations.

The general scheme for model selection in SUPERQUAD is as follows. The best model is taken as the one which has the lowest sample standard deviation and no ill-defined formation constants (i.e., positive values with standard deviations less than 33% of their value). If after refinement a formation constant is found to be ill-defined, a new model is automatically generated from which the corresponding species has been rejected. Negative constants are not rejected during the refinement, but only at the end of it if they remain negative. Each successive model uses as initial estimates the "best" constants stored for the previous best model, before a new refinement is started. It must be mentioned that some problems can appear when there is a strong correlation between the refined parameters. It is open to discussion if a constant with a high standard deviation can be considered at the same level as a negative constant, because in the latter case, the concentration of the corresponding species is vanishingly low, whereas in the former it can be high.

ESTA has two facilities which provide useful information on the identity of the species that constitute a model. In one, plots of the formation and of the deprotonation functions can be obtained; the nature of dominant species can often be deduced from the shapes of these curves, which provide a useful means of comparing observed and calculated data. In the other, formation constants for individual species regarded as the predominant complex can be estimated as required to produce agreement between calculated and observed data at the point considered. Such information can be useful in choosing species as well as providing initial estimates of their formation constants.

Model selection is often complicated in systems where polynuclear species are present; selection of the best model requires a large amount of calculation and critical judgement of the results. In mixed-ligand systems, several species may be present at the same pH. The presence or absence in the model of mixed species affects the fit of the potentiometric experimental data in a rather limited way, even when the mixed species predominates, because in the course of the refinement the absence of a mixed species can be compensated by higher concentrations of the related binary complexes. In these cases, direct comparison of experimental and calculated titration curves is of considerable help in ascertaining the presence of mixed-ligand complexes.

REFINEMENT OF TITRATION PARAMETERS

The titration or group parameters can be refined with LETAGROP, SUPERQUAD or ESTA. LETAGROP, as in other aspects of data treatment, is the pioneer in this approach. The procedure used involves the refinement of the group parameters at a lower level after each change in the values of the common parameters (stability constants) at a higher level. In this way, the best set of group parameters is obtained for each set of stability constants. In LETAGROP (version ETITR [27]), the refinable group parameters are the standard potential of one or two electrodes, the initial acid concentration and/or an impurity in the solution titrated, the titrant or both solutions, and the metal-ion concentration. The group parameters can be refined by using either individual titrations or a set of them. However, simultaneous refinement of group and common parameters in LETAGROP has been found to be very extravagant of computer time.

In SUPERQUAD, group parameters are called "dangerous parameters" to emphasize the fact that their refinement is questionable unless their values cannot be established with sufficient accuracy by any known chemical method. The refinable parameters are the standard potentials, the slope response of the electrode, and the analytical concentrations of all the reactants in the titrand and in the titrant. It is possible to constrain a certain parameter, setting the condition that during the refinement only equal relative shifts of its value for all the titrations are calculated. This can be applied, for instance, to one of the constituents when its purity cannot be exactly known.

ESTA can refine the following parameters: initial test solution volume, vessel and burette concentrations, and intercept and slope of the electrode responses. The effectiveness of optimizing different sets of parameters can be tested by examining several sets of simulated titration data generated by ESTA with random errors in any of the titration parameters except the formation constants [14].

The sources of systematic errors in potentiometric experiments and their influence on the results were discussed above. It might be thought that the refinement of group parameters could be used to eliminate the systematic errors in concentrations and calibration parameters. At this point, several observations should be made: (a) the refinement of titration parameters can never be a substitute for a careful experimental procedure; (b) the refinement of titration parameters can have a negative effect on the selection of the right model, because the concentration of minor species can be compensated by small changes in titration parameters; (c) the random error associated with each of the titration parameters becomes systematic for the corresponding titration points, and its presence at certain levels is unavoidable; (d) when the work has been done over a properly selected range of conditions, it can be accepted that a limit of precision and accuracy has been achieved, and that then it is nonsense to try to improve the fit by refinement of titration parameters, although some systematic trends may still appear in the residuals.

Following Sillén and coworkers [27], the simultaneous refinement of common and titration parameters usually produces three kinds of situation: (a) better fit and precision with reasonable values of the refined parameters; (b) better fit but worse precision and also reasonable values of the parameters; and (c) better fit, worse precision and completely unreasonable values of the parameters. The third case is unacceptable; a false minimum of the error-square function has been found. A group parameter has an unreasonable value when it is too distant from the value proposed from experiment (i.e., it has been changed by more than 5%). The second case is commoner; it happens when group parameters and common parameters are correlated. Great care must then be taken and the refinement order must be carefully planned. Nevertheless, if the precision is low, it is better to accept the results obtained without the simultaneous refinement of group parameters. The first case is, of course, the only one which can assure the correctness of the approach; the refined estimation of group parameters is then better than the experimental one, but this situation is quite rare.

The authors are grateful for the computer time made available through grant CAICYT-657/81.

REFERENCES

1 P. Gans, Coord. Chem. Rev., 19 (1976) 99.
2 F. Gazier, Coord. Chem. Rev., 27 (1979) 195.
3 F. J. C. Rossotti, H. Rossotti and R. J. Whewell, J. Inorg. Nucl. Chem., 33 (1971) 2051.
4 C. W. Childs, P. S. Hallman and D. D. Perrin, Talanta, 19 (1969) 629.
5 F. R. Hartley, C. Burgess and R. Alcock, Solution Equilibria, Horwood/Wiley, Chichester, 1980.
6 W. E. Deming, Statistical Adjustment of Data, Wiley, New York, 1943.
7 L. C. W. Dixon, Non-Linear Optimization, The English Universities Press, London, 1972.
8 I. G. Sayce, Talanta, 15 (1968) 1397.
9 L. G. Sillén, Acta Chem. Scand., 16 (1962) 159; 18 (1964) 1085.
10 N. Ingri and L. G. Sillén, Acta Chem. Scand., 16 (1962) 173; Ark. Kemi, 23 (1964) 97.
11 L. G. Sillén and B. W. Warnqvist, Ark. Kemi, 31 (1968) 315; 31 (1968) 341.
12 A. Sabatini, A. Vacca and P. Gans, Talanta, 21 (1974) 53; Inorg. Chim. Acta, 18 (1976) 237.
13 P. Gans, A. Vacca and A. Sabatini, J. Chem. Soc. Dalton Trans., (1985) 1195.
14 P. M. May, K. Murray and D. R. Williams, Talanta, 32 (1985) 483.
15 N. Drapper and H. Smith, Applied Regression Analysis, 2nd edn., Wiley, New York, 1981.
16 A. Sabatini and A. Vacca, J. Chem. Soc. Dalton Trans., (1972) 1693.
17 R. Fletcher and M. J. D. Powell, Comp. J., 6 (1963) 163.
18 D. W. Marquardt, J. Soc. Ind. Appl. Maths, 11 (1963) 431.
19 I. Nagypal, L. Päka and L. Zékány, Talanta, 25 (1978) 549.
20 G. Anderegg, Acta Chem. Scand., Ser. A, 33 (1979) 74; Ser. A, 34 (1980) 467.
21 A. Braibanti, F. Dallavalle, G. Mori and B. Veroni, Talanta, 29 (1982) 725.
22 E. Casassas and R. Tauler, J. Chim. Phys., 82 (1985) 1067.
23 A. Vacca, A. Sabatini and M. A. Cristina, Coord. Chem. Rev., 8 (1972) 45.
24 R. Tauler, E. Casassas, M. J. A. Rainer and B. M. Rode, Inorg. Chim. Acta, 105 (1985) 165.
25 R. Tauler, E. Casassas and B. M. Rode, Inorg. Chim. Acta, 114 (1986) 203.
26 E. Casassas and R. Tauler, J. Chim. Phys., 83 (1986) 409.
27 P. Brauner, L. G. Sillén and R. Whiteker, Ark. Kemi, 31 (1968) 365.

Analytica Chimica Acta, 191 (1986) 413—423
Elsevier Science Publishers B.V., Amsterdam — Printed in The Netherlands

ASSESSMENT OF THE RESULTS OBTAINED FROM DIFFERENT COMPUTER PROGRAMS APPLIED TO POTENTIOMETRIC COMPLEXATION DATA

ENRIC CASASSAS, MONTSERRAT FILELLA* and ROMÀ TAULER

Departament de Química Analítica, Universitat de Barcelona, Diagonal 647, 08028 Barcelona (Spain)

(Received 19th June 1986)

SUMMARY

The calculation of equilibrium constants in solution by means of five published computer programs is critically evaluated. Three equilibrium systems were chosen to illustrate the capabilities of these programs. A trend toward better reliability, increasing amount of information supplied and inclusion of facilities which can be of great help for the user, is observed in the more recent programs such as SUPERQUAD and ESTA.

One of the main aims of analytical chemistry is to extract as much reliable information as possible from experimental data. The achievement of such an aim has been greatly strengthened by the general adoption of computers which have changed the quality and style of analytical work. Solution chemistry is an area in which the application of computer-assisted methods of data reduction was pioneered. As early as 1962, Ingri and Sillén [1] published LETAGROP, the first attempt to build a computer program which could cope with complex equilibria data. Although LETAGROP was conceived initially as a supplement to the graphical methods then used, numerical methods progressively abandoned their supplementary status and became independent tools for the treatment of solution data.

Computer programs have permitted great strides to be taken in fields where simplifying assumptions are needed (model selection) or where complicated and/or repetitious calculations have to be done. The trend toward a sounder interpretation of experimental data involves a need for critical evaluation of the performance and abilities of such programs. As has been already pointed out [2], reliability is the main feature to be considered in comparison of programs, and reliability seems to depend greatly on the nature of the chemical problem being investigated in a way that has not yet been clearly characterized. Therefore, any critical evaluation requires the application of the programs under comparison to some real systems comprising different types of complex formation equilibria.

In the work described here, the programs selected for comparison purposes were Sillén's pioneering LETAGROP [1, 3—7], two programs of widespread

0003-2670/86/$03.50

popularity, SCOGS [8] and MINIQUAD [9, 10], and two recently published programs, ESTA [11, 12] and SUPERQUAD [13]. The main features of these programs were tabulated in the preceding paper [14]. The comparison was made by applying the programs to three equilibrium systems, which represent those most usually found in the examination of solution equilibria: (1) the copper(II)/ammonia system involving formation of complexes of one metal ion with one ligand; (2) the lead(II)/*N*-(2-mercaptopropionyl)glycinate system involving formation of protonated complexes and polynuclear complexes of one metal ion with one ligand; and (3) the copper(II)/salicylate/pyridine system involving the formation of mixed-ligand complexes.

The calculations were done on VAX 11/750 and IBM 3083 computers. The terms used are explained in Table 1.

RESULTS AND DISCUSSION

Copper(II)/ammonia system

This is a well-known binary system. It was studied here [15] by an adaptation of the procedure proposed by Bjerrum: a large excess of the proto-

TABLE 1

Glossary of terms

Symbol	Definition
T_i	Total concentration of component i.
C_i^V	Initial concentration of component i in titration vessel.
C_i^B	Concentration of component i in the burette.
$[X_i]$	Free concentration of component i.
pqr	Vectorial notation for complex $M_pL_qH_r$.
$pqq'r$	Vectorial notation for mixed-ligand complex $M_pL_qL'_{q'}H_r$.
$\log \beta_{pqr}$	$[M_pL_qH_r]/[M]^p[L]^q[H]^r$.
$\log \beta_{pqq'r}$	$[M_pL_qL'_{q'}H_r]/[M]^p[L]^q[L']^{q'}[H]^r$.
N	Number of experimental points.
n_p	Number of refined parameters.
σ_E, σ_V	Estimated standard deviation of e.m.f. and titrant volume.
d	Standard deviation of $\log \beta$.
SIGY	LETAGRÓP's standard deviation of residuals based on (a) T_H in the millimolar scale (val 1), (b) e.m.f. (val 4).
U	Sum of squared residuals. (a) SCOGS: $U = \Sigma(V^o - V^c)^2$ where V is the titrant volume; (b) MINIQUAD: $U = \Sigma(T_i^o - T_i^c)^2$; (c) ESTA: $U = [\Sigma(y^o - y^c)^2]/(N - n_p)$, where y is either e.m.f. or total ion concentration sensed.
σ	Residuals standard deviation from MINIQUAD output.
Sigma	Sample standard deviation from SUPERQUAD output.
R	Hamilton R-factor.
R_{lim}	Hamilton R-limit.
$\bar{Z}_M$	Metal formation function = $[T_L - [A](1 + \Sigma_n \beta_{LH_n}[H]^n)]/T_M$
$[A]$	$(T_H - [H] + [OH])/(\Sigma_n n\beta_{LH_n}[H])$
$\bar{Q}$	Deprotonation function = $(T_H^* - T_H)/T_M$

nated ligand (NH_4^+) was present, and its concentration was kept constant during the titration, in order to favour complex formation and to avoid metal hydrolysis and precipitation. The experimental conditions were as follows: 7 titrations with 311 experimental points, T = 25°C, I = 1.0 mol l^{-1} ammonium nitrate, C^V_{Cu} = 2.4—9.0 mmol l^{-1}, and −log[H] = 3.6—7.6.

Because the model has long been established, it was taken for granted that the species 110, 120, 130 and 140 are formed in this system. Table 2 shows the results obtained from the application to the experimental data of the different programs tested, i.e., log values of the formation constants of the four species formed, their standard deviations as given by the programs and all the complementary information from the programs in relation to the goodness of the fit achieved.

Examination of these results shows that the values of the constants obtained with the different programs are equivalent for practical analytical purposes, notwithstanding the small differences between them. Of special interest is the complete accord observed when a weighted objective function is used in the minimization procedure regardless of which sum of squared residuals is used (e.m.f. in SUPERQUAD and option OBJE of ESTA, or total ion concentration sensed in option OBJT of ESTA).

The different standard deviations reported in Table 2 are very similar, especially considering that LETAGROP supplies three times the value of the standard deviations.

TABLE 2

Copper(II)/ammonia system. Logarithms of formation constants obtained from different computer programs with standard deviations in parentheses

Program	Option	$\log \beta_{110}$	$\log \beta_{120}$	$\log \beta_{130}$	$\log \beta_{140}$	Complementary information
LETAGROP	val 1	4.084	7.573	10.311	12.380	SIGY = 0.318
		(0.051)	(0.041)	(0.053)	(0.046)	
	val 4	4.080	7.557	10.307	12.361	SIGY = 1.454
		(0.014)	(0.026)	(0.038)	(0.053)	
MINIQUAD		4.103	7.580	10.327	12.389	$U = 2.54 \times 10^{-6}$; χ^2 = 193;
		(0.008)	(0.008)	(0.012)	(0.012)	$\sigma = 5.22 \times 10^{-5}$, skewness = −0.96; kurtosis = 12.5
ESTA	OBJT	4.100	7.582	10.324	12.380	$U = 8.96 \times 10^{-8}$
	unw.[a]	(0.011)	(0.009)	(0.012)	(0.010)	R = 0.0003
	OBJT	4.099	7.561	10.318	12.346	U = 17.0
	w.[b]	(0.006)	(0.006)	(0.008)	(0.009)	R = 0.0002 (R_{lim} = 0.00004)
	OBJE	4.102	7.557	10.326	12.349	U = 1.62
	unw.[a]	(0.003)	(0.005)	(0.008)	(0.012)	R = 0.018
	OBJE	4.098	7.561	10.317	12.345	U = 17.3
	w.[b]	(0.006)	(0.006)	(0.008)	(0.009)	R = 0.026 (R_{lim} = 0.006)
SUPERQUAD[a]		4.099	7.559	10.315	12.346	sigma = 4.14; χ^2 = 27.2
		(0.009)	(0.008)	(0.011)	(0.013)	

[a]Unweighted. [b]Weighted: σ_E = 0.2 mV; σ_V = 0.01 ml.

*Lead(II)/(*N*)-(2-mercaptopropionyl)glycinate system*

Lead complexes with *N*-(2-mercaptopropionyl)glycinate (MPG) were studied under biological conditions in order to include the formation constants obtained in a model for blood plasma simulation [16]. The experimental conditions were as follows: 10 titrations with 474 experimental points, T = 37°C, I = 150 mmol l^{-1} chloride, C^{V}_{Pb} = 1.7—3.4 mmol l^{-1}, C^{V}_{MPG} = 1.8—16.1 mmol l^{-1}, and —log[H] = 2.0—8.0.

The essential difficulty in the study of solution equilibria lies in model selection. Strictly speaking, the model includes all the mathematical relationships required to describe an equilibrium system, including the parameter values, but the term is often used to mean only the set of species present. The identities of such species are not generally known in advance but they are required for the optimization procedures usually applied. The model chosen must be the one which gives the most satisfactory account of the data from both chemical and statistical points of view, but the model selection process is often far from straightforward.

The following model selection procedure was applied to solve this system: (a) plotting of experimental $\bar{Z}_M$ (vs. −log[A]) and $\bar{Q}$ (vs. —log[H]) curves (Figs. 1a and 2a); (b) analysis of the curves and deduction of probable species; and (c) proposal of possible models. Then for each model, the residuals functions obtained are compared and the minimum value is sought (Table 3). Comparison of the calculated and experimental $\bar{Z}_M$ and $\bar{Q}$ curves

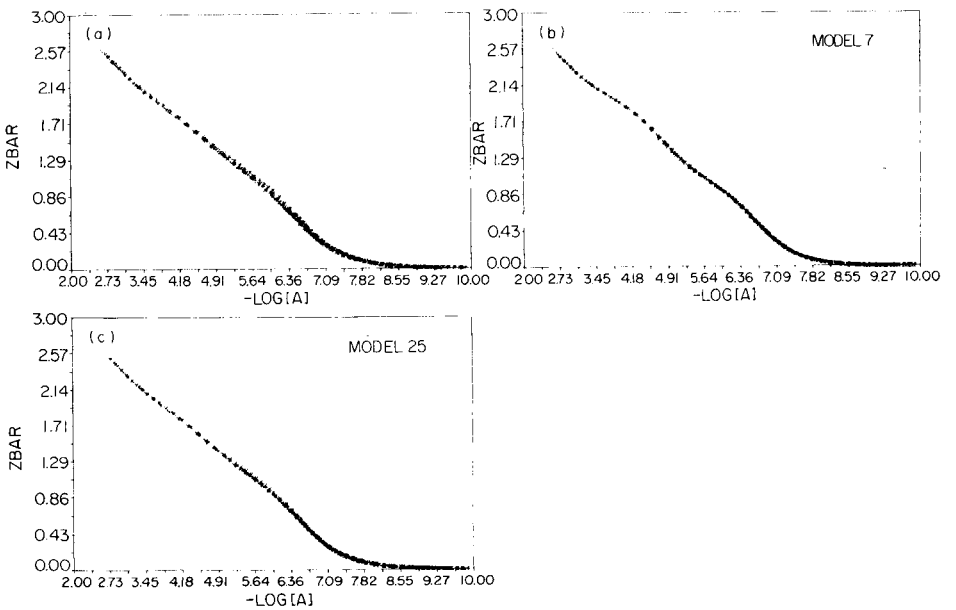

Fig. 1. Formation curves for the lead(II)/*N*-(2-mercaptopropionyl)glycinate system: (a) experimental; (b) calculated for model 7; (c) calculated for model 25.

TABLE 3

Model selection procedure

Model	Species (pqr)	U^a	Model	Species (pqr)	U^a
1	110	6.41×10^{-7}	15	110, 120, 130, 231	231 rejected
2	120	4.38×10^{-7}	16	110, 120, 130, 232	5.38×10^{-9}
3	130	1.41×10^{-6}	17	110, 120, 130, 340	4.80×10^{-9}
4	110, 120	2.91×10^{-8}	18	110, 120, 130, 341	341 rejected
5	110, 130	1.67×10^{-7}	19	110, 120, 130, 342	342 rejected
6	120, 130	4.21×10^{-7}	20	110, 120, 130, 230, 340	340 rejected
7	110, 120, 130	5.44×10^{-9}	21	110, 120, 130, 220	220 rejected
8	110, 120, 130, 111	2.96×10^{-9}	22	110, 120, 130, 221	4.99×10^{-9}
9	110, 120, 130, 112	112 rejected	23	110, 120, 130, 222	2.81×10^{-9}
10	110, 120, 130, 121	121 rejected	24	110, 120, 130, 460	3.97×10^{-9}
11	110, 120, 130, 122	3.82×10^{-9}	25	110, 120, 130, 230, 111	1.01×10^{-9}
12	110, 120, 130, 131	131 rejected	26	110, 120, 130, 460, 111	1.15×10^{-9}
13	110, 120, 130, 132	132 rejected	27	110, 120, 130, 230, 460, 111	1.01×10^{-9}
14	110, 120, 130, 230	4.31×10^{-9}			

[a]ESTA OBJT unweighted.

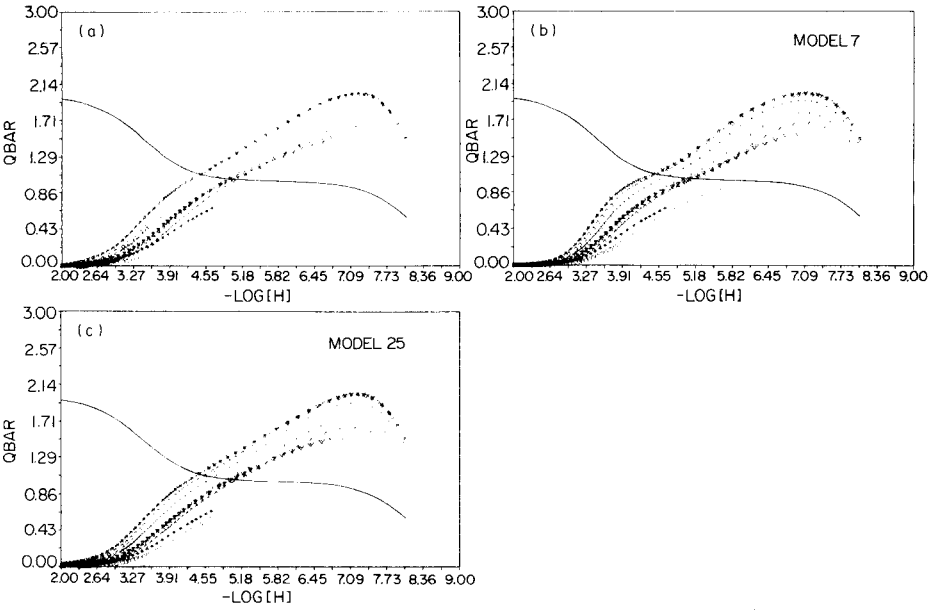

Fig. 2. Deprotonation curves for the lead(II)/*N*-(2-mercaptopropionyl)glycinate system: (a) experimental; (b) calculated for model 7; (c) calculated for model 25. On each deprotonation curve a plot of $\bar{n}$ vs. $-\log[H]$ appears as a solid line.

then indicates the best fit; for instance, the different fitting of the curves corresponding to model 7 (Figs. 1b and 2b) and model 25 (Figs. 1c and 2c) with the experimental ones is easily observed. The extent of formation of each species is then calculated. It is very important to check that all the

proposed species exist in significant concentrations over a certain range of data. In the final steps of the procedure, chemical knowledge is applied and the "best" model is selected.

The application of this procedure resulted in the selection of 111, 110, 230, 120 and 130 (model 25) as the "best" model.

Some of the programs compared (ESTA and SUPERQUAD) include facilities which help to select the "best" model. SUPERQUAD's model selector automatically generates a new model when, after refinement, a formation constant is found to be ill-defined (its calculated standard deviation is more than 33% of its value or its value is negative) and the "best" model is taken as the one with the lowest sample standard deviation and no ill-defined formation constants. This selector was applied to the ten most probable species (110, 120, 130, 111, 122, 230, 340, 221, 222, 460) and the model obtained was the one above proposed. The selection steps are shown in Table 4. It is worth emphasizing that model selection should not be based exclusively on numerical information.

Some of the facilities provided by the ESTA program package [17] proved to be very useful in the search for the identity of the species present. For instance, experimental and calculated formation and deprotonation curves can be plotted and formation constants can be calculated for individual species at each titration point, each species being regarded as the only remaining complex required to produce agreement between calculated and observed data at that point (BETA task). The results obtained with the BETA subroutine are shown in Table 5.

The results obtained from the different programs are presented in Table 6 following the criteria used in Table 2. The computer program LETAGROP was not able to perform, after many refinement cycles, the simultaneous optimization of the five constants necessary to define this system. Table 6 indicates that there is an inverse relationship between the dispersion of the log β values and the definition of the species, so that better defined species (e.g., 110 and 120) present less disperse values. As in the copper(II)/ammonia

TABLE 4

SUPERQUAD's model selector applied to the lead(II)/*N*-(2-mercaptopropionyl)glycinate system

Step	sigma[a]	χ^2	Species rejected
1	26.29	208	222
2	18.78	309	460
3	13.99	298	122
4	1.94	47	340
5	1.95	49	221
6	1.95	43	None

[a] σ_E = 0.05 mV; σ_V = 0.005 ml.

TABLE 5

Output of the BETA task (ESTA)[a]

Species	$\log \beta_{pqr}$	d	No. of points	Species	$\log \beta_{pqr}$	d	No. of points
110	6.71	0.07	170	231	26.95	0.58	167
120	11.97	1.27	239	232	31.22	0.75	126
130	16.07	3.51	283	340	31.61	1.48	199
111	10.67	0.45	91	341	36.60	0.79	167
112	13.13	0.32	10	342	41.03	0.87	134
121	17.40	0.47	158	220	16.25	0.32	170
122	21.45	0.71	99	221	20.56	0.53	126
131	23.02	1.36	211	222	24.22	0.73	91
132	28.14	0.86	146	460	46.77	2.86	210
230	21.83	1.30	211				

[a]Only the points with complex formation percentages between 10 and 90 are considered.

TABLE 6

Lead(II)/*N*-(2-mercaptopropionyl)glycinate system. Logarithm of formation constants obtained from different computer programs with standard deviations in parentheses

Program	Option	$\log \beta_{111}$	$\log \beta_{110}$	$\log \beta_{230}$	$\log \beta_{120}$	$\log \beta_{130}$	Complementary information
SCOGS		9.810 (0.013)	6.704 (0.002)	20.749 (0.014)	11.444 (0.004)	14.225 (0.005)	$U = 9.67 \times 10^{-3}$
MINIQUAD		9.809 (0.013)	6.706 (0.002)	20.781 (0.018)	11.452 (0.006)	14.250 (0.009)	$U = 1.50 \times 10^{-7}$; $\chi^2 = 233$ $\sigma = 1.03 \times 10^{-5}$ skewness 0.58; kurtosis = 4.95
ESTA	OBJT unw.[a]	9.795 (0.009)	6.703 (0.002)	20.760 (0.013)	11.446 (0.004)	14.244 (0.005)	$U = 1.02 \times 10^{-9}$ $R = 0.002$
	OBJT w.[b]	9.820 (0.009)	6.705 (0.002)	20.766 (0.011)	11.449 (0.003)	14.246 (0.004)	$U = 3.75$ $R = 0.003$ ($R_{lim} = 0.001$)
	OBJE unw.[a]	9.883 (0.020)	6.708 (0.003)	20.824 (0.008)	11.459 (0.003)	14.266 (0.005)	$U = 0.69$ $R = 0.004$
	OBJE w.[b]	9.820 (0.009)	6.705 (0.002)	20.766 (0.011)	11.449 (0.003)	14.246 (0.004)	$U = 3.75$ $R = 0.001$ ($R_{lim} = 0.000$
SUPERQUAD[b]		9.818 (0.012)	6.705 (0.002)	20.767 (0.015)	11.449 (0.004)	14.246 (0.006)	sigma = 1.95; $\chi^2 = 42.9$

[a]Unweighted. [b]Weighted; $\sigma_E = 0.05$ mV; $\sigma_V = 0.005$ ml.

system, coincident values are obtained when the objective function used is weighted. The well known assumption that it is not advisable to use unit-weighted sums of squared residuals based on e.m.f. is reinforced by the outlying values obtained from option OBJE (unweighted) of ESTA.

Copper(II)/salicylate/pyridine system

This system has usually been considered as an example of the formation of mixed-ligand complexes. Its study by potentiometric techniques is not

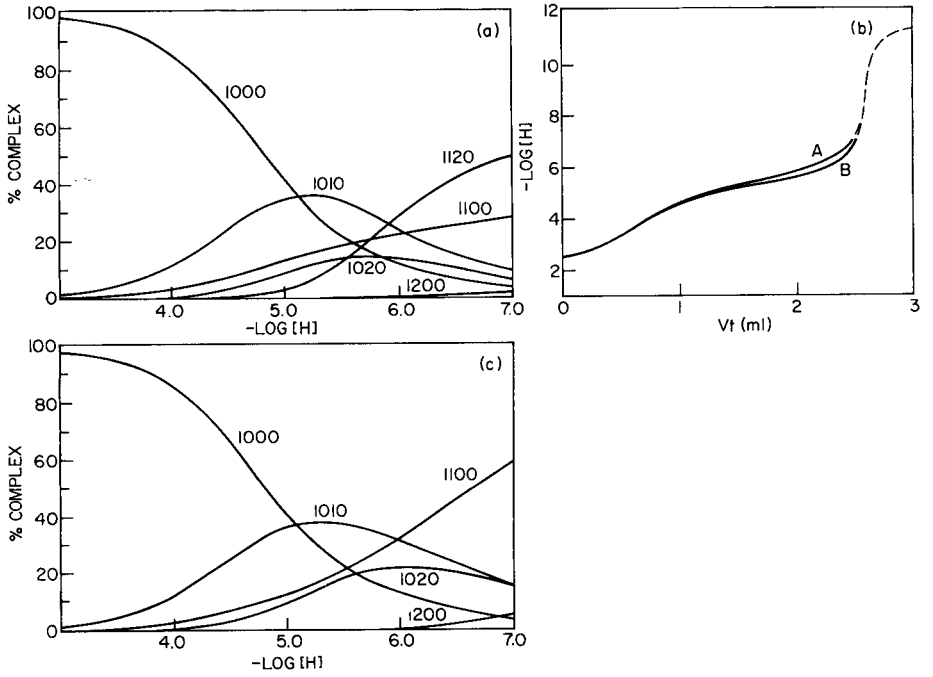

Fig. 3. Copper(II)/salicylate/pyridine system with C^{V}_{Cu} = 5 mmol l^{-1}, C^{V}_{sal} = 5 mmol l^{-1} and C^{V}_{py} = 15 mmol l^{-1}. (a) Species distribution as a function of $-\log[H]$ including the mixed-ligand species 1120. (b) Simulated titration curves with (curve A) and without (curve B) the inclusion of the mixed-ligand species 1120; C^{V}_{H} = 16 mmol l^{-1} and C^{B}_{OH} = 500 mmol l^{-1}. (c) Species distribution as a function of $-\log[H]$ without any mixed-ligand species.

TABLE 7

Copper(II)/salicylate/pyridine system. Logarithms of formation constants obtained using the different programs

Program	Option	Species	Set of data	log $\beta_{pqq'r}$	Complementary information
LETAGROP	val 1	1110	A	12.2(2)[a]	SIGY = 0.441
			B	12.0—12.2	SIGY = 0.372
		1120	A	14.1—14.3	SIGY = 0.437
			B	13.8—14.0	SIGY = 0.345
		1110	A	11.8—12.3	SIGY = 0.437
		1120		13.9—14.3	
			B	max. 12.0	SIGY = 0.346
				13.9—14.1	
MINIQUAD		1110	A	12.01(9)	$\sigma = 0.12 \times 10^{-3}$; $\chi^2 = 518$
			B	12.91(7)	$\sigma = 0.14 \times 10^{-3}$; $\chi^2 = 44.8$
		1120	A	13.83(9)	$\sigma = 0.11 \times 10^{-3}$; $\chi^2 = 363$
			B	14.96(6)	$\sigma = 0.13 \times 10^{-3}$; $\chi^2 = 46.9$

TABLE 7 (continued)

Program	Option	Species	Set of data	log $\beta_{pqq'r}$	Complementary information
		1110	A	rej. 1110	
		1120			
			B	rej. 1110	
ESTA	OBJT	1110	A	11.90(8)	$U = 1.50 \times 10^{-7}$
	unw.[b]		B	11.96(7)	$U = 1.36 \times 10^{-7}$
		1120	A	13.72(8)	$U = 1.42 \times 10^{-7}$
			B	13.80(7)	$U = 1.20 \times 10^{-7}$
		1110	A	rej. 1110	
		1120			
			B	rej. 1110	
	OBJT	1110	A	12.04(2)	$U = 20.2$
	w.[c]		B	12.03(2)	$U = 12.0$
		1120	A	14.21(2)	$U = 22.5$
			B	14.20(2)	$U = 14.6$
		1110	A	rej. 1120	
		1120			
			B	rej. 1120	
	OBJE	1110	A	11.5(2)	$U = 77.9$
	unw.[c]		B	11.5(2)	$U = 93.7$
		1120	A	13.1(2)	$U = 78.0$
			B	13.1(2)	$U = 93.8$
		1110	A	rej. 1120	
		1120			
			B	rej. 1120	
	OBJE	1110	A	12.04(2)	$U = 20.5$
	w.[c]		B	12.02(2)	$U = 11.7$
		1120	A	14.21(3)	$U = 23.4$
			B	14.19(2)	$U = 15.2$
		1110	A	rej. 1120	
		1120			
			B	rej. 1120	
SUPERQUAD[c]		1110	A	12.06(3)	sigma = 4.82; χ^2 = 43.9
			B	12.05(3)	sigma = 4.09; χ^2 = 24.2
		1120	A	14.24(4)	sigma = 5.08; χ^2 = 35.9
			B	14.22(3)	sigma = 4.48; χ^2 = 34.3
		1110	A	rej. 1120	
		1120			
			B	rej. 1120	
SUPERQUAD[d]		1110	A	11.96(4)	sigma = 2.64; χ^2 = 42.9
			B	11.8(1)	sigma = 2.49; χ^2 = 37.9
		1120	A	14.05(4)	sigma = 2.75; χ^2 = 48.4
			B	13.9(1)	sigma = 2.39; χ^2 = 31.1
		1110	A	rej. 1110	
		1120			
			B	rej. 1110	

[a]Standard deviations affecting the last figure appear in parentheses. [b]Unweighted. [c]Weighted: σ_E = 0.2 mV; σ_V = 0.02 ml. [d]Simultaneous refinement of total acid concentrations.

simple because, in order to favour the formation of the mixed-ligand complexes, a relatively large excess of pyridine has to be present to prevent the formation of binary copper salicylate complexes or copper hydroxide precipitates [15]. The experimental conditions were as follows: 7 titrations with 246 experimental points, T = 25°C, I = 1.0 mol l^{-1} ammonium nitrate, C^V_{Cu} = 1.1—2.3 mmol l^{-1}, C^V_{sal} = 1.6—2.9 mmol l^{-1}, C^V_{py} = 5.4—60 mmol l^{-1}, and $-\log[H]$ = 2.8—7.4.

Model selection in systems where two ligands are present is not straightforward because the inclusion of mixed-ligand complexes in the model affects the fit of the data in a rather limited way even when the mixed species predominate. For instance, in the system under study, the inclusion of a mixed-ligand complex with a high extent of formation (Fig. 3a) causes only a very slight variation in the calculated titration curves (Fig. 3b) probably because the lack of formation of the mixed-ligand complex is compensated by an increase in the percentage of formation of the binary copper salicylate (Fig. 3c) which has a similar effect on the e.m.f. values. That the model selection in the copper/salicylate/pyridine system is not easy is corroborated by the results obtained from the different programs (Table 7). Although the evidence for the existence of a mixed-ligand complex is strongly supported, the results do not permit the model to be established with certainty.

Because the mixed-ligand complex is formed in a rather narrow range of $-\log[H]$ values, two sets of data were used to calculate the values which are presented in Table 7: (A) all experimental points, and (B) all points where mixed-ligand complexes appear to form (132 experimental points, $-\log[H]$ = 5.1—7.4).

All the programs calculate values for the logarithmic formation constants when only a mixed-ligand complex is considered. Precision, however, is low as can be seen from the large standard deviations. But when two mixed-ligand complexes are simultaneously taken into consideration one of them is systematically rejected by all programs except LETAGROP. Even though not always the same species is rejected, some trends can be observed in the results obtained. Thus the 1110 species is rejected when the sum of squared residuals is unit-weighted and based on total concentrations (MINIQUAD and option OBJT unweighted of ESTA) whilst the 1120 species is rejected when the sum of squared residuals is weighted and/or based on e.m.f. (SUPERQUAD, option OBJE unweighted of ESTA, and options OBJT and OBJE weighted of ESTA). It can be concluded that, in this system, potentiometric techniques cannot be used alone to identify the species present and that several alternative methods must be applied.

The results presented in the discussion of each of the above systems suggest that the most recent programs (i.e., those which can use a weighted objective function) are more reliable. Nevertheless, it is worth reiterating that although a main object of analytical chemistry is to extract as much reliable information as possible from experimental data, this information can never be better than the data from which it has been obtained.

This research was supported by CAYCIT grant 657/81.

REFERENCES

1 N. Ingri and L. G. Sillén, Acta Chem. Scand., 16 (1962) 173.
2 P. Gans, Adv. Mol. Relaxation Interact. Processes, 18 (1980) 139.
3 L. G. Sillén, Acta Chem. Scand., 16 (1962) 159.
4 L. G. Sillén, Acta Chem. Scand., 18 (1964) 1085.
5 N. Ingri and L. G. Sillén, Ark. Kemi, 23 (1964) 97.
6 L. G. Sillén and B. Warnqvist, Ark. Kemi, 31 (1968) 315.
7 L. G. Sillén and B. Warnqvist, Ark. Kemi, 31 (1968) 341.
8 I. G. Sayce, Talanta, 15 (1968) 1397.
9 A. Sabatini, A. Vacca and P. Gans, Talanta, 21 (1974) 53.
10 P. Gans, A. Sabatini and A. Vacca, Inorg. Chim. Acta, 18 (1976) 237.
11 K. Murray and P. M. May, ESTA. Equilibrium Simulation for Titration Analysis, UWIST, Cardiff, 1984.
12 P. M. May, K. Murray and D. R. Williams, Talanta, 32 (1985) 483.
13 P. Gans, A. Sabatini and A. Vacca, J. Chem. Soc. Dalton Trans., (1985) 1195.
14 E. Casassas, R. Tauler and M. Filella, Anal. Chim. Acta, 191 (1986) 399.
15 E. Casassas and R. Tauler, J. Chim. Phys., 82 (1985) 1067.
16 M. Filella and D. R. Williams, Inorg. Chim. Acta, 106 (1985) 49.
17 K. Murray and P. M. May, Anal. Proc. (London), 21 (1984) 364.

Analytica Chimica Acta, 191 (1986) 425—432
Elsevier Science Publishers B.V., Amsterdam — Printed in The Netherlands

THE ALES LABORATORY AUTOMATION SYSTEM

ELIO FUCINI and GIANNI SPADARO
SIP Direzione Generale Laboratori, Via Borgaro 27, 10149 Torino (Italy)
MICHELE PENNISI
Digital Equipment Corp., Via Silvio d'Amico 40, 00145 Roma (Italy)
(Received 28th May 1986)

SUMMARY

A system for the automation of the analytical activities of a chemical laboratory is described. The system deals with investigations of physical and chemical characteristics of telecommunication materials for prototype development and quality control. The architecture, software development and interfacing of different analytical instruments (mainly for calorimetry, spectroscopy, electrochemistry, chromatography and mechanics) for the ALES (Automatzione del Laboratorio Elettrochimico SIP) system are discussed in terms of analytical and management performance.

The Italian Telecommunication Company (SIP) has for many years had a chemical testing laboratory for materials of interest. Materials and equipment manufactured in metal, plastic, ceramic and composite materials are examined in order to evaluate their characteristics and to assess product quality, ageing effects and lifetimes. The purpose of the work is to evaluate at the test stage the properties of purchased materials, to direct the development of new equipment and material prototypes, and to understand environmental effects on the materials. Such studies are also very useful in establishing the causes of anomalies or malfunctions, suggesting suitable remedies, and avoiding work safety problems in dealing with potentially dangerous materials.

In the SIP chemical laboratory, various analytical instruments are organized around work stations which are homogeneous as regards the type of analytical technique and related expertise. The materials to be examined, arriving in the SIP laboratory from all over the country, fall into the following categories: prototype material, material to be purchased, material in the course of its lifetime, degraded material, etc. The SIP division commissioning the investigation may be primarily concerned with system planning, purchases, quality assurance, operating and maintenance, or work safety. Every requirement coming from a SIP Division or from the laboratory itself comprises a job involving studies and tests on materials, and the results are presented as a technical report on completion.

The use of a data-processing system for quicker, easier and more accurate

0003-2670/86/$03.50

performance of the most important laboratory activities, was considered essential in order to solve the increasing technical problems in the analytical field, as well as the problems of management and organization of job information. A data base of materials, suppliers, response of materials to environmental conditions, etc., was also needed.

DEVELOPMENT OF THE AUTOMATION PROJECT

Starting in the late 1970's, the ALES project (Automazione del Laboratorio Elettrochimico SIP) has been developed with particular attention to the following aspects: (1) the state of art in the analytical instruments used in the laboratory and short/mid-term expectation of future equipment acquisition; (2) the automation needed in testing and management in the laboratory; (3) technical and market trends in the area of LIMS (laboratory information management system) and automated test software [1]; and (4) evaluation of practicable automation projects and their cost-benefit.

In the planning stage of the system, the laboratory was equipped with several analytical instruments, which ranged from instruments without automation capability because of lack of analog or digital output signals, through instruments fitted with analog and/or simple TTL signals, to microprocessor-controlled instruments which output the main test results. Some other instruments had dedicated personal computers [2] capable of setting and control of analytical variables, calculating test results, storing analytical methods and test results and printing numerical and graphic reports. About 1000 samples are submitted to the laboratory per annum, approximately 9000 tests and analyses are done, the test results are certified and are sent with the overall job reports to the commissioning division (Fig. 1).

The automation priorities in ALES system were set as follows: jobs and samples classification; test planning and programming for each sample; certification and storage of test results; printing of final technical paper for each job; technical/economic reports on laboratory activities; setting and monitoring of analytical parameters; raw-data acquisition and optimization; data processing and calculation of test results; and the creation of data bases containing information on standards, suppliers, material characteristics, test results, material quality index, technical bibliography, etc. In addition to immediate benefits, automation of the above-mentioned procedures makes it possible to standardize report formats for both individual tests and certificates, to optimize test programming after assessing all the jobs, and to define work lists according to job priority.

In the early 1980's, commercial analytical instrumentation favoured dedicated computers and applications software which precluded modification by the user. Only a few instrument manufacturers were then starting to offer software packages (LIMS) that automated their own instruments and could, with difficulty, be modified for the requirements of each particular laboratory, especially with regard to management aspects. Accordingly, a "home-

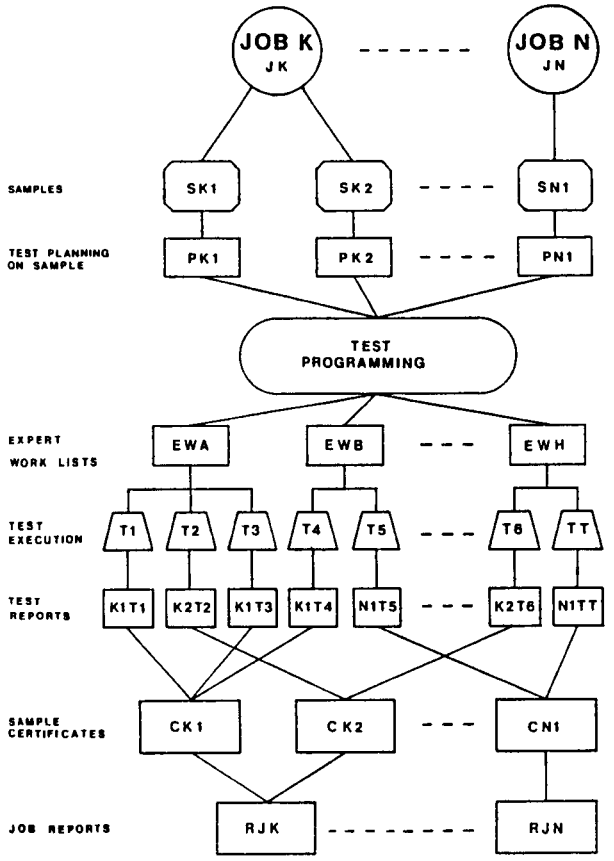

Fig. 1. Outline of job flow in ALES system.

made" system had to be chosen because of the difficulties encountered in effectively adapting existing LIMS to the needs of this laboratory.

Given these needs, the decision was taken to construct a system with a master computer and, so far as possible, slave computers dedicated to each instrument. All the instruments that had only analog output were linked to a single computer which performed functions equivalent to those of the dedicated computers [3], so as to provide a uniform data flow from each instrument to the master computer. This arrangement made it possible to keep the entire range of instrumental performances already available and, at the same time, to complement them with new software programs for each different kind of test.

In the Digital project, three technicians were employed for about 2.5 years: a year was devoted to analysis and system design, 10 months to software development, and 8 months to system implementation. A 1-year training course on basic information theory and the ALES package was initiated. Simultaneously, the SIP staff liaised with Digital Equipment Corp. (DEC)

staff, using its own system manager for over 90% of total working time, its laboratory chief (25%) and other laboratory chemists (15%).

ARCHITECTURE OF THE ALES SYSTEM

The architecture of the ALES system (Fig. 2) is based on the logical ordering of local area networks, apart from the electrical connection mode and the methods used in the reduction of background noise. The hardware requirements included the use of several CPU linked together in order to ensure system reliability [4] with at least six work stations provided with graphic terminals and hard-copy printers. High-quality printers were needed for compiling reports. Other essentials were the capability to acquire digital

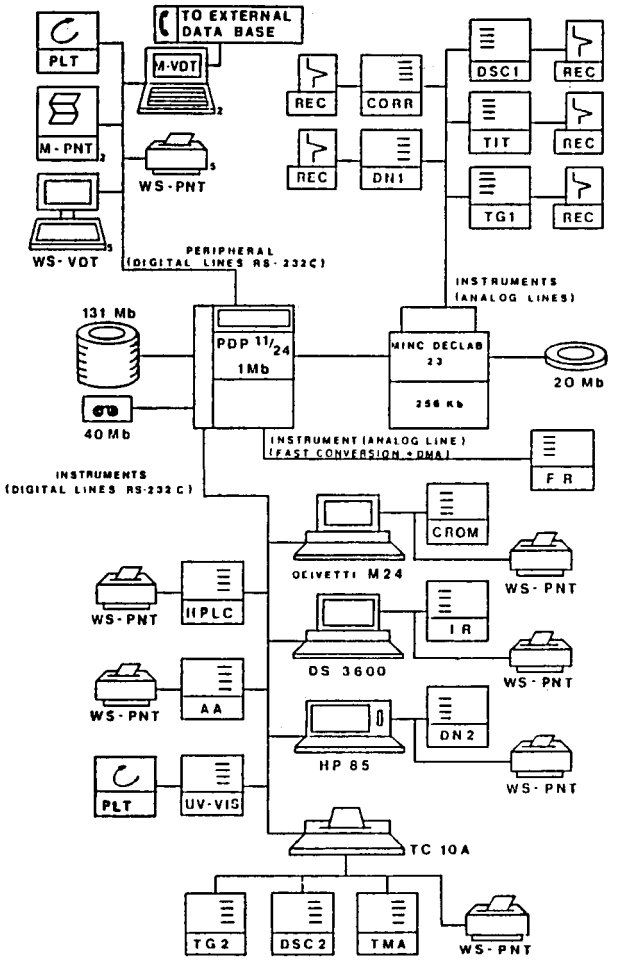

Fig. 2. ALES system architecture. For explanation, see text and Table 1.

data (RS-232-C, TTY, ON/OFF), analog data for medium-frequency sampling (0.1—5 Hz) and the provision of TTY output. Furthermore, all analog signals had to be matched with the acquisition parameters of the computer converters.

In order to meet such varied requirements, the master computer chosen was a DEC PDP 11/24 with 1Mb memory, 121 Mb Winchester disk, 10 Mb removable disk, 18 EIA RS-232-C I/O ports and 4 analog-to-digital converters able to acquire 150 000 data per second/clock. The slave computer chosen was a PDP 11/23 MINC with 16 digital inputs, 16 digital outputs, 32 analog inputs (single-ended) able to convert 20 000 data per second/clock, with two removable disks (10 Mb each). The instruments and peripherals connected via the RS-232-C to the master computer [5] are listed in Tables 1 and 2. The instruments provided only with analog output channels were connected to the MINC and to a local recorder (REC); these are also listed in Table 1. Linkage of the instruments provided with RS-232-C ports was quite simple. Linkage with analog ports required more attention [6], as the signal levels and their impedance characteristics caused problems in such an electrically noisy ambience as a chemical laboratory. Special care was given to the manufacture of amplifiers, and to noise shielding.

STANDARD SOFTWARE AND APPLICATION SOFTWARE

The ALES package under the RSX11-M V 4.1 operating system was developed by DEC. All software programs were written in Fortran-77,

TABLE 1

Instruments used

Technique	Instrument	Code
Digital output		
Calorimetry	Calorimeter, Mettler TA-3000	DSC 2
	Thermogravimetric, Mettler TG-50	TG 2
	Thermomechanic, Mettler DM-40	DMA
Chromatography	High-performance liquid, HP-1084B	HPLC
Mechanics	Dynamometer, Instron 4301	DN 2
Spectroscopy	Atomic absorption, PE-5000	AA
	Colour analyzer, Optronik	CROM
	Infrared, PE-398	IR
	U.v.-visible, HP-8450A	UV-VIS
Analog output		
Calorimetry	Calorimeter, Mettler TA-2000	DSC 1
	Thermogravimetric, Mettler HE-20	TG 1
Electrochemistry	Automatic titration, Mettler DK	TIT
	Corrosion analyzer, Amel	CORR
Mechanics	Dynamometer, Instron 1193	DN 1
	Resilience analyzer, Ceast 6545	FR

TABLE 2

Peripherals

Peripheral	Terminal	Code
Video-terminal	5 DEC VT125 — Analytical station	WS-VDT
	2 DEC VT220 — Management station	M-VDT
Printer	5 DEC LA34 — Analytical station	WS-PNT
	1 DEC LA120 — Management station	M-PNT
	1 DEC LQP02 — Management station	M-PNT
Plotter	1 HP 7450A — General purpose	PLT

except for the kernel of the acquisition program for which Macro-11 was used; this is indispensable for real-time sampling of all input channels. The six standard software packages used were as follows. The RMS (record management services) package provides keyed access for the RSX operating system; it comprises a set of run-time service routines and utility programs that enable keyed-access data files to be defined, populated, updated and maintained on random-access storage devices. The FMS (form management system) package is designed to aid in the development of programs that use video-forms with characters, lines and window attributes, scroll, blink, reverse, bold, etc. The RGL/FEP (remote graphics instructions set) package contains picture-drawing and data-plotting subroutines for the Fortran enhancement package operating on a VT125-AB graphic terminal. The SSP (scientific subroutine package) is a collection of over 100 mathematical and statistical routines, written in Fortran-77, which are commonly required in scientific programming and data processing.

The LSP (laboratory subroutine package) is a set of Fortran-callable subroutines that perform various standard analytical routines such as data acquisition, peak processing, fast Fourier transform, phase-angle and amplitude spectrum, power spectrum, correlation, integration and envelope processing. The DECnet (Digital network package) extends the facilities of DEC operating systems so that they can be interconnected to form computer networks and to share devices, data files and other resources.

Each work station has at its disposal several software programs developed jointly by SIP and DEC to meet the requirements of each routine analysis used. The programs are used to integrate existing software performances, running on microprocessors and dedicated computers.

Management and analytical software included in the ALES package are listed in Table 3.

Conclusion

The ALES system has been in operation for about a year. Experience so far has confirmed that the general policy underlying the choices made was satisfactory, particularly the selection of the star configuration of the

TABLE 3

Management and analytical software in ALES

MANAGEMENT SOFTWARE	
Enquiry	External scientific library and data base.
File management	Analytical methods, standard and technical library.
Planning	Analysis and test.
Print	Job reports, sample reports, statistical laboratory activity reports.
Programming	Instruments and manpower available, job execution priority, new work scheduling, state of work in progress, technician work.
Storage	Jobs log-in data, samples log-in data.
ANALYTICAL SOFTWARE – COMMON PROGRAMS	
Acquisition	Analytical parameters, raw data and results.
Calibration	Instruments.
Control	Liquid and gas flow during analysis, environment temperature and pressure.
Graphic plot	Analytical curves.
Print	Test reports (graphic on request).
Setting	Instrumental parameters.
Storage	Analytical results, raw data (on request).
ANALYTICAL SOFTWARE – SPECIFIC PROGRAMS	
Calorimetry	Specific heat, coefficient of expansion, elasticity, melting and crystallization, evaporation and drying, glass transition, crystallinity, heat and temperature of fusion, kinetics of reaction, oxidation stability, purity.
Chromatography	Qualitative composition (retention time), quantitative composition (peak high and peak area), medium molecular weight.
Electrochemistry	Primary passivation potential, breakdown potential, passivation potential, passive current density, transpassive current density, transpassivation potential, pH, quantitative composition (Gran method), conductance.
Mechanics	Breaking load and strain, Young modulus, load to proportional limit, compression tension and torsion, Charpy and Izod impact test, coefficient of elasticity.
Spectroscopy	Qualitative composition, quantitative composition, colour formula.

system with full autonomy of each work station. There have been visible improvements in laboratory efficiency and test result reliability, both qualitatively and quantitatively, leading to increased productivity. These results have been achieved by widespread standardization in the laboratory procedures.

The problems initially posed by the knowledge gap between the laboratory experts and the automation experts should, however, be mentioned. These difficulties were partly overcome when an expert technician with a chemical background and complementary knowledge of electronics and computers was called in.

Further implementation of the ALES system is being examined in relation to the introduction of new instruments (image analyzer, gas chromatography/

mass spectrometry, etc.) and new test and management procedures. A short-term assessment of the technical and economic advantages of replacing the PDP 11/24 by a 32-bit computer will then be needed, with a view to achieving maximum hardware and software compatibility (VAX 730 or 750 or μVax II).

REFERENCES

1 R. Dessy, Anal. Chem., 55 (1983) 70A.
2 P. Lykos, Personal Computers in Chemistry, Wiley-Interscience, New York, 1981.
3 J. Justice and T. Isenhour, Digital Computers in Analytical Chemistry, Academic Press, New York, 1982.
4 S. Heller and R. Potenzone, Computer Application in Chemistry, Elsevier, New York, 1983.
5 M. Salit and M. Parsons, Anal. Chem., 57 (1985) 715A.
6 M. Starling, Anal. Chem., 57 (1985) 310A.

Analytica Chimica Acta, 191 (1986) 433—437
Elsevier Science Publishers B.V., Amsterdam — Printed in The Netherlands

Short Communication

ROUTINE ANALYSES OF CRUDE OIL FRACTIONS BY PRINCIPAL COMPONENT MODELLING OF GAS CHROMATOGRAPHIC PROFILES

MAGNUS O. EIDE and OLAV M. KVALHEIM*
Department of Chemistry, University of Bergen, N-5000 Bergen (Norway)
NILS TELNAES
Norsk Hydro A/S, Lars Hilles gt. 30, N-5000 Bergen (Norway)
(Received 26th May 1986)

SUMMARY

The naphtha fraction of 13 crude North Sea oils was analyzed by high-resolution gas chromatography. Principal component modelling shows that prior normalization to percentages is unnecessary if logarithmic data are used. When the variation in absolute amounts is large (e.g., as a result of manual injection or complicated work-up of samples), the first principal component accounts for differences in absolute amounts. Smaller differences in absolute amounts are masked by differences in chromatographic profiles. In this case, normalization does not change the relations between samples as is observed on the dominant principal components.

It was recently shown [1] that a logarithmic transformation is preferable to standardizing each variable to unit variance in principal component modelling [2—4] of gas chromatographic (g.c.) and similar analytical data. Transforming the data to percentages prior to conversion to logarithms produced only minor changes in the clustering of samples on the principal components. Thus, the problem of closure [5] appeared avoidable for gas chromatographic data. The logarithmic transformation has other advantages: (i) systematic variation in small variables is revealed because the total variance is distributed more equally among the variables; and (ii) the distribution of each variable between the samples approaches normality, an important feature for reliable outlier testing. One objection that can be raised against the previous recommendation [1] is the limited variability among the total areas of the gas chromatograms used. A factor of three between the largest and smallest areas may not span the range occurring naturally in routine g.c. Accordingly, a more thorough survey was undertaken to establish the interpretability of data when logarithms of raw g.c. profiles are used as input to principal component modelling.

Experimental

The naphtha fraction of crude oils from thirteen wells in the Norwegian sector of the North Sea was analyzed on a HP 5880 gas chromatograph

0003-2670/86/$03.50

equipped with a methylsilicone-coated silica column.

Two different injection methods (autosampling and manual injection) were used. Manual injection was used to ensure differences in absolute amounts comparable to the variation in more complicated analytical work-ups. The samples were analyzed over a period of eight weeks during which time the column was also used extensively for other samples. Over this period, some samples were analyzed several times, which provided an opportunity to investigate the possibility of systematic time variation (e.g., column-aging).

Areas of 58 major peaks were selected to represent the g.c. profiles (Fig. 1). Tentative assignments of these peaks are given in Table 1. The data were analyzed by using the SIMCA program [6] implemented on a UNIVAC 1100/82 computer [7].

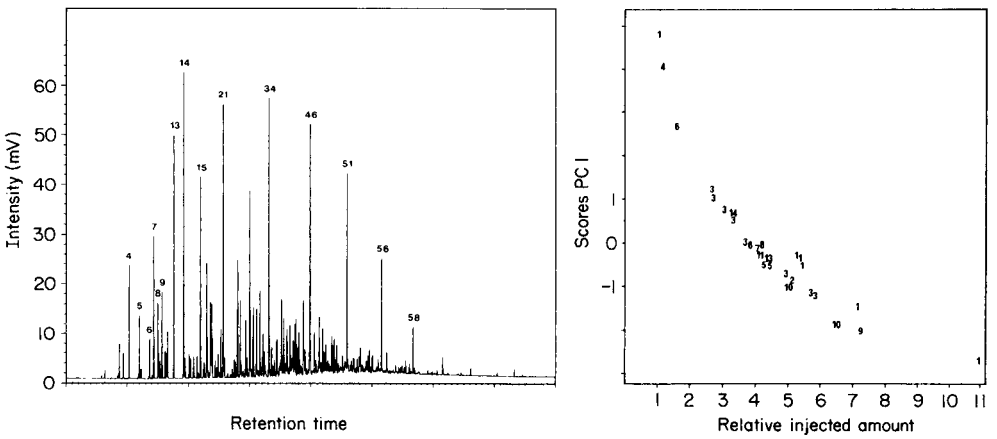

Fig. 1. Gas chromatogram for a naphtha fraction from one oil sample. Numbering refers to Table 1.

Fig. 2. Areas of gas chromatograms for different oil samples plotted vs. scores on PC1 for logarithms of raw data.

RESULTS AND DISCUSSION

Differences between total areas of the gas chromatograms by a factor larger than 10 before logarithmic conversion confirm that differences in absolute amounts constitute a major source for variation between samples. Principal component modelling of the logarithms of peak areas reveals that the scores on the PC1 correlate well with the total areas (amounts injected) of the chromatograms. Figure 2 shows the scores on PC1 plotted against summed peak areas for the chromatograms; the exponential relationship between scores and total areas is a result of using the total areas and not their logarithms.

The pattern displayed on PC2 and PC3 (Fig. 3A) matches completely

TABLE 1

Assignments of peaks used

Peak no.	Retention time (min)	Constituent	Peak no.	Retention time (min)	Constituent
1	1.41	Isopentane	26	14.77	Ethylbenzene
2	2.09	2-Methylpentane	27	15.46	*m*-Xylene
3	2.30	3-Methylpentane	28	16.05	4-Methyloctane
4	2.64	Hexane	29	16.94	*p*-Xylene
5	3.11	Methylcyclopentane	30	17.40	2-Methyloctane
6	3.72	Benzene	31	17.62	3-Methyloctane
7	3.96	Cyclohexane	32	17.76	*o*-Xylene
8	4.53	2-Methylhexane	33	18.92	Tetramethylcyclohexane
9	4.84	3-Methylhexane	34	19.74	Nonane
10	4.90	*cis*-1,3-Dimethylcyclo-	35	20.90	Isopropylcyclohexane
		pentane	36	22.01	Propylcyclohexane
11	5.00	*trans*-1,3-dimethylcyclo-	37	22.38	Butylcyclopentane
		pentane	38	22.68	Propylbenzene
12	5.12	*trans*-1,2-Dimethylcyclo-	39	22.77	3-Ethyltoluene
		pentane	40	23.27	4-Ethyltoluene
13	5.98	Heptane	41	23.84	1,3,5-Trimethylbenzene
14	6.49	Methylcyclohexane	42	25.07	4-Methylnonane
15	8.34	Toluene	43	25.30	2-Methylnonane
16	9.69	2-Methylheptane	44	26.17	3-Methylnonane
17	9.79	3-Methylheptane	45	26.95	1,2,4-Trimethylbenzene
18	10.09	*cis*-1,3-Dimethylcyclo-	46	27.71	Decane
		hexane	47	29.00	(5-Methyldecane)
19	10.66	*trans*-1,4-Dimethylcyclo-	48	29.51	(4-Methyldecane)
		hexane	49	29.76	(2-Methyldecane)
20	10.79	1,1-Dimethylcyclohexane	50	31.68	(3-Methyldecane)
21	12.02	Octane	51	35.41	Undecane
22	13.35	*cis*-1,2-Dimethylcyclo-	52	36.75	(5-Methylundecane)
		hexane	53	36.86	(4-Methylundecane)
23	13.72	2,4-Dimethylheptane	54	37.40	(2-Methylundecane)
24	14.15	1,1,3-Trimethylcyclo-	55	37.88	(3-Methylundecane)
		hexane	56	42.69	Dodecane
25	14.57	1,1,4-Trimethylcyclo-	57	43.75	(2-Methyldodecane)
		hexane	58	49.58	Tridecane

both with replicate information and with the geographical location of the wells where the oils were sampled. Principal component modelling of the chromatograms normalized to mean area before logarithmic transformation shows the same pattern on PC1 and PC2 (Fig. 3B) as observed on PC2 and PC3 (Fig. 3A) for logarithmically transformed raw data. Accordingly, the common variance of the data set splits into two approximately orthogonal parts: (i) differences in amount injected; and (ii) differences in composition as reflected in the g.c. profiles. Accordingly, differences in injected amount

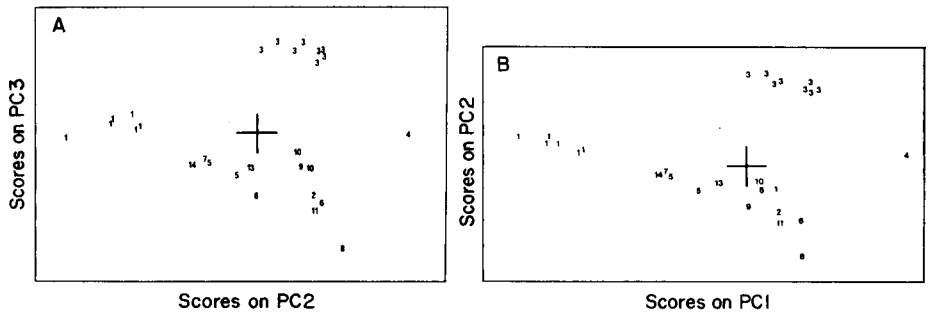

Fig. 3. Scores: (A) on PC2 vs. PC3 for logarithms of raw data; (B) on PC1 vs. PC2 for logarithms of percentage data.

can be projected from the data matrix by subtracting the product of scores (t) and loadings (b) on the size component, i.e., $\mathbf{X} \leftarrow \mathbf{X} - tb$. After the removal of this component, separate class models can be obtained by means of SIMCA [6].

For most of the samples, chromatograms were obtained with autosampler and manual injection. When the autosampler was used, the total areas differed by less than a factor of three. In this case, differences in amount injected were masked by differences in the composition of samples (compare Fig. 3A with Fig. 4). The replicated chromatograms were obtained over a period of 8 weeks. No systematic variation with time was observed in any of the score plots (Figs. 3 and 4).

The loading plot on PC2 and PC3 (Fig. 5) based on the logarithms of raw

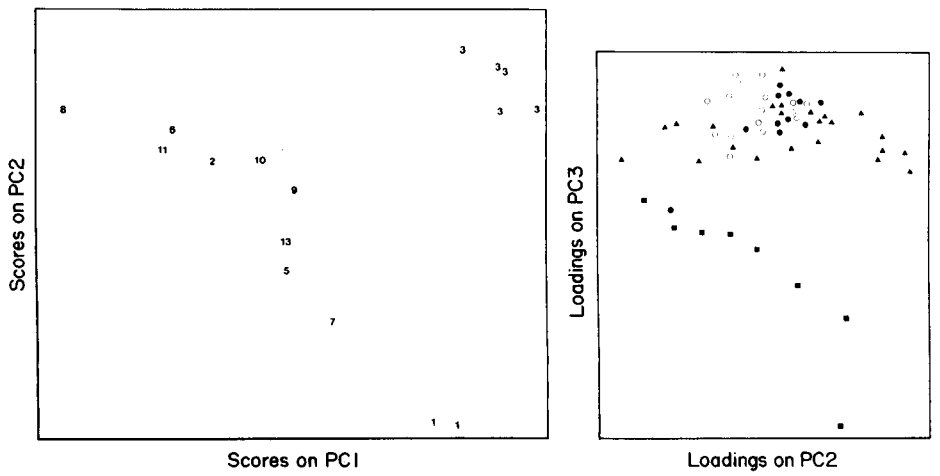

Fig. 4. Scores on PC1 vs. PC2 for logarithms of percentage data. Only gas chromatograms obtained with the autosampler were included in the principal component modelling.

Fig. 5. Loadings on PC2 and PC3 for logarithms of raw data. (■) n-alkanes; (▲) branched alkanes; (○) cycloalkanes; (●) aromatics.

data shows that the oils used in this investigation differ mainly in the ratio between light and heavy constituents on PC2, and in relative abundances of n-alkanes on PC3; PC2 is attributed mainly to differences in maturity [8] because all these oils come mainly from the Kimmeridge Clay Formation. The differences in distribution of n-alkanes observed on PC3 are probably caused by biodegradation [8].

Because all the oils used here are from the same source, they are rather similar in composition. Depending on the injection method and the complexity of the analytical work-up, the differences in absolute amounts are either masked or revealed on the first principal component. Accordingly, it appears that g.c. profiles of oils can be examined routinely by principal component modelling of the logarithms of raw data, avoiding the problem of closure inherent in any procedure for normalizing data.

REFERENCES

1 O.M. Kvalheim, Anal. Chim. Acta, 177 (1985) 71.
2 E. R. Malinowski and D. G. Howery, Factor Analysis in Chemistry, Wiley, New York, 1980.
3 D. L. Massart and L. Kaufman, in The Interpretation of Analytical Chemical Data by the Use of Cluster Analysis, Wiley, New York, 1983.
4 S. Wold, C. Albano, W. J. Dunn III, U. Edlund, K. Esbensen, P. Geladi, S. Hellberg, E. Johansson, W. Lindberg and M. Sjöström, in B. R. Kowalski (Eds.), Chemometrics — Mathematics and Statistics in Chemistry, Reidel, Dordrecht, 1984.
5 E. Johansson, S. Wold and K. Sjödin, Anal. Chem., 56 (1984) 1685.
6 S. Wold, Pattern Recognition, 8 (1976) 127.
7 O. M. Kvalheim, Simca User's Guide, University of Bergen, 1985.
8 B. P. Tissot and D. H. Welte, Petroleum Formation and Occurrence — A new approach to oil and gas exploration, Springer Verlag, Heidelberg, 1984.

Analytica Chimica Acta, 191 (1986) 439—443
Elsevier Science Publishers B.V., Amsterdam — Printed in The Netherlands

Short Communication

THE USE OF SIMPLEX OPTIMIZATION IN EVALUATING COMPLEX CHROMATOGRAMS OF MIXTURES

X. TOMÀS and L. G. SABATÉ

Department of Chemometrics, Institut Químic de Sarrià, 08017 Barcelona (Spain)

(Received 4th April 1986)

Summary. The application of simplex optimization to the qualitative and quantitative evaluation of chromatograms of complex mixtures is outlined. The chromatogram is considered as a linear combination of pure component chromatograms (assuming no interactions are present); if suitable components are selected and the coefficients of the linear combination are properly evaluated, the experimental chromatogram can be reproduced numerically. The simplex method is then used to evaluate the solution with minimal error. The quantitation of polychlorobiphenyls from Aroclor mixtures in marine sediments and fish, and the identification of essential oils in a perfume base extract are outlined. Errors of $\leqslant 10\%$ (25% in environmental samples) between the experimental and reconstructed chromatograms were achieved.

The simplex optimization method, devised by Spendley et al. [1] and modified by Nelder and Mead [2], is simple and effective for optimizing chemical systems which have several experimental variables. The method has been applied to most analytical techniques, usually to find the experimental conditions giving optimal response [3, 4]. Various modified procedures have been suggested for different purposes [5]. A problem arises if the optimal response cannot be easily characterized by a single number [6]. An example of this problem is mixture resolution by chromatography; quality criteria in selecting the best chromatogram must be sought cautiously, because some compromise between factors (separation time, resolution, etc.) is usually necessary.

On the basis that a mixture response can be considered as a linear combination of the responses of pure and known components, many analytical problems have been solved successfully. However, if the response is a complex chromatogram, if the components are mixtures of pure compounds (e.g., formulations, essential oils, natural extracts) and if the number of components present is large or unknown, then the problem becomes so magnified that numerical aids (combinatory or optimization) are needed. In this preliminary communication, a modified simplex method is applied to this type of problem, in an attempt to avoid the difficulties found with classical methods such as iterative least-squares or linear programming in solving overdetermined systems [7].

0003-2670/86/$03.50

Mathematical model

The chromatogram considered shows p peaks from a sample mixture of n components or standards. Each standard consists of a specified number of compounds. Mathematically, the problem can be expressed by a system of equations: $\mathbf{AX}^0 = \mathbf{B}^0$, where $\mathbf{B}^0$ is a column vector with dimension p. Its elements are the areas (or heights) of the p peaks of the mixture chromatogram: $B^0 = (b_1^0, b_2^0, \ldots, b_p^0)^T$ (for $b_i^0 \geqslant 0$). The matrix of coefficients, $\mathbf{A}$, is a row hypermatrix ($1 \times n$). Each element is a column vector reproducing the chromatogram of a pure standard:

$$\mathbf{A} = (A_1, A_2, \ldots, A_n)$$

$$\mathbf{A}_i = (a_{1i}, a_{2i}, \ldots, a_{pi})^T \text{ (for } a_{ji} \geqslant 0)$$

$\mathbf{X}^0$ is a column vector with dimension n, the elements of which are the fractions of the diverse standards which allow $\mathbf{B}^0$ to be reproduced:

$$\mathbf{X}^0 = (x_1^0, x_2^0, \ldots, x_n^0)^T \quad (0 \leqslant x_i^0 \leqslant 1)$$

If the chromatogram of the mixture has been generated by a linear combination of the chromatograms of n standards, the system will have, in general, a number p of equations higher than the number n of unknowns. Therefore, it can be solved by reduction to an equivalent system of n equations with n unknowns by using some classical method.

There is also the possibility of considering all the equations and using mathematical optimization techniques to find the solution. From this point of view, the solution will be the $\mathbf{X}^0$ vector which best reproduces the $\mathbf{B}^0$ chromatogram. This vector can be calculated through an iterative process in which an error function $D(x)$ is minimized. This $D(x)$ function is usually defined as the norm of first order of the difference vector $\mathbf{B}^k - \mathbf{B}^0$, where $\mathbf{B}^k$ is the chromatogram generated by linear combination of some n standards:

$$D(\mathbf{X}^k) = \Sigma\,(|b_j^r - b_j^k|)$$

where $b_i^k = \Sigma_{j=1}^n\, x_j\, a_{ji}$ (for $i = 1, \ldots, p$). The norm, a surface in the space of $n + 1$ dimensions, has a minimum for $\mathbf{X} = \mathbf{X}^0$ corresponding to the solution sought (ideally $D(X^0) = 0$), but if experimental error is present or the selection of standards is not quite accurate, the surface is perturbed and the minimum is no longer found at $\mathbf{X}^0$, because some other $\mathbf{X}'$ may reproduce the chromatogram with $D(\mathbf{X}') > 0$. The surface response is limited by the boundaries affecting the fractions of standards in the mixture: $0 \leqslant x_i \leqslant 1$ and $\Sigma_1^n\, x_i = 1$. The latter implies that a mixture can be defined with $n - 1$ standards, because the nth component is obtained by difference. This condition must be modified if standards do not explain the whole chromatogram, and then $\Sigma_1^n\, x_i \leqslant 1$.

On this basis, the modified simplex method will be applied in order to minimize the discrepancy function $D(x)$ or its normalized expression towards the identified proportion of the chromatogram: $N(x) = 100\ D(x)/\Sigma b_i$ for i = 1, 2, . . . , p. Thus if $x = 0, N(x) = 100$ and $x = x'$ with $N(x') \geqslant 0$.

A Basic program, implemented on an IBM PC computer (256K RAM, two 360K floppy disks), for the procedure described was prepared and applied to the determination of polychlorobiphenyls (PCB's) in diverse samples and essential oils in some extracts of perfume bases.

Results

Determination of polychlorobiphenyls. The chromatograms of three samples containing known amounts of Aroclors 1254, 1260 and 1268 were obtained as described by Broto et al. [8]. Separate standards were processed under the same conditions. The results obtained (Table 1) are in good agreement, and the errors are quite acceptable for such procedures.

Four samples of red mullet from L'Ametlla (Tarragona) and two marine sediments from the same place in the Catalan Sea were also analyzed. This area, near the Ebro river delta, was studied in the MEDPOL UNEP program as a zone of conflicting agricultural, industrial and urban pollution [9]. The red mullet samples were found to contain about 405 $\mu g\ kg^{-1}$ total PCB's; of the total Aroclor standard compounds, 75 ± 4% was Aroclor 1260 and 24 ± 4% was 1254; there was no Aroclor 1268 present. The sediments contained about 0.5 mg kg^{-1} PCB's; of the total Aroclor compounds, about 86% was Aroclor 1260 and 14% was Aroclor 1268 with no Aroclor 1254. The differences between the experimental and calculated chromatograms (about 25% overall) were greater than those obtained for the simple mixtures of Aroclors, but the errors can be ascribed to the low ranges of the measured values, and to biodegradation of PCB's and the variations of natural specimens, which mean that experimental chromatograms will contain peaks not matched by the standards used.

Analysis of extracts of perfume bases. A synthetic sample of a mixture of four essential oils, armoise, bergamot, orange and rosemary, was prepared. From the chromatogram obtained, twelve peaks were selected as significant, and on this basis, the simplex method was applied to reconstruct the mixture composition. Table 2 summarizes the results expressed as essential oils and as each of the twelve selected compounds (chromatographic peaks). Good agreement is achieved in both solutions. A synthetic sample of natural extracts was also analyzed. It contained some of the 21 essential oils

TABLE 1

Determination of polychlorobiphenyls in Aroclor mixtures

Sample	Aroclor (%)					
	Taken			Found		
	1254	1260	1268	1254	1260	1268
1	19.9	44.1	35.9	18.4	46.2	33.3
2	34.4	39.1	26.6	35.1	38.0	26.6
3	47.6	29.7	22.7	46.8	31.3	22.6

TABLE 2

Analysis of a mixture of four essential oils and the significant peaks used

Oil	Armoise	Bergamot	Orange	Rosemary
% taken	10	50	30	10
% found	10.1	50.0	29.9	9.9

Significant peak	Area (%)		Significant peak	Area (%)	
	Measured	Reconstructed		Measured	Reconstructed
Myrcene	1.4	1.32	α-Thujone	1.7	2.6
α-Pinene	2.8	3.0	β-Thujone	0.3	0.67
Camphene	1.4	0.85	Linalool	7.0	7.50
β-Pinene	3.1	4.36	Linalyl acetate	17.5	17.0
Limonene + cineole	50.7	48.88	Borneol	0.9	0.7
γ-Terpinolene	2.4	34.5	Camphor	7.8	5.6

TABLE 3

Analysis of a sample of natural extracts

Essential oil[a]	Proposed solution (area)		True solution	Essential oil[a]	Proposed solution (area)		True solutic
	1	2			1	2	
Basil	0.020	—	0.020	Lemon	0.367	0.300	0.300
Bergamot	0.186	0.097	0.200	Litsea C.	0.013	—	0.010
Cardamom	0.019	0.010	0.020	Mandarin	0.031	0.110	0.070
Coriander	0.026	—	0.020	Petit grain B.	0.200	0.111	0.200
Fennel	—	0.041	—	Rosemary	0.015	—	0.020
Lavandula	0.100	0.188	0.100	Salvia Sc.	0.041	0.051	0.040
Lavandin	—	0.089	—	Error (%)	2.1	3.6	

[a]Essential oils considered as possible components of the mixture but which were not present in the synthetic mixture and were not in fact identified, were citronella, lavender, eucalyptus C., eucalyptus, geranium, lemon grass, marjoram and orange.

mentioned in Table 3 and its major component (lemon) was present in the chromatogram. Qualitative and quantitative interpretation of the chromatograms was done by the simplex procedure; the two possible solutions obtained are summarized in Table 3. Differences can be explained by the age and natural variation of the standards, but the data are adequate for starting an organoleptic reconstitution of the perfume base extract.

REFERENCES

1 W. Spendley, G. R. Hext and F. R. Himsworth, Technometrics, 4 (1962) 441.
2 J. A. Nelder, R. Mead, Comput. J., 7 (1965) 308.
3 S. N. Deming and S. L. Morgan, Anal. Chim. Acta, 150 (1983) 183.

4 M. F. Delaney, Anal. Chem., 56 (1984) 261R.
5 D. Betteridge and A. P. Wade, Talanta, 32 (1985) 723.
6 J. J. Leary, A. E. Brookes, A. F. Dorrzapf and D. W. Golightly, Appl. Spectrosc., 36 (1982) 37.
7 M. G. R. Zobel, J. Assoc. Off. Anal. Chem., 57 (1974) 791.
8 F. Broto, M. Gassiot, R. Martínez, VIe J. Étud. Pollutions, CIESM, Cannes, 1982, Abstracts, p. 449.
9 J. Obiols, X. Tomàs, M. Gassiot, J. Ros, F. Faraco, VIe J. Étud. Pollutions, CIESM, Cannes, 1982, Abstracts, p. 461.

Analytica Chimica Acta, 191 (1986) 445—450
Elsevier Science Publishers B.V., Amsterdam — Printed in The Netherlands

Short Communication

PARTIAL LEAST-SQUARES MODELLING OF DYE FASTNESS TO LIGHT

ROSARINA CARPIGNANO*, PIERO SAVARINO, ERMANNO BARNI and GUIDO VISCARDI

Istituto di Chimica Organica Industriale, Università di Torino, Corso M. D'Azeglio 48, 10125 Torino (Italy)

SERGIO CLEMENTI and GIANFRANCO GIULIETTI

Dipartimento di Chimica, Università di Perugia, Via Elce di Sotto 10, 06100 Perugia (Italy)

(Received 25th March 1986)

Summary. Several physicochemical properties (^{13}C-n.m.r., spectrophotometric, chromatographic, calorimetric) were measured for a series of 38 azo dyes in order to test the existence of relationships between one or more of these data sets and the fastness of the dyes on polyester fabric. The partial least-squares method was applied; it had previously proved useful in establishing structure/property relationships for the same dyes. It is shown that ^{13}C-n.m.r. data can be used successfully to predict dye fastness to light. These data are quickly and cheaply obtained with small amounts of compound.

In recent work on azo dyes, a chemometric procedure was developed for modelling dye fastnesses in terms of molecular structure descriptors. The procedure was applied to a series of monoazo dyes for polyamide derived from 4-alkylamido-2-hydroxybenzoic acids [1] and a series of diethylamino-azobenzene dyes [2]. In both cases, the results showed that it is possible to work out mathematical models to relate physicochemical properties to molecular structure as in quantitative structure/activity relationships, provided that the statistical tool is appropriate. In particular, it was shown that the partial least-squares (PLS) method [3, 4] was by far the best approach. Modelling the fastnesses by traditional structural descriptors permitted prediction of the same properties for dyes not yet synthesized.

It would also be of interest to estimate dye fastnesses even when the compound is available. In fact, a procedure able to predict fastness to light on the basis of simple, fast, cheap analytical measurements requiring small amounts of dye would be very useful. Accordingly, this study was aimed at collecting n.m.r., spectrophotometric, chromatographic and calorimetric data, in order to select those suitable for a property/property relationship.

The multivariate statistical approach is again the PLS method, which has already been shown to be useful in various branches of chemistry [5—7]. The PLS approach relies on SIMCA method of principal component analysis

0003-2670/86/$03.50

(PCA) and is particularly suitable for detecting cause/effect relationships without any preliminary assumptions on the relevance of individual variables. The PLS algorithm has been described in detail [4] and only a brief summary is given here. In this analysis, there is one dependent variable y, fastness to light, and a number of independent variables, the physicochemical properties (X block). The method models the dependencies between the variables, extracting the principal components of the X block under the constraint of maximizing the relationship with the dependent variable. Cross-validation is used to estimate the number of dimensions that give the model the best possible predictive properties.

The study is based on the series of diethylaminoazobenzene dyes of general formula I, which was examined previously [2]; four new compounds synthe-

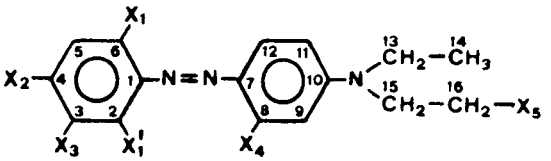

(I)

sized because of their predicted high fastness to light were added. Some compounds were no longer available so that the investigation involved 38 dyes.

Experimental

Dyes and fastness to light. The new compounds are nos. 35—38 (see Table 3). Dye synthesis, dyeing on polyester fabric and assessment of fastness to light were done as previously described [2].

Measurements of chemical properties. Carbon-13 n.m.r. spectra were recorded at 68.70 MHz on a JEOL GX270 spectrometer in DMSO-d_6 solutions (ca. 0.2 M). Chemical shifts were measured relative to the central peak of the solvent (39.60 ppm). The observed shifts can be obtained from the authors on request.

Electronic absorption spectra were recorded with a Unicam SP8—100 spectrophotometer for 1×10^{-5} M solutions of the dyes in neutral methanol and in methanolic 1 M perchloric acid. The absorption maxima are listed in Table 1.

The R_f values were measured under three sets of conditions (Table 1). Melting points (m.p.) and molar heats of fusion (L_f) were measured with a Mettler TA-3000 system. The values found are also listed in Table 1.

Calculations. The calculations were done on a IBM AT personal computer using the SIMCA-MACUP package [5].

Results and discussion

The results of the chemometric investigations are reported in Tables 2 and 3. The n.m.r. block of data and the other properties used are kept separate.

TABLE 1

Spectrophotometric, chromatographic and calorimetric data

Dye no.	λ_{max} (nm)		$R_f(1)$[a]	$R_f(2)$[b]	$R_f(3)$[c]	M.p. (°C)	L_f (kJ mol^{-1})
	Neutral	Acidic					
1	462	509	0.45	0.23	0.65	125.0	24.13
2	456	511	0.65	0.00	0.01	145.5	27.66
3	487	470	0.51	0.01	0.22	153.9	31.46
4	458	515	0.59	0.08	0.35	180.4	37.91
5	485	510	0.37	0.53	0.75	156.1	32.06
6	480	513	0.57	0.01	0.02	165.2	32.08
7	505	473	0.44	0.04	0.24	198.3	39.35
8	428	522	0.74	0.12	0.33	111.5	35.04
9	452	512	0.58	0.57	0.79	109.4	37.62
10	448	517	0.73	0.02	0.01	96.3	32.95
11	480	473	0.44	0.07	0.34	101.7	24.56
12	503	509	0.74	0.06	0.19	153.6	32.21
13	434	469	0.55	0.21	0.55	144.8	39.57
14	405	559	0.66	0.08	0.43	102.2	28.33
15	418	518	0.66	0.02	0.03	128.7	31.28
16	516	503	0.73	0.01	0.01	149.5	27.83
17	450	545	0.50	0.53	0.80	124.6	36.03
18	479	472	0.38	0.05	0.31	—	—
19	474	510	0.43	0.14	0.50	144.1	33.57
20	436	472	0.37	0.11	0.61	—	—
21	411	460	0.48	0.69	0.92	—	—
22	434	—	0.39	0.77	0.96	70.2	24.91
23	416	514	0.50	0.24	0.62	68.2	28.84
24	422	511	0.52	0.32	0.65	—	—
25	467	501	0.39	0.45	0.74	—	—
26	470	509	0.40	0.38	0.73	—	—
27	414	516	0.52	0.22	0.65	68.9	26.99
28	435	—	0.35	0.78	0.95	66.6	23.67
29	440	520	0.62	0.07	0.29	—	—
30	484	472	0.38	0.02	0.23	—	—
31	435	514	0.63	0.03	0.18	—	—
32	402	521	0.59	0.13	0.48	—	—
33	446	—	0.40	0.75	0.85	—	—
34	487	472	0.37	0.07	0.50	—	—
35	391	464	0.60	0.16	0.44	122.4	28.15
36	423	441	0.55	0.11	0.35	150.6	38.52
37	437	472	0.45	0.19	0.47	148.4	37.24
38	434	469	0.50	0.20	0.46	—	—

[a]On hydrophobic h.p.t.l.c. plates (RP-18 F-254s) with methanol eluent. [b]On silica gel plates (60 F-254) with benzene eluent. [c]On alumina plates (F-254) with benzene eluent.

TABLE 2

Fraction of variance explained (%V) by each model expansion

A[a]	%V		
	Model: I[b]	II[c]	III[d]
1	55.1	31.1	65.2
2	65.2	36.0	74.0
3	71.9	—[e]	—[e]
4	79.7	—	—

[a]Dimensionality of the model. [b]The X block is constituted by the n.m.r. data. [c]The X block is constituted by the data in Table 1. [d]The X block is constituted by the structure descriptors used in the previous work [2]. [e]The third dimension proved to be not significant for the model.

TABLE 3

Comparison of experimental and predicted values of fastness to light

Dye		Fastness to light				Dye		Fastness to light			
No.	Symbol[a]	Exper.[e]	Predicted by model			No.	Symbol[a]	Exper.[e]	Predicted by model		
			I[b]	II[c]	III[d]				I[b]	II[c]	III[d]
1	HCHHHH	4.5	4.41	4.02	3.95	21	XHHXHH	5.5	4.83	6.44	5.09
2	HCHHHO	3	3.81	3.37	3.73	22	XHHHHH	4.5	3.39	4.42	4.24
3	HCHHAH	4.5	4.48	4.81	4.18	23	YHHHHC	6.5	5.28	4.71	5.78
4	HNHHHC	5.5	5.91	4.48	5.61	24	YHHHTC	4.5	5.50	4.68	6.09
5	HNHHHH	4	4.85	3.41	4.15	25	CHHHTH	5	5.06	3.86	3.45
6	HNHHHO	3.5	3.83	3.70	3.92	26	HCHHTH	5	4.81	3.86	4.27
7	HNHHAH	5	5.26	4.60	4.37	27	XHHHHC	6.5	4.77	4.85	5.71
8	NHHHHC	3.5	4.50	4.66	4.23	28	YHHHHH	4.5	3.81	3.58	4.31
9	NHHHHH	3	3.16	4.13	2.77	29	HCHHTC	5	6.00	4.36	5.73
10	NHHHHO	3	2.40	4.15	2.54	30	CHHHAH	5	5.12	4.57	3.35
11	NHHHAH	3.5	3.29	4.54	2.99	31	HCHHHC	5.5	6.05	4.56	5.42
12	CNHHHC	6	6.59	3.36	4.71	32	HHHHHC	5	5.33	5.11	5.49
13	YNHXTC	7	6.35	6.21	7.16	33	YNHXHH	4.5	5.22	3.24	5.38
14	HMHHHC	5	4.54	4.07	5.42	34	YNHXAH	5	5.66	4.82	5.60
15	HHHHHO	3	3.20	4.87	3.80	35	XHHXHC	6.5	6.24	6.99	6.56
16	NNHHHO	3	3.06	3.04	2.66	36	XNHXHC	7	6.37	7.24	6.68
17	NMHHHH	1.5	2.00	3.30	2.69	37	XNHXTC	7.5	6.85	5.94	6.99
18	NMHHAH	1.5	2.23	5.06	2.92	38	YNHYTC	7	6.16	6.04	7.23
19	NMHHIH	1	0.71	4.01	2.50			r[f]	0.90	0.70	0.87
20	XHHXAH	6	5.82	6.06	5.39						

[a]The symbol is formed with a letter for each of the positions: X_1, X_2, X_3, X'_1, X_4, X_5 in formula I. Each letter represents a substituent: H=H; N=NO_2; C=CN; Y=Br; X=Cl; M=OCH_3; A=$NHCOCH_3$; T=CH_3; I=NH_2; O=OH. [b–d]See footnotes in Table 2. [e]Fastnesses are expressed in terms of numerical scales. For fastness to light the 1—8 scale is used, grade 1 corresponding to poor fastness and grade 8 to maximum fastness. [f]Correlation coefficient of the linear regression $y_{calc.}$ vs. $y_{exper.}$

The results show that when the X block is constituted by the n.m.r. data, the PLS model requires four latent variables to account for a fraction of variance of y of ca. 80%. In contrast, the model based on the other seven measurements is poor; it explains a much lower fraction of variance than the two-dimensional model based on n.m.r. data.

The data in Table 3 list the predicted fastnesses on the basis of the PLS models, compared with the experimental values. When the descriptors are the n.m.r. shifts (model I), the predicted level differs from the real value by more than one unit, with a maximum of 1.7, for only three dyes out of 38. As many as 14 predicted values differ from the experimental ones by more than one unit, with a maximum of 3.5, when the descriptors are the other properties (model II). An overall view of the goodness of the modelling is given by the correlation coefficients of the simple linear regression of y(calculated) vs. y(experimental), which are 0.90 and 0.70, respectively. The former value can be considered satisfactory, owing to the imprecision of the technological measurements.

The last column of Table 3 lists the predicted fastnesses on the basis of the same eleven descriptors as used previously [2]. Obviously, the computations were repeated to include the same 38 objects. The results show that modelling via n.m.r. is of the same order of precision as that via the traditional descriptors.

Consequently, it is clear that ^{13}C-n.m.r. data can be used successfully to predict dye fastness, whereas the other kinds of physicochemical measurement considered here cannot. Nuclear magnetic resonance spectra are fast and cheap data (especially because they require small amounts of material), and are particularly suitable for multivariate statistical analysis because each compound is represented by a bundle of numbers. Nevertheless, the property/structure descriptors relationship is still considered to be much more important, both because it allows a straightforward interpretation of the structural features responsible for the property, and because it can be used for predictions before a new dye is actually available.

This work was supported by a contribution from Progetto finalizzato CNR Chimica Fine e Secondaria to R. C., P. S., E. B., G. V. and a research grant from the Italian Ministry of Education (M.P.I.) to S. C. The authors thank Drs. P. G. Cargnino and A. Menozzi (Vagnone & Boeri S.p.A., Orbassano-Turin) for the calorimetric measurements.

REFERENCES

1 R. Carpignano, P. Savarino, E. Barni, S. Clementi and G. Giulietti, Dyes and Pigments, 6 (1985) 189.
2 R. Carpignano, P. Savarino, E. Barni, G. Di Modica and S. S. Papa, J. Soc. Dyers Colour., 101 (1985) 270.
3 S. Wold and M. Sjöström, in B. R. Kowalski (Ed.), Chemometrics: Theory and Application, American Chemical Society, Washington, DC, 1977, p. 243.

4 S. Wold, C. Albano, W. J. Dunn III, K. Esbensen, S. Hellberg, E. Johansson and M. Sjöström, in H. Martens and H. Russwurm (Eds.), Food Research and Data Analysis, Applied Science, London, 1983, p. 147.
5 S. Wold, C. Albano, W. J. Dunn III, U. Edlund, K. Esbensen, P. Geladi, S. Hellberg, E. Johansson, W. Lindberg and M. Sjöström, in B. R. Kowalski (Ed.), Chemometrics. Mathematics and Statistics in Chemistry, Reidel, Dordrecht, 1984, p. 17.
6 M. L. Bisani, D. Faraone, S. Clementi, K. H. Esbensen and S. Wold, Anal. Chim. Acta, 150 (1983) 129.
7 W. Lindberg, J. Öhman, S. Wold and H. Martens, Anal. Chim. Acta, 174 (1985) 41.

Analytica Chimica Acta, 191 (1986) 451—456
Elsevier Science Publishers B.V., Amsterdam – Printed in The Netherlands

Short Communication

A PARTIAL LEAST-SQUARES MODEL FOR THE PERMEABILITY OF STEROIDS ACROSS A POLY(ETHER-URETHANE) MEMBRANE

M. MARSILI* and G. SCAVIA

CNR-Progetto Finalizzato Chimica Fine e Secondaria, Via Nizza 128, 00198 Roma (Italy)

(Received 29th July 1986)

Summary. Six descriptors (volume and charge densities of two substituents, melting point and water solubility) for 8 steroids are used to study permeability across the membrane. The PLS treatment shows that a reduced training set gives reliable predictions for compounds of similar type.

The understanding of diffusion phenomena of steroids across artificial membranes is very important in the study and design of contraceptives which can be released in a controlled manner [1]. A useful measure of the behaviour of a diffusing molecule through a given matrix is its permeability, P [2]. Permeability is defined as the product of the maximum flux of the substance across the membrane, J_{max}, and the thickness, l, of the membrane, or as the product of the diffusion coefficient, D (kinetic parameter) and the solubility of the substance in the polymer matrix, C_p (thermodynamic parameter) [2]: $P = J_{max}\ l = D\ C_p$.

A partial least-squares (PLS) treatment was made on the permeability of eight steroids (Fig. 1) across a poly(ether-urethane) (E-type) membrane, in order to find a statistical model for relating structural features of the steroids to P. Comprehension of the parameters responsible for permeability

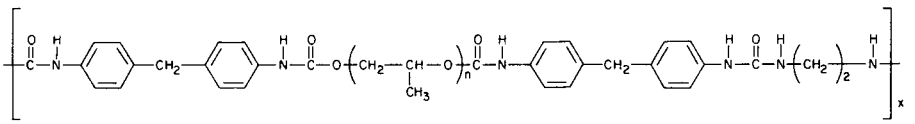

should make it possible to design molecules with a specific permeability. In this communication, it is shown that modern statistical techniques can deal with a reduced set of objects and still produce a high predictive performance.

Methods and results

The PLS method has been described extensively elsewhere [3—6]. The algorithms attempt to generate simultaneously a set of rotated eigenvectors in an X matrix (block of independent variables) and in a Y matrix (block of dependent variables), which will best describe the Y matrix and so minimize

0003-2670/86/$03.50

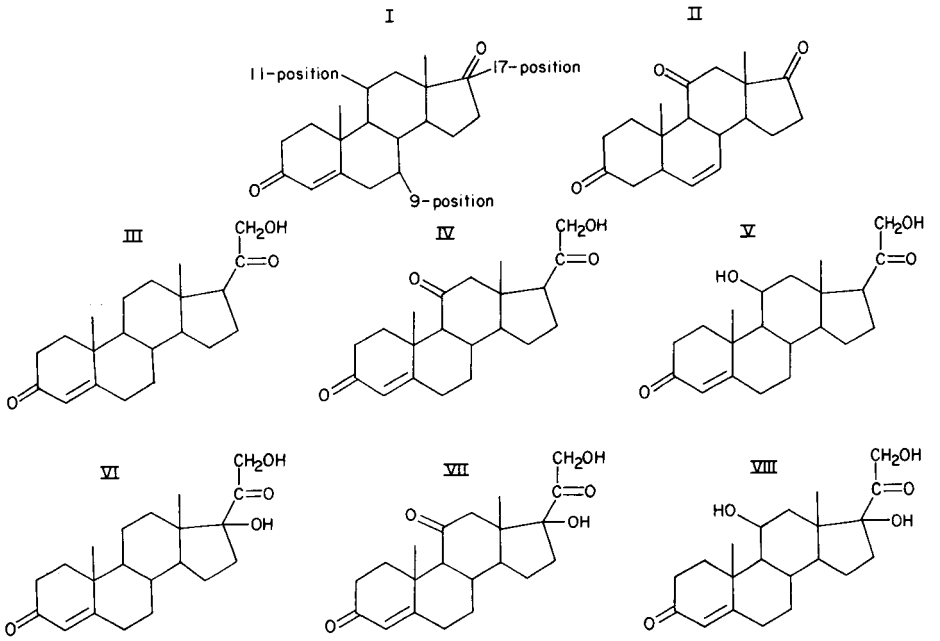

Fig. 1. Steroids tested: (I) androstenedione; (II) adrenosterone; (III) 11-deoxycorticosterone; (IV) 11-dehydrocorticosterone; (V) corticosterone; (VI) 11-deoxy-17-hydroxycorticosterone; (VII) cortisone; (VIII) hydrocortisone.

the prediction error of y. These PLS eigenvectors (factors), generated within the X and Y matrices, also called latent variables, are characterized by coefficients (weights), which represent the importance of a given variable in covering the variance explained. In a PLS treatment, the least number of dimensions necessary to give a stable model with the best predictive power is the one at which the predicted residual sum of squares (PRESS) reaches a minimum value [3—5].

In the present study, the descriptors used to define the variables of the x block are (Table 1) the charge density [7] of atoms of the common skeleton of the steroids which are subject to changes by substitution (C-11 and C-17), the volume of the substituents [8], the melting points and water solubilities [2]. The y block is a vector containing the experimentally-obtained permeability values (Table 2) which were obtained under the experimental conditions used by Lee et al. [2]).

The results of the PLS treatment are reported in Table 3. The lowest value of the PRESS is actually reached in the third dimension. However, the change of the PRESS from the second to the third dimension is very small, so only two dimensions are used for the model. In a typical case, the PRESS changed from 2.0 for one dimension to 0.125 for 2 dimensions, 0.1 for 3 dimensions and 0.4 for 4 dimensions. In the second dimension, the model explains 98%

TABLE 1

Descriptors used to define the variables of the x block

No.	V_1[a]	V_2[b]	V_3[c]	V_4[d]	V_5[e]	V_6[f]
1	−48.0	−296.0	0.11	1.00	174.0	39.0
2	137.0	−296.0	1.00	1.00	212.0	110.0
3	−48.0	−682.0	0.11	6.30	142.0	89.0
4	136.0	−682.0	1.00	6.30	179.0	460.0
5	60.0	−682.0	1.81	6.30	181.0	220.0
6	−48.0	−1060.0	0.11	8.00	209.0	72.0
7	136.0	−1060.0	1.00	8.00	222.0	230.0
8	60.0	−1060.0	1.81	8.00	219.0	290.0

[a]σ charge on C-11 (me). [b]Negative σ charge on the substituent in position 17 (me). [c]Volume of the substituent in position 11 (Å^3). [d]Volume of the substituent in position 17 (Å^3). [e]Melting point (°C). [f]Water solubility (μg ml^{-1}).

TABLE 2

The y vectors used

No.	Permeability[a]	Solubility[b]	Diffusion[c]	No.	Permeability[a]	Solubility[b]	Diffusion[c]
1	0.90	1.00	0.90	5	0.69	1.10	0.63
2	0.45	0.50	0.89	6	0.44	0.78	0.56
3	1.40	2.50	0.54	7	0.28	0.49	0.58
4	0.94	1.80	0.52	8	0.24	0.49	0.48

[a]10^{-12} g steroid/cm s. [b]10^{-4} g steroid/cm^3 polymer. [c]10^{-9} cm^2 s^{-1}.

TABLE 3

Results of the PLS treatment

		y = PERMEABILITY		y = SOLUBILITY		y = DIFFUSION	
Dimension		I	II	I	II	I	II
Variance explained in X block		0.46	0.65	0.38	0.65	0.43	0.74
Variance explained in Y block		0.72	0.98	0.68	0.94	0.84	0.95
Dimension	Variable	Weight		Weight		Weight	
I	V_1	−0.369		−0.366		−0.025	
	V_2	0.378		0.205		0.626	
	V_3	−0.416		−0.415		−0.192	
	V_4	−0.189		0.072		−0.705	
	V_5	−0.821		−0.992		−0.011	
	V_6	−0.104		0.095		−0.416	
II	V_1	0.263		0.401		0.539	
	V_2	−0.165		−0.263		0.017	
	V_3	0.224		0.301		0.449	
	V_4	0.422		0.462		−0.187	
	V_5	−0.490		−0.230		0.735	
	V_6	0.688		0.669		0.083	

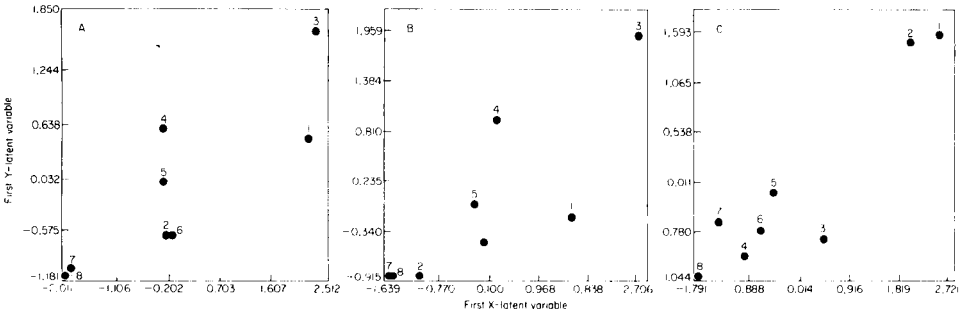

Fig. 2. Plots of the first x latent variable vs. the first y latent variable for the PLS model with different dependent variables: (A) permeability of the steroids in the polymer; (B) solubility in the polymer; (C) diffusion across the polymer.

of the variance of the experimental permeabilities. This result is good considering that the residual variance (2%) is due more to noise than to any systematic variation of molecular properties. Figure 2A reveals a discrete correlation between the x latent variable and the y latent variable of the first dimension. The first dimension explains a very high percentage of the variance of the y block (72%). The interpretation of the importance of the different descriptors in influencing the dependent variable is based on the weights, w_i, of this dimension; large absolute values of w_i refer to important x-variables. From Table 3, it is evident that the melting point is the variable most correlated with the permeability; the negative weight indicates a negative dependence of the permeability on this descriptor. The other descriptors give a less significant contribution, although the charges on substituents in positions 11 and 17 and the volume in position 11 seem to have some importance.

In a second study, eight PLS models were built by removing one steroid at a time and using the remaining seven objects for each model. The omitted case was used as a test set for prediction of its permeability from that model (leave-one-out method, LOOM). Table 4 shows the difference between the

TABLE 4

Effectiveness of the models tested by LOOM

Case no.[a]	Permeability (y) (exper.)[b]	(pred.)	Δy[c]	Case no.[a]	Permeability (y) (exper.)[b]	(pred.)	Δy[c]
1	0.90	1.05	−0.15	5	0.69	0.71	−0.02
2	0.45	0.42	0.03	6	0.44	0.55	−0.11
3	1.40	1.20	0.20	7	0.28	0.24	0.04
4	0.94	0.80	0.14	8	0.24	0.23	0.01

[a]This refers to the steroid put in the test set. [b]SD = 0.40. [c]The error for the predicted permeability given by a model constructed on the other seven steroids.

experimental and predicted values. The predictive powers of the models are obviously good: Δy is, in all cases, smaller than the standard deviation of y. The eight models confirm the results obtained in Table 3 and show that seven objects are sufficient to give a stable model.

As discussed above, permeability is defined as the product of the diffusion coefficient and the solubility of the substance in the polymer matrix. The next step was then to investigate the descriptors which D and C_p separately depend, and to compare the results with those obtained for permeability. Two PLS models were built by using the original x block (Table 1) and the diffusion and solubility data of the same eight steroids in the same polymeric membrane (see Table 2) as the y vectors. The results of these two PLS treatments are also reported in Table 3. The corresponding plots of the first y latent variable vs. the first x latent variable are shown in Fig. 2B, C.

According to the weights of the first dimension, it is evident that the descriptors which influence the diffusion of this set of steroids across the membrane are different from those which influence the solubility in the polymer matrix, C_p. The influence of the dipolar characteristics of these steroids on the melting points suggests that electrostatic interaction between solute (steroid) and solvent (membrane) is important in explaining C_p. In contrast, the descriptors which influence the diffusion separate the androstene derivatives (cases 1 and 2) from pregnene derivatives (other cases) (Fig. 2C) and refer to the substitution in position 17, i.e., molecules with the bulky substituent $-COCH_2OH$ in position 17 diffuse much less easily than the others and form a well-defined class.

By comparing the results obtained with the three different y vectors, it is clear that the permeability, within this set of data, is more similar to C_p than to diffusion; probably, the change of the volume of the substituents is too small to influence P. The release of steroids similar to those examined is, therefore, more influenced by their solubility in the polymer than by their diffusion properties. According to these results, the electronic characteristics rather than the steric characteristics of the molecule should be utilized in the design of a steroid with a desired release property.

Conclusions

This study is only a first step in attempting to understand the mechanism involved in the release of steroids and, therefore, in designing more efficient controlled-release systems. Although the statistical models obtained have good stability, their predictive power will obviously be limited to steroids with substituents similar to those examined in the present data set; more powerful models would require increased variety of the substituents on positions 11 and 17. Furthermore, only a few steroids (estrogens and progestins) act as contraceptives. Therefore, in the study of the controlled drug release, it is more realistic to alter the polymer matrix than to vary the steroid. Different polymeric membranes will be examined in later tests.

We are grateful to Professor E. Drioli for helpful discussion. Financial support from the Istituto Mario Negri, Milan is gratefully acknowledged.

REFERENCES

1 R. S. Langer and D. L. Wise, Medical Application of Controlled Release, Vol. 1, CRC Press, Boca Raton, FL, 1984.
2 K. Lee, H. K. Lonsdale, R. W. Baker, E. Drioli and P. A. Bresnahan, J. Membr. Sci., 24 (1985) 125.
3 S. Wold, A. Ruhe, H. Wold and W. Dunn, SIAM J. Stat. Comput., 5 (1984) 735.
4 K. Mardia, J. Kent and J. Bibby, Multivariate Analysis, Academic Press, London, 1980, pp. 452—485.
5 H. Martens and H. Russwurm, Food Research and Data Analysis, Applied Science, London, 1983, pp. 147—188.
6 B. Kowalski (Ed.), Chemometrics: Mathematics and Statistics in Chemistry, Reidel, Dordrecht, 1984, pp. 17—95.
7 J. Gasteiger and M. Marsili, Tetrahedron, 36 (1980) 3219; Croat. Chem. Acta, 53 (1980) 601.
8 M. Marsili and Ph. Floersheim, Comp. Chem., 7 (1983) 175.

Analytica Chimica Acta, 191 (1986) 457—460
Elsevier Science Publishers B.V., Amsterdam — Printed in The Netherlands

Short Communication

APPLICATION OF PARTIAL LEAST-SQUARES MODELLING IN THE OPTIMIZATION OF A WASTE-WATER TREATMENT PLANT

PÄIVI AARNIO* and PENTTI MINKKINEN

Lappeenranta University of Technology, P.O. Box 20, SF-53851 Lappeenranta (Finland)

(Received 28th May 1986)

Summary. The partial least-squares method was applied to data collected at a municipal waste-water treatment plant to estimate the relationship between the process parameters and effluent quality. The main reason for poor treatment efficiency was the so-called bulking phenomenon of the activated sludge. The PLS model of the data representing a normal period of operation and the bulking period thereafter showed that high temperature and decreasing concentrations of carbon and phosphorus contributed to the bulking state.

The aim of this study was to improve the performance of a municipal waste-water treatment plant consisting of mechanical, chemical, and biological treatment units. A major problem in the operation of activated sludge plants is the phenomenon called "bulking" which is caused by the overgrowth of filamentous micro-organisms. As a result, the sludge settles slowly and thickens poorly and the sludge volume index is high (SVI > 250).

Model of the effluent quality

The partial least-squares (PLS) model was applied to data collected at the plant during one year to estimate the relationship between the treatment efficiency and the process parameters. The SIMCA-3B computer package modified for a HP-3000/40 computer was used in the calculations. The number of objects was 48, and the operational conditions of the waste-water treatment plant were described by 22 variables (X block). The treatment efficiency was described by three variables (Y block), i.e., total phosphorus concentration, chemical oxygen demand, and turbidity of the effluent. A simplified scheme of the plant and sampling points is shown in Fig. 1. The variables used in the PLS models are listed in Table 1.

The PLS model with one principal component explained 73% of the variance of the Y block variables. The most important independent variables were the flow rate of the stream passing through the biological unit, the flow rate of return sludge, and the sludge volume index. The modelling powers of these variables exceeded 0.25. High sludge loading and high pH decreased the effluent quality; the other variables were less significant. These results are illustrated in Figs. 2 and 3.

0003-2670/86/$03.50

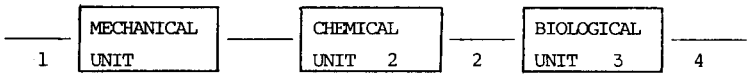

Fig. 1. A simplified scheme of the waste-water treatment plant and the sampling points: (1) influent water; (2) primary sedimentation; (3) aeration basin; (4) effluent.

TABLE 1

The variables used in the PLS models

1. INFLUENT WATER

No. Variable

1. Flow, m^3/day
4. Phosphorus concentration, mg l^{-1}
5. Sedimentation rate, ml l^{-1} h^{-1}
6. pH
7. Chemical oxygen demand, mg l^{-1}
8. Suspended solids concentration, mg l^{-1}

2. PRIMARY SEDIMENTATION

No. Variable

3. Added polymer, g m^{-3}
11. Phosphorus concentration, mg l^{-1}
12. Suspended solids concentration, mg l^{-1}
13. pH
14. Chemical oxygen demand, mg l^{-1}
15. Sedimentation rate, ml l^{-1} h^{-1}

3. AERATION BASIN

No. Variable

2. Added $FeSO_4$, g m^{-3}
9. Flow, m^3/day
10. Flow passing by the aeration basin, m^3/ day
16. Sedimentation rate, ml l^{-1} h^{-1}
17. pH
18. Sludge volume index
19. Sludge age, day
20. Return sludge flow, m^3/day
21. Excess sludge flow, m^3/day
22. Sludge loading, kg COD/kg MLSS/day

4. EFFLUENT

No. Variable

23. Phosphorus concentration, mg l^{-1}
24. Chemical oxygen demand, mg l^{-1}
25. Turbidity, NTU
26. Temperature, °C

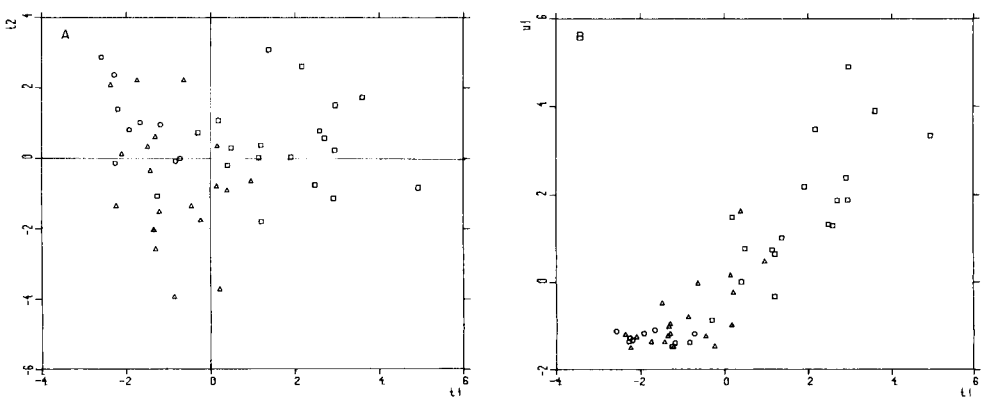

Fig. 2. PLS model of the effluent quality. The first latent X block variable t_1 plotted against: (A) the second latent X block variable t_2 (only t_1 is significant); (B) the first latent Y block variable u_1. (□) SVI ≥ 300; (○) 250 ≤ SVI ≤ 300; (△) SVI ≤ 250.

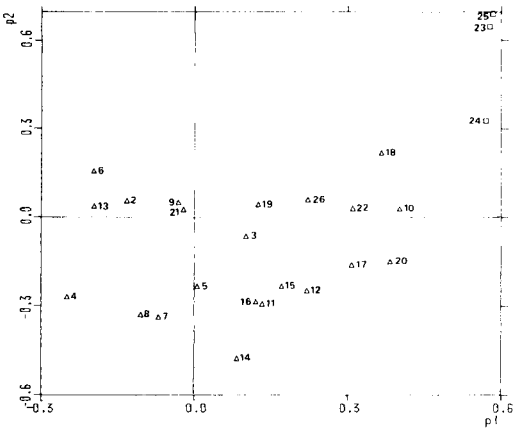

Fig. 3. PLS model of the effluent quality. Loadings of the variables: (□) Y variables; (△) X variables.

Model of the bulking phenomenon

The most effective way to improve the effluent quality is to avoid excessive growth of filamentous micro-organisms, i.e., the bulking phenomenon. To find the reasons for bulking, 39 objects were chosen, 21 of which represented a normal period when the sludge volume index was below 250 (group A), and the other objects represented the bulking period thereafter (group B, SVI > 300). A dummy matrix with two variables 1 and 0 for group A and 0 and 1 for group B was constructed (Y block), and 19 of the above-mentioned 26 variables were chosen as independent variables (X block). The X and Y blocks were analyzed by the PLS model to find the differences between these two groups.

A model with two significant principal components was obtained. The t vectors are plotted against each other in Fig. 4A; as can be seen the groups are well separated. The loading plot in Fig. 4B gives the discrimination powers

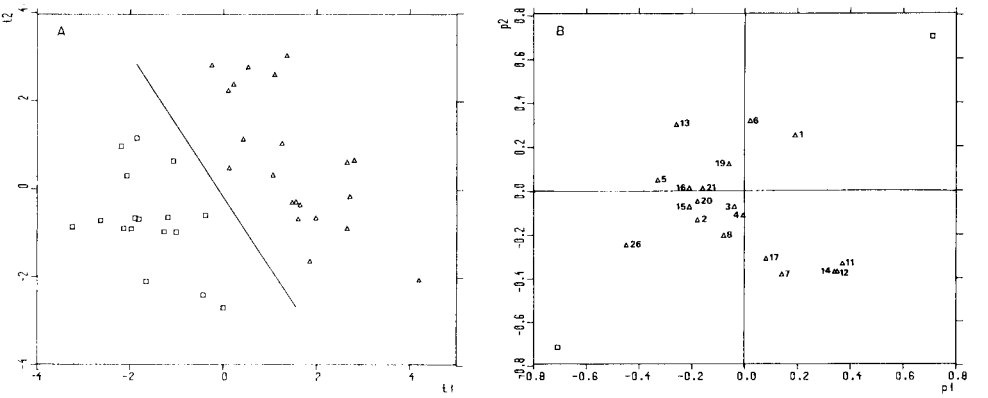

Fig. 4. PLS model of the bulking phenomenon. (A) The first latent X block variable t_1 plotted against the second latent X block variable t_2: (□) group B (bulking period); (△) group A (normal period). (B) The loadings of the variables: (□) Y variables; (△) X variables.

of the X variables. The phosphorus concentration, the suspended solids concentration and the chemical oxygen demand (COD) of the chemically treated water as well as the temperature in the biological unit have the highest discrimination powers and have modelling powers above 0.25. The range and the mean values of these variables in groups A and B are listed in Table 2.

TABLE 2

The range and the mean of the variables with the highest discrimination powers

No. Variable	Group A		Group B	
	Range	$\bar{x}$	Range	$\bar{x}$
11. Phosphorus, mg l^{-1}	0.9—5.5	3.0	0.9—3.4	1.8
12. Suspended solids, mg l^{-1}	40—148	101	38—110	69
14. COD, mg l^{-1}	32—106	54	23—50	36
26. Temperature, °C	5—9	7	9—19	14

Conclusions

From the measured variables, the decreasing concentrations of the nutrients phosphorus and carbon, together with rising temperature, seem to have contributed to the bulking state at the waste-water treatment plant. To avoid this, the concentration of phosphorus and the chemical oxygen demand after primary sedimentation should be kept above 3 mg l^{-1} and 40 mg l^{-1}, respectively. The bulking phenomenon is the main reason for decreasing effluent quality. The other process parameters within the range examined in this study have little effect on the treatment efficiency. Because these results were not based on designed experiments, they are being confirmed on a pilot scale. The results of this study formed the basis of the experimental design.

Analytica Chimica Acta, 191 (1986) 461—466
Elsevier Science Publishers B.V., Amsterdam — Printed in The Netherlands

Short Communication

INVESTIGATION OF THE HOMOGENEITY OF SOLIDS WITH A LINEAR REGRESSION MODEL

A. PARCZEWSKI

Jagiellonian University, Faculty of Chemistry, ul. Karasia 3, PL-30-060 Kraków (Poland)

K. DANZER* and R. SINGER

Friedrich-Schiller-Universität, Sektion Chemie, Steiger 3, DDR-6900 Jena (German Democratic Republic)

(Received 26th May 1986)

Summary. Testing of the homogeneity of solids is usually based on the comparison of the variance of measurements at several sample points with the variance of repeated measurements. In the case of destructive analytical methods, empirical mathematical models are needed because repetitions at the same subsample are impossible. Successful application of such models depends on the adequacy of the mathematical model and the type of distribution observed. Gradients and textures with low or medium local frequency require other tests than stochastic distributions with high local frequency. A simple regression model based on a 2^2 factorial allows conclusions about the type of distribution without great mathematical effort.

The distribution of an element in a solid sample is regarded as homogeneous if the variance of measurements obtained with a lateral resolving method at different sample points is not significantly greater than the variance of repeated measurements [1]. Because repetitions at the same point in the sample are impossible when a destructive analytical method is used, this simple and direct comparison cannot be utilized. In this case, empirical mathematical methods like analysis of variance (ANOVA), two-dimensional analysis of variance [2] or regression models are applied for characterizing the investigated distribution [3]. The successful application of these models depends on the adequacy of the theoretical assumptions and on the real distribution. Stochastic concentration fluctuations with high local frequency are most conveniently characterized by single analysis of variance [4, 5] of the results of stochastically arranged measuring points, whereas the detection of systematic inhomogeneities like textures or gradients with medium or low local frequency requires a regular arrangement of the measuring points and an exploration by two-dimensional analysis of variance or regression models. The limitation of the different procedures to certain types of distributions means that prior information is an essential primary condition for the application of such empirical mathematical models, because differences between the theoretical model and reality leads to fundamental errors. If

0003-2670/86/$03.50

no prior information about the expected inhomogeneity is available, a regular arrangement of the measuring points on the sample is to be recommended for three reasons: first, it provides more information yield than a stochastic arrangement [6]; secondly, with the help of efficient graphics in microcomputers, SPLINE-interpolation calculations can be done to construct graphics of the investigated distribution, allowing visual estimation of the element distribution [7]; and thirdly, regular arrangements of the measuring points allow the application of regression models.

Mathematical model

A regression model based on the principle of a 2^2 factorial was proposed by Parczewski [8]. In this model, the concentration x of the measured element is treated as a function of the normalized space coordinates z_1 and z_2 corresponding to the equation

$$x = B_0 + B_1 z_1 + B_2 z_2 + B_{12} z_1 z_2 \tag{1}$$

where B_0 is the mean concentration, B_1 the coefficient in direction z_1, B_2 the coefficient in direction z_2, and B_{12} the coefficient of interaction between the two coordinates. The coefficient B_{12} becomes significant when the concentration gradient $\partial x/\partial z$ is not constant within the square formed by the four measuring points (x_{11}, x_{12}, x_{22}, x_{21}) used for the calculation of the coefficients:

$$\begin{aligned} B_0 &= (x_{12} + x_{22} + x_{11} + x_{21})/4 \\ B_1 &= (x_{12} + x_{22} - x_{11} - x_{21})/4 \\ B_2 &= (x_{12} - x_{22} + x_{11} - x_{21})/4 \\ B_{12} &= (x_{12} - x_{22} - x_{11} + x_{21})/4 \end{aligned} \tag{2}$$

For a regular array of r rows and c columns of measuring points, sets of $m = (r - 1)(c - 1)$ coefficients can be calculated in this way. It must be noted that each measured concentration x is affected by the analytical error, numerically expressed as standard deviation s_A. By linear combination of four concentrations in each Eqn. 2 in the case of a homogeneous distribution, this error will propagate on the values of the coefficients B corresponding to $s_B = s_A/2$.

The investigated distribution is therefore regarded as inhomogeneous if the standard deviation of the regression coefficients s_{B_0}, s_{B_1}, s_{B_2} and/or $s_{B_{12}}$ is significantly greater than half the analytical error. In the case of destructive methods, the analytical error can be estimated by using two-dimensional analysis of variance. This test is most conveniently done by comparing a test value $F = 4s_{B_i}^2/s_A^2$ with the corresponding quantile $F(P; f_1; f_2)$ of the FISHER distribution, where P is the confidence coefficient, and $f_1 = (r - 1)(c - 1) - 1$ and f_2 are the degrees of freedom underlying the estimation of analytical error. In the case of estimating s_A by two-dimensional analysis of variance, $f_2 = (r - 1)(c - 1)$. The decision whether an

inhomogeneity so detected is a gradient or a stochastic one was described earlier [9]; the absolute value of the sum of the gradients, V, is compared with the sum of the absolute values of the gradients, S. For a stochastic distribution the value of V/S is near zero; for a gradient distribution it approaches unity. This estimation has the disadvantage that previously the statistical distribution of the V/S values was unknown and therefore could not be tested using the quantiles $F(P; f_1; f_2)$ of a theoretical distribution. This disadvantage is now eliminated by using new test values:

$$P_1 = \sum_1^m B_{1i} \qquad P_2 = \sum_1^m B_{2i} \tag{3}$$

$$Q_1 = \sum_1^m |B_{1i}| \qquad Q_2 = \sum_1^m |B_{2i}| \tag{4}$$

$$R_1 = P_1/Q_1 \qquad R_2 = P_2/Q_2 \tag{5}$$

The standard deviation of these values can be calculated by the rules of error propagation:

$$s_{P_1}^2 = (2r-3)\, s_A^2/4 \qquad s_{P_2}^2 = (2c-3)\, s_A^2/4 \tag{6}$$

$$s_{Q_1}^2 = \sum_1^m b_{1i}^2 s_A^2 \qquad s_{Q_2}^2 = \sum_1^m b_{2i}^2 s_A^2 \tag{7}$$

$$s_{R_1}^2 = \sum_1^m (a_{1i} + R_1 b_{1i})^2 s_A^2/Q_1^2 \qquad s_{R_2}^2 = \sum_1^m (a_{2i} + R_2 B_{2i})^2 s_A^2/Q_2^2 \tag{8}$$

where a and b are the coefficients in the formulae for P and Q, $P = \Sigma a_i x_i$ and $Q = \Sigma b_i x_i$, which take into account the correlation between coefficients B corresponding to adjacent quartets of measuring points. The significance of P, Q and R can be tested according to Student's t-test: $t = P/s_P$; Q/s_Q; R/s_R.

It must be noted that the test of R/s_R should be considered tentative because the distribution of R deviates from the normal one. The proposed characteristics P, Q and R give the following information. If P_1 and/or P_2 are significant, it can be concluded that a gradient exists in direction z_1 and/or z_2; in this case, R_1 or R_2 does not differ much from 1. If P_i ($i = 1,2$) is not significant, while Q_i proves to be significant, a stochastic inhomogeneity exists along z_i axes; in this case, R_i does not differ much from zero. If both P_i and Q_i are insignificant, inhomogeneity is not detectable.

Examples

For presentation of the advantages of the regression test, four examples were selected, which were earlier investigated with other empirical mathematical methods [2, 8]. These examples involved: (1) the distribution of boron (homogeneous) on an iron surface; (2) the distribution of boron (inhomogeneous) on an iron surface; (3) the distribution of chromium in an

alloy steel; (4) the distribution of manganese in alloy steel. Figures 1—4 are computer plots of isolines (lines of constant concentration or measured signal) calculated on the basis of the regression model. Table 1 shows the proposed test values Y ($Y = P$, Q or R) and their standard deviations calculated from Eqns. 6—8. The t values were calculated from the t-test formulae described above. The analytical errors s_A were evaluated by using two-dimensional analysis of variance [2].

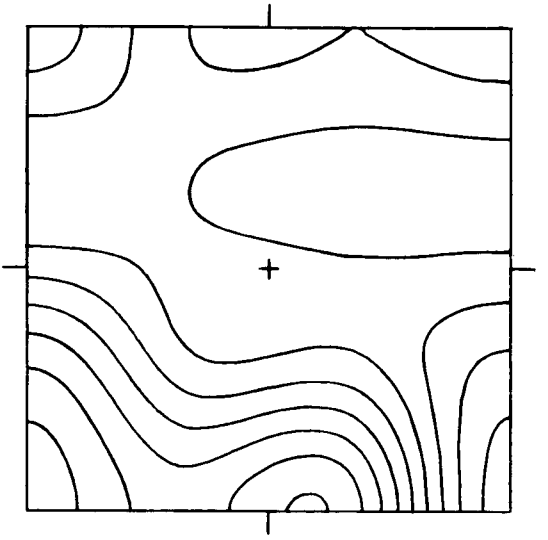

Fig. 1. Distribution of boron on iron surface (homogeneous).

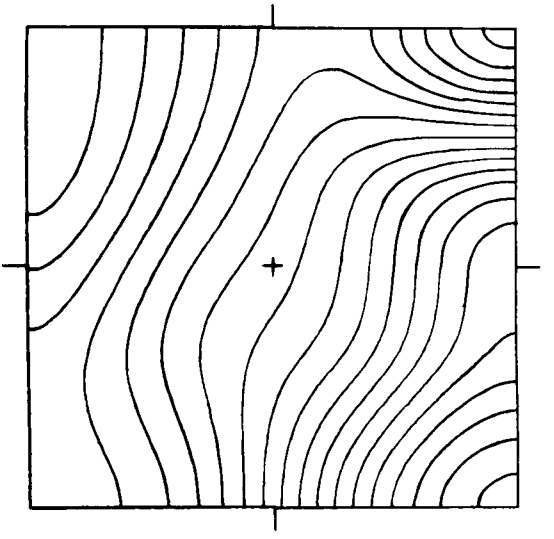

Fig. 2. Distribution of boron on iron surface (inhomogeneous).

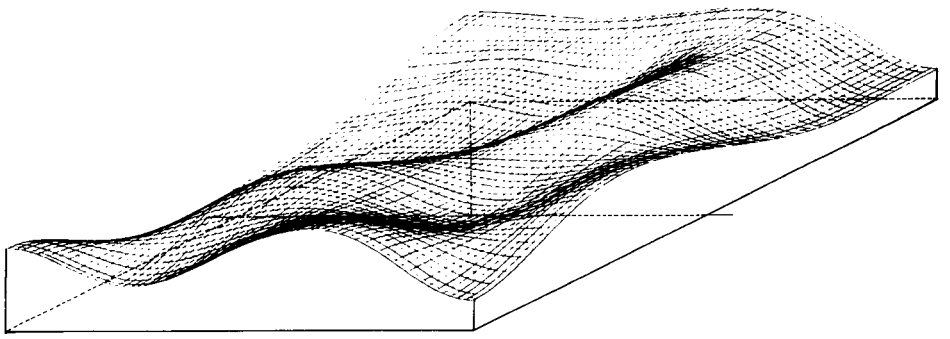

Fig. 3. Distribution of chromium in alloy steel.

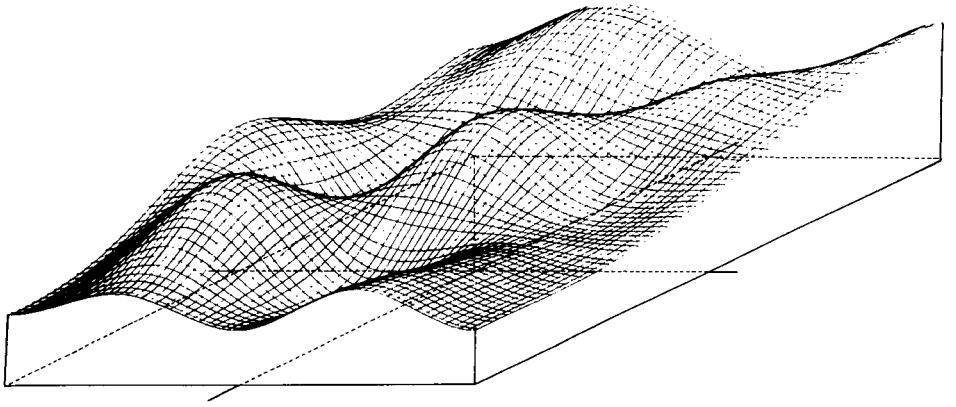

Fig. 4. Distribution of manganese in alloy steel.

TABLE 1

Results of the examination of homogeneity of solids[a]

	Y[b]	s_Y	t[c]	Y	s_Y	t[d]
Case 1				*Case 3*		
P_1	−0.097	0.047	2.04	−0.002	0.172	0.01
P_2	−0.109	0.047	2.30*	−0.137	0.172	0.80
Q_1	0.118	0.106	1.11	0.962	0.313	3.08*
Q_2	0.153	0.085	1.80	0.852	0.269	3.17*
R_1	−0.822	0.67	1.23	−0.003	0.179	0.02
R_2	−0.715	0.40	1.80	−0.161	0.199	0.81
Case 2				*Case 4*		
P_1	−0.558	0.173	3.22*	0.45	0.268	1.68
P_2	−0.802	0.173	4.63*	−0.84	0.268	3.14*
Q_1	0.579	0.19	3.05*	2.25	0.43	5.24*
Q_2	0.830	0.19	4.37*	2.16	0.526	4.11*
R_1	−0.964	0.212	4.55*	0.20	0.133	1.50
R_2	−0.966	0.183	5.28*	−0.389	0.145	2.69*

[a]Significant values are indicated by asterisks. [b]$Y = P$, Q or R, see Eqns. 3—5. [c]$t(0.95;9) = 2.262$. [d]$t(0.95;8) = 2.306$.

Discussion

From the data presented in Table 1, the following conclusions can be drawn. For the distribution of boron in iron, which was supposed to be homogeneous, a gradient in the z_2 direction is detected. For the inhomogeneous distribution of boron in iron, distinct gradients in both directions are proved. A significant stochastic inhomogeneity of chromium in alloy steel is detected. For manganese in the alloy steel, the stochastic distribution of manganese along the z_1 axes and a gradient along the z_2 axes (possibly overlaid with stochastic fluctuations) proves to be significant.

Comparison of the results of these tests with those of former empirical mathematical models [2, 8] clearly shows the advantages of the new method. It has proved to be successful, especially in the case of stochastic distributions which are otherwise difficult to detect. The method should be preferred for the examination of distributions which are characterized by only one element concentration and without repeated measurements.

REFERENCES

1 H. Malissa, Fresenius Z. Anal. Chem., 273 (1975) 449.
2 K. Danzer and G. Marx, Anal. Chim. Acta, 110 (1979) 145.
3 K. Danzer and G. Ehrlich, 4. Tagung Festkörperanalytik, 1984, Tagungsber. Techn. Hochsch. Karl-Marx-Stadt, Heft 12, Bd. 2, p. 547.
4 K. Danzer, K. Doerffel, H. Ehrhard, G. Ehrlich, P. Gadow and M. Geissler, Anal. Chim. Acta, 105 (1979) 1.
5 K. Danzer, Spectrochim. Acta, Part B, 39 (1984) 949.
6 K. Danzer, 3. Tagung Festkörperanalytik, 1981, Tagungsber. Techn. Hochsch. Karl-Marx-Stadt, 1981, p. 19.
7 Ch. Opitz, K. Danzer, K. Lösche, G. Enke and G. Baumert, Posterbeitrag, 3. Tagung COMPANA, 1985.
8 A. Parczewski, Anal. Chim. Acta, 130 (1981) 221.
9 R. Singer and K. Danzer, Z. Chem., 9 (1984) 339.

Analytica Chimica Acta, 191 (1986) 467—472
Elsevier Science Publishers B.V., Amsterdam — Printed in The Netherlands

Short Communication

LE TRAITEMENT DES FORMES EN CHIMIE ANALYTIQUE

HERVÉ RIX

Laboratoire Signaux et Systèmes, U.A. 814 CNRS, Université de Nice, 41 boulevard Napoléon III, 06041 Nice Cédex (France)

(Reçu le 26 Mai 1986)

Summary. (Signal-shape processing in analytical chemistry.) When signal evolution (e.g., spectra) has to be detected or measured, shape processing can be useful. The distribution function method enables all the information in the signal shape to be utilized, by working with normalized integrals. The concept of shape also helps in estimating resolution parameters of overlapped peaks. The principles are outlined and some applications in chromatography and Mössbauer spectrography are summarized.

Résumé. Dans les cas où l'on a à détecter ou à mesurer l'évolution d'un signal (d'un spectre par exemple) on a souvent intérêt à traiter la forme. La méthode des fonctions de répartition permet de prendre en compte toute l'information contenue dans la forme, en travaillant sur les intégrales normées. La notion de forme peut aussi intervenir dans une hypothèse de conservation pour estimer des paramètres de séparation de pics mal résolus. L'article passe en revue les principes et une série d'applications réelles en chromatographie et en spectrographie Mössbauer.

Le traitement des spectres obtenus en chimie analytique a pour but initial la localisation (en temps ou en fréquence) de phénomènes purs (pics chromatographiques, raies spectroscopiques) ainsi qu'une mesure de leurs intensités. Le traitement du signal vise dans ce cas, d'une part à éliminer le bruit de mesure, d'autre part à accroitre le pouvoir séparateur de l'appareil. Là se pose le problème du test de la pureté du phénomène, pureté du corps associé à un pic unique pour citer l'exemple de la chromatographie qui sera développé plus loin. Mais l'objet de l'analyse peut être non pas l'énchantillon mais l'appareil lui-même: pour une excitation donnée, on étudie la réponse en fonction de conditions expérimentales variables.

Le rôle de la chimiométrie est alors de donner une mesure objective de l'évolution des observations. Pour détecter ou mesurer une différence entre deux signaux, deux approches sont possibles: mesurer des indices synthétiques (moments par exemple) ou mesurer une différence de forme. La méthode des moments proposée par Grushka et al. [1—3] ainsi que la méthode d'analyse de pente [3, 4] permettent, par exemple, de différencier un pic pur d'un pic double, à partir de quantités directement reliées à la forme. La méthode des fonctions de répartition (MFR) qui compare les intégrales normées des signaux [5, 6] utilise tout l'information contenue dans la forme d'un signal. Elle permet donc de faire du traitement de

0003-2670/86/$03.50

"formes de signaux". L'objet de cet article est de montrer l'intérêt d'un tel traitement de formes au travers d'applications empruntées aux techniques de la chimie analytique.

Les méthodes

On rappelle brièvement le principe de la MFR [5, 6], de la décomposition de formes qui en dérive [7] et d'une méthode de séparation de deux pics serrés dans le cas où ils sont de même forme [8, 9].

La méthode des fonctions de répartition. Soit $s(t)$ et $v(t)$ deux signaux positifs sur leurs intervalles d'observation et soit $S(t)$ et $V(t)$ leurs intégrales normées respectives (rappelons que l'intégrale normée d'un signal, à l'instant t, s'obtient en intégrant le signal jusqu'à t et en divisant cette quantité par l'aire totale, positive par hypothèse, située sous le signal). On peut interpreter S et V comme les fonctions de répartition de deux variables aléatoires homogènes à la variable d'abscisse t et notées $T(s)$ et $T(v)$, respectivement. Si l'on définit la fonction $\phi(t)$ par $S(t) = V[\phi(t)]$, on peut interpréter $T(v)$ comme la transformée de $T(s)$ par la transformation croissante ϕ: $T(v) = \phi[T(s)]$. Si la notion de similitude de forme est prise au sense usuel, c'est-à-dire invariance par translation et changements d'échelle, les fonctions ϕ laissant la forme inchangée sont les fonctions affines. Plus généralement, il est montré [6] comment on peut généraliser cette notion de similitude de forme. Partiquement, pour mesurer la différence de forme entre deux signaux $s(t)$ et $v(t)$, on calcule, à partir des signaux échantillonnés, une série de couples (t_i, t'_i) définis par $S(t_i) = V(t'_i)$. La variation de t'_i en fonction de t_i est une discrétisation de la fonction $\phi(t)$ et l'écart de forme entre s et v doit être une mesure de l'écart à la linéarité de la courbe $t' = \phi(t)$.

Suivant les applications, plusieurs mesures de cet écart ont été proposées, que l'on notera ici: (i) Δ_1 = écart quadratique moyen entre les points de la courbe $\phi(t)$ et la droite de régression de t' par rapport à t; (ii) Δ_2 = écart quadratique moyen entre les points de la courbe $\phi(t)$ à l'exterieur d'une fenêtre (t_i, t_{i+L}) et la droite des moindres carrés ajustée sur les points à l'intérieur de la fenêtre; (iii) Δ_3 = maximum des écarts précédemment définis lorsqu'on fait glisser la fenêtre entre ses deux positions extrêmes; (iv) Δ_4 = coéfficient de corrélation linéaire entre les t_i et les t'_i; (v) Δ_5 = coéfficient du terme en t^2 lorsqu'on ajuste une parabole sur les couples (t_i, t'_i).

L'étude en simulation des performances de la MFR a été faite en traçant la limite de détectabilité d'un pic double, somme de deux composantes de même forme et de même largeur, en fonction des trois paramètres: distance entre les composantes (d), rapport des aires (k), rapport signal à bruit (S/B). On obtient ainsi dans un diagramme (d, k) un réseau de courbes iso-S/B [10, 11]. En outre, les performances numériques de la MFR ont été récemment étudiées dans le problème de la séparation de deux sources radar; la nette supériorite de la MFR sur les méthodes classiques (méthode des moments, méthode du seuil) a été clairement établie [12].

Décomposition de forme. En relation avec la MFR, Massiot [7] propose une méthode de décomposition d'un signal en une somme de deux signaux de forme donnée, en travaillant au niveau des fonctions de répartition. Supposons que le signal $v(t)$ apparaisse comme ayant une forme intermédiaire entre celles des signaux $s_1(t)$ et $s_2(t)$. On approchera (au sens des moindres carrés) la fonction de répartition $V(t)$ associée à $v(t)$ par une fonction de répartition de la forme

$$F(t) = p\,S_1(a_1 t + b_1) + (1-p)\,S_2(a_2 t + b_2) \tag{1}$$

où les paramètres p, a_1, b_1, a_2, b_2 sont à estimer.

Séparation de deux pics voisins, de même forme. Les hypothèses de travail sont ici plus restrictives. Soit un signal $s(t)$ ayant une forme de pic (un seul maximum). Soit $v(t)$ un deuxième signal somme de deux pics de la même forme que $s(t)$,

$$v(t) = C\left\{s(t) + (k/a)\,s[(t-d)/a]\right\} \tag{2}$$

Avec ces notations, d représente la distance entre les composantes, a le rapport des largeurs et k le rapport des aires de la deuxième à la première composante. Le problème à résoudre est l'estimation de ces trois paramètres quand on dispose des profils échantillonnés de $s(t)$ et de $v(t)$. Deux procédures ont été proposées: l'une qui suppose des composantes de même largeur ($a = 1$) [8], l'autre en laissant a intervenir comme paramètre [9].

Hypothèse "a = *1*"*: estimation de* d *et* k. Dans ce cas Eqn. 2 devient

$$v(t) = C[s(t) + k\,s(t-d)] \tag{3}$$

Soit $\tilde{s}(t)$ (respectivemment $\tilde{v}(t)$) le profil normé (par la surface) de $s(t)$ (respectivement $v(t)$). L'équation 3 s'écrit, avec les profils normés:

$$\tilde{v}(t) = (\tilde{s}(t) + k\,\tilde{s}(t-d))/(1+k) \tag{4}$$

On peut voir sur la Fig. 1 la propriété mathématique permettant d'estimer le parametre d: d est la différence d'abscisse entre le point d'intersection des courbes $\tilde{s}(t)$ et $\tilde{v}(t)$ et le point de même ordonnée sur $\tilde{s}(t)$. L'estimation $\hat{d}$ de d ainsi obtenue permet alors d'estimer le paramètre k qui intervient linéairement, soit par un ajustement classique au sens des moindres carrés, soit comme proposé en [9] de la façon suivante. Si l'on extrait k de l'Eqn. 4, on obtient

$$k = [\tilde{s}(t) - \tilde{v}(t)]/[\tilde{v}(t) - \tilde{s}(t-d)] \tag{5}$$

En présence de bruit, on n'utilise pas une estimation ponctuelle de k pour une valeur unique de t: pour une série de valeurs échantillonnées t_i, on calcule les quantités $Y(t_i) = \tilde{s}(t_i) - \tilde{v}(t_i)$ et $X(t_i, \hat{d}) = \tilde{v}(t_i) - \tilde{s}(t_i - \hat{d})$. La droit régression $Y = \alpha X + \beta$ donne avec α une estimation $\hat{k}$ de k relative à notre estimation $\hat{d}$ de d. Les résultats de simulation [8] montrent le précision de la méthode dans des cas de résolution où les techniques d'ajustement de modèle sont inutilisables, même sans bruit [13].

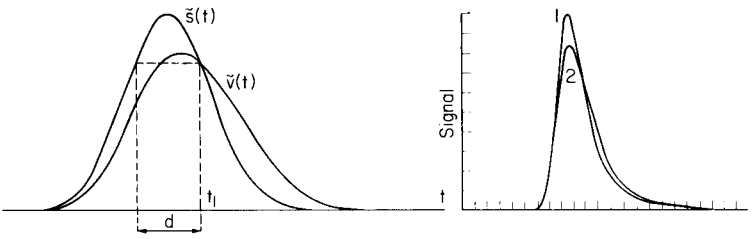

Fig. 1. Détermination graphique de la séparation de 2 composantes de même forme et de même largeur.

Fig. 2. Profils normés: (1) pic simple (iso-butylbenzene); (2) pic double (iso+n-butylbenzène).

Estimation conjointe de d, k, a. Dans le cas où le paramètre a intervient, la relation 4 devient

$$\tilde{v}(t) = \left\{\tilde{s}(t) + (k/a)\,\tilde{s}[(t-d)/a]\right\}/(1+k) \tag{6}$$

d'où l'on peut tirer

$$k = [\tilde{s}(t) - \tilde{v}(t)]/\left\{\tilde{v}(t) - (1/a)\,\tilde{s}[(t-d)/a]\right\} \tag{7}$$

Posons maintenant: $Y(t_i) = \tilde{s}(t_i) - \tilde{v}(t_i)$ comme précédemment et $X(t_i, \hat{d}, \hat{a}) = \tilde{v}(t_i) - (1/\hat{a})\,\tilde{s}[(t_i - \hat{d})/\hat{a}]$. La pente α de la droite de régression $Y = \alpha X + \beta$ donne une estimation $\hat{k}(\hat{d}, \hat{a})$ associée aux estimations $\hat{d}$ de d et $\hat{a}$ de a. Les estimations retenues sont celles qui minimisent la fonction de dispersion:

$$D(d,a) = \sum_i [Y(t_i) - \alpha(d,a)\,X(t_i) - \beta(d,a)]^2$$

L'étude numerique [9] montre dans quelle mesure on peut considerer que $a = 1$.

Applications en chimie analytique

Les méthodes rappelées ci-dessus ont été appliquées à divers problèmes de traitement du signal principalement en chimie analytique. Les résultats essentiels sont présentés ci-dessous.

Détection d'une impureté en chromatographie. La MFR a été appliquée à la détection de la contamination d'un corps pur par une impureté provoquant un pic secondaire de faible intensité, proche du pic principal [5, 14]. On compare la forme d'un pic de n-hexane pur à celle d'un pic de n-hexane contaminé par quelques pourcents de n-heptane. Dans une première procédure, les conditions expérimentales sont maintenues constantes et identiques pour le pic pur et le pic double. Elles sont choisies de façon à obtenir une résolution de l'ordre de 0,25: le pic double apparait alors visuellement unique. Une étude expérimentale statistique montre qu'une impureté de 1% est nettement détectée. On propose aussi une deuxième procédure utilisant la différence d'évolution de forme d'un pic pur et d'un pic double lorsque

l'on fait varier les conditions expérimentales (température et débit). La MFR permet de détecter, et de mesurer, une très petite variation de forme entre deux profils: on ne peut attribuer cette variation à la présence d'une impureté (ici n-heptane) que si toutes les autres causes de variation de la forme sont éliminées. En particulier, les pics à comparer doivent avoir pratiquement la mème hauteur. Ce problème de non-linéarité de la réponse a été étudié dans les travaux décrits ci-dessous.

Variation de la forme d'un pic chromatographie en fonction de la masse injectée. La mise en évidence, grace à la MFR, de la variation de forme d'un pic en fonction de sa hauteur, montrant ainsi la non linéarité du système, a été publiée dans [15]. Une étude plus fine et systématique a ensuite été réalisée par Excoffier et al. [16]. La variation de forme d'un pic de cyclohexane est mesurée en fonction de la masse injectée, celle-ci variant d'un facteur 100 de la plus petite à la plus grande valeur. La mesure de l'écart de forme est celle notée Δ_3 ci-dessus. Dans cette application le rapport *S/B* favorable a permis de réduire au maximum la fenêtre d'ajustement, c'est-à-dire de considérer la tangente à la courbe $\phi(t)$. Les résultats obtenus montrent une variation continue croissante et très significative de l'écart de forme, alors que l'étude classique des premiers moments ne permet aucune conclusion.

Evolution de spectres Mössbauer. La MFR a été utilisée par Massiot [7] pour comparer les formes de spectres Mössbauer du fer dans des verres silicatés d'intérêt géologique. L'évolution de forme du spectre, lorsqu'on synthétise la même composition chimique sous des fugacités d'oxygène différentes de façon à faire varier le rapport Fe^{3+}/Fe^{2+}, suggère des spectres "intermédiaires" entre une "forme reduite" et une "forme oxydée", qui sont chacune un doublet. La méthode de décomposition de forme permet de réduire le nombre de paramètres de 13 (quand on ajuste quatre pics indépendants) à 5 (quand on décompose en une somme de deux doublets de forme donnée), avec de meilleurs résultats.

Séparation de composantes serrées. La méthode de super-résolution rappelée plus haut a été appliquée à la séparation d'isomères de position: n-, iso- et tertio-butylbenzene, en chromatographie liquide. Les résultats [9], montrent les points suivants: (i) les hypothèses d'égalité des formes et des largeurs de pics (a = 1 à moins de 3% près) pour les trois isomères semblent justifiées; (ii) la méthode proposée permet d'estimer, avec une bonne précision, une résolution de l'ordre de 0,22 dans le cas le plus délicat "iso/n" et pour trois valeurs différentes du rapport de concentration (0,14; 0,33; 0,6); la Fig. 2 illustre un de ces cas où le pic double "iso + n" est visuellement simple; (iii) en outre, la confrontation avec des cas réels a montré l'utilité pratique de la formule 5: en effet, la représentation graphique du second membre en fonction de t, qui est théoriquement une droite horizontale si les hypothéses de départ sont vérifiées, permet d'éliminer les mauvais enregistrements et de ne faire des estimations que dans des cas où elles ont une signification.

Conclusion

Les exemples d'application précédemment regroupés et empruntés au traitement des spectres physico-chimiques, montrent que pour utiliser la notion de forme d'un signal il est nécessaire de normer son aire. En travaillant au niveau de l'intégrale normée du signal (supposé ou rendu positif) on peut caractériser, grace à la MFR, une différence de forme indépendamment de toute modélisation a priori. En travaillant au niveau du profil normé (dans le cas des pics) on peut utiliser une hypothèse de conservation de la forme. Cette hypothèse permet d'estimer avec précision des paramètres de séparation en mettant, en quelque sorte, cette forme "en facteur". La conservation de la forme intervient en fait dans le traitement de tous les signaux répétitifs. Cette propriété a d'ailleurs été mise à profit dans un autre domaine que la chimie analytique: l'analyse des signaux biologiques tels que les signaux cardiaques. La technique de sommation synchrone, utilisée pour extraire des signaux faibles noyés dans un bruit élevé, a ainsi pu être notablement améliorée grace à un algorithme de synchronisation fondé sur l'hypothèse de conservation de la forme [17, 18]. Enfin, la MFR donnant une mesure de la ressemblance entre deux signaux, est toute indiquée pour les problèmes de classification des formes.

REFERENCES

1 E. Grushka, M. N. Myers, P. D. Schettler and J. C. Giddings, Anal. Chem., 41 (1969) 889.
2 E. Grushka, M. N. Myers and J. C. Giddings, Anal. Chem., 42 (1970) 21.
3 E. Grushka, Anal. Chem., 44 (1972) 1733.
4 E. Grushka and G. C. Monacelli, Anal. Chem., 44 (1972) 484.
5 H. Rix, Thése d'Etat es Sciences, Université de Nice (1980).
6 H. Rix and J. P. Malengé, IEEE Trans. Syst. Man. Cybern., 2 (1980) 90.
7 D. Massiot, J. Non-Cryst. Solids, 69 (1985) 371.
8 H. Rix, Signal Processing, 5 (1983) 97.
9 M. Ahmad, H. Rix, H. Colin and G. Guiochon, X Colloque sur le Traitement du Signal et ses Applications, Nice, Mai 1985.
10 H. Rix and J. P. Malengé, Chromatographia, 9 (1976) 554.
11 H. Rix and J. P. Malengé, VI Colloque sur le Traitement du Signal et ses Applications, Nice, Avril 1977.
12 S. D. Morgera and N. K. Garg, Signal Processing, 10 (1986) 153.
13 A. Baruya and W. F. Maddams, Appl. Spectrosc., 32 (1978) 563.
14 H. Rix and J. P. Malengé, J. High Resolut. Chromatogr. Chromatogr. Commun., 4 (1980) 172.
15 H. Rix, J. Chromatogr., 204 (1981) 163.
16 J. L. Excoffier, A. Jaulmes, C. Vidal-Madjar and G. Guiochon, Anal. Chem., 54 (1982) 1941.
17 H. Rix and S. Jesus, C.R. Acad. Sci., Série II, 299 (1984) 399.
18 S. Jesus and H. Rix, Melecon '85, Madrid, Octobre 1985.

Analytica Chimica Acta, 191 (1986) 473–480
Elsevier Science Publishers B.V., Amsterdam — Printed in The Netherlands

Short Communication

IMAGE ANALYSIS AND CHEMICAL INFORMATION IN IMAGES

PAUL GELADI*,[a] and SVANTE WOLD
Research Group for Chemometrics, Umeå University, S-901 87 Umeå (Sweden)
KIM ESBENSEN
Norwegian Computing Center, Postboks 355, Blindern, 0314 Oslo (Norway)
(Received 29th May 1986)

Summary. Image analysis and its different aspects are presented with emphasis on the difference between technology, conceptual modelling (psychology) and chemical information. An overview is given of how the information in image analysis is presented. The distinction between univariate and multivariate image analysis is taken up. The different data analysis techniques that are in common in both chemometrics and image analysis play a major role here.

The manner in which data are collected and used in the laboratory is important in the choice of a method of data analysis. The way in which a problem is specified and questions are asked establishes how data-array structures will be set up, simplified and analyzed. Figure 1 shows a number of possible data-array configurations; they are all combinations of object structure and variable structure.

Image analysis is concerned with (object × object) types of data structures. With one variable measured, this is the classical analysis of grey images. A more interesting challenge is the multivariate analysis of images, where each pixel represents a feature vector for p measured variables. Possible extensions are measuring (variable × variable) per pixel as in fluorescence microscopy and the less obvious (object × object × object) structure of holograms (3-D images). These possibilities are shown schematically in Fig. 2.

In order to study 2-dimensional (object × object) structures with a complex variable structure, one has to master some basics of image analysis, but equally important is knowledge of chemical and physical processes that generate the "images". Three important points must be made. First, 90% of the theory and applications of standard image analysis has no real relevance for current chemical research and applied chemistry. Secondly, no matter how sophisticated are the computers and memory configurations available, one is critically dependent on a physical interface with the imaging

[a]P. Geladi is affiliated to both institutions.

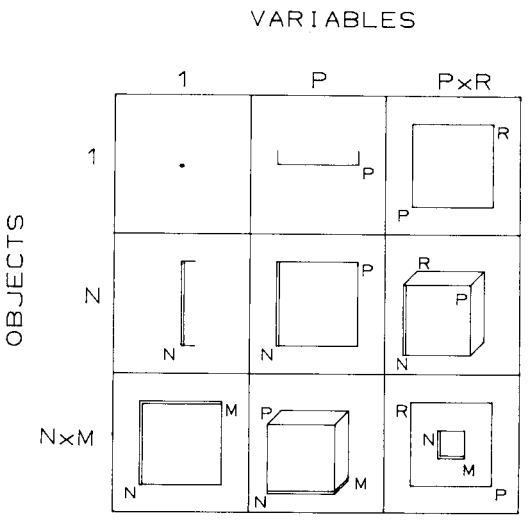

Fig. 1. The nine simplest data-array structures. One variable measured for one object (upper left) is uninteresting for data analysis. The interesting structures are the well-known data matrix (N objects × P variables; middle square), the univariate image (lower left corner), the variable × variable matrix (for "hyphenated" methods such as l.c./u.v., g.c./m.s.; upper right) and their more complex developments, data parallellepipeds (shown here as cubes) and hyperparallellepipeds (the easiest example shown here is a square inside another square). The object ways are indicated by double lines.

instrumentation. Thirdly, univariate deterministic methods cannot solve the complicated chemical and physical problems that appear in nature and in the laboratory. Because of this, multivariate methods must be chosen. In multivariate methods, correlated variables, often with an ill-defined physical meaning, can be used to construct latent variables that do a better job in data analysis and interpretation than do many single variables.

Image analysis was needed even early in this century when pictures were sent by telephone cable and required processing. In the sixties, space exploration made the use of image-correcting algorithms necessary and this was the start of most of the activity that has led to the theories and instrumentation known today. In the seventies, image analysis stepped down from the custom-built installations of the space sciences to cartography, geology and agriculture (macroscopic) on one hand and medicine, pathology and biology (microscopy) on the other. Recently, there has been an explosion in hardware and software and image analysis is making its way into analytical, clinical, geochemical and metallurgical laboratories. The last step is one from visualization and shape analysis of univariate images to analysis in the multivariate domain.

Classical image analysis

Classical operations on grey-level images of size 512 × 512 pixels have been well described [1—9]. Digital image analysis has mainly been used for

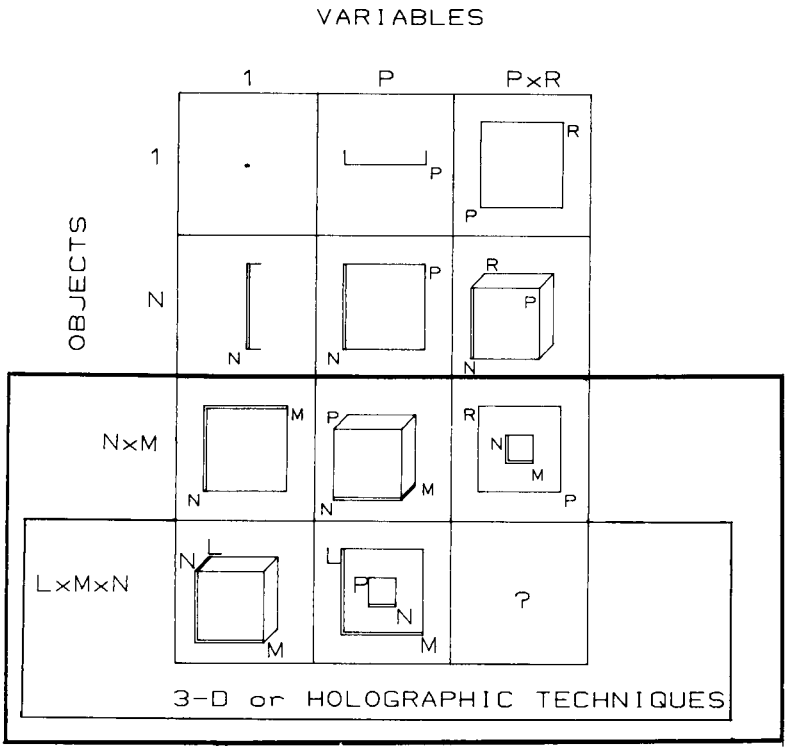

Fig. 2. Image analysis techniques are enclosed in the large rectangle; 3-D techniques (small rectangle) are a special case.

the following purposes: restoration or correction of optical errors caused by lenses and atmospheric disturbances, i.e., focussing a defocussed picture; data compression, which is necessary if more pictures are to be sent on a narrow communications channel; enhancement or adaptation of pictures to the physiology of the human eye (many image analysis operations are concerned with grey levels and enhancement of contrast to increase visual appreciation, as in the treatment of x-ray plates, but the information in the data is not used in any complex way); microscopy automation because image analysis techniques are faster and more objective than the human eye and not susceptible to fatigue. This list shows that although most of these items can be made chemically useful in one way or another, they are not immediately relevant for extracting chemical information from data as it is presently produced, e.g., from spectrometry. This leads to the peculiar situation that either crude properties are measured over a whole sample (image), or very accurate measurements are done with parts of a sample.

Many of the traditional fields of image analysis are only marginally useful for analyzing 2-dimensional chemical data, especially where multivariate data or processes are concerned.

Two-way object structures in chemistry

This article is generally concerned with 2-way data arrays ($m \times n$ object structures), i.e., a data vector of variables is measured in points characterized by an x-coordinate and a y-coordinate. In the univariate case, this vector becomes a scalar (grey level). The samples of most interest for such data measurements are heterogeneous solids (geochemistry, metallurgy, forensic science) and heterogeneous liquids or suspensions (biological systems). There is a certain correspondence to geography and the related remote (satellite) sensing, but there is also a big difference. The structures studied by remote sensing have a definite geometry, where positioning and relative positioning are important. In the chemical laboratory, the 2-dimensional geometry of a sample is only a random representation of some bulk material. In oil prospecting, for instance, one 1-cm^2 slide of 0.2 mm thickness is supposed to represent, say, 100 m^2 of solid rock. Here only global properties deduced from the study of the object are of importance.

In some sorts of microscopy, shapes and structures are a representation of a stochastic property. Very often one is only interested in a global property of a material that is related to shape and structure parameters.

Chemical and related methods leading to 2-dimensional data. Microscopic methods as used in biology and medicine and in the chemical laboratory are typical examples of methods producing data suitable for image analysis. The related optical macroscopy is also of interest. In these optical methods, many variables can be chosen and changed to obtain more relevant data. One can use diascopy, combined with polarization, dark field, phase contrast and different wavelengths in the range 200—1000 nm. In episcopy, fluorescence is possible; many combinations of excitation and emission wavelengths can be chosen. The variety of microscopic methods is so large that using univariate methods would appear perverse.

Related to microscopy is electron microscopy. Here the choice is primarily between transmission electron microscopy, scanning electron microscopy and scanning transmission electron microscopy. Different energy levels of electrons can be detected, giving different information about the sample. Even more interesting is the possibility of measuring x-ray emission, which can provide a whole x-ray spectrum in every pixel of the image. More of a macroscopic nature is proton-induced x-ray emission. Again, an image with a vector of x-ray intensities can be obtained for every pixel of the sample. Secondary-ion mass spectrometry is a method where ion images are measured; the data consist of a stack of images, each for a different ion. Laser-activated mass spectrometry is another method for which one mass spectral vector per pixel is the result. X-ray and nuclear magnetic resonance (n.m.r.) tomography are not primarily meant for chemical analysis, but they produce multivariate image data. Their role might increase considerably in the future.

This list is not exhaustive, nor are all the methods immediately ready for interfacing with image analysis equipment, but the potential exists. Many

methods used in the laboratory can generate 2-way multivariate data. One can represent these data either as a stack of single-variable images or as a vector in every pixel (Fig. 3).

A hypothetical microscopic image analysis. A microscopic sample consisting of liquid and a number of cells is to be analyzed. Some illustrations are given in Fig. 4. First, there is not enough contrast, so the sample must be stained and a wavelength or filter chosen. The cell nuclei then show very clearly; traditional image-analysis techniques can be used on this image to get an idea of the number of nuclei and their size-distribution histogram. One can also produce a mask blackening out all but the nuclei. After that, one might consider measuring absorbances for each nucleus so that Beer's law would give DNA concentrations. But many factors influence absorbances so that Beer's law is inadequate [10]. A microscope is not a spectrophotometer. This is a typical example of a case where deterministic laws fail when applied

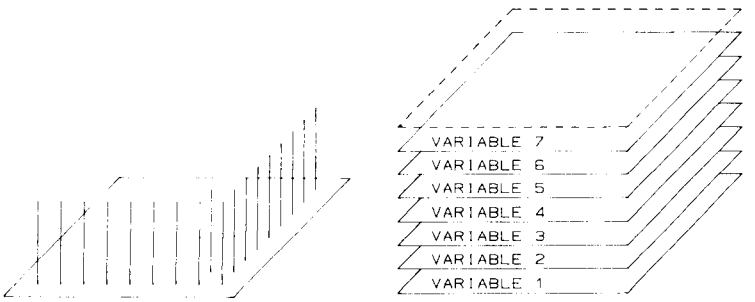

Fig. 3. A multivariate image can be seen as a collection of vectors, one for each pixel (only shown partly to avoid confusion) or as a stack of univariate images for the different variables.

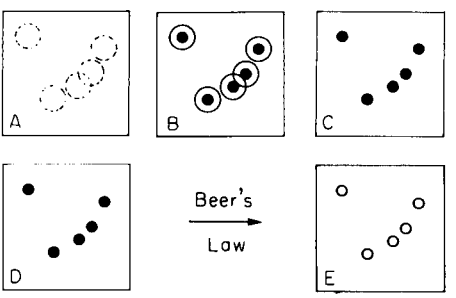

Fig. 4. A hypothetical analysis of a microscopic sample. Two-dimensional techniques work well; techniques based on strict laws in the variable space are more difficult. (A) Normal sample with bad contrast; (B) stained sample with nuclei visible; (C) nuclei isolated with binary imaging; (D) binary mask to give absorbance in nuclei; (E) DNA concentration in nuclei.

to univariate situations. Multivariate analysis may allow a better scheme of calibration or error detection.

Univariate deterministic laws often fail because of the complex nature of the samples studied and of the imaging interface.

Regression of microscopic images against bulk properties. Geometric properties extracted from grey-level images have been used for multivariate regression against bulk properties of the material, often measured on a similar sample of a different size. These geometric properties can take the form of a histogram. A schematic representation is given in Fig. 5.

In oil prospecting, one is interested in porosity of minerals (e.g., sandstone) and their permeability for liquids (hydrocarbons). Microscopic analysis of thin sections of cores reveals a complex structure of pores and cracks. It would be rather difficult to calculate a dynamic property such as permeability from this structure by means of physical laws and geometry of the material studied. It is equally difficult to describe this pore structure completely. Classical porosity and permeability tests are very time-consuming and expensive.

Ehrlich et al. [11] used automated image analysis on thin sections. They used the classical dilation and erosion operations cleverly to obtain a histogram of pore sizes. These histograms for different samples were analyzed by the principal component method to provide a classification of samples. A further application of the data [11] was the use of regression of pore size histograms (X) to measured permeability (Y). This regression relation allowed the prediction of permeability from the image-analysis results of new samples. This is a typical example of how structural elements of a material help to describe bulk properties.

Another example of regression of image data with external bulk data was published by Martens et al. [12]. They used grey levels in x-ray tomographic images from living pigs and regressed them by a partial least-squares (PLS) method against fat/lean meat concentrations measured after slaughtering. The data from the tomogram could then be used to predict meat quality from the regression model before an animal was slaughtered. Thus it is

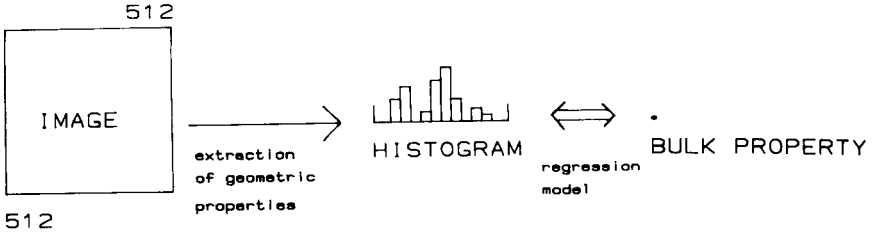

Fig. 5. Geometric properties can be extracted from images and represented as histograms. With successive histograms as an **X** block, a multivariate regression model against a bulk property can be calculated. This requires a large number of objects in order to make the regression methods work reliably.

clearly possible to set up a regression model between bulk parameters of a material and microscopic structure parameters measured by image analysis.

Principal component analysis on multivariate images

A multivariate image can be seen as a stack of sheets or layers, where each sheet is a univariate image for a certain variable (e.g., wavelength) or one can view it as an image with a p-dimensional feature vector in every pixel (Fig. 3). A method for analyzing such data structures has been described [13, 14]. Principal component analysis of a multivariate image is shown schematically in Fig. 6. The scores obtained from such a data block are images themselves (eigenpictures). Although this method works well, it is not practical if one thinks of an image of size 512 X 512 pixels X 10 variables. In the absence of the appropriate technology, some shortcuts have to be taken [15].

After principal component analysis, the results are visible images not just tables of numbers. Principal component images may show more interesting or more concentrated information than single variable images. One can also use score plots and try to find classes. Very often these classes in variable space are confined to a certain locality in image space. These classes can then be described by their own local PCA model and this model can be used to project the rest of the data into an image where contrasts show interclass distances. An example for geochemical data has been reported [16].

Contextual information is very important in images. Information from neighbouring pixels can often be used advantageously (Fig. 7). Often the four or eight nearest neighbours of a pixel are used for introducing contextual data. But this increases the size of the data arrays by a factor of 4 or 8. Selected principal-component data from neighbouring pixels in multivariate

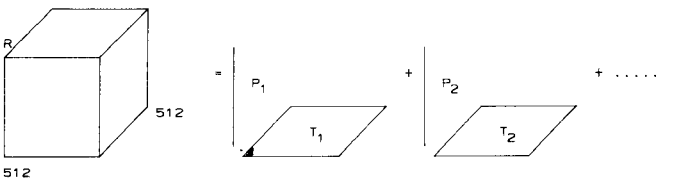

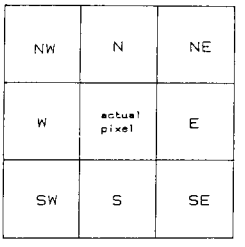

Fig. 6. A multivariate image can be decomposed by generalized principal-component analysis. The result consists of loading vectors (**p**) and score images (T) (eigenpictures).

Fig. 7. Contextual data for a pixel. The pixels shown here can be scalars or vectors. Each time a certain pixel (actual pixel) is used in a calculation, one can consider using data from its neighbours. A mean taken over the 8 neighbours would represent a local "neighbourhood grey level". Other combinations could give directional derivatives. These are used as extra variables in a variable vector for a pixel.

images can be used as a "concentrated" context. They are added as extra variable planes.

Multivariate image analysis via holography and tomography

It is not difficult to extend the existing univariate methods of 2-dimensional image analysis to three dimensions. A problem is that holography only shows the exterior of an object and not its interior. Tomography allows viewing of interiors [17], e.g., with x-rays and n.m.r. Eventually, multivariate tomography of heterogeneous solid objects may be combined with 3-D image analysis and representation to provide an analytical technique. A 3-D reconstruction from electron micrographs has been reported [18].

Figure 2 indicates how further developments might be imagined. All the basic techniques necessary for this method are technologically possible. Their integration requires better technology but such is being developed. Such techniques do not require supercomputers. A cleverly designed hardware interface, an advanced array processor and a Unix-based microcomputer for control would be sufficient.

The help of Hans Isaksson and Lennart Lindquist, Swedish Geological Survey, Luleå, and Arne Dunberg and Christer Albano, Peat Dewatering Project, Umeå, is gratefully acknowledged.

REFERENCES

1 A. Rosenfeld and A. Kak, Digital Picture Processing, 1982, Academic Press, New York.
2 R. Gonzalez and P. Wintz, Digital Image Processing, Addison-Wesley, Reading, 1977.
3 W. Pratt, Digital Image Processing, Wiley, New York, 1978.
4 R. Clarke, Transform Coding of Images, Academic Press, London, 1985.
5 T. Huang (Ed.), Picture Processing and Digital Filtering, Springer, Berlin, 1979.
6 D. Harris, Computer Graphics and Applications, Chapman and Hall, London, 1984.
7 J. Serra, Image Analysis and Mathematical Morphology, Academic Press, London, 1982.
8 V. Kovalevsky, Image Pattern Recognition, Springer, Berlin, 1980.
9 B. Vandeginste and B. Kowalski, Anal. Chem., 55 (1983) 557.
10 H. Martens, Ph.D. Thesis, University of Trondheim, 1985.
11 R. Ehrlich, S. Kennedy, S. Crabtree and R. Cannon, J. Sediment. Petrol., 54(4) (1984) 1365.
12 H. Martens, O. Vangen and E. Sandberg, in Proc. Nordic Symp. Appl. Statist., Stavanger, Stokkand Forlag, Stavanger, 1983.
13 S. Wold, P. Geladi, K. Esbensen and J. Öhman, in Proc. Symp. Appl. Stat., Copenhagen, 1986.
14 J. Lohmöller and H. Wold, Europ. Meeting of Psychometrics Society, Groningen, Netherlands, June 1980.
15 K. Esbensen, P. Geladi and S. Wold, in Proc. Symp. Appl. Stat., Copenhagen, 1986.
16 K. Esbensen, I. Lundholm, L. Lindqvist, D. Nisca and S. Wold, 1985. Swedish Geological Report STU 83-5733, Luleå.
17 G. Herman, Image Reconstruction from Projections, Springer, Berlin, 1979.
18 D. DeRosier, Contemp. Phys., 12(5) (1971) 437.

Analytica Chimica Acta, 191 (1986) 481—485
Elsevier Science Publishers B.V., Amsterdam — Printed in The Netherlands

Short Communication

CHEMOMETRICS ALSO NEED DATA

LÁSZLÓ DOMOKOS* and CLEMENS JOCHUM
Beilstein Institut, Varrentrappstr 40—42, 6000 Frankfurt/M 90 (Federal Republic of Germany)

(Received 25th June 1986)

Summary. One of the crucial points in using chemometric algorithms is to obtain a large number of reliable and representative data. Beilstein owns one of the largest collections of critically evaluated factual and structural data of organic compounds abstracted from the literature. The Beilstein Online system will give easy access to this data base.

Chemometrics can be considered as an interaction between mathematically-minded chemists, the data and the algorithms. Recently, many algorithms have been developed using multivariate mathematical and statistical methods. To demonstrate and prove the applicability and performance of these algorithms, large representative data sets would be necessary. In practice, however, methods are tested often only with one or very few data sets containing few data. This is especially the case if the software is developed not by chemists but by mathematicians, statisticians, etc. who do not have easy access to measurement data. The Beilstein Institute, which owns the largest collection of physical and chemical factual data of organic chemical compounds, hopes to help in this regard by starting the Beilstein-Online project which will give online access to its data.

The projected numerical and factual data base Beilstein-Online represents a natural extension of the Beilstein Handbook of Organic Chemistry which has been published for more than 100 years.

The present Beilstein information pool contains handbook and registry data of the literature time-frame from 1830 to 1960. As the handbook has mostly been printed by conventional typesetting methods, this information pool is available only in printed form. However, the most recent 25% of published volumes has been printed by electronic typesetting methods and is therefore available in computer-readable form. In addition, the primary literature from 1960 to 1980 has been completely abstracted. Over 7 million abstract cards contain the structural formula, numerical physical data, reaction pathways and original literature citations (Fig. 1a). This entire information pool will gradually be transferred to computer-readable form and extended by additional new sources of information (see below). All future Beilstein information products will be generated from this information pool

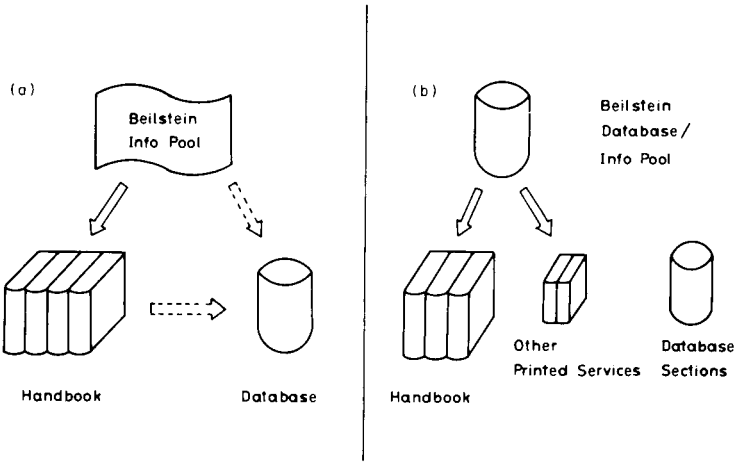

Fig. 1. (a) Present state; (b) future development.

which will be organized in an internal data base (Fig. 1b).

Information sources of the data base

The Beilstein data base will be generated from three sources of information. The first source is the printed handbook series from the basic series up to the fourth supplementary series (H to E-IV). These series are almost completed and contain the literature from 1830 to 1960. These volumes contain factual data for ca. 1.5 million organic compounds, which makes this data base unique. The second source is the printed handbook material of the fifth supplementary series which contains the literature from 1960 to 1980, covering ca. 1 million heterocyclic compounds. As in the previous handbook series, these data have been thoroughly checked for errors and redundancies. Publication of the fifth supplementary series will continue. The primary literature from 1960 to 1980 has been completely abstracted in more than 7 million excerpts. Some of these excerpts will be added to the data base in their original (unchecked) form in order to give scientists limited access (see below) to these data as soon as possible.

Recently, electronic abstracting of the factual data of the primary literature from 1980 was started. These abstracted data are no longer written out but entered directly in a structured manner into microcomputers and stored on magnetic diskettes. After several automatic plausibility and redundancy checks, the data are copied onto the mainframe computer and loaded into the data base. Thus ready access to the factual data of the current literature is available.

The data-base concept

With respect to the different sources of available information, the data base can be divided into a short file and a full file (Fig. 2). The full file will consist

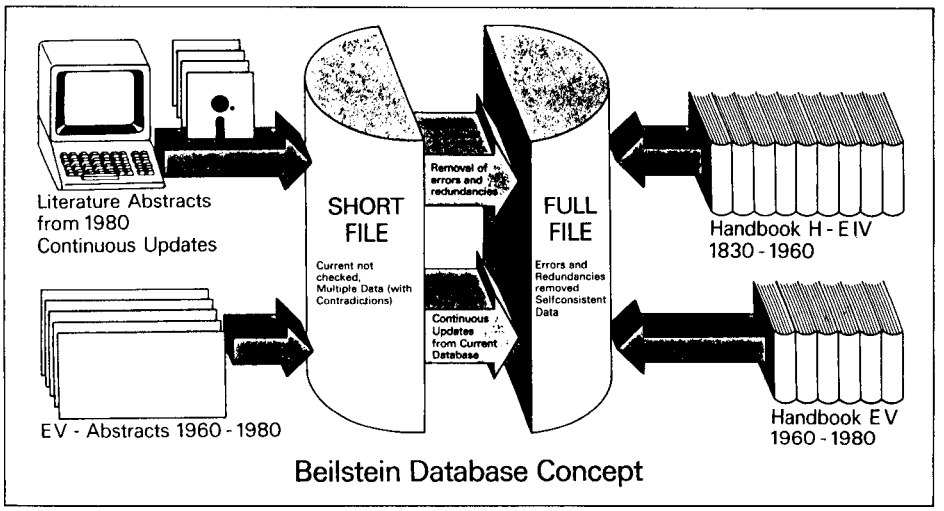

Fig. 2. Beilstein data-base concept.

of almost all the data which have been published in the Handbook series and which have been checked for errors and redundancies by Beilstein information specialists. The short file is built directly from the abstracts of the primary literature without any further checking. Factual data of the current, primary literature will be added to the short file on a regular basis. The full file will be continuously extended by processing the raw material from the short file after error-checking and removal of redundancies.

The data structure will be completely defined during the systems-analysis phase. More than 500 different factual or numerical terms or fields can be stored for each compound. Of these 500 fields, more than 300 are retrievable independently or in combination. More than 60 fields consist of numerical physical data which may also be retrieved separately or combined with a substructure search (see below).

The process of loading the data base

The Beilstein data base is loaded in three steps. First, the data from the various sources (see above) are entered manually into IBM-PC-compatible microcomputers and stored on floppy disks. Secondly, the disks are uploaded onto the mainframe and stored in an intermediate file. Automatic plausibility checks are performed on this intermediate file and if necessary, corrections are made. Thirdly, the data are loaded into the ADABAS-managed data base. ADABAS-based retrieval programs will allow Beilstein chemists to search the data base and to convert data from the short file to the full file.

Three microcomputer programs have been developed which allow the chemist to enter all the information from its respective source in a structured manner without any specific computer knowledge. All programs work on IBM-PCs and 100%-compatibles with at least 256K of memory and two

floppy-disk drives. EKSTASE is used to input data from the Beilstein Handbook. Numeric and factual data are entered separately from the structural formulas as most of the structures are converted automatically to a topological representation (see below). The person who enters the input can choose from various panels to enter different kinds of data (e.g., reactions, physical parameters or citations). To make corrections, he can scroll back and forth on the screen or can go back to a specific data entry. The systematic IUPAC names of the reference compounds are automatically copied from the Registry tapes so as to avoid manual input errors. EXCERP allows the paperless abstracting of the primary literature. The abstracter first enters the structure using a mouse on a PC-compatible graphics screen. The graphic-structure input program MOLMOUSE is optimized for speed and maximum error-checking and not for beauty of screen presentation. MOLMOUSE generates the connection table, a topological representation of the stereochemistry, calculates the molecular formula and lastly compares it against the manual-input molecular formula to avoid errors. After leaving MOLMOUSE, the abstracter can choose from more than 25 different screens to enter numerical and factual data in a predefined way according to the Beilstein data structure outlined above. Corrections are possible at any time during this input process. BIZEPS is a stripped-down version of EXCERP for inputting the abstract cards of the Fifth Supplementary Series. As each abstract card usually contains fewer physical parameters than the final Handbook article (which is the summary of many abstract cards), this program is further optimized for input speed by using function keys for entering numerical and factual data. The graphic structure input part (MOLMOUSE) is identical to EXCERP.

All three programs store the input information on floppy disk. Most of the input is done by voluntary collaborators who send the disks at certain times to the Institute for further processing. To avoid most of the manual input of the Handbook structural formulas, the program VICA was developed; this converts systematic chemical names (IUPAC nomenclature) to topological representations. On a test data set of approximately 700 000 names, the program was able to convert 84% to connection tables without error. It is important to point out that the program either gives a message that it cannot convert a given name with its internal set of name fragments or it correctly converts the name. So far, no errors have been encountered.

After having been converted to the same file structure, the data will be loaded into an ADABAS-managed data base. More than 10 commercial database management systems were evaluated during the systems-analysis phase. The two highest scoring systems have been benchmarked with an artificial Beilstein structured data base with 200 000 compounds. ADABAS scored best on practically all tests (loading, updating, retrieval, etc.).

An ADABAS-based system for update and retrieval is currently being developed. This system will be used to make final corrections on the data base, append compounds and retrieve compounds for checking and writing Handbook articles. It will also be licensed to inhouse customers (see below) of the

Beilstein data base. There will be a micro- and a mainframe-based version of this software.

Data-base access

The data structure of the Beilstein data base will permit many different methods of access to the information dependent only on the retrieval software used. The following methods are planned: (1) via a graphical or alphanumeric input, depending on the type of computer terminal (structure or substructural search); (2) by searching for numerical or alphanumeric terms (physical data, keywords or Boolean terms, such as existence of spectra, etc.) which can be sought separately or in Boolean combinations ("and", "or", "not"); (3) by combination of (1) and (2); (4) by searching other key fields, such as the molecular formula, the CAS registry number or the molecular, structure-related so-called Beilstein Lawson-Number.

The Beilstein factual data base can be accessed through various institutions and computers: (1) via public online hosts; (2) large chemical companies can acquire a licence for the data base to run it on their own computer center; (3) individual customers can access selected parts of the data base with their own microcomputers when attached to a Winchester or optical storage device.

Beilstein and chemometrics

The possibility of easy online access to this data base combined with a flexible structure and numerical search will open new perspectives for chemists to apply chemometric algorithms. Also data not contained in the data base, e.g., complete spectra, can be accessed in other data bases using the structure or CAS registry number.

Of course, chemometric tools are needed at the different stages of the development of the data bank. For example, the data must be checked for reliability. Many physical features described in Beilstein were measured under various conditions. For example, the boiling point is given at a certain pressure, or the diffraction at a certain temperature, etc. In these cases, algorithms are necessary to evaluate the physical value for a given standard condition to permit a well defined search. Beilstein contains several hundreds of chemical and physical data of compounds, although only a portion of these may be known. The others were not measured or are not yet published. Deterministic or statistical methods could be used for calculating missing values. There are also plans to provide access for users of Beilstein Online to software packages which operate on the retrieved data.

Analytica Chimica Acta, 191 (1986) 487—493
Elsevier Science Publishers B.V., Amsterdam — Printed in The Netherlands

Short Communication

CLUSTER ANALYSIS OF THE ELEMENTAL COMPOSITION OF FIVE AUSTRIAN PEATS

WALTER KOSMUS* and REINHOLD PIETSCH

Institute for Analytical Chemistry, Karl-Franzens University, A-8010 Graz (Austria)

KURT J. IRGOLIC

Center for Energy and Mineral Resources Texas A&M University, College Station, Texas 77843 (U.S.A.)

(Received 26th May 1986)

Summary. The elemental composition of peat depends on the plant residues from which the peat was formed. The concentrations of 45 elements were determined for five peat samples by plasma emission spectrometry. Literature data on the composition of three bogs was added. The elemental abundances of six rock or soil categories, the elemental compositions of several peat-forming plants, and the results of the elemental analyses of bog samples, were examined by the SIMCA method. A clear difference was found between fens and raised bogs. Factor analysis of the elemental compositions shows that the concentrations of most of the elements reflect their natural abundance in the surrounding region. Some concentrations are influenced by anthropogenic pollution, e.g. lead, and by plant metabolism. The cluster analysis together with the training sets shows the degree of the deposition of mineral material from adjacent rivers and the type of plant growth which formed the peat.

Peat-bogs or moors are found all over the world, particularly in temperate zones. Little is known about the chemistry of peat and the reasons for the curative or preservative power of peats. There is no generally accepted classification of peat-lands; classification systems proposed include the topological system based on mode of formation, the climatological system based on climatic conditions at the time of the peat formation, the botanic system based on the plants covering the peat surfaces, the geological system based on the geological formation in which the peat is embedded, and the hydrological system based on the mode of interaction between peat and water. Most descriptions of peat environments use several of these systems concomitantly.

In this communication, only two types of peat-land, the minerotrophic peat deposits called fens and the ombrotrophic peat deposits called raised bogs or simply bogs are considered. These two types of peat deposits should have different elemental composition. Fens are always in contact with ground water, which is generally a rich source of dissolved inorganic salts. An extreme case of a fen is a peat-land that is periodically flooded by an adjacent river. Deposited sediments and materials derived from dissolved matter

0003-2670/86/$03.50

increase the content of inorganic substances in the peat. The inorganic materials in the peat are determined as ash content. Bogs receive nutrients only from the air mostly as precipitation that has low concentrations of dissolved materials, or from air-borne dust; certain plants fix atmospheric nitrogen while others are insect-catchers. The chemical composition of peat from a bog should be largely governed by the vegetation. During decomposition of the organic matter in the deeper layers of peat-lands, the chemical composition and the properties of peat change. For instance, the aerobic zone contains nitrate, sulphur, and iron(III), whereas ammonia, hydrogen sulphide, and iron(II) are found in the anoxic zone. The pH in the anoxic zone is generally much lower than in the aerobic zone. Substances such as the ill-defined humic and fulvic acids are produced. Proteins of different molecular weights are present. The chemical composition of a peat layer governs the mobility of elements and the changes in concentrations with depth.

To check whether peats can be classified according to their elemental composition, samples were taken from the black, well-decomposed layer of five Austrian peat-lands, the peat from which is used for medical purposes.

Althofen. This fen, exposed to 800—1000-mm rainfall per year, is situated at 610-m height in a U-shaped valley well drained by an adjacent river that floods the valley periodically. Under the vegetation layer (20 cm) consisting mainly of sphagnum and eriophorum, there is a well-decomposed black peat of nearly neutral pH. The surrounding geological formation is alluvial.

Garanas. This is a raised bog located at 1230-m height and exposed to 1000—1500-mm rainfall per year. The most abundant plants are sphagnum and eriophorum with some vaccinium, calluna, and isolated pines. The several layers of peat are distinguishable by the degree of decomposition of the organic material. The deepest layer, a black peat, has a pH of 3—4. Under the microscope, small silicate particles were detected.

Tatzmannsdorf. This fen at 316-m height and exposed to 800—1000-mm rainfall per year is dominated by rhynchospora, carex, scirpus, and alnus. The neutral peat is dark brown. The shale content of the peat increases with depth.

Neydharting. This extensively used fen, located at 380-m height and exposed to 1000—1500-mm rainfall per year, is covered by sphagnum, eriophorum, carex and other plants. Below the vegetation layer of about 30 cm, the black neutral peat has some silty components such as muscovite and other silicates.

St. Felix. This fen, located at 430-m height and exposed to 1000—1500-mm rainfall per year has a black peat of pH 5 that was formed mainly from vaccinium and eriophorum. The peat developed in a bowl-like depression in a flat landscape and is sealed against ground seepage by an impermeable layer of grey-blue shale.

Experimental

Lithological categories. The elemental abundances in igneous rock, shale, sandstone, carbonate, oceanic clay, and oceanic carbonate as the main sedimentary and marine materials of the earth's crust were taken from a model of geochemical balances by Horn and Adams [1]. Bismuth, Pd, Pt, and Te, which were not included in this model, were excluded from the cluster analysis.

Plant species. The elemental compositions of the most abundant species growing on peat-lands were included in the cluster analysis. Only the concentrations of the elements P, K, Na, Ca, Mg, Mn, Fe, S, and Si were considered, because only these were available for all the relevant plant species. The concentrations were not determined specially but were taken from the literature [2, 3].

The following species were included: white beak-sedge, rhynchospora alba, mud sedge, carex limosa, deer-grass, scirpus caespitosus, peat moss, sphagnum (cuspidatum, magellanicum and rubellum), bogbean, menyanthes trifoliata, eriophorum latifolium, purple moor grass, molinia coerulea, cowberry, vaccinium vitis idaea, mountain pine, pinus mugo, Scots pine, pinus sylvestris, common alder, alnus glutinosa, black alder and frangula alnus.

Chemical analysis. Neydharting peat was collected from the building in which the peat was prepared for oral application. All other peat samples were taken in the field. The samples were placed in plastic containers. After drying at 105°C to constant weight, each peat sample was ground in an agate ball mill. The powder (0.25—0.5 g) was refluxed with 25 ml of concentrated nitric acid for 2 h. The mixture was cooled to room temperature and then filtered through a medium-porosity sintered-glass filter funnel. The beaker and filter were rinsed three times with water, the filtrate and washings were transferred quantitatively to a 50-ml volumetric flask, and the flask was filled to the mark with distilled, deionized water. These solutions were analyzed with an ARL model 34000 argon-plasma emission vacuum spectrometer with 48 elements on the array. For the determination of the major elements Al, Ca, P, S, and Si, the samples were ashed and the ash dissolved. The elements were determined in the resulting solutions by classical techniques.

Pattern recognition. SIMCA was applied for classification. All terms used here are defined in the paper by Wold [4]. Each variable (element concentration) was weighted by the inverse of the standard deviation calculated for each range of the element concentrations.

Results and discussion

Principal component analysis. The chemical analyses of the five peat samples produced ca. 220 elemental concentrations. For correlation purposes, six lithologic materials and twelve plant species were considered, which contributed a further 340 concentrations. Chemometric methods should be useful for classifying peat-lands on the basis of the elemental composition of peats even on an unsupervized level.

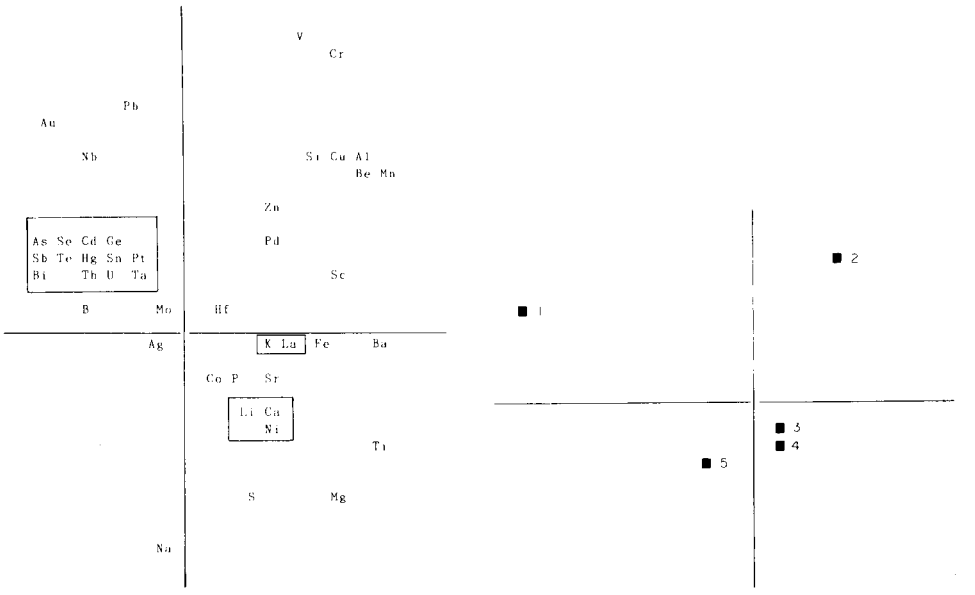

Fig. 1. The projection of the peat samples in the plane spanned by two principal components. Boxed elements are at the same position.

Fig. 2. Principal component plot of the five peat samples: (1) Garanas; (2) Neydharting; (3) Althofen; (4) Tatzmannsdorf; (5) St. Felix.

As the first step in classification of the peats, principal component analysis (PCA) was applied to the elemental concentrations from all five peat samples. Figure 1 shows the projection of the elemental concentration vectors for the five samples onto the plane spanned by the two principal components (Karhunen-Loeve transformation). These two principal components account for 38% of the total variance. The 38% variance indicates that the five peats do not have the same characteristics. The distribution and the concentrations of elements in peat are influenced by several factors. During the formation of peat, the plant material loses 50–80% of its mass [5] by degradation to volatile CO_2, H_2S, NH_3, and CH_4. Additional material is removed by leaching with water, mainly rain. The mobility of the elements depends strongly on the chemical conditions. Humic acid, fulvic acid, proteins with thiol groups, and ammonia form complexes with a variety of metal ions and either prevent or promote leaching. Under anoxic conditions, hydrogen sulphide precipitates insoluble metal sulphides. All these interactions and changes of pH as a function of depth make a peat-land a very complex chemical system that is difficult to characterize in detail. All these factors combine to distribute even chemically similar elements such as sodium and potassium [6] or cadmium and lead [7] quite differently as a function of depth.

During times of low rainfall, the transpiration of the vegetation can transport some elements from deep strata to the surface [8]. This redistribution of elements caused by changing climatic conditions can produce large temporal variations in element concentrations and can make comparison of data obtained at different times very difficult. For this reason, elemental concentrations in peat samples from other laboratories were not included in the factor analysis.

The interpretation of the projection shown in Fig. 1 requires great care to avoid unwarranted conclusions. Although no information about the chemical relationships among elements was built into the mathematical analysis, some clustering of elements with similar properties is obvious in Fig. 1. Elements known to be essential to plants are situated in the lower half of the projection, whereas elements that have mineral or anthropogenic origin are found in the upper half. Most of the elements that form insoluble sulphides appear in the left upper quadrant. Elements for which the solubilities are controlled by their valence states (Cr, Fe, Mn, Mo, V), are scattered over the entire projection. The position of lead, away from the sulphide-forming elements, is probably caused by the introduction of lead through combustion of leaded gasoline and the distance of the sampling location from traffic. The unexpected location of Cr and V in the projection is probably due to contamination during sampling of the Neydharting peat. The clustering of Al and Si indicates input of aluminosilicates into the peat.

Cobalt and nickel appear in that area of the projection in which elements important to plants are clustered. Because peat-land plants must be nitrogen-fixing in order to survive in an environment deficient of nitrogen compounds, the location of cobalt and molybdenum, two elements needed for nitrogen fixation [9], in this area of the projection is not surprising. Nickel displaces calcium from the walls of plant cells that consist of pectins [10]. Sphagnum, the major peat-forming plant, is rich in pectins and so accumulates nickel [11]. Similarities between the elemental compositions of the peats and their precursor materials should be easily established with statistical methods based on similarity such as SIMCA. In the geometric representation of the results of cluster analysis, similar objects fall on a straight line. Such a representation for the five peat samples is shown in Fig. 2. The four fens lie almost on a straight line and belong, therefore, to the same class of peat-lands. The Garanas bog has such a large class distance that it appears as an outlier. However, the straight line connecting Garanas with Althofen, Tatzmannsdorf, and St. Felix could also define a class analogy, with Neydharting as the outlier. The location of Neydharting in Fig. 2 is caused by contamination of the sample taken after it had been transported from the fen to the preparation facility through steel pipes with some brass parts, which accounts for the high concentrations of Cr, V, and Cu.

To improve the understanding of the ecological system of the peat-lands, the elemental compositions of major mineral materials and peat-forming plants were introduced sequentially into the model. When only the composi-

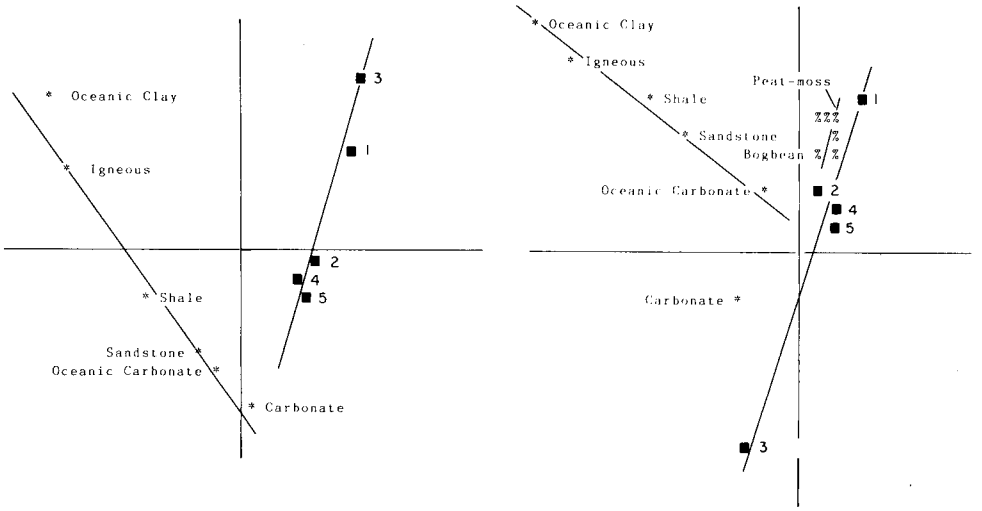

Fig. 3. Principal component plot of peat (■) and the rock or soil categories (*) in a single model. Numbering as in Fig. 2.

Fig. 4. Principal component plot of peat (■), rock or soil categories (*) and vegetation (%) in a single model. Numbering as in Fig. 2.

tion of the minerals or rocks was used, all the peats formed one class (Fig. 3). When the elemental compositions of the plants (nine elements, only) and the rock or soil types and the peats were added in the cluster analysis, the objects fell into the expected three classes (Fig. 4). The Garanas bog is close to the plants, from which it is almost exclusively formed. The three fens form a tight cluster; the contaminating elements in the Neydharting sample were not considered in this analysis. The Althofen fen is clearly different from the other fens, because of considerable input of mineral matter by the river.

Discrimination between models. The use of SIMCA to evaluate multivariate data in order to find similarities can be extended to test if an object fits a class model within a certain tolerance interval. Because the residual standard deviation of the variables is approximately F-distributed, the F-test at a confidence level of 0.99 was chosen to decide if the elemental distribution in peat samples is significantly different from the distribution in the vegetation or the mineral environment. Elemental concentrations for peat samples taken just under the vegetation layer from three bogs (Die Schwemm, Austria; Venner Moor, F.R.G.; Stordalen, Sweden) taken from the literature [2] were added to the data from the five peats, to check whether all these bogs still belonged to the same class. A plot of the results clearly showed a distinct separation of the peats from the mineral material and the vegetation.

The discrimination power of the elements between peat and mineral matter increases in the order (Zn, Pb, Al) < (Cd, Mg, S, Cu) < (Ca, Cr, Mn, Se).

Iron and manganese discriminate well between peat and vegetation, whereas magnesium and phosphorus are less discriminatory. It is surprising that nine elements are sufficient to distinguish between peat and plants. The discrimination between peat and vegetation is still an open question [6, 13]. The statistical analysis presented here should help to resolve some questions about the classification of peat-lands [12]. The results of the SIMCA treatment show that the description of an ecosystem improves as the number of features is increased.

The authors express their appreciation to the Jubiläumsfond der Österreichischen Nationalbank, which supported this project.

REFERENCES

1 M. K. Horn and J. A. S. Adams, Geochim. Cosmochim. Acta, 30 (1966) 279.
2 B. Markert and H. Lieth, Veröff. Naturforsch. Ges. zu Emden v. 1814, Jahresbericht 1985, p. 27.
3 N. Malmer and H. Sjörs, Bot. Notiser, 108 (1955) 46.
4 S. Wold, Pattern Recognition, 8 (1976) 127.
5 F. Overbeck, Botanisch-Geologische Moorkunde, Karl Wachholtz Verlag, Neumünster, 1975, p. 302.
6 A. W. H. Damman, Oikos, 30 (1978) 480.
7 K. Kalcher, W. Kosmus and R. Pietsch, Telma, 13 (1983) 173.
8 F. F. Hooper and L. S. Morris, Ecology, 63 (1982) 1411.
9 P. J. Peterson and C. A. Girling, in N. W. Lepp (Ed.), Effect of Heavy Metal Pollution on Plants, Vol. 1, Applied Science, London, 1981, p. 231.
10 M. M. Cole, J. Appl. Ecol., 10 (1973) 269.
11 K. Brehm, Biol. Z., 5 (1975) 85.
12 R. L. Mitchell and J. W. S. Reith, J. Sci. Food Agric., 17 (1966) 437.
13 W. G. Chaloner, Phil. Trans. R. Soc. London, Ser. B, 311 (1985) 139.

Analytica Chimica Acta, 191 (1986) 495—504
Elsevier Science Publishers B.V., Amsterdam — Printed in The Netherlands

Short Communication

A SIMPLIFIED APPROACH TO THE GENERALIZED STANDARD-ADDITION METHOD AND ITS APPLICATION IN ELECTROTHERMAL ATOMIC ABSORPTION SPECTROMETRY

SULO PIEPPONEN*

Food Research Laboratory, Technical Research Centre of Finland (VTT), Biologinkuja 1, SF-02150 Espoo (Finland)

TIMO ALANKO

Computing Service, Technical Research Centre of Finland (VTT), Lehtisaarentie 2 A, SF-00340 Helsinki (Finland)

PENTTI MINKKINEN

Lappeenranta University of Technology, P.O. Box 20, SF-53851 Lappeenranta (Finland)

(Received 28th May 1986)

Summary. A simple and general standard-addition method for a single-component determination is presented. The method uses two independent variables for the calculation of the analyte concentration (the amount of sample taken and the amount of analyte added) and one dependent variable, the response. The sensitivity and the response of the blank can also be estimated from the model by changing the amount of the sample and the amount of the analyte addition. In the simplest case, a linear equation is assumed to exist between the variables. Geometrically, the model can be expressed by the response plane in the variable-space. The method has all the advantages of the ordinary standard-addition method but also includes automatic blank elimination and versatile matrix-interference control. Two examples of the use of the method are based on graphite-furnace atomic absorption spectrometry of chromium and lead. Standard statistical packages are applied.

The conventional standard-addition method is widely used in analytical chemistry. Different known amounts of the analyte are added to a series of samples of the same size and the concentration of analyte in the sample is calculated by using linear regression. The method allows various interferences to be overcome, but nonspecific background signals are not eliminated.

In recent years, increasing interest has been focused on making the standard-addition method more general. Saxberg and Kowalski [1] proposed the generalized standard-addition method (GSAM), which is able to correct for many matrix effects and interferences in multicomponent determinations. The GSAM uses multiple linear regression to process data obtained for multi-component samples in which the response/analyte concentration relationship is of some arbitrary polynomial form. For a non-linear polynomial relationship, the GSAM requires an iterative solution. Later, a recursive version of the GSAM was presented [2], in which some new properties were added.

0003-2670/86/$03.50

Applications of experimental designs and non-linearly transformed factors were also proposed for inclusion in the GSAM [3, 4]. Theoretical approaches and experimental examples of the use of the GSAM have been reported in many papers [5—14].

The method presented here is a greatly simplified approach to the GSAM; it has various differences from, and some similarities to the GSAM of Saxberg and Kowalski. The fundamental difference between the two methods is that whereas Saxberg and Kowalski concentrated on multicomponent determinations, the main emphasis here is placed on single-component determinations. Because of its multicomponent nature and widely generalized form, the GSAM has a complicated mathematical expression. The mathematics becomes easier for single-component systems, although many of the advantages of the multicomponent system are then lost.

The traditional standard-addition method is able to correct only for matrix effects affecting the slope of the calibration line. The generalized standard-addition method also corrects for interferences caused by the matrix components and limited selectivity of the sensors used. However, only particular interferences for which a sensor is available can be corrected. In atomic absorption spectrometry, matrix effects are normal but interferences such as overlapping absorption peaks are rare. The graphite-furnace method has very low detection limits and, consequently, contamination of reagents and laboratory vessels can be troublesome, especially at concentrations near to the detection limits. The aim of this work, therefore, was to develop a method which could overcome both the matrix effect and the contamination problem. In this paper, only the linear model of the method and its applicability are discussed.

Theory

The method uses two independent variables for the calculation of the analyte concentration, namely the amount of sample used for the analysis and the amount of analyte added, and one dependent variable, the response of the measurement. A linear relationship is assumed to exist between the variables:

$$R_i = B + S\,a_i + S\,C\,m_i + \epsilon_i \qquad (1)$$

where $i = 1, 2, \ldots N$, N being the number of points; R_i is the total response for point i, a_i the addition of analyte for point i, m_i the amount of sample for point i, B the response of background and/or blank, S the sensitivity (slope), C the analyte concentration in the sample, and ϵ_i an error term related to point i. The unknown parameters to be estimated are B, S and C. R is the dependent variable and a and m are the independent observed variables. The customary assumptions about the error term are made, i.e., that the error terms of different observations are independent, with zero mean and a common variance (denoted σ^2) and that the error term distribution is Gaussian.

Nonlinear regression by the least-squares method. In the form of Eqn. 1, the regression model is non-linear in the parameters S and C. The usual estimation method for such models is the method of least squares. With a minimum of four observations, the least-squares method can be applied to this model to obtain point estimates for the unknown parameters B, S, C and σ^2. Approximations of the standard deviations and confidence limits of B, S and C can also be obtained. The advantage of the non-linear approach is that it is implemented in all widely-used statistical packages and is thus available without programming effort in most research environments. In the present work both the SPSS [15] and BMDP [16] packages were used with a Cyber 180-840 computer for the calculations. The disadvantage of the non-linear approach is that the confidence limits and standard deviations obtained, particularly for C, are only linear approximations of the true values. As shown below, precise confidence limits can be obtained by using a slightly different approach to the model. In practice, however, the differences in confidence limits are not very significant.

Deriving exact confidence limits. By using different parameters, the model expressed by Eqn. 1 can be made linear:

$$R_i = B + S\,a_i + D\,m_i + \epsilon_i \tag{2}$$

where $D = S\,C$. It is obvious that this model is a linear regression model and that the parameter of interest, C, is the ratio of two regression coefficients, $C = D/S$. The theory of linear regression models can then be applied to derive and calculate statistically optimal least-squares estimates, standard deviations and confidence limits for B, S and D. Furthermore, it can be shown that the least-squares estimate of D/S is the ratio of the least-squares estimates of D and S, respectively. The problem is that the statistical properties of this least squares estimator are not as good as those of the estimators of B, S and D. In fact, the estimator of C has the distribution of the ratio of two correlated normal variables. This distribution does not in general have moments, so that it is formally not meaningful to calculate its mean and standard deviation or to talk about its bias. In addition, the distribution is often skewed. A statistical discussion of the distribution is available [17]. Moran and Kowalski [10] discussed essentially the same distribution (without the correlation assumption) in a GSAM context to show the approximate bias caused by the ratio estimator.

However, despite the statistical difficulties in the point estimator of C, it is possible to obtain exact confidence limits for the true value of C [18]. In most applications, these limits are skewed about the point estimate, reflecting the shape of the distribution of this estimator. The calculation of these limits is based on the results obtained from a linear regression on at least four points in model 2. The limits were calculated here on a Cyber 180-840 computer with a program based on NAG Fortran [19] subroutines. The normal assumption in the calculation of confidence limits is that the error variance (σ^2) is unknown and must be estimated from the data simultaneously with

other unknowns. When the number of points is limited, this leads to very large confidence limits, as shown below. However, with repeated routine analyses (with the same apparatus, the same analyte and the same concentration range) it may be appropriate to regard the error variance as known from previous experience. With this information, the practical confidence limits can be greatly reduced by using the normal distribution with known error variance instead of the *t*-distribution in the calculation of the confidence limits. This approach is not pursued further here. Thus, as far as the assumptions of the present model are concerned, the remaining problem has to do with the mathematical properties of the point estimate of the concentration parameter *C*. The problem remains largely a formal exercise because the non-linear approach (Eqn. 1) gives results which are acceptable from the practical point of view.

Geometric expression of the model. Geometrically, the model can be expressed by the response plane (in step one) in the variable-space (Fig. 1). The analyte concentration is not seen directly in the figure. If the response plane is continued, it will intersect the sample-addition plane and the slope of the intersection line will be equal to the analyte concentration (Fig. 2). The slope of this line is not affected by a constant blank. The analyte concentration can be also seen in the figure if the intersection of a parallel plane to the sample-addition plane and response plane is projected onto the sample-addition plane. The projection line intersects the sample axis at point *M* and the addition-axis at point *A*. The ratio *A/M* is the concentration *C*. The ratio is not affected by the response of the blank.

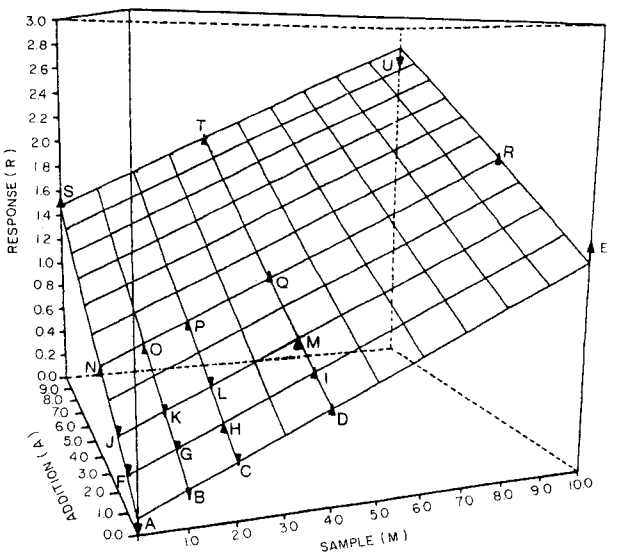

Fig. 1. Response plane in the variable-space. The response plane and the residuals represent the case of the analysis of chromium in tap water. $R = B + S\,a + S\,C\,m$, where B = 0.103 (A s), S = 0.135 (A s μg^{-1}) and C = 1.018 (μg ml^{-1}).

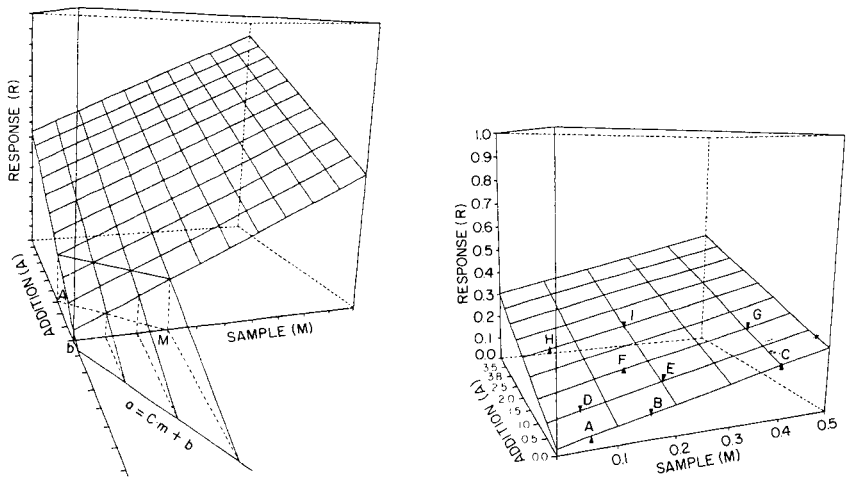

Fig. 2. The geometric solution of the concentration (C). $C = A/M$ and is the slope of the line $a = C\,m + b$.

Fig. 3. The response plane and the residuals in the case of the determination of lead in NBS tomato leaves (SRM 1573) $R = B + S\,a + S\,C\,m$, where $B = 0.022$ (A s), $S = 0.071$ (A s μg^{-1}) and $C = 6.38$ ($\mu g\ g^{-1}$).

The limitations of the model. Because the model presented here has a linear equation, it has some limitations concerning the non-linearity of the response plane. The model is exact provided that: (1) sensitivity (S) is constant under the conditions used (i.e., S does not depend on the concentration or the amount of matrix); (2) non-specific response (background) is not a function of the amount of the sample (if so, the background must be corrected); and (3) contamination is constant in all the experiments (points).

The curvature of the response plane can be seen in the residuals. In some cases, the linear model gives good approximations for non-linear cases. For example, if the curvature is caused only by a deviation from Beer's law, the linear model gives a correct value for concentration (C) but incorrect values for blank (B) and sensitivity (S). In the three-dimensional model, presented here, the concentration is less sensitive to curvature than in the two-dimensional model (standard addition line), because the concentration is a ratio of the two parameters. Work is under way to develop a method that will also work when the sensitivity is dependent on the amount of sample.

Experimental design. In general, an experimental design should be such that the position of the response plane in the variable-space is covered as completely as possible. This guarantees that the analyte concentration can be calculated easily and accurately. By varying the amount of sample taken and the amount of analyte addition, the response points can be located on the response plane so that they support the regression model. The theory of experimental design can also be used [3]. The points can in practice be

TABLE 1

Experimental design of five points

Addition[a]	Sample[a]				
	0	m	$2m$	$3m$	$4m$
0		X			
a	X				X
$2a$			X		
$3a$					
$4a$		X			

[a]Mass or volume.

chosen freely, the only restriction being that all the points must not be located on the same line.

When the case is known well, 4—8 points should suffice to give reasonable results. A larger experimental design is recommended when a model or a new analytical pathway is being tested. An example of experimental design for 5 points is given in Table 1. The sensitivity of the measurement and the limitations of the optimum response region must be considered when the experimental design is planned. As discussed above, the value of a constant blank does not affect the calculation of the analyte concentration. This means that traditional blanks are not usually needed, but the information obtained from the blank points is valuable if a new model or method is being tested. The method also gives the value of the blank, even if real blank solutions are not prepared and measured. The units are easy. After the units for the addition of the analyte (mass or volume) and for the amount of the sample (mass or volume) have been chosen, the analyte concentration automatically has the dimension [addition]/[sample amount]. The concentrations of the measured solutions are not needed in any phase of the calculation. The only demand applicable to these experiments is that all the solutions for the measurement must have the same volume.

Experimental

The theory was tested in practice by using flameless atomic absorption spectrometry. A Perkin-Elmer 5000/Zeeman atomic absorption spectrometer was used with a HGA-400 graphite-furnace programmer, AS-40 autosampler and 3600 data station. The stabilized-temperature platform furnace system was used in all measurements. Instrumental conditions are given in Table 2. The calculations for the estimation of the unknown parameters were done as described in the theoretical section.

Determination of chromium in water. A tap-water sample, spiked with 1.00 μg ml^{-1} chromium, was analyzed directly as an unknown sample. An experimental design of 21 points was used (Table 3). The standard-addition

TABLE 2

Conditions for atomic absorption spectrometry with Zeeman background correction

Parameter	Cr	Pb	Parameter	Cr	Pb
Wavelength (nm)	357.9	283.3	Furnace program	Temperature/ramp/hold	
Slit (nm)	0.7	0.7		(°C/s/s)	
Integration (s)	10	5	step 1	180/20/20	180/20/20
Signal (A s)	Area	Area	step 2	1650/10/10	1000/5/10
Injection volume (μl)	10	10	step 3	2500/0/10	1800/0/5
Matrix modifier	0.05 mg $Mg(NO_3)_2$	0.5 mg $NH_4H_2PO_4$	step 4	2650/1/2	2650/1/4
			step 5	20/5/10	20/5/10
			Gas	argon (stop flow in step 3)	

TABLE 3

Experimental parameters of the standard-addition method for the determination of chromium in spiked tap water

Point	Sample (ml)	Cr addition (μg)	Response (A s)	Point	Sample (ml)	Cr addition (μg)	Response (A s)
A	0	0	0.004	L	2	2	0.636
B	1	0	0.176	M	4	2	0.937
C	2	0	0.353	N	0	4	0.662
D	4	0	0.673	O	1	4	0.791
E	10	0	1.602	P	2	4	0.935
F	0	1	0.239	Q	4	4	1.247
G	1	1	0.353	R	10	4	2.038
H	2	1	0.518	S	0	10	1.558
I	4	1	0.813	T	4	10	2.051
J	0	2	0.370	U	10	10	2.642
K	1	2	0.480				

solution was 1.00 μg ml^{-1} chromium in 0.3% (v/v) nitric acid. Solutions for measurements were diluted, after addition of sample and standard aliquots, to 100 ml with 0.3% (v/v) nitric acid. The data in Table 3 were used for the calculations.

Determination of lead in NBS tomato leaves. NBS standard reference material 1573 (tomato leaves) was decomposed by wet digestion (concentrated nitric acid and hydrogen peroxide) in an aluminium block electrothermal heater. An experimental design of 9 points is presented in Table 4. The additions of lead to the sample were made before the digestion step from a standard solution (1.00 μg ml^{-1}). After digestion and evaporation to near dryness, the residues were dissolved and diluted with 0.3% (v/v) nitric acid to 50 ml.

TABLE 4

Experimental parameters of the standard-addition method for the determination of lead in tomato leaves (NBS 1573)

Point	Sample (g)	Pb addition (μg)	Response (A s)	Point	Sample (g)	Pb addition (μg)	Response (A s)
A	0.055	0.0	0.047	F	0.154	1.0	0.171
B	0.155	0.0	0.087	G	0.404	1.0	0.269
C	0.400	0.0	0.209	H	0.050	2.0	0.194
D	0.055	0.5	0.076	I	0.200	2.0	0.242
E	0.201	0.5	0.147				

Results and discussion

The goodness of fit of the measured points to the response plane of the model was good in both experimental cases (Figs. 1 and 3). This implies that the assumption of linearity was valid for these cases, even though the measured responses in the case of chromium included very high absorbance values. In fact, a slight curvature of the response surface can be seen in the case of chromium. A moderate curvature of the response surface because of deviation from Beer's law does not much affect the analyte concentration (C), whereas it does affect the calculated values of sensitivity (S) and blank (B). This was also confirmed in practical experiments. The curvature of the response surface for other reasons, such as matrix effects and background absorption, has a greater influence on the analyte concentration.

The results obtained for chromium are presented in Table 5. Because the data fit the model rather well, as discussed above, the number of points used for the calculation does not affect the results appreciably. Obviously, the confidence limits increase considerably as the number of points used for the calculations decreases. In Table 5 the exact confidence limits are given. The measured sensitivity, given as characteristic mass (pg/0.0044 A s), was in reasonable agreement with the manufacturer's value. The analyte concentration was in good agreement with the expected value (1.00 μg ml^{-1}). The tap water used actually contained <0.01 μg ml^{-1} chromium. The relative standard deviation varied from 1.8% to 10.6% depending on the number of points used for the calculations. The calculated blank value, 0.103 A s, is different from the measured blank value, 0.004 A s, because of the curvature of the response surface. In general, the curvature can be seen if the model residuals are plotted.

The results obtained for lead are also presented in Table 5. The mean concentration found was in very good agreement with the certified value. Depending on the number of points used for the calculation, the standard deviation of the concentration varied from 4.6% to 8.2%. The 95% confidence limits (exact) were large, especially when only 4 points were used for the calculation. The measured sensitivity was in good agreement with the

TABLE 5

Results obtained for chromium in spiked tap water (1.0 $\mu g\ ml^{-1}$ Cr) and for lead in NBS tomato leaves

Number of points	Sensitivity (CM) (pg/0.0044 A s)[a]	Concentration		
		Estimate	St. dev.	95% conf. limits
Chromium ($\mu g\ ml^{-1}$)				
21	3.3	1.018	0.055	0.908—1.142
18	2.9	1.024	0.018	0.986—1.065
12	2.9	1.032	0.031	0.965—1.107
8	3.0	1.007	0.055	0.875—1.160
6	2.9	1.007	0.070	0.801—1.266
5	3.0	1.002	0.106	0.620—1.620
4	3.0	1.017	0.051	0.467—2.261
3	3.0	—	—	—
Lead ($\mu g\ g^{-1}$)[b]				
9	14.0	6.38	0.43	5.41—7.55
7	12.8	6.47	0.53	5.15—8.21
5	11.4	6.30	0.29	5.17—7.75
4	11.6	6.33	0.37	2.7—20
3	11.0	6.25	—	—

[a]Reference values of sensitivity given by the manufacturer are 3.5 pg/0.0044 A s for chromium and 11 pg/0.0044 A s for lead.
[b]Certified value, 6.3 ± 0.3 $\mu g\ g^{-1}$ lead.

manufacturer's value. The calculated blank value was 0.022 A s, which corresponds to a theoretical blank concentration of 0.006 $\mu g\ ml^{-1}$ in the measured solutions.

Conclusions

The geometric expression of the model helps the analyst to understand the system as a whole and also to recognize the effects of interfering substances. The method presented should provide new ways of investigating and eliminating matrix interferences and background absorption in atomic absorption spectrometry. It can also be used for the testing of new analytical pathways. Because the method has a good capability of eliminating the response of the blank, an experimental design with a constant matrix can be utilized. The effects of the sample matrix can then be eliminated and a variety of samples can be analyzed by means of standard pretreatment.

The authors are greatly indebted to Risto Mannonen and Jari Tuominen for their ideas and technical assistance.

REFERENCES

1 B. E. H. Saxberg and B. R. Kowalski, Anal. Chem., 51 (1979) 1031.
2 B. Vandeginste, J. Klaessens and G. Kateman, Anal. Chim. Acta, 150 (1983) 71.

3 P. Kościelniak and A. Parczewski, Mikrochim, Acta, II (1984) 359.
4 P. Kościelniak, Mikrochim. Acta, II (1984) 369.
5 R. W. Gerlach and B. R. Kowalski, Anal. Chim. Acta, 134 (1982) 119.
6 J. H. Kalivas and B. R. Kowalski, Anal. Chem., 53 (1981) 2207.
7 M. Raymond, C. Jochum and B. R. Kowalski, J. Chem. Educ., 60 (1983) 1072.
8 D. W. Osten and B. R. Kowalski, Anal. Chem., 57 (1985) 908.
9 J. H. Kalivas and B. R. Kowalski, Anal. Chem., 55 (1983) 532.
10 M. G. Moran and B. R. Kowalski, Anal. Chem., 56 (1984) 562.
11 F. H. Walters, Anal. Lett., 16 (1983) 667.
12 E. A. G. Zagatto, A. O. Jacintho, F. J. Krug, B. F. Reis, R. E. Bruns and M. C. U. Araujo, Anal. Chim. Acta, 145 (1983) 169.
13 J. H. Kalivas, Anal. Chem., 55 (1983) 565.
14 A. Lorber, Anal. Chem., 57 (1985) 954.
15 SPSS-6000 (Statistical Package for the Social Sciences), Northwestern University, Evanston, IL.
16 BMDP (1983) Biomedical Computer Programs, BMDP Statistical Software, Los Angeles, CA.
17 G. Marsaglia, Journal of the American Statistical Association, 60 (1965) 193.
18 C. R. Rao, Linear Statistical Inference and Its Applications, Wiley, New York, 1965, p. 199.
19 NAG FORTRAN Library, Mark 11, Numerical Algorithms Group, Oxford (U.K.), 1983.

Analytica Chimica Acta, 191 (1986) 505—512
Elsevier Science Publishers B.V., Amsterdam — Printed in The Netherlands

Short Communication

RATIO LOGARITHMIC DIAGRAMS IN CHEMICAL EQUILIBRIUM STUDIES

ANTONIO QUIRANTE

Instituto Nacionale Bachillerato, INBAD, Extensión de Murcia, Avda. Fama s/n, Apdo. 197, Murcia (Spain)

(Received 29th April 1986)

Summary. Ratio logarithmic diagrams are useful not only in the qualitative approximation stage for solving chemical equilibrium problems, but in the quantitative stage of choosing and ranking a sequence of equations iteratively leading to a solution. The procedures can also be used to find the best equilibrium constants appropriate to experimental concentrations and a predefined theoretical model. Some simple systems are used for illustration.

The advantages of using logarithmic diagrams and ratio logarithmic diagrams [1—5] are well known and the present availability of microcomputers makes it possible to study and teach problems in chemical equilibrium by numerical iterative procedures [6—8].

In this communication, the possibilities of ratio logarithmic diagrams are explored not only in the qualitative approximation stage for solving chemical equilibrium problems, but also in the quantitative stage of choosing and ranking a sequence of equations which lead iteratively to the solution. The procedures can also be used in handling the reverse problem of finding the stability constants most appropriate to experimental concentrations, given a theoretical model.

In the procedure described, the following steps can be achieved systematically: (a) a possibly defective approximate model can be amended to another model nearer the correct solution; (b) the equations can be ranked so that iteration will provide the correct solution with quick convergence; (c) initial suitable values of concentrations can be chosen for the calculations. Once the first step is complete, by using easily constructed ratio logarithmic diagrams, all the chemical species involved in the problem can be classified as three types: (1) predominant species, the relative concentrations of which are never significantly changed from the initial approximation to the final correct solution; (2) determinant species, the presence of which has a decisive influence on the relative concentrations of the remaining species from the first approximation to the correct solution, but do not modify the predominant species significantly; and (3) negligible species, which can be removed from the numerical treatment of the problem without significant

0003-2670/86/$03.50

relative changes in the concentrations of remaining species (within stated error limits).

This article gives three examples of problems in chemical equilibrium which can be treated by the proposed method. Example 1 deals with the relatively simple problem of evaluating concentrations from data on stability constants. Example 2 shows the usefulness of the method in evaluating concentrations with several unknown features. Example 3 is concerned with finding the best set of parameters (stability constants and absorptivities of the species) for a set of experimental data, given a mathematical model.

Evaluation of concentrations from stability constants

The first example concerns the concentrations of the species present in 0.01 mol l^{-1} cobalt chloride. The equilibria (charges are omitted in numerical expressions) are:

$$Co^{2+} + Cl^- \rightleftharpoons CoCl^+; [CoCl]/[Co]\,[Cl] = 10^{2.4} \quad (1)$$

$$CoCl^+ + Cl^- \rightleftharpoons CoCl_2; [CoCl_2]/[CoCl]\,[Cl] = 10^{1.5} \quad (2)$$

$$CoCl_2 + Cl^- \rightleftharpoons CoCl_3^-; [CoCl_3]/[CoCl_2]\,[Cl] = 10^{-0.4} \quad (3)$$

Graphical approach. The initial approximate hypothesis is that $CoCl_2$ is the predominant species and the concentration 0.01 mol l^{-1}. For the ratio logarithmic diagram, pCl is considered as the independent variable and the predominant species $CoCl_2$ as the reference species. Equation 2 and the approximate hypothesis yield log [CoCl] = −3.5 + pCl. Similarly, Eqn. 3 yields log $[CoCl_3]$ = −2.4 − pCl. Equation 1 with the equation for log [CoCl] yields log [Co] = −5.9 + 2pCl. Figure 1A shows the lines plotted from these three equations on the ratio logarithmic diagram; a horizontal line at ordinate −2 for $CoCl_2$ and a line of slope −1 passing through the origin for Cl^- are also shown.

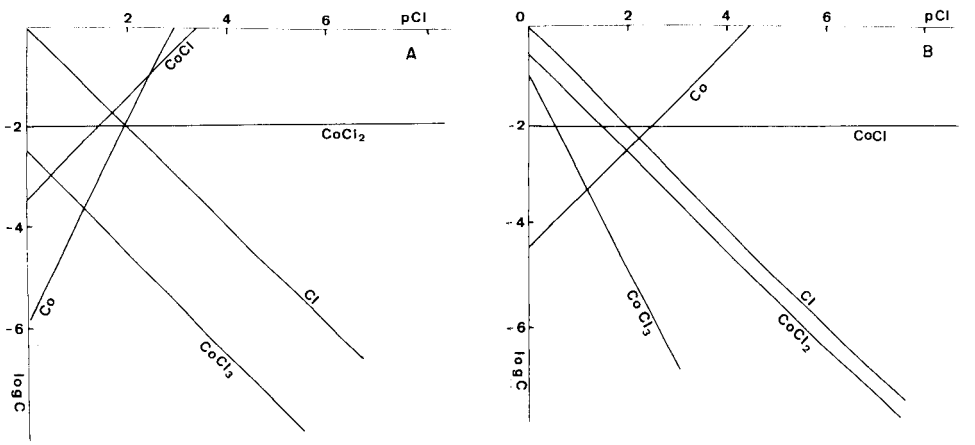

Fig. 1. Ratio logarithmic diagrams for example 1: (A) initial hypothesis; (B) corrected hypothesis.

To obtain an approximate solution from the diagram, mass balances are needed:

$$[Co] + [CoCl] + [CoCl_2] + [CoCl_3] = 10^{-2} \quad (4)$$

$$[Cl] + [CoCl] + 2\,[CoCl_2] + 3\,[CoCl_3] = 2 \times 10^{-2} \quad (5)$$

To obtain an equation from the mass balances which does not contain the predominant species, Eqn. 4 is multiplied by -2, Eqn. 5 is added. Then, rearrangement gives

$$2\,[Co] + [CoCl] = [Cl] + [CoCl_3] \quad (6)$$

To establish an approximate graphical solution, it is noted that in Fig. 1 the Cl line, from the top corner, meets the CoCl line first. If the other concentrations in Eqn. 6 are ignored, the pCl corresponding to the approximate solution and the concentration of every species involved are obtained. Checking this hypothesis, the graphic solution obtained provides results which show that $[CoCl] > [CoCl_2]$, which is obviously wrong.

The results previously obtained show the possibility of correcting the approximate hypothesis by taking CoCl as the reference and predominant species. This new hypothesis, with $[CoCl] = 0.01$ for later calculations, enables the entire above procedure to be repeated. Figure 1B shows the ratio logarithmic diagram at the step corresponding to Fig. 1A. The new mass-balance step gives the equation

$$[Co] + 10^{-2} = [Cl] + [CoCl_2] + 2[CoCl_3] \quad (7)$$

Now, in Fig. 1B, the Cl line, followed down, meets the 10^{-2} term first. If the other concentrations in Eqn. 7 are ignored, this intersection gives the pCl for the approximate solution and the corresponding concentrations of the various species involved in the chemical equilibrium. When this new hypothesis is checked, the graphic solution obtained from the corrected approximate hypothesis provides results in agreement with that hypothesis, showing [CoCl] to be higher than any other species containing cobalt.

Numerical approach. The graphical results can be utilized to establish a better iterative calculation with low risk of divergence or break by display of absurd values. Once the approximate solution has been obtained in the graphical step, the following rules can be applied: (1) the mass balance of the central group (Co in this problem) is used to obtain the concentration of the principal species of this central group (CoCl here); (2) the stability constant equations are used to calculate the concentration of nonpredominant species starting from predominant species; (3) the species which the graphical step showed to be negligible under the conditions of the problem, are neglected (here $CoCl_3$). Once the calculation is complete, the concentration of a neglected species can be calculated, if necessary, by using stability constants and a concentration already obtained for another species.

The approximate solution obtained in the graphical step enables realistic values of input data to be chosen for the iterative procedure. This shortens

TABLE 1

Calculation process for the numerical approach to the cobalt chloride example

Input data	*Successive log [Cl] values*	*Final results*
log [Co] = −3	−2.000	log [Cl] = −2.286
log [$CoCl_2$] = −3	−2.368	log [$CoCl_2$] = −3.072
log [Cl] = −2	−2.264	log [Co] = −2.4
Calculation order	−2.294	
[CoCl] = 0.01 − [Co] − [$CoCl_2$]	−2.284	
[Co] = [CoCl]/[Cl] × $10^{2.4}$	−2.287	
[Cl] = 0.01 − [Co] − [$CoCl_2$]	−2.286	

the time needed for iteration, which may be advantageous in a slightly convergent procedure.

Table 1 summarizes the calculations needed, which use the above-stated rules and the graphical results as input data. The final results are also given. The condition for stopping the iteration was that the difference between two consecutive values of log (X) was <0.001.

Evaluation of concentrations from data with unknown constants

In this example, 0.035 mol of potassium thiocyanate is dissolved in 1 l of a solution 0.01 M in iron(III) and 0.01 M in cadmium(II). Only the following equilibria are considered (X = SCN^-):

$$Fe^{3+} + X^- \rightleftharpoons FeX^{2+};\ [FeX]/[X]\ [Fe] = 10^{3.1} \quad (8)$$

$$FeX^{2+} + X^- \rightleftharpoons FeX_2^+;\ [FeX_2]/[FeX]\ [X] = 10^{1.6} \quad (9)$$

$$FeX_2^+ + X^- \rightleftharpoons FeX_3;\ [FeX_3]/[FeX_2]\ [X] = 10^{0.3} \quad (10)$$

$$Cd^{2+} + X^- \rightleftharpoons CdX^+;\ [CdX]/[Cd]\ [X] = 10^{1.4} \quad (11)$$

$$CdX^+ + X^- \rightleftharpoons CdX_2;\ [CdX_2]/[CdX]\ [X] = 10^{0.7} \quad (12)$$

The mass balances for the Fe, Cd and X components give:

$$[Fe] + [FeX] + [FeX_2] + [FeX_3] = 0.01 \quad (13)$$

$$[Cd] + [CdX] + [CdX_2] = 0.01 \quad (14)$$

$$[X] + [CdX] + 2\,[CdX_2] + [FeX] + 2\,[FeX_2] + 3\,[FeX_3] = 0.035 \quad (15)$$

This gives a system of 8 equations for 8 unknowns.

Graphical approach. For the initial hypothesis, it is assumed that most of the iron is present as FeX_2^+ and most of the cadmium as CdX^+. A ratio logarithmic diagram is thus drawn with pX as the independent variable and CdX^+ and FeX_2^+ as the predominant species with 0.01 M concentrations. Figure 2A shows the lines for the various species involved in the equilibrium

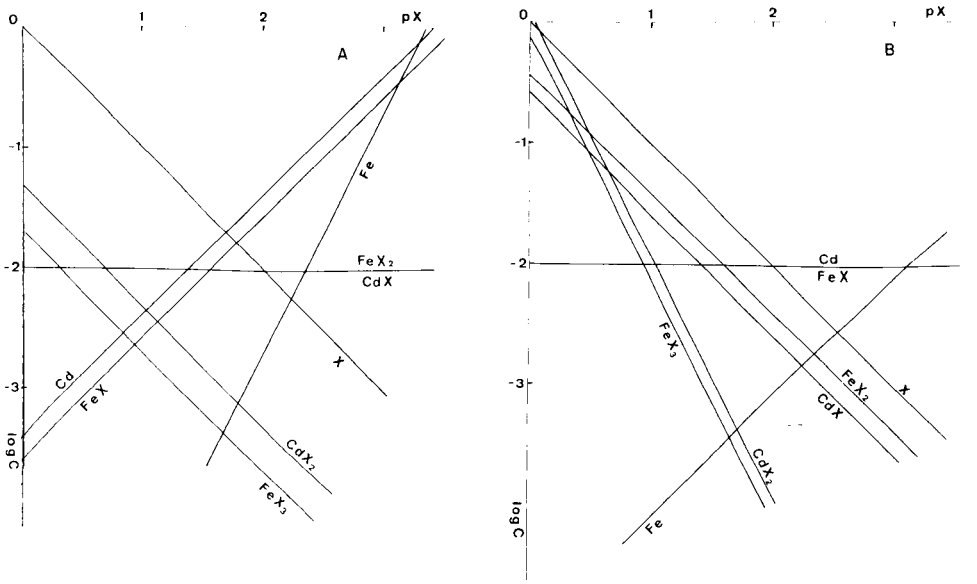

Fig. 2. Ratio logarithmic diagrams for example 2: (A) initial hypothesis; (B) corrected hypothesis.

according to this initial hypothesis. As in the procedure described for the first example, Eqn. 13 is multiplied by -2 and Eqn. 14 by -1, and the resulting equations are added to Eqn. 15 to give

$$[X] + [CdX] = 0.05 + [Fe] + [Cd] + [FeX] \quad (16)$$

From the top corner of Fig. 2A, the X line meets Cd first. The pX for this intersection is then a suitable approximation for the solution of Eqn. 16.

The results obtained from this initial hypothesis showed the diagram to be inaccurate and suggested Cd^{2+} and FeX^{2+} as the predominant species. This new approximate hypothesis was used to draw the ratio logarithmic diagram in Fig. 2B. Then Eqns. 13 and 14 were multiplied by -1 and added to Eqn. 15 to give

$$[X] + [CdX] + [FeX_2] + 2\,[FeX_3] = 0.015 + [Fe] + [Cd] \quad (17)$$

Figure 2B indicates that $[X] = 0.015$ can replace Eqn. 17 as a pX value corresponding to the approximate solution. Thus: $\log [X] = -1.88$, $\log [Cd] = -2$, $\log [FeX] = -2$, $\log [FeX_2] = -2.24$, $\log [CdX] = -2.44$, $\log [Fe] = -3.26$, $\log [CdX_2] = -3.54$ and $\log [FeX_3] = -3.8$.

Numerical approach. The above results allowed the concentrations of Fe^{3+}, CdX_2 and FeX_3 to be neglected in the numerical approach. This approximation was used in Eqns. 13–15, and Eqns. 9 and 11 were used to obtain the concentrations of the FeX_2^+ and CdX^+ species. Table 2 summarizes the input data, iterative procedure, successive values of log X obtained at each step,

TABLE 2

Calculation process for the numerical approach to the Fe/Cd/SCN problem

Input data	*Successive log [X] values*	*Final results*
log $[FeX_2]$ = −2.24	−1.8	log [X] = −1.749
log [CdX] = −2.44	−1.76	log [CdX] = 2.23
log [X] = −1.88	−1.732	log [FeX] = −2.23
Calculation sequence	−1.752	log $[FeX_2]$ = −2.38
$[FeX] = 0.01 - [FeX_2]$	−1.748	
$[Cd] = 0.01 - [CdX]$	−1.751	
$[FeX_2] = 10^{1.6}$ [FeX] [X]	−1.749	
$[CdX] = 10^{1.4}$ [Cd] [X]	−1.750	
$[X] = 0.015 + [Cd] - [FeX_2]$		

and the final results. Again, the iteration was stopped when two consecutive values of log X differed by <0.001.

Estimation of acidity constant and molar absorptivity

A 4×10^{-5} M solution of picoline-2-aldehyde thiosemicarbazone (HX) showed the following absorbances at different pH:

pH	1.6	2.7	3.3	3.6	3.9	4.2	4.4	4.6	4.75	4.95	5.20	6
A	1.07	1.07	1.05	1.01	0.72	0.52	0.40	0.3	0.22	0.17	0.13	0.1

The problem was to obtain the best values of the molar absorptivities, ϵ_{HX} and ϵ_{X^-}, and the acidity constant K_a on the assumption that only the HX/X^- couple caused the absorbance change. The acid/base equilibrium and acidity constant are

$$HX \rightleftharpoons H^+ + X^-; K_a = [H]\,[X]/[HX] \qquad (18)$$

The mass balance for X is $[HX] + [X] = 4 \times 10^{-5}$. The absorbance ($A$) of the solution as a function of the molar absorptivities and concentrations of HX and X is $A = \epsilon_{HX}\,[HX] + \epsilon_X\,[X]$. As a first approximation, ϵ_{HX} and ϵ_X can be obtained from the maximum and minimum absorbances in the A/pH table: $\epsilon_{HX} = 1.07/4 \times 10^{-5} = 2.67 \times 10^4$ and $\epsilon_X = 0.12/4 \times 10^{-5} = 0.3 \times 10^4$.

Graphical approach. The ratio logarithmic diagram used above is not useful for this problem, because no species shows a sufficiently constant concentration with change in pH. However, it is advantageous to plot log ([HX]/[X]) as a function of pH; this gives, from Eqn. 18, a line of slope −1 intercepting the y-axis at pH = pK_a. The [HX]/[X] ratio can also be obtained from the experimental A/pH data, given a correct model. If A_{HX} and A_X are defined as the maximum and minimum absorbances from the A/pH table, then from the above equations,

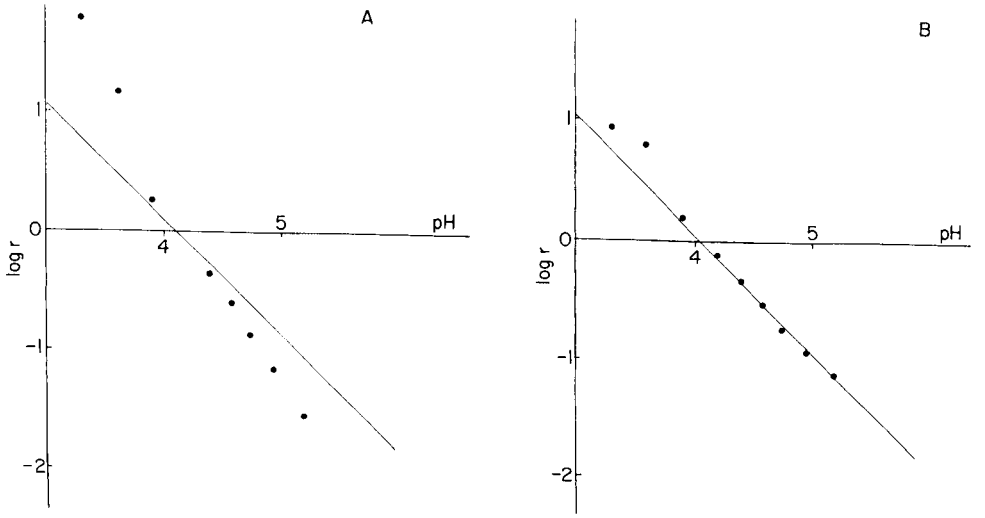

Fig. 3. Plots of log r as a function of pH: (A) initial approach; (•) from experimental absorbance data; (B) after numerical optimization (•) from experimental absorbance data and optimized values of ϵ_{HX} and ϵ_X.

$$[HX]/[X] = (A - A_X)/(A_{HX} - A) = r \tag{19}$$

If the model is correct, a plot of log r vs. pH will have a slope of -1. Figure 3A shows such a plot of the experimental log r/pH data for $A_{HX} = 1.07$ and $A_X = 0.12$. The theoretical line of slope -1 that crosses the pH axis at the same pH as the line joining the experimental points deviates greatly from these points at low and high pH. But it is impossible to decide whether the model or the choice of parameters is wrong.

Numerical optimization. Here, the best values of ϵ_{HX}, ϵ_X and K_a for the proposed model are obtained from the A/pH data. The procedure comprises three steps. First, the A/pH function is calculated from the selected values. From Eqn. 18, the mass balance and the A/ϵ dependence, the sequence of calculation is $[X] = 4 \times 10^{-5}/(1 + [H]/K_a)$, $K_a [HX] = [H] [X]$, and $A = \epsilon_{HX} [HX] + \epsilon_X [X]$. Then, the deviation of the model from the experimental A/pH data is estimated. For this purpose, the sum of the differences between the theoretical absorbances calculated in the first step and the experimental absorbances is used. This difference is termed D. The third step provides partial optimization of parameters. An arbitrary approximate (but presumably high) value of the parameter to be optimized is selected and the best known values for the remaining parameters are used to provide a first estimate of D. The value of the parameter to be optimized is then decreased slightly and a new value of D is calculated. If this new value of D is smaller than the previous one, the procedure is repeated. Optimization of this parameter is considered complete when D reaches a minimum. This

procedure is repeated successively for each parameter until an absolute minimum of D is achieved. The numerical optimization of parameters in this example gave the values: $\log K_a = 9.44$, $\epsilon_{HX} = 3.19 \times 10^4$ and $\epsilon_X = 1.365 \times 10^4$, with $D = 0.522$.

Graphical verification. With the best set of values from the above procedure, the log r vs. pH plot can be redrawn; log r is calculated from the experimental absorbances and the optimized absorptivities. Figure 3B shows the improvement achieved after the numerical optimization. The optimization improved the agreement with experimental data at high pH, but the results at low pH suggest a failure of the model.

REFERENCES

1 J. N. Butler, Chemical Equilibrium, Addison-Wesley, Massachusetts, 1964.
2 A. J. Bard, Chemical Equilibrium, Harper and Row, New York, 1966.
3 J. Inczedy, J. Chem. Educ., 47 (1970) 769.
4 D. W. Barnum, J. Chem. Educ., 59 (1982) 809.
5 R. de Levi, J. Chem. Educ., 47 (1970) 187.
6 J. Butcher and Q. Fernando, Anal. Chim. Acta, 36 (1966) 65.
7 N. G. Sellers and J. A. Caruso, J. Chem. Educ., 50 (1973) 547.
8 R. J. Vong and R. J. Charlson, J. Chem. Educ., 62 (1985) 141.
9 J. M. Cano, Doctoral Thesis, Anales de la Universidad Hispalense, Sevilla, 1971, p. 30.

ANALYTICA CHIMICA ACTA, VOL. 191 (1986)

AUTHOR INDEX

0003-2670/86/$03.50

'rinted in The Netherlands

CONTENTS

(Abstracted, Indexed in: Anal. Abstr.; Biol. Abstr.; Chem. Abstr.; Curr. Contents Phys. Chem. Earth Sci.; Life Sci.; Index Med.; Mass Spectrom. Bull.; Sci. Citation Index; Excerpta Med.)

Special issue on Chemometrics in Analytical Chemistry III, Proceedings of a Conference held in San Terenzo di Lerici, La Spezia, Italy, May 25–30, 1986

(For Contents list see preliminary pages vii–ix.)